Sunil Kumar Sharma
Ram Krishna Upadhyay
Vikram Kumar
Hardikk Valera *Editors*

Transportation Energy and Dynamics

Springer

Energy, Environment, and Sustainability

Series Editor

Avinash Kumar Agarwal, Department of Mechanical Engineering, Indian Institute of Technology Kanpur, Kanpur, Uttar Pradesh, India

AIMS AND SCOPE

This books series publishes cutting edge monographs and professional books focused on all aspects of energy and environmental sustainability, especially as it relates to energy concerns. The Series is published in partnership with the International Society for Energy, Environment, and Sustainability. The books in these series are edited or authored by top researchers and professional across the globe. The series aims at publishing state-of-the-art research and development in areas including, but not limited to:

- Renewable Energy
- Alternative Fuels
- Engines and Locomotives
- Combustion and Propulsion
- Fossil Fuels
- Carbon Capture
- Control and Automation for Energy
- Environmental Pollution
- Waste Management
- Transportation Sustainability

Review Process

The proposal for each volume is reviewed by the main editor and/or the advisory board. The chapters in each volume are individually reviewed single blind by expert reviewers (at least four reviews per chapter) and the main editor.

Ethics Statement for this series can be found in the Springer standard guidelines here https://www.springer.com/us/authors-editors/journal-author/journal-author-helpdesk/before-you-start/before-you-start/1330#c14214

Sunil Kumar Sharma · Ram Krishna Upadhyay ·
Vikram Kumar · Hardikk Valera
Editors

Transportation Energy and Dynamics

Editors
Sunil Kumar Sharma
School of Engineering and Applied Science
Gati Shakti Vishwavidyalaya
Vadodara, Gujarat, India

Ram Krishna Upadhyay
School of Engineering and Applied Science
Gati Shakti Vishwavidyalaya
Vadodara, Gujarat, India

Vikram Kumar
Department of Mechanical Engineering
Indian Institute of Technology Kanpur
Kanpur, Uttar Pradesh, India

Hardikk Valera
Engine Research Laboratory
Indian Institute of Technology Kanpur
Kanpur, Uttar Pradesh, India

This Springer imprint is published by the registered company Springer Nature Singapore Pte Ltd.
The registered company address is: 152 Beach Road, #21-01/04 Gateway East, Singapore 189721,
Singapore

Preface

Energy in transport systems plays an essential role in terms of the functioning, efficiency, and ecology of transport systems and sustainable urban mobility. The wider context of these issues is transport systems, in which energy is an element of synergy in the functioning of all aspects of smart cities.

The International Society for Energy, Environment and Sustainability (ISEES) was founded at the Indian Institute of Technology Kanpur (IIT Kanpur), India, in January 2014 to spread knowledge/awareness and catalyse research activities in the fields of Energy, Environment, Sustainability, and Combustion. Society's goal is to contribute to the development of clean, affordable, and secure energy resources and a sustainable environment for society, spread knowledge in the areas mentioned above, and create awareness about the environmental challenges the world is facing today. The unique way adopted by ISEES was to break the conventional silos of specialisations (engineering, science, environment, agriculture, biotechnology, materials, fuels, etc.) to tackle the problems related to energy, environment, and sustainability in a holistic manner. This is quite evident in the participation of experts from all fields to resolve these issues. The ISEES is involved in various activities, such as conducting workshops, seminars, and conferences, in the domains of its interests. The society also recognises the outstanding works of young scientists, professionals, and engineers for their contributions in these fields by conferring them awards under various categories.

Sixth International Conference on 'Sustainable Energy and Environmental Challenges' (VI-SEEC) was organised under the auspices of ISEES from 27 to 29 December 2021 in hybrid mode due to restrictions on travel because of the ongoing COVID-19 pandemic situation. This conference provided a platform for discussions between eminent scientists and engineers from various countries, including India, Spain, Austria, Australia, South Korea, Brazil, Mexico, USA, Malaysia, Japan, Hong Kong, China, the UK, Netherlands, Poland, Finland, Italy, Israel, Kenya, Turkey, and Saudi Arabia. At this conference, eminent international speakers presented their

views on energy, combustion, emissions, and alternative energy resources for sustainable development and a cleaner environment. The conference presented two high-voltage plenary talks by Prof. Ashutosh Sharma, Secretary, DST, and Dr. V. K. Saraswat, Honourable Member, NITI Ayog.

The conference included 12 technical panel discussions on energy and environmental sustainability topics. Each session had 6–7 eminent scientists who shared their opinion and discussed the trends for the future. The technical sessions at the conference included Rail and Road Transportation, Sustainable Energy and Environment, Materials and Design, Treatment, and Possible Solutions.

About 500+ participants and speakers from around the world attended this three-day conference.

This conference laid out the roadmap for technology development, opportunities, and challenges in Energy, Environment, and Sustainability domains. All these topics are very relevant for the country and the world in the present context. We acknowledge the support from various agencies and organisations for conducting the Sixth ISEES Conference (VI-SEEC) where these books germinated. We want to acknowledge our publishing partner Springer (special thanks to Ms. Swati Mehershi).

The editors would like to express their sincere gratitude to many authors worldwide for submitting their high-quality work on time and revising it appropriately at short notice. We want to express our special gratitude to our prolific set of reviewers, Dr. Chandan Pandey, Dr. Prakash Kumar, Dr. Jaesun Lee, Dr. Sunho Choi, and Dr. Mohammed Aslam who reviewed various chapters of this monograph and provided their valuable suggestions to improve the manuscripts.

This book is based on featuring in-depth coverage of passenger and freight transportation. This comprehensive resource discusses modern transportation systems and options for improving their sustainability. The book addresses vehicle and infrastructure design, economics, environmental concerns, energy security, and alternative energy sources and platforms. Worked-out examples, case studies, illustrations, equations, and end-of-chapter problems are also included in this practical guide. This essential multi-authored work reflects a new sustainable transportation planning paradigm. It explores sustainable development and transportation concepts, describes practical techniques for a comprehensive evaluation, provides tools for multi-modal transport planning, and presents innovative mobility management solutions to transportation problems. This text reflects a fundamental change in transportation decision-making. It focuses on accessibility rather than mobility, emphasises the need to expand the range of options and impacts considered in the analysis, and provides practical tools to allow planners, policymakers, and the general public to determine the best solution to the transportation problems facing a community. Chapters include recent results and focus on current trends in the transport sector.

In this book, readers will get an idea about the transportation ecosystem, its components, its challenges, its contribution to economic growth, and the interplay between the stakeholders that govern the system. The book will examine the background and history of transportation, emphasising the industry's fundamental role and importance in companies, society, and the environment in which transportation service is

provided. The book will also provide an overview of carrier operations, management, technology, and the strategic principles for successfully managing different modes of transportation. We hope the book will greatly interest the professionals and post-graduate students involved in transportation, energy, and environmental research.

Vadodara, India   Sunil Kumar Sharma
Vadodara, India   Ram Krishna Upadhyay
Kanpur, India   Vikram Kumar
Kanpur, India   Hardikk Valera

Contents

Sustainable Energy and Environment

Materials and Design

Technology Driven Application

Editors and Contributors

About the Editors

Dr. Sunil Kumar Sharma is an Assistant Professor and the Assistant Program Director of the Engineering and Applied Science Department at the Gati Shakti Vishwavidyalaya, Vadodara, a Central University, established by the Ministry of Railway, Government of India. He has received his Ph.D. from the Indian Institute of Technology, Roorkee. He worked at the Non-destructive Evaluation and Structural Health Monitoring Laboratory at C. N. University, South Korea. His research interests are vehicle dynamics, contact mechanics, mechatronics, and real-time software-enabled control systems for high-speed rail vehicles. He published several research articles in a national and international journals. Dr. Sharma is also featured among the top 2% of scientists in a global list compiled by Stanford University, USA.

Dr. Ram Krishna Upadhyay is currently working as an Assistant Professor at the Gati Shakti Vishwavidyalaya, Vadodara, a Central University, established by the Ministry of Railway, Government of India. He has received his Ph.D. and M.Tech. from the Indian Institute of Technology (ISM) Dhanbad in Mechanical Engineering with a broad specialization in Surface Engineering and Tribology. Before joining Gati Shakti Vishwavidyalaya, Vadodara, Dr. Ram worked as Postdoctoral Fellow at the Indian Institute of Technology Kanpur for over three and a half years. His research interests include lubrication and materials wear for

industrial application, tribology of additive manufactured parts, and nanocomposites. He is a recipient of the SERB-ACS NPDF best poster competition award by the Science and Engineering Research Board, New Delhi, and the American Chemical Society, USA. He published several journal papers, book chapters, edited a book, and completed a project funded by the Science and Engineering Research Board, New Delhi.

Dr. Vikram Kumar is currently at IIT Kanpur. He received his Ph.D. in Mechanical Engineering from the Indian Institute of Technology Kanpur, India, in 2018. His areas of research include Polymer and composite coating; wear, friction, and lubrication; IC engine tribology; alternative fuels; advanced low-temperature combustion; engine emissions measurement; particulate characterization. Dr. Kumar has edited two books and authored nine book chapters and 19 research articles in international journals and conferences. He has been awarded with 'ISEES Best Ph.D. Thesis Award' (2018), 'Senior Research Associateship under 'SCIR-POOL Scientist' (2018–2021). He is a lifetime member of ISEES.

Hardikk Valera is pursuing Ph.D. from the Engine Research Laboratory (ERL), Department of Mechanical Engineering, Indian Institute of Technology (IIT) Kanpur. He has completed his M.Tech. and B.Tech. from the National Institute of Technology (NIT) Jalandhar, India, and Ganpat University, respectively. His research interests include methanol fuelled SI engines, methanol fuelled CI engines, optical diagnostics, fuel spray characterization, and emission control from engines.

Contributors

Yakubu Khartum Abubakar Department of Mechanical Engineering, Federal Polytechnic Idah, Idah, Nigeria

Abiodun Oluwatosin Adeoye Department of Chemistry, Federal University Oye-Ekiti, Oye, Ekiti State, Nigeria

Henry Afolabi Department of Urban and Regional Planning, Obafemi Awolowo University, Ile-Ife, Osun, Nigeria

Folaranmi Olufisayo Akinosun Department of Public Administration, Ambrose Alli University, Ekpoma, Edo, Nigeria

Olamide Akintifonbo Ministry of Housing, Physical Planning and Urban Development, Ado-Ekiti, Ekiti, Nigeria

Muhammed Toyyib Aliyu Department of Chemical Engineering, Ahmadu Bello University Zaria, Zaria, Nigeria

Mohd Avesh Star Saidham Services Solutions, Doiwala, Dehradun, India

Duppala Azad Department of Mechanical Engineering, Aditya Institute of Technology and Management, Tekkali, Andhra Pradesh, India

B. A. Ranganath Department of Mechanical Engineering, MVGR College of Engineering, Vizianagaram, Andhra Pradesh, India

A. Bhargavi Prism Johnson Limited, Mumbai, India

Levent Bilgili Department of Naval Architecture, Maritime Faculty, Bandirma Onyedi Eylul University, Bandirma, Balikesir, Türkiye

Amit Kumar Chaurasia Amity Institute of Biotechnology, Amity University Uttar Pradesh, Noida, India

Gyang Emmanuel Dang Department of Electrical and Electronic Engineering, Abubakar Tafawa Balewa University, Bauchi, Nigeria

Raghuveer Dontikurti Department of Mechanical Engineering, Aditya Institute of Technology and Management, Tekkali, Andhra Pradesh, India

Sreeramulu Dowluru Department of Mechanical Engineering, Aditya Institute of Technology and Management, Tekkali, Andhra Pradesh, India

Azad Duppala Department of Mechanical Engineering, Aditya Institute of Technology and Management, Tekkali, Andhra Pradesh, India

Victor Great Edidem Department of Mechanical Engineering, Federal University of Technology Minna, Minna, Nigeria

Elissavet Emmanouilidou Department of Chemistry, School of Science, International Hellenic University, Kavala, Greece;
Petroleum Institute, International Hellenic University, Kavala, Greece

Emmanuel Oghenero Emojevu Department of Chemistry, University of Benin, Benin, Nigeria

Hadj-Mabrouk Habib Vice-Presidency Research (VPR), University Gustave Eiffel, Marne La Vallée, France

Baba Nwunuji Hikon Department of Chemical Sciences, Federal University Wukari, Wukari, Taraba State, Nigeria

Ismail Hossain School of Natural Sciences and Mathematics, Ural Federal University, Yekaterinburg, Russia

Shailendra Jain Department of Electrical Engineering, Maulana Azad National Institute of Technology, Bhopal, MP, India

Hong-Lae Jang School of Mechanical Engineering, Changwon National University, Changwon-Si, Republic of Korea

Nikolaos C. Kokkinos Department of Chemistry, School of Science, International Hellenic University, Kavala, Greece;
Petroleum Institute, International Hellenic University, Kavala, Greece

Subhadeep Kuila School of Engineering and Applied Sciences, National Rail and Transportation Institute, Vadodara, India

Vikram Kumar Mechanical Engineering Department, Indian Institute of Technology Kanpur, Kanpur, India

Prashant Kumbhkar Department of Chemical Engineering, Ujjain Engineering College, Ujjain, India

Alexander V. Lagerev Academician I G Petrovskii Bryansk State University, Bryansk, Russia

Igor A. Lagerev Academician I G Petrovskii Bryansk State University, Bryansk, Russia

Shilpi Lavania Department of Electronics and Communication Engineering, Institute of Engineering and Technology, Dr. Bhimrao Ambedkar University, Agra, India

Olayide Samuel Lawal Department of Chemistry, Federal University Oye-Ekiti, Oye, Ekiti State, Nigeria

Jaesun Lee School of Mechanical Engineering, Changwon National University, Changwon-Si, Republic of Korea

Musa Joshua Maikato Department of Mechanical Engineering, Ahmadu Bello University Zaria, Zaria, Nigeria

Dosu Malomo Department of Chemistry, Federal University Oye-Ekiti, Oye, Ekiti State, Nigeria

Pankaj Malviya Department of Chemical Engineering, Indore Institute of Science and Technology, Indore, India

Swati Mohapatra School of Science, Gujarat State Fertilizers and Chemicals University, Vadodara, Gujarat, India

Venkatesh Muddada Department of Mechanical Engineering, Aditya Institute of Technology and Management, Tekkali, Andhra Pradesh, India

Onyeka Francis Offor Department of Pure and Industrial Chemistry, University of PortHarcourt, PortHarcourt, Nigeria

Olorunfemi Ayodeji Olojede Department of Urban and Regional Planning, Obafemi Awolowo University, Ile-Ife, Osun, Nigeria

Oluwatimilehin Gabriel Oluborode Department of Urban and Regional Planning, Obafemi Awolowo University, Ile-Ife, Osun, Nigeria

Oluyemisi Omotayo Omonije Department of Biochemistry, Federal University of Technology Minna, Minna, Nigeria

Srihari Palli Department of Mechanical Engineering, Aditya Institute of Technology and Management, Tekkali, Andhra Pradesh, India

Hemant Parmar Department of Mechanical Engineering, Ujjain Engineering College, Ujjain, India

Karthik V. N. P. Perla Grasim Industries Limited, Mumbai, India;
School of Engineering and Applied Sciences, National Rail and Transportation Institute, Vadodara, India

Boniface Eche Peter Department of Pure & Applied Chemistry, Usmanu Danfodiyo University, Sokoto, Nigeria

Nisha Prasad Research Scholar, Department of Electrical Engineering, Maulana Azad National Institute of Technology, Bhopal, MP, India

Oleg Pudovikov Russian University of Transport (MIIT), Moscow, Russian Federation

Rukayat Oluwatobiloba Quadri Department of Chemistry, Federal University Oye-Ekiti, Oye, Ekiti State, Nigeria

Sivasankara Raju Rallabandi Department of Mechanical Engineering, Aditya Institute of Technology and Management, Tekkali, Andhra Pradesh, India

Duppatla Rambabu Department of Mechanical Engineering, Aditya Institute of Technology and Management, Tekkali, Andhra Pradesh, India

D. Bhanuchandra Rao Department of Mechanical Engineering, Aditya Institute of Technology and Management, Tekkali, Andhra Pradesh, India

Pavankumar Rejeti Department of Mechanical Engineering, Aditya Institute of Technology and Management, Tekkali, Andhra Pradesh, India

Kumar Saurav School of Engineering and Applied Sciences, National Rail and Transportation Institute, Vadodara, India

Palak Shah Department of Chemical Engineering, Indore Institute of Science and Technology, Indore, India

Rakesh Chandmal Sharma Mechanical Engineering Department, Graphic Era (Deemed to be University), Dehradun, India

Sunil Kumar Sharma Gati Shakti Vishwavidyalaya, Vadodara, Gujarat, India

Angela Shvets Ukrainian State University of Science and Technologies, Dnipro, Ukraine

Ezeaku Henry Sochima Department of Metallurgical and Materials Engineering, University of Nigeria Nsukka, Nsukka, Nigeria

Annie Srivastava Rail India Technical and Economic Service Limited, New Delhi, India

Hema Shreaya Sura Mahindra Logistics Limited, Mumbai, India

Lokendra Singh Thakur Department of Chemical Engineering, Ujjain Engineering College, Ujjain, India

Ram Krishna Upadhyay Gati Shakti Vishwavidyalaya, Vadodara, Gujarat, India

Hardikk Valera Engine Research Laboratory, Indian Institute of Technology Kanpur, Kanpur, India

Anil Kumar Verma Department of Chemical Engineering, Assam Energy Institute, Sivasagar, India

Sudhanshu Yadav School of Engineering and Applied Sciences, National Rail and Transportation Institute, Vadodara, India

Mohammed Giwa Yahaya Department of Mechanical Engineering, Federal University of Technology Minna, Minna, Nigeria

Nikita Zhukhin Russian University of Transport (MIIT), Moscow, Russian Federation

General

Introduction to Sustainable Transportation System

Sunil Kumar Sharma, Ram Krishna Upadhyay, Vikram Kumar, and Hardikk Valera

Abstract Transportation plays a substantial role in the modern world; it provides tremendous benefits to society and imposes high economic, social, and environmental costs. Sustainable transport planning requires integrating environmental, social, and economic factors to develop optimal solutions to our many pressing issues, especially carbon emissions and climate change. This book explores sustainable development and transportation concepts, describes practical techniques for a comprehensive evaluation, provides tools for multi-modal transport planning, and presents innovative mobility management solutions to transportation problems. Moreover, it focuses on accessibility rather than mobility, emphasizes the need to expand the range of options and impacts considered in the analysis, and provides practical tools to allow planners, policymakers, and the general public to determine the best solution to the transportation problems facing a community.

This multi-authored book reflects new sustainable transportation design and planning techniques. It explores sustainable development and transportation concepts, describes practical techniques for a comprehensive evaluation, provides tools for multi-modal transport planning, and presents innovative mobility management solutions to transportation problems.

The Part I of this book includes one chapter based on the introduction of different sections and presents the important aspects of each section.

S. K. Sharma (✉) · R. K. Upadhyay
Gati Shakti Vishwavidyalaya, Vadodara, Gujarat 390004, India
e-mail: sk.sharma@gsv.ac.in

V. Kumar
Mechanical Engineering Department, Indian Institute of Technology Kanpur, Kanpur 208016, India

H. Valera
Engine Research Laboratory, Indian Institute of Technology Kanpur, Kanpur 208016, India

The Part II of this book is based on rail and road transportation. Chapter 2 of this part discusses recent trends of biodiesel-blended powered trains worldwide with a focus on feedstock availability, blending limits, infrastructure, and maintenance cost indicating their potential for a rapid shift to a sustainable railway sector. Chapter 3 investigates the longitudinal oscillations arising in a train using a mathematical modeling technique. Chapter 4 explains how the international standards were analyzed to derive the strength requirements for the interior plate for the rolling-type gangway, which the authors have developed for the application of urban railroad vehicles in Korea using finite element analysis. Chapter 5 shows that if the operation and patronage dynamics of the Lagos Shuttle Train Services were improved on passengers' welfare and NRC's effectiveness would be enhanced with many beneficial spinoffs. Toward this end, workable policies are recommended. Chapter 6 gives a basic understanding of the high-speed rail transportation systems. It describes the various constituents of high-speed rail transportation systems in detail, focusing on the advancement of different countries in this technology to make the system efficient and sustainable. This chapter also highlights the relevance of linear motor-based high-speed rail transit systems in today's scenario. A comparison of these technologies to analyze their applicability to India was also discussed. Chapter 7 of this part proposes a new hybrid method based on three machine learning algorithms for rail safety measures. Chapter 8 predicts the land values after the introduction of Mumbai Ahmedabad High-Speed Rail (MAHSR) in the cities with the high-speed rail (HSR) stations. Chapter 9 gives the comparative analysis of regenerative braking at different gradients for Indian Railways WAP-7 locomotive incorporating a flywheel model. Chapter 10 of this part presents a mathematical model which describes the spatial oscillations of a train of freight railcars moving along a section of the track with vertical and horizontal irregularities.

The Part III of the book is based on sustainable energy and environment. Chapter 11 of this part is based on sustainable energy via the thermochemical and biochemical conversion of biomass wastes for biofuel production. Chapter 12 provides an overview of process management in green manufacturing with a case study. Chapter 13 gives a technique to treat the high metals' contaminants that threaten the environment. This study further focused on the occurrence and allocation of heavy metals and the possible eco-friendly environmental remedies. Chapter 14 discusses and draws attention to the life cycle perspective in the calculation of greenhouse gas emissions and compares the short-, medium-, and long-term effects of transportation modes both with themselves and each other.

The Part IV of this book is based on materials and design, which covers the design and operation of mobile aerial ropeways based on an autonomous self-propelled chassis and the effect of different composite materials on turbocharger wheels.

The Part V of this book includes four chapters. Chapter 17 is based on deploying machine learning models for predictive maintenance of high-value assets of Indian Railways. The objective is to understand the current maintenance policies used by Indian Railways and then outline the potential advantages of implementing predictive maintenance. To signify the importance of predictive maintenance, an analysis is performed over real-world data of rolling stock by training a machine learning model

over the data and predicting the remaining useful life of the components. Chapter 18 develops and validates a verbal alert utility scale for intelligent transportation systems to address the safety of transportation cyber-physical systems. Chapter 19 describes the framework for digital supply chains and analysis of the impact of challenges on implementing digital transformation. Chapter 20 of this part discusses the design and modeling of digital twin technology to improve freight logistics. It also examines whether this technology is a viable opportunity to venture into freight logistics policymaking and infrastructure planning.

This monograph presents the different technologies which can be used to increase the energy efficiency of the transportation sector and sustainability. Specific topics covered in the monograph include:

- Conventional, hybrid, and electric drive systems
- Transport infrastructure as a power supply for transport systems
- Human drive vehicles, autonomous vehicles, connected vehicles
- Various communication environments and innovative new mobility service
- Energy networks in smart cities
- Demand-responsive transport and demand-responsive service
- Deep learning, machine learning, and artificial intelligence in transportation systems and applications.

The topics are organized into five different sections: (i) General, (ii) Rail and Road Transportation, (iii) Sustainable Energy and Environment, (iv) Materials and Design, and (v) Technology-Driven Application. Particular topics covered in this book are as follows:

- Introduction to Sustainable Transportation System
- Sustainable Rail Fuel Production from Biomass
- Automatic Speed Control of Heavy-Hauler Trains
- A Study on the Strength Analysis of Interior Plate for Rolling-Type Gangways of Urban Railroad Vehicle
- Operation and Patronage Dynamics of the Lagos Shuttle Train Services, Lagos, Nigeria
- Linear Motors for High-Speed Rail Transit System: A Sustainable Approach
- Approach to Assist in the Discovery of Railway Accident Scenarios Based on Supervised Learning
- Predicting the Effect on Land Values After Introducing High-Speed Rail
- Comparative Study of Regenerative Braking at Different Gradients for Indian Railways WAP-7 Locomotive Incorporating a Flywheel Model
- Multibody Model of Freight Railcars Interaction in a Train
- Sustainable Energy via Thermochemical and Biochemical Conversion of Biomass Wastes for Biofuel Production
- Process Management in Green Manufacturing
- Heavy Metals Contaminants Threat to Environment: Its Possible Treatment
- Operational Greenhouse Gas Emissions of Air, Rail, Road, and Sea Transport Modes in Life Cycle Perspective

- Mobile Aerial Ropeways Based on an Autonomous Self-propelled Chassis: Design and Operation
- Design and Analysis of Turbo Charger Turbine Wheel Using Composite Materials
- Deploying Machine Learning Models for Predictive Maintenance of High-Value Assets of Indian Railways
- Developing and Validating a Verbal Alert Utility Scale for Intelligent Transportation Systems: To Address the Safety of Transportation Cyber-Physical Systems
- Framework for Digital Supply Chains and Analysis of Impact of Challenges on Implementation of Digital Transformation
- Design and Modeling of Digital Twin Technology to Improve Freight Logistics.

Rail and Road Transportation

Sustainable Rail Fuel Production from Biomass

Nikolaos C. Kokkinos and **Elissavet Emmanouilidou**

Abstract Decarbonization of the transportation sector is a crucial concern in order to mitigate climate change and reduce the dependency on fossil fuels. The contribution of the transportation sector to global greenhouse gas emissions accounts for about one-fourth. In spite of the fact that the rail sector is considered the most energy-efficient and environmentally friendly transportation mode, diesel still dominates as fuel. Toward to the net-zero greenhouse gas emissions target by 2050, the rail industry needs to deploy sustainable technologies for locomotives. The electrification of locomotives is costly, and battery-powered trains, as well as hydrogen trains, are not yet feasible for long-distance journeys. However, the utilization of biodiesel blends is the most promising option in the short-to-medium term allowing the use of the current diesel fleet. Biomass conversion technologies for biodiesel production from non-edible sources could promote the sustainability of biodiesel adoption in railway transport. The current chapter highlights recent trends of biodiesel-blended powered trains over the world focused on feedstock availability, blending limits, infrastructure, and maintenance cost indicating their potential for a prompt shift to a sustainable railway sector.

Keywords Sustainability · Railway sector · Biofuels · Biodiesel · Transportation

1 Introduction

The transport sector remains one of the major consumers of fossil fuels, and its decarbonization is a crucial concern in order to reduce greenhouse gas (GHG) emissions and meet the goals of the Paris Agreement [1]. Specifically, in 2015, over 100 countries agreed to keep the increase in global average temperature below 2 °C and

N. C. Kokkinos (✉) · E. Emmanouilidou
Department of Chemistry, School of Science, International Hellenic University, Ag. Loukas, 654 04 Kavala, Greece
e-mail: nck@chem.ihu.gr

Petroleum Institute, International Hellenic University, Ag. Loukas, 654 04 Kavala, Greece

continue to pursue efforts to limit the temperature rise to 1.5 °C above pre-industrial thresholds by 2050. "Net zero" is defined as the balance between anthropogenic emissions by sources and removals by sinks of greenhouse gases (GHGs) in the second half of this century. Neutrality target requires eliminating all CO_2 and other GHG emissions for every end-use sector [2, 3].

Moving the transportation system toward sustainability requires innovative technologies and mobility services. Reduction of CO_2 emissions through optimization of combustion engines, electrification of propulsion systems, and development of battery technologies are some of the main large-scale trends in transport technologies. Autonomous driving systems, electrification of conventional drivetrains, hydrogen drive fuel cells technology, additive manufacturing using 3D printing, regulation, and transport policies are some examples of future transport technologies and drivers [4].

Rail is considered the most energy-efficient, fast, and environmentally friendly transport mode. In fact, rail requires 12 times less energy and emits 7–11 fewer GHGs per passenger-km traveled compared to road transport and the aviation sector. Moreover, freight rail is the least carbon-intensive way to transport goods. Toward a sustainable shift to a low-carbon mode of transport, the rail sector can significantly improve the wider move toward transport decarbonization [5–7].

Despite the fact that the rail sector is currently the most electrified transport subsector, however, oil accounted for 55% of total energy consumption. The most popular locomotive engine is an internal combustion engine that operates with diesel. The popularity of diesel engines in rail applications relies on their high compression ratio and thermal efficiency percentage, which is above 45% during the ignition process. Typically, 88% of this energy is sent to the wheels by the linked electric drive system, alternator, and traction motors. Therefore, as more stringent standards have to be implemented regarding GHG emissions reduction, several alternative solutions have been reported [7–9].

Alternative fuels present differentiations in their origin and production methods; however, they are all produced through sustainable processes without additional emissions of CO_2. The main representatives of alternative fuels include electro-fuels, hydrogen, ammonia, biodiesel, alcohol-derived fuels, dimethylether (DME), etc. Nevertheless, at present, the majority of alternative fuels have not been commercialized [8, 10].

Biodiesel presents a high potential to be used as an alternative fuel in the railway sector as a blend with fossil diesel and in the future as an independent fuel in existing diesel locomotive engines [11]. An increase in the biodiesel blend limit could be an intermediate solution that can result in over 50% on environmental impact. Non-edible feedstocks as well as biomass-waste materials for biodiesel production can be utilized in order to meet biodiesel demand needs for transportation. Technological improvement and cost elimination of advanced bio-mass-to-liquid conversion technologies such as pyrolysis, gasification, and hydrothermal liquefaction (HTL) will be definitely beneficial [12, 13]. However, environmental, social, and economic sustainability are the three main facets of global biodiesel challenges to meet future demand. The sustainability of biodiesel production is still uncertain, due to the current high production costs. Rapeseeds and sunflower seeds (EU), soybeans (Argentina, Brazil,

USA), palm oil, and Jatropha oil (Indonesia) are currently the most widely utilized raw materials among the major producers [14].

Over time, conventional diesel-powered locomotives are going to be replaced with electric and hybrid ones. Hydrogen is more likely to be used in the far future due to high infrastructure cost and concerns associated with its transportation, storage, and handling [8].

2   Energy Supply and Demand in the Transport Sector

Currently, world transportation energy demand is mainly based on fossil fuels. Automobile gasoline is the principal fuel, and its share of total transportation energy consumption is projected to be decreased from 39% in 2012 to 33% in 2040. Diesel is considered the second-largest transportation fuel, and its share is going to be reduced from 36% in 2012 to 33% in 2040 [15]. According to US Energy Information Administration (EIA) [16], liquid fuels will dominate as an energy source; however, renewable energy use will increase to almost the same level. Moreover, global gas production will grow by approximately 30% between 2020 and 2050. High oil dependence and increased energy use the in transport sector necessitate the adoption of alternative fuels in order to mitigate climate change and improve energy security [17]. Nevertheless, in most developing countries, non-renewable energy is commonly used [18].

Without prompt action, carbon dioxide emissions would be more than double by 2040 and will have a negative impact on the climate. However, conventional methods are mostly used to produce biofuels in developing nations. In general, inadequate infrastructure, ineffective conversion technologies, a lack of readily available feedstock, and limited funding choices are to blame for the greater cost of biofuel production in developing nations [19]. Communities in developing countries are using less biofuel because of rising production cost, which is deterring producers from investing in the industry. Developing nations that have already moved their investment priorities to the renewable energy sector and passed the take-off stage are those where the impact of using renewable energy on economic growth is positive and greater than the impact of using non-renewable energy. For long-term economic development, they can implement cutting-edge policy measures including feed-in tariffs, renewable portfolio standards, green certificates, and divesting from fossil fuels [20].

According to International Energy Agency's (IEA) Report [21], biofuel demand in the transport sector was definitely affected by the COVID-19 pandemic from 2019 to 2021; however, it was expected to reach pre-COVID-19 levels in 2021. In Net Zero Emissions Scenario by 2050, biofuels comprise the most important option for transportation compared to other low-carbon technology perspectives. Feedstocks that do not compete with food crops are going to be extensively utilized for biofuel production, while their demand is estimated to be 45% of total biofuel demand by

2030. In order to fulfill the "two-degree scenario", the use of 29.6 EJ of biofuels along with other renewable energy sources is required by 2060 [22].

To date, biomass is one of the largest renewable and abundant energy sources and accounts for 10% of the global energy supply and 13% of energy consumption. In Europe, the majority of biomass (59%) is used for feed and food production, whereas its share in bioenergy production is 21%. Toward net-zero GHG emissions target, bioenergy production and consumption are going to be increased; however, the EU is still heavily dependent on fossil fuels [23]. In 2016, biomass covered 11% of global energy consumption, while biofuel use in the transport sector reached 4% [24].

In 2016, biodiesel production in Europe was five times higher than ethanol production as the transport sector in the EU uses higher amount of diesel compared to gasoline [25]. Global biodiesel production is expected to be increased by 9% from 2017 to 2027, while EU will continue to be the major producer of biodiesel, followed by the USA and Brazil [26].

2.1 Environmental Impact Legislation

The transport sector is considered one of the major energy consumers globally. Specifically, it contributes to 29% of global energy consumption and 65% of petroleum products consumption. Among several regions, USA and China presented the highest cumulative CO_2 emissions from 2000 to 2015, although the utilization of renewable energy and electricity improved [27].

Decarbonization of the transport sector is a global concern as 15% of global greenhouse gas (GHG) emissions and 20% of energy-related CO_2 emissions are generated by this sector. The main drivers for transportation emissions include economic growth, changes in fuel quality, and the adoption of stricter policies regarding emissions control on vehicles and engines. Hence, there are variations in transportation emissions around the globe [28].

Association between transport energy consumption and CO_2 emissions has to be taken into serious consideration. In the developing counties, the implementation of stricter policies is crucial to reduce CO_2 emissions. Regulations on the import of used cars need to be more rigorous as they emit more emissions compared to cars in developed countries. Moreover, efficient policies have to be adopted in the urban settlements due to overcrowding [18].

According to Directive 2003/30/EC of the European Parliament and the European Council [29], EU-27 Member States were obliged to promote the use of biofuels or other alternative fuels for transport between 2006 and 2010. Emphasis was given in the need for commercialization of a minimum percentage of biofuels and other alternative fuels by EU national markets. Biofuel consumption increased during the aforementioned period; however, heterogeneity was observed in consumption increment between EU-27 Member States [30]. Toward a policy of binding objectives, Directive 2009/28/EC was introduced in order to establish that in each State Member, 10% of the energy consumed is generated from renewable sources and mainly biofuels

by 2020 [31]. Tax incentives and the implementation of biofuel blending mandates seemed to promote biofuels consumption in most of the countries [30].

In 2015, Paris Agreement that was adopted by 196 parties set a long term to limit global temperature rise to 2 °C with a strong aim for limiting temperature rise to 1.5 °C above pre-industrial levels by the end of the century. Developed countries will provide \$100 billion of climate finance per year by 2025 where higher goals will be set [32].

The European New Green Deal and the Renewable Energy Directive Recast (REDII) that was adopted in 2018 set ambitious targets to decarbonize transport sector in Europe by 2050. Road and rail transport is expected to operate with renewable energy of at least 14%. Moreover, REDII included measures for biofuels uptake in aviation and maritime sectors [33].

As stated the European Council, 27% of total energy consumption has to come from renewable sources such as biomass by 2030. Moreover, 0.5% of bioenergy supply for transport sector should be generated by second generation biofuels [34]. European railway companies agreed the following CO_2 reduction emission targets, defining as base year 1990: 30% by 2020, 50% by 2030, and 100% by 2050 [35].

3 Energy in the Railway Sector

The first age of bioenergy in transportation lasted all nineteenth century and part of twentieth century, where steam boilers used solid biomass to power locomotive and ship engines. Moreover, first cars, buses, and trucks used biofuels in their initial stages, while bioethanol and biodiesel were tested by Henry Ford (1896) and Rudolf Diesel (1895), respectively. However, due to large oil reserves discovery and low prices of gasoline and diesel, those fossil fuels dominate in the energy sector since the earlier part of the last century [22].

Decarbonization of the transport sector necessitates the utilization of new technologies and energy sources. Alternative fuels are produced through sustainable and environmental processes and can be used in vehicles with little or no modifications of combustion engines. In the transport sector, liquid and some gaseous fuels are the most promising options including vegetable oils and biodiesel, natural gas (NG), liquefied petroleum gas (LPG), hydrogen, electric/fuel cell, etc. Biofuels, especially biodiesel and solid biomass, are already used in the commercial level in the transport sector and industries [36, 37].

Electric modes of transport present high potential to contribute in the total energy mix in the future. Under existing technology in Europe today, it has been calculated that 72.3% of energy demand in the European transport sector could be electrified, whereas for the remaining part, biofuels comprise a promising approach [38]. Purely electric engines are commonly used in medium-power locomotives on connections where electric traction or catenary is available. Moreover, large investments are required [8].

Fig. 1 Alternative fuels for
the railway
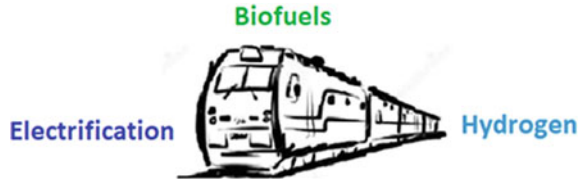
Hydrogen presents potential as an alternative fuel for locomotives in far future. Main drawbacks are high infrastructure cost as well as transportation, storage, and handling issues. One the other hand, ammonia and natural gas (in form of LNG) are more likely to be used due to economic and environmental attractiveness [8, 13].

Rail is considered one of the most energy-efficient and lowest-emitting transport modes for freight and passengers. According to IEA's Report 2021 [39], rail accounts for 8% of global passenger travel and about 9% of freight activity, whereas only 3% of transport energy use. Net Zero Emissions Scenario foresees alternative options for rail energy supply such as electrification, hydrogen, low-carbon fuels, and biofuels (Fig. 1). Nevertheless, oil accounted for 55% of total energy consumption in rail. In 2019, rail services consumed 0.6% of global oil use and 1.2% of global electricity consumption and emitted about 0.3% of direct CO_2. Rail infrastructure for both urban and high-speed rail expanded threefold between 2005 and 2015, while China presented the most infrastructure growth. In order to achieve Net Zero Scenario, hydrogen or battery electric trains coupled with partial track electrification need to replace diesel trains by 2030 [7].

International Railway Association (IRA) mainly focuses on GHG emissions reduction by 2030 and on the adoption of more sustainable traction modes by 2050. Diesel trains emit higher levels of GHGs, and they are noisier compared to electric ones [40]. Electric trains, as the name suggests, run on electricity rather than the conventional fossil fuels diesel and coal. Large-scale power plants, including those that provide electricity for homes, are used to produce electricity at first. Thus, depending on the power plant, the electricity may be produced using any energy source, such as coal or hydroelectricity [41]. The phenomenon of engine noise creation is quite complex in and of itself. There are three main causes of the noise that a diesel engine makes: combustion of gases, mechanical components of the engine, and exhaust gases [42]. Electrification of railway lines presents high capital and infrastructure costs, and it is difficult for all routes to be electrified. Hence, hybrid trains will continue to be developed over the following years [40].

The most common locomotive engine is an internal combustion engine that operates on diesel fuel. Cleaner fuel utilization is of great significance in order to mitigate GHG emissions. Hybrid combined locomotive engines using several alternative fuels such as natural gas, methanol, ethanol, hydrogen, and dimethyl ether have been recently modeled. However, multi-objective optimization is essential in the near future [10].

The majority of vehicles used in the transportation sector are trucks. However, there are several drawbacks of using road trucks for transportation, including: sensitivity to traffic in urban areas, accidents or breakdowns brought on by poor road conditions or unfavorable weather, limited load capacity for operations that require transportation of large quantities of materials over long distances, and high emissions of GHG. On the other hand, trains are more suited to move large loads over long distances avoiding most weather- and traffic-related issues [43].

Europe's ambition to shift road freight transport to rail could potentially open the way for significant deployment of hydrogen. Technologies based on hydrogen are ideal for large loads and high-energy demand, because they provide long-range solutions with quick refueling times. Hydrogen-powered trains can be a great way to replace diesel engines on non-electrified lines, and it should become a required component of national policy frameworks to further the goal of decarbonizing rail. The regional rail should be taken into account as one of the sectors where hydrogen might play a crucial role in achieving decarbonization at a reasonable cost. Some hydrogen-powered trains are already in operation, and others are being tested in several countries such as Germany, Netherlands, Austria, and France [44].

3.1 Biofuels Contribution

3.1.1 Biofuel Generations

Biofuels are renewable fuels derived from biomass, and they can be in gaseous, liquid, and solid forms. According to the degree of commercialization status regarding technological maturity, biofuels are generally categorized as conventional and as advanced. Conventional biofuels are produced through commercialized methods and include bioethanol, biodiesel, and biogas [45]. Typically, feed-based or food crops are used to produce first-generation (conventional) biofuels. Esterification, transesterification, hydrolysis, and fermentation are frequently commercialized methods used in the production process. Sugarcane, oilseeds, animal feed, and oil-containing food crops are often the feedstocks utilized to produce first-generation biofuels. Bioethanol is produced through the fermentation of sugar from beets, cane, or wheat starch, as well as starch from root crops. Alcohols, animal fat, or vegetable oils (palm, soybean) are esterified or transesterified to form fatty acid methyl esters (FAME) [46]. On the other hand, advanced biofuels include hydrotreated vegetable oil, lignocellulosic bioethanol, microalgae biodiesel, biohydrogen, etc. that are produced through conversion technologies that are still under development or in early commercialized stages [45, 47].

Depending on the feedstock used for biofuel production, three generations of biofuels exist. First-generation (1G) biofuels are derived by edible plant materials and crops. Most familiar 1G biofuels include vegetable oils, bio-alcohols, biodiesel, biogas, and solid biofuels. However, due to several disadvantages, such as land use competition, food vs. energy debate, higher carbon footprint utilization

of 1G biofuels is considered as unfavorable. Second generation (2G) or "advanced" biofuels are produced by non-edible feedstocks including dedicated energy crops, waste cooking oil (WCO), waste animal fats, lignocellulosic-based materials, agricultural and forestry residues, etc. Bioalcohols, bio-oil, biodiesel, bio-dimethyl ether (DMF), biosyngas Fischer–Tropsch (FT) biodiesel, and biohydrogen are some of main 2G biofuels. In the near future, 2G biofuels will be a promising solution for bioenergy demand fulfillment as most of conversion technologies are close to being commercialized even if production cost is still challenging. Finally, third- (3G) and fourth (4G)-generation biofuels are produced by algae and genetically or metabolically engineered microorganisms, respectively. Production methods involve several "algae-to-biofuels" technologies that are still under development stage [47–51].

3.1.2   Bioethanol and Biodiesel

The two most widely used biofuels in the transport sector are bioethanol and biodiesel [52]. They are mainly produced by lignocellulosic materials and vegetable oils and seeds, respectively. Bioethanol can be used as substitute of petrol, whereas biodiesel as substitute of diesel. Fermentation of sugar and starch-based materials is mostly used as production method of bioethanol. Lignocellulosic feedstocks could contribute over the next years in the production of "advanced" cellulosic bioethanol toward to a more sustainable waste-to-energy perspective [52–54].

Biodiesel is a mixture of fatty acid alkyl esters, and it is considered as a renewable and low-carbon substitute of fossil diesel for transport sector. Biodiesel can be produced by a variety of feedstocks such as edible oils, non-edible oils, and WCO as well as algae. The most common and effective production method is base-catalyzed transesterification of triglycerides with short chain alcohols (mainly methanol, ethanol). To date, feedstock accounts for about 80%, whereas catalyst 3–5% of total production cost [55, 56]. The quality of biodiesel is affected by several parameters such as feedstock composition, transesterification reaction conditions, etc. Hence, in order to be commercialized, it is mandatory to meet quality specifications and requirements established by institutions like the European Committee of Standardization (ISO) and the American Society for Testing and Materials (ASTM). Biodiesel blend that is the most frequently used in several vehicles' diesel engines without any engine modification is B20, while B5 is commonly used in fleets [56, 57].

Biodiesel has been extensively analyzed from the technological point of view; however, limited studies include successful implementation and supply chain of biodiesel in railway sector. Risks associated with fossil fuels and biofuels are different. Supply chain decisions can be categorized as strategic and operational. Certain supply risk management strategies for biodiesel involve raw material supply, transportation and logistics, production, and storage as well as market prices and government uncertainties [58].

Disposal of WCO in landfills can cause environmental contamination. Hence, sustainable waste management is crucial under the principles of the circular economy. The idea of circular economy has acquired substantial traction worldwide in the

recent years. The technological capacity for sustainable value creation is the driving force behind the circular economy. Early research on circular economies stressed the necessity for closed-loop material flow and technological innovation [59]. In terms of sustainable waste management, the following principles need to be applied following the hierarchy: (a) prevention, (b) preparing for reuse, (c) recycling, (d) other recovery, including energy recovery, and (e) disposal [60]. Among several strategies, WCO utilization as feedstock for biodiesel production is an attractive option that can also reduce production cost. However, since free fatty acids (FFAs) concentration is high in WCO, acid-catalyzed esterification is required before the transesterification process. Economic evaluation results indicate that biodiesel production from WCO can be economically feasible if special waste management policies will be implemented and WCO recycling will be improved [61–63].

Drop-in fuel production from biomass is an ongoing challenge that needs to be addressed in order to avoid first-generation biofuel drawbacks and mitigate GHG emissions under a more sustainable way. Production cost is currently higher than fossil fuels, while feedstock availability still remains uncertain. Utilization of waste biomass as feedstock could eliminate production cost and GHG emissions. Thermochemical conversion routes such as pyrolysis, gasification-Fischer–Tropsch (GFT) synthesis, and hydrothermal liquefaction (HTL) are in the forefront of development for a variety of biomass-based feedstocks [12]. Definitely, the rail sector and companies have to understand the benefits of biodiesel utilization. It is very important to be efficiently educated in engineering, the practical side of biodiesel use as well as in making biodiesel marketable to consumers [64].

4   Current Status and Future Perspectives in the Railway Sector

Most light railway networks in urban areas are electrified. However, there are still diesel-fueled railways. One promising way to reduce GHG emissions is the utilization of renewable fuels and specifically biodiesel in the railway sector [11].

The development of locomotive and the improvement of rail transportation is very important in order to reduce the dependence on fossil fuels. Alternative fuels such as methanol, DME, and biodiesel can resolve the energy crisis in the near future [6]. Locomotives are compression ignition engines fueled with diesel, and their technology is the same used in the automotive sector before 30–40 years. Despite the fact that diesel locomotives are environmental pollutants, total replacement by electrified locomotives is not feasible as electricity supply is not available in all areas. The electrification of transportation necessitates the integration of vehicles into a reliable, affordable, and user-friendly infrastructure for the supply of energy, such as in rail transportation via the catenary and in other modes via static or dynamic charging, battery swapping (questionably economical), or hydrogen tank filling [65].

Moreover, diesel locomotives are more efficient in the conversion of chemical energy into electricity [66].

Biodiesel can be used directly in both freight and passenger locomotives. Several countries use biodiesel as a blend in locomotive diesel engines such as UK, USA, and India. In fact, the British railway ran the first biodiesel-fueled train using 20% of biodiesel and 80% of fossil diesel [55].

Diesel traction of EU railway operations accounts only for 20%, and diesel fleet characteristics vary among the countries. In Baltic States, Ireland, and Greece, the majority of fleets are diesel-fueled, whereas in Germany and France, diesel traction is mainly used in sections with low transport [5]. Specifically, in Germany, railway sector is mainly electrified. In fact, the rate of electric operation reached 99%, 79%, and 87% for long-distance rail passenger transport, regional transport, and freight transport, respectively [67].

Indian Railways operate mainly electric and diesel locomotives. In fact, it has over 5000 diesel locomotives. The Ministry of New and Renewable Energy stated a minimum share of biofuels in the market to meet energy demand needs in the future. An indicative target of 20% blending of biofuels has been proposed by 2017. Several studies on the effect of biodiesel on locomotive emissions indicated that in the case of unsaturated feedstocks, lower NO_x emissions occurred. Lower blends of biodiesel can be used without any major engine modifications; however, issues such as storage, handling, and usage need to be addressed [68].

Railway transport will be strengthened in the future. Two main goals that EU set are: (a) road freight over 300 km should shift by 30% to other modes including rail and waterborne transport by 2030 and more than 50% by 2050, and (b) the majority of medium-distance passenger transport should be by rail. Biodiesel use in rail transport could be enhanced as most engine manufacturers can improve biodiesel blends. Moreover, tax incentives for biofuels are less compared to road transport [69].

5 Conclusion

The rail sector is considered the most energy-efficient and lower GHG emitter among all transport modes. Toward the decarbonization of transport sector, rail contribution will be of great significance. Pure electrified and hydrogen-fueled trains are still under demonstration scale, and the main drawback is the major infrastructure cost. Since diesel still dominates in rail sector, biodiesel could be a promising alternative rail fuel toward a sustainable future. As feedstock cost definitely affects the overall production cost of biodiesel, biomass-waste materials could be used in near future; however, most of advanced conversion methods are still in demonstration scale of technological maturity. Moreover, maintenance cost of locomotive engines needs also to be addressed. Rail companies should cooperate with manufacturers in order to promote higher blends of biodiesel in rail engines over the next years.

References

1. Zhang, R., Zhang, J.: Long-term pathways to deep decarbonization of the transport sector in the post-COVID world. Transp. Policy (Oxf) **110**, 28–36 (2021)
2. van Soest, H.L., den Elzen, M.G.J., van Vuuren, D.P.: Net-zero emission targets for major emitting countries consistent with the Paris Agreement. Nat. Commun. **12**(1), 2140 (2021)
3. Deutch, J.: Is net zero carbon 2050 possible? Joule **4**(11), 2237–2240 (2020)
4. Hoppe, M., Trachsel, T.: Emerging trends in transport technologies: the potential for transformation towards sustainable mobility (2018)
5. UIC-International Union of Railways, First Report: Railways and Biofuel Railways and Biofuel, 2007. https://uic.org/IMG/pdf/railways_and_biofuels_final_report.pdf. Accessed 20 June 2022
6. Agarwal, A.K., et al.: Introduction to the locomotives and rail road transportation. In: Agarwal, A.K., et al. (eds.) Locomotives and Rail Road Transportation: Technology, Challenges and Prospects, pp. 3–7. Springer Singapore, Singapore (2017)
7. IEA (2021). Rail, IEA, Paris. https://www.iea.org/reports/rail. Accessed 20 June 2022
8. Pielecha, J., et al.: The latest technical solutions in rail vehicles drives. MATEC Web of Conf. **118** (2017)
9. Sun, Y., et al.: A review of hydrogen technologies and engineering solutions for railway vehicle design and operations. Railway Eng. Sci. **29**(3), 212–232 (2021)
10. Seyam, S., Dincer, I., Agelin-Chaab, M.: Development and assessment of a cleaner locomotive powering system with alternative fuels. Fuel **296**, 120529 (2021)
11. Mogila, V., Vasyliev, I., Nozhenko, O.: The use of biofuel on the railway transport. Transp. Probl.: An Int. Scien. J. **7**, 21–26 (2012)
12. Kargbo, H., Harris, J.S., Phan, A.N.: "Drop-in" fuel production from biomass: Critical review on techno-economic feasibility and sustainability. Renew. Sustain. Energy Rev. **135** (2021)
13. Dincer, I., Zamfirescu, C.: A review of novel energy options for clean rail applications. J. Nat. Gas Sci. Eng. **28**, 461–478 (2016)
14. Mizik, T., Gyarmati, G.: Economic and sustainability of biodiesel production—a systematic literature review. Clean Technol. **3**(1), 19–36 (2021)
15. IEA (2016). World Energy Outlook 2016, IEA, Paris. https://www.iea.org/reports/world-energy-outlook-2016. Accessed 01 July 2022
16. EIA, International Energy Outlook 2021 with projections to 2050, Narrative. https://www.eia.gov/outlooks/ieo/pdf/IEO2021_Narrative.pdf. Accessed 30 June 2022
17. Ahlgren, E., Hagberg, M., Grahn, M.: Transport biofuels in global energy-economy modelling—a review of comprehensive energy systems assessment approaches. GCB Bioenergy **9** (2017)
18. Mehmood, U.: Transport energy consumption and carbon emissions: the role of urbanization towards environment in SAARC region. Integr. Environ. Assess. Manag. **17**(6), 1286–1292 (2021)
19. Subramaniam, Y., Masron, T.A.: The impact of economic globalization on biofuel in developing countries. Energy Convers. Manage.: X **10** (2021)
20. Ahmed, M., Shimada, K.: The effect of renewable energy consumption on sustainable economic development: evidence from emerging and developing economies. Energies **12**(15)
21. IEA (2021). Transport Biofuels, IEA, Paris. https://www.iea.org/reports/transport-biofuels. Accessed 15 July 2022
22. Nogueira, L.A.H., et al.: 9—Biofuels for Transport. In: Letcher T.M. (ed.), in Future Energy (Third Edition), pp. 173–197. Elsevier (2020)
23. Popp, J., et al.: Bioeconomy: biomass and biomass-based energy supply and demand. N Biotechnol **60**, 76–84 (2021)
24. Szalay, D.: Development of biomass and biofuel usage. In: Palocz-Andresen, M., et al. (eds.) International Climate Protection, pp. 145–153. Springer International Publishing, Cham (2019)

25. Drabik, D., Venus, T.: EU biofuel policies for road and rail transportation sector. In: Dries, L., et al. (eds.) EU Bioeconomy Economics and Policies, vol. II, pp. 257–276. Springer International Publishing, Cham (2019)
26. OECD, Food, and A.O.o.t.U. Nations, OECD-FAO Agricultural Outlook 2018–2027 (2018)
27. Solaymani, S.: CO_2 emissions patterns in 7 top carbon emitter economies: the case of transport sector. Energy **168**, 989–1001 (2019)
28. Du, H., et al.: What drives CO_2 emissions from the transport sector? A linkage analysis. Energy **175**, 195–204 (2019)
29. Directive 2003/30/EC of the European Parliament and of the Council of 8 May 2003 on the promotion of the use of biofuels or other renewable fuels for transport, Brussels, 2003. https://eur-lex.europa.eu/legal-content/EN/TXT/PDF/?uri=CELEX:32003L0030&from=en Accessed 02 July 2022
30. Cansino, J.M., et al.: Promotion of biofuel consumption in the transport sector: an EU-27 perspective. Renew. Sustain. Energy Rev. **16**(8), 6013–6021 (2012)
31. Directive 2009/28/EC of the European Parliament and of the Council, of 23 April 2009, on the promotion of the use of energy from renewable sources and amending and subsequently repealing Directives 2001/77/EC and 2003/30/EC, Brussels, 2009. https://eur-lex.europa.eu/legal-content/EN/TXT/PDF/?uri=CELEX:32009L0028. Accessed 02 July 2022
32. Pánovics, A.: From Copenhagen to Paris: the way towards a new international climate change agreement. In: Palocz-Andresen, M., et al. (eds.) International Climate Protection, pp. 233–238. Springer International Publishing, Cham (2019)
33. Chiaramonti, D., et al.: The challenge of forecasting the role of biofuel in EU transport decarbonisation at 2050: a meta-analysis review of published scenarios. Renew. Sustain. Energy Rev. **139** (2021)
34. European Council (Euco169/14 EC). 2030 climate and energy policy framework, https://www.consilium.europa.eu/uedocs/cms_data/docs/pressdata/en/ec/145397.pdf. Accessed 05 July 2022
35. UIC (2012). Moving towards sustainable mobility. A strategy for 2030 and beyond for the European railway sector. Summary. International Union of Railways (UIC), https://www.cer.be/sites/default/files/publication/CER-UIC_Sustainable_Mobility_Strategy_-_SUMMARY.pdf. Accessed 10 July 2022
36. Stančin, H., et al.: A review on alternative fuels in future energy system. Renew. Sustain. Energy Rev. **128** (2020)
37. Ramadhas, A.S.: Alternative Fuels for Transportation. CRC Press (2016)
38. Dominković, D.F., et al.: The future of transportation in sustainable energy systems: opportunities and barriers in a clean energy transition. Renew. Sustain. Energy Rev. **82**, 1823–1838 (2018)
39. IEA (2020), Tracking Rail 2020, IEA, Paris. https://www.iea.org/reports/tracking-rail-2020-2. Accessed 17 July 2022
40. Polater, N., Tricoli, P.: Technical review of traction drive systems for light railways. Energies **15**(9) (2022)
41. Givoni, M., Brand, C., Watkiss, P.: Are railways 'climate friendly'? Built Environ. (1978–) **35**(1), 70–86 (2009)
42. Tiwari, N.: Diesel locomotive noise sources, reduction strategies, methods and standards, pp. 41–69 (2017)
43. Pinto, J.T.d.M., et al.: Road-rail intermodal freight transport as a strategy for climate change mitigation. Environ. Dev. **25**, 100–110 (2018)
44. Hydrogen Europe, Alternative fuels infrastructure as the key to unlock the potential of hydrogen-fuelled mobility. https://hydrogeneurope.eu/wp-content/uploads/2021/12/Hydrogen-Europe-Alternative-Fuels-Infrastructure-Regulation.pdf. Accessed 25 June 2022
45. Awogbemi, O., et al.: An overview of the classification, production and utilization of biofuels for internal combustion engine applications. Energies **14**(18) (2021)
46. Banerjee, S., Kaushik, S., Tomar, R.S.: Global scenario of biofuel production: past, present and future. In: Rastegari, A.A., Yadav, A.N., Gupta, A. (eds.) Prospects of Renewable Bioprocessing in Future Energy Systems, pp. 499–518. Springer International Publishing, Cham (2019)

47. Ruan, R., et al.: Biofuels: introduction, in biofuels: alternative feedstocks and conversion processes for the production of liquid and gaseous biofuels, pp. 3–43 (2019)
48. Datta, A., Hossain, A., Roy, S.: An overview on biofuels and their advantages and disadvantages. Asian J. Chem. **31**(8), 1851–1858 (2019)
49. Nanda, S., et al.: A broad introduction to first-, second-, and third-generation biofuels. In: Recent Advancements in Biofuels and Bioenergy Utilization, pp. 1–25 (2018)
50. Kumar, M., et al.: Algae as potential feedstock for the production of biofuels and value-added products: opportunities and challenges. Sci. Total Environ. **716**, 137116 (2020)
51. Mat Aron, N.S., et al.: Sustainability of the four generations of biofuels—a review. Int. J. Energy Res. **44**(12), 9266–9282 (2020)
52. Hassan, M.H., Kalam, M.A.: An overview of biofuel as a renewable energy source: development and challenges. Procedia Eng. **56**, 39–53 (2013)
53. Wyman, C.E., Cai, C.M., Kumar, R.: Bioethanol from lignocellulosic biomass. In: Encyclopedia of Sustainability Science and Technology, pp. 1–27 (2017)
54. Liu, Y., et al.: Biofuels for a sustainable future. Cell **184**(6), 1636–1647 (2021)
55. El-Gharbawy, A., et al.: A review on biodiesel feedstocks and production technologies. J. Chil. Chem. Soc. **66**, 5098 (2021)
56. Ramos, et al.: Biodiesel production processes and sustainable raw materials. Energies **12**(23) (2019)
57. Firoz, S.: A Review: Advantages and Disadvantages of Biodiesel (2017)
58. Gangwar, M., Sharma, S.M.: Risks, determinants, and perspective for creating a railway biodiesel supply chain: case study of India. J. Clean. Prod. **133**, 182–187 (2016)
59. Jawahir, I.S., Bradley, R.: Technological elements of circular economy and the principles of 6R-based closed-loop material flow in sustainable manufacturing. Procedia CIRP **40**, 103–108 (2016)
60. Official Journal of the European Union.: DIRECTIVE 2008/98/EC OF THE EUROPEAN PARLIAMENT AND OF THE COUNCIL of 19 November 2008 on waste and repealing certain Directives, https://eur-lex.europa.eu/legal-content/EN/TXT/PDF/?uri=CELEX:32008L0098&from=EN. Accessed 19 June 2022
61. Hosseinzadeh-Bandbafha, H., et al.: Environmental life cycle assessment of biodiesel production from waste cooking oil: a systematic review. Renew. Sustain. Energy Rev. **161**, 112411 (2022)
62. Liu, Y., et al.: Economic evaluation and production process simulation of biodiesel production from waste cooking oil. Curr. Res. Green Sustain. Chem. **4** (2021)
63. Sahar, et al.: Biodiesel production from waste cooking oil: An efficient technique to convert waste into biodiesel. Sustain. Cities Soc. **41**, 220–226 (2018)
64. Stead, C., et al.: Introduction of biodiesel to rail transport: lessons from the road sector. Sustainability **11**(3) (2019)
65. Meyer, G., Bucknall, R., Breuil, D.: Electrification of the transport system (2017)
66. Tiwari, N.: Diesel locomotive noise sources, reduction strategies, methods and standards. In: Agarwal, A.K., et al. (eds.) Locomotives and Rail Road Transportation: Technology, Challenges and Prospects, pp. 41–69. Springer Singapore, Singapore (2017)
67. Breuer, J., et al.: An overview of promising alternative fuels for road, rail, air, and inland waterway transport in Germany. Energies **15**(4) (2022)
68. Gautam, A., Misra, R., Agarwal, A.: Biodiesel as an alternate fuel for diesel traction on Indian railways, pp. 73–112 (2017)
69. European Technology and Innovation Platform Bioenergy (ETIP Bioenergy).: Biofuels for rail transport. 02/07/2022. Available from: https://www.etipbioenergy.eu/value-chains/products-end-use/end-use/rail

Automatic Speed Control of Heavy-Haulers Trains

Oleg Pudovikov and **Nikita Zhukhin**

Abstract During the movement of heavy-haulers trains, longitudinal oscillations occur, accompanied by significant longitudinal forces. In some cases, for example, in case of violation of the traction control technology of locomotives, the values of these forces reach values that can cause damage and destruction of autocoupler devices of wagons and train rupture, which is a serious violation of traffic safety. In some cases, the problem is complicated by the factor of fatigue wear, which has a significant impact on the resistance of components to mechanical stress. Also, in addition to dynamic forces, slowly changing quasi-static forces are also dangerous, which can cause cars to be squeezed out of the track and derail them. In the work, longitudinal oscillations arising in a train are investigated using mathematical modeling methods. To solve the problems considered, a multi-mass model of the train was used, taking into account the nonlinear and nonlinearizable characteristics of the absorbing devices of the automatic couplers, the nonlinear nature of the change in the resistance forces acting on the train, and the location of the train on several elements of the track profile. An assessment of the stability reserves against squeezing was performed, when calculating which the vertical and lateral forces of interaction between the wagon wheel and the rail are taken into account. Based on the research carried out, the concept of constructing a system for automatic control of the speed of a freight train is proposed; for this purpose, a system of criteria is proposed to assess the quality of control of the speed of a freight train from the point of view of traffic safety, recommendations are given on the structure of the speed control loop, and the method of selecting the parameters of the speed control law using multi-criteria optimization methods is considered.

Keywords Heavy-haul train · Longitudinal oscillations of the train · Automatic speed control · Parametric synthesis · Optimal train control

O. Pudovikov (✉) · N. Zhukhin
Russian University of Transport (MIIT), GSP-4, Obraztsova Str., 9 P. 9, 127994 Moscow, Russian Federation
e-mail: olegep@mail.ru

1 Introduction

One of the ways to increase the carrying capacity of railways that do not require significant capital expenditures for the modernization of their infrastructure is the introduction into circulation and widespread use of trains of increased weight and length. However, in such trains, longitudinal oscillations with a significant amplitude of forces occur. Additional negative factors affecting the values of these forces are possible errors that occur when performing technological operations to control the train, as a result of which the values of the longitudinal dynamic forces can significantly exceed the value established under the conditions of static and fatigue strength for auto-couplings and absorbing devices of rolling stock. Among these errors is an incorrect choice of the speed of increasing the traction force or braking, the absence of a time delay when increasing the traction force or electric braking, and the absence or insufficient amount of delay between the release of the air brake and the increase in traction force. As a result, the probability of sudden and gradual failures increases, consisting in the destruction of the harness devices of the wagons and, consequently, the rupture of the train. The latter is a serious violation of traffic safety, leading to significant material losses, and in some cases to human casualties [1]. An additional hazard factor operating in heavy trains on sections with a heavy and flat track profile is the possible appearance of conditions that contribute to the loss of stability of cars in the rail track (pulling or squeezing) [2, 3].

One of the ways to improve the safety of trains, including freight, is the use of automation tools for speed control, one of the tasks of which is to reduce the influence of the so-called human factor on the control process. Automatic train guidance systems, including those built according to the multi-circuit principle, are used in railway transport [4] (Fig. 1). In such systems, the external control loop is the train-running time controller, whose task is to select such a combination of train modes to ensure the execution of a given train running time along a stretch or section of railway, provided that the selected trajectory is realized with minimal expenditure of fuel and energy resources for train traction. When solving the optimization problem, restrictions on the values of the maximum permissible speeds of movement on different sections of the track $v_n^{\max}(S)$ are also taken into account, as well as the value of the permissible speed of movement coming from the system of interval regulation of train movement.

The internal, subordinate circuit for the travel time controller is the automatic speed control system, the setting signals for which are the speed and mode of movement of the train, as well as the control circuit of the pneumatic brake. The output coordinate of the automatic speed control system is the set value of the traction or braking force for the automated traction drive, or the operating mode of the pneumatic brake of the train [4]. The automatic speed control system must provide the required quality of control, including taking into account specific criteria, which allows taking into account the features of dynamic processes occurring in the train during transient modes of movement, as well as the magnitude of quasi-static longitudinal forces that directly affect the stability of the cars.
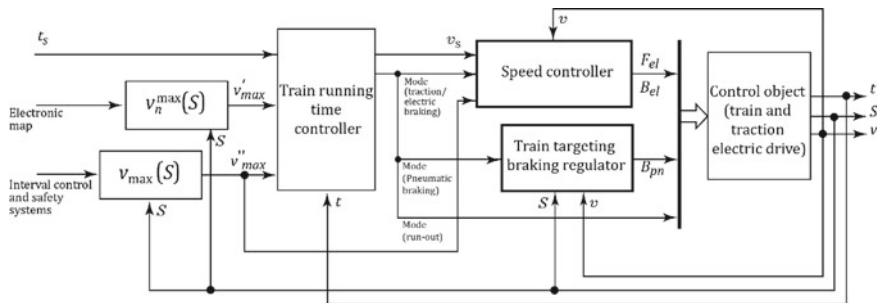
Fig. 1 Multi-circuit automatic speed control system trains

2 Model of Automatic Speed Control System

A train is a complex, multi-mass mechanical system consisting of several dozen (and sometimes hundreds) interacting crews (locomotives and wagons) with nonlinear and nonlinearized connections between them. In the process of movement, external forces of different magnitude and direction act on different crews in the same train, representing the resultant forces of resistance to movement, the components of traction or braking forces, as well as reactions in inter-wagon connections. All this leads to the occurrence of longitudinal oscillations in the train [3, 5–10].

To perform the analysis of dynamic processes occurring in the train, models that consider the train as a system of solids are most suitable [3, 5–10].

When constructing such a model, the train is represented as a chain of n masses of wagons and locomotives connected by connections (Fig. 2). Each mass of a discrete model moves under the action of forces transmitted to it from elastic or elastic-viscous bonds, as well as external forces. Representing a train in this way, each wagon is considered an absolutely solid body of a certain mass, and each inter-wagon connection is considered a body without mass. Such a representation of the train makes it possible to take into account gaps in the mechanisms of absorbing devices and automatic couplings, which significantly affect the propagation of disturbances along the train composition and the magnitude of the forces arising (Fig. 3).

Taking into account the assumptions made, the movement of each train crew is described by the following differential equations [7]:

$$
\begin{cases}
\dot{v}_i = \frac{S_i - S_{i+1} + F_i}{m_i}, & i = 1, \ldots, n; \ S_{n+1} = 0; \\
\dot{q}_i = v_{i-1} - v_i, & i = 2, \ldots, n; \\
\dot{x}_1 = v_1 = -\dot{q}_1,
\end{cases}
\tag{1}
$$

where n—number of carriages on the train; q_i—deformation of the i-th intercar connection; $\dot{q}_i$—deformation rate; m_i—weight of the i-th wagon or locomotive; v_i—the speed of the center of mass of the crew; S_i—reaction in the i-th intercar connection; and F_i—total external force acting on the i-th crew.
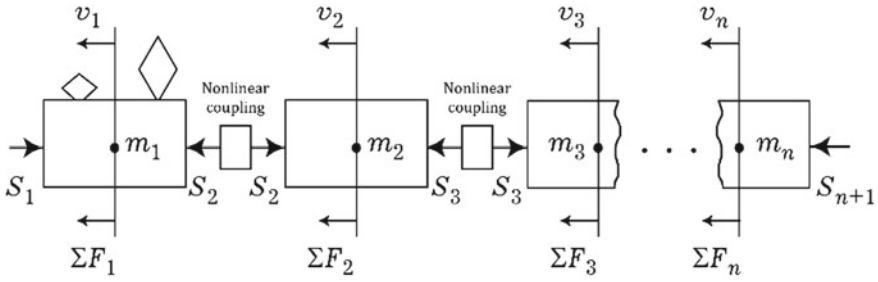
Fig. 2 Train model as a system of solids

Fig. 3 Inter-wagon communication model
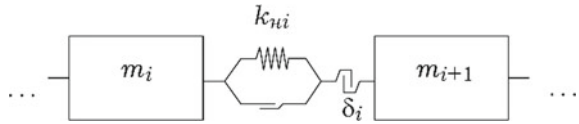
The total external force F_i acting on the i-th crew is the resultant of the thrust F_{eli}, the braking force (electric B_{eli} and pneumatic B_{pni}), and forces the main W_{oi} and additional W_{ai} resistance to the movement of the train:

$$F_i = F_{ki} - B_{eli} - B_{pni} - W_{oi} - W_{ai} \tag{2}$$

When performing calculations, it is assumed that in addition to automatic couplings, spring-friction shock absorbers (absorbing devices) are used as part of the intercar communication with the static characteristic shown in Fig. 4.

The amount of deformation of the i-th intercar connection is determined as follows:

Fig. 4 Dependence of the force on the deformation of the inter-wagon connection. k_H—stiffness on the loading branch, $k_к$—body stiffness, η—the coefficient characterizing the energy dissipation in the apparatus, Δ—the course of the absorbing apparatus, S_0—the value of the initial tightening (preload), and δ_0—clearance in the coupling device
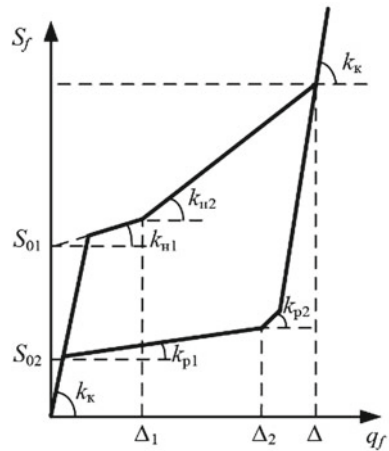
$$q_i = x_i + x_{i-1} - \frac{l_{i-1} + l_i}{2}$$

where x_i is the coordinate (along the trajectory) of the position of the center of mass of the i-th crew and l_i is the length of the crew.

The magnitude of the longitudinal force in each inter-wagon connection is determined from the expression:

$$S_i = S_{fi}(q_{fi})\operatorname{sign} q_i, \tag{3}$$

Где

S_i—the longitudinal force arising in the i-th intercar connection;
S_{fi}—the longitudinal force arising in the absorbing devices of the inter-wagon connection;
q_{fi}—actual deformation of absorbing devices and crew bodies.

The amount of deformation of the absorbing apparatus q_{fi} is determined from the conditions (4):

$$q_{fi} = \begin{cases} q_i, & \text{when } q_i \geqslant \delta_{0i} \\ 0, & \text{when } 0 \leqslant q_i < \delta_{0i} \\ -q_i, & \text{when } q_i < 0 \end{cases} \tag{4}$$

where the value $S_{\Phi i}$ is calculated as follows:

$$S_{fi} = \begin{cases} \min\{S_{Hi}; S_{\kappa i}\}, & \text{when}\left(q_{fi} < \Delta_i\right) \wedge \left(q_{fi}(t) \geqslant q_{fi}(t-h)\right) \\ \max\left\{S_{pi}; S_{\kappa i}\right\}, & \text{when}\left(q_{fi} < \Delta_i\right) \wedge \left(q_{fi}(t) < q_{fi}(t-h)\right) \\ S_{\kappa i}, & \text{when } \left(q_{fi} \geqslant \Delta_i\right) \end{cases} \tag{5}$$

$$\begin{cases} S_{Hi} = S_{01i} + k_{H1i}q_{fi}, \text{ when } \left(q_{fi} < \Delta_{1i}\right) \\ S_{Hi} = S_{01i} + k_{H1i}\Delta_{1i} + k_{H2i}(q_{fi} - \Delta_{1i}), \text{ when}\left(q_{fi} \geqslant \Delta_{1i}\right) \wedge \left(q_{fi} < \Delta_i\right) \\ S_{pi} = S_{02i} + k_{p1i}q_{fi}, \text{ when}\left(q_{fi} < \Delta_{2i}\right) \\ S_{pi} = S_{02i} + k_{p1i}\Delta_{2i} + k_{p2i}(q_{fi} - \Delta_{2i}), \text{ when}\left(q_{fi} \geqslant \Delta_{2i}\right) \wedge \left(q_{fi} < \Delta_i\right) \\ S_{\kappa i} = S_i + k_{\kappa i}\left(q_{fi}(t) - q_{fi}(t-h)\right) + \beta_i \dot{q}_i \operatorname{sign}q_i \\ S_i = S_{Hi}(t-h) \vee S_{pi}(t-h), \text{ when } S_{fi}(t-h) = S_{Hi}(t-h) \vee S_{pi}(t-h) \\ \text{else } S_i = S_{fi}(t-h) - \beta_i \dot{q}_i(t-h)\operatorname{sign} q_i(t-h) \end{cases}$$
$$\tag{6}$$

where

Δ_{1i}—the sum of deformations of absorbing devices at which both springs of each device come into operation under load;
Δ_{2i}—the sum of deformations of absorbing devices at which both springs of each device come into operation during unloading;

k_{H1i} and k_{H2i}—stiffness coefficients during operation of one and two springs of the apparatus on the loading branch;

k_{p1i} and k_{p2i}—also, on the unloading branch;

S_{01i} and S_{02i}—the force of the initial tightening of the absorbing apparatus on the loading and unloading branches.

A long-composite train is located on several elements of the track profile with different steepness, radius of curves, and slope of rails. This feature has a significant impact on the course of transients in the train and on the magnitude of dynamic and quasi-static forces in it. Therefore, when solving problems related to the study of longitudinal dynamics, the forces of resistance to movement must be determined separately for each engine, locomotive or wagon. The magnitude of the resistivity force to motion depends nonlinearly on the velocity [11] and in general can be calculated in accordance with the following expression:

$$W_{oi} = a_0 + \frac{a_1 + a_2 v + a_3 v^2}{q_0}$$

Here a_0, a_1, a_2 и a_3—coefficients depending on the characteristics of the rolling stock and track design; q_0—weight per axle.

The strength of additional resistance to the movement of wagons and locomotives from the slope and curves is constantly changing. This, in turn, affects the trajectory and longitudinal oscillations of the train, complicating the process of automatic control. To take into account the influence of the track profile on the automatic control of a freight train, it is advisable to use a model with a wagon definition of additional resistance forces from the slope.

The algorithm for calculating the amount of resistance to movement from the slope acting on the i-th crew is based on the assumption that the longitudinal profile of the track section consists of $(m + 1)$ rectilinear sections with slopes i_k and length $L_k(k = \overline{0, m})$ and m curved, each of which is an arc of radius $R_k(k = \overline{1, m})$.

These arcs match the segments of the path of a constant slope (Fig. 5). The value of the specific forces of additional resistance to movement from the slope w_{ai} depends on the position of the crew on the track profile, which is calculated at each step of integrating the equation of motion of the train.
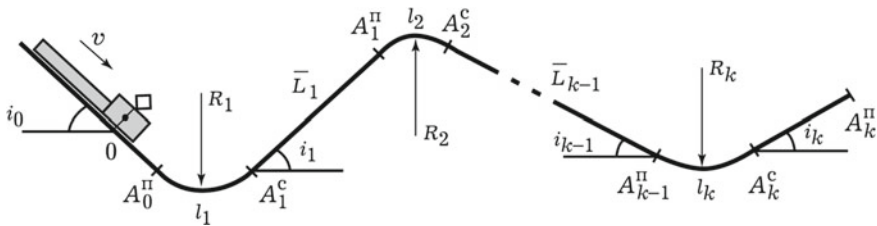
Fig. 5 Example of the representation of the longitudinal profile of the path

The magnitude of the specific (N/kN) force acting on the i-th crew is determined by the following relations:

$$w_{ai} = \begin{cases} i_{\kappa,i} & \text{when } A_k^c \leqslant x_i \leqslant A_k^{\Pi} \\ i_{\kappa,i} + \frac{y}{R_{\kappa,i}} & \text{when } A_k^{\Pi} \leqslant x_i \leqslant A_k^c \end{cases}$$

where $i_{\kappa,i}$ is the slope angle with the number k on which the crew with the number i is located; x_i is the coordinate of the i—th crew; $R_{\kappa,j}$ is the radius of the arc of the interface of the corresponding section; and y is an auxiliary variable, $y = x_i - A_k^{\Pi}$, $k = \overline{0, m}$.

Next, the value of the additional resistance to movement W_{ai} acting on the locomotive and the train cars is determined:

$$w_{ai} = \begin{cases} w_{ai} P_i, & \text{for a locomotive} \\ w_{ai} Q_i, & \text{for the carriage} \end{cases}$$

Here P_i, Q_i are the weight of the locomotive and the wagon, respectively, kN.

In the future, the calculated values of the force of additional resistance to movement from the slopes W_{ai} are used when integrating the system of differential equations of train motion (1).

The traction electric drive is used to create a torque on the wheels of the rolling stock, which is converted into the tangential force of traction or braking of the locomotive. When modeling an automatic control system, an electric locomotive with continuous control of traction or braking forces (with collector motors and pulse-width voltage regulation or with brushless, synchronous or asynchronous motors) traction characteristics presented in Fig. 6 is adopted as a prototype electric locomotive. In this study, quasi-continuous control of the traction force is considered, i.e., we will assume that the traction electric drive is able to realize any value of the traction force (or braking) from the zone determined by the restrictions imposed on the characteristics of the electric drive.

The automated traction electric drive of an electric rolling stock, in general, includes a control device that implements the necessary control law, a converter unit, and traction motors.

Fig. 6 Example of traction and braking characteristics of an electric locomotive with continuous traction and braking force control
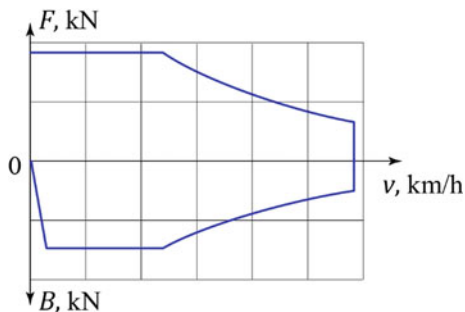
The voltage and speed control circuit of traction motors can be described by an aperiodic link of the first order due to the fact that the time constant of the electromagnetic system in question, which is a fraction of a second, is several orders of magnitude smaller than the train time constant, which takes a value of several thousand seconds:

$$F_{el}\left(B_{el}\right) = T_{el}\frac{\mathrm{d}F_s(B_s)}{\mathrm{d}t} + F_s(B_s)$$

where T_{el}—the time constant of the traction electric drive; $F_s(B_s)$—the set value of the traction force (braking) at the input of the control circuit of the traction electric drive; and $F_{el}(B_{el})$—the force of traction (braking) (Fig. 1).

As noted, the use of control automation tools contributes to improving the safety of train traffic. Figure 7 shows as an example a functional diagram of an automatic control system, which includes a train parameter setter 1, the output of which contains a set of data on the parameters of cars and locomotives in the train [Train], an electronic map with track and profile data 2 [Track], an auto guidance system 3, and a speed setter 4. The speed setter and the auto-driving system form the values of the set speed v_{s1} and v_{s2}, and element 5 selects the minimum of these two values.

Freight train parameters (number of wagons, their mass) can vary widely. To compensate, it is advisable to build an automatic control system according to an adaptive principle that allows adjustment of the parameters of the control law depending on the parameters of the train. For this purpose, an adaptation module 6 has been introduced into the system under consideration, which determines the parameters of the automatic control system based on the train parameters: the vectors of the parameters $[k_1]$ and $[k_2]$. In device 7, based on the parameters of the train (number and mass of cars), track and profile, the magnitude of the traction force of the locomotive,
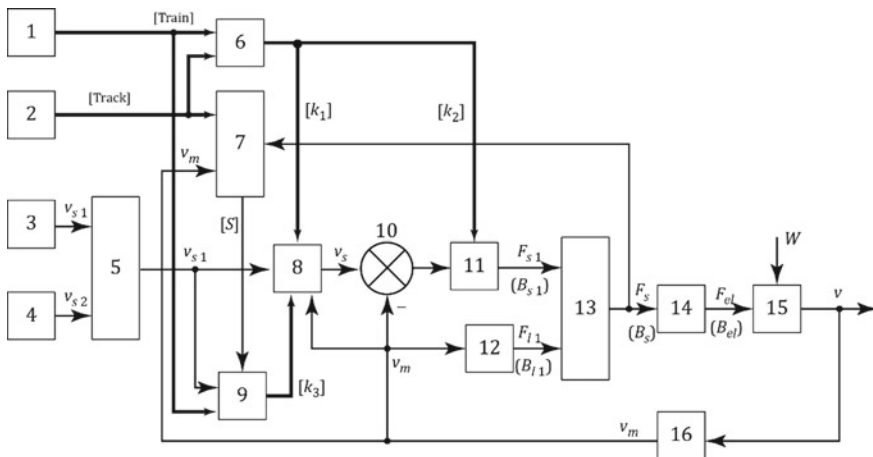
Fig. 7 Functional diagram of the automatic speed control system of a freight train

as well as the measured speed of movement, the values of the longitudinal forces for each inter-wagon connection of the train are calculated, as well as the values of the coefficients of the stability margin of the cars. The calculated values of the longitudinal forces are transmitted to the correction device 9. The signal of a given speed changes abruptly; therefore, a smoothing device 8 is provided to smooth it, and therefore to limit the rate of change in traction or braking force. As will be shown below, the smoothing device makes a significant contribution to ensuring the quality of speed control in transient driving modes. The correction device 9 at each moment of time receives from the device 7 an array of calculated values of longitudinal forces $[S]$ defined for each inter-wagon connection. Based on these values, as well as the parameters of the train, a signal is generated in device 9 that corrects the value of a given acceleration or deceleration, thereby reducing the set value of the traction or braking force.

The comparison device 10 calculates the mismatch between the values of the corrected set and the actual measured speeds of movement $v = v_s - v_m$. This value, as well as the values of the control coefficients k_1^1 and k_1^2, is received at the inputs of the control device 11, which implements the proportional-integral law of speed control.

In order to avoid the output of the traction force (braking) for the restrictions imposed on the traction electric drive of the locomotive, a device of restrictions 12 is provided. Based on the information about the actual measured speed of movement, it determines the maximum permissible value of the traction force (braking) F_{l1} (B_l). The device 13 selects the minimum of two values of the traction force (braking) calculated by the control device 11 and the restriction device 12. The selected value of the traction force (braking) enters the actuator 14—an automated traction electric drive of the locomotive, at the output of which the actual value of the traction force (braking) is formed. The traction (braking) force F_{el} (B_{el}) performs a force effect on the control object 15—train, which is also affected by the forces of the main and additional resistance of movement W. To measure the actual speed of the v_m locomotive, a measuring device 16 is provided, which takes into account time sampling and the current averaging of the measured signal.

In this system, to ensure the quality of control in transient driving modes, a device is installed at the input of a closed speed control loop that smooths the intermittently changing master signal. To ensure the required quality of control in transient driving modes and to reduce the values of longitudinal dynamic forces arising during acceleration and braking of the train, this device provides for a two-stage change of the master signal. During the first stage, the train is pre-stretched (compressed) with reduced acceleration (deceleration). After the completion of the stretching (compression) of the train, the second stage of acceleration (braking) is carried out with maximum acceleration (deceleration). This approach makes it possible to reduce the magnitude of the longitudinal dynamic forces arising in the train in transient modes of movement.

The smoothing device of the considered automatic speed control system is implemented on the basis of a second-order aperiodic link with a transition function of the form [12]:

$$f_1(t) = x_1 a_s^* \left[1 - \frac{k_2^1}{k_2^1 - k_2^2} \exp\left(-\frac{t}{k_2^1}\right) + \frac{T_2}{k_2^1 - k_2^2} \exp\left(-\frac{t}{k_2^2}\right) \right]$$

Here, $f_1(t)$ is a transient function; a_s^* is the value of a given acceleration of the train; x_1 is the fraction of a given acceleration realized during the first stage of acceleration or deceleration; k_2^1, k_2^2 are the time constants of the link; and t is the current time.

The delay value from the beginning of the first stage of acceleration (deceleration) to the beginning of the second stage is defined as the estimated stretching time of the pre-compressed train [12]:

$$t_s = \sqrt{\frac{2(N-1) \cdot \Delta_{0i}}{x_1 a_3^*}} + \sqrt{\frac{2 \cdot \sum_{i=1}^{N} \Delta_{api}}{x_1 a_3^*}};$$

where t_s is the stretching time of the pre-compressed train; N is the number of cars in the train; Δ_{0i} is the gap in the absorbing apparatus of the i-th automatic coupling; and $\sum_{i=1}^{N} \Delta_{api}$ is the total maximum elongation of the absorbing devices of the train.

At the second stage of increasing the traction force (braking), the smoothing device implements a similar transient function $f_2(t)$ [12]:

$$f_2(t) = (1 - x_1) a_3^* \left[1 - \frac{k_2^1}{k_2^1 - k_2^2} \exp\left(-\frac{t - t_{Tp}}{k_2^1}\right) + \frac{k_2^2}{k_2^1 - k_2^2} \exp\left(-\frac{t - t_{Tp}}{k_2^2}\right) \right]$$

The resulting function of increasing the thrust force (braking) $f(t)$ is described by Formulas (7 and 8) for the first and second stages of acceleration (braking), respectively:

$$f(t) = f_1(t) \tag{7}$$

$$f(t) = f_1(t) + f_2(t) \tag{8}$$

The device 11, as noted, implements the proportional-integral control law and is a control device as part of the automatic control system and forms a control action for the actuator (within the framework of this work—an automated traction electric drive) aimed at eliminating the mismatch between the value proportional to the set value of the speed of movement v_s formed by the device 8 and a value proportional to the actual velocity v_m.

The proportional-integrating law described by the equation is used as the law according to which the control device functions.

$$F_{s1}(B_{s1}) = k_1^1 \Delta v + \frac{1}{k_1^2} \int_0^t \Delta v \, \mathrm{d}t,$$

where k_1^1, k_1^2 are the parameters of the control law.

3 Assessment of the Quality of Freight Train Speed Control

There are a number of requirements for automatic train speed control systems. First of all, they must be stable, which is ensured by the correct choice of corrective links in the automatic control system.

In the case of a predefined structure, the quality of control is ensured by a rational choice of the parameters of the corrective links, which allows you to influence the nature of the transients in the automatic control system and the operation in steady-state mode, and hence the values of the indicators by which the quality of control is evaluated. It is convenient to select the values of the link parameters using multi-criteria optimization methods, one of which, applied in the work, will be discussed later. The following system of criteria was used to assess the quality of the freight train speed control:

- the time of the transition process t_p; this parameter characterizes the time after which, after changing the setting effect, the output coordinate of the automatic control system (in this case, the speed) reaches the set value, taking into account the accepted level of accuracy. In general, for automatic control systems, the speed of rolling stock is determined by the highest value of the traction or braking force. In the case of using a system with the proposed structure, the minimum transition time is determined by the parameters k_2^1, k_2^2 k_2^1, k_2^2 of the links installed at the input of the closed speed control circuit;
- the value $F_{\max}$ of the greatest longitudinal force that occurs with a relatively rare combination of extreme loads. In operation for freight cars, it corresponds to the settling and starting of a heavy train, collisions during maneuvering operations, as well as emergency braking at low speeds; this value is taken based on the condition of preventing the appearance of residual deformations (damages) in the nodes or parts of cars, as well as the occurrence of sudden failure associated with their possible destruction [13];
- the value of a is the sum of accumulated fatigue damage from the action of variables in magnitude, "moderate" loads that occur in normal operating conditions—moving at an acceptable speed along straight and curved sections of the track, along switches, etc. This parameter allows you to take into account high-frequency oscillations that occur in the train as a result of collisions of cars during the transition from stretched to compressed state and vice versa. These oscillations occur when the train starts moving, when the profile fractures occur, when

the train mode changes, when the train or its individual parts change their state from stretched to compressed, and vice versa. Since these fluctuations are accompanied by a change in the magnitude and direction of the longitudinal force, the consequence of this is the accumulation of fatigue damage in the structure of structural materials used in the manufacture of shock-traction devices, namely auto-couplings. Due to the influence of accumulated metal fatigue, the destruction of the auto-coupling can occur under the action of a longitudinal force significantly less than the calculated value, especially under the action of unfavorable factors, such as low temperature, when the fragility of the structural material used increases. When performing calculations, a linear hypothesis of fatigue damage summation is adopted—linear—assuming that fatigue failure occurs when the condition is met:

$$\sum_i a_i = \sum_i \frac{n_i}{N_i} = 1$$

where N_i is the number of cycles before the failure of the part at the amplitude σ_{ai}, determined by the fatigue curve and n_i is the number of cycles of the amplitude σ_{ai};

$$N_i = N_0 \left(\frac{\sigma_{-1}}{\sigma_{ai}} \right)^m.$$

Here, m is an indicator of the fatigue curve of the material; N_0 is the base number of cycles.

- the coefficient of stability margin from derailment k_y. As noted earlier, not only fast-flowing dynamic, but also slow-changing quasi-static forces arise in the train during movement. In addition to the danger of breaking the automatic coupling from quasi-static tensile forces, there is a significant danger from quasi-static compressive forces leading to the derailment of wagons. Such compressive forces, leading to loss of stability and derailment of wagons, act in the mode of electric braking, and in the case of multiple locomotives in different locations of the train, also in traction modes [3]. Consider the factors affecting the stability of the wagon. The composition of cars with automatic couplings is a multi-link hinge-rod mechanism (Fig. 8). The links of such a mechanism (wagons and auto-couplings) under the action of tensile forces are located on the same line. Under the action of compressive forces, the links tend to be skewed and to keep them in a coaxial position, transverse connections are needed, the role of which is performed by trolleys with springs and wheel pairs interacting with the rail track. Since these bonds are not rigid, but elastic, the skew of the links will occur only when the compressive forces F reach a certain critical value $F_{\kappa p}$. This value is calculated from the equilibrium condition of the system (cars in the train) in a state of skew under the action of longitudinal forces $F_{\kappa p}$ and reactions of transverse elastic bonds.
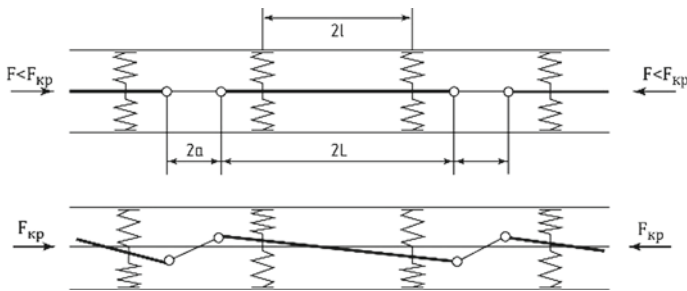
Fig. 8 Design scheme of the train composition and the distortions of its elements in the plan under the action of compressive forces. F is the value of the longitudinal force; here $F_{\kappa p}$ is the critical value of the compressive force; $2L$ is the length of the frame of the car; $2l$ is the base of the car; and a is the length of the body of the automatic coupling

In the case of a wagon moving along a curved section of the track, the reaction forces at the points of contact of the wheel and the rail R_a and R_b are calculated for both the case of the wheel running into the outer (case I) and the inner rails (case II), since it is difficult to predict which of them in a particular case will be more dangerous. In these cases, the expression coefficient of stability margin $k_{yI,II}$ will be defined as [3]:

$$k_{yI,II} = \frac{tg\beta - \mu}{1 + \mu tg\beta} \cdot \frac{P_t + \frac{F}{1 - \frac{F}{F_{\kappa pa}}}\left[\frac{\delta L}{l^2}\left(1 + \frac{L}{a}\right)\frac{h_b}{h_{cm}} \pm \alpha\frac{L_c}{R}\right]\frac{h_{cm}}{s}}{\mu P_t + \frac{2F}{1 - \frac{F}{F_{\kappa pa}}}\left\{\left[\frac{\delta L}{l^2}\left(1 + \frac{L}{a}\right) \pm \alpha\frac{L_c}{R}\right]\left(1 - \mu\frac{h_{cm}}{s}\right) \mp \alpha\frac{L_c}{R}\cdot\frac{h_{cm} - h_b}{2s}\right\}}, \quad (9)$$

where β is the angle between the forming ridge of the wheel and the horizontal; μ is the coefficient of friction between the wheel and the rail; α is the angle of the wagon skew; F is the magnitude of the longitudinal force; $F_{\kappa pa}$ is the critical value of the compressive force; δ is the initial skew of the wagon in the rail track; $2L$ is the length of the wagon frame; $2l$ is the base of wagon, a—the length of the coupling body; $2s$—the distance between the wheels of the wheelset; $⟦2L_c$—the length of the wagon along the coupling axes of the couplers; R—the radius of the curved section of the track; h_{cm}—the height above the rail head of the center of gravity of the wagon; h_b—the height above the rail head of the plane of the support; P_t—vertical load from the trolley onto the rails.

The wagon is resistant to derailment if $k_y \geq 1.3$, i.e., $k_{ymin} = 1.3$. However, random factors depending on a set of values, such as:

- the condition of the track and the quality of its maintenance (e.g., an unoiled inner surface of the rail head will lead to the derailment of the wagon due to an increase in the friction force between the wheel crest and the rail head and, as a result, a faster rolling of the side surface of the wheel onto the rail);
- technical condition of the mechanical part of the wagon (condition of wheel sets, bogies, spring suspension), etc.

Therefore, the loss of stability in a real system, in contrast to a mathematical model, can also occur at values of longitudinal compressive forces much smaller than the calculated ones. In this regard, it is assumed that the minimum allowable value of the stability coefficient is the value $k_y = 3.3$.

The vector quality criterion used consists of heterogeneous partial criteria, i.e., in order to obtain their best values, different requirements must be imposed on the speed control system; therefore, it is not possible to find automatic control parameters that meet all criteria simultaneously. To overcome this difficulty, it is advisable to reduce the multi-criteria optimization problem to a single-criteria one, for which a generalized optimality criterion (objective function) should be used. To perform this transition, good results are shown by the criterion formed on the basis of the deviation of particular criteria from the "ideal" alternative—the criterion of total losses G [14, 15]:

$$G = \sqrt{\frac{1}{z} \sum_{i=1}^{z} \left\{ \frac{U_i - U_i^*}{U_i^{**} - U_i^*} \right\}^2}$$

where U_i^* is the minimum value of the i-th criterion obtained when solving the problem of single-criteria optimization according to this i-th criterion; U_i^{**} is the maximum or permissible value of the i-th criterion; and z is the number of partial optimization criteria.

Minimization of the objective function involves alternately finding the minima of the values of particular criteria, after which, using the found minimum values, the minimization of the objective function itself is performed. To minimize both particular criteria and the objective function, the method of deformable polyhedron Nelder-Meade was used [16]. As a result of solving the problem of parametric synthesis of the automatic speed control system, the system parameters were found, and the simulation of the automatic speed control system was repeated.

4   Results and Discussion

To study the operation of the automatic control system, a program was developed in the Delphi language. The movement of a train consisting of 69 loaded wagons driven by an eight-axle electric locomotive with a total weight of 6050 tons was simulated. Figures 9 and 10 show graphs of transients occurring in a train when implementing a given driving mode using an automatic speed control system with parameters found by performing trial calculations and the smoothing device turned off (Fig. 9) and with parameters found as a result of solving the parametric synthesis problem according to the considered technique. The figures show the following results: the speed of the locomotive $v(t)$ (Figs. 9, 10a), the traction force of the locomotive $F_{el}(t)$, and the force in the automatic coupling between 34 and 35 cars of the train F_{35} (Figs. 9, 10b–d). The mode of starting a pre-compressed train with its further acceleration to

a speed of 40 km/h, speed stabilization when moving along profile fractures, and subsequent repeated acceleration to 60 km/h was studied.

At the initial moment of time $t = 0$, the speed of the train v, as well as the studied values of the forces F_{el} and F_{35}, is equal to 0. After a gradual increase in the traction force of the electric locomotive F_{el} from zero to a maximum value of 500 kN (Fig. 9c), the acceleration of the train begins.

Acceleration is carried out under the action of a constant thrust force until the speed reaches 40 km/h. After that, the thrust force gradually decreases to the level necessary to maintain a constant speed. The passage of the train along the profile elements with a greater or lesser slope is accompanied by a corresponding change in the traction force (Fig. 9b). At time $t = 550$ s, the value of the set speed increases from 40 to 60 km/h, which causes a reciprocal increase in the traction force of the electric locomotive and subsequent acceleration of the train (Fig. 9b).

Let us take a closer look at the process of changing the force F_{35} acting in the automatic coupling between the cars located in the middle of the train. On the graph F_{35} (Fig. 9b), several areas can be distinguished that differ in the nature of the
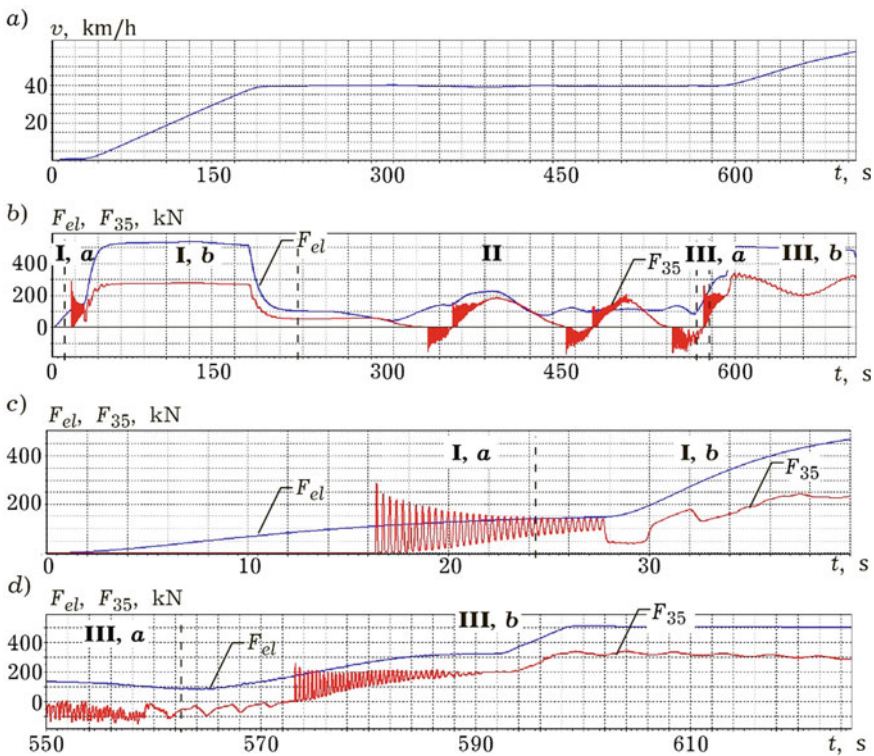
Fig. 9 Results of modeling the operation of the automatic speed control system with the parameters obtained as a result of performing trial calculations: the speed of the train $v(t)$ (a), the traction force of the locomotive F_{el} (t), and the force $F_{35}(t)$ acting in the 35th inter-wagon connection (b–d)
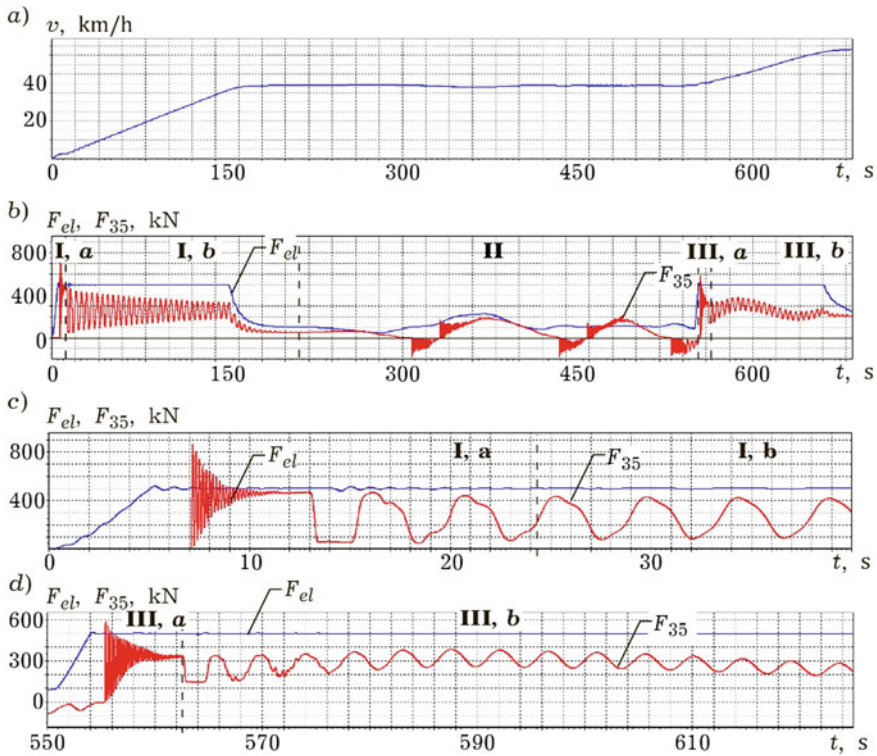
Fig. 10 Results of modeling the operation of the automatic speed control system with the parameters obtained as a result of parametric synthesis: the speed of the train $v(t)$ (**a**), the traction force of the locomotive $F_{el}(t)$, and the force $F_{35}(t)$ acting in the 35th inter-wagon connection (**b–d**)

behavior of the presented curve. In area I (corresponding to the train starting from its place), the change in force is oscillatory, which is caused by alternately driving the cars of the compressed train located behind it in the direction of the tail section. The magnitude of the greatest force achieved in this case is 870 kN at a frequency of about 5 Hz, which is 1.75 times greater than the traction force on the automatic coupling between the locomotive and the first wagon (Fig. 9b). Despite the fact that further acceleration of the train is carried out under the action of a constant traction force F_{el} (Fig. 9b, c), on the graph F_{35}, there are damped oscillations with a frequency of about 0.2 Hz caused by the propagation of forward and reverse stretching waves along the train (Fig. 9b, c, time interval $t = 13 - 160$ s). The end of acceleration is accompanied by a decrease in the thrust force F_{el} and, consequently, a decrease in the force F_{35} (region II).

The frequency of fluctuations in the magnitude of the force F_{35} caused by changes in the traction force and resistance to movement (region III) is determined by the speed of the train and the length of the profile elements and is 0.01–0.1 Hz.

When the train follows the profile elements of a different sign, a group of cars located in the rear of the train runs into the head part, which manifested itself in the form of successive transitions of the train from a stretched to a compressed state (force F_{35} is positive or negative, respectively, time intervals $t = 310 - 350, 430 - 470$ s). As can be seen from Fig. 9b, the presence of gaps in the harness during the transition of the train from one state to another caused high-frequency oscillations (with a frequency of the same order as when starting).

During the subsequent acceleration to a higher speed (area IV in Fig. 9b) due to the fact that before that part of the train was in a compressed state (force F_{35} is negative), an increase in the traction force F_{el} to the maximum level caused the train to stretch, which, in turn, again led to the appearance of high-frequency oscillations, as well as the appearance of a stretching/compression wave.

When modeling the automatic speed control system with the parameters found as a result of solving the synthesis problem, it was found that in the process of starting the train from the place, the largest value of the longitudinal force F_{35} was ≈ 300 kN (Fig. 9b, c). The frequency of force fluctuations is approximately equal to the frequency obtained as a result of calculations with the first version of the automatic management.

In the second variant, there are practically no fluctuations in the region I, b, as a result of which there is no accumulation of fatigue damage. It is established that the frequency of oscillations of the forces F_{el} and F_{35} caused by a change in the resistance to movement (region II) is determined by the speed of the train and the length of the profile elements and is about 0.01–0.1 Hz, while the magnitude of the traction force, as well as the forces acting in the train, is determined by the magnitude of the resistance to movement at a given speed. For both variants, the average value of the longitudinal dynamic force was 75 kN, and the maximum amplitude was 150 kN. However, due to the very low frequency of force changes caused by changes in resistance to movement, this mode has practically no effect on the process of accumulation of fatigue damage and may not be considered in the future.

When the traction was switched on again in the second case, as well as in the first, an increase in the traction force F_{el} to the maximum value caused the train to stretch, which, in turn, again led to the appearance of high-frequency oscillations, the largest amplitude of which was approximately 120 kN, which is more than 1.5 times less than in the first case.

As can be seen, the parameters of the speed controller have the greatest influence on the course of transients in the areas corresponding to the train starting from its place, as well as acceleration (braking), which, in turn, affects the rate of accumulation of fatigue damage. At the same time, the type and parameters of the regulator have no influence on the nature of the change in the values of the longitudinal forces in region II corresponding to the speed stabilization mode and consequently on the amount of fatigue damage.

Taking the following parameters of the fatigue curve of the auto-coupling body: endurance limit $\sigma_{-1} = 148$ MPa, the base number of loading cycles $N_0 = 2 \times 10^6$,

the fatigue curve index $m = 4.11$, the relative value of fatigue damage accumulated in the auto-couplings of the train a, using the linear summation hypothesis, for the considered first variant of the control system implementation the speed will be equal to:

$$a_1 = 3.615 \times 10^{-6}$$

At the same time, the implementation of similar motion modes considered earlier using the second version of the control system allows to improve the flow of transients, which manifests itself in the form of a more than 30-fold reduction in the relative magnitude of accumulated fatigue damage:

$$a_2 = 1.157 \times 10^{-7}$$

5   Conclusion

The use of the automatic control system of the proposed structure with the parameters found as a result of solving the parametric synthesis problem has significantly reduced the values of longitudinal dynamic forces and improved the nature of transient processes in the train, reducing the likelihood of rupture of harness devices due to the occurrence of sudden and gradual failures as a result of exceeding the maximum permissible values by longitudinal forces and accelerated accumulation of fatigue damage.

References

1. Pudovikov, O.E.: Automatic speed control of a long-component freight train. Mechatronics. Automation. Management. No. 8, pp. 51–57 (2010). [Russian]
2. Pudovikov, O.E.: Systems for automatic control of locomotive speed of a freight train with distributed traction. In: Pudovikov, O.E., Sidorenko, V.G., Sidorova, N.N., Kiselev, M.D. (eds.), Russian Electr. Eng. **90**(9), 653–660 (2019)
3. Danilov, V.N., Chesnokov, I.I.: Dynamics of the wagon: textbook for universities of railway transport. Ed. 2nd, reprint. additional/S.V. Vershinsky, – M.: Transport, 352 p (1978). [Russian]
4. Baranov, L.A., Golovitcher, Ya.M., Erofeev, E.V., Maximov, V.M.: Microprocessor-based systems of electric rolling stock auto driving. Baranov, L.A. (ed.), M.: Transportation, 272 p (1990). [Russian]
5. Lazaryan, V.A.: Dynamics of wagons—stability of movement and oscillations. M.: Transzheldorizdat, 255 p (1964). [Russian]
6. Garg, V.K., Rao, V.D.: Dynamics of railway vehicle systems. Academic Press (1984). [Russian]
7. Blokhin, E.P.: Train dynamics (unsteady longitudinal oscillations). Blokhin, E.P., Manashkin, L.A. (eds). – M.: Transport, 222 p (1982). [Russian]
8. Lisitsyn, A.L., Muginstein, L.A.: Unsteady traction modes (Traction support of the transportation process). Narskikh, G.I., Petushkova, I.K. (eds.) M.: Intext, 159 p (1996). [Russian]

9. Wu, Q., Luo, S., Cole, C.: Longitudinal dynamics and energy analysis for heavy haul trains. J. Mod. Transport. **22**, 127–136 (2014). https://doi.org/10.1007/s40534-014-0055-x
10. McClanachan, M., Cole, C.: Current train control optimization methods with a view for application in heavy haul railways. Proc. Inst. Mech. Eng., Part F: J. Rail Rapid Transit. **226**(1), 36–47 (2012). https://doi.org/10.1177/0954409711406352
11. Rosenfeld, V.E.: Theory of electric traction: textbook for universities. In: Rosenfeld, V.E., Isaev, I.P., Sidorov, N.N. (eds,) M.: Transport, J.-D. transp, 294 p (1995). [Russian]
12. Pudovikov, O.E.: Management of long–compound heavy freight trains. Electronic scientific periodical "Management of large systems" Issue 29 State Reg. number 0421000023\0024. IPU RAS, pp. 214–231 (2010). [Russian]
13. Baranov, L.A., Savoskin, A.N., Pudovikov, O.E.: Criteria for the quality of regulating the speed of a train. **4**, 50–56 (2009). [Russian]
14. Dekhtyarenko, V.A., Svoyatytsky, D.A.: Methods of multicriteria optimization of complex systems in design. Publishing house of the Academy of Sciences of the Ukrainian SSR, Kiev, 41 p (1976). [Russian]
15. Brahman, T.R.: Multicriteria and the choice of alternatives in technology. Radio and Communications, Moscow, 288 p (1984). [Russian]
16. Himmelblau, D.M.: Applied nonlinear programming. McGraw-Hill Book Company (1972)

A Study on the Strength Analysis of Interior Plate for Rolling-Type Gangway of Urban Railroad Vehicle

Jaesun Lee and Hong-Lae Jang

Abstract A gangway system is a flexible connector fitted to the end of a railway coach, enabling passengers to move from one coach to another without danger of falling from the train. Recently, a gangway system with an added interior plate is gradually being applied to urban railroad vehicles, and various types have been developed and applied to the corresponding vehicles according to the types of urban railroad vehicles in each country. In the case of gangways with interior plates, it is gradually expanding because it is advantageous for insulation, sound absorption performance, and passenger safety. Interior plates are widely used as interior materials for railway vehicles including gangways and generally have requirements such as mechanical properties and fire safety performance. In particular, the interior plate for gangway must be designed to flexibly withstand movements such as yaw, pitch, lateral, vertical, and roll, so the mechanical strength requirements are variously defined. In this study, related international standards were analyzed to derive the required strength requirements for the interior plate for rolling-type gangway, which is being developed for the application of urban railroad vehicles in Korea, and mechanical strength analysis was performed through the finite element analysis (FEA) accordingly. Experiments were also performed to obtain the mechanical properties of the fiber reinforced plastics (FRP) interior plates manufactured through the application of aramid-based materials for fire safety. As a result of performing the FEA in boundary conditions derived from the EN 16286-1 standard, it was confirmed that the FRP interior plate under development can be applied to the rolling-type gangway of urban railroad vehicles.

Keywords Gangway systems · Finite element analysis · EN 16286-1

J. Lee · H.-L. Jang (✉)
School of Mechanical Engineering, Changwon National University, Changwon-Si 51140, Republic of Korea
e-mail: hjang@changwon.ac.kr

1 Introduction

The gangway of railroad vehicles is changing from the existing bellows to gradually applying interior plates for insulation, sound absorption performance, and passenger safety. Therefore, the type in which the interior plate is added to the gangway of the railway vehicle is being gradually expanded and applied worldwide [1–7]. Various types of built-in-type gangway have to be developed and applied to railway vehicles according to the characteristics of each country's railway vehicles. In the case of Korean urban railway vehicles, related products have not yet been developed. Interior plates are widely used as interior materials for railway vehicles and have requirements such as mechanical properties and fire safety performance. In particular, the internal plate for rolling-type gangway must be designed to flexibly withstand movements such as yaw, pitch, lateral, vertical, and roll, so the requirements for mechanical strength are defined in various ways by standards [8–14].

The rolling bracket for gangway is a device that flexibly withstands the movement of the gangway and is a device that bends and restrains the interior plate by rolling it in the longitudinal direction [15–19] (Fig. 1).

In this study, related international standards were analyzed to derive the required strength requirements for the interior plate of rolling-type gangway, which is being developed for the application of urban railroad vehicles in Korea, and mechanical strength analysis was performed through the finite element analysis (FEA) accordingly. Experiments were also performed to obtain the mechanical properties of interior plates manufactured through the application of aramid-based materials to FRP for fire safety.
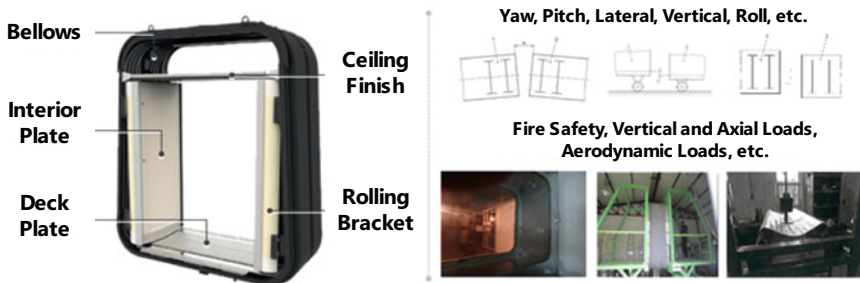
Fig. 1 Overview of interior plates for gangways

2 Mechanical Property Testing of Rolling-Type Interior Plate

2.1 Manufacture of Rolling-Type Interior Plate

The rolling-type interior plate for gangway was manufactured by vacuum infusion method, and the procedure is as follows:

Mold release agent treatment Apply release wax for smooth demolding [20, 21].

Material alter Cut glass fiber reinforcement and materials for vacuum application according to the size of application [22, 23].

Resin preparation Mix the main agent and hardener according to the mixing ratio.

Mat lamination Laying the prepared mat [24–26].

Vacuum application After applying release film, breather, peel fly, vacuum film, etc., apply vacuum [27–29].

Curing Hardening of laminated products at high temperatures [30–32].

Demolding and cutting After the product molded in the mold, it is cut to size.

Painting Paint the product [33–35].

Others Avoid leakage when vacuum is applied. The curing temperature should be 60° or higher [36–38] (Figs. 2 and 3).
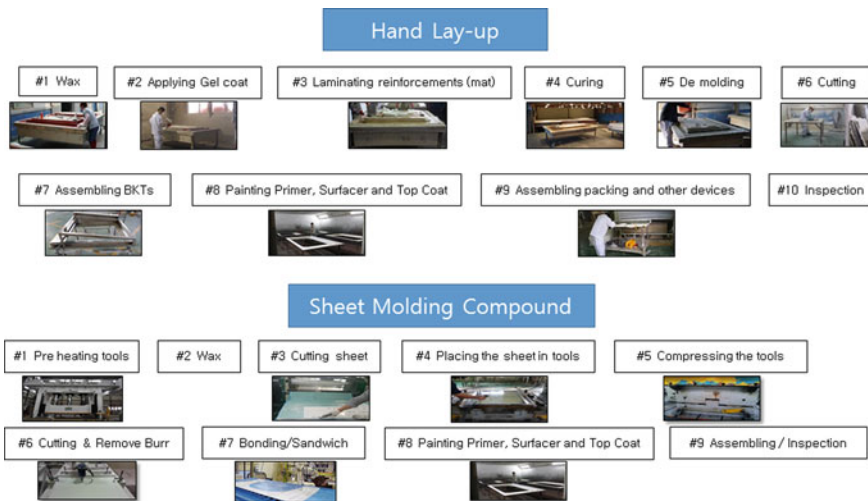
Fig. 2 Forming process of interior plate for gangway
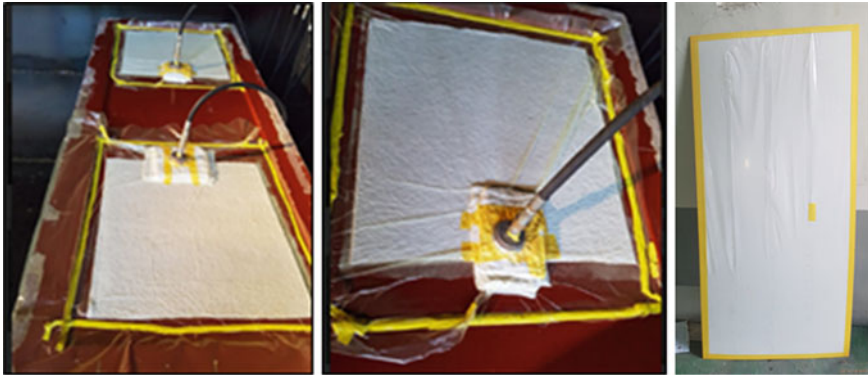
Fig. 3 Vacuum infusion process and finished interior plate prototype

2.2 Specimens for Measuring Mechanical Properties

For structural analysis according to the load requirements presented in EN 16286-1[39], it is first necessary to measure the mechanical properties of the FRP material of the interior plate for rolling-type gangway [40–43]. Unlike general ductile materials, FRP is a brittle material, so when tensile tests for measuring elastic modulus and Poisson's ratio, premature rupture due to stress concentration in the grip area has been reported. For this reason, the tensile test standards for FRP materials such as ASTM D3039 [44], ISO 527-4 [45], and ACI 440.3R [46] recommend that a specimen be prepared separately by using a reinforcing material in the grip part. Dumbbell-type specimens, which are general tensile specimens, are not particularly proposed for multiaxial FRP materials [45], because stress concentration in curved areas causes fiber breakage and reduces tensile strength [47–51]. In Fig. 4, the shape of the tensile test specimen required for each standard is shown. In common, specimens with reinforcing materials attached to grips on rectangular specimens are presented, and the sizes of specimens are slightly different for each standard (Table 1).
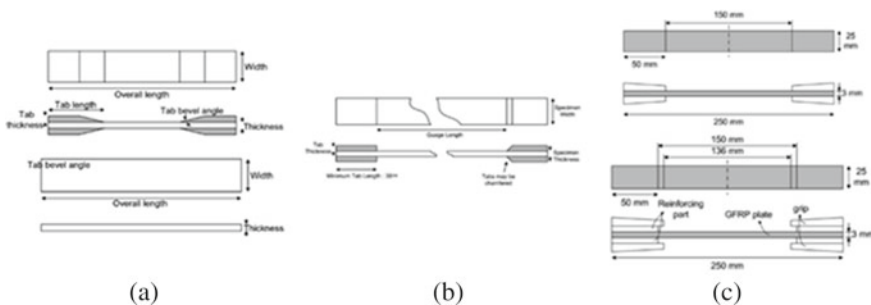
Fig. 4 Shape and dimensions of tensile test specimens and reinforcing materials for each standard of FRP material. **a** ASTM D3039, **b** ACI 440.3R, and **c** ISO 527-4

Table 1 Specimen size

Test	Standard	Size (mm)	Orientation (deg)
Tensile	ASTM D3039	250 × 15 × 1	0°
Bending	ASTM D7264	40 × 13 × 1	0°
Tensile	ASTM D3039	175 × 25 × 1	90°
Bending	ASTM D7264	40 × 13 × 1	90°

Fig. 5 Produced specimens

Since bending is dominant in the mechanical behavior of interior plates for rolling-type gangway, bending tests of materials for measuring flexural strength are also essential [52–56]. The bending test was to be performed according to ASTM D7264 [57], and specimens for tensile and bending tests were cut and processed. Specimens were prepared by dividing the fiber direction (0°) and the fiber perpendicular direction (90°) for each test (Fig. 5).

2.3 Tests on Mechanical Properties of Interior Plate

A tensile test was performed on the fabricated specimen according to ASTM D3039 standard as shown in Fig. 6. The test speed was set to 2 mm/min, and an extensometer for measuring elongation was attached, and a strain gauge was attached to the specimen to measure Poisson's ratio [58–63]. The bending test was performed at a test speed of 1 mm/min according to ASTM D7264 standard as shown in Fig. 6. The span distance was set to 32 mm considering the thickness of the specimen 1 mm. MTS 100 kN fatigue tester and 100 kN universal testing machine were used for the test.

As a result of the tensile test, the modulus of elasticity in the fiber direction was about 19 GPa, and the tensile strength was about 330 MPa. In the direction perpendicular to the fiber, 6.5 GPa and 55 MPa were measured, respectively, which were 1/3 and 1/6 respectively compared to the fiber direction. The Poisson's ratio was measured to be 0.13 and 0.1 for the fiber direction and the fiber perpendicular

Tensile test (ASTM D 3039)   3-point Bending test (ASTM D 7264)

Fig. 6 Material property measurement tests

direction, respectively. It was confirmed that there was a large difference in physical properties depending on the glass fiber insertion direction. Also, through the stress–strain curves, it was possible to confirm the properties of brittle materials in which yield and fracture occur almost simultaneously. Brittle material breaks while little to no energy is absorbed when stressed. The specimen of FRP interior plate fractures with no plastic deformation as shown in Fig. 8, so that we confirm the brittleness of the material we used. It is noteworthy that the tensile strength compared to the modulus of elasticity was recorded significantly higher than that of other FRP materials. Therefore, it could be inferred that the material was manufactured to meet the requirements of the interior plate for a rolling-type gangway that should not be destroyed while being flexibly deformed according to the operation of the railway vehicle (Fig. 7).

Through the bending test, the flexural strength in each direction was investigated. In the 0° direction, the strength was about 250 MPa, while in the 90° direction, the strength was about 1/3, 75 MPa (Figs. 9 and 10).

3 Strength Analysis of Rolling-Type Interior Plate

3.1 EN 16286-1 Load Requirements for Interior Plates for Gangways

The load-bearing conditions for gangway interior plates are not specified in the domestic regulations. Therefore, Part 1: Main applications of EN 16286-1:2013 "Railway applications—Gangway systems between vehicles" was referred to. EN 16286-1 is a document that specifies the requirements for the overall gangway system and covers the overall gangway scaffold, ceiling, sidewall, bellows, etc. In particular, the load requirements for gangway interior plates are dealt with in 7.5 load requirements.
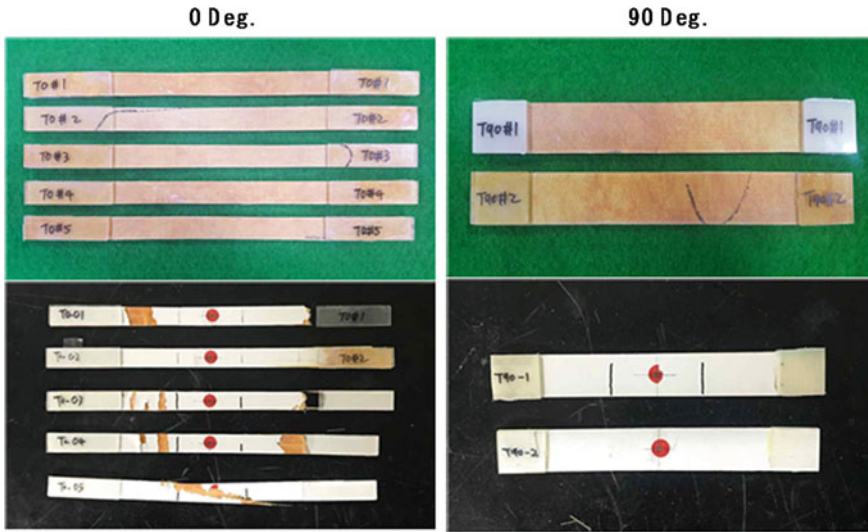
Fig. 7 Specimens before and after tensile tests
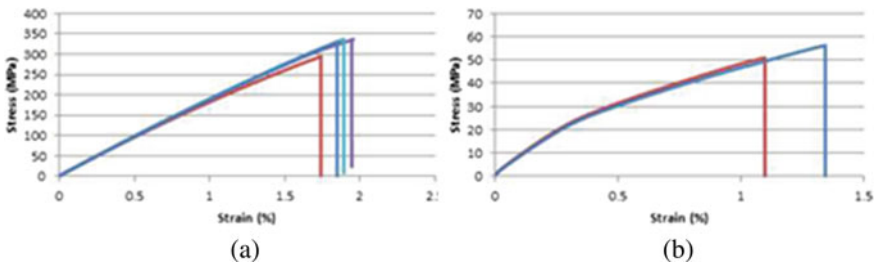
Fig. 8 Stress–strain curves for tensile tests **a** 0° **b** 90°

General information Flexible members used for floors and side walls must have sufficient strength and rigidity to safely support passengers and crew.

Vertical load condition of connecting passage The load-bearing condition of the bottom of the connecting passage can be verified by calculation or test. Considering the static load of the passenger according to EN 15663 [64] and the acceleration condition of EN 12663-1 [65], the load applied to the floor plate area of the connecting passage is applied. It shall withstand a vertical load of 800 N on an arbitrary area of 100 mm * 200 mm above the floor of the connecting passage. For verification requirements, refer to EN 12663-1.

Dynamic load and fixation applied to the gangway system Forces due to acceleration and relative motion as defined in EN 12663-1 for device mounting must be considered.
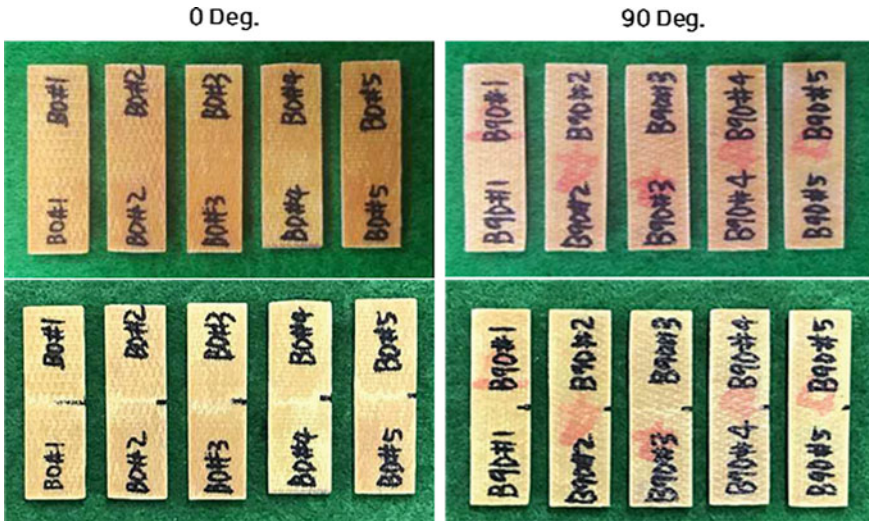
Fig. 9 Specimens before and after 3-point bending tests
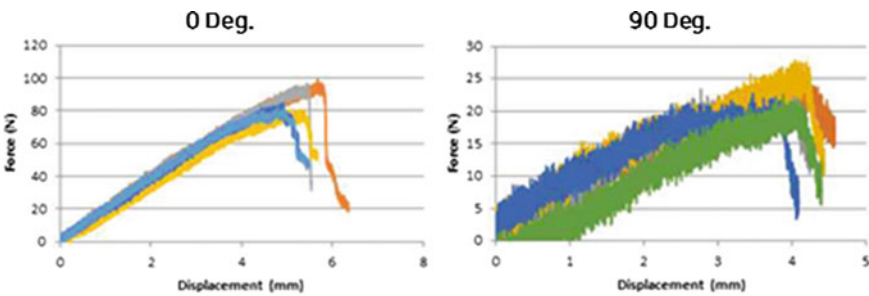
Fig. 10 Force–displacement curves for bending tests

Horizontal load The sidewall interior plates for the gangway of the passage must withstand the load of one person leaning against the sidewall. It must withstand the concentrated vertical load applied in the gangway without any permanent deformation. The detailed conditions are as follows.

- When a load of 15% * 80 kg * 9.81 m/s^2 = 120 N is applied to any 100 mm * 100 mm point of the interior plate for the gangway (assuming that a person leans on his/her hand).
- When a load of 80 kg * 9.81 m/s^2 = 800 N is applied as a distributed load from a height of 1.3 m by 0.2 m in the height direction and 0.5 m in the width direction (assuming that a person leans on his/her shoulder) (Fig. 11).

Fig. 11 Application of interior plate for gangway and load requirements

3.2 Structural Analysis of Interior Plate According to Load Requirements

Based on the test results of measuring the material properties, a structural analysis model of the rolling-type interior plate was constructed. First, the material model, which assumed that the interior plate was a linear elastic body and entered the properties obtained through the tensile test, was verified using the bending test data. Modeling for finite element analysis was performed for the test method specified in ASTM D7264 and the size of the actually used specimen. The bending test jig was modeled as a rigid cylinder with $R = 3$ mm, and the bending specimen was modeled using 8-node 3D solid elements, and an in-plane contact condition was applied between the two components. Support boundary conditions and load boundary conditions are simulated like actual experimental conditions by interaction by contact. The load was applied in the form of a displacement load to the rigid body above the specimen, and it was set to move up to 6 mm. The material constants applied to the bent specimen were derived from the experimental results as shown in Table 2.

The result of nonlinear static finite element analysis considering geometric nonlinearity as contact is shown in the Fig. 12.

Figure 13 shows the results of analyzing the bending test based on the data obtained from the experiment and comparing them with the results of the bending test. In the case of bending stiffness, the analysis result appears to be about 15% higher than the test result. However, since the scale of the gangway interior plate to be analyzed later is relatively large and the contact between the curved surface of the rolling

Table 2 Material constants for bending test specimens of FRP

Mechanical properties	Value
Elastic modulus, GPa	19
Poisson's ratio	0.13
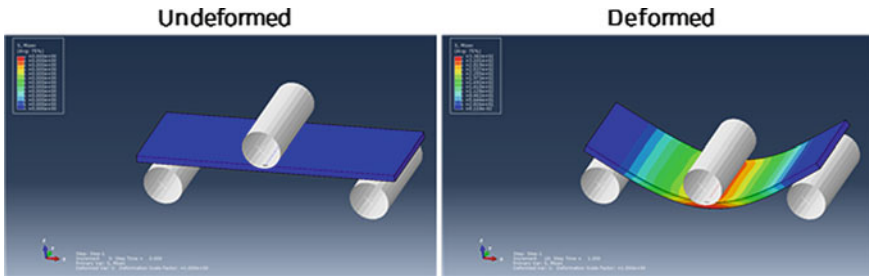
Fig. 12 FEA results on 3-point bending tests **a** undeformed **b** deformed

bracket and the interior plate is the dominant factor in the rolling mechanism of the gangway interior plate, a nonlinear analysis with excessive calculation cost is essential. Therefore, for the sake of computational efficiency, it is assumed that the linear elastic body is used.

Using the verified material model, a structural analysis model of the rolling-type gangway interior plate was constructed. The cylindrical rolling bracket was modeled as a rigid body, and TIE constraint was applied to the end of the modeled flat FRP interior plate with reference to the drawings. The rotation was made by applying a moment to the center of the rolling bracket, and the bending phenomenon was simulated as the inner plate joined by the TIE constraint was naturally rolled on the bracket. The interior plate was modeled as a shell element, and a mesh was created using S4R5 elements with 5 degrees of freedom at each node assuming a small membrane strain. The built-in internal plate structural analysis model and the rotation of the rolling bracket for each given moment, along with the behavior and stress distribution of the entire system, can be seen in Fig. 14.

The stress distribution of the inner plate was examined by gradually increasing the torque of the rolling bracket until a torque corresponding to 500 N·m was applied.
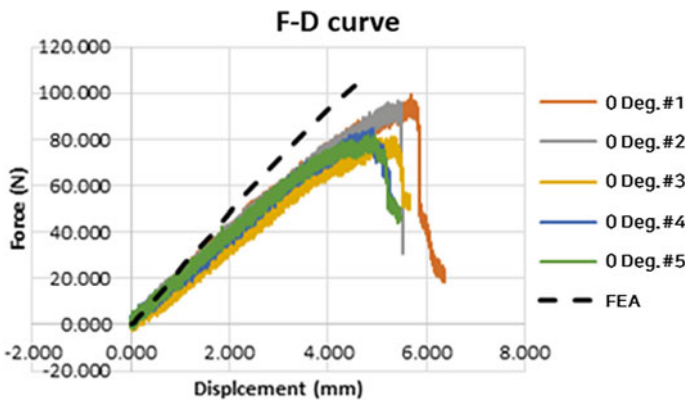
Fig. 13 Comparison between *F–D* curves from experiments and FEA
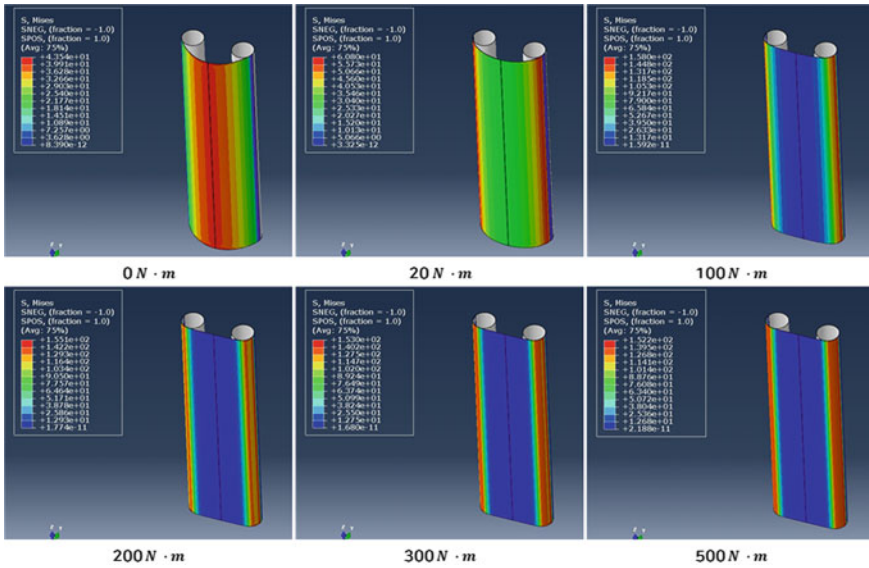
Fig. 14 Stress distribution of interior plates according to various torques

When installed for the first time, bending of the inner plate occurs in the center, and the inner plate begins to roll on the rolling bracket in a state in which stress is generated, and it is relieved. As the torque reaches 20 N·m, contact occurs between the curved surface of the bracket and the upper surface of the interior plate, and accordingly, it can be seen that high stress is generated in the contact between the bracket and the interior plate. When it was installed on the gangway of a railroad car after the rotation was completed, the maximum stress was about 152 MPa, and it was found that it occurred in the vicinity of the interior plate attached to the bracket. Through this, it can be inferred that, as the interior plate for rolling-type gangway is installed in the vehicle, the part where the initial stress is highest when it is rolled on the bracket is the bolted part between the interior plate and the bracket. While the tensile strength of the interior plate was 330 MPa, it was confirmed that half the stress occurred analytically.

The EN 16266-1 standard suggests two load conditions for the inner plate for gangway and assumes the load conditions applied by the hand and the shoulder, respectively. For the structural analysis model of the gangway interior plate constructed previously, an additional analysis was performed by applying the torque corresponding to 500 N·m to the bracket and applying the load requirements suggested in the standard while it was attached to the railroad car.

It was possible to confirm the predictable shape of deformation when load condition #1 was applied to the interior plate. The point where the maximum stress occurred was previously expected to be the bolted part, and it was confirmed that the maximum stress occurred in the area where the bracket and the interior plate were in direct contact when the load condition #1 was applied, and the maximum value is about

Fig. 15 Stress distribution
of interior plates according to
load requirement #1 (hand)
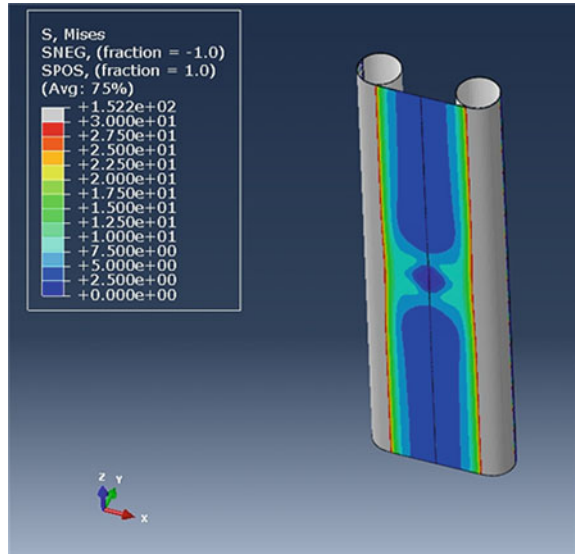
152 MPa, which is about 1/2 of the tensile strength of the interior plate measured
through the experiment of 330 MPa.

Even when load condition #2 by the shoulder was applied, it was possible to
confirm the predictable shape of the deformation, and the point of maximum stress
was different from the load condition #1 at the area where the bracket and the interior
plate contacted outside the surface to which the load was applied could be seen to
occur. In addition, for load condition #2, the maximum stress is about 164 MPa,
and it can be confirmed that the maximum stress increases by about 10 MPa when
a load condition is applied to the shoulder rather than a human hand load. From the
requirements, it can be inferred that the size of the load by the shoulder is larger than
the load by the human hand. However, it is still a value corresponding to about 1/2
of the tensile strength of the interior plate material of 330 MPa, and it was confirmed
that permanent deformation does not occur, and the manufactured interior plate for
gangway will satisfy the EN 16286-1 standard (Figs. 15 and 16).

4   Conclusion

The interior plate for gangway must be designed to flexibly withstand movements
such as yaw, pitch, lateral, vertical, and roll, so the mechanical strength requirements
are variously defined. In this study, related international standards were analyzed
to derive the required strength requirements for the interior plate for rolling-type
gangway, which is being developed for the application of urban railroad vehicles in
Korea, and mechanical strength analysis was performed through the finite element

Fig. 16 Stress distribution of interior plates according to load requirement #2 (shoulder)
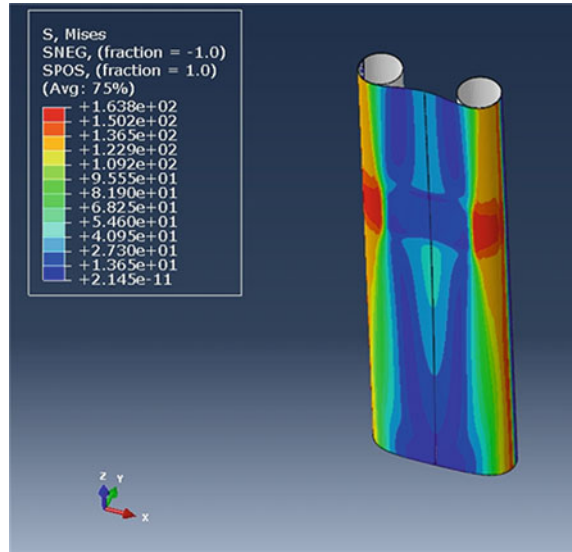
analysis (FEA) accordingly. Experiments were also performed to obtain the mechanical properties of the fiber reinforced plastics (FRP) interior plates manufactured through the application of aramid-based materials for fire safety. As a result of performing the FEA in boundary conditions derived from the EN 16286-1 standard, it was confirmed that the FRP interior plate under development can be applied to the rolling-type gangway of urban railroad vehicles.

References

1. Sharma, S.K., Sharma, R.C., Lee, J.: In situ and experimental analysis of longitudinal load on carbody fatigue life using nonlinear damage accumulation. Int. J. Damage Mech. **31**, 605–622 (2022). https://doi.org/10.1177/10567895211046043
2. Sharma, S.K., Lee, J., Jang, H.-L.: Mathematical modeling and simulation of suspended equipment impact on car body modes. Machines **10**, 192 (2022). https://doi.org/10.3390/machines10030192
3. Vishwakarma, P.N., Mishra, P., Sharma, S.K.: Characterization of a magnetorheological fluid damper a review. Mater. Today Proc. **56**, 2988–2994 (2022). https://doi.org/10.1016/j.matpr.2021.11.143
4. Sharma, R.C., Sharma, S.K.: Ride analysis of road surface-three-wheeled vehicle-human subject interactions subjected to random excitation. SAE Int. J. Commer. Veh. **15**, 02-15-03-0017 (2022). https://doi.org/10.4271/02-15-03-0017
5. Sharma, S.K., Sharma, R.C., Lee, J., Jang, H.-L.: Numerical and experimental analysis of DVA on the flexible-rigid rail vehicle car body resonant vibration. Sensors. **22**, 1922 (2022). https://doi.org/10.3390/s22051922
6. Vishwakarma, P.N., Mishra, P., Sharma, S.K.: Formulation of semi-active suspension system and controls in rail vehicle. SSRN Electron. J. (2022). https://doi.org/10.2139/ssrn.4159616

7. Sharma, S.K., Mohapatra, S., Sharma, R.C., Alturjman, S., Altrjman, C., Mostarda, L., Stephan, T.: Retrofitting existing buildings to improve energy performance. Sustainability **14**, 666 (2022). https://doi.org/10.3390/su14020666

8. Lee, J., Han, J., Sharma, S.K.: Structural analysis on the separated and integrated differential gear case for the weight reduction. In: Joshi, P., Gupta, S.S., Shukla, A.K., Gautam, S.S. (eds.) Advances in Engineering Design. Lecture Notes in Mechanical Engineering, pp. 175–181 (2021). https://doi.org/10.1007/978-981-33-4684-0_18

9. Choi, S., Lee, J., Sharma, S.K.: A study on the performance evaluation of hydraulic tank injectors. In: Advances in Engineering Design: Select Proceedings of FLAME 2020, pp. 183–190. Springer Singapore (2021). https://doi.org/10.1007/978-981-33-4684-0_19

10. Sharma, S.K., Sharma, R.C., Lee, J.: Effect of rail vehicle-track coupled dynamics on fatigue failure of coil spring in a suspension system. Appl. Sci. **11**, 2650 (2021). https://doi.org/10.3390/app11062650

11. Mohapatra, S., Mohanty, D., Mohapatra, S., Sharma, S., Dikshit, S., Kohli, I., Samantaray, D.P., Kumar, R., Kathpalia, M.: Biomedical application of polymeric biomaterial: polyhydroxybutyrate. In: Bioresource Utilization and Management: Applications in Therapeutics, Biofuels, Agriculture, and Environmental Science, pp. 1–14. CRC Press (2021). https://doi.org/10.21203/rs.3.rs-1491519/v1

12. Wu, Q., Cole, C., Spiryagin, M., Chang, C., Wei, W., Ursulyak, L., Shvets, A., Murtaza, M.A., Mirza, I.M., Zhelieznov, К., Mohammadi, S., Serajian, H., Schick, B., Berg, M., Sharma, R.C., Aboubakr, A., Sharma, S.K., Melzi, S., Di Gialleonardo, E., Bosso, N., Zampieri, N., Magelli, M., Ion, C.C., Routcliffe, I., Pudovikov, O., Menaker, G., Mo, J., Luo, S., Ghafourian, A., Serajian, R., Santos, A.A., Teodoro, Í.P., Eckert, J.J., Pugi, L., Shabana, A., Cantone, L.: Freight train air brake models. Int. J. Rail Transp., 1–49 (2021). https://doi.org/10.1080/23248378.2021.2006808

13. Sharma, S.K., Lee, J.: Crashworthiness analysis for structural stability and dynamics. Int. J. Struct. Stab. Dyn. **21**, 2150039 (2021). https://doi.org/10.1142/S0219455421500395

14. Sharma, R.C., Palli, S., Sharma, N., Sharma, S.K.: Ride behaviour of a four-wheel vehicle using H infinity semi-active suspension control under deterministic and random inputs. Int. J. Veh. Struct. Syst. **13**, 234–237 (2021). https://doi.org/10.4273/ijvss.13.2.18

15. Bhardawaj, S., Sharma, R.C., Sharma, S.K., Sharma, N.: On the planning and construction of railway curved track. Int. J. Veh. Struct. Syst. **13**, 151–159 (2021). https://doi.org/10.4273/ijvss.13.2.04

16. Sharma, R.C., Sharma, S., Sharma, S.K., Sharma, N., Singh, G.: Analysis of bio-dynamic model of seated human subject and optimization of the passenger ride comfort for three-wheel vehicle using random search technique. Proc. Inst. Mech. Eng. Part K J. Multi-body Dyn. **235**, 106–121 (2021). https://doi.org/10.1177/1464419320983711

17. Sharma, R.C., Sharma, S., Sharma, N., Sharma, S.K.: Linear and nonlinear analysis of ride and stability of a three-wheeled vehicle subjected to random and bump inputs using bond graph and simulink methodology. SAE Int. J. Commer. Veh. **14**, 02-15-01-0001 (2021). https://doi.org/10.4271/02-15-01-0001

18. Sharma, S.K., Sharma, R.C.: Multi-objective design optimization of locomotive nose. In: SAE Technical Paper, pp. 1–10 (2021). https://doi.org/10.4271/2021-01-5053

19. Sharma, S.K., Phan, H., Lee, J.: An application study on road surface monitoring using DTW based image processing and ultrasonic sensors. Appl. Sci. **10**, 4490 (2020). https://doi.org/10.3390/app10134490

20. Sharma, S.K., Lee, J.: Design and development of smart semi active suspension for nonlinear rail vehicle vibration reduction. Int. J. Struct. Stab. Dyn. **20**, 2050120 (2020). https://doi.org/10.1142/S0219455420501205

21. Sharma, R.C., Sharma, S.K., Sharma, N., Sharma, S.: Analysis of ride and stability of an ICF railway coach. Int. J. Veh. Noise Vib. **16**, 127 (2020). https://doi.org/10.1504/IJVNV.2020.117820

22. Sharma, S.K., Lee, J.: Finite element analysis of a fishplate rail joint in extreme environment condition. Int. J. Veh. Struct. Syst. **12**, 503–506 (2020). https://doi.org/10.4273/ijvss.12.5.03

23. Sharma, S., Sharma, R.C., Sharma, S.K., Sharma, N., Palli, S., Bhardawaj, S.: Vibration isolation of the quarter car model of road vehicle system using dynamic vibration absorber. Int. J. Veh. Struct. Syst. **12**, 513–516 (2020). https://doi.org/10.4273/ijvss.12.5.05

24. Sharma, R.C., Sharma, S.K., Palli, S.: Linear and non-linear stability analysis of a constrained railway wheelaxle. Int. J. Veh. Struct. Syst. **12**, 128–133 (2020). https://doi.org/10.4273/ijvss.12.2.04

25. Acharya, A., Gahlaut, U., Sharma, K., Sharma, S.K., Vishwakarma, P.N., Phanden, R.K.: Crashworthiness analysis of a thin-walled structure in the frontal part of automotive chassis. Int. J. Veh. Struct. Syst. **12**, 517–520 (2020). https://doi.org/10.4273/ijvss.12.5.06

26. Sharma, S.K., Sharma, R.C., Sharma, N.: Combined multi-body-system and finite element analysis of a rail locomotive crashworthiness. Int. J. Veh. Struct. Syst. **12**, 428–435 (2020). https://doi.org/10.4273/ijvss.12.4.15

27. Palli, S., Sharma, R.C., Sharma, S.K., Chintada, V.B.: On methods used for setting the curve for railway tracks. J. Crit. Rev. **7**, 241–246 (2020)

28. Bhardawaj, S., Sharma, R., Sharma, S.: Ride analysis of track-vehicle-human body interaction subjected to random excitation. J. Chinese Soc. Mech. Eng. **41**, 237–236 (2020). https://doi.org/10.29979/JCSME

29. Bhardawaj, S., Sharma, R.C., Sharma, S.K.: Analysis of frontal car crash characteristics using ANSYS. Mater. Today Proc. **25**, 898–902 (2020). https://doi.org/10.1016/j.matpr.2019.12.358

30. Bhardawaj, S., Sharma, R.C., Sharma, S.K.: Development in the modeling of rail vehicle system for the analysis of lateral stability. Mater. Today Proc. **25**, 610–619 (2020). https://doi.org/10.1016/j.matpr.2019.07.376

31. Sharma, R.C., Sharma, S., Sharma, S.K., Sharma, N.: Analysis of generalized force and its influence on ride and stability of railway vehicle. Noise Vib. Worldw. **51**, 95–109 (2020). https://doi.org/10.1177/0957456520923125

32. Bhardawaj, S., Sharma, R.C., Sharma, S.K.: Development of multibody dynamical using MR damper based semi-active bio-inspired chaotic fruit fly and fuzzy logic hybrid suspension control for rail vehicle system. Proc. Inst. Mech. Eng. Part K J. Multi-body Dyn. **234**, 723–744 (2020). https://doi.org/10.1177/1464419320953685

33. Mohapatra, S., Pattnaik, S., Maity, S., Mohapatra, S., Sharma, S., Akhtar, J., Pati, S., Samantaray, D.P., Varma, A.: Comparative analysis of PHAs production by Bacillus megaterium OUAT 016 under submerged and solid-state fermentation. Saudi J. Biol. Sci. **27**, 1242–1250 (2020). https://doi.org/10.1016/j.sjbs.2020.02.001

34. Lee, J., Sharma, S.K.: Numerical investigation of critical speed analysis of high-speed rail vehicle. 한국정밀공학회 학술발표대회 논문집 (Korean Soc. Precis. Eng. **696** (2020)

35. Goswami, B., Rathi, A., Sayeed, S., Das, P., Sharma, R.C., Sharma, S.K.: Optimization design for aerodynamic elements of Indian locomotive of passenger train. In: Advances in Engineering Design, pp. 663–673. Lecture Notes in Mechanical Engineering. Springer, Singapore (2019). https://doi.org/10.1007/978-981-13-6469-3_61

36. Sinha, A.K., Sengupta, A., Gandhi, H., Bansal, P., Agarwal, K.M., Sharma, S.K., Sharma, R.C., Sharma, S.K.: Performance enhancement of an all-terrain vehicle by optimizing steering, powertrain and brakes. In: Advances in Engineering Design, pp. 207–215 (2019). https://doi.org/10.1007/978-981-13-6469-3_19

37. Sharma, S.K., Sharma, R.C.: Pothole detection and warning system for Indian roads. In: Advances in Interdisciplinary Engineering, pp. 511–519 (2019). https://doi.org/10.1007/978-981-13-6577-5_48

38. Bhardawaj, S., Chandmal Sharma, R., Kumar Sharma, S.: A survey of railway track modelling. Int. J. Veh. Struct. Syst. **11**, 508–518 (2019). https://doi.org/10.4273/ijvss.11.5.08

39. EN 16286-1:2013 Railway applications—Gangway systems between vehicles—Part 1: Main applications (2013)

40. Choppara, R.K., Sharma, R.C., Sharma, S.K., Gupta, T.: Aero dynamic cross wind analysis of locomotive. In: IOP Conference Series: Materials Science and Engineering, p. 12035. IOP Publishing (2019)

41. Bhardwaj, S., Chandmal Sharma, R., Kumar Sharma, S.: Development and advancement in the wheel-rail rolling contact mechanics. IOP Conf. Ser. Mater. Sci. Eng. **691**, 012034 (2019). https://doi.org/10.1088/1757-899X/691/1/012034

42. Sharma, S.K., Saini, U., Kumar, A.: Semi-active control to reduce lateral vibration of passenger rail vehicle using disturbance rejection and continuous state damper controllers. J. Vib. Eng. Technol. **7**, 117–129 (2019). https://doi.org/10.1007/s42417-019-00088-2

43. Sharma, S.K.: Multibody analysis of longitudinal train dynamics on the passenger ride performance due to brake application. Proc. Inst. Mech. Eng. Part K J. Multi-body Dyn. **233**, 266–279 (2019). https://doi.org/10.1177/1464419318788775

44. ASTM D3039/D3039M-08 Standard Test Method for Tensile Properties of Polymer Matrix Composite Materials (2014). https://doi.org/10.1520/D3039_D3039M-08

45. ISO 527-4:1997—Plastics—Determination of tensile properties—Part 4: Test conditions for isotropic and orthotropic fibre-reinforced plastic composites (2021)

46. ACI 440.3R Guide Test Methods for Fiber-Reinforced Polymer (FRP) Composites for Reinforcing or Strengthening Concrete and Masonry Structures (2004)

47. Goyal, S., Anand, C.S., Sharma, S.K., Sharma, R.C.: Crashworthiness analysis of foam filled star shape polygon of thin-walled structure. Thin-Walled Struct. **144**, 106312 (2019). https://doi.org/10.1016/j.tws.2019.106312

48. Palli, S., Koona, R., Sharma, S.K., Sharma, R.C.: A review on dynamic analysis of rail vehicle coach. Int. J. Veh. Struct. Syst. **10**, 204–211 (2018). https://doi.org/10.4273/ijvss.10.3.10

49. Sharma, R.C., Palli, S., Sharma, S.K., Roy, M.: Modernization of railway track with composite sleepers. Int. J. Veh. Struct. Syst. **9**, 321–329 (2018)

50. Sharma, R.C., Sharma, S.K., Palli, S.: Rail vehicle modelling and simulation using Lagrangian method. Int. J. Veh. Struct. Syst. **10**, 188–194 (2018). https://doi.org/10.4273/ijvss.10.3.07

51. Sharma, S.K., Sharma, R.C.: Simulation of quarter-car model with magnetorheological dampers for ride quality improvement. Int. J. Veh. Struct. Syst. **10**, 169–173 (2018). https://doi.org/10.4273/ijvss.10.3.03

52. Sharma, S.K., Kumar, A.: Disturbance rejection and force-tracking controller of nonlinear lateral vibrations in passenger rail vehicle using magnetorheological fluid damper. J. Intell. Mater. Syst. Struct. **29**, 279–297 (2018). https://doi.org/10.1177/1045389X17721051

53. Sharma, S.K., Kumar, A.: Impact of longitudinal train dynamics on train operations: a simulation-based study. J. Vib. Eng. Technol. **6**, 197–203 (2018). https://doi.org/10.1007/s42417-018-0033-4

54. Sharma, R.C., Sharma, S.K.: Sensitivity analysis of three-wheel vehicle's suspension parameters influencing ride behavior. Noise Vib. Worldw. **49**, 272–280 (2018). https://doi.org/10.1177/0957456518796846

55. Sharma, S.K., Kumar, A.: Ride comfort of a higher speed rail vehicle using a magnetorheological suspension system. Proc. Inst. Mech. Eng. Part K J. Multi-body Dyn. **232**, 32–48 (2018). https://doi.org/10.1177/1464419317706873.

56. Sharma, S.K., Sharma, R.C.: An investigation of a locomotive structural crashworthiness using finite element simulation. SAE Int. J. Commer. Veh. **11**, 235–244 (2018). https://doi.org/10.4271/02-11-04-0019

57. ASTM D7264/D7264M-07 Standard Test Method for Flexural Properties of Polymer Matrix Composite Materials (2015). https://doi.org/10.1520/D7264_D7264M-07.

58. Sharma, S.K., Kumar, A.: Impact of electric locomotive traction of the passenger vehicle Ride quality in longitudinal train dynamics in the context of Indian railways. Mech. Ind. **18**, 222 (2017). https://doi.org/10.1051/meca/2016047

59. Sharma, S.K., Kumar, A.: Ride performance of a high speed rail vehicle using controlled semi active suspension system. Smart Mater. Struct. **26**, 055026 (2017). https://doi.org/10.1088/1361-665X/aa68f7

60. Kulkarni, D., Sharma, S.K., Kumar, A.: Finite element analysis of a fishplate rail joint due to wheel impact. In: International Conference on Advances in Dynamics, Vibration and Control (ICADVC-2016) NIT Durgapur, India February 25–27, 2016. National Institute of Technology Durgapur, Durgapur, India (2016)

61. Sharma, S.K., Chaturvedi, S.: Jerk analysis in rail vehicle dynamics. Perspect. Sci. **8**, 648–650 (2016). https://doi.org/10.1016/j.pisc.2016.06.047
62. Sharma, S.K., Kumar, A.: Dynamics analysis of wheel rail contact using FEA. Procedia Eng. **144**, 1119–1128 (2016). https://doi.org/10.1016/j.proeng.2016.05.076
63. Sharma, S.K., Kumar, A.: The Impact of a rigid-flexible system on the ride quality of passenger bogies using a flexible carbody. In: Pombo, J. (ed.) Proceedings of the Third International Conference on Railway Technology: Research, Development and Maintenance, Stirlingshire, UK, p. 87. Civil-Comp Press, 2016, Stirlingshire, UK (2016). https://doi.org/10.4203/ccp.110.87
64. EN 15663:2017 Railway applications—Vehicle reference masses (2017)
65. EN 12663-1:2010 Railway applications—structural requirements of railway vehicle bodies—Part 1: Locomotives and passenger rolling stock (and alternative method for freight wagons) (2010)

Operation and Patronage Dynamics of the Lagos Shuttle Train Services, Lagos, Nigeria

Olorunfemi Ayodeji Olojede ⓘ**, Olamide Akintifonbo** ⓘ**,**
Oluwatimilehin Gabriel Oluborode ⓘ**, Henry Afolabi** ⓘ**,**
and Folaranmi Olufisayo Akinosun ⓘ

Abstract This study examined the operation and patronage dynamics of the Lagos Shuttle Train Services, the only intra-urban rail transit in Nigeria, a country of over 200 million people. Using multistage sampling, six sets of respondents were surveyed over two survey periods—before the onset and in the wake of COVID-19. Two key-informant interviews and four sets of questionnaires were administered. Participant observation was used to complement the data obtained. The interviewees were the Head of Operations Department and a senior staff member of the Nigerian Railway Corporation (NRC). Three sets of questionnaires were administered on all the 20 engineers, 79 conductors, and 14 ticket vendors in the employ of NRC, while the fourth set of questionnaires was administered on 216 passengers selected from both the Mass Transit Trains (MTT) and the Diesel Multiple Unit (DMU) trains operated along the Lagos Shuttle Train Services' corridor. Findings revealed that the operation dynamics of the Lagos Shuttle Train Services comprise both desirable and undesirable factors that could enhance and undercut, respectively, the effectiveness of its service. On the other hand, its patronage dynamics were found to reflect the socio-economic and locational attributes as well as the aspirations and desires of passengers. The study concluded that if the operation and patronage dynamics of the Lagos Shuttle Train Services were improved on, passengers' welfare and NRC's effectiveness would be enhanced with many beneficial spin-offs. Towards this end, workable policy recommendations were proffered.

Keywords Nigerian Railway Corporation (NRC) · Lagos Shuttle Train Services · Mass Transit Train (MTT) · Diesel Multiple Unit (DMU) · Operation and patronage dynamics · Maglev

O. A. Olojede (✉) · O. G. Oluborode · H. Afolabi
Department of Urban and Regional Planning, Obafemi Awolowo University, Ile-Ife 220282, Osun, Nigeria
e-mail: olojedeo@oauife.edu.ng

O. Akintifonbo
Ministry of Housing, Physical Planning and Urban Development, Ado-Ekiti 360261, Ekiti, Nigeria

F. O. Akinosun
Department of Public Administration, Ambrose Alli University, Ekpoma 310006, Edo, Nigeria

1 Introduction

Rail transport is the most important mode of transport in developed and developing countries for both freight and passenger services [10, 34, 36]. Apart from its pronounced environmental benefits over road and air transport, it also has the capacity to carry a large number of passengers and goods safely and securely over long distances at a cheaper rate, and unaffected by traffic congestion [36, 53]. This makes it a suitable pivot of the transport system of any nation.

Rail transport has provided veritable solutions to the insufficiency in urban transport service to cope with increasing passenger demand [31]. With the introduction of new urban rail systems, metros, and light rail systems globally, railway now serves as the backbone of transit services in major cities, the reason being that it is capable of providing automobile competitive public transport service throughout sprawling cities [45, 52]. Globally, according to UIC (2015), railway accounts for about 3000 billion passenger-kilometres with India having the highest passenger travel (almost 40% of the total passengers carried).

In Nigeria, railway transportation is considered the oldest transport mode [14]. The first railway line in the country became operative in 1898, and other lines were later constructed to link the northern and southern parts of the country [27, 34]. However, it has hardly developed over the past 100-plus years compared to what obtains in developed countries, and it plays an insignificant role in urban mass transit services [33, 43]. Much attention has been given to road transport, which was initially developed to complement it, thus creating huge pressure on road transport and resulting in traffic congestion as well as underutilization of infrastructure.

Lagos, like other cities of the world, has witnessed rising transport demand and problems associated with growing population. Efforts to tackle these problems are more often than not disjointed, uncoordinated, and poor, and have not been able to solve the problems effectively. The rail transport system, which has been thought to have the potential of mitigating these problems, has not been able to solve them either. Consequently, there is the need to investigate why the Nigerian rail system has not been efficacious in solving problems similar to what rail systems in other countries have been solving. A good inlet into this is the examination of its operation and patronage dynamics.

Irrespective of the source consulted, Nigeria has a population of over 200 million people. With at least eight cities populated by millions of people, over 80 cities with a population of between 100,000 and one million people, and at least 248 urban centres that boast between 10,000 and 100,000 people in the country, according to the World Population Review [54], the Lagos Shuttle Train Services is the only functional intra-urban rail transit system. In the context of this study, its operation dynamics consist in the factors that determine or influence the nature and characteristics of rail services provided for its passengers, while its patronage dynamics are the factors that determine or influence the nature and characteristics of urban rail transit services enjoyed by its passengers. These two sets of attributes go a long way in determining the success or otherwise of any intra-urban rail transit. Against this background, this

study intends to examine the operation and patronage dynamics of the Lagos Shuttle Train Services with a view to determining its efficacy in meeting the transit need of the Metropolitan Lagos people and proffering practicable policy recommendations towards its functional revamp.

2 Literature Underpinnings

2.1 Rail Transport Operation Dynamics

As evident in the literature, some indices are important in the assessment of the operation and patronage of any transit system. These are the dynamics of rail transport operation. Arbitrarily, indices of patronage can be said to be broadly categorized into service quality and service quantity. The service quality factors include reliability, fare, safety and security of system, cleanliness, comfort, coverage, accessibility, and information system. Service quantity factors, on the other hand, include service coverage and frequency. The service coverage of a transit system is especially crucial in examining the operation of the transit system as transit is not a viable option if the service is not provided to the locations where people want to go and at the times they need to travel [20]. Also, transit service within walking distance is not necessarily considered as available if it does not meet the travel demand. Service frequency has to do with the number of scheduled transit system trip per hour. It mostly affects passengers waiting time at terminals.

Access to public transport is the distance (proximity) from passengers' trip origin to the terminal, otherwise known as the first mile distance. It is usually measured in terms of travel time. Passengers' comfort in terms of ventilation and presence of air conditioner, seat comfort, rest comforts (serenity), sanitary condition of transit system, and capacity (passenger load) of the system are important in measuring the quality of service. System safety includes safety during trip and at stations, and it indicates the efficiency and effectiveness of service. Reliability is often used to describe service punctuality, and it has to do with stick adherence to schedules. Moreover, the provision of reliable information about schedules to passengers at stations, prior to the trip (pre-trip information), and information on-board are used in assessing the operation of rail transport system.

According to Babalik [18], the operation of rail transit system is greatly influenced by such factors as government policy, urban form (spatial distribution of human activities), and funding. Government policies regulates the operation and management of transport systems, consistency in policy making and execution results in improved services; urban form determines the relative location of different activities and consequently determines the cost-effectiveness of rail transport operation. Funding is also essential as capital and enormous resources are required for transit operation. Other identified factors are the number and capacity of available vehicles (which influences service frequency and coverage), number of staff, population of the transit system

service area, and the type of vehicles (in terms of design and condition), which affects speed, reliability, availability, and consumption rates.

2.2   Rail Transport Patronage Dynamics

According to Taylor and Fink [51], rail transport patronage or ridership is the sum of the number of people using rail transport over a period of time for a given service or set of services, and it is influenced by many factors which can be classified into extrinsic (exogenous) and intrinsic factors. Exogenous factors are those that are external to the system and its management. They include population and socio-economic characteristics of passengers. Intrinsic factors, on the other hand, are factors that are associated with the system itself. They are those factors the management have control over, such as fare, services provided, and station characteristics [26]. They also include service quality and service quantity factors such as service coverage, frequency, safety, security, speed, information provision, food service, as well as comfort and reliability, among other factors. Another important factor influencing the patronage of transit system is availability or proximity. Also, people who live or work close to a transit station tend to patronize the transit system. Hour of service or schedule of any transit system also makes it attractive to passengers [21].

In line with the findings of Armbruster [16], Eric [22], Taylor and Fink [51], and Taylor [50], the dynamics of rail transit patronage include passengers' socio-economic characteristics such as income, employment status, household size, and car ownership. These are in addition to employment status which influences the number of trips made using the transit system. Moreover, increase in car ownership often results in decrease in-transit patronage. Gender is also a crucial factor as it has been found that men are most likely to travel than women.

Furthermore, the population of cities with a transit system influences its patronage: the larger the population of an area, the higher the patronage of the transit system. Higher population density depicts more potential passengers using the transit system for their travel. Other external factors that are ordinarily beyond the control of policy makers include topography and weather [26]. In addition, the availability of other modes of transport leads to competition among the modes, thereby affecting the patronage level of transit system.

Funding is another influencing factor. The level of funding for transit subsidies greatly influences transit patronage [51]. Generally, government-owned public transit systems tend to be adequately funded with cheaper fares, thus attracting higher patronage levels. Transit agencies can influence patronage through service adjustment and reduction of fare rate. All things being equal, a decrease in fare can result in an increase in patronage.

2.3   Rail Transport Operation and Patronage in Nigeria

Rail system in Nigeria is operated by the Nigeria Railway Corporation (NRC), a public enterprise. The corporation renders both passenger and cargo services; however, it is used mainly for passenger services. As observed by Ademiluyi [1], of all transport modes commonly used in Nigeria, the rail subsector remains the relatively most neglected in terms of investment and transformation. It has been static and highly unresponsive to changing technology and innovations [5]. This near-stagnation in rail expansion has not allowed rail network to link major cities or major growth points that have since emerged [14]. Therefore, railway system in Nigeria, when compared with those in developed countries of the world, plays an insignificant role in urban mass transit and transportation. In Nigeria, rail transport accounts for one per cent of land transportation. The highest number of passengers carried (over 4 million) was recorded in 2014. Consequently, the total revenue generated from both passenger and freight service in the year was record highest. In 2015, however, the number plummeted drastically.

Many factors have been identified as contributing to the decline or rail transport patronage in Nigeria. According to Oni and Okanlawon (2011), the collapse of the agrarian economy is one of these factors as it led to low output of agricultural produce, necessitating redundancy in the existing rail facilities owing to underutilization of capacity. Another factor is the dilapidated nature of the present railway infrastructure, caused by years of neglect by successive governments. Other factors inhibiting the performance of the railway system include high cost of operation and maintenance, inadequate funding and huge operating losses, full government ownership, corruption and weak management, static and poor response to emerging needs, and loss of patronage to the road transport sector [14, 32].

2.4   Empirical Studies on Rail Transport Operation and Patronage

Many studies have been conducted on the operation and patronage of rail transport across the globe [5, 25, 44, 47]. Agunloye and Ilechukwu [5] examined the travel pattern and socio-economic characteristics of rail transport passengers in Lagos Metropolis, Nigeria. Their findings revealed that most passengers were low-income earners who engaged in work-related trips and who depended heavily on train than any other mode. Age, income, travel cost, and travel purpose influenced their trip frequency. Nathanail [30], Basorun and Rotowa [19], Adeyinka [2], as well as Obasanjo and Francis [31] assessed the quality of rail transport service. Their studies suggested that train personnel behaviour is an important factor in measuring service quality. These studies came up with important findings that aid our understanding of rail transport operation, however, the major emphasis of their scope was beyond rail transport operations.

Studies that assessed rail transport operation and patronage include Ibidapo-Obe and Ogunwolu [24] and Olayiwola et al. [35]. These studies examined level of service, management, passengers' volume, traffic (trip) characteristics, and operational efficiency. In addition, Agunloye and Oduwaye [6] identified factors such as arrival time, weekly trip frequencies, cleanliness of train, and smoothness of ride. The findings of these studies revealed poor condition of rail service, insufficient locomotive stock, overcrowding of passenger coaches in peak period, and operational delay, among others. The implications of the findings were also well articulated. However, the dynamics of the identified factors were not emphasized.

Arguably, a general dearth of studies holistically examining both the operation and patronage dynamics of rail transport in Nigeria has been observed. This study is an attempt to fill part of this gap. It assesses these dynamics with a specific reference to the Lagos Shuttle Train Services which happens to be the only transit system that provides a metropolitan rail transit service in Nigeria.

3 Methodology

3.1 Study Area

The study area is Lagos State, the former capital of Nigeria. It is located in southwest Nigeria and lies between Latitude 6° 22′ and 6° 52′ North of the Equator and with a longitudinal stretch of between 2° 42′ and 3° 42′ East of the Greenwich Meridian (Fig. 1). The state's southern boundary is formed by about 180 kms of Atlantic coastline, while the western boundary is formed by the Republic of Benin. The northern and eastern boundaries are framed by Ogun State. The state occupies an area of 3577 km^2, and it is the smallest state in Nigeria in terms of land area despite being the most densely populated with an estimated population of 14 million people. Lagos State is considered the economic capital as well as the financial and commercial nerve centre of Nigeria. This is because it accounts for 65% of the country's commercial activities, 33.5% of its industrial establishment, and 45% of its skilled manpower [7, 12, 43, 46].

Lagos is the only city in Nigeria where all transport modes—air, water, road, and rail—are well represented. It is a major intra- and intercity travel generation and attraction area in Nigeria. The roads in the state are frequently congested with over one million vehicles plying it on a daily basis [15]. The traffic in the state is characterized by heavy congestion, pollution, accident, breakdown of transport infrastructure, and other negative externalities.

The Lagos Railway started under the management of the Lagos Government Railway. It continued under the Government Department of Railways on 3 October 1912 with the amalgamation of the Lagos Government Railway and the Baro-Kano Railway which brought about a nationwide rail service. With the passing of the
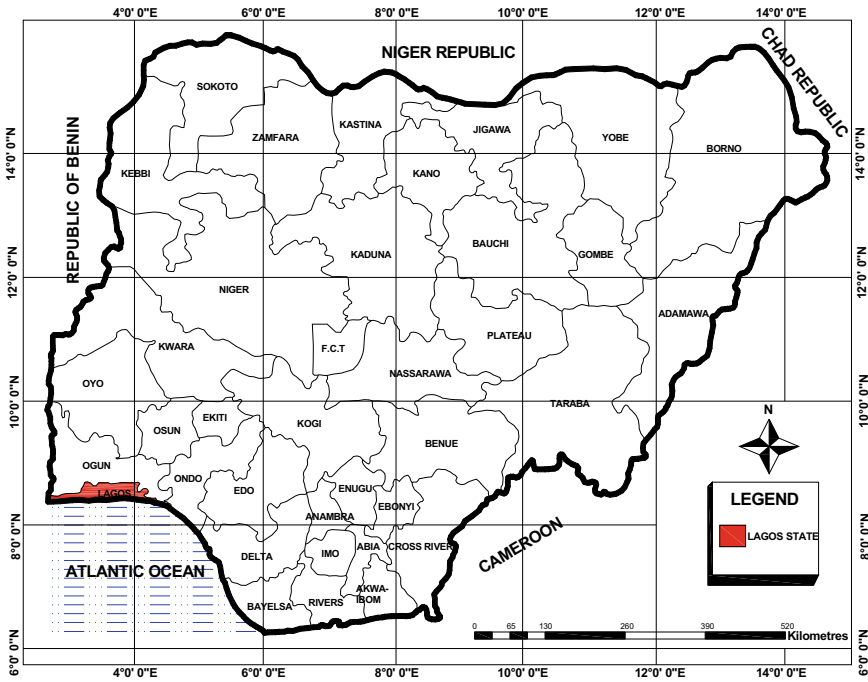
Fig. 1 Map of Nigeria indicating Lagos State. *Source* National Airspace Research and Development Agency (NASRDA, 2012)

Nigerian Railway Corporation Act of 1955, as amended in the Laws of the Federation of Nigeria 1990, the name Government Department of Railways changed to the Nigerian Railway Corporation (NRC), the current name by which the corporation is known [17, 49]. The Lagos Urban Rail Transit Service was launched in 1989 with the assistance of Federal Urban Mass Transit Programme using existing infrastructure, coaches, and locomotives of NRC. This led to the dualization of a 16-km track, creation of link between rail and ferry services, and provision of suburban rail services. The suburban trains were later converted for long express train services because the coaches were not suitable for urban transport services [10].

The rail line in Lagos State provides both long-distance travel rail services and intercity shuttle services for both passenger and freight transport [43]. The intercity shuttle services runs from Iddo terminus to Ijoko/Kajawla in Ogun State, while the long-distance travel rail services link the southern part of the country with the North. In 1992, the Lagos State government under lease-type agreement with NRC launched the Jubilee Rail Service to improve rail commuter service. In 2001, the Lagos Shuttle services started operation as Lagos Metropolitan Mass Transit Train Service with its terminus at Iddo and covering about 26 kms [24]. The shuttle services involve the movement of passengers from Iddo to Ijoko and sometimes to Kajawla at cheaper rates.

At inception, the NRC of Lagos District operated only a Mass Transit Train (MTT) daily to convey passengers and goods from Iddo to Ifo Junction, Ifo to Idogo, and from Ebute Metta to Apapa [11]. Later, the service was extended to Ijoko, and passengers are only conveyed from Iddo terminus to Ijoko in the afternoon [35]. However, it has extended its passenger services to Kajawla, and at present, NRC operates an average of 10 MTTs daily. In 2014, three Diesel Multiple Unit (DMU) trains were provided to improve the rail transport system (Premium Times, 2014). The rail line falls within the Lagos Megacity region (Fig. 2). Iddo is within Lagos Mainland Local Government of Lagos State, while Ijoko is in Ado-Odo/Ota Local Government Area of Ogun State.

The rail system between Ido and Ijoko/Kajawla comprises 14 train stations out of which four stations are in Ogun State and ten are in Lagos State. The four stations in Ogun State are Kajawla (KA), Ijoko (JK), Itoki (IT), and Agbado (GD). While the ten stations in Lagos State are Iju Junction (IJ), Agege (GE), Ikeja (IK), Shogunle (SG), Oshodi (SH), Mushin (MU), Yaba (YA), Ebute Metta (EB), Ebute Metta Junction (EGJ), and Ido Terminus (DD) (NRC, 2016). These stations are all stopping points for the transit service and are principally used for loading and unloading of goods and passengers. Some of these stations, such as Agege, Oshodi, Mushin, Ebute Metta junction, and the Ido terminus have multiple-track facilities for coach attachment and detachment [24].

The MTT is generally considered as the economy train because of its cheaper fare charges, the number of coaches hauled, and the seating capacity, while the DMU is considered as a first-class train because of the availability of air condition (A/C) in coaches, small number of coaches hauled, and reduced seating capacity which makes it more expensive. The rail service operates from Monday through Saturday
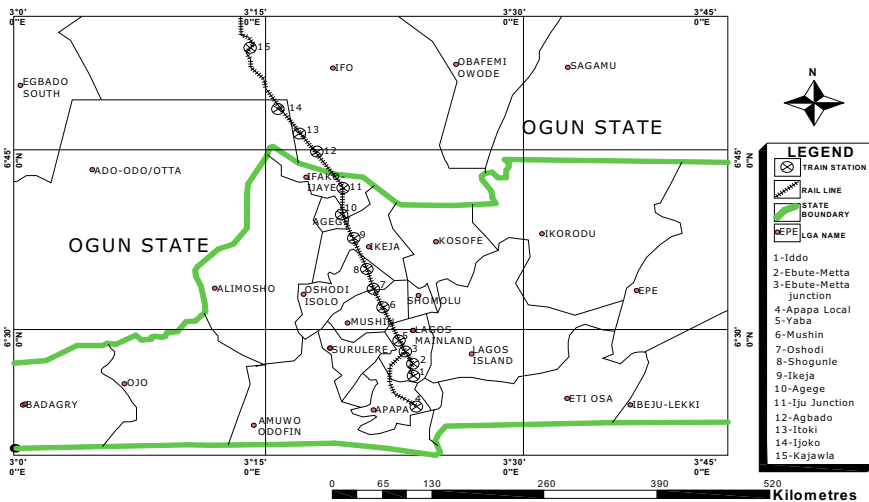
Fig. 2 Rail network map of Lagos Shuttle Train. *Source* Nigerian Railway Corporation (NRC, 2016)

and runs three shifts: the morning shift (6 a.m. to 2 p.m.), the afternoon shift (2 p.m. to 10 p.m.), and the night shift (10 p.m. to 6 a.m.). Until September 2020, the fare charged per trip either way regardless of the boarding station was N230 for MTT. N300 was charged for DMU during off-peak period and N750 during peak period. The peak period is in the morning (6:00 a.m. to 12:59 p.m.) and evening (4:01 p.m. to 9:00 p.m.), while the off-peak period was in the afternoon (1 p.m. to 4 p.m.).

It is on record that there was an increase in the number of passengers carried by MTT from 2010 to 2013. The passenger traffic flow was at its peak in 2013, with almost 4 million passengers. However, the volume of passengers carried has begun to dwindle in a consistent manner since then. This may be attributed to the introduction of the DMU train in 2014 which attracted so many passengers because of its added executive features such as air conditioner, posh physical appearance, and high speed. However, the highest number of trips was made by MTT in 2014 with attendant decrease in the number of passengers carried [43].

In the wake of the COVID-19 pandemic, the first case of which was recorded in Lagos, Nigeria, in February 2020, and following a global restriction and ban on transportation, the management of NRC suspended its operations for 25 weeks from Monday, 23 March to Monday, 14 September 2020. The expedient measure was taken to curtail the spread of the pandemic as it is generally acceptable to both common knowledge and scientific analyses that transportation aids the spread of infectious diseases and pandemics [28, 42, 55, 56].

3.2 Sampling Procedure

The primary data for this study were collected over two different periods. The first survey was before the onset of COVID-19 pandemic (pre-suspension survey), while the second survey was executed after the resumption of train services (post-resumption survey). Six sets of respondents were sampled: five in the pre-suspension survey and one in the post-resumption survey. In the pre-suspension survey, the respondents were the head of Operations Department, engineers, conductors, ticket vendors, and a set of passengers (for questionnaire administration). In the post-resumption survey, the respondent was a senior staff member (who granted a key-informant interview under the condition of anonymity). Participant observation was used to complement both surveys.

Baseline information obtained from NRC and preliminary investigation prior to the pre-suspension survey revealed that there were 20 engineers, 79 conductors, and 14 ticket vendors. They were all selected for questionnaire administration. The sampling of passengers began with the identification and selection of stations in the Lagos Shuttle Train Services corridor. There were 14 stations in the study area and every train took off from the Iddo terminus, with an average of ten trains taking off daily. There were three DMU trains and seven MTT trains along the corridor. One DMU train operated at each hour of service; two MTT trains operated in the morning

Table 1 Schedule for each train type

Train type	Scheduled hour of service		
	Morning	Afternoon	Evening
DMU (three trains)	1	1	1
MTT (seven trains)	2	2	3

Table 2 Coaches and number of passengers sampled

Train type	Seating capacity	No. of trains	Ave. no. of coaches	Total no. of coaches	Coaches selected	Total no. of passenger	Selected passengers (10%)
DMU	72	3	3	9	5	360	36
MTT	90	4	10	40	20	1800	180
Total	162	7	13	49	25	2160	216

and afternoon service hours, while the remaining three operated in the evening hour of service (Table 1).

Both train types were stratified by hour of service (or shift), and 50% of each train type operating in each shift were sampled. Thus, all the three DMU trains were sampled (50% of 1 being 0.5 or approximately 1), one for each shift. For the MTT, one train each was sampled (50% of 2 being 1) for the morning and afternoon shifts, while two trains were sampled in the evening shift (50% of 3 being 1.5 or approximately 2). Thus, in all, three DMU and four MTT trains were sampled (Table 2).

Each selected train was stratified according to the number of coaches hauled. The DMU hauled an average of three coaches, while the MTT hauled an average of ten coaches. In each train selected, 50% of the coaches were sampled. For the five coaches of the DMU sampled, two were selected for each of the morning and afternoon shifts, while one was selected for the evening shift. For the 20 coaches of the MTT sampled, five were selected for each of the morning and afternoon shifts, while ten were selected for the evening shift. The capacity of the DMU was 72, while that of the MTT was 90. Thus, the total number of passengers in the selected coaches was 360 for the DMU and 1800 for the MTT. A tenth (10%) of these passengers were then sampled using the judgemental sampling technique. In all, 216 passengers were sampled. The summary of the sampling process is presented in Table 2.

3.3   Survey Instruments

As earlier stated, the data used for this study were collected in two batches. The pre-suspension data were collected with the aid of structured interview and questionnaire, complemented with participant observation. Structured interview was conducted on the head of Operations Department of NRC, while different sets of questionnaires

were administered on the engineers, conductors, ticket vendors, and passengers. In the post-resumption survey, the head of Operations Department of NRC was not available. Therefore, a senior staff member of the corporation was interviewed based on availability and willingness given the condition of anonymity. In addition, a cross section of passengers was interviewed in the post-resumption survey. Participant observation was also used to complement the data collected. The goal for the post-resumption survey was to determine the effect of the COVID-19 pandemic on the operation and patronage dynamics of the Lagos Shuttle Train Services.

3.4 Data Analysis

The quantitative data obtained were analysed using cross-tabulation, frequency distribution, percentages, and Respondent Agreement Indices (RAI), while the qualitative data were analysed using content analysis. For the RAI, respondents were asked to rate their level of agreement with factors influencing patronage using a five-point Likert scale (1 = Strongly Disagree, 2 = Disagree, 3 = Undecided, 4 = Agree, and 5 = Strongly Agree). The designated values of 1, through 5, were used to allot weight to the options from Strongly Disagree through Strongly Agree, respectively. The weight value (WV) for each criterion is expressed as

$$WV = F_i V_i \tag{1}$$

where F_i was the frequency of response for variable i, V_i was the weight attached to responses on variable i, and i was the designated value of the Likert point response under consideration. The sum of weighted value (SWV) for each variable was obtained by summing up the product of the number of responses of each rating for a variable, and the respective weight of the value is expressed as

$$SWV = \sum_{i=0}^{5} F_i V_i, \tag{2}$$

where SWV was the total weight value, F_i is the frequency of respondents rating for variable i, V_i was the weight attached to variable i, and i was the designated value of the Likert point response under consideration. The mean index for each variable was obtained by dividing the SWV of each variable by the total number of respondents ($N = 183$). This was then computed as the RAI which is expressed as

$$RAI = \frac{SWV = \sum_{i=0}^{5} F_i V_i}{N}. \tag{3}$$

Similar uses of agreement indices abound in scientific literature [3, 4, 8–10, 37–40, 48].

4 Results and Discussion of Findings

4.1 Profiles of Operators of Lagos Shuttle Train

According to Basorun and Rotowa [19] and Adeyinka [2], there is a correlation between the profile of operators and service quality. In line with this, some socio-economic attributes of operators of the Lagos Shuttle Train were examined. These were gender, age, educational status, income, and work experience in the corporation. Summarized in Table 3 are the attributes of these operators.

It was found that most of the operators were male. Specifically, all the engineers and most of the conductors were male, while a larger proportion of the ticket vendors were females. This is a true reflection of what typically obtains in Nigeria where most technical jobs are an exclusive reserve of the male gender.

Most of the operators were in the active/productive age (under 40). However, this is untrue of the engineers the majority of whom were at least 40 years old. The most likely reason for this is that their job requires a long formal training and cognate

Table 3 Profile of operators

Attribute	Engineers		Ticket vendors		Conductors	
	Frequency	%	Frequency	%	Frequency	%
Gender						
Male	20	100	6	42.9	74	93.7
Female	0	0	8	57.1	5	6.3
Age						
< 30	–	–	2	14.3	14	17.7
30–40	3	15.0	11	78.6	55	69.6
40–50	11	55.0	1	7.1	10	12.7
> 50	6	30.0	–	–	–	–
Education						
Senior/technical	11	55.0	4	28.6	60	75.9
Tertiary	9	45.0	10	71.4	19	24.1
Monthly income (in ₦)						
30,000–40,000	–	–	4	28.6	39	49.4
41,000–50,000	20	100	10	71.4	40	50.6
Work experience (years)						
< 6	–	–	3	21.5	10	12.7
6–10	–	–	11	78.5	51	64.5
10–20	15	75	–	–	18	22.8
> 20	5	25	–	–	–	–

experience. Besides, they possess personal fitness qualities that cannot be compromised, stamina and clear vision, for example. Thus, they are not easily replaceable unlike the conductors and ticket vendors who can be replaced in a matter of days.

Generally, the operators are poorly paid given the cost of living in Nigeria. A monthly income of at most N50,000 is not in any way commensurate with the level of education, formal training, and cognate experience required for operating trains, especially of those who are engineers. A cursory look at the profile of the engineers shows that they were sufficiently experienced with none of them having less than 10 years' work experience in the corporation. Further analysis reveals that all the engineers could operate both the MTT and DMU train types. Also, none of them had less than two years of formal training.

4.2 Socio-economic Characteristics of Passengers

The socio-economic characteristics considered relevant in this study were those that were generally deemed as strong predictors of transit patronage in such previous studies as Alam et al. [13], Armbruster [16], Eric [22], Litman [29], Taylor [50], and Taylor and Fink [51]. In this study, these socio-economic characteristics were analysed using descriptive statistics (Table 4). Findings revealed a near-balanced proportional representation of both genders among the respondents. The distribution of the marital status, education, occupation, and age of the respondents were also not unexpected considering the generally obtainable demographic patterns and trends in the country.

Further analysis reveals that there were significant variations in the socio-economic characteristics of passengers that took the two train types, especially in socio-economic characteristics that relate to standards of living. For instance, most of the respondents in the MTT (79.4%) were middle-income earners. This is also reflected by their private vehicle ownership status that strongly suggests that most (77.8%) of them were captive riders (people who must take public transport because they do not have their own personal vehicles). These findings corroborate the earlier submissions of Agunloye and Ilechukwu [5]. Moreover, considering the household size distribution of the respondents, it is deducible that passengers of the DMU generally had a desirable occupancy ratio.

4.3 Operation and Patronage Dynamics

Operation and patronage attributes constitute a key indicator of quality of service and patronage of a transport system [5, 23, 44]. More importantly, they are what informs the dynamics of a transport system. Consequently, the operators were asked for information on how they carried out their services as well as the underlying influences or motivating factors that constituted the operation dynamics.

Table 4 Profile of passengers

Attribute	Train type		Total
	MTT	DMU	
Gender			
Male	96 (53.3%)	25 (68.8%)	121 (56.0%)
Female	84 (46.7%)	11 (31.2%)	95 (44.0%)
Marital Status			
Single	27 (15.0%)	8 (22.2%)	35 (16.2%)
Married	146 (81.1%)	25 (69.5%)	171 (79.2%)
Divorced/widowed	7 (3.9%)	3 (8.3%)	10 (4.6%)
Education			
None	8 (4.4%)	0 (0%)	8 (3.7%)
Primary/adult	5 (2.7%)	1 (2.8%)	6 (2.8%)
Secondary	61 (33.9%)	8 (22.2%)	69 (31.9%)
Post-secondary	98 (54.4%)	18 (50.0%)	116 (53.7%)
Postgraduate	8 (4.4%)	9 (25.0%)	17 (7.9%)
Occupation			
Schooling	19 (10.6%)	2 (5.6%)	21 (9.7%)
Business	28 (15.6%)	1 (2.6%)	29 (13.4%)
Private sector	68 (37.8%)	29 (80.6%)	97 (44.9%)
Public sector	65 (36.0%)	2 (5.6%)	67 (31.0%)
Retired	0 (0.0%)	2 (5.6%)	2 (0.9%)
Age			
< 18	4 (2.2%)	0 (0.0%)	4 (1.9%)
18–30	36 (20.0%)	5 (12.5%)	41 (19.0%)
31–60	131 (72.8%)	30 (85.4%)	161 (74.5%)
> 60	9 (5.0%)	1 (2.1%)	10 (4.6%)
Household size			
< 4	31 (17.2%)	12 (33.3%)	43 (19.9%)
4–6	132 (73.3%)	24 (66.7%)	156 (72.2%)
> 6	17 (9.5%)	0 (0.0%)	17 (7.9%)
Vehicle ownership			
Yes	40 (22.2%)	23 (63.9%)	63 (29.2%)
No	140 (77.8%)	13 (36.1%)	153 (70.8%)
Vehicle type			
Motorcycle	2 (5.0%)	1 (4.3%)	3 (4.8%)
Car	34 (85.0%)	20 (87.0%)	54 (85.7%)
Minibus/Bus	4 (10.0%)	2 (8.7%)	6 (9.5%)
Monthly income			

Table 4 (continued)

Attribute	Train type		Total
	MTT	DMU	
≤ ₦20,000	4 (2.2%)	1 (2.8%)	5 (2.3%)
₦20,001–₦70,000	143 (79.4%)	2 (5.6%)	145 (67.1%)
> ₦70,000	33 (18.3%)	33 (91.7%)	66 (30.6%)

Operation Dynamics. Findings on the operation dynamics of the Lagos Shuttle Train Services reveal that most of the engineers (80.0%) operated on the Iddo–Ijoko route, while the rest operated on the Iddo–Kajawla route. It was also found that the DMU trains operated only on weekdays, while the MTT operated from Monday through Saturday. This implies that the DMU did not provide any passenger service on weekends and neither of the train types operated on Sundays. Further, the minimum and mean time spent by engineers on both coach attachment and detachment was 2 min and 5.8 min, respectively, while the maximum time was 10 min (with a standard deviation of 2.2). However, this only applies to the MTT as the DMU train only hauls three coaches and has an engine at each end.

The mean dwelling time (time spent by a train in station for boarding and deboarding of passengers) ranged from 2 to 10 min with a mean value of approximately 5 min and standard deviation of 2.9. With 14 stations along the corridor, it is implied that the total dwelling time for passengers travelling the entire corridor would be at least an hour. This simply translates to increased travel time. Meanwhile, the trains are run at low speeds of between 35 and 40 kms per hour. The engineers identified nine different reasons for the low speeds. These are presented in Table 5.

Further analysis reveals that 15 (75.0%) of the engineers had experienced their trains breaking down during operation. Following each breakdown experienced, the response of the engineer was to either rectify the fault (46.2%) or call for another locomotive (53.8%). Incidentally, all the 20 engineers had had an accident with the trains. In terms of severity, a loss of life was recorded in three (15.0%) of the

Table 5 Causes of low speeds of trains

Cause	Frequency	(%)	Rating
Poor condition of route	18	90	First
Trading on railway	2	10	Eighth
Intercession with roads	6	30	Sixth
Railway gauge	15	75	Third
Poor condition of train	18	90	First
Poor condition of locomotive	15	75	Third
Crossing of other trains	13	65	Fifth
Brake inefficiency	3	15	Seventh
Weather condition	1	5	Ninth

accidents in which the engineers were involved. According to the head of Operations Department:

> The train is very safe. The rate of accidents is low. The maximum number of accidents that occur in a year is five, and there is hardly any casualty. These accidents are minor ones.

On issues pertaining to safety, four (20.0%) of the engineers admitted that they used their mobile phones during operation. Also, 18 (90.0%) of the engineers admitted to overloading the train. While this might indicate inadequate rolling stock, it was an action that had implications for the comfort, convenience, and safety of passengers. Nevertheless, the servicing of the trains was prioritized. The head of Operations Department submitted as follows:

> The trains are serviced…on a daily basis, except on weekends, to ensure proper functioning of the train. Also, the track is inspected and serviced daily by the gangers for safety reasons. The gangers check the tracks every morning…to check for any loosening…The gangers notify the engineer about any fault observed on the track for quick repairs.

He stated further thus

> The safety of passengers, goods and trains are considered germane by NRC…the management services the rail daily and also has a logbook that is to be filled up by engineers after every trip. This is done so that the corporation could be aware of the condition of the trains, what happened during the trip, and how safe the trains are to passengers.

Further on safety, findings reveal that series of tests were carried out on the engineers. According to the head of Operations Department:

> …the engineers are tested by the medical team of the corporation to ensure their fitness to drive the train. The tests include the eye/visual test, alcohol test, physical standard test, and mental test. These tests are conducted periodically. For instance, the alcohol test is carried out on the engineer after every accident to ensure that the engineer was not driving under the influence of alcohol. The eye visual test and physical standard test are carried out monthly, while mental test is carried out yearly.

Contrary to the claims of the head of Operations Department, ten (50.0%) of the engineers reported that they had never been subjected to any physical standard test or mental test. In addition, 14 (70.0%) of the engineers claimed they had never been tested on alcohol level. However, most (70.0%) of them reported that the eye/visual standard test was carried out on them annually. The remaining six engineers (30.0%) claimed that the eye/visual standard test, physical standard test, mental test, and alcohol test were all carried out on them monthly by the NRC medical team. A similar trend was found on the reassessment of the engineers. According to the head of Operations Department, the engineers were periodically reassessed on a quarterly basis at the headquarters of the Lagos District of NRC in addition to weekly training aimed at improving their skills. Conversely, 14 (70.0%) of the engineers claimed that they were reassessed weekly, while the remaining six (30.0%) claimed they were reassessed monthly. With all the claims, counterclaims, and discrepancies, it is difficult to ascertain that all the necessary tests on and reassessment of the engineers were conducted as and when due.

Ticket racketeering constituted another operation issue along the Lagos Shuttle Train Services corridor. This was duly acknowledged by both the management and staff of NRC. Some people bought tickets in bulk just for the purpose of reselling them at a higher price outside the corporation. Actions taken towards curbing this illegality were instructing ticket vendors not to sell more than a ticket to a passenger, appending authorized signature on tickets, selling of tickets only 10 min before the departure time, and the self-production of tickets to guard against the printing of fake tickets. It was the duty of the conductors to verify and validate all tickets used in boarding the trains. Specifically, they checked the date, amount, emblem, train type, design and colour, and series on all tickets. Validation took no more than 5 s, and it was done both at the point of boarding and en route. Despite all the safeguards, rooftop riding, ticket transferring, and passengers alighting before validation were all perpetrated by some unscrupulous passengers. Apprehended stowaways were usually forcefully required to buy the ticket at double the price or charged to court. Rooftop riders arrested with the help of police were also charged to court.

COVID-19 Pandemic. Following the resumption of the shuttle train services after the 25-week COVID-19-induced suspension of operations, a set of non-pharmaceutical protocols were imposed including the compulsory wearing of face-masks and physical distancing which brought about a reduction in the carrying capacity of the trains. Consequently, all fares were increased by 100 per cent. For instance, MTTS started charging N460 flat per trip, and the trains no longer stop at some stations. Before COVID-19, fares between Iddo in Lagos and Ijoko/Kajola in Ogun were N230 per trip. In the new regime, trains originating from Ijoko only stopped at Ebute Metta Junction and Iddo stations. The return trains originating from Iddo terminated at Ijoko only. The MTT train left Ijoko by 0630 and Iddo by 1730.

In strict adherence to NCDC's guidelines for public engagement, no passenger was allowed to board the train without a facemask and hand sanitizer. This was in addition to the measures the NRC management has taken to ensure proper social distancing while boarding and on-board the MTTS. In addition to strict social distancing measures on-board the MTT, seats marked 'X' were not to be sat on. Standing or hanging on the train was no longer tolerated with provision that defaulters of the laid down rules would be prosecuted. Before the new rule, trains originating from Iddo usually stopped in various railway stations, including Ebute Metta, Yaba, Mushin, Oshodi, Sogunle, Agege, Iju, Agbado, Itoki, Opo Suuru, and Ijoko before terminating at Kajola.

Another measure NRC put in place was the sensitization and awareness campaign against COVID-19 among its staff and those residing in railway compound in Lagos after the suspension. Acknowledging the imperativeness of observing the non-pharmaceutical protocols of COVID-19, all the staff and residents were mandated to use facemasks and adhere strictly to social distancing directive as well as personal and environmental hygiene to prevent the pandemic from spreading. All staff were directed to comply with the precautionary protocols outlined by the Federal Ministry of Health and the Nigeria Centre for Diseases Control. The campaign was carried out in all the districts of the corporation. It also became compulsory for all passengers and other categories of NRC facilities to cooperate with NRC frontline staff

who subjected them to body temperature measurement at the entry points of the corporation's facilities. The management also decontaminated offices, workshops, residential quarters, and train stations to curb the spread of the virus.

According to a senior staff member of NRC, train passengers were complying with COVID-19 protocols. The NRC management ensured that all passengers and employees of the corporation adhered to COVID-19 protocols. Passengers were aware of the 'No nose mask no boarding' policy. Safety was prioritized over turnover before and after boarding. That some people did not believe in COVID-19 notwithstanding, it was the duty of NRC workers to ensure that rules were rules and that they must be enforced. Passengers were reported and seen to be complying. Moreover, soaps and hand sanitizers were provided in the train for the use of passengers. Thus, there was no excuse for any passenger to not comply.

Patronage Dynamics. With a view to uncovering the patronage dynamics of the Lagos Shuttle Train Services, passengers were asked to state the underlying factors that informed or affected their patronage. Patronage attributes deemed most relevant to this study are summarized in Table 6.

According to Table 6, findings on the patronage attributes of Lagos Shuttle Train Services passengers revealed that most of the respondents (80.6%) were commuters who accounted for 82.8% and 69.4% of the respondents in MTT and DMU trains, respectively. It was also found that the largest proportion of the passengers took the trains over the five weekdays. This implies that the respondents were frequent riders who likely heavily depended on the trains for non-discretionary commuting. Another pointer to this is that a total of 72.2% of the passengers took the trains twice daily. These were most likely their morning and evening commutes.

Another important finding based on Table 6 is that over 73% of the passengers lived within 500-m radius of their take-off station. Thus, the relative shortness of their first mile distance (the distance they had to cover to get to the rail transit station) was likely a strong factor in their commuting mode choice. Strengthening this inference is the finding that a significant overall proportion (30.6%) of the passengers chose walking as their first mile mode. Another 22.2% chose public transport as a first mile mode choice. It then follows that a total of 52.8% of the passengers chose active transport modes for their first mile travel. A similar situation was also obtained for the last mile mode. This is a good index for transport decarbonization which advocates the promotion of active transport modes [41].

An important attribute of the MDU is also revealed in the analysis. None of the passengers on that train experienced the presence of illegal passengers. This contrasts with the MTT where an overwhelming majority (98.9%) of the passengers noticed the presence of illegal passengers. This could be linked to design and executive nature of the DMU train which probably made it unattractive to undesirable co-travellers.

Generally, it is deducible that most of the passengers would choose the trains over any other mode. This is as revealed by the existence of alternative modes by which the passengers could commute. Only the Bus Rapid System (BRT) accounted for as high as 52.8% of all the alternative modes with the minibus coming second at a distance. Together, these two modes accounted for 83.4% of all the alternative

Table 6 Patronage attributes of the Lagos Shuttle Train Services

Attribute	Train type		Total
	MTT	DMU	
Trip frequency (no. of days per week)			
1	18 (10.0%)	5 (13.9%)	23 (10.6%)
2	12 (6.7%)	2 (5.6%)	14 (6.5%)
3	15 (8.3%)	7 (19.4%)	22 (10.2%)
4	17 (9.4%)	1 (2.8%)	18 (8.3%)
5	93 (51.7%)	21 (58.3%)	114 (52.8%)
6	25 (13.9%)	0 (0.0%)	25 (11.6%)
Trip purpose			
Work	149 (82.8%)	25 (69.4%)	174 (80.6%)
Leisure	4 (2.2%)	1 (2.8%)	5 (2.3%)
Medical	2 (1.1%)	1 (2.8%)	3 (1.4%)
Educational	10 (5.6%)	1 (2.8%)	11 (5.1%)
Shopping	8 (4.4%)	5 (13.9%)	13 (6.0%)
Other	7 (3.9%)	3 (8.3%)	10 (4.6%)
First mile distance			
< 300 m	34 (18.9%)	5 (13.9%)	39 (18.1%)
300–500 m	93 (51.7%)	26 (72.2%)	119 (55.1%)
501–1000 m	36 (20.0%)	3 (8.3%)	39 (18.1%)
> 1000 m	17 (9.4%)	2 (5.6%)	19 (8.8%)
First mile mode			
Walking	61 (33.9%)	5 (13.9%)	66 (30.6%)
Motorcycle	57 (31.7%)	2 (5.6%)	59 (27.3%)
Car	21 (11.7%)	13 (36.1%)	34 (15.7%)
Public transport	33 (18.3%)	15 (41.7%)	48 (22.2%)
Other	8 (4.4%)	1 (2.8%)	9 (4.2%)
Daily trip frequency			
1	45 (25.0%)	15 (41.7%)	60 (27.8%)
2	135 (75.0%)	21 (58.3%)	156 (72.2%)
Awareness of illegal passengers			
Yes	178 (98.9%)	0 (0.0%)	178 (82.4%)
No	2 (1.1%)	36 (100.0%)	38 (17.6%)
Alternative mode			
Car	10 (5.6%)	8 (22.2%)	18 (8.3%)
Taxi	2 (1.1%)	4 (11.1%)	6 (2.8%)
BRT	102 (56.7%)	12 (33.3%)	114 (52.8%)
Minibus	61 (33.9%)	5 (13.9%)	66 (30.6%)

Table 6 (continued)

Attribute	Train type		Total
	MTT	DMU	
Official vehicle	1 (0.6%)	0 (0.0%)	1 (0.5%)
Motorcycle	1 (0.6%)	5 (13.9%)	6 (2.8%)
Other	3 (1.7%)	2 (5.6%)	5 (2.3)
Last mile mode			
Walking	77 (42.8%)	13 (36.1%)	90 (41.7%)
Motorcycle	46 (25.6%)	9 (25.0%)	55 (25.5%)
Car	14 (7.8%)	2 (5.6%)	16 (7.4%)
Public transport	39 (21.7%)	8 (22.2%)	47 (21.8%)
Other	4 (2.2%)	4 (11.1%)	8 (3.7%)

modes. This finding is important as it shows that the railway is a mode of choice among commuters in the study area.

Further, responses were asked to identify factors that most likely influenced their patronage of the Lagos Shuttle Train Services. From extant literature, these factors include service frequency, accessibility, availability of alternative mode, cleanliness, speed, and staff behaviour, among other factors [29, 51]. According to the assessment of the respondents, measured psychometrically, the most prominent factors influencing their patronage were proximity or closeness of station to other mode terminals (4.07) and ease of access to the train station (4.03). Next to these were closeness of station to the point of destination (3.99), closeness of station to the point of origin (3.85), and the rail type (3.60). Closeness of station to other mode terminals ranked the highest (4.05) for the MTT, while ease of access to station (4.40) ranked the highest for the DMU.

Moreover, MTT passengers strongly disagreed that such features as extra services offered, availability of air conditioner in coaches, travel time, less crowdedness, provision of safety equipment, condition of coaches, provision of schedule of information, ease of purchasing tickets, provision of on-board safety information, and ventilation of coaches were among factors influencing their patronage. On the other hand, the DMU passengers strongly disagreed that factors such as operation on weekends, extra services offered, capacity, availability of toilet in coaches, alternative mode unavailability, punctuality, and provision of on-board safety instruction influenced their patronage.

5 Summary, Conclusion, and Recommendations

It was found by this study that time wastage, low speeds, delays, in-transit breakdowns, unsafety, overloading, as well as illegal activities and passage punctured the effectiveness and desirability of the Lagos Shuttle Train Services. Nevertheless, the service featured several desirable attributes including competence on the part

of the engineers, proactivity on the part of the management as regards some unacceptable behaviours among undesirable co-travellers, and the pandemic-responsive stance taken by the management which in turn is capable of promoting responsible transport. These constitute the operation dynamics of the Lagos Shuttle Train Services.

Concerning the patronage dynamics of the Lagos Shuttle Train Services, it was found that most of the passengers were commuters who took the trains twice daily over the five weekdays, most likely for their morning and evening commutes. Also, most of passengers enjoyed relative proximity to the station which implies a good index for transport decarbonization. Moreover, income was found to be an important determinant of a passenger's experience in transit, especially in relation to comfort and convenience. Generally, it is shown that the railway was a mode of choice in the study area. The most prominent factors influencing patronage were proximity and access. Meanwhile, passengers would be happy to see other desirable features.

The operation and patronage dynamics of the Lagos Shuttle Train Services, if improved on, would promote the welfare of passengers and enhance the effectiveness of NRC. These would, in turn, contribute to the progress and prosperity of Nigeria as Nigerians would reap more benefits from a top-notch urban transit. Towards this end, the following policy recommendations are proffered.

There should be a holistic overhauling of the operations of and services rendered by both the Lagos Shuttle Train Services and NRC in its entirety. All the problems identified here and elsewhere should be thoroughly dissected and conscientiously tackled. For example, all the old rolling stock should be discarded and replaced with modern ones. Nigeria and Nigerians can never reap the full benefits of a contemporary railway system while still retaining antiquated infrastructure and antediluvian rolling stock. If all the intrinsic problems that have to do with low speeds, delays, and in-transit breakdowns must be solved, then a complete structural revamp is indispensable. Meanwhile, the recommended upgrading of rolling stock and infrastructure should be done along with a commensurate honing of skills as well as the transformation of the welfare package of the operators, especially the engineers. There is a way staff welfare contributes to efficiency.

In addition, every form of stowing away, rooftop riding, ticket racketeering, and all other irresponsible behaviours on trains should be decisively and vehemently resisted. Then, the hitherto strict stance taken on pandemic responsiveness by the management should be sustained for guaranteed rail transport safety. Any passenger who refuses to fully comply should be ejected. This is expedient as every stakeholder has a significant role to play in responsible transport.

Moreover, every effort should be made to make rail transport not only attractive to commuters, irrespective of their socio-economic status, but also desirable. Consequently, as much as possible, cognizance should be taken of their expressed desires that have to do with the offer of extra services, installation and/or retrofitting of coaches with air conditioners, provision of safety equipment, reliable weekend services, punctuality, and other desirable features. Provision of information schedule is also important. Adequate and timely information is needed and should be provided

to passengers through every possible medium. Meanwhile, all schedules should be strictly monitored and followed.

Efforts should be redoubled on guarding against the illegality perpetrated by undesirable co-travellers. Also, random inspection should be done on-board the trains both before and after ticket validation. These would also improve revenue generation. Fares should be prorated such that no passenger would feel cheated. The charging of flat rates irrespective of distance should be discontinued on all the routes. Prorated charging should be adopted as opposed to the charging of flat rates. This is important so that passengers travelling over short distances would not feel unduly cheated.

On their own part, passengers should also be ready to pay for the improvements where and when necessary. As an appendage to this, researchers should embark on studies to examine the affordability and willingness of passengers to pay for improvements in railway services. A situation whereby the corporation cannot break even let alone make profit can never engender the much-needed sustainability in the nation's railway subsector.

Even though magnetic levitation (maglev) is not yet a feasible railway technology in Nigeria, considering the country's economic profile, however, a long-range plan for it would not be totally out of place. The maglev technology is arguably the future of train transportation. Nigeria should not be left behind. Maglev boasts incredible speed of up to 620 kms per hour, and it is rated to be safe. Meanwhile, it runs on sustainable and environment-friendly energy source, namely liquid nitrogen. Thus, it does not emit any harmful gas. Its huge upfront investment is a major intimidating factor as it is a typical greenfield project that requires the design and construction of completely new infrastructure; however, workable and practicable finance sources can be explored. All things considered, it is a worthwhile option that should not be ignored.

References

1. Ademiluyi, I.A.: Historical evolution and characteristics of transport modes in Nigeria. Babcock J. Manage. Social Sci. **5**(1), 91–111 (2006)
2. Adeyinka, A.M.: Assessment of the quality of urban transport services in Nigeria. Acad. J. Interdiscip. Stud. **2**(1), 49–58 (2013)
3. Afon, A.: The use of residents' satisfaction index in selective rehabilitation of urban core residential areas in developing countries. Int. Rev. Environ. Strateg. **6**(1), 137–152 (2006)
4. Afon, A.O.: The use of residents' environmental quality indicator (EQI) data in the core residential housing improvement. In: Akinbamijo, O.B., Famehinmi, A.S., Ogunsemi, D.R., et al. (eds.) Effective Housing in the 21st Century Nigeria, pp. 115–122. Global Environmental Strategies (IGES), Kanagawa (2000)
5. Agunloye, O.O., Ilechukwu, V.U.: Travels pattern and socio-economic characteristics of rail transport passengers in Lagos Metropolis, Nigeria. Int. J. Econ. Dev. Res. Invest. **2**(1), 115–126 (2011)
6. Agunloye, O.O., Oduwaye, L.: Factors influencing the quality of rail transport services in Metropolitan Lagos. J. Geogr. Region. Plann. **4**(2), 98–103 (2011)
7. Aigbe, G.O., Ogundele, F.O., Aliu, I.R.: road facility availability and maintenance in Lagos State, Nigeria. Br. J. Arts Soc. Sci. **4**(2), 135–149 (2012)

8. Akinosun, F.O.: A psychometric assessment of the Osun Youth Empowerment Scheme (OYES) of the Osun State Government of Nigeria. IOSR J. Human. Soc. Sci. (IOSR-JHSS) **27**(5), 22–31 (2022)
9. Akinosun, F.O.: Assessment of the efficacy of poverty alleviation programmes in Osun State, Nigeria. Ph.D. Thesis. Department of Public Administration, Ambrose Alli University, Edo State, Nigeria (2011)
10. Akintifonbo, O.: A study of the operation and patronage of the Lagos Shuttle Train. M.Sc. Thesis. Department of Urban and Regional Planning, Obafemi Awolowo University, Ile-Ife, Nigeria (2017)
11. Akpomrere, O.R., Nyorere, O.: Bus Rapid Transit (BRT) and railway transport system: geographic information system approach. Int. J. Econ. Dev. Res. Invest. **4**(1), 53–63 (2013)
12. Alabi, M., Bello, K.A., Omirin, O.M.: Ratification: Mode of securing tenure within government acquired land in Lagos State, Nigeria. Ife Plann. J. **4**(1), 66–84 (2011)
13. Alam, B., Nixon, H., Zhang, Q.: Investigating the determining factors for transit travel demand by bus mode in US Metropolitan Statistical Areas, Mineta Transportation Institute (2015)
14. Amba, D.A., Danladi, J.D.: An appraisal of the Nigerian transport sector: evidence from the railway and aviation sub-sectors. J. Econ. Sustain. Dev. **4**(10), 163–170 (2013)
15. Amiegbebhor, D., Dickson, O.F.: Impact assessment of Bus Rapid Transit on commuters satisfaction in Lagos State, Nigeria. JORIND **22**(2), 198–208 (2014)
16. Armbruster, B.: Factors affecting transit ridership at the metropolitan level 2002–2007. M.Phil. Thesis. Faculty of the Graduate School of Arts and Sciences of Georgetown University, Washington, DC (2010)
17. BPE: Nigerian Railway Corporation. Bureau of Public Enterprises, Presidency, Abuja, Nigeria (2018)
18. Babalik, E.: Urban rail systems: a planning framework to increase their success. Ph.D. Thesis. Centre for Transport Studies, University of London, London (2000)
19. Basorun, J.O., Rotowa, O.O.: Regional assessment of public transport operations in Nigerian cities: the case of Lagos Island. Int. J. Dev. Soc. **1**(2), 82–87 (2012)
20. Bhat, C.R., Guo, J.Y., Sen, S., Weston, L.: Measuring access to public transportation services: a review of customer-oriented transit performance measures and methods of transit submarket identification. Texas Department of Transportations (2005)
21. Cervero, R.: Rail-oriented office development in California: how successful. Transp. Q. **48**(1), 33–44 (1994)
22. Eric, C.T.: A comparative analysis of railway patronage in two metropolitan cities: Hong Kong and New York City. M.Phil. Thesis. Department of Geography, University of Hong Kong, Hong Kong (2009)
23. Geetika, N., Shefali, N.: Determinants of customer satisfaction on service quality: a study of railway platforms in India. J. Public Transp. **13**(1), 97–113 (2010)
24. Ibidapo-Obe, O., Ogunwolu, L.: An operational appraisal of the Ido-Ijoko rail mass transit system service. Paper presented at the international conference in engineering, Lagos, Nigeria, 23–26 May, pp. 30–47 (2005)
25. Irfan, S.Y., Hung Kee, D.M., Shahbaz, S.: Service quality and rail transport in Pakistan: a passenger perspective. World Appl. Sci. J. **18**(3), 361–436 (2012)
26. Kuby, M., Barranda, A., Upchurch, C.: Factors influencing light-rail station boardings in the United States. Transp. Res. Part A **38**, 223–247 (2004)
27. Labisi, A.: Rail transport. In: Balogun, Y., et al. (eds.) Lagos State in Maps, pp. 66–67. Rex Charles Publication in Association with Connel Publications, Ibadan (1999)
28. Li, J., Xiang, T., He, L.: Modeling epidemic spread in transportation networks: a review. J. Traffic Transp. Eng. **8**(2), 139–152 (2021)
29. Litman, T.A.: Evaluating public transit benefits and costs. Victoria Transport Policy Institute (2017)
30. Nathanail, E.: Measuring the quality of service for passengers on the Hellenic Railways. Transp. Res. Part A: Policy Pract. **42**(1), 48–66 (2008)

31. Obasanjo, O.T., Francis, M.: Quality of Intra-urban passenger bus service in Kaduna Metropolis, Nigeria. Int. J. Traffic Transp. Eng. **4**(1), 1–7 (2015)
32. Odeleye, J.A.: Public-private participation to rescue railway development in Nigeria. Japan Railway Transp. Rev. **23**, 42–49 (2000)
33. Okanlawon, K.R.: Towards enhancement of light rail system in efficient transportation of commuters in Lagos State. J. Social Policy Soc. **1**(1), 22–27 (2006)
34. Okanlawon, K.R.: A study of rail mass transit in Lagos and its environs. Ph.D. Thesis. University of Lagos, Lagos, Nigeria (2011)
35. Olayiwola, K.O., Okesoto, J.O., Akinpelu, A.A.: Assessment of rail transport services on Iddo-Ijoko corridor. Paper presented at the first National Conference on Technological Advancement and the Built Environment. School of Environmental Studies, Yaba College of Technology, Yaba, 13–14 June, pp. 1–12 (2012)
36. Olojede, O.A.: The hell-bound bandwagon: train rooftop riding in Lagos Metropolis, Nigeria. Urban Rail Transit **5**(1), 29–38 (2019)
37. Olojede, O.A.: Urban transport security: analysis of transit crime in Osogbo, Nigeria. Analele Universităţii din Oradea, Seria Geografie **29**(1), 9–18 (2019)
38. Olojede, O.A., Agbola, S.B., Samuel, K.J.: Residents' assessment of local government road infrastructure delivery in Ile-Ife, Nigeria. Local Econ. **34**(4), 346–363 (2019)
39. Olojede, O., Daramola, O., Olufemi, B.: Metropolitan transport safety and security: an African experience. J. Transp. Saf. Secur. **9**(4), 383–402 (2017)
40. Olojede, O., Yoade, A., Olufemi, B.: Determinants of walking as an active travel mode in a Nigerian city. J. Transp. Health **6**, 327–334 (2017)
41. Olojede, O.A.: Transport decarbonisation in South Africa: a case for active transport. Scien. J. Silesian Univ. Technol. Series Transp. **110**, 125–142 (2021)
42. Olojede, O.A., Oluborode, O.G.: Transportation: The agathokakological vehicle of pandemic transmission and management. Scientific J. Silesian Univ. Technol. Series Transport. **115**, 107–120 (2022)
43. Oni, S.R., Okanlawon, K.R.: An assessment of the usage of Lagos mass transit trains. Int. J. Railway **5**(1), 29–37 (2012)
44. Rajeswari, V., Santa Kumari, K.: Satisfaction and service quality in Indian Railways: a study on passenger perspective. IOSR J. Econ. Fin. **4**(1), 58–66 (2014)
45. Renner, M., Gardner, G.: Global Competitiveness in the Rail and Transit Industry. Worldwatch Institute, Washington, DC (2010)
46. Salami, B.M., Faletiba, D.E., Fatoba, J.O., Ajala, M.O.: Integrated geophysical and geotechnical investigation of a bridge site: a case study of a swamp/creek environment in South East Lagos, Nigeria. Ife J. Sci. **14**(1), 75–82 (2012)
47. Salkonen, R., Paavilainen, J.: Measuring railway traffic punctuality from the passenger's perspective. In: The 12th World Conference on Transport Research. Lisbon, Portugal. July 11–15 (2010)
48. Sambasivan, M., Soon, Y.W.: Causes and effects of delays in Malaysian construction industry. Int. J. Project Manage. **25**, 517–526 (2007)
49. Stocker, J.: Nigerian Railway Jubilee, 1901–1951: an illustrated and descriptive history of the Nigerian Railway (Lagos Railway, Wushishi Tramway, Baro Kano Railway). Railway Printer, Michigan (1951)
50. Taylor, B.D.: Transit's little secret: Analysing transit patronage in the U.S. UCLA Institute of Transportation Studies (2007)
51. Taylor, B., Fink, C.: The factors influencing transit ridership: a review and analysis of the ridership literature. In: Working Paper, UCLA Department of Urban Planning, pp. 1–17 (2003)
52. Urban Transport Fact Book: Commuter rail (suburban rail, regional rail) in the United States: International Context (2003)
53. Whiteing, T., Menaz, B.: Thematic research summary: rail transport. Transport Research Knowledge Centre—European Commission (2009)
54. World Population Review: Population of Cities in Nigeria (2022). World Population Review (2022). https://worldpopulationreview.com/countries/cities/nigeria

55. Zheng, Y.: Estimation of disease transmission in multimodal transportation networks. J. Adv. Transp., 1–16 (2020)
56. Zhou, J., Dong, S., Ma, C., Wu, Y., Qiu, X.: Epidemic spread simulation in an area with a high-density crowd using a SEIR-based model. PLOS Digit. Health **16**(6), e0253220 (2021)

Linear Motor-Based High-Speed Rail Transit System: A Sustainable Approach

Nisha Prasad and Shailendra Jain

Abstract Rapidly rising economies and urbanization have immensely increased the energy concerns in transportation sector. The road transportation system is unable to provide long-term solutions to these problems due to raging fuel prices, rising environmental concerns, and worsening traffic congestion as a result of the increasing private vehicle ownership. Thus, to improve the energy security in this sector, emphasis must be given to the development of mass rail transit systems. The actual challenge lies in developing such rail transit systems that can reduce the dependency on road transport with lesser carbon footprints. However, conventional rail transit systems based on rotary motors possess many limitations in terms of speed, efficiency, automation, and sustainability. The development of a linear motor-based high-speed rail transportation system can provide a viable solution to these problems. The use of linear motors in these systems offers many advantages as compared to rotary motor-based conventional rail transportation systems. Being fully electrified, such a system also decreases the dependency on oil products making it a greener and more contemporary alternative to conventional rail transportation systems. This chapter gives a basic understanding of high-speed rail transportation systems. It describes the various constituents of high-speed rail transportation systems in detail, with a focus on the advancement attained by different countries in this technology, to make the system efficient and sustainable. This chapter also highlights the relevance of linear motor-based high-speed rail transit systems in today's scenario. A comparison of these technologies to analyze their applicability in context with India is also discussed.

Keywords High-speed railways · Advancements in rail technology · Linear motor-propelled railways

N. Prasad (✉)
Research Scholar, Department of Electrical Engineering, Maulana Azad National Institute of Technology, Bhopal, MP, India
e-mail: nishaprasad2402@gmail.com

S. Jain
Department of Electrical Engineering, Maulana Azad National Institute of Technology, Bhopal, MP, India
e-mail: jainsh@manit.ac.in; sjain68@gmail.com

1 Introduction

Reducing the carbon footprints is the biggest challenge every industrial sector is facing today for one or the other reasons. Transportation sector is also dealing with this issue worldwide due to rapidly increasing industrialization [1]. In addition to this, major dependency on road transportation is making this problem worse as this leads to traffic congestions, fatalities, fuel and parking problems, air, and noise pollutions [1, 2]. As per the latest report issued by International Union of Railways (UIC), road transportation is the major contributor of carbon emissions in global transport model.

Thus, the figures given by the UIC report show that the rail transportation is one of the most environment-friendly and energy-efficient transport system [2, 3]. However, this is not the end of the story, it is just the beginning. Developing the rail systems is not the challenge in this technical era. The main problem is to break the mental barrier of the public for curbing the use of private vehicles and to motivate them for accepting rail transport as part of their daily life. For this to happen, it is mandatory to develop efficient, faster, reliable, cheaper, compact, and high-quality traction systems. Thus, high-speed rail technology is not the luxury, but it is the need of today's era [3].

Rail transport technology has seen many modifications since its advent [4–9]. Still its technology is going through lot of changes for its betterment. Figure 1 gives the chronological developments in traction motors technology [3–10]. First electric locomotive was built in 1837, which was battery powered [4]. Later in 1837, DC motors were first introduced in an electric tram [4, 5]. In 1891, capabilities of three-phase AC motors were realized by developing first AC electric locomotive [4]. However, until 1990s DC motors were primarily used in traction propulsion systems with tap control using diode rectifiers. These rectifiers were replaced by phase-controlled thyristors when Ward Leonard control was introduced. During 1990s, AC squirrel cage induction motors were adopted in traction propulsion systems due to their robustness, cost-effectiveness, reliability, and low maintenance needs [4, 5].

However, long before these developments, history of high-speed rail technology can be traced back to the starting of nineteenth century during the industrial revolution. Those were the times when train speeds were considered a matter of competition. At that time, Stephenson's rocket locomotive made a history by attaining remarkable 50 km/h [1, 4]. Later during twentieth century, major modifications and developments in high-speed rail technology took place in different parts of Europe and Japan. These developments changed the perspective about this technology. Since then, this technology is still evolving with new innovations in all parts of this world.

European countries mainly experimented with different types of rotary motors and train body materials for its improvement. However, Japan started with rotary motor and then attained breakthrough during 1969–70 by using linear motor-propelled superconducting magnetic levitation technology in SCMaglev high-speed rail system [6, 7]. This development highlighted the advantages of using linear motors over rotary motors for the first time.
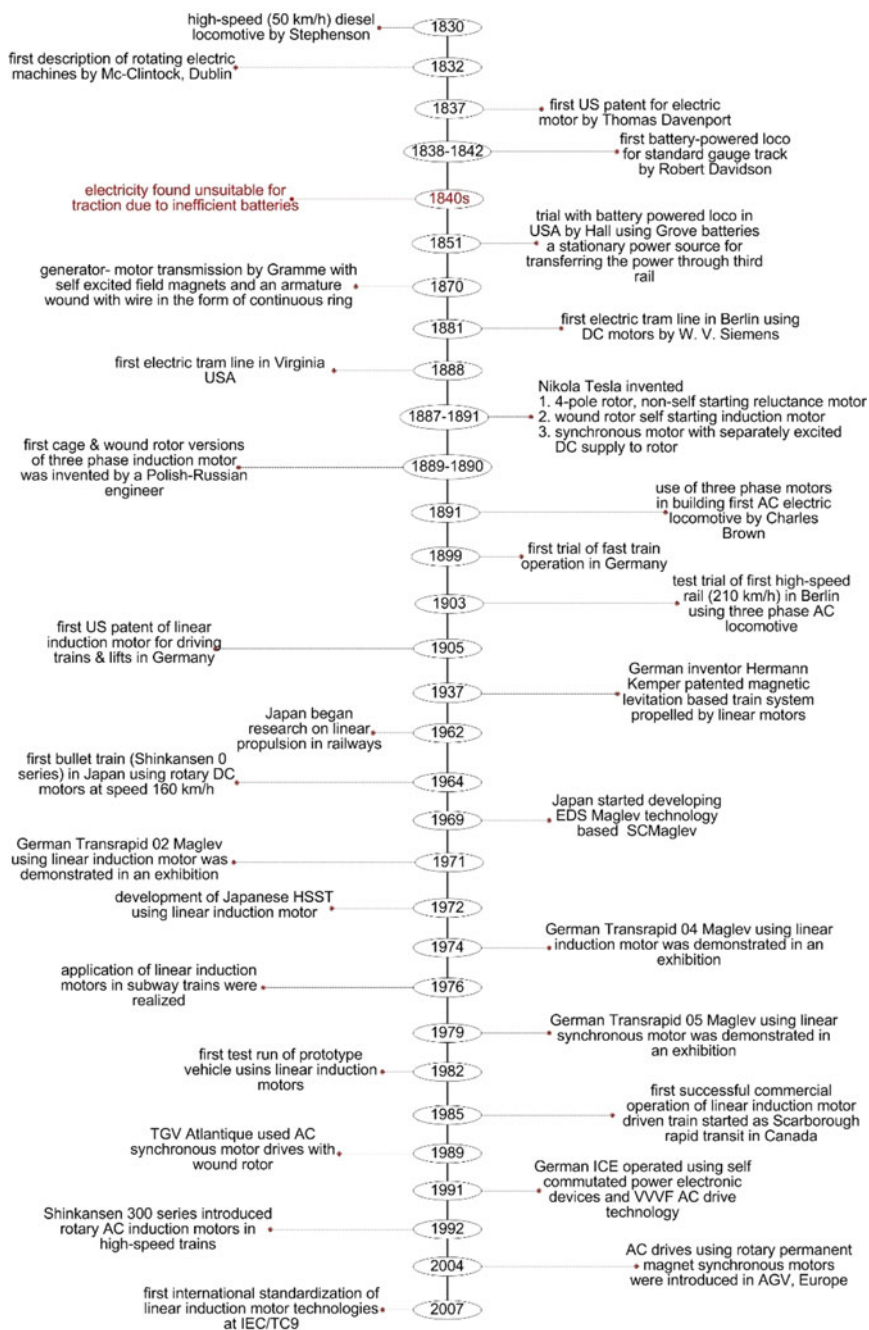
Fig. 1 Chronological history of application of traction motors in railways and evolution of high-speed rail

Linear motors produce translational motion with any gear mechanism as needed by rotary motors to convert rotary motion into translational motion [8–10]. Thus, linear motors give the advantage of noiseless operation, better traversing of track outlines, independence from adhesion between rail and wheel with more reliability [9, 10]. Therefore, other than Japan countries like China, Germany, and USA are focusing more on developing linear motor-propelled high-speed rail systems [8, 9]. Since this technology is still evolving, there is a lot of scope for improvement. Its excruciating capital cost is its major drawback which makes it unaffordable for developing countries like India.

Thus, to ensure sustainability of this technology reduction in its cost is necessary. As every high-speed rail system consists of many components, thus modifying its components as per the conditions and requirements of different countries can help in its capital cost reduction for that country. To understand these modifications, it is important to first understand these components.

Thus, to gain a better insight about this technology, this chapter therefore discusses different components of high-speed rail technology from technical point of view. It also presents the development achieved by different countries to enhance this technology. Later, this chapter also gives insight about the suitability of this technology for developing countries like India.

2   High-Speed Rail as a Traction System

Depending upon the operating power levels, traction systems can be classified as light rail vehicles (LRV), metros, monorails, commuters, locomotives, and high-speed rail. The power levels of these systems range from few kW to few MW, whereas speed varies from 50 to 500 km/h as seen in Fig. 2 [9–13]. Light rail vehicles come under the low power range vehicles. Tram systems are an example of LRVs, which are generally used for intercity/suburban transport. Metros, monorails, and commuters are the medium power range vehicles as they require traction motors with higher ratings as compared to LRVs. Locomotives need high effort especially during acceleration; thus, they require traction motors with the highest torque and power rating. The power level of high-speed rail varies in the range of MW. However, it is slightly lesser than locomotives.

However, as per UIC, any rail system attaining 250 km/h on dedicated track or 200 km/h on modified track is termed as high-speed rail [1, 2]. To achieve such speeds, different countries have adopted different methods. In the first method, the conventional rail systems are upgraded and modified that is known as upgraded wheeled rail systems, while in the second method the magnetic levitation-based linear motor-propelled rail systems are developed to run on dedicated tracks known as Maglev rails [14, 15]. Both of these high-speed rail systems mainly consist of three main technical components: rolling stock formation, electric power supply system, and operation and maintenance hierarchy of the traction system.
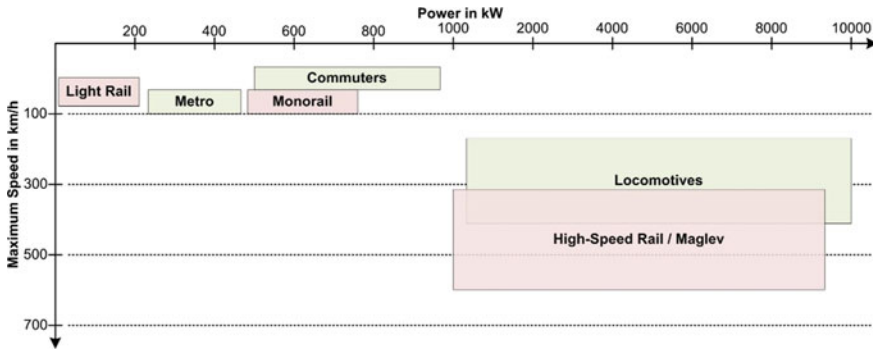
Fig. 2 Comparison of different traction systems based on power and speed

2.1 Rolling Stock Formation

In general, the rolling stock formations in traction systems can be of two types: concentrated type and distributed type [16–18]. Concentrated type formation is generally used in conventional railways, in which train sets are hauled by one or more locomotives as explained in Fig. 3a. The number of locomotives depends upon the required power by the rolling stock that further depends upon the weight to be hauled [16], whereas in distributed type formation, several electrical units or motor coaches are installed at equal distances along the train set as shown in Fig. 3b. Thus, it is known as electric multiple unit (EMU) trains. Distributed type formation is known for its capabilities such as high acceleration, fast deceleration, high axle loads, better adhesion, and transport capacity as compared to concentrated type [17, 18]. Therefore, distributed type formation is preferably used in all the high-speed rails including both upgraded wheeled rails and Maglev rails.

Fig. 3 Rolling stock formations **a** concentrated type/locomotives and **b** distributed type/electric multiple units
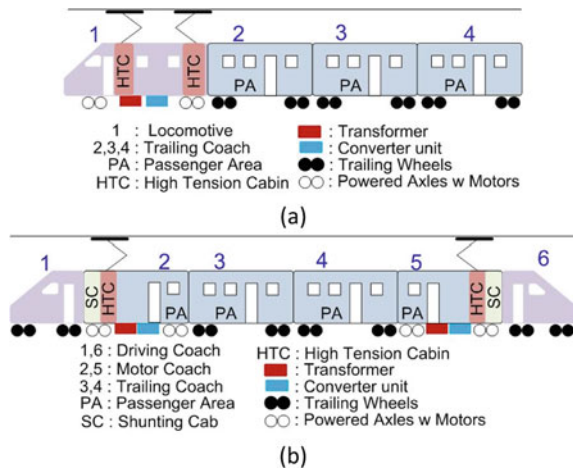
2.2 General Power Circuit of Electric Multiple Units

Every electric multiple unit (EMU) train set consists of number of motor coaches (MC) and trailing coaches (TC) arranged in a fixed configuration depending upon the requirement. Trailing coaches are non-powered coaches as they contain non-powered axles or axles with no traction motor as shown in Fig. 2 [18, 19]. Figure 4 shows the block diagram of power circuit present in motor coach of an EMU rail system [20–22]. This block diagram is for wheeled EMU system. As per the diagram, motor coach contains all the electrical equipment that are placed in a high-tension cabin. The axles corresponding to these cabins are connected to the traction motors. The coach contains two traction converter units. The converters are the devices to convert one form of electricity into another form. In case of traction converters, single-phase (1-φ) AC is first converted to DC with the help of a rectifier. The voltage level of this DC is changed with the help of chopper that is known as DC-to-DC converter. This converted DC further gets converted to three-phase (3-φ) AC with the help of inverters. Thus, traction converter unit is a combination of a rectifier, a chopper, and an inverter. Each traction converter unit supplies two traction motors.
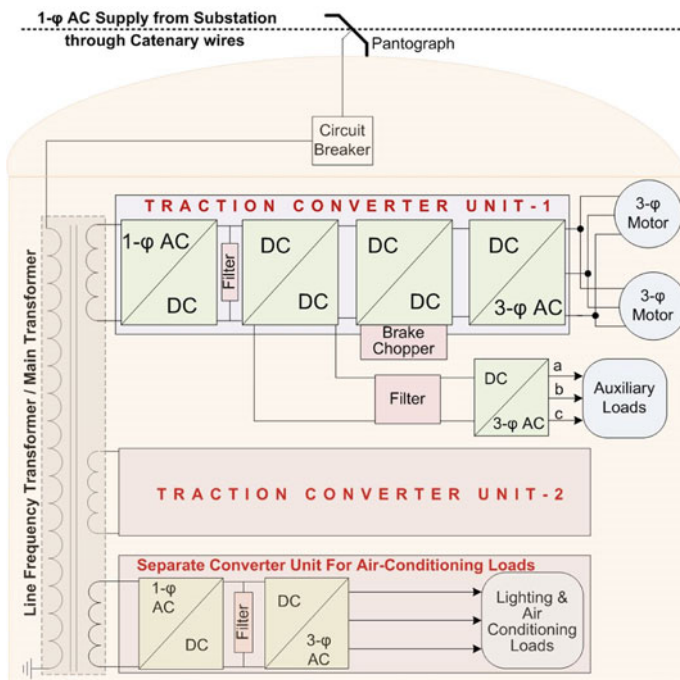
Fig. 4 Power supply arrangement in motor coach of high-speed wheeled rail system

The pantograph collects the single-phase supply and transfers it to the main transformer that is known as line frequency transformer (LFT). The line frequency transformers are the transformers that work at fixed line frequency, which is 50 Hz for India. When used in traction systems, the primary of these transformers is connected to the main traction line supply of 25 kV AC, whereas the secondary of these transformers supplies the traction converters after stepping down the voltage. Converters convert the supply to AC–DC–DC–AC, to produce a three-phase supply for the traction motors [20, 21]. An additional DC chopper stage is added in the converter drive train to power the auxiliary loads such as cooling units, compressors, water pumps, and blowers. Other than that, separate power is needed for hotel loads like air-conditioning and lighting units. A number of auxiliary converters are adjusted as per the auxiliary loads.

Maglev rail systems also use EMU configuration [17, 18, 20]. However, in high-speed Maglevs using linear synchronous motors (LSM) generally the converters are installed on ground. As shown in Fig. 5, the ground side supply energizes the converters. These converters convert this supply to AC–DC–AC to form three-phase supply that energizes the LSM stator coils. These stator coils are laid on along the complete track. The translator part of the LSM is installed on the train coach. As the train moves, the translator starts translating over the stator coils due to electromagnetic induction principle [23, 24]. Thus, in high-speed Maglev rails power is transferred through magnetic coupling between ground coils and onboard coils without using any pantograph.

Japanese SC Maglev, Chinese Shanghai Maglev, and German Transrapid are examples of such systems [8, 9, 17]. In medium speed Maglev rails, power supply system is installed onboard and only non-powered system forms the track [8, 9, 23]. This method is generally used in systems that use linear induction motors for their propulsion. Japanese HSST is an example of such system [6, 8, 9].
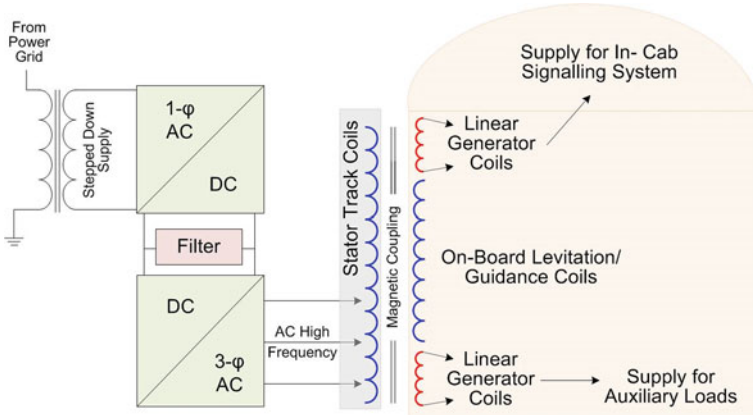
Fig. 5 Power supply arrangement of high-speed Maglev rail system

2.3   Operation and Maintenance Routing of High-Speed System

When any rail system operates at speeds above 200–300 km/h, then control hierarchy becomes a major concern for such a system. To assure safety at higher speed, synchronization among different onboard monitoring systems, ground control systems, and communication systems with other vehicles becomes mandatory. The generalized control routing of a high-speed rail system is explained in Fig. 6 with the help of a block diagram.

The operation of multiple high-speed rails in a section is monitored by a centralized ground controlling unit (GCU). The GCU communicates with the vehicle through ground signals. The train control and monitoring system (TCMS) manages the operation of vehicle depending upon the instructions received through ground signals and vehicle control unit (VCU) [20, 25, 26]. The VCU is the prime controller that controls the complete characteristics of the vehicle dynamically and assures vehicle safety. It communicates with every system inside the vehicle, e.g., traction converters, traction motors, auxiliary systems, driver display unit (DDU), and remote I/O signal system. The VCU reports every fault occurrence using the DDU that displays fault values and occurrence time [20]. The VCU generates signals for traction control unit (TCU) through an interfacing system. The TCU passes these signals to a controller and generates required PWM signals for the power electronic converters. These converters thus control the motoring and braking operation by controlling the traction motors [25, 26]. The auxiliary control unit (ACU) controls the auxiliary systems of the vehicle in a similar way. The ACU also communicates with VCU and receives signals through a common bus that is used by main systems to communicate with the VCU.
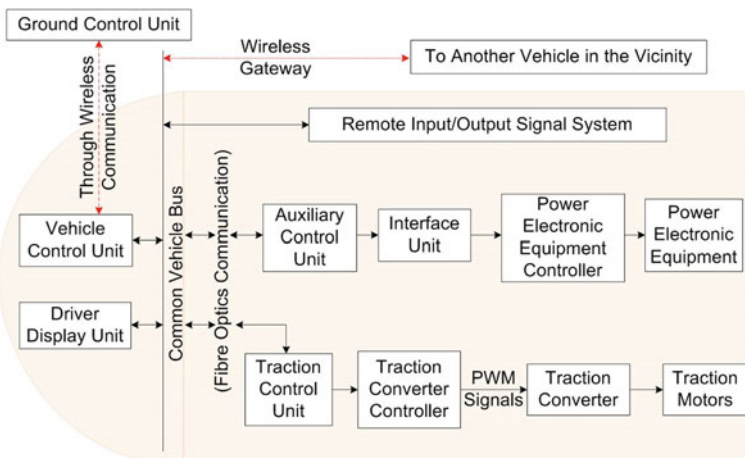
Fig. 6 Block diagram of control system routing in high-speed rail system

Other than these technical components, high-speed rail system has some non-technical components like infrastructure that deals with civil design of track, station, power supply, etc., and commercial aspect that mainly concerns with finance and marketing of rail system. All these components are crucial to assure the safety and success of any high-speed rail system. Advancements and modifications in these components lead to the development of suitable high-speed rail system in any country. The further section describes the different modifications adopted by different countries to develop suitable high-speed rail system for their country.

3 Advancements Achieved for Betterment of High-Speed Rail Technology

For an evolving technology like high-speed rails, advancements become inevitable part of both wheeled and non-wheeled high-speed rail systems. Many modifications are also done in conventional railways to achieve betterment in performance of high-speed rails. To understand the pros and cons of these modifications, it is important to understand and learn about these changes. These developmental modifications are explained in the subsequent subsections.

3.1 Advancements in Power Electronic Transformer Technology

Expanding high-speed rail networks has increased the demand for highly efficient power electrical drive system with high-power density. While achieving this requirement in EMU with distributed propulsion systems, the passenger space gets compromised.

Use of articulated vehicle mechanism with distributed power mechanism is adopted by some countries to increase the passenger space and speed of the vehicle. Alstom's AGV is one such example, in which a vehicle is developed in different sections that are connected by a pivot bar [27]. This helps the vehicle in taking sharper turns in lesser time, which increases its speed.

However, in a distributed system, the weight and size of line frequency transformer (LFT) pose a major space concern due to the presence of higher number of powered axles. The LFTs are designed for minimum power density and efficiency [28]. But, increasing demand for railway vehicles imposes restriction on weight, size, and efficiency of different rail equipment.

Optimization of different components such as dielectric materials, cooling methods, winding material, and its designs is tried to achieve this objective. However,
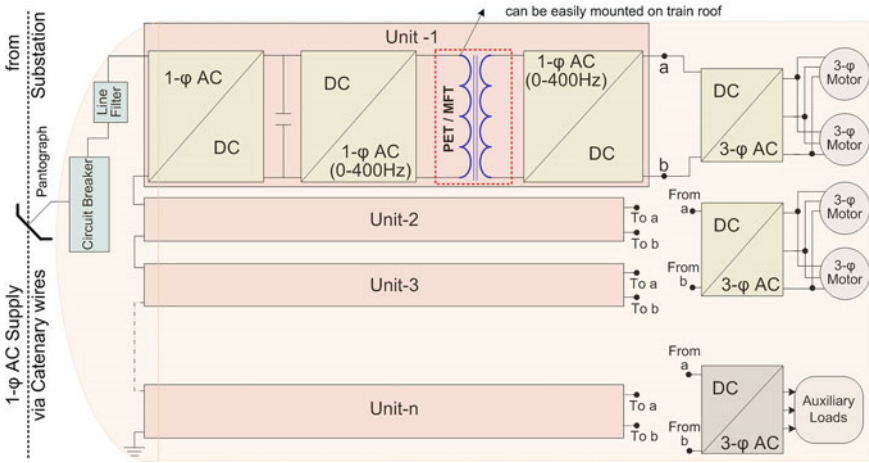
Fig. 7 Traction power converter unit using PET technology

these methods have not produced the required results. Thus, use of power electronic transformer (PET) is seen as an effective alternative to LFT for increasing the efficiency and power density of the railway vehicles [27–29].

The PET is a solid-state transformer that operates at medium frequency of more than 400 Hz. The PET-based traction conversion system needs direct connection of high-voltage catenary with the converter; thus, a few converter train units with high-power switches are connected in cascade at high-voltage input side, and parallelly connected output of these units supplies different traction motors and auxiliary systems [20, 28]. A block diagram of a single unit is shown in Fig. 7.

In this converter system, an additional conversion stage is given which makes the conversion train as high-voltage AC–DC–AC (high frequency)-AC (high frequency)-DC–AC (three-phase).

The PET-based technology uses medium frequency transformers (MFTs) that can be easily fitted on the train roof, which increases the space inside the train [27].

The PET-based drive combines LFT and AC–DC conversion step of conventional LFT-based traction system; thus, it increases the power density and efficiency of the traction drive. It also gives improved power quality with additional benefits of fault current limitation and fault isolation [20, 28].

However, this technology is facing lots of challenges and still evolving to achieve its full potential. The biggest challenge in using this technology is the direct connection of catenary supply with HV side AC–DC converter and selection of suitable switching frequency for its high-power switches. Due to this constraint, maintaining the continuity of power supply becomes mandatory especially during load variations, pantograph oscillations, and neutral section passage. Also, because of this configurational modification, the design of auxiliary system becomes more challenging.

3.2 Advancements in Power Converter Drive

As discussed in above section, every PET converter drive consists of a line side filter, high-voltage end single-phase AC–DC converter, second harmonic filter, DC–AC (high frequency) converter, MFT, AC (high frequency)-DC, and a three-phase inverter to feed the traction motors.

Many configurations for these drives are developed since its advent. The high-voltage end converter in PET-based drive system requires AC–AC conversion. This conversion can be done in two ways: (i) two-stage conversion, i.e., AC–DC–AC and (ii) single-stage conversion, i.e., AC–AC. Many topologies of two-stage conversion are studied in different papers. However, these topologies face common problem of second harmonics that demands the filter and oversized capacitors [28–31].

Thus, single-stage conversion becomes a suitable option in advanced PET drives. Half-bridge AC–AC configuration is a common choice in such converters to simplify the power circuit [20, 28]. The cycloconverters and matrix converters are generally used for AC–AC conversion in traction drives as they reduce capacitor needs thus increases the power density and reliability of the system. However, they require large number of switches that complicates the control circuit [28–31].

Other converters such as current source inverters with fly back transformers and modular multilevel converters are also proposed in literature [32–34]. Siemens 5 MW is an example of AC–AC multilevel modular converter with concentrated multi-winding MFT [35]. It has also developed a 98% efficient 2 MW drive using a multilevel modular converter with a switching frequency of 10 kHz [36].

Other than that, Swiss railways have developed a PET-based drive containing cascaded H-bridge converter in combination with resonant DC–DC converters [37]. The H-bridge converters are the converters that resemble the shape of English letter 'H'. In these converters, the four power electronic switches are connected on the four vertical limbs of letter 'H', whereas the load is connected on the horizontal limb of letter 'H'. This converter allows the bidirectional flow of current through the load. Therefore, it provides four-quadrant operation of the load. For example, if the load is a DC motor, four-quadrant operation could mean forward motoring, forward braking, reverse motoring, and reverse braking. The use of H-bridge also reduces the harmonic distortion of the supply and thus increases the efficiency of the circuit.

Bombardier has also developed a similar 5 MW configuration with full-bridge DC–DC converter. In this drive, the switching frequency is kept 8 kHz [38]. ABB has developed a 1.2 MVA PET-based drive containing a cycloconverter along with a parallel output rectifier for high-speed applications [39].

Alstom has developed a 2 MVA PET-based drive using series cascaded H-bridge on AC side along with a parallel cascaded H-bridge phase-controlled multilevel converter. Devices like IGBTs and SiCs are used in these converters [40].

In addition to the research in drive configurations, different soft switching techniques like zero current switching and zero voltage switching are also evolving to operate these converter drives at high switching frequencies [41, 42]. These techniques are required to reduce switching loses in these converters. In future PET drives,

simplifying the controlling of modular multilevel converter, reducing the count of converter modules, and utilizing the high switching frequencies with soft switching techniques are going to be the main challenges.

3.3 Advancements in Power Electronic Devices

As discussed in previous section, high-speed rail technology requires the operation of its converters at high-power and voltage levels. Thus, it becomes mandatory to use switches having high-voltage and power ratings in these converters. To increase the ratings to these switches, its material becomes a point of concern as increased ratings demand for better thermal characteristics with low losses [43].

The commonly used silicon-based switches generally provide inferior thermal characteristics that not only increases the cooling requirements of the circuit but also reduces its overall efficiency [28, 44]. Almost all the silicon (Si)-based devices have unsuitable thermal and power characteristics for application in high-power converters that are used in high-speed traction converter drives. The power electronic devices (PEDs) used in traction converters operate under harsh conditions such as high temperatures. These high temperatures generally occur due to heat dissipation by the motors, engines, losses dissipated as heat by PEDs, and operating ambient temperatures. Thus, PEDs must be capable of withstanding high temperatures at their junctions. The Si devices generally have maximum allowable junction temperature of around 150 °C [44]. Thus, operating temperature of Si devices must be kept under this temperature to avoid breakdown of the devices. To maintain this temperature, different heat sinks are used with these devices which generally increase the cost and size of the devices. However, silicon-based IGBTs (Si-IGBTs) and PiN diodes have shown their capability for use in traction converters due to improvement in their thermal characteristics. But their weight and operating temperatures pose limitations on their use in high-power traction converters. Also, both the bipolar devices give higher losses. The unipolar devices like MOSFETs and Schottky diodes possess far better characteristics as compared to IGBTs and PiN diodes. However, both the devices do not exist for high-voltage ratings. Increasing the voltage rating of these devices requires increase in silicon width that results in high manufacturing costs of the devices. Also, the switching frequency of these Si devices is restricted due to the heat dissipated by the devices. Higher switching frequency operation is desirable in high-power converters as it lessens filter requirements, decreases harmonic distortions, and gives smoother output. Thus, Si devices have reached their theoretical limits. Therefore, they are not suitable for use in modern high-speed rail transportation industry due to such limitations.

Thus, wide band gap power electronic devices (WBG-PEDs) such as silicon carbide (SiC) and gallium nitride (GaN) possess qualities that can make them a suitable alternative to these Si devices. These WBG-PEDs have maximum operating junction temperatures of around 600 °C [44]. Other than that, these devices possess

low losses, lesser weight, low resistance, high thermal conductivity, higher breakdown voltages, faster reverse recovery characteristics, and high switching frequencies of more than 20 kHz. Thus, WBG-PEDs are now replacing the Si-based PEDs in modern high-speed rail transportation systems.

The silicon carbide (SiC)-based Schottky barrier diode is added in antiparallel with these Si-IGBTs (SiC-SBD/Si-IGBT) to improve their thermal characteristics [45]. These new generation materials with wide bandgap are under consideration due to their high temperature withstanding capability and high breakdown voltages as compared to common silicon devices.

Use of such SiC-based hybrid devices in Japanese railways has resulted in 60% reduction in volume, 35% reduction in overall converter losses, 17% reduction in diode switching losses, and 50% reduction in IGBT conduction loss [28, 46, 47]. Reduction in these losses has resulted in 33% reduction in size for same current rating [20]. By further optimizing the cooling techniques, this reduction in size, weight, and volume is found to be 40% as compared to normal silicon-based devices [46, 47].

Further improvement in performance of SiC-SBD/Si-IGBT is done by Japanese electric equipment company Fuji Electric by using Sn-Sb alloy solder [48]. Addition of this alloy resulted in major reduction in losses and size along with higher operating temperature and strength. Also, this has improved the overall thermal characteristics of the converter drive. The SiC-based inverter modules are employed in both Japanese metro and Japanese Shinkansen high-speed rail system that are designed by Mitsubishi Electric Corporation [49].

These systems have shown tremendous improvement in switching losses and energy consumption at all speeds. This has also resulted in size reduction by more than 60% and weight decrease by 30% as compared to normal converters using IGBTs [20]. Thus, use of SiC-SBD/Si-IGBT gives improvement in voltage characteristics, switching losses, thermal characteristics that results in lesser cooling requirements, and more efficiency [20, 28, 49]. However, these devices pose limitation on maximum drain to source breakdown voltage due to restrictions of fabrication process. The maximum breakdown voltage value of this device is 1200 V. But, connecting these devices in series and parallel help in obtaining higher voltage and current ratings, respectively [20, 28].

To counter the voltage limitations of Si-IGBT devices, SiC-MOSFETSs are slowly replacing these IGBTs. Many series–parallel hybrid topologies using SiC-MOSFETs are studied in literature [50–52]. SiC-MOSFETs are preferred due to their high current-carrying and high-voltage withstanding capability, which makes them suitable for traction applications [50, 51].

The selection of suitable device for high-power traction converters is still an evolving research topic. Thus, in future it is expected to achieve high efficiency with lesser weight and volume, increased loading capability, increased reliability, lesser maintenance, higher levels of auxiliary onboard power, and lesser cost through these converters.

3.4   Advancements in Energy Storage Systems

High-speed rail systems are fully electrified worldwide. Thus, in such systems, utilizing and storing the energy of braking is a point of concern as all of them generally use regenerative braking. Employing such energy storage systems increases the efficiency and cost-effectiveness of the system by reducing the wastage of energy.

Many methods are proposed in literature for utilizing this braking energy. First one is the method of feeding the braking energy back to the grid through reversible stations employing thyristorized from where it is transferred to the other vehicle passing through the same section [53]. Mostly, the excess energy is utilized in mechanical braking process. However, off-board energy storage systems are another option for storing the braking energy [54]. The off-board energy storage systems generally employ lithium-ion battery, nickel-metal hydride battery, supercapacitors, and flywheels [55]. Washington metro rail system utilizes such off-board storage system using nickel-metal hydride batteries [56]. Bombardier and Kinetic traction systems have developed such energy storage systems using supercapacitors and flywheels, respectively [20, 56].

The maintenance and capital cost of off-board storage systems are more as compared to reversible grid feeding technology. However, both of these techniques require catenary for transmitting and receiving brake energy. Thus, they do not contribute much in betterment of vehicle performance.

Therefore, the onboard energy devices came into existence to make the energy transmission catenary free [20]. However, use of onboard energy storage systems increases the weight and assembling cost of the train vehicles. But as per the comparative studies given in literature, the onboard energy systems are the most effective method. Using the onboard energy storage system reduces the energy consumption, peak power demand, voltage regulation, and burden on power supply system. It also improves the acceleration/braking characteristics during high-speed operation. These systems also help in handling the supply discontinuities during transition through neutral sections and non-electrified sections [20, 57].

The onboard energy devices must possess capability of storing braking energy along with features such as high operating power levels, high energy density, and high maximum power value. Onboard energy storage device is formed using devices such as flywheels, lithium-ion batteries, lithium air batteries, lithium polymer batteries, and supercapacitors [58]. The supercapacitors are most commonly used for energy storage as it possesses high-power density and longer life span. Its faster charging and discharging capability make it suitable for storing energy during braking and releasing energy during acceleration operations [59, 60].

Bombardier experimented with onboard supercapacitors on light rail vehicle MITRAC and DEMUs that resulted in 30% energy saving along with fuel savings and carbon reduction [20, 61]. Later, lithium-ion batteries were tested on commuter trains of SEIBU rail company [62]. Bombardier also tested the flow batteries as an alternative to supercapacitors in EMUs for short-term energy storage requirements [63]. However, combination of batteries and supercapacitors is found as the most

effective solution for catenary free EMUs and DEMUs. This hybrid combination is tested in Japanese series EV-E301 [64]. Assembly of different energy storages like batteries, fuel cells, and supercapacitors in diesel engines is tested in diesel loco-motives for achieving complete catenary free operation [65]. This combination is currently under use by Canadian railways to achieve remarkable savings in energy [66].

Thus, energy storage technology is still evolving and perfect blend of different resources is yet to be achieved.

3.5   Advancements in Maintenance Technology

With the increase in high-speed rail lines and rail vehicles worldwide, the mainte-nance of these rail systems and its different components becomes a prime concern. The regular maintenance ensures the reliability and safety of these rail systems. To maintain such a rapidly expanding rail network, the advanced maintenance tech-nologies are needed. The traction maintenance technologies have seen many changes since its beginning where it started from the maintenance of component only after its failure. Later this developed into a preventive maintenance technology where each component is checked after certain period to ensure its proper working [67].

After the modern maintenance technology came, condition-based maintenance started. This has now changed to prognostic and health monitoring (PHM) tech-nology. However, at present three types of maintenance technology are under use in high-speed rails worldwide [67]. This includes.

- Reliability-centered maintenance technology
- Condition-based maintenance technology
- Prognostic and health monitoring (PHM) technology.

The concept of reliability-centered maintenance was first started in 1960s in US aviation industry and army. Later, in 1970s China applied this technology in civil aviation industry. This technology started with the time when maintenance used to be done only after failure. Later it included preventive maintenance in which components used to be inspected after a certain time interval. In its present form, reliability-centered maintenance is a method in which operation and failures of the system are analyzed to optimize the maintenance system by determining whether preventive maintenance is required by any component or not [68, 69]. For that the system is analyzed using its operational and design characteristics. These charac-teristics are matched with the available safety and reliability data to monitor the present state of the system and its components. This helps in determining the need for maintenance. At present, maintenance of high-speed trains in China is based on this principle [70].

Later, in 1980s the condition-based maintenance technology was developed due to the development of advanced computers. Conventional preventive maintenance techniques involve useless inspections of different parts. However, that problem is

taken care of by using condition-based monitoring in which the system is monitored in real time [71, 72]. This helps in determining the potential failures before their occurrences. Thus, it is not a time-based maintenance system but a condition-based maintenance. This system determines the degradation of the system at an early stage. The development of this system is going on for improving the maintenance technology of Japanese Shinkansen [73, 74].

Due to the development of sensor-based fault detection and maintenance technology, Prognostic and Health Management (PHM) technology came into existence to further enhance the condition-based monitoring systems [75, 76]. The PHM is a fault prediction and health management technology, which is achieved through advanced transmission technology.

The sensor technology picks up the system status information and uses the intelligent algorithm to carry out the system condition analysis, fault diagnosis, and prediction, make maintenance suggestions, and support users in decision-making [77]. PHM technology focuses primarily on systems state awareness, data analysis, health status monitoring, frequent failure locations with time, failure occurrence, and evolution prediction. This technology also helps in determining the life tracking of different traction components that is not possible in earlier maintenance systems. It can greatly improve the operation and maintenance efficiency of the system. America uses this system in aerospace and other industries [67, 77]. China has upgraded its maintenance of high-speed rail systems by using PHM-based system [77, 78].

The onboard PHM system of high-speed rails mainly consists of onboard system, communication system, ground system, application promotion platform, etc. The onboard PHM system preprocesses the train status, including fault diagnosis, health assessment, and intelligent decision-making, combining state features and preprocessing results. Then it transfers it to the ground PHM system through the vehicle-ground data transmission system. The ground PHM system receives the operation data from the train cluster and then optimizes the vehicle loading analytical models in PHM systems to develop its maintenance content.

3.6 Advancements in High-Speed Rail Body Material

The body and bogie structure becomes very important during high-speed operations. The lightweight design of the high-speed vehicle body can not only reduce the material but it can reduce the vehicle cost and the force of the wheel and rail. This in turn reduces maintenance costs for trains and tracks. It is important to improve the strength, stiffness, and natural vibration frequency of the vehicle for its safe operation [79]. The application of high-quality and high-strength materials is achieved by using carbon. The transformation of steel car body to stainless steel car body and aluminum alloy car body has helped in fulfilling this objective. The problem of corrosion resistance is currently under development and exploration in carbon fiber body.

The high-speed rail body design using aluminum alloys is under use in China that is suitable for the operation at a speed of 300–350 km/h [80]. In this the main structure is still made of large section, ultra-thin hollow, full-length aluminum alloy. Further increase in train speed and axle load demands for the improvement in the design standard of the strength and stiffness of vehicle body. Thus, future rail vehicles require comprehensive new materials and structures with excellent performance and breakthroughs in traditional metals, material limitations for providing efficient, reliable, energy-saving, and environmentally friendly solutions [80, 81].

Carbon fiber and other composite material structures, with their lightweight, high-strength, high-grade composite material structures, with their excellent comprehensive properties of lightweight, high-strength, and high weather resistance can be the suitable solution. This material after showing comprehensive performance and mature applications in aviation, aerospace, shipbuilding, automotive, and sports medical fields has become an excellent choice in the fields of traction [81–83].

Carbon fiber-reinforced plastics (CFRP) provide a reference for the application in the field of high-speed rails. Many research institutions in China have carried out systematic research on carbon fiber composite materials for trains [79–81]. This material is found suitable for the application at a speed of up to 600 km/h. The application research in fiber-reinforced composite materials in the field of rail transit started late, but developed rapidly. Trial operation of carbon fiber equipment cabin apron for intercity EMU reduced the weight of alloy by more than 30% as compared to aluminum [79]. This material is used for development of parts and components, such as high-speed train cab head hoods, skirts, pantograph shrouds, interior panels, sides of low-floor vehicles wall and roof, urban rail vehicle driver's cab hood, driver's platform, and intercity vehicle crew skirts in Chinese high-speed rail industry [79, 81–83]. This area is still evolving to find the perfect and suitable material for application in high-speed rail worldwide.

3.7 Advancements in High-Speed Rail Body Shape

With the continuous improvement in the running speed of high-speed EMUs, the air-to-air interactions have become more pronounced. Thus, it requires deep study on aerodynamic theory, evaluation, design, and manufacturing of vehicle-tunnel-environment coupling.

Research is needed on integrated design technology for overcoming aerodynamic effect, tunnel effect, wind effect, and ground effect. As the aerodynamic drag is proportional to the square of the rail speed, the aerodynamics puts significant influence on running stability and energy consumption of high-speed rail by affecting the train drag [84, 85]. The aerodynamics performance of any high-speed rail is mainly related to the shapes/designs of train head and tail; therefore, optimizing the head and tail design of the train becomes imperative at high speeds.

The design of the aerodynamic shape is mainly carried out from two aspects: streamlining the head shape and surface smoothing of the train [84]. The comprehensive improvement of the two aspects is carried out to improve the aerodynamics of the train. Vehicle aerodynamic development is based on aerodynamic design technology analysis, summary of previous technical analysis, summary of design experience, and learn from the other models.

The surface smoothing design mainly includes smoothing and streamlining of collector system, main switch from the collector system, bogie area, vehicle end connection, frame area, vehicle end connection, roof antenna, door, window, car, and other parts. Many key technical problems of aerodynamic design faced by China's high-speed EMUs are resolved by smoothing and streamlining of these parts [84, 85]. This is done to reduce aerodynamic resistance, aerodynamic noise and to meet the needs of safety, reliability, energy saving, environmental protection, comfort at different speeds and in different operating environments [85].

The main objectives of any aerodynamic design mainly include improvement in safety performance, comfort performance, environmental performance, and energy saving. For selecting any aerodynamic design, the main performance indicators include surface pressure, aerodynamic resistance, aerodynamic lift, aerodynamic noise, train crossing pressure wave, train-induced airflow, and tunnel aerodynamics performance.

The design parameters mainly focus on surface smoothness, longitudinal section head shape, horizontal section head shape, train car body area, train car body shape, inclination angle of the cab, and slenderness ratio whose value is proportional to the ratio of streamlined head length and cross-sectional area of train body. The increase in slenderness ratio helps in decreasing the aerodynamic pressure along the nose of the train head [84, 85]. Thus, modern high-speed rail systems like Maglevs use shapes that resemble the beak of a bird to decrease the aerodynamic drags.

According to the characteristics of different parts, combined with the previous research results, a variety of aerodynamic shape design schemes are finally selected through simulation optimization, wind tunnel test and dynamic model test, comprehensive analysis, experimental tests, and evaluation.

3.8 Advancements in High-Speed Rail Bogie

The bogie is the key that determines the safety characteristics of high-speed EMUs as they are the key subsystems for sitting comfort. With new materials, new structures, with high-strength, lightweight materials, intelligent high-speed bogies and rack formations are developed. However, the bogie as a key bearing component for running, its structural safety, and system stiffness matching is restricted by lightweight.

The weight of a train car is of two types: sprung weight and unsprung weight. The sprung weight mainly includes weight lying over the suspension springs, e.g., engine, passenger bogie, and electrical and mechanical components. The unsprung

weight includes the weight attached to the bottom of the suspension system, e.g., wheel weight, braking system, etc. The stiffness of suspension springs affects the movements of sprung weight, and thus, it is adjusted as per the requirement. Low stiffness increases ride comfort by absorbing jerks, however, at the cost of increased rolling and diving during turning, braking and acceleration. The unsprung weight of the vehicle mainly affects the propulsion force requirement. Higher unsprung weight increases the force required to move the vehicle forward, which directly increases the force exerted on the suspension springs. Thus, it also affects the balance of sprung weight of the vehicle. Therefore, reducing the unsprung weight becomes important in high-speed railways along with the reduction of sprung weight [86, 87].

The unsprung weight can also be of two types: static and dynamic. Static weight is the weight of vehicle at rest. However, dynamic weight is the additional weight added over the static weight during movement because of the effects of high-frequency wheel-rail interaction, inertial effects, damping and stiffness effects, etc. According to the research results of high-speed EMU with the increase of vehicle speed, the larger unsprung weight increases the amount of track subsidence [86]. This increases the cost of line maintenance and thus also reduces the safety of vehicle operation. To reduce the unsprung weight, the method is to follow a lightweight design for the unsprung, inter-sprung, and sprung weight of the bogie [86, 87]. However, reducing the unsprung weight is found most effective in reducing the dynamic wheel weight of the vehicle [87].

The unsprung components of high-speed trains mainly include wheel sets, axle boxes, and gears box. Components such as hollow axles and small diameter wheels are chosen to target weight and strength safety factors. Then reducing the weight of unsprung part and lightweight design of the framework is necessary to reduce the axle load. In addition, the integrated base brake technology and application of permanent magnet motor technology are also for reducing the spring mass of high-speed trains [87]. The lightweight provides a wider space.

For this purpose, a carbon fiber frame is developed and tested in China. It is found to achieve 40% weight reduction as compared with aluminum alloy frame. At the same time, a carbon-ceramic brake disk is also developed, which is similar to the steel brake disk to achieve a weight loss of more than 30% [83].

Research is still going on to further improve the safety, stability, comfort of train ride, and economy of use at high speeds. The use of Jacobian bogies (articulated train sets) started in 1930s to fulfill the same purpose [6, 15]. Figure 8 represents the bogie arrangement in articulated train set. Use of such train sets starts in Germany that was later followed by USA. Today, this set configuration is used in almost all high-speed rail sets worldwide [15].

In articulated train sets also known as Jacobian bogies, train bogie is fitted between the two train cars as shown in Fig. 8, whereas in conventional set, each car is supported on two bogies. Thus, articulated train set needs a lesser number of bogies as compared to conventional one that helps in reducing the train weight per length. This not only increases the strength of the train set, eases the high-speed operation, faster turning, and reduces the wheel to rail squeaking noise. This configuration is also known for its safety, as it has reduced the severity of many train accidents, e.g., TGV train accident
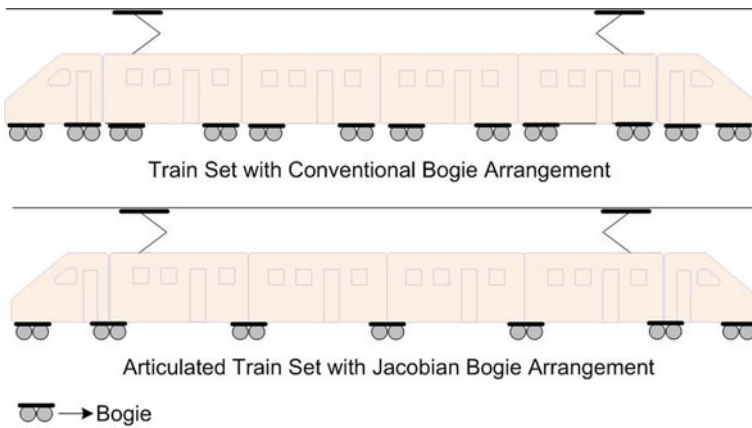
Fig. 8 Train bogie arrangements

in 2000, in which the use of articulated train sets had prevented any major life loss from happening [88].

Other than articulated train sets, titling train technology as shown in Fig. 9 is also been used by some European countries for increasing speed of train especially at turns [16, 89]. Tilting technology enhances the average speed of the train. This is achieved by generating inward tilt at turnouts to reduce lateral acceleration. This helps in traversing the curves at higher speeds.

The train sets are generally tempered to implement this technique [16, 89]. This technology has helped in achieving speeds up to 200–250 km/h. At present, this technology is under use by many parts of the world for increasing the train speeds, e.g., Japanese Shinkansen, German ICE, Spanish Talgo trains, etc. [15, 16, 88, 89].

Fig. 9 Tilting train mechanism for enhancement in average speed at turns
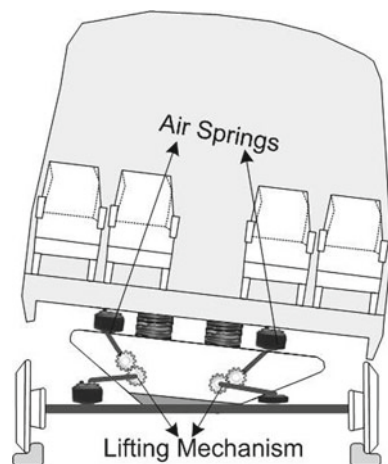
3.9 Advancements in Traction Motors

The motors used in high-speed rails are an important concern as operation of these trains requires high propulsion force. Thus, for attaining high-speed operations, many modifications are done in electrical motors worldwide. The selection of motors is generally done on the basis of their weight, size, electrical loading, magnetic loading, power density, efficiency, maintenance needs, acoustic noise, fault tolerance, cost, vibration, ruggedness, capability to operate in adverse environments, etc.

The use of three-phase induction motors (IM) has been dominant in rail propulsion applications since the day when the importance of using three-phase AC motors for traction applications was realized [36, 90].

In 1990s, three-phase permanent magnet synchronous motors (PMSMs) were incorporated in European AGV [91]. This motor is occasionally used in French TGVs also. Since PMSMs reduce inherent rotor losses, possess high-power density, high efficiency with high-power factor hence in last 15 years, PMSMs are slowly replacing the IMs in many rail systems, e.g., Tokyo metro [92]. However, this motor suffers from disadvantages like demagnetization due to high currents or temperature, need of individual inverter per motor, complex control, and less fault tolerance capability. Thus, the search for a perfect traction motor for high-speed rails has attracted the researchers toward motors such as switched reluctance motors (SRMs) and synchronous reluctance motors (SynRMs) [20, 91].

The SRMs have the capability to be a suitable alternative to PMSMs due to their simple construction, robustness, high fault tolerance, absence of magnets, low inertia, low manufacturing cost, and capability to operate at high temperature [93, 94]. However, due to its high torque ripples, high vibrations, high acoustic noise, complex control, and lesser efficiency than PMSMs, this motor is still under trial for traction applications.

Similar is the case with SynRM. These motors are said to be the best alternative to IMs due to their high torque density and high efficiency [95]. However due to low power factors and speed limits, this motor is also under trial for traction applications [90].

At present, PMSMs are used by Alstom and some Japanese companies for traction purposes, whereas IMs are used by Siemens, ABB, and many other Japanese companies [27, 90]. PMSMs and SRMs are found to be suitable for low-floor train sets due to low inertia and low gear losses that helps in reducing the bogie size.

Since the use of rotary motors as a propulsion drive in traction systems, the development of high-speed rail has seen many changes around the world [8, 9]. However, the torque produced by rotary motors is converted into translational force by mechanical gears and wheels [96], whereas linear motors generate translational motion without the use of any gear mechanism. Thus, they provide reliable and noiseless train operation, free from adhesion between rail and wheels. Linear motors eliminate not only compressor pipe valves losses but also reduce backlash problems that may arise due to the use of gears [8, 9]. Linear drives give easy traversing of sharper track profiles. Direct linear drives are free from acceleration and speed

restrictions due to adhesion between wheel and rail. Thus, they provide much better speed performance. Therefore, linear motors are becoming popular as propulsion drives in high-speed rail systems [96]. The next section provides insight about linear motor-propelled high-speed rail systems.

4 Development of Linear Motor-Propelled Rail Technology

Continuous struggle to achieve betterment in high-speed rail technology has accelerated the development of linear motor-propelled rail system worldwide. These systems are generally based on magnetic levitation technology and commonly known as Maglevs. Due to global adversities related to transport, fuel, and environments, Maglevs are rapidly finding their place in mainstream of public transport.

Maglev systems are characterized by predominant use of magnets in place of rail wheels. Figure 10 represents the basic components of a Maglev system. These systems generally consist of major components such as magnetic levitation, linear propulsion, guidance, contactless power supply, operation, and control.

4.1 Magnetic Levitation

Magnetic levitation technology is the major part of this rail system as it generates sufficient levitating force to lift the train set in upward direction. This allows the vehicle to move freely over the tracks without any use of rail wheels. Magnetic levitation force is achieved by using different magnets in the system such as electromagnets (EMs), permanent magnets (PMs), superconducting magnets (SCMs), and hybrid magnets (HMs). As shown in Fig. 11, with the use of different magnets, different technologies are developed to generate levitation force based on which Maglev systems can be classified as electrodynamic suspension system (EDS), PM EDS, electromagnetic suspension system (EMS), and hybrid EMS [6, 8, 9, 97].

Basic Components of a Maglev System

Magnetic Levitation Mechanism	Linear Propulsion Mechanism	Guidance Mechanism	Contactless Power Supply Mechanism	Operation & Control Mechanism
• provides upward push to the vehicle to make it glide over the track	• propels the vehicle forward • uses linear motors	• controls the lateral shift of the vehicle • keeps it centralized at all times	• transfers power from ground to vehicle • uses magnetic coupling • no physical contact like pantographs	• monitors the operation of complete system • controls & maintains synchronism between ground stations & vehicles

Fig. 10 Basic components of a Maglev system

Fig. 11 Maglev systems based on different levitation techniques [100]

The basic representation of all these systems is shown in Fig. 11. The EDS system generates the levitation by using repulsion between magnets fitted on tracks and onboard magnets as shown in Fig. 11. This technology generally uses SCMs as it requires strong magnets. It produces levitation of the order of 10–15 cm [98]. At present, Japanese SCMaglev uses this technology for producing levitation [97]. However, use of SCMs not only increases the capital cost and cryogenic requirements but also increases the ride discomfort due to high magnetic field thus further increases the cost of magnetic shielding [3, 98].

To counter these drawbacks, PM EDS technology is developed in which SCMs are replaced by PMs as shown in Fig. 11. However, like EDS system, system based on this levitation technology also needs wheels on which the vehicle must roll at the start to generate required levitation force. In this the PMs are arranged in the form of Halbach array that is known to produce the sinusoidal field on one side and nullifying it on the other side [99]. This field interacts with short-circuited track coils to produce levitation. At present, this technology is under testing in the USA. China is also testing the combination of SCMs and PMs since 2002 [98, 99]. One of the drawbacks of this technology is the higher-order harmonics generated by the PMs Halbach array that introduces oscillations in the system.

Due to problems associated with EDS systems, EMS system came into existence. In this system, levitation is generated at rest thus requires no wheels. This system uses magnetic attraction between magnets fitted on track and onboard electromagnets.

The use of EMs vastly reduces the capital cost of the system [100]. However, it only produces levitation of the order of 1–2 cm [101]. The existing EMS technology mainly uses two configurations: one with integrated levitation and guidance circuit and another with separated levitation and guidance circuit as shown in Fig. 11. The EMS system with integrated levitation and guidance circuit is presently under use in Shanghai Maglev, Korean UTM, and Japanese HSST [100]. This configuration helps in cutting down the number of power ground converters and electromagnets however, at the cost of increased interference. To counter these problems German Transrapid (TR09) uses EMS technology with separated levitation and guidance circuit however that results in increased capital cost due to more converters and electromagnets [8, 9, 98–100]. The major concern of EMS system is the controlling of small air-gap throughout the run of the vehicle [101, 102].

Thus, to increase the air-gap in EMS system, hybrid EMS technology is developed [103]. At present, this technology is under use in China. This system uses a combination of EMs and PMs to achieve higher air-gaps as shown in Fig. 11. Use of PMs reduces the power requirement of the system. In this, at the start of the vehicle both magnets power the vehicle, and once the levitation stability is reached, the EMs are de-energized to save energy. This system produces levitation of the order of 2–3 cm.

4.2 Linear Propulsion

Currently, high-speed Maglev rail systems generally operate at maximum speeds higher than 400–500 km/h. At such high speed, the system requires contactless propulsion mechanism. Thus, linear motors become a natural choice for such applications as they produce propulsion force without any gear transmission. Also, the propulsion produced by these motors is free from wheel-rail adhesion. Linear motors not only produce propulsion but they also generate required braking force for this system. Thus, these linear motors must possess characteristics like high power and force density with high efficiency, high fault tolerance, low losses, etc. [104]. The commonly used linear motors for producing linear translation motion are shown in Fig. 12.

The linear motors can be broadly classified as linear DC and linear AC motors. Linear DC has two versions: brushed and brushless DC, whereas linear AC can be asynchronous motors and synchronous motors. Asynchronous motors include induction and reluctance motors. The working principle of each linear motor is similar to their rotary counterpart. Every rotary motor has two parts: a rotor and a stator. As shown in Fig. 13, the formation of a linear motor can be imagined as if its associated rotary motor is cut along its axis of rotation (Y–Y′) and flattened after it is opened. After cutting, rotor part of rotary motor forms the translator of linear motor.

Every linear motor consists of two main parts: a stator and a translator. Out of these two parts, one remains stationary and other moves or glides over the stationary part to produce the required propulsion force. As per the application, any of the two parts can be made stationary or moving. This design flexibility gives birth to many possible configurations of each linear motor. However, linear motors with flat configurations are most effective in traction applications as shown in Fig. 14. Because they produce higher propulsion force along with the capability of the direct drive transmission. They not only decrease the mechanical gear transmission losses but also produce smoother translation as compared to rotary motors.

Based on the location of the stator, motor can be short stator or long stator type [104]. In short stator type, stator forms the moving part, while translator forms the

Fig. 12 Classification of linear motors used for traction applications
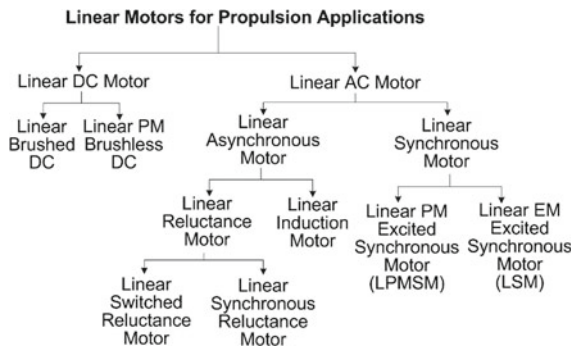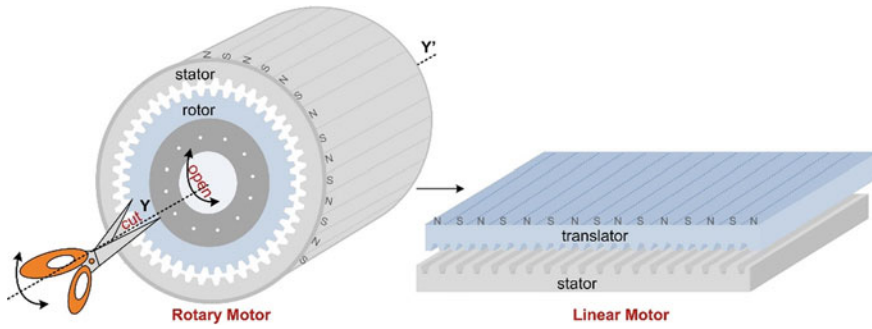
Fig. 13 Conversion of linear motor from rotary motor
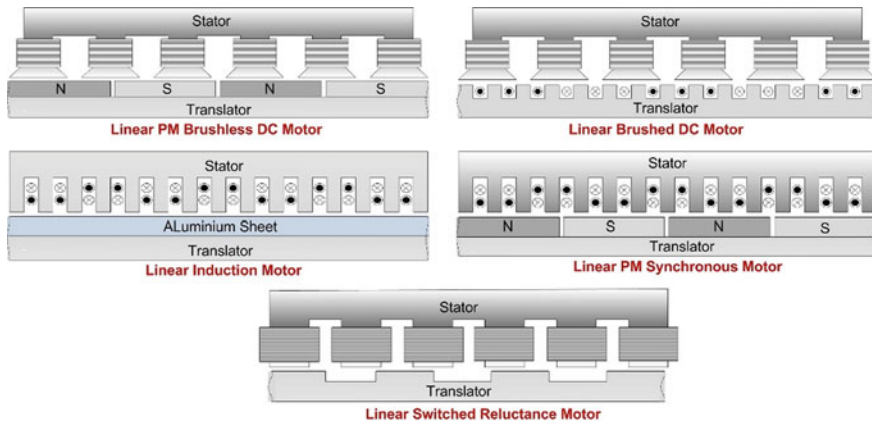
Fig. 14 Flat configurations of different linear motors

track. While in its long stator variant, translator moves along the motion track formed by the stator.

Short stator configuration reduces the cost of track construction and makes the controlling of the motor easier, but additional onboard supply arrangement and controllers increase the weight of the vehicle [3, 6–10]. This configuration is preferred for low to medium speed applications of up to 250 km/h, due to requirement of current collection arrangement to feed the onboard stator coils. This configuration also possesses low energy efficiency due to high drag force and high leakage inductance because of end effect of the motor. In short stator motor, exit side end effect produces backward force on the translator, which decreases the net propulsion force of the motor.

In practical high-speed Maglev systems, long stator motor configuration is a popular choice [8–10]. This configuration is preferred as it does not require any current collector. Ground side converters control the supply of the stator windings. The stator coils are laid into various sections to form the guide way. Separate inverters

are installed to energize each of these sections. Thus, long stator configuration needs an extra control circuit to check and maintain the section supply as the train passes from one track section to the next track section.

Linear DC motor is one of the options available for producing linear propulsion. However, its brushed version is not found suitable for use in high-speed Maglev systems due to the presence of commutator and brushes. In its brushless version, PMs are used along with the electronic switchers to replace mechanical brushes. However, brushless linear DC is found to be suitable for servo applications rather than high-power traction applications [105]. It is preferred in applications requiring translational range of 1–10 cm such as digital cameras and disk drives chart recorders.

Thus, linear induction motors are generally chosen for Maglev applications [106, 107]. At present, this motor is under use in Japanese HSST Maglev system that is a medium speed system [8]. In this system, the motor stator is attached to the underframe that moves with the vehicle which gives it a short stator configuration as described earlier, whereas the translator consisting of an aluminum sheet laid over a ferromagnetic slab forms the track structure. Energized distributed stator windings generate moving magnetic flux. This flux links with the translator to produce eddy currents. These eddy currents when interact with stator flux generate required propulsion.

Advantages of this structure include simple and comparatively cheaper tracks [6–9]. However, it produces heating of tracks due to eddy currents that also increase the losses in the system. This motor also suffers from faults such as single phasing, crawling, overvoltage, under voltage, and inter-turn faults [106, 107].

Thus, to overcome these drawbacks, linear synchronous motor evolved as its alternative. This motor possesses high force density along with high efficiency and high-power factor as compared to linear induction motors. Therefore, it is under use in almost all the high-speed Maglev systems worldwide including Chinese Shanghai Maglev, Japanese SCMaglev, German Transrapid, etc. [3, 6–9].

Since it is a doubly excited motor, it incorporates a DC excitation source in its structure. To make the system contactless, generally PMs are used for DC excitation and fitted in the translator. The translator forms the onboard part and moves with the vehicle [108]. The distributed stator windings are laid on the tracks and energized with the help of ground converters which gives it a long stator configuration. Excitation of stator windings generates moving flux that moves at synchronous speed. DC magnets fitted on translator generate constant flux [106–108]. When both of these fluxes interact, a magnetic locking is produced that impels the translator to move at synchronous speed.

However, this motor requires precise position monitoring to maintain synchronism with the moving flux generated by stator windings, which makes the track structure complex and costly [109]. Also, use of double excitation sources increases its cost and losses. Vehicles propelled by linear synchronous motor have limitations such as accommodation of only one vehicle at a time in any track section. The other vehicle cannot enter the section unless the first one clears it to maintain the synchronism. Thus, operation of more trains needs more tracks that not only increases control and monitoring needs but also increases converter requirements [106–109].

To counter these limitations, the linear switched reluctance motor is being seen as a suitable alternative to all these motors for traction applications. As this motor possess simple construction, low cost, high starting force, low losses, absence of magnets with single excitation, and high fault tolerance due to phase independence, it is under trial for traction applications in many parts of the world [110]. Thus, the search for finding perfect motor for traction propulsion is still going on.

4.3 Guidance

Guidance mechanism in Maglevs is inevitable as it helps in controlling the lateral displacement of the vehicle. Technology in guidance systems uses either repulsive forces or attractive forces between the two magnets to centralize the vehicle [111]. These two magnets are laid on the sideway tracks and side of the vehicle. Every guidance system contains two pairs of such magnets that produces unidirectional force [111–113]. Both of these left and right magnets are connected with the suspension under frame in systems using attractive forces for guidance as shown in Fig. 15a.

In guidance using attractive forces, the left pair of magnet generates force toward right and right magnet pair produces force toward left as shown in Fig. 9a. Lateral forces generated by these magnet pairs are transferred through suspension frame. The magnitude of these forces changes as per the position of the vehicle to maintain the centralized position of the vehicle. At stable position, the net force produced by the magnet pairs remains nearly zero. But when the vehicle displaces, the force on the other side of the magnet pair increases that pulls the vehicle toward its original position [112, 113].

While using repulsive forces in guidance, the direction of force produced by the two magnet pairs remains toward the sideway tracks as shown in Fig. 15b. It means left magnet pair produces force toward left and right magnet pair produces force toward right. At normal position, the net force produced by these magnet pairs equals nearly zero. However, when the vehicle shifts sideways, the repulsive force
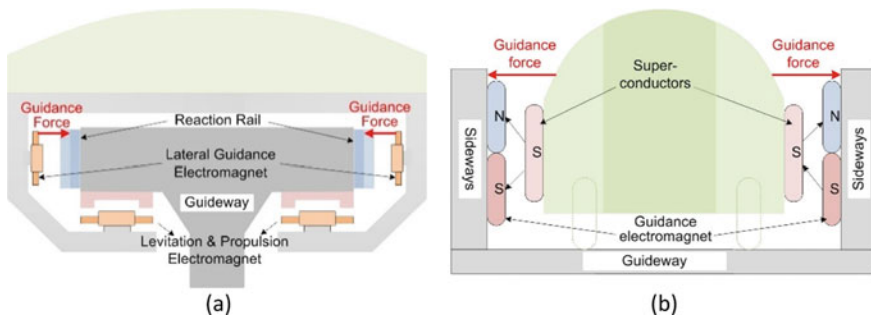
Fig. 15 Guidance system using **a** attractive forces and **b** repulsive forces

on that side of the magnet pair increases that pushes the vehicle toward its original position.

Japanese MLX and MLU uses magnetic repulsive forces in their guidance system. German Transrapid also uses repulsive force-based guidance technology [3, 8, 9, 111], whereas Japanese HSST Maglev uses magnetic attractive forces in their guidance system [8, 111].

The operating characteristics of this system change according to the guideway design and weather conditions. Thus, this system has higher uncertainties and needs precise control mechanism.

4.4 Contactless Power Supply

In high-speed Maglevs operating at 400–500 km/h, mechanism to transfer the power supply to the vehicle becomes crucial. At such high speeds, transfer through mechanical contacts like pantograph is not feasible [114, 115]. Thus, different contactless supply systems are designed for use in different high-speed rail systems worldwide. The input power supply received inside the vehicle powers the levitation coils, propulsion coils, and other onboard equipment. For transfer of power, generally linear transformers and linear generators are used.

Power supply network of any Maglev system consists of supply substations, feeder cables, track coils, switching stations, converters, and other equipment. In Chinese Maglev, 110 kV AC is taken from a power grid, which is stepped down to 20 kV AC and 1.5 kV AC [114, 115]. This is converted to DC that later gets converted to variable frequency AC (0–300 Hz) [115]. This AC output excites the stator windings of linear synchronous motors laid on the guideway. To transfer this ground supply to the vehicle Chinese Shanghai Maglev uses two methods. When speed is less than 100 km/h, the third rail is used for power transfer, and when the speed is more than 100 km/h, power is transferred electromagnetically using linear generator coils fitted on the vehicle [114]. These onboard generator coils derive power from energized long stator coils laid on tracks wirelessly.

German Transrapid Maglev system also uses similar system in which generator coils are integrated with levitation electromagnets. Coils energized with supply of frequency 6 times more than the synchronous frequency are laid on tracks that transfers this energy to onboard generator coils [115, 116].

Japanese MLX uses concentrated type and distributed type linear generators along with a gas-turbine generator [24, 116]. Thus, this system does not require installation of any high-frequency transferring coils neither does it need current collecting rails. Longitudinally fitted onboard coils perform the functioning of distributed generator's coils that are integrated with onboard superconductors. The concentrated generator's coils are laid at both ends of the vehicle. As the vehicle moves, constant flux produced by superconductors links with guidance and levitation coils on both sides of the track. The flux from these sideway coils further links with onboard generator coils. Thus, in this process constant flux by superconductors changes into AC via linear generator.
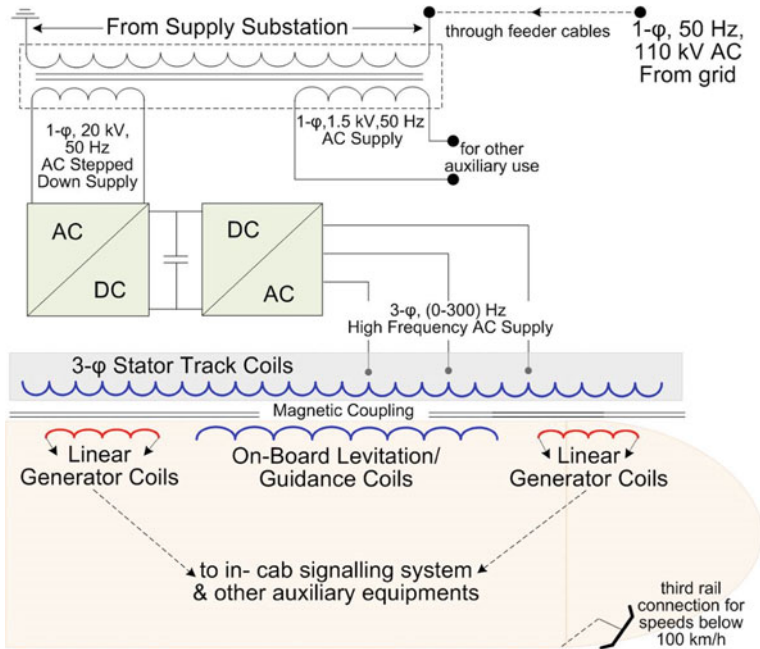
Fig. 16 Contactless power supply arrangement

The major disadvantage of this system is the use of onboard gas turbines which increases vehicle's weight [24] (Fig. 16).

However, high-speed trains carry auxiliary power sources of a few kW to energize air-conditioners, lights, cryogenic cooling systems, and other accessories. Thus, this explains the importance of suitable power transfer method in a high-speed rail system [114–116].

4.5 Operation and Control

A high-speed Maglev system mainly consists of components such as ground supply system including converters, traction transformers, track coils, levitation system, guidance system, high-speed rail set, etc.

To ensure the safety and reliability of all these components, their operation and control mechanism is highly crucial. This mechanism monitors the operation of the complete system as shown in Fig. 17.

The operation and control of the system need real-time data collection through vehicle-ground, vehicle to vehicle, and vehicle's onboard communication channels. To manage high-speed systems, the wireless channel is used for communication. Thus, the control circuitry forms an important part of any Maglev system [96].
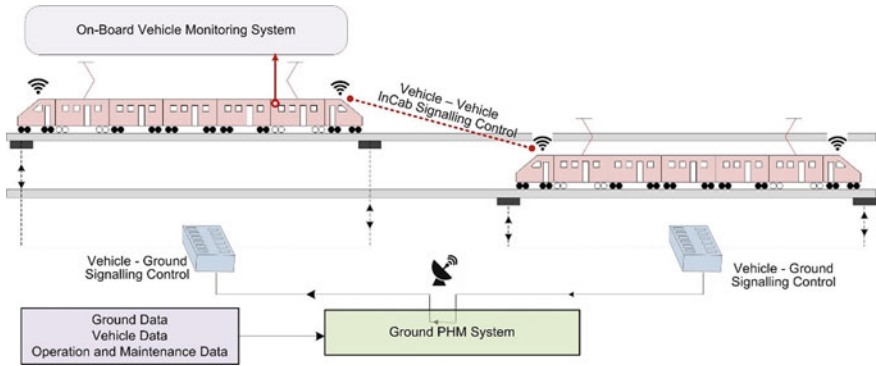
Fig. 17 Block diagram representation of operation and control

To accomplished the task of monitoring such a fast-expanding high-speed rail network, requirement of high-performance and intelligent sensor technology is inevitable.

A normal function of a sensor is to detect and convert the sensed value into electrical signals as per the settings [117]. Thus, the installed sensors sense transient changes in the values due to external factors. These sensed signals are transmitted to a control and logic unit that reads and compares these values with the reference values. The identified error is transmitted to a conditioning unit for taking the suitable action. Therefore, sensors play an important role in safety of train operation, identifying the system condition in real time, acquiring data to support intelligent train controlling mechanism and intelligent monitoring system [102, 103].

Thus, in Maglev systems to develop a fully automatic and intelligent control system, the use of these sensors is imperative. Therefore, the Chinese high-speed rail CRH380A uses more than 1000 sensors [117].

In a rail system, the sensors are generally employed for sensing currents, voltages, speeds, and temperatures. The conventional sensors are not suitable to fulfill these sensing requirements in a high-speed rail system due to the presence of heavy insulation and electromagnetic interference.

Thus, intelligent sensing technology using optical fiber sensors is rapidly finding its place in intelligent rail control systems. The main advantages of the optical fiber sensors include immunity to electromagnetic interference, smaller weight and size, high sensitivity, immunity of adverse environment conditions, etc. [20, 25]. The block diagram representation of intelligent control circuit using intelligent sensors is given in Fig. 18.

Intelligent sensing system contains a built-in microprocessor that processes the sensed value and converts the signal into appropriate form before sending it to the output terminal of network interface.

These intelligent sensing systems have self-learning, self-correcting, and self-diagnosing abilities. The potential of artificial intelligence realizes energy saving,
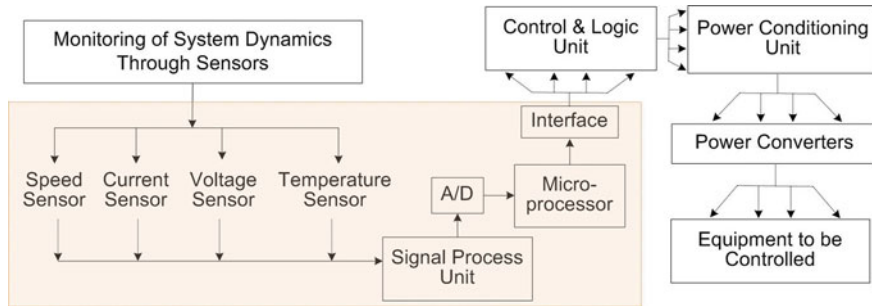
Fig. 18 Block diagram representation of intelligent control system

cost reduction, and efficiency improvement. It has promoted the development of the industrial chain.

The application directions of artificial intelligence in train equipment include data-driven predictive modeling and analysis, forecast-based resource effectiveness and operations, decision optimization, and cyber-physical systems modeling. The deepening of industry-based Ethernet network, fusion control technology, and realization of artificial intelligence technology have promoted the realization of intelligent operation and maintenance, unmanned driving, and modern intelligent service.

5   Present Scenario of High-Speed Rail Technology and Its Relevance to Country like India

After reviewing the progress achieved by various countries in high-speed rail technologies, it has been found that mainly either wheel-based systems are modified to achieve improvements in speed performance or linear motor powered Maglev systems are developed to achieve even greater speed. Figure 19 shows the various high-speed wheeled rail systems around the world [6–10, 27, 107].

It is clearly seen that these systems although adopted various structural modifications, but mainly used rotary motors such as induction or PM synchronous motors for their propulsion. This technology is mainly adopted by European countries.

To deal with the growing transportation crisis and environmental issues around the world, linear motorized Maglev systems are gradually taking their place in mass transportation systems. Shanghai Maglev (China) and HSST (Japan) have been operating since December 2002 and March 2005, respectively. Based on indigenous Chinese technology, the low-medium speed Maglev in Changsha (China) has been operating since 2016.

Currently, China has the largest commercial HSR network in the world [1, 2]. Following this leap taken by China, countries such as Morocco, Saudi Arabia, USA, Australia, Italy, and Spain are also developing HSR [1, 2]. Figure 20 shows the major linear motor-propelled rail systems operating worldwide [3, 6–10, 24, 104,

- Italo & Frecciarossa
- Italy
- Speed : 300-350 km/h
- Propulsion : Rotary PMSM/IM
- Tilting, High-Speed

- Eurostar
- Europe
- Speed : 300-320 km/h
- Propulsion : Rotary IM
- High-Speed Rail

- Fuxing Hao
- China
- Speed : 350-420 km/h
- Propulsion : Rotary IM
- High-Speed Rail

- Shinkansen
- Japan
- Speed : 250-300 km/h
- Propulsion : Rotary IM
- High-Speed Rail

SOME OF THE ROTARY MOTOR PROPELLED WHEELED RAIL SYSTEMS WORLDWIDE

- Renfe (AVE)/ Talgo
- Spain
- Speed : 300-350 km/h
- Propulsion : Rotary IM
- Multi-Gauge, High-Speed

- Korail (KTX)
- South Korea
- Speed : 300-330 km/h
- Propulsion : Rotary PMSM/IM
- High-Speed Rail

- Deutsche Bahn ICE
- Germany
- Speed : 250-300 km/h
- Propulsion : Rotary IM
- High-Speed Rail

- Thalys
- Europe
- Speed : 250-300 km/h
- Propulsion : Rotary SM
- High-Speed Rail

- Haramain Railway
- Saudi Arab
- Speed : 300-350 km/h
- Propulsion : Rotary IM
- High-Speed Rail

Fig. 19 Some rotary motor-propelled wheeled rail systems worldwide

107]. USA's Inductrack and Korea's UTM have been under research since the 1990s. It is clearly seen that Maglev systems are far better in achieving higher speeds.

However, Maglev technology is the most expensive rail technology. It is also been observed that this technique is mainly adopted by the developed countries. These systems also see the predominant use of linear induction motors and linear synchronous motors.

Developing countries like India are also trying to develop high-speed rail network. India has not only modified its existing rails, but has also shown its readiness to join the global high-speed group by forming the High-Speed Rail Cooperation (HSRC) in 2012 [118]. The country is investing heavily in the manufacture of Maglev rail system in India. However, Maglev technology in its present form is not feasible in the Indian scenario due to its excruciating capital cost.

India needs to develop its technology according to its demographic and economic needs. Linear motor-propelled wheeled rail technology can help India to achieve its goal. The use of motors such as the linear switched reluctance motor may offer cheaper technological advancements for a developing country such as India. Thus,

- TELMAG Monorail
- Venezuela
- Under trial
- Propulsion : linear reluctance motor
- Non-Maglev

- Transrapid
- Germany
- Speed : 450–500 km/h
- Propulsion : LSM
- Under Trial
- High-Speed Rail

- Linear Metro
- Metro Rail, Japan
- Speed: 60–70 km/h
- Propulsion : LIM
- Rapid Transit

SOME OF THE
WHEELED/NON-WHEELED
LINEAR MOTOR PROPELLED
RAIL SYSTEMS WORLDWIDE

- SCMAglev
- Japan Railways
- Speed : 500–600 km/h
- Propulsion : LSM
- High-Speed Rail

- General Atomics
- USA
- Speed : 150–160 km/h
- Propulsion : LSM
- Under Testing
- Maglev (EDS w PM)

- Innovia Metro
- Bombardier, Alstom
- Speed: 80–100 km/h
- Propulsion : LIM
- Adv. Rapid Transit

- Moscow Monorail
- Russia
- Speed : 60–70 km/h
- Propulsion : LIM
- Wheeled, Non-Maglev
- Rapid Transit

- Shanghai Maglev
- China
- Speed : 500–600 km/h
- Propulsion : LSM
- High-Speed Rail

*Image courtesy : https://en.wikipedia.org/wiki/TELMAG
https://i.pinimg.com/originals/df/fb/07/dffb0753cb12cd9115b4b9f359dae6c7.jpg
https://en.wikipedia.org/wiki/Transrapid
https://www.maglev.net/media/articles/72/general%20atomics%20maglev%20test%20track.jpg
https://image.shutterstock.com/image-photo/yamanashi-japan-june-12-linear-260nw-287697098.jpg
https://en.wikipedia.org/wiki/Bombardier_Innovia_Metro
https://en.wikipedia.org/wiki/Moscow_Monorail
https://en.wikipedia.org/wiki/Shanghai_maglev_train

Fig. 20 Some linear motor-propelled rail systems worldwide

it is being suggested to develop such rail technology, which combines the features
of both the wheeled rail and Maglev rail high-speed technologies. Currently, such
mergers are used by Russia in its Moscow monorail system as shown in Fig. 18
[119]. It is a wheeled rail system that uses linear induction motor for its propulsion.
However, the operating speed of this non-Maglev monorail system is only 60 km/h.
Similar technology using linear reluctance motors in non-Maglev system is under
trial in Venezuela [120].

In such a situation, the merger of technologies can prove to be a boon for countries
like India. After reviewing the inherent benefits of linear switched reluctance motors,
it is concluded that using linear switched reluctance motors in wheeled rail systems
for their propulsion can help develop a new rail technology that can further reduce
capital costs with improved performance features.

The use of linear switched reluctance motor can open myriad opportunities for developing countries like India. The applicability of linear switched reluctance motor-based technology extends its benefits not only in high-speed technologies but also in suburban transport technologies.

Similarly, the concept of using hybrid-excited magnets in Maglev applications is under testing and research. This technology also shown its capabilities to reduce the use of costly PM and superconducting magnets in Maglev systems, which can further help in reducing its cost.

6   Conclusion

Concurrent and futuristic global concerns have given consistent stimulus to the development of high-speed rail systems, since their materialization.

This chapter presented a comprehensive review about the existing high-speed rail technologies worldwide along with their components. This kind of rail system depends upon its components. The eclectic review of components of high-speed rail systems indicates that the modification and customization of these components change a system completely. This flexibility enticed different countries to modify and develop this system as per their stipulations. Because of which this rail system varies from country to country. Though, search for better transportation systems encouraged the development of high-speed rails systems worldwide. Still only, a few countries have the knowledge and expertise to develop such a system.

It is seen that mainly either the components of wheeled rail systems are modified to develop high-speed wheeled rail systems or the levitation-based linear motor-propelled Maglev systems is developed to get high-performance and faster rail systems.

European countries have mainly relied on revising the wheeled rail system, which makes it a low-cost setup as compared to the Maglev system. However, these kinds of system suffer from speed limitations. The use of rotary induction and rotary synchronous motors is predominant in such systems.

The rotary motors increase the losses due to the use of gear transmission assembly required to transform rotary motion into linear motion. The high-speed wheeled rail systems suffer from performance limitations posed due to dependency on track-wheel adhesion. This system also faces losses due to mechanical contact.

Conversely, it is also found that linear motor-propelled Maglev systems have far better performance due to the natural benefits of using linear motors for propulsion. The Maglev technology, used by countries like Japan, China, and Germany, relies on developing dedicated structure which offers huge range of speed. However, initial cost of building such a system is humongous.

India is also stepping toward accepting this HSR technology. India is either modifying its existing rail system or developing a dedicated corridor for Maglev system. However, just like other countries, India needs to develop a system as per their demographic and economic requirements. It is seen that the Maglev systems are though

popular but not feasible for developing countries like India due to their extremely high capital cost.

Thus, replacement of rotary motors with linear motors in the rail propulsion system can help in developing a new high-speed rail technology with a combination of both the existing HSR technologies. This new technology can help countries like India to increase the speed of their existing system at a comparatively lower cost.

References

1. UIC, O.: Railway Handbook 2018: High Speed Rail Fast Track to sustainable Mobility (2018)
2. UIC, O.: Railway Handbook 2017: Energy Consumption and CO_2 Emissions (2017)
3. Zhou, L., Shen, Z.: Progress in high-speed train technology around the world. J. Mod. Transp. **19**(1), 1–6 (2011)
4. Duffy, M.C.: Electric Railways: 1880–1990. The Institution of Engineering and Technology, Chicago (2003)
5. Richmond, V.: Milestones: Richmond Union Passenger Railway, 1888. IEEE Richmond Section (1992). https://ethw.org/Milestones:Richmond_Union_Passenger_Railway,_1888
6. Campos, J., de Rus, G.: Some stylized facts about high-speed rail: a review of HSR experiences around the world. Transp. Policy **16**(1), 19–28 (2009)
7. Powell, J., Danby, G.: Maglev: transport mode for the 21st century. Executive Intell. Rev. **737**, 44–55 (2007)
8. Uzuka, T.: Faster than a speeding bullet: an overview of Japanese high-speed rail technology and electrification. IEEE Electrification Mag. **1**(1), 11–20 (2013)
9. Koseki, T.: Technical trends of railway traction in the world. In: International Power Electronics Conference (ECCE ASIA), pp. 2836–2841, Sapporo, Japan (2010)
10. Boldea, I., Tutelea, L.N., Xu, W., Pucci, M.: Linear electric machines, drives, and MAGLEVs: an overview. IEEE Trans. Industr. Electron. **65**(9), 7504–7515 (2018)
11. Sekar, S.P., Gangopadhyay, D.: Impact of rail transit on land use and development: case study of suburban rail in Chennai. J. Urban Plann. Dev. **143**(2), 1–10 (2017)
12. Anson, E.H., Kimball, R.L.: An electric system for monorail rapid transit. Trans. Am. Inst. Electr. Eng. Part II: Appl. Ind. **73**(5), 225–227 (1954)
13. Bhargava, B.: Railway electrification systems and configurations. In: IEEE Power Engineering Society Summer Meeting. Conference Proceedings, vol. 1, pp. 445–450, Edmonton, Canada (1999)
14. Mundrey, J.S.: Tracking for high-speed trains in India. RITES J **12**(7), 1–20 (2010)
15. Sharma, S.: Future of high speed trains in India and its comparative study with Japan, France, Germany and South Korea. IOSR J. Mech. Civ. Eng. Ver. III **12**(5), 2278–1684 (2015)
16. Agarwal, M.M., Miglani, K.K.: Challenges and possible solutions for appropriate track technology for mixed traffic regime of semi high speed and heavy axle loads based on global experience. In: Institution of Permanent Way Engineers, vol. 2, pp. 196–225, Mumbai, India (2017)
17. Uzuka, T.: Trends in high-speed railways and the implications on power electronics and power devices. In: IEEE 23rd International Symposium on Power Semiconductor Devices and ICs, pp. 6–9, San Diego, USA (2011)
18. Singh, B., Bhuvaneswari, G., Garg, V.: Improved power quality AC–DC converter for electric multiple units in electric traction. In: IEEE Power India Conference, pp. 1–6, New Delhi, India (2006)
19. Eckel, H.G., Bakran, M.M., Krafft, E.U., Nagel, A.: A new family of modular IGBT converters for traction applications. In: European Conference on Power Electronics and Applications, pp. 10–15, Dresden, Germany (2005)

20. Ronanki, D., Singh, S.A., Williamson, S.S.: Comprehensive topological overview of rolling stock architectures and recent trends in electric railway traction systems. IEEE Trans. Transp. Electrification **3**(3), 724–738 (2017)

21. Boora, A.A., Zare, F., Ghosh, A., Ledwich, G.: Applications of power electronics in railway systems. In: Australasian Universities Power Engineering Conference, pp. 1–9, Perth, Australia (2007)

22. Faddoul, R.Y., Stone, S.R.: Auxiliary inverters for traction. In: IEE Colloquium on GTO's, Rival Devices and Applications, pp. 4/1–4/9, London, UK (1988)

23. Shanghai Maglev Official Website: http://www.smtdc.com/en/gycf3.html. Accessed: 12 Apr 2022

24. Mochizuki, A.: Part 2: speeding-up conventional lines and Shinkansen. Breakthroughs in Japanese railways. Jap Railway Transp. Rev. **9**(58), 51–60 (2011)

25. Neil, G.: On board train control and monitoring systems. In: Proceedings of IET Professional Development Course on Electric Traction Systems, pp. 223–246, London, UK (2012)

26. Dong, H., Ning, B., Cai, B., Hou, Z.: Automatic train control system development and simulation for high-speed railways. IEEE Circuits Syst. Mag. **10**(2), 6–18 (2010)

27. Mermet-Guyennet, M.: New power technologies for traction drives. In: IEEE International Symposium on Power Electronics, Electrical Drives, Automation and Motion (SPEEDAM), pp. 719–723, Pisa, Italy (2010)

28. Ronanki, D., Williamson, S.S.: Evolution of power converter topologies and technical considerations of power electronic transformer-based rolling stock architectures. IEEE Trans. Transp. Electrification **4**(1), 211–219 (2018)

29. Kolar, J.W., Ortiz, G.I.: Solid State Transformer Concepts in Traction and Smart Grid Applications, pp. 1–185. Power Electronic Systems Laboratory, Swiss Federal Institute of Technology (ETH), Zurich (2013)

30. Adamowicz, M., Szewczyk, J.: SiC-based power electronic traction transformer (PETT) for 3 kV DC rail traction. Energies 13(21):5573, 1–30 (2020)

31. Kjaer, P.C., Norrga, S., Ostlund, S.: A primary-switched line-side converter using zero-voltage switching. IEEE Trans. Ind. Appl. **37**(6), 1824–1831 (2001)

32. Roy, S., De, A., Bhattacharya, S.: Current source inverter based cascaded solid state transformer for AC to DC power conversion. In: International Power Electronics Conference (IPEC-ECCE ASIA), pp. 651–655, Hiroshima, Japan (2014)

33. Zadeh, M.B., Fazel, S.S.: A new simple control approach of M2LC for AC railway applications. In: 4th Annual International Power Electronics, Drive Systems and Technologies Conference, pp. 407–415, Tehran, Iran (2013)

34. Liu, W., Zhang, K., Chen, X., Xiong, J.: Simplified model and submodule capacitor voltage balancing of single-phase AC/AC modular multilevel converter for railway traction purpose. IET Power Electron **9**(5), 951–959 (2016)

35. Glinka, M., Marquardt, R.: A new AC/AC multilevel converter family. IEEE Trans. Industr. Electron. **52**(3), 662–669 (2005)

36. Glinka, M.: Prototype of multiphase modular-multilevel-converter with 2 MW power rating and 17-level-output-voltage. In: IEEE 35th Annual Power Electronics Specialists Conference, vol. 4, pp. 2572–2576, Aachen, Germany (2004)

37. Zhao, C., Lewdeni-Schmid, S., Steinke, J.K., Weiss, M.: Design, implementation and performance of a modular power electronic transformer (PET) for railway application. In: Proceedings of the 2011 14th European Conference on Power Electronics and Applications, pp.1–10, Birmingham, UK (2011)

38. Steiner, M., Reinold, H.: Medium frequency topology in railway applications. In: European Conference on Power Electronics and Applications, pp. 1–10, Aalborg, Denmark (2007)

39. Hugo, N., Stefanutti, P., Pellerin, M., Akdag, A.: Power electronics traction transformer. In: European Conference on Power Electronics and Applications, pp. 1–10, Aalborg, Denmark (2007)

40. Martin, J., Ladoux, P., Chauchat, B., Casarin, J., Nicolau, S.: Medium frequency transformer for railway traction: Soft switching converter with high voltage semi-conductors. In:

International Symposium on Power Electronics, Electrical Drives, Automation and Motion, pp. 1180–1185, Ischia, Italy (2008)

41. Bhajana, V.V., Drabek, P.: A new ZVS-ZCS multilevel DC/DC converter with current fed dual active circuits for traction applications. In: Proceedings of the 2014 15th International Scientific Conference on Electric Power Engineering (EPE), pp. 547–552, Brno-Bystrc, Czech Republic (2014)

42. Tan, X., Ruan, X.: Equivalence relations of resonant tanks: a new perspective for selection and design of resonant converters. IEEE Trans. Industr. Electron. **63**(4), 2111–2123 (2016)

43. Huber, J.E., Kolar, J.W.: Optimum number of cascaded cells for high-power medium-voltage AC–DC converters. IEEE J. Emerg. Sel. Top. Power Electron. **5**(1), 213–232 (2017)

44. Ozpineci, B., Tolberti, L.M.: Comparsion of Wide Bandgap Semiconductors for Power Applications, pp. 1–34. Oak Ridge National Laboratory, Department of Energy, U.S.A (2003)

45. Zhang, H., Tolbert, L.M.: Efficiency impact of silicon carbide power electronics for modern wind turbine full scale frequency converter. IEEE Trans. Industr. Electron. **58**(1), 21–28 (2011)

46. Ishikawa, K., Yukutake, S., Kono, Y., Ogawa, K., Kameshiro, N.: Traction inverter that applies compact 3.3 kV/1200 A SiC hybrid module. In: International Power Electronics Conference (IPEC-ECCE ASIA), pp. 2140–2144, Hiroshima, Japan (2014)

47. Ishikawa, K., Ogawa, K., Onose, H., Kameshiro, N., Nagasu, M.: Traction inverter that applies hybrid module using 3-kV SiC-SBDs. In: International Power Electronics Conference—ECCE ASIA, pp. 3266–3270, Sapporo, Japan (2010)

48. Kaneko, S., et al.: Compact, low loss and high reliable 3.3kV hybrid power module. In: International Exhibition and Conference for Power Electronics, Intelligent Motion, Renewable Energy and Energy Management (PCIM), pp. 1–7, Nuremberg, Germany (2016)

49. (2015). Train trial shows a 40% energy saving for SiC inverters [Online]. Available: http://drivesncontrols.com

50. Xiao, Q., Yan, Y., Wu, X., Ren, N., Sheng, K.: A 10kV/200A SiC MOSFET module with series-parallel hybrid connection of 1200V/50A dies. In: Proceedings of IEEE 27th International Symposium on Power Semiconductor Devices & IC's (ISPSD), pp. 349–352, Hong Kong, China (2015)

51. Casarin, J., Ladoux, P., Lasserre, P.: 10 kV SiC MOSFETs versus 6.5 kV Si-IGBTs for medium frequency transformer application in railway traction. In: Proceedings of International Conference on Electrical Systems for Aircraft, Railway, Ship Propulsion and Road Vehicles (ESARS), pp. 1–6, Aachen, Germany (2015)

52. Fabre, J., Ladoux, P.: Parallel connection of SiC MOSFET modules for future use in traction converters. In: Proceedings of International Conference on Electrical Systems for Aircraft, Railway, Ship Propulsion and Road Vehicles (ESARS), pp. 1–6, Aachen, Germany (2015)

53. Cornic, D.: Efficient recovery of braking energy through a reversible dc substation. In: Proceedings of Electrical Systems for Aircraft, Railway and Ship Propulsion, pp. 1–9, Bologna, Italy (2010)

54. Killer, A., Armstorfer, A., Dez, A.E., Biechl, H.: Ultracapacitor assisted regenerative braking in metropolitan railway systems. In: Proceedings of IEEE Colombian Intelligent Transportation Systems Symposium (CITSS), pp. 1–6, Bogota, Colombia (2012)

55. Vazquez, S., Lukic, S.M., Galvan, E., Franquelo, L.G., Carrasco, J.M.: Energy storage systems for transport and grid applications. IEEE Trans. Industr. Electron. **57**(12), 3881–3895 (2010)

56. Zelinsky, M.: Market Advancement of NiMH Batteries for Stationary Applications. (2016) [Online]. Available: http://www.battcon.com/Papers2016/Zelinsky%20Paper%202016.pdf

57. Steiner, M., Scholten, J.: Energy storage on board of railway vehicles. In: Proceedings of European Conference on Power Electronics and Applications, vol. 10, pp. 1–10, Dresden, Germany (2005)

58. Lukic, S.M., Cao, J., Bansal, R.C., Rodriguez, F., Emadi, A.: Energy storage systems for automotive applications. IEEE Trans. Industr. Electron. **55**(6), 2258–2267 (2008)

59. Iannuzzi, D.: Improvement of the energy recovery of traction electrical drives using supercapacitors. In: Proceedings of 13th International Power Electronics and Motion Control Conference, pp. 1469–1474, Poznan, Poland (2008)

60. Morand, J., Bergogne, D., Venet, P., Sari, A., Bevilacqua, P.: An energy saver for tramway networks using double active bridge and supercapacitors. In: Proceedings of 15th European Conference on Power Electronics and Applications (EPE), pp. 1–9, Lille, France (2013)

61. Steiner, M., Klohr, M., Pagiela, S.: Energy storage system with ultracaps on board of railway vehicles. In: Proceedings of European Conference on Power Electronics and Applications, pp. 1–10, Aalborg, Denmark (2007)

62. Ayata, M., et al.: Traction inverter system with Lithium-ion batteries for EMUs. In: Proceedings of 17th European Conference on Power Electronics and Applications (EPE'15 ECCE-Europe), pp. 1–9, Geneva, Switzerland (2015)

63. Campillo, J., Ghaviha, N., Zimmerman, N., Dahlquist, E.: Flow batteries use potential in heavy vehicles. In: Proceedings of International Conference on Electrical Systems for Aircraft, Railway, Ship Propulsion and Road Vehicles (ESARS), pp. 1–6, Aachen, Germany (2015)

64. Kono, Y. Shiraki, N., Yokoyama, H., Furuta, R.: Catenary and storage battery hybrid system for electric railcar series EV-E301. In: International Power Electronics Conference (IPEC-Hiroshima 2014—ECCE ASIA), pp. 2120–2125, Hiroshima, Japan (2014)

65. Pouget, J., Riffonneau, Y.: Signal hardware-in-the-loop simulator of hybrid railway traction for the evaluation of energy management. In: Proceedings of the IEEE Vehicle Power and Propulsion Conference, pp. 914–919, Seoul, Korea (South) (2012)

66. Cousineau, R.: Development of a hybrid switcher locomotive the railpower green goat. IEEE Instrum. Meas. Mag. **9**(1), 25–29 (2006)

67. Xu, S., Chen, C., Lin, Z., Zhang, X., Dai, J., Liu, L.: Review and prospect of maintenance technology for traction system of high-speed train. Transp. Saf. Environ. **3**(3), 1–20 (2021)

68. D'Addio, G.F., Savio, S., Firpo, P.: Optimized reliability centered maintenance of vehicles electrical drives for high speed railway applications. In: Proceeding of the IEEE International Symposium on Industrial Electronics (ISIE), vol. 2, pp. 555–560, Guimaraes, Portugal (1997)

69. Singh, S., Suresha, R., Sachidananda, K.H.: Reliability centered maintenance used in metro railways. J. Européen Systèmes Automatisés **53**(1), 11–19 (2020)

70. Wang, Z.: Optimization model for EMU collaborative scheduling problem among multiple china railway high-speed depots. In: International Conference on Electronic Information Engineering and Computer Science (EIECS), pp. 298–305, Changchun, China (2021)

71. Fumeo, E., Oneto, L., Anguita, D.: Condition based maintenance in railway transportation systems based on big data streaming analysis. Procedia Comput. Sci. **53**, 437–446 (2015)

72. Prajapati, A., Bechtel, J., Ganesan, S.: Condition based maintenance: a survey. J. Qual. Maint. Eng. **18**(4), 384–400 (2012)

73. Quatrini, E., Costantino, F., Gravio, G.D., Patriarca, R.: Condition-based maintenance—an extensive literature review. Machines **8**(31), 1–28 (2020)

74. Sato, K., Kato, H., Fukushima, T.: Outstanding technical features of traction system in N700S Shinkansen new generation standardized high speed train. IEEJ J. Ind. Appl. **10**(4), 402–410 (2021)

75. Shengkui, Z., Pecht, M.G., Wu, J.: Status and development of fault prediction and health management (PHM) technology. J. Aeronaut **26**(5), 626–632 (2006)

76. Lu, C., Jian, M.: A state of the art review on PHM technology. Comput. Measur. Control **9**, 1–4 (2016)

77. Zhang, J., Bo, J., Li-Ming, H.: Wireless sensor networks prototype system for PHM. In: 8th World Congress on Intelligent Control and Automation; pp. 6836–6841, Jinan, China (2010)

78. Meng, Z.: Beijing metro vehicle PHM technology research and application. Roll Stock **5**, 35–38 (2020)

79. Panrawee, R., Sakdirat, K., Zuo-Jun, S.: An improvement on the end-of-life of high-speed rail rolling stocks considering CFRP composite material replacement. Front. Built Environ. **5**(89), 1–9 (2019)

80. Tan, P., Ma, J., Zhou, J., Fang, Y.: Sustainability development strategy of China's high speed rail. J. Zhejiang Univ. Sci. A 17, 923–932 (2016)

81. Rochard, B.P., Schmid, F.: Benefits of lower-mass trains for high speed rail operations. Proc. Inst. Civ. Eng—Transp. **157**(1), 51–64 (2004)

82. Klinger, C., Bettge, D.: Axle fracture of an ICE3 high speed train. Eng. Fail. Anal. **35**, 66–81 (2013)
83. Zeuner, T., Stojanov, P., Sahm, P.R., Ruppert, H., Engels, A.: Developing trends in disc bralke technology for rail application. Mater. Sci. Technol. **14**(9–10), 857–863 (1998)
84. Tian, H.: Review of research on high-speed railway aerodynamics in China. Transp. Saf. Environ. **1**(1), 1–21 (2019)
85. Yang, G., Guo, D., Yao, S., Liu, C.H.: Aerodynamic design for China new high-speed trains. Sci. China Technol. Sci. **55**, 1923–1928 (2012)
86. Deng, X., Shi, X., Guo, J., Zhu, H.: European high-speed bogie technology review. Int. J. Veh. Des. **79**(1), 43–62 (2019)
87. Mistry, P., Johnson, M.: Lightweighting of railway axles for the reduction of unsprung mass and track access charges. Proc. Inst. Mech. Eng. Part F: J. Rail Rapid Transit **234**(9), 958–968 (2020)
88. BBC News: Eurostar Train Derails in France. 5 June 2000. Last retrieved 10 May 2009
89. Persson, R.: Tilting trains enhanced benefits and strategies for less motion sickness. Ph. D. Thesis, Stockholm, U.K. (2011)
90. Nategh, S., Boglietti, A., Liu, Y., Barber, D., Brammer, R., Lindberg, D., Aglen, O.: A review on different aspects of traction motor design for railway applications. IEEE Trans. Ind. Appl. **56**(3), 2148–2157 (2020)
91. Torrent, M., Perat, J.I., Jiménez, J.A.: Permanent magnet synchronous motor with different rotor structures for traction motor in high speed trains. Energies **11**(6), 1–17 (2018)
92. Shikata, K., Nomura, H., Fukasawa, S., Kawai, H., Aoki, H., Tasaka, Y.: PMSM propulsion system for Tokyo Metro. In: Proceedings of the IEEE Electrical Systems for Aircraft, Railway and Ship Propulsion, pp. 1–6, Bologna, Italy (2012)
93. Prasad, N., Jain, S., Gupta, S.: Review of linear switched reluctance motor designs for linear propulsion applications. CES Trans. Electr. Mach. Syst. **6**(2), 179–187 (2022)
94. Mitra, A., Emadi, A.: On the suitability of large switched reluctance machines for propulsion applications. In: Proceedings of IEEE Transportation Electrification Conference and Expo (ITEC), pp. 1–5, Dearborn, USA (2012)
95. Germishuizen, J.J., Van der Merwe, F.S., Van der Westhuizen, K., Kamper, M.J.: Performance comparison of reluctance synchronous and induction traction drives for electrical multiple units. In: Proceedings of the Thirty-Fifth IAS Annual Meeting and World Conference on Industrial Applications of Electrical Energy, vol. 1, pp. 316–323, Rome, Italy (2000)
96. Hellinger, R., Mnich, P.: Linear motor-powered transportation: history, present status, and future outlook. Proc. IEEE **97**(11), 1892–1900 (2009)
97. Thornton, R.D.: Efficient and affordable maglev opportunities in the United States. Proc. IEEE **97**(11), 1901–1921 (2009)
98. Schultz, L., de Haas, O., Verges, P., Beyer, C., Rohlig, S., Olsen, H., Kuhn, L., Berger, D., Noteboom, U., Funk, U.: Superconductively levitated transport system—the Supratrans project. IEEE Trans. Appl. Supercond. **15**(2), 2301–2305 (2005)
99. Long, Z., He, G., Xue, S.: Study of EDS & EMS hybrid suspension system with permanent-magnet Halbach array. IEEE Trans. Magn. **47**(12), 4717–4724 (2011)
100. Prasad, N., Jain, S., Gupta, S.: Electrical components of maglev systems: emerging trends. Urban Rail Transit **5**, 67–79 (2019)
101. Banerjee, S., Prasad, D., Pal, J.: Large gap control in electromagnetic levitation. ISA Trans. **45**(2), 215–224 (2006)
102. Meins, J., Miller, L., Mayer, W.J.: The high speed maglev transport system TRANSRAPID. IEEE Trans. Magn. **24**(2), 808–811 (1988)
103. Zhang, W., Li, J., Zhang, K., Cui, P.: Design of magnetic flux feedback controller in hybrid suspension system. Math. Probl. Eng. **2013**(4), 1–8 (2013)
104. McLean, G.W.: Review of recent progress in linear motors. IEE Proc. B (Electr. Power Appl.) **135**(6), 380–416 (1988)
105. Neogi, S.K., Chatterjee, K.: Torque ripple reduction in high power BLDC motors utilizing an auxiliary DC to DC converter. In: IEEE International Electric Machines and Drives Conference (IEMDC), pp. 1663–1669, San Diego, CA, USA (2019)

106. Lu, Q.F., Mei, W.H.: Recent development of linear machine topologies and applications. CES Trans. Electr. Mach. Syst. **2**(1), 65–72 (2018)
107. Gerada, D., Mebarki, A., Brown, N.L., Gerada, C., Cavagnino, A., Boglietti, A.: High-speed electrical machines: technologies, trends, and developments. IEEE Trans. Industr. Electron. **61**(6), 2946–2959 (2014)
108. Lee, J., Jo, J., Han, Y., Lee, C.: Development of the linear synchronous motor propulsion testbed for super speed Maglev. In: International Conference on Electrical Machines and Systems, ICEMS 2013, pp. 26–29, Busan, South Korea (2013)
109. Otkun, Ö, Sefa Akpınar, A.: An experimental study on the effect of thrust force on motor performance in linear permanent magnet synchronous motors. Electr. Power Compon. Syst. **45**(18), 2017–2024 (2017)
110. Wang, D., Wang, X., Du, X.F.: Design and comparison of a high force density dual-side linear switched reluctance motor for long rail propulsion application with low cost. IEEE Trans. Magn. **53**(6), 1–4 (2017)
111. Lee, H.W., Kim, K.C., Lee, J.: Review of maglev train technologies. IEEE Trans. Magn. **42**(7), 1917–1925 (2006)
112. Lutzemberger, G., Musolino, A., Rizzo, R.: Automated people mover: a comparison between conventional and permanent magnets MAGLEV systems. IET Electr. Syst. Transp. **7**(4), 295–302 (2017)
113. Zhai, M., Hao, A., Li, X., Long, Z.: Research on the active guidance control system in high speed maglev train. IEEE Access **7**, 741–752 (2018)
114. Wang, Y., Weiguo, L., Hongyun, H., Zongjian, L., Yang, X., Da, L.: Research on contactless power supply of high speed maglev train based on MCR-WPT. In: 14th IEEE Conference on Industrial Electronics and Applications (ICIEA), pp. 2297–2302. Xi'an, China (2019)
115. Shanghai Maglev Transportation Development Co. Ltd: Maglev Technology (2005). http://www.smtdc.com/en/gycf3.html. Last accessed 01 June 2019
116. Uzuka, T.: Trends in high-speed railways and the implications on power electronics and power devices. In: IEEE 23rd international symposium on power semiconductor devices and ICs, ISPSD 2011, 23–26 May 2011, San Diego, CA (2011)
117. Feng, J., Xu, J., Liao, W., Liu, Y.: Review on the traction system sensor technology of a rail transit train. Sensors **17**(6), 1–16 (2017)
118. High Speed Rail Corporation of India Limited: http://hsrc.in/. Last accessed 01 June 2022
119. Railway-Technology Website: Moscow Metro—Railway Technology. https://www.railway-technology.com/projects/moscow-metro/. Last accessed 27 Feb 2021
120. Diario El Universal: Informan a Chávez sobre tren a La Guaira (2006). Retrieved 6 Aug 2013

Approach to Assist in the Discovery of Railway Accident Scenarios Based on Supervised Learning

Hadj-Mabrouk Habib (ORCID)

Abstract The European Community has developed a real turning point in the common rail transport policy by defining new ambitions to rebalance sustainably the sharing between modes of transport, develop intermodality, fight congestion, and finally place safety at the heart of European action. To consolidate the usual methods of railway safety analysis, this chapter proposes two complementary railway safety assessment methods based on AI techniques and in particular on machine learning (ML). The study seeks to exploit, by machine learning, the lessons resulting from "Experience Feedback" (REX) in order to help and assist safety experts, technical investigators, and certification bodies to assess the level of safety of a new rail transport system. Unfortunately, safety in rail transport improves essentially on the basis of in-depth knowledge of accidents and incidents resulting from "experience feedback". As stipulated by European regulations, all players in rail transport and in particular infrastructure managers and railway undertakings are obliged to set up a system of "experience feedback" in order to understand the causes and the seriousness of the consequences engendered by rail accidents and incidents. So, the knowledge of accidents and incidents results essentially from the contribution of lessons learned and experiences acquired. To explain and understand the causes and circumstances of accident risks and therefore at least avoid the reproduction of similar accidents, we have oriented our study toward the use of approaches derived from AI and machine learning. From experience feedback, the main objective is to exploit a set of insecurity events in order to anticipate and prevent the reproduction of the risks of accidents or similar incidents and possibly to discover and identify new scenarios of potential accidents liable to jeopardize safety. This chapter proposes a new hybrid method based on three machine learning algorithms. The first stage of acquiring knowledge led to the development of two accident scenario databases. The first base relates to the analysis of "functional safety", and the second base relates to the analysis of the "security of critical software". The second step, which is based on a concept classification algorithm, makes it possible to group the accident scenarios into coherent classes such as the class relating to train collision or derailment problems. For each

H.-M. Habib (✉)
Vice-Presidency Research (VPR), University Gustave Eiffel, 14/20 Boulevard Newton, 77447
Marne La Vallée, France
e-mail: habib.hadj-mabrouk@univ-eiffel.fr

class of accident or incident scenarios, the third step implements a learning technique based on production rules in order to identify some relevant safety rules. In the fourth step, the previously generated production rules are transferred to an expert system in order to deduce the potential accident risks. Finally, a case-based reasoning (CBR) system makes it possible to search, on the basis of "experience feedback", for the cases closest to this new risk of accident and proposes the most appropriate prevention or protection measures.

Keywords Rail transport · Classification · Assessment · Accident scenarios · Functional safety · Software safety · Rule-based machine learning · Case-based reasoning · Expert system

1   Introduction

The rail transport sector is now one of the foundations of the European project. From the beginning and in the context of the 1957 Treaty of Rome and the 1992 Maastricht Treaty, the Member States stressed the importance of a common transport policy.

As a result, transportation was one of the European Community's initial shared policy sectors. In the previous 30 years, the transport sector has been seen as a priority area and a critical component in the development of Europe, as it is not only the physical manifestation of free movement of people and commodities, but also a critical sector in the implementation of a single market. The European Community has marked a watershed moment in the common rail transport strategy by outlining new goals to rebalance sustainable mode sharing, enhance intermodality, combat congestion, and ultimately place safety at the center of European action.

To complement the traditional techniques of railway safety analysis, this paper presents a novel approach of safety analysis and assessment based on machine learning. The project aims to use machine learning to utilize the lessons learned through "Experience Feedback" (REX) in order to aid and assist safety experts, technical investigators, and certification authorities in determining the degree of safety of a new rail transportation system.

The harmful consequences of railway accidents, which sometimes result in loss of life and destruction of the system and its environment, are the foundation for the establishment of a "Feedback of Experience" (REX) system, which is regarded as an essential means of promoting railway safety improvement. As a result, it is vital to implement a REX process to remember and capitalize all accidents and occurrences in order to minimize the recurrence of new comparable mishaps. The investigation of accidents and events in the area of accidentology and safety theoretically allows for continual development of safety. The goal of REX for a train operator is to increase the degree of safety in its operation by leveraging bad historical experiences (accidents, major incidents, near-accidents, etc.) or positive occurrences (good practice, reference, etc.). The REX strives not only to decrease the quantity and/or severity of system dysfunctions (people, installations, processes, environment), but also to

adopt the most effective strategies to mitigate the risks associated with the life cycle of railway systems (design, construction, operation, maintenance). The primary goal of REX is to learn from lived experience in order to prevent replication. In the face of a dangerous circumstance, the REX, as a process of obtaining information and learning, enables not only the identification of knowledge, but also its sharing among the people involved. It is a strategy aimed at highlighting the weaknesses, dysfunctions, and incompatibilities of the safety system and developing suggestions to prevent or mitigate such occurrences.

This study concerns two methods of rail safety analysis: Functional Safety Analysis (FSA) and Software Errors and Effects Analysis (SEEA) methods. This manuscript is structured around six paragraphs. After presenting in the second paragraph a bibliographic study on the contribution of ML to the field of railway safety, the third paragraph presents the motivations and objectives to be achieved. Referring to the bibliographic study, we considered using the "Charade" [1] system for the generation of rules, the tool "ReCall" for CBR, and system "Clasca" [2] for the classification of accident scenarios. The results obtained to date are successively presented in the fourth and fifth paragraphs. The validation of the proposed methodology took place in two phases. The first phase consisted of an overall assessment of the feasibility model based on its application to all the accident scenarios archived to date relating only to the risk of an accident: train collision. The second phase focused on an internal evaluation of the "Clasca" classification module based on a set of test scenarios provided by the experts. This validation revealed not only the interests but also the current limitations of the completed model and resulted in prospects for improvement presented in the seventh and final paragraphs dedicated to the discussion of the results obtained.

2   Literature Review

There are now many applications that are based on the use of AI techniques, particularly machine learning, neural networks, Big Data Analytics (BDA), "data mining", and "text mining", to solve decision support problems in the rail transport sector. These applications were developed relatively recently. This study is related to the assessment of threats to the security of urban rail transport in China [3], the management of railway maintenance operations [4], the examination of texts and reports of railway accidents and events [5], and the identification of flaws on rail surfaces [6]. Big Data is being used by Siemens in their development of the Internet of trains [7]. Shirazi et al. [8] employ natural language processing (NLP) and machine learning in their investigation of the causal relationship between causes and safety shortcomings in the rail sector. Data mining approaches based on association rules and classification algorithms were used by Ghomi et al. [9] in order to determine the elements that contribute to the degree of injuries sustained in incidents involving pedestrian crossings. Zhang et al. [10] created a technique based on machine learning in order to differentiate between primary and secondary accidents. This was done in the interest

of improving the identification of accidents. In order to get a better understanding of the factors that lead to railway accidents, Heidarysafa et al. [11] conduct in-depth learning research on accident narratives.

Case-based reasoning, often known as CBR, is becoming an increasingly popular topic of discussion among researchers and industry professionals working in the rail transportation industry. CBR is a well-established topic of study that is mostly focused on machine learning (ML) and other AI-related methodologies. This line of thinking, which is predicated on the idea of resemblance, places primary emphasis on the process of problem resolution that is informed by previous experience. It is a cognitive method of human reasoning that mainly depends on how individuals learn a new skill based on their previous routines and experiences. It is called inductive reasoning. CBR refers to the process of drawing from and making use of one's previous experiences in order to better comprehend, explain, interpret, or solve contemporary problems that are analogous to those encountered in the past. CBRs are finding a growing amount of usage in a variety of commercial applications, including technical diagnostics, medical diagnostics, image processing, law, design, and planning, among others. Our literature search in the topic of transportation encompassed three different modes of transportation: the air, the road, and the train. When it comes to the industry of air transportation, one example that comes to mind is the forecasting of mishaps and events [12]. Planning [13] and traffic management at junctions [14] are two examples that come to mind when thinking about the field of road transportation. We may highlight the avoidance of operational accidents [15], the diagnosis of locomotive failures [16], and the identification of failures in the rail switching system [17] as examples of important work in the area of rail transportation.

3 Positioning of the Study in Relation to the State of the Art

The decision support tool presented in this chapter is based on the implementation of a hybrid reasoning approach that revolves around five main phases (Fig. 1): (1) acquisition of knowledge, (2) classification of scenarios, (3) evaluation, (4) suggestion of dangerous events, and (5) search for solutions.

The first phase of acquiring knowledge and more particularly of the railway accident scenarios required the use of several data collection sessions not only from experts in the field of safety but also from the safety files drawn up by the manufacturers of the railway systems. Several knowledge collection techniques were used such as the interview, the questionnaire, the conceptual sorting, and the analysis of the protocols. This phase finally led to several databases of accident and/or incident scenarios.

The second phase of scenario classification uses a classification algorithm CLASCA [2]. This is an inductive learning system that makes it possible to search, in the database of historical scenarios derived from experience feedback, for the class to which a new potential accident scenario belongs.

Fig. 1 Different types of reasoning involved in the proposed approach

```
┌──────────────────────────────┐
│  Acquisition of knowledge    │◄─────┐
│   ┌──────────────────────┐   │      │
│   │ Historical Scenario  │   │      │
│   │ Knowledge Base (HSKB)│   │      │
└───┴──────────┬───────────┴───┘      │
               ▼                      │
┌──────────────────────────────┐      │
│  Classification of scenarios │◄─────┤
│        ┌──────────────────┐  │      │
│        │  CLASCA system   │  │      │
└────────┴────────┬─────────┴──┘      │
                  ▼                   │
┌──────────────────────────────┐      │
│         Assessment           │      │
│      ┌──────────────────┐    │      │
│      │ CHARADE system   │    │      │
└──────┴────────┬─────────┴────┘      │
                ▼                     │
┌──────────────────────────────┐      │
│ Suggestion of dangerous events│     │
│    ┌──────────────────────┐  │      │
│    │ Knowledge-Based System│ │      │
└────┴────────┬──────────────┴─┘      │
             ▼                        │
┌──────────────────────────────┐      │
│     Search for solutions     │──────┘
│   ┌──────────────────────┐   │
│   │ Case-Based Reasoning │   │
│   │   "ReCall" system    │   │
└───┴──────────────────────┴───┘
```
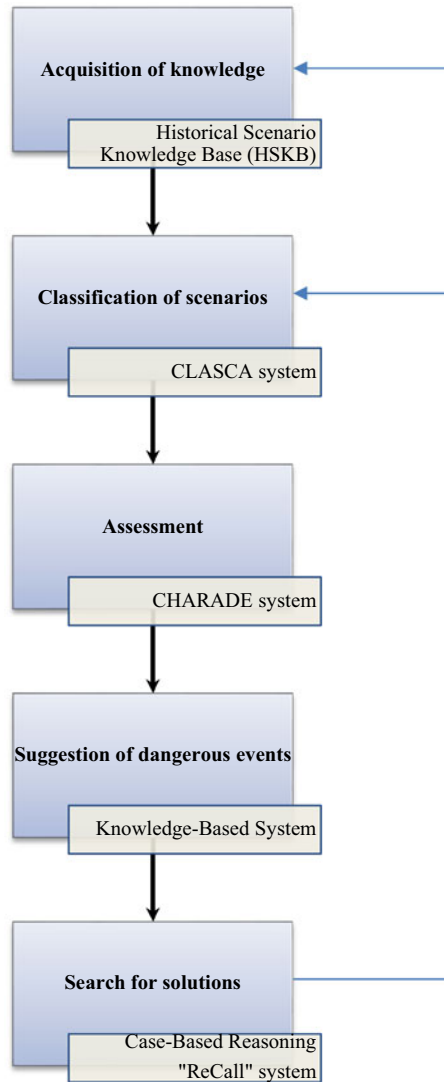
The third phase of the study makes it possible to generate a base of production rules that can be used by an expert system. This is a stage of research into the regularities and similarities present between all the historical scenarios in the database. The objective is to learn lessons from historical data relating to rail accident investigations. The realization of this stage required the recourse to the learning system of the rules CHARADE [1].

The fourth phase seeks to find the dangers or dangerous events likely to jeopardize the safety of the system. To this end, all the rules previously generated by the Charade

system are used by an expert system (knowledge-based system) in order to deduce any potential risks.

The fifth and final phases of the study allow the search for potential solutions to combat a particular danger previously deduced by the expert system. During this phase, we used another type of reasoning: case-based reasoning (CBR).

In the end, the approach that we have implemented is a hybrid method and calls on several modes of reasoning: induction for the classification phase, the search for regularities to generate production rules, deduction (forward chaining) by the expert system, and finally, reasoning by analogy (search for similarity) for case-based reasoning.

4 Motivations and Objectives

Also called Rex, "experience feedback" is a method that consists of sharing the lessons and conclusions of an experience (positive or negative) with a view to improving and optimizing practices in the future. In the field of rail transport, the harmful consequences and the terrible cost of accidents are the basis for the establishment of a "Rex" system as one of the essential means to encourage the improvement of rail safety. In France, and in the land transport sector, any serious accident occurring on the rail system is the subject of a technical investigation carried out by the land transport accident investigation bureau (BEA-TT). This investigation aims to improve, as far as possible, railway safety and accident prevention.

Each investigation into a railway accident or incident is the subject of a report drawn up in an investigation form which includes "feedback" on the technical, organizational, and human aspects:

1. A detailed description of the dangerous event and its context: description of the event, its location, the presumed causes, the consequences, the condition of the rolling stock and the infrastructure, the measures taken to avoid recurrence of such an event. These measures may relate to the application of certain design rules, the implementation of appropriate maintenance rules, the strict application of safety rules and procedures, the training of personnel, in particular those performing safety tasks, the implementation of technical "catch-up loops" to compensate for human errors such as speed control systems that cause the train to stop if the authorized speed is exceeded or automatic train stop devices in the event of inadvertent crossing of a closed signal.
2. The history of the investigations, in particular, on the safety management system (means and procedures aimed at improving railway safety on a continuous basis), the National and European rules and regulations applied (general requirements relating to the operation, skills, communications between agents, documentation, traceability, etc.), the operation of rolling stock and technical installations, documentation on the operating system and previous events of a comparable nature.

3. An analysis and conclusions on the causes of the event, including the factors that contributed to the event and in particular (a) the factors related to the measures taken by the operator; (b) factors relating to the condition of rolling stock or technical installations; (c) factors related to personnel skills, procedures, or maintenance; (d) factors relating to the conditions of the National and European regulatory framework; and (e) factors related to the application of the safety management system.

The proposed study is part of this "feedback" process in railway safety. The proposed method aims to exploit, through ML techniques, data on accidents and incidents involved in several rail transport systems put into service in France. To this end, the safety reports that were analyzed led to the development of several databases. This study covers two databases: the first concerns the functional analysis of safety and currently includes around a hundred accident and/or incident scenarios. The second database includes around 200 scenarios (cases) and concerns software error safety analyses. From these historical databases, the objective is to avoid at least the reproduction of these accident scenarios during the operation of a new rail transport system and therefore contribute to the prevention of rail accidents.

The analysis and evaluation of the safety of a rail transport system require experts to implement several safety methods and techniques. Commonly used methods are as follows (Fig. 2):

- "Preliminary Hazard Analysis" (PHA) [18].
- "Functional Safety Analysis" (FSA).
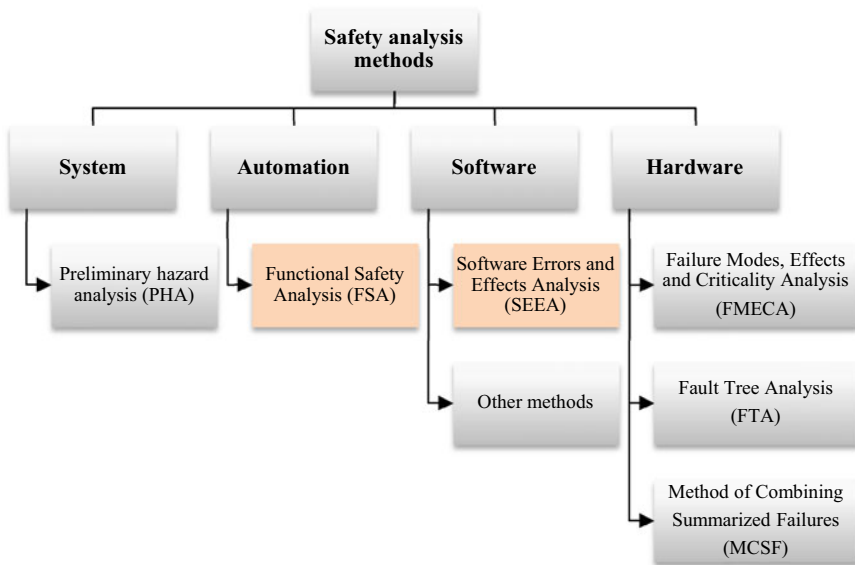
Fig. 2 Some methods of railway safety analysis

- "Software Error and Effects Analysis" (SEEA).
- "Fault Tree Analysis" (FTA).
- "Analysis of Failure Modes, their Effects and their Criticality" (AFMEC).
- "Method of Combining Summarized Failures" (MCSF).

Within the framework of the MCSF method, certain failures known as "simple failures" generally have benign consequences on the behavior of the system. These failures are then grouped together by following a well-determined order with a view to discovering new, much more dangerous failures. These failures are called "Summary Failure" (SF). The method proposed in this article takes into account this SF [19].

To help experts in their decisive task of safety assessment and therefore decision-making, this manuscript proposes a new method based on AI in order to suggest new risks of accidents likely to call into question the rail safety. This study concerns the two safety analyses previously mentioned: FSA and SEEA. Two main phases are necessary. Based on experience feedback, the first phase is to collect a representative set of accident scenarios. This important phase required not only about thirty interviews with safety experts, but also the examination of several safety. These accident scenarios are then stored in two separate databases. The first base concerns the FSA method and is called the "Historical Scenario Knowledge Base" (HSKB). The second basis concerns software safety analysis (SEEA). The second phase of the proposed method aims to exploit these historical data in order to uncover possible adverse safety situations. This second phase implements several machine learning techniques: concept classification learning (or conceptual grouping), rule-based machine learning (RBML), and case-based reasoning (CBR). The bibliographic study led us to use the "Clasca" system for the classification of scenarios [2], the "Charade" system [1] for generation of rules, and finally, the "ReCall" system from the "ISoft" based on Quinlan's ID3 algorithm [20].

5   Result 1: Functional Safety Assessment Approach

In the field of railway safety, experts in the field use several methods of analysis and evaluation in order to successively identify dangerous elements or equipment, dangerous situations (or hazard), potential accidents such as collision or the derailment of the system as well as the seriousness of the resulting consequences. The use of predictive analysis methods for dependability advantageously contributes to eliminating failures or reducing their probability of occurrence. Several analysis methods exist such as Preliminary Hazard Analysis (PHA), Functional Safety Analysis (FSA), Software Error Effect Analysis Software Safety analysis (SEEA), Failure Modes, Effects and Criticality Analysis (FMECA), Fault Tree Analysis (FTA), and Method of Combining Summarized Failures (MCSFs).

The MCSF method from the field of aeronautics was formalized jointly by the National Society of Aeronautical and Space Industries (SNIAS) and the Certification Authorities of the French Ministry of Air, for the analysis of the safety of Concorde

aircraft and Airbus. The FMECA, which generally highlights single failures, must be complemented by the study of combinations of failures that result in adverse events. The MCSF, used as an extension of FMECA, inductively determines such combinations of failures. The MCSF is used by safety experts as the "Research Combination of Significant Faults" (RCSF) method. Three types of failures are distinguished according to their consequences on the safety of the transport system: EF: Elementary Failure, SF: Summarized Failures, and PF: Global Failure. The term Elementary Failures (EFs) include failures whose consequences are identical on the behavior of the transport system. Their usually large number makes them difficult to operate. It is customary to group together in a single failure called "Summarized Failures" (SFs) the EFs whose consequences on the system are generally benign. Combined together, SFs can aggravate the consequences on the system; their combination constitutes a Global Failure (GF). GFs are often dangerous and result from a combination of SFs taken in a well-determined order of occurrence. The MCSF, a purely inductive method, first analyzes the effects of component failure modes and then studies the combinations of these failure modes in order to define sets of failures corresponding to abnormal operations or undesirable events for the systems to be analyzed. The MCSF therefore endeavors to extract only the combinations that are significant in terms of safety and is then presented as an extension of FMECA.

In the following, for the formalization and structuring of safety knowledge, we are mainly interested in SFs which have a universal character due to their independence from technology. An SF is a generic failure resulting from the grouping of a set of elementary failures having the same consequence on the behavior of the system. Each scenario involves one or more SFs. A list of the SFs of all the scenarios acquired to date relating to the risk of "collision" has been drawn up. A sample of some SF is given below:

- SF1: Failure of an anti-collision transmitter in a train.
- SF2: Train in reverse in an occupied block.
- SF3: Masking of an alarm by initialization.
- SF4: Penetration by recoil of a train on an occupied block.
- SF5: Wrongly maintaining a Route by the Autopilot on hold.
- SF6: Permanent traction failure.
- SF7: Unexpected switching of Entry/Exit mode.

The railway safety assessment approach is centered on the "Summarized Failures" (SFs) involved in an accident scenario. The aim is to compare the SFs proposed in a new scenario with the list of historical PRs (feedback). From a set of historical scenarios, the "Charade" [1] rules' learning system exploits this base of examples to produce "summarized failures" (SFs) recognition functions. All production rules are oriented from symptoms to causes (or consequences). In other words, the premise of a rule groups together the set of descriptors of a scenario and the conclusion of the rule contains the descriptor SF. It involves learning SF recognition functions in the form of production rules that establish a relationship between a set of facts (descriptive parameters of a scenario or descriptors) and the SF fact. This logical dependency relationship can be described in the following form: IF the facts (or

descriptors): Geographical area, Principle of cantonment, Danger, Safety function, etc. are verified, THEN their consequence is the fact (or descriptor): SF.

The evaluation knowledge base (base of rules produced by learning) is exploited by an inference engine with a view to deducing the SFs to be considered in the new scenario to be evaluated. The expert system uses the rules produced by the rule learning system (Charade) to deduce the possible SFs which must be considered by the new scenario submitted for evaluation by the safety experts. This evaluation approach favors the generation of new scenarios by the deduction of one or more SF likely to call into question the safety of the transport system. In this sense, it helps the experts to judge the completeness of the safety file.

Figure 3 details all of the steps involved in the functional safety assessment approach. These ten steps can be synthesized into three activities: knowledge acquisition [21], scenario classification [2], and scenario evaluation [22–25].

5.1 Collection of Historical Data

Remember that one of the tasks of safety assessment and therefore of certification of railway equipment consists in examining in depth the completeness and consistency of the safety file proposed by the system manufacturer. The safety expert must prove the safety nature of a new safety system or equipment by demonstrating that the safety criteria and functions are well respected. Each risk of accident liable to jeopardize the safety of passengers or to cause the system's ability to perform the required safety functions to be altered is translated by the experts into a potential accident scenario. Rail safety experts are often called upon to imagine new accident scenarios to complete the comprehensiveness of the study. An accident scenario is an orderly sequence of events that lead to a potential accident risk such as collision or system derailment. In this complex process, a major difficulty consists of finding the abnormal scenarios that can lead to a particular risk. This is the fundamental point that motivated the present work. Researching and imagining potential accident scenarios rely not only on the know-how of experts in the field but also on the use of traditional safety analysis methods. Generally, the first method, called "Preliminary hazard analysis" (APR), essentially aims to identify potential accidents related to the system and its interfaces in order to assess them and propose solutions to eliminate, reduce, or control them. The second method, called "Functional safety analysis" (FSA), focuses on justifying that the design architecture of the system is safe with respect to the potential accidents identified by the APR and therefore to ensure that all safety provisions are considered to cover potential dangers or accidents.

In terms of railway safety, there are generally three types of functions (or equipment): (1) "Safety functions" generally called critical functions such as the speed instruction management system, (2) "Monitoring functions" which make it possible to monitor trains, and (3) "Functional functions" that ensure the operation and availability of the system. This technical and functional analysis of the system first
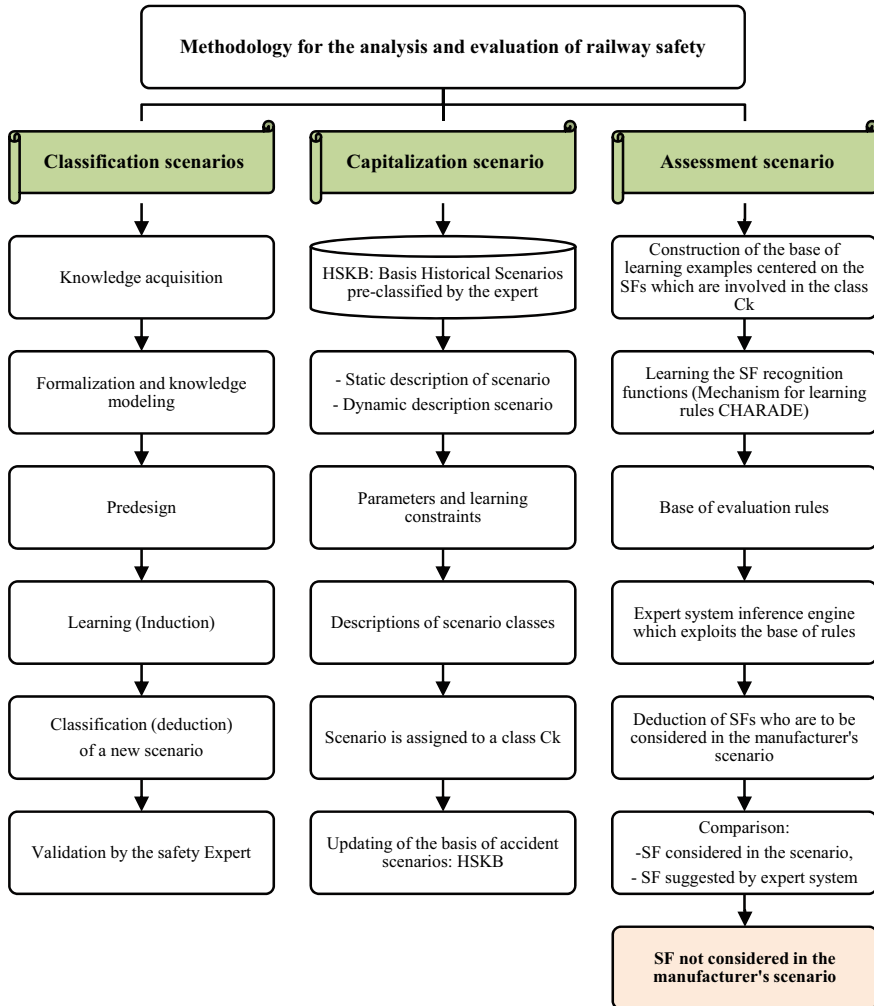
Fig. 3 Steps involved in the process of assisting the evaluation of the SFA

requires a hierarchical breakdown of the system into its constituent functions up to the designation of the most elementary functions.

Knowledge relating to the fundamental concepts involved in the risks of railway accidents has been structured in a hierarchy organized according to several levels: types of accidents (collective or individual accident), risks of accidents (collision, derailment, electrocution, training, fall, etc.), safety functions (initialization, docking, alarm management, location of trains, etc.), accident scenarios (retreat of a train on a section being initialized, incorrect processing of the penetration alarm on an occupied block, loss of a mute element during the initialization phase, etc.), and descriptive parameters of a scenario (risk or danger, safety function, incident function,

geographical area, actors involved, etc.). This hierarchy has been validated by the experts.

After around thirty interview sessions with safety experts as well as the analysis of several safety files, the knowledge acquisition led to the inventory around a hundred accident or incident scenarios. This study was deliberately limited to the problem of "train collisions". The collected scenarios are grouped together in a database (HSKB). These scenarios were then grouped by the experts into nine classes of scenarios such as the "Train docking" class or the "Emergency braking management" class.

Each accident or incident scenario has been formalized and characterized by eight key descriptors such as type of block (TB), hazard (H), hazard-related functions (HRFs), summarized failures (SFs) (see Fig. 4), and for each descriptor, we have identified several possible values. For example, the descriptor hazard (H) can take the value "Collision" or "Derailment" or "Electrocution" or "Fall", etc.

These descriptive parameters of a scenario are then exploited by the learning system with a view to seeking empirical regularities between several scenarios and subsequently generating dangerous situations that are likely to occur in a particular context and which require special attention from railway safety experts and evaluators.

5.2 Classification Step

"Clasca" is an algorithm for learning concepts in order to generate descriptions' characteristic of accident scenarios. In the presence of a new scenario submitted for evaluation by the experts, the "Clasca" system uses the HSKB sample database to find the class to which it belongs: initialization phase, docking phase of trains, etc. The classification step is based on the descriptions learned in the previous step to find the class to which a new scenario belongs. The HSKB database is constantly updated to consider the new characteristics of new scenarios. The safety experts are involved in to validate the proposed classification [2].

5.3 Assessment Step

Each class of the HSKB base is then used by the "Charade" learning system to produce the rules necessary for the discovery of the dangers and risks of potential. The potential dangers generated by the "Charade" system are called "Summarized Failures" (SFs). The "Charade" learning system [1] is based on a method of searching for the regularities present in a class Ck of the HSKB base (identified by "Clasca") in order to generate a production rule base that can be used directly by an expert system. Figure 5 shows an example of production rules generated by the "Charade" system. The base of the rules is then exploited (forward chaining) by an expert system in

Type of block (TB)	
Fixed blocks	Moving blocks

Hazard (H)				
Collision	Derailment	Electrocution	Evacuation	Entrainement de l'individu...

Hazard related functions (HRF)					
Management of automatic driving	Localisation des trains	Control Input/Output	Tracking trains	Speed setpoint	Management of trains Stops...

Geographical zones (GZ)				
Terminus	Station	Line	Train entry zone	Section limit...

Elements involved (EI)		
The trains	The operator at the control centre (CC)	The automatic driver (AD)...

Incident functions (IF)		
Route management; Traffic control	Transmission	Operating instructions ...

Summarized failures (SF)		
SF1: train reversing into an occupied block,	SF2: collision avoidance transmitter failure in a train,	SF3: masking of an alarm by initialization, ...

Adopted solutions (AS)		
AS1: changing the switching position,	AS2: counting the trains on the line,	AS3: increasing the length of the moving variable block, ...

Fig. 4 Eight descriptive parameters of an accident scenario

order to deduce the potential dangers or risks which require a particular examination by the safety experts [26, 27].

The feasibility study of a rail safety assessment support system was voluntarily limited to the risk of accidents linked to "rail collisions". The scenarios collected to date are collected in a database called the "Historical Scenarios Knowledge Base" (HSKB). In the presence of a new scenario submitted for evaluation by safety experts, the classification learning system called "Clasca" uses the HSKB to find the class to which it belongs. Each class of the HSKB database is then used by the rule learning system "Charade" [1] to produce the rules necessary for the discovery of potential dangers. These generated hazards are called "Summary Failures" (SFs) which result

---

R1:

If   Elements_involved = Traveling_operator,

     Incident_functions = instructions

     Elements_involved = command_post_controller.

Then Summarized_Failures = SF11 (Invisible element on the zone of completely automatic driving),

     Elements_involved = Automatic_pilot_with_redundancy,

     Hazard_related_functions = train_localization,

     Geographical_zones = terminus. [0]

R2:

If   type_of_block = fixed_canton,

     hazard_related_functions = initialization,

     incident_functions = instructions

Then summarized_failures = SF10,

     hazard_related_functions = authorization_CI_HT,

     hazard_related_functions = management_of_alarms,

     hazard_related_functions = location_of_trains. [0]

R3:

If hazard_related_functions = location_of_trains,

  elements_involved = PA_without_redundancy

Then summarized_failures = SF9,

  geographic_zones = line,

  type_of_block = fixed_canton. [0]

R4:

If geographical_zones = zone_injection_de_rame,

  hazard_related_functions = docking,

  type_of_block = mobile_canton

Then summarized_failures = SF20. [0]

Fig. 5 Example of a production rule spawned from the learning system "Charade"

from a grouping of elementary failures carried out by the safety experts during the knowledge acquisition phase. The "Charade" learning system is based on a method of researching the regularities present in a class C_k (initialization, docking, etc.) of the HSKB database in order to generate a base of production rules that can be used directly by an expert system.

In data analysis, research based on observation and experience is generally called empirical study and the collection of information is called "empirical data". Data mining seeks to find patterns or relationships unknown a priori in large volumes of data. Based on the Galois lattice (or concept lattice) to construct an ordered set of facts (or regularities), the "Charade" system automatically learns rules from a description language and a set of examples. The Galois lattice is built from a set of objects (concepts) described by a set of conjunctions of binary attributes. The construction process of the lattice starts from the most general concept (describing all the objects) and, by successive specializations, results in a set of concepts. The Galois lattice also makes it possible to generate the implications of attributes called rules and is generally used for the construction of knowledge bases, for example, production rules in expert systems. Learning through the lattice will limit the number of implications to only relevant rules of the context, insofar as they will be verified by many examples. The development of rules in "Charade" is based on the search and discovery of empirical regularities present on the training set. A regularity corresponds to an observed correlation between descriptors of the base of training examples: if all the examples of the training set which have the descriptor d_1 also have the descriptor d_2, we can infer that $d_1 \rightarrow d_2$ on the learning set. This process of obtaining rules is based on the use of two Boolean lattices: a lattice of descriptors C and a lattice of examples D. The first function C goes from the lattice of descriptors to the lattice of examples: it associates with each description (d_i) consisting of a conjunction of descriptors, the subset (E) of the examples of the training set covered by this description. The other function D makes to correspond to each subset (E) of the training set, the description (d_j) formed from the conjunction of descriptors common to all the examples of E. The composite function CoD which associates to the conjunctive description (d_i) the conjunctive description (d_j), generates the rule $d_i \rightarrow d_j$.

In addition to these logical rules, "Charade" also makes it possible to generate approximate rules which translate the statistical correlations observed between the descriptors. To adapt the format of the rules to the characteristics and properties sought by the user of an expert system, "Charade" implements several constraints and learning parameters such as the "noise factor" which makes it possible to set the minimum number of examples necessary to detect a regularity, the "limitation of the number of descriptors" by premise of the rules generated or the "structuring of the system of rules". This last constraint forces the rules produced to go from one set of descriptors to another set of descriptors. For example, for an SBC intended for diagnosis, the desired rules are oriented from symptoms to causes and from causes to remedies. Within the framework of our application to the evaluation of railway safety, this last constraint is essential to orient all the rules generated toward the "Summary Failures" (SFs) descriptor in order to understand the context (or the characteristic parameters) in which the scenario can lead to a particular risk or hazard.

Thus, from the base of examples of historical scenarios (HSKB), the rule learning step seeks to generate a system of rules translating the recognition functions of SFs in the form: IF the facts: type of block (TB) and geographical zones (GZs) and elements involved (EI) and hazard (H) and hazard-related functions (HRFs) and incident functions (IFs) are checked, THEN they result in the single fact "Summary Failures" (SFs). The automatic induction of a system of rules and not of isolated rules as well as the possibility of structuring the rules to elaborate functions of recognition of SF confers to "Charade" an undeniable interest.

Here is part of the system of rules generated by "Charade", under the following induction constraints (Fig. 5):

- Terminal condition = summary failures (SFs).
- Noise = 0 (we consider a low degree of evaluation to avoid the loss of information).
- Maximum number of descriptors per premise = 33 (the descriptors of the scenarios identified are 33 in number).

An initial evaluation by safety experts showed, on the one hand, the consistency of the rules generated and, on the other hand, their interest in stimulating the search for new situations of insecurity.

6 Result 2: Software Safety Assessment Method

We have just presented the methodology implemented for help with FSAs. This paragraph details a second complementary approach to help assess software security (SEEA). As shown in Fig. 6, the PHD can identify all potential accidents of the system such as collision, derailment of a train. As for the FSA, for each potential accident, it proposes the functions and equipment needed to guard against these accidents. The safety assessment method is organized around two closely related phases. To improve the FSA, we proposed a new method based in particular on the learning of the rules of production with a view to generate potential hazards (SF). This second method to analyzing software safety (SEEA) focuses on identifying the solutions (or recommendations) necessary to cover the danger previously generated. This second evaluation phase, which is based on the use of case-based reasoning (CBR), aims to look for the most similar and analogous case in the historical accident and incident database (source case base) the problem to be addressed (target case) in order to propose the appropriate measures to avoid the occurrence of such a danger and consequently of a potential accident.

Figure 7 details the nine steps of the method adopted for the assessment of SEEAs [28, 29]. The left part of Fig. 7 presents the evaluation steps and the right part of the figure shows the results obtained following each step of the approach. For example, Step 1 on knowledge acquisition and modeling allowed the development of a generic SEEA representation model. From the study of the safety files of already certified software (experience feedback), we developed a database of 224 cases (base of
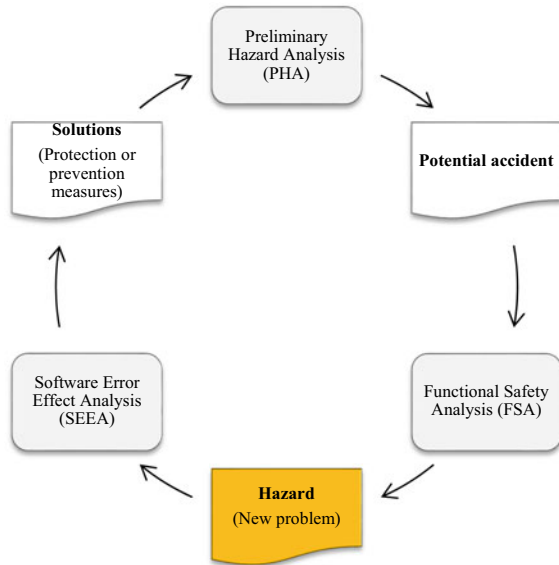
example scenarios). Each SEEA case example is described by several descriptive
parameters such as type of error, feared danger, severity of damage (Fig. 8).

To show the feasibility of the proposed method and the interest of case-based
reasoning (CBR), a feasibility model of the SEEA assessment assistance tool was
implemented using the "ReCall" software, marketed by the "ISoft" company. This
tool requires prior entry of the database of examples (case database) which currently
includes 224 cases. Because the "dreaded event" concept descriptor reflects the
answer that we are trying to find in the case base, its status as unknown will be
maintained throughout this phase of the development of the case base. We make
use of indexing rules that allow us, on the one hand, to arrange the case memory
and, on the other hand, to represent the relevant properties of the entries (the target
cases) in terms of indexes. This is made possible by the fact that indexing rules make
it feasible. In this particular example, the hierarchy is constructed by first taking
into account all of the descriptors and then imposing the descriptors "researched
system" and "studied subsystem" as the top and second levels of the decision tree,
respectively. After that, a decision tree classification technique called the Quinlan
ID3 algorithm [30] will choose the most appropriate descriptors for the subsequent
levels from the set of remaining descriptors.

The ID3 algorithm makes use of a heuristic search strategy that is based on the
gradient technique and works by maximizing a numerical criterion known as gain of
information. This criterion is derived from the entropy of SHANNON, which was
established by Claude Shannon in the early 1940s [20]. ID3 uses a recursive process
to build a decision tree. At each stage of the recursion, the algorithm determines,
from among the remaining characteristics for the current branch, the one that will
most readily categorize the cases at this level of this branch of the tree. This attribute

Fig. 7 Method for acquisition, modeling, and evaluation of SEEA
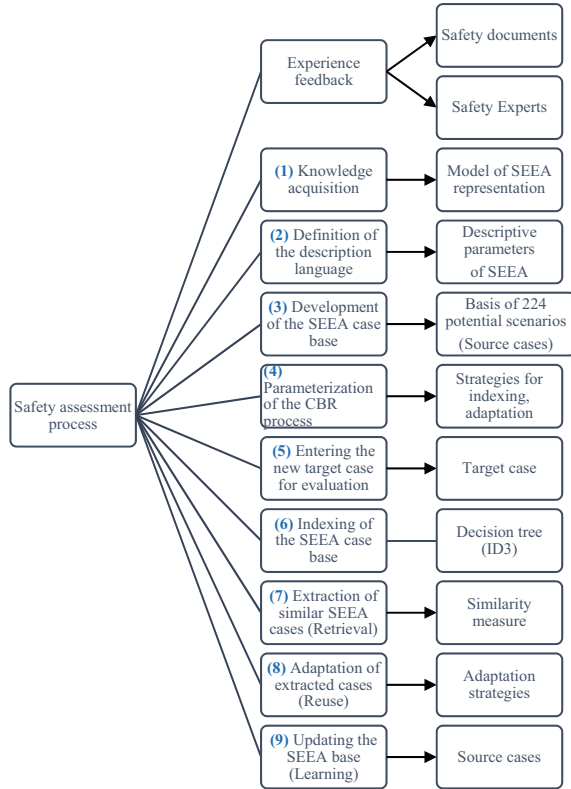
is then used as the basis for the determination of the next stage. To be more specific, the attribute that will result in the greatest amount of information gained. The name for this kind of computation is Shannon's entropy [29].

From:

- A collection of unique classes denoted by the notation "$C_1, C_2, \ldots C_k$".
- A set of instances denoted by the notation "$E_1, E_2, \ldots E_n$" and expressed as pairs (attribute/value) and partitioned into classes C_i.

ID3 generates a decision tree that may be used to identify (or otherwise categorize) all of the instances E_i. The generated categorization rules may then be applied to this tree for further analysis.

QUINLAN's approach involves doing a series of tests on each characteristic in order to determine which one should be used first in order to maximize the amount of information obtained. That is, the characteristic is most useful for differentiating between instances of the various classes. The decision tree is a decision support tool that is used in a range of sectors such as data mining, business intelligence, medical, and safety, among others. It represents a collection of alternatives in the form of graphical data, and it is used to help make decisions (tree).
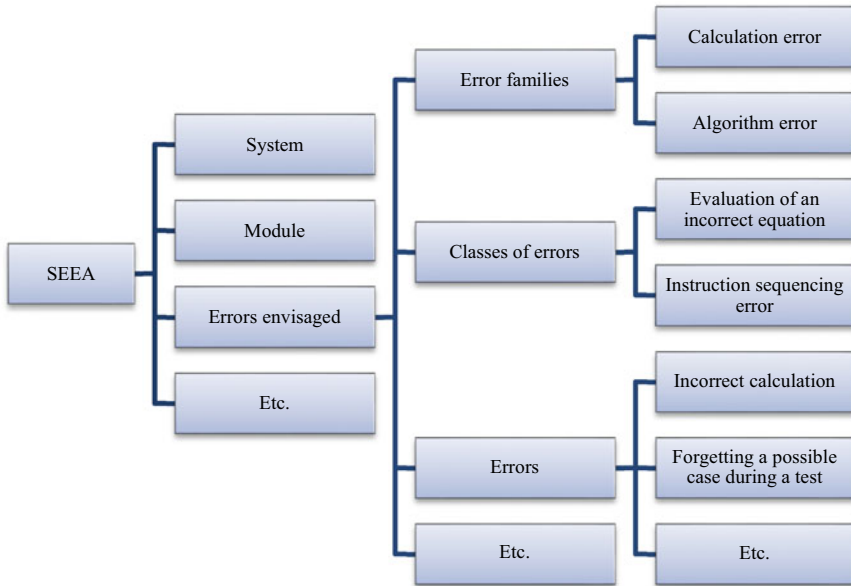
Fig. 8 Main descriptors involved in the SEEA formalism

It is necessary, given a new issue that needs to be addressed (the target case), to search through a base of existing instances (the source cases) to locate the case or cases that are most comparable to the new problem and significant to its resolution. In most cases, there are two different possibilities: (1) The problem can be solved immediately if the case that was found in the database (the source case) is the same as the new problem that needs to be solved (the target case); (2) if the case that was found presents a certain similitude (or analogy) with the new case, then an adaptation procedure is required. In our example, this modification may be carried out in a number of different ways: It can be done implicitly by the safety domain expert, it can be done by comparing examples that are comparable to the target case, or it can be done by the voting mechanism. In the second scenario, the value of the characteristic that has to be modified is determined by calculating it across all of the examples that are comparable using a vote that is weighted according to the proportion of similarity that each case possesses. The tool suggests a single option for the "dreaded event" property in our illustration (Fig. 9), and that option is: Accident involving a train. As a result, the subject matter expert in the field may modify the scenario that is the most comparable to the problem at hand (which was provided by the tool) by giving the "Feared Event" concept the value "Collision" as a remedy to the issue.

The case database will then be updated, which is the last stage in the CBR process. In this step, the newly revised target case is included into the SEEA's historical case database (source cases), after approval by the safety expert [29].
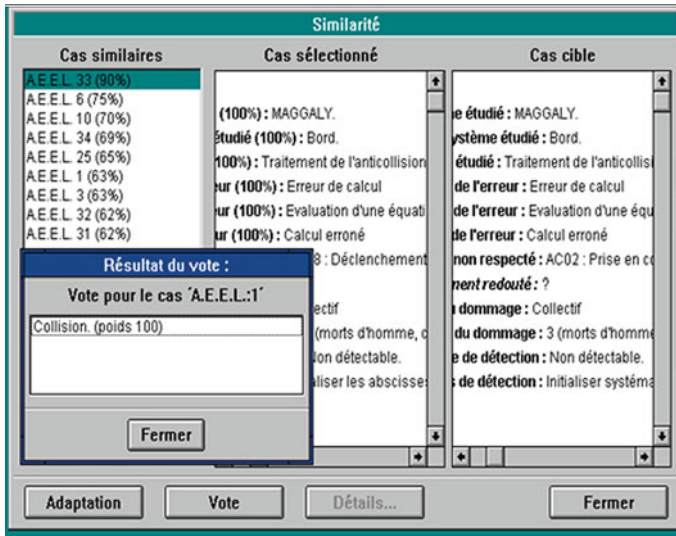
Fig. 9 "Feared event" proposed by the tool: "Collision"

In practice, we are often faced with a problem that we have already encountered in the past, and similar problems often have similar solutions. A new problem is solved by finding a similar past case and reusing it in the new situation. CBR is a progressive and evolutionary process that aims to find solutions to a new problem (the case) from previous similar problems already experienced (case base).

In the case of reasoning from examples, the concepts are defined as a class of examples. Solving a problem (classifying a new example) is based on finding the class that best matches the example. In this context, the set of solutions contained in this class represents the solution for the example in question, and the solutions are not modified according to the input data of the learning system. Conversely, in CBR, the proposed solutions can be modified and adapted to the new problem to be solved. As evidenced by the problem of safety analysis and certification of rail transport: to find potential accident scenarios likely to jeopardize safety, experts refer to past accident cases (experience feedback). CBR is particularly well suited to applications whose task is performed by human experts and whose experiences are available in a database, in historical documents resulting from feedback (for example, accident investigation reports and railway incidents) or in human experts. In the case of our application of CBR to the evaluation of railway safety, it is not necessarily a question of finding the concrete and applicable solution for a new problem. It can also be a question of justifying, criticizing, or interpreting the solutions proposed by the CBR.

A CBR process involves going through the following major phases [28, 29]:

1. Identification and characterization of the new problem to be solved. In our application, it is a new accident or incident scenario described by a set of characteristic descriptors of a scenario. More specifically, it is a new case of accident or incident

submitted to the experts for assessment in terms of completeness and consistency. This first stage of the CBR process required a long phase of collecting knowledge from experts and from historical safety files. This step finally made it possible not only to develop an indexing vocabulary, but also to constitute the basis of learning cases (set of experiences structured in the form of accident or incident scenarios).

2. Search for the case most similar to the problem. During this step, it is a question of carrying out measurements of similarity between two or more cases. These measures are defined according to the common characteristics between the scenarios archived in the database and the new scenario submitted for evaluation by the experts.

3. The most similar case (scenario) is used to suggest a new solution. For example, proposing the potential risks (or dangers) likely to occur in a given situation or configuration described by the new scenario or even proposing the solutions (prevention and/or protection measures) already envisaged in the past from the base of source cases (learning base or historical cases).

4. Evaluation of this solution. The proposed solution must be evaluated by interaction with the safety expert. Either the solution is immediately found in a similar case from historical data or the CBR process does not offer an immediate solution to the problem but rather a plausible solution that requires an important adaptation step. In this last hypothesis, it is necessary that the CBR system has knowledge of adaptation specific to the problem to be solved. There are several adaptation techniques and approaches: (a) substitution methods which includes zero adaptation approaches, re-instantiation, adjustment of parameters, etc., (b) transformation methods such as the model-driven transformation technique. As part of our feasibility study, we used the simplest adaptation method to implement: "Zero adaptation". This approach is generally used when the new problem corresponds exactly to an existing case in the learning base. The "zero adaptation" approach occurs when the new problem is close enough or when an exact match is found, which may be more or less common depending on the application. To our knowledge, in industrial applications, few CBR systems adapt automatically. For most systems, human intervention is required to partially or completely generate a solution from historical examples stored in the case base.

5. Update of the source case database with the new case. Once the solution has been adapted to the target problem, this new experience should be archived and stored as a new case in the initial database (source cases). It is a stage of learning and updating to enrich the experience in a given field.

Thus, by analogy to inductive machine learning, CBR starts the learning cycle with a set of learning cases or examples; he then proceeds by a process of generalizing these examples (inductive learning) by identifying the common points between a case retrieved from the base of examples and the target problem.

7   Validation

Two major steps were performed to show the feasibility of the approach. The first phase consisted of an overall evaluation of the feasibility model based on its application to all the accident scenarios archived to date relating only to the risk of an accident: train collision.

Most of the knowledge relating to the field of safety assessment and certification of rail transport derives essentially from the analysis of the risks of accidents and incidents represented in the form of potential accident scenarios. These are designed by design engineers and safety experts or archived in safety files and investigation reports. The development of a new accident scenario is based in particular on the history relating to the transport systems that have already been certified. The extraction and formalization of all the scenarios tested to date are a substantial work (about thirty knowledge acquisition sessions). Indeed, the operational safety of guided rail transport systems requires considering all the risks of accidents (collision, derailment, electrocution, fall, etc.) to which many scenarios can be associated. As part of a feasibility study, we have voluntarily limited developments to a single accident risk: "collision". Nevertheless, the architecture of the system produced is open and can therefore accommodate other types of accident risks such as derailment.

If this downward revision of the number of accident scenarios does not in any way affect the quality of the database of learning examples dedicated to the risk of collision, the problem of evaluating the performance of the learning system developed laid. Remember that this is initially a feasibility study to show the contribution and the merits of machine learning to railway safety.

The second phase focused on an internal evaluation of the "Clasca" classification module based on a set of test scenarios provided by the experts. This validation revealed not only the interests but also the current limitations of the completed model and resulted in prospects for improvement. The quality of learning is measured by assessing the validity and usefulness of the knowledge learned. An acquaintance is valid if it is adequate and consistent with what is already known in the field of railway safety. It is useful if it helps to achieve the defined goals. The control of these two criteria is the responsibility of safety experts. To test the prediction capacity of the system and therefore the representativeness of the results obtained by the learning system, there are two solutions: either the expert has a list of control cases constituting the basis of test examples or the all initial data available is shared in "learning base" and "test base" according to a distribution law given by the domain expert. Initially estimated at several hundred accident scenarios, the number of examples acquired so far is 80 scenarios for the learning base and 13 for the test (validation) scenarios. While this downward revision of the number of scenarios does not in any way affect the quality of the basis of examples of learning dedicated to collision risk, the problem of assessing the performance of the "Clasca" learning module arises.

Table 1 presents the evaluation results obtained for the thirteen test scenarios. The classification results of these thirteen scenarios can be interpreted as follows:

Table 1 Result of the validation of the module "Clasca"

Test scenarios	Prediction of "Clasca"		Decision expert	Comparison of results
	Class	Adequacy rate		
SV1: divergence between output control and input control	C7	1.00	C7	Well ranked
SV2: premature registration of an item on a section	C7	0.77	C3	Misclassified
SV3: late discrimination involving follower identification	C7	0.99	C7	Well ranked
SV4: transmission fault between two adjacent PAs	C1	0.88	C1	Well ranked
SV5: splitting a multiple unit on a DN	C7	1.00	C7	Well ranked
SV6: three elements train	C7	0.83	C9	Misclassified
SV7: lifting of the FU at zero speed after an evacuation request	?	< SS	C4	Unclassified
SV8: manual driving on a section in evacuation request	C9	0.78	C9	Well ranked
SV9: needle movement in manual control	?	< SS	?	Unclassified
SV10: localization fault and needle movement	C3	0.94	C3	Well ranked
SV11: reverse order of registration	C8	0.76	C8	Well ranked
SV12: train in manual operation not respecting distance instructions	C9	0.91	C9	Well ranked
SV13: counter-sense target	C6	0.83	C6	Well ranked

- Nine scenarios are "well classified": they are classified in the same way by the system and the expert.
- Two scenarios are "unclassified": their class matching rate is lower than the current similarity threshold, and the system does not offer any class of membership. Since the similarity threshold is evaluative, these scenarios are momentarily put on hold and may be reclassified later. For one of these cases, the expert proposed a class, and for the other case, he agreed with the decision of the system by not classifying the scenario.

- Two scenarios are "misclassified": the classification of the system does not approve the expert. The main cause of this failure comes from the non-representative of the class descriptions learned on the basis of a small number of scenarios.

Although this first evaluation demonstrates the validity of the method implemented on the "Clasca" model, a more detailed evaluation is needed to measure and eventually optimize the system's performance. For this, it is imperative to enrich the base of learning examples with additional scenarios relating to the risk of collision as well as scenarios relating to all other risks of accidents such as derailment. The main originality of "Clasca" lies in considering the non-monotone incrementality. This raises the problem of the influence of the order in which the examples are considered. Learning in CLASCA is non-monotonous: the description of a class learned at time t is called into question at time $t + 1$ and the frequency of appearance of a descriptor is sometimes increasing, sometimes decreasing. Although better suited to noisy data, non-monotonous learning does not guarantee the convergence of the process. In "Clasca", the convergence problem is controlled by the introduction of an evolutionary similarity threshold. The non-monotony of learning influences the sensitivity of "Clasca" to the order of arrival of the scenarios. An example that is integrated in a class at time t is not guaranteed to return to the same class at time $t + n$ because of the evolution of the description of the class. This is even truer at the beginning of learning, when the description of the class is not yet well typed. To date, we have admitted to a first degree that the involvement of the expert in the control of classification results can circumvent this problem. A study on this point will however have to be conducted.

The expected objective is to study the feasibility of a final decision support system through the treatment of a sub-problem representative of the field of railway safety: train collision. This feasibility model presents a reduced form of the final system and attempts to identify all the characteristics of safety assessment knowledge. It required a knowledge extraction step to identify the safety data in terms of source, nature, form as well as the strategies and modes of reasoning developed by the expert for the resolution of the studied sub-problem (the collision). The modeling phase ends with a procedure for evaluating and validating the methods and tools used and ultimately allows a conclusion to be drawn on the feasibility of the system.

The validation of this methodology took place in two phases. The first phase consisted of an overall assessment of the feasibility model of the system developed on the basis of its application to all the scenarios archived to date for the risk of collision. The second phase focused on an internal evaluation of the "Clasca" classification module based on a set of test scenarios provided by the experts. This validation revealed the interests but also the current limits of the model produced and led to prospects for improvement.

This model attests to the interest and validity of the methodology developed to classify and assess accident scenarios, which was our initial objective. Although this first evaluation demonstrates the soundness of the approach implemented on the model, a more detailed evaluation is necessary to measure and ultimately optimize

the performance of the system. In order for this system to be evaluated in an industrial environment, it is necessary to provide for certain improvements and extensions. The safety analysis knowledge acquired to date is far from being representative of the field and needs, on the one hand, to be supplemented by other scenarios relating to the risk of collision in order to enrich the base of examples learning and on the other hand, to be extended to several other additional accident risks such as derailment. Initially, the design of an integrated version of a prototype is necessary to finalize the results of the model and consider the comments made. Other limits are still being studied and concerned in particular the influence of the order in which the learning examples (scenarios) are considered ("Clasca" module), the relevance of certain evaluation rules (module "Charade"), and finally, the procedure for adapting certain solutions produced by the case-based reasoning (CBR) module.

8 Conclusion

The analysis of the field of railway safety has shown that the process of knowledge transfer from experts to the machine is complex and little studied and that the famous "bottleneck" of the development of a knowledge-based system (KBS) is not limited to the single phase of knowledge extraction but is also linked to the characteristics and formalization of knowledge. The know-how of the experts is based on subjective, empirical, and sometimes implicit and ambiguous knowledge which can generate several interpretations. There is generally no scientific explanation to justify this compiled expertise. This knowledge is not always conscious in the expert, understandable by a novice or even expressible through language. The transcription of verbal (natural) language into formal language interpretable by a machine often causes a distortion of expert knowledge. This introduces a bias between the expert's cognitive model and the implemented model. This discrepancy is due not only to the fact that the representation languages used in AI are not sufficiently rich to explain the cognitive functioning of the expert, but also to the subjective interpretation of the developers of AI-based systems. In addition, the expert who is generally the only one with the know-how to solve certain crucial problems may show a lack of motivation and availability. All these constraints restrict the field of investigation of knowledge acquisition. The joint use of knowledge acquisition and machine learning techniques is a solution to weaken these constraints. Experts generally consider that it is easier to describe examples or experimental cases than to explain decision-making processes. The introduction of automatic learning systems operating on examples makes it possible to generate new knowledge likely to help the expert to solve a particular problem. The expertise of a domain is not only held by the experts but also distributed and stored implicitly in a mass of historical data that the human mind finds difficult to synthesize. Extracting relevant knowledge from this mass of information for an explanatory or decision-making purpose is one of the objectives of machine learning characterized by improved performance with experience. However, learning from examples is insufficient to acquire all of the experts' know-how and requires

the use of knowledge acquisition to identify the problem to be solved, extract and formalize knowledge accessible by the usual means of learning acquisition. In this sense, each of the two approaches can overcome the weaknesses of the other. To improve the process of transferring expertise, it is therefore interesting to reconcile these two approaches in the iterative process of acquiring knowledge.

From the initial knowledge of the domain (expert and historical knowledge), the acquisition of knowledge makes it possible to build a model of the reasoning of the expert and a model of representation of the examples and to obtain a set of examples and classes of objects. This acquired knowledge is exploited by learning to produce new learned knowledge which will then be evaluated by the domain expert. The confrontation of the knowledge discovered by learning with the knowledge acquired from the expert makes it possible to enrich the initial knowledge of the field. There is always a gap between the knowledge acquired and the knowledge actually held by the expert. Indeed, we can rarely extract all the expert knowledge on the first try but when we present to the expert the knowledge learned by the system, he is aware of their interest and identifies contradictions, "holes", or rules relevant. It can provide an opinion on the choice of examples and descriptors, interpret the results produced by learning, improve the previously acquired expertise model, correct and complete the example description language, and adjust the learning parameters. By encouraging the expert to better verbalize his expertise, we therefore contribute to the enrichment of knowledge in the field. In this, taking the expert into account in the process is essential to improve the transfer of expertise. We therefore find here a new aspect of the concept of expert/system cooperation which must go beyond the goal of the sole implementation of ergonomic dialogue interfaces and move toward an increase in the decision-making capacities of the systems in order to establish a "partnership" with the human operator.

Based on the examination of the manufacturer's safety file, the expertise of the experts, the history of the incidents that occurred and considering a certain number of constraints (safety objectives), the certifying expert relying on safety analysis tools and methods is required to develop a certification report. As long as the certifying expert demonstrates through accident scenarios that the safety objectives are not achieved, the designer must review and improve the transport system in terms of safety. These iterative processes of safety evaluation, which relies on several modes of reasoning and uses several types of knowledge, confirm that a conventional computing solution is inappropriate and that the use of AI techniques seems more appropriate.

To improve the usual methods and techniques for evaluating railway safety, we have agreed to use machine learning techniques: learning classification procedures (module "Clasca"), rule-based machine learning (module "Charade"), case-based reasoning (module "ReCall"), and knowledge-based system (KBS). The first step of collecting knowledge, not only from experts in the field, but also from several safety files (feedback), finally led to the development of two formalisms of knowledge involved, respectively, in safety functional (FSA) and software security (SEEA). These two models make it possible to assist experts in their safety analysis tasks by helping them to better structure and conceptualize the knowledge involved. These

safety knowledge representation models were then used by several safety experts and researchers to develop two databases: a database of 224 SEEA scenarios and a database of 80 AFS scenarios. When it comes to ML, our work is part of supervised learning. Indeed, the presence of the safety expert is essential to ensure effective and relevant learning. We used three learning systems. The first "Clasca" which is an inductive and incremental learning algorithm allows grouping and classifying the historical accident scenarios. The second "Charade", which was kindly provided by the Prf. Jean-Gabriel Ganasca (LIP6-Jussieu-Paris 6), strives to look for regularities present in a class of accident scenarios (proposed by the "Clasca" module) in order to produce a rule base that can be exploited by an expert system. For the third case-based reasoning algorithm (CBR), we used a CBR generator called "ReCall" from ISOFT. Despite the undeniable interest of these tools "Clasca", "Charade", and "ReCall", several shortcomings were noted during the evaluation phase. As stated above, for the "Clasca" system, it is necessary firstly to enrich the learning base so that it is representative. With regard to the system "ReCall", several shortcomings have been noted in particular for coping strategies. Finally, the system "Charade", despite its undeniable interest, some rules generated are not of direct interest to assess safety. It is therefore essential to check the veracity and the relevance of certain rules.

References

1. Ganascia, J.-G.: Agape et Charade : deux mécanismes d'apprentissage symbolique appliqués à la construction de bases de connaissances. Thèse d'État, Université Paris-sud, France (1987)
2. Hadj-Mabrouk, H.: CLASCA: learning system for classification and capitalization of accident scenarios of railway. J. Eng. Res. Appl. **6**(8), 91–98 (2016a)
3. Li, J., Wang, J., Xu, N., Hu, Y., Cui, C.: Importance degree research of safety risk management processes of urban rail transit based on text mining method. J. Inf. **9**(2), 26 (2018)
4. Hayward, V.: Big Data and the Digital Railway (2018). Available from: https://on-trac.co.uk/big-data-digital-railway/
5. Williams, T., Betakbc, J.: A comparison of LSA and LDA for the analysis of railroad accident text. Procedia Comput. Sci. **130**, 98–102 (2018)
6. Faghih-Roohi, S., Hajizadeh, S., Núñez, A., et al.: Deep convolutional neural networks for detection of rail surface defects. In: International Joint Conference on Neural Networks (IJCNN), July 2016, Canada, pp. 24–29 (2016)
7. Marr, B.: How Siemens is Using Big Data and IoT to Build the Internet of Trains (2017). Available from: https://www.forbes.com/sites/bernardmarr/2017/05/30/how-siemens-is-using-big-data-and-iot-to-build-the-internet-of-trains/#2b7a4b6e72b8
8. Shirazi, K.N., Ul Hassan, N., Naqvi, S.A.-A., Parkinson, H.J., Bamford, G.: Big data and natural language processing for analysing railway safety. In: Innovative Applications of Big Data in the Railway Industry, pp. 240–267. IGI Global Publishing (2017)
9. Ghomi, H., Bagheri, M., Fu, L., Miranda-Moreno, L.-F.: Analyzing injury severity factors at highway railway grade crossing accidents involving vulnerable road users: a comparative study. Traffic Inj. Prev. **17**(8), 833–841 (2016)
10. Zhang, X., Green, E., Chen, M., Souleyrette, R.R.: Identifying secondary crashes using text mining techniques. J. Transp. Saf. Secur. (2019). https://doi.org/10.1080/19439962.2019.1597795

11. Heidarysafa, M., Kowsari, K., Barnes, L.-E., Brown, D.-E.: Analysis of railway accidents' narratives using deep learning. In: International Conference on Machine Learning and Applications (IEEE ICMLA) (2018). arXiv: 1810.07382 [cs.CL]. https://doi.org/10.1109/ICMLA.2018.00235
12. Zubair, M., Khan, M.J., Awais, M.: Prediction and analysis of air incidents and accidents using case-based reasoning. In: Third Global Congress on Intelligent Systems, 6–8 Nov 2012, Wuhan, China (2012)
13. Khattak, A., Kanafani, A.: Case-based reasoning: a planning tool for intelligent transportation systems. Transport. Res. C—Emer. Technol. **4**, 267–288 (1996)
14. Louati, A., Elkosantini, S., Darmoul, S., et al.: A case-based reasoning system to control traffic at signalized intersections. IFAC-PapersOnLine **49**, 149–154 (2016)
15. Cui, Y., Tang, Z., Dai, H.: Case-based reasoning and rule-based reasoning for railway incidents prevention. In: Proceedings of ICSSSM '05. 2005 International Conference on Services Systems and Services Management, Chongquing, China, pp. 13–15 (2005)
16. Varma, A., Roddy, N.: ICARUS: design and deployment of a case-based reasoning system for locomotive diagnostics. Eng. Appl. Artif. Intel. **12**, 681–690 (1999)
17. Zhao, H., Chen, H., Dong, W., Sun, X., Ji, Y.: Fault diagnosis of rail turnout system based on case-based reasoning with compound distance methods. In: 29th Chinese Control and Decision Conference (CCDC), pp. 4205–4210 (2017). https://doi.org/10.1109/CCDC.2017.7979237
18. Hadj-Mabrouk, H.: Preliminary hazard analysis (PHA): new hybrid approach to railway risk analysis. Int. Refereed J. Eng. Sci. **6**(2), 51–58 (2017)
19. Hadj-Mabrouk, H.: Machine learning from experience feedback on accidents in transport. Published in 7th International Conference on Sciences of Electronics, Technologies of Information and Telecommunications, pp. 246–251(2016b). https://doi.org/10.1109/SETIT.2016.7939874
20. Quinlan, J.R.: Induction of decision trees. Mach. Learn. **1**, 81–106 (1986)
21. Hadj-Mabrouk, H.: Contribution of learning Charade system of rules for the prevention of rail accidents. Intell. Decis. Technol. **11**, 477–485 (2017)
22. Hadj-Mabrouk, H.: A hybrid approach for the prevention of railway accidents based on artificial intelligence. In: Vasant, P., Zelinka, I., Weber, G.W. (eds.) International Conference on Intelligent Computing and Optimization, pp. 383–394 (2018a)
23. Hadj-Mabrouk, H.: New approach of assessing human errors in railways. Trans. VSB—Tech. Univ. Ostrava, Saf. Eng. Ser. **13**(2), 1–17 (2018b)
24. Hadj-Mabrouk, H.: Contribution of artificial intelligence to risk assessment of railway accidents. J. Urban Rail Transit **5**(2), 104–122 (2019a)
25. Hadj-Mabrouk, H.: Contribution of artificial intelligence and machine learning to the assessment of the safety of critical software used in railway transport. J. AIMS Electron. Electr. Eng. **3**(1), 33–70 (2019b)
26. Hadj-Mabrouk, H.: Contribution of machine learning to rail transport safety. Chapter 10. In: Vasant, P., et al. (eds.) Advances of Machine Learning in Clean Energy and the Transportation Industry, pp. 277–312. Nova Science Publishers. https://doi.org/10.52305/SJDR3905
27. Hadj-Mabrouk, H.: Decision support approach for assessing of rail transport: methods based on AI and machine learning, Chapter 5. In: Hassan, S., Mohamed, A. (eds.) Handbook of Research on Decision Sciences and Applications in the Transportation Sector, pp. 124–146. IGI Global (2021). https://doi.org/10.4018/978-1-7998-8040-0.ch005
28. Hadj-Mabrouk, H.: Application of case-based reasoning to the safety assessment of critical software used in rail transport . Saf. Sci. **131**, 104928 (2020). https://doi.org/10.1016/j.ssci.2020.104928
29. Hadj-Mabrouk, H.: Case-based reasoning for safety assessment of critical software. Intell. Decis. Technol. **14**(4), 463–479 (2020). https://doi.org/10.3233/IDT-200016
30. Shannon, C.E.: A mathematical theory of communication. Bell Syst. Tech. J. **27**, 379–423 (1948)

Predicting the Effect on Land Values After Introducing High-Speed Rail

Annie Srivastava, Shilpi Lavania, and Swati Mohapatra

Abstract This graduation project/thesis is aimed at predicting the land values after the introduction of Mumbai–Ahmedabad High-Speed Rail (MAHSR) in the cities having the High-Speed Rail (HSR) stations. Evidences from various countries are collected and studied in order to understand the effect of population on land value and determining the relationship between them, through predictive regression analysis. After the quantitative analysis, other factors like accessibility and other physical attributes like location, density, and working population have been studied in order to conclude the population spread over the various cities under study with the rising industrial growth and employment opportunities. Research recommendations that include topics of technological implementation, sustainable development, and land use planning are included in order to gain the maximum benefits out of the implementation of High-Speed Rail in the route.

Keywords Land value · Population · High-speed rail

1 Introduction

High-Speed Rail is a complex system constituting of the components like infrastructure, rolling stock, signaling systems, station emplacement, maintenance systems, operation rules, and other legal and financial entities [1–5]. HSR is a system adaptable to any country like any other railway system having various commercial and operational considerations. HSR offers the society a range of advantages due to

A. Srivastava
Rail India Technical and Economic Service Limited, New Delhi, India

S. Lavania
Department of Electronics and Communication Engineering, Institute of Engineering and Technology, Dr. Bhimrao Ambedkar University, Agra, India

S. Mohapatra (✉)
School of Science, Gujarat State Fertilizers and Chemicals University, Vadodara, Gujarat 391750, India
e-mail: swatimohapatraiitr@gmail.com

its high capacity up to 400,000 passengers per day, positive environmental impact by reducing congestion, efficient use of land up to 1/3 of that of a motorway, and increasing energy efficient to 9 times that of airplanes or 4 times that of cars and high safety such that no accidents with injured passengers at a speed of 200 km/h have been reported as per UIC [6]. High commercial speed, shorter total time of travel make the last mile travel time shorter as well highly reliable in nearly any kind of weather, high frequency leading to high accessibility unlike long waiting time at airports, affordable price, higher comfort when compared to bus or car making it a highly efficient system [7–11]. Seatbelts are not a necessity and electronic devices are not limited to use providing customers the freedom to make their trip a happy one. It helps in boosting the economy the place and acts as a regulatory measure in controlling urban sprawl leading to a logical territory structure [12–15].

Precisely, the need for speed became eminent in the nineteenth century during the Industrial Revolution of Europe with the rising need of fast movement of passengers for trade [16–19]. With increase in speed from 50 km/h to average of 135 km/h electric powered rail systems still competent with other faster means of transport like airways, it marked an evidence and scope for technological development in the advanced countries of the time [20–23]. European countries like UK, Germany, Italy, and France (331 km/h in 1955) were making significant records as per speed was concerned until in 1964, on October 1, Japan surprised the world when the Tokaido Shinkansen, the very 1st High-Speed Rail running between Tokyo Central and Shin Osaka was introduced on a brand-new standard gauge line over 515 km which was 1435 mm apart from the conventional meter gauge used in Japan [24–28]. Japan, introducing the very first High-Speed Rail, Tokaido Shinkansen in 1964, was promoted as a new transport system by then JNR president Shinji Sogo and Vice President for Engineering Hideo Shima was a boost in Japan's economy due to the innovation of High-Speed Rail which turned out to be Japan's backbone of passenger transport operational at speeds as high as 210 km/h powered at 25 kV ac, Centralized Traffic Control (CTC), Automatic Train Control (ATC), and with other modern improvements, it has now reached the top speed of 320 km/h [29–36].

The success of the operations of Shinkansen in Japan led to the technical progress in rail speed in European countries like UK, Germany, Italy, and France, which aimed at the future of railway passengers. Though the future was uncertain due to Concorde, political opposition, 1973 first petroleum crisis, and other events and even though there emerged other means of transportation, the national French railway company SNCF started its first operations in 1971, on September 27 between Paris and Lyon, the HSR having a speed of 260 km/h [37–42]. Unlike the Japanese concept of the Shinkansen which was operational on a new standard gauge, the Europeans developed it on the existing railways itself. The big success stories of the development of HSR in Japan and some if the European countries set a trend of adoption in various other countries around the world, some of them being Spain in 1992, Netherlands in 1997, China in 2003, South Korea in 2004, Taiwan in 2007 and Turkey in 2009. France set the highest speed record of 574.8 km in 2007. In 2008, on August 1, China with its 120 km HSR line connecting Beijing and Tianjin was a major transformation for the country with the highest population [43–50]. China set high records of implementing

almost 20,000 km of High-Speed Rail (HSR) lines serving 800 million customers per annum as per 2014 which constituted more than ½ of passenger traffic of HSR around the world. It has an enormous number of fleet of 1200 train sets. Taking the example from these countries, various other nation states like Saudi Arabia, Morocco, USA, etc. [51–56] have their lines under construction. It is indicated that the emergence and the development of HSR need to be done continuously in the coming 50 years and beyond in order to acquire and keep the hold in the passenger commute market.

India as it is moving toward adopting the HSR technology and implementing it as a move toward matching world standards in terms of transport and accessibility which is a major boost to the nation's economy and trade as is evident of the fact that speed and for that matter the first HSR were first introduced as a result of industrialization in Japan and other European countries [57–66]. With industrialization, urbanization became the developing factor as a consequence which allowed more people with higher frequency to move in distant place with reduced time for trade. No doubt, HSR has been a major factor contributing to transit-oriented and sustainable development of the various positive technological and environmental impacts; it has shown in the countries where it has been implemented [1, 4, 5, 36].

This study is determining land value along the cities where HSR line will be introduced using population dynamics and circle rate as variables to design regression model for prediction that will be useful for transit-oriented development and economic growth of the country. Section 2 explains the methodologies that would be used in the course of this research to predict land values along the routes. Section 3 provides a base to the various qualitative factors that affect land values along the cities having the HSR station when a new transport system, i.e., HSR line in this case is introduced. The next two sections, i.e., 4 and 5 contain the case study of the HSR line that is being studies and the parameter like population dynamics and circle rate that are used in the quantitative analysis followed by a discussion on the results combining both the qualitative and the quantitative analyses in Sect. 6. Section 7 provides the research recommendations that must be done after the land value analysis like the transit-oriented and sustainable development to gain most out of the HSR line being introduced along a route. The study is then concluded completing the aim of the research, i.e., predicting land values after introducing HSR in India. Land value determination will be useful in sustainable development, transit-oriented development, and land use planning along the HSR route to gain the maximum benefits out of this transport infrastructure development in trade, economy, and positive impact on climatic conditions.

2   Research Methodologies

2.1   Integration Between Theory and Case Studies

The study is a combination of both quantitative and qualitative analyses based on evidences that are collected resulting from the theoretical and empirical studies on the various countries around the world where High-Speed Rail has been introduced and implemented. The prediction of land value along the HSR line after the introduction of the Mumbai–Ahmedabad High-Speed Rail (MAHSR) corridor which is the case study of this paper will allow better planning of land use for a well-developed future socioeconomic structure leading to nation's economic and environmental benefits [67].

2.2   Analysis Method

The research is aimed at finding and establishing a relation between the yearly changes in circle rate with the change in population. To establish the relationship, data are collected for population and circle rate for the various cities having proposed stations along the MAHSR route as the proposed operation is estimated to start in 2025 and regression analysis is applied to predict the land value as per the trend. After which, other factors like accessibility will be used as to determine if there will be a positive or negative impact on land values in the given areas under study. The type and formula of regression analysis will be determined based and specific to the particular area of study as provided in section. R^2 which is the coefficient of determination will be used to check the proportion of the variance as derived for the predicted dependent variable determined from the independent variable. The closer the value of R^2 to 1, the better the regression model fits to the actual values.

3   High-Speed Rail System and the Impact on Land Values

The various evidences collected from places around the world show that there is a heterogeneous effect on land value with the introduction of HSR. While China, a part of Spain, and UK show a positive impact, other places like Milan and Paris in France, Rome, showed negative results. Also, there were places like Berlin in Germany, Tainan in Taiwan, Strasbourg, Le Creusot, and Florence represented in the table above showing only a marginal impact on land values with the coming of High-Speed Rail in these places. This heterogeneous observation is related to mirroring the impacts seen for the various urban transport systems in cities.

3.1 Impact on Different Places

The heterogeneous impact of the introduction of HSR line in various cities is explained in detail in this section.

UK

The UK as per 2020 has an estimated population of 67,363,000 ranking 21 in the world as per 2019. The projected population for 2030 is shown to be 70,338,000. The total area is 242,500 km². (93,630 sq. mi) with density being 709.6/km². (274 per sq. mi) as per the data recorded in 2018. It is one of the most developed island countries due to its early industrialization, situated in the North Western coast of Europe, constituting of the Great Britain which comprises England, Scotland, Whales, and Northern part of Ireland. The urbanization has resulted in incremental change in the employment pattern making it a great center of urbanization. This is clearly depicted that around 83.4% of the population is settled in the urban area as per the data in 2018 ("United Kingdom—Urban settlement"). Greater London is a metropolitan area and the largest industrial center because of the greatest port being located there. Due to the need of business expansion, the population is moving from inner to outer areas of London leading to development of urban centers leading to urbanization.

London Borough of Camden

London Borough of Camden has an area of 22 km². (8.4 sq. mi) with a population of 220,338 as per 2011 which showed 11.27% growth since 2001 (198,020) which constituted more than 1/5th of the population ethnic minorities from South Asia and Africa. As with the growth in population, the expansion of the railways, and canal system, there was an increase shown in urbanization ("Camden|borough, London, United Kingdom"). The Town of Camden turned to the production house of crafts oriented to tourism has taken over the piano and furniture making market trade. Hatton Garden is being London's center for trading silver and gold while a concentrated shopping center has been developed at the Tottenham Court. The place also has a lot of historical landmarks, namely, the chapel of St. Etheldreda in Ely Place, Gray's Inn which is the legal center in Holborn, Staple Inn, the museum of Sir John Soane in Lincoln's Inn Fields. Bloomsbury resides the neoclassical British Museum, the British Library at St. Pancras since 1998, and many more that makes the place tourist attraction. With the introduction of High-Speed 1 (HS1) line, Camden with its station named as St. Pancras International Station showed an increment of 20% in its housing prices in 2007 while showing a slower growth rate of 7% in 2008.

After the arrival of HS1 line, there was an immediate increase in housing prices by 15% in 2007, whereas there was no significant change in 2008 in London. Before the arrival of High Speed 1 (HS1) line, Camden showed similar trends in terms of housing prices as that of London considered as a whole. This result showed an increase in property prices at adjacent lying area due to increased accessibility to HSR transport system. With evidence found from a statistical study conducted by Preston and Wall in 2008, it showed a 6% increase in employment and 3% in housing prices in Ashford

when compared to the whole of South East England with the introduction of Ashford HSR station.

France

France is a county with Paris as capital city. It has a population of about 64,958,000 as per 2020 ranking 22 in 2019 in the world. The projected population for 2030 is about 68,379,000. The total area is 543,965 km². (210,026 sq. mi) with density being 118.5/km². (306.9 per sq. mi) as per the data recorded in 2018. The urban population constitutes of about 80.4% and rural being 19.6% as per the data in 2018. The Gross National Income (GNI) in U.S. $'000,000 was 2,548,257, and GNI per capita (U.S.$) was recorded to be 37,970 in 2017.

A country in the northwestern region in Europe, the nation is of high cultural as well as historical importance among the countries of the west. The country being bounded by the Mediterranean Sea and the Atlantic Ocean has been a major player in the colonizing various parts of the world, and also, it has bridged the north and the south of Europe through its geography, language, and economy. Not to be forgotten, it serves as Europe's most powerful industrial leadership as well as one of the most important producers in agriculture.

Paris

There are 20 arrondissements in Paris, out of which the tenth arrondissement is called as the "warehouse" which is located at the bank of the Seine River constituting a huge area of the Saint Martin canal. It has six main railway stations, and Gare de l'Este and Gre du Nord are two of them which were constructed in the nineteenth century which were among the busiest in the whole of Europe. The city has a population of 88,557 and a density of 30,643/km² (79,370 per sq. mi) as per January 2018. The area is 2.89 km² (1.12 sq. mi). The tenth arrondissement is densely populated and is a center for business activities employing a large number of inhabitants as can be denoted by 71,962 jobs among 89,612 inhabitants in 1999.

The Gare de l'Est station is located in the tenth arrondissement of Paris connecting Paris to Strasborg. The station was redeveloped in 2006 for TGV trains. The property values increased by 2.18% in 2007 which was lower rate as compared to 4% increase in the whole of Paris. In 2005, before the redevelopment of the station, there was 1% increment since 2004, but it decreased to 9% in 2009 and 2% in 2007. The growth rate of property values was although higher in tenth arrondissement of Paris as compared to the rest of Paris before the redevelopment of the station. Some empirical studies suggested that negative externalities faced due to very close infrastructure overpower the positive impact of the benefits of easier accessibility.

Lyon

Lyon is located in the east central part of France between Paris and Marseille and is the third largest city in the country. It is the capital of two places, namely the Rhone department and Auvergne Rhone Alpes region. It is a metropolis famous for its historical and architectural heritage recognized by the UNESCO as a world heritage site. It is also one of the larger urbanized areas or agglomeration in the whole

of France apart from Paris. The estimated population in 2014 was 1,422,331. Lyon marks its presence with its unique location which is strategic as per the economy is concerned it lies between northern and southern Europe with a great room for world trade. It has also made significant efforts in the development of cinematography and is a key player in gastronomic heritage along with its rich cultural and architectural presence. With the opening of TGV Southeast between Paris and Lyon which was opened in 1981, Lyon's Part-Dieu station had a 43% increase in land prices.

Le Mans and Nantes
Le Mans has an estimated population of 143,813 as per 2014. It is known for its world famous automobile race while is called "24 h of Le Mans" at Sarthe road racing circuit where there is also a museum showcasing old motorcars. France has Le Mans Mayet transmitter, one of the tallest radio mast situated in Mayet and of the height 342 m. Nantes is located in the western region of France which has seen a significant change in the twenty-first century as compared to the previous one due to the implementation of the urban renewal plan in the year 1920. It has Paris on its south west side also joined by rivers Erdre and Sevre at river Loire. It is a business center having different economic activities like engineering, food processing, manufacturing industry for aeronautics and has also shown growth and development in the biotechnology industry having a large section to pursue higher education. With the redevelopment of docklands and specialized towers with conference facilities, it also created attracted tourism. Also, with the opening of TGV Atlantique between Paris and Le Mans which was opened in 1989, it showed an absolute 100% increase in 3 years in property value in Le Mans. In Nantes along the same TGV line, there was 20% increment land value.

Italy
Italy has an estimated population of 60,553,000, ranking 23 in the world as per the fiscal year 2020 and projected population for 2030 being 60,286,000 which actually shows a decline. The total area is 302,073 km^2 (116,631 sq. mi) having density of 200.1/km^2 (518.3 per sq. mi). It has an urban population of 70.4% and rural being 29.6% as per the data in 2018. Its Gross National Income (GNI) in U.S.$'000,0000 as per 2017 is 1,878,330 and GNI per capita (IN U.S.$) standing at 31,020 as per 2017. Located in the southcentral region of the European continent, surrounded by the Mediterranean Sea, Italy is a land of scenic beauty also referred to a boot-like-shaped country. It homes the world's most rugged mountains, the Alps that is one of the factors making the people of the country to be independent and self-efficient.

Cit Turin
It is known as the intellectual and its political center in the nineteenth century and became the first capital of a united Italy between 1861 and 1865 undergoing a large amount of damage in the World War II. It is known for its museum of ancient art along with mineralogy, zoology, palaeontology, and natural history. Its monuments also showcase artillery, cinema, mountains, and collection of automobiles. The place is also filled with literature excellence as can been seen from the number of fine

libraries it has. The Turin–Milan HSR line in Italy was opened in 2006. Before 2006, the land value in the Cit Turin area was less as compared to the whole city, but it increased to 30% which was significantly higher than the whole city at 9.5% as the scenario changes [68].

Milan

Situated in the northern region of Italy, Milan is the financial center and manufacturing hubs making it one of the most important commercial places in the whole of Italy. Although many arguments have been raised in history regarding Milan to be the capital of united Italy instead of Turin, it still is industrial center identifying itself a modern nation state with an area of city being 182 km^2 (70 sq. mi) and population of 1,399,860 as per 2020. It has a density of 7700/km^2 (20,000 per sq. mi), the city is of great historical importance [68]. The Turin–Milan HSR line in Italy was opened in 2006. There was decreasing trend in the areas nearing the Milan station as opposed to the trends shown in Cit Turin.

Rome

Rome situated in the central region of Italy is a place with historical importance. It has a population of 2,837,332 as per 2020, an area of 5352 km^2 (2066 sq. mi), and a density of 2232/km^2 (5781 per sq. mi). The city is rich in its art and spirituality making it a religious center. The Rome–Naples HSR was opened in 2006. The areas surrounding the HSR station showed 5.1% growth in land value as compared to the whole of the city of Rome showing an increment 5.8% but were less as compared to the previous year which was 6.5% and 6.7%, respectively.

Naples

Naples is situated near the center of the hills extending from Posillipo in the north to Sorrentine Peninsula in the south. It is the principal port which is at decline, rich in culture creating attraction for tourists and with commercial importance. With the opening of Rome–Naples HSR in 2006, Naples central station showed a significant growth from 2.8% in 2005 jumping to 15.5% in 2006. On the other hand, it also led to the decrement in land value in the whole city as it went from 16.1% in 2005 to 10.8% in 2006 [68–70].

3.2   Heterogeneous Impacts of HSR on Land Values and Property Prices

There are various factors, mainly revolving around circle rate, interest rates, overall real estate value, land market and land use pattern that have an impact and are used while determining the land value in any region [48, 50–53]. Despite of the large

number of possibilities determining land value, the following can be referred to as the major categories and which the various other factors are grouped into:

Physical Attribute
It is one of the initial factors that include geography, topology, climatic condition, and basic amenities like water supply and sewage system in a place. It has a relation to the construction and development cost, leading to higher cost in areas on a rough terrain than on the plains leading to higher land value in that area to incur the cost.

Last Mile Accessibility Economic Activity
The central business district or CBD has higher land value due to its economic nature and good last mile accessibility reducing travel time. Some examples of CBD are London, Beijing, and Mumbai with some of the world's largest real estate and thus land value. The higher circle rates are the indicators of these urban agglomerations.

Location
Raised from a higher demand to be near the workplace and other public amenities like hospitals, schools, parks, market, shopping malls, and entertainment zones for an ease of life due to reduced travel time, the CBDs have a higher land value as result of higher accessibility to these places.

Existing and future Plans of Land Use
The higher investment in economic activities such as setting up of industrial institutions has a major impact on increased land value of any place. It calls for a higher migration of people in order to gain from the employment opportunities provided by the industries [45–47, 49]. This leads to integration of various transport facilities in order to boost the economic process.

Although land value is determined using the factors mentioned above, the ultimate selling price is determined by the capacity of the average population to pay. The negative impact is suffered when land is too close to the terminals as a result of negative externalities like noise pollution over its benefits. Based on the above categories when combined with the key observations made from the various cities, we can separate the places into two categories, namely large and small or relatively small cities, and develop an understanding and application on the conceptual part based on evidences.

3.3 Key Observations Made from Large Cities

Out of the large cities like London, Lyon, Paris, Rome showed slower growth. Paris and Rome as situated around the center of the large cities. As a result of already existing high accessibility and high land value, they experienced a decremented impact on land value due to which the positive factors were negated out by other external factors like noise pollution. Milan not having being near the center of the

city saw a negative impact on land value with the introduction of HSR line due to lack of last mile connectivity and accessibility [54–58, 71]. Camden in London was associated high criminal activity and poverty, hence the reason for lower land value, but with the introduction of HSR line along the route, it showed significant improvement ultimately leading to higher land value as the opening of the line called for more investors in the redevelopment project, though with a decreasing trend from 20% in 2007 to 7% in 2008. Lyon established France's government office complex, tallest skyscraper in the area, largest shopping center showing a great hike in land prices due to increasing business activities in the area leading to a rise on the need to travel and higher accessibility around the Part-Dieu HSR station area.

3.4 Key Observations Made from Small Cities

There was a land value increase shown with the development of HSR in smaller cities like Turin, Naples, Le Mans, and many more as a result of increased accessibility. This is because these cities have huge potential for industrial growth and development with the implementation of High-Seed Rail in the area allowing economic establishment in these areas. Le Creusot being a remote area lacked even the infrastructure of road connectivity for last mile connectivity due to which it could not gain much of the benefits of economic growth with the development of HSR line in that area [59–61].

In general, on the basis of the evidences collected from the different cities, it appeared that smaller cities had greater scope for economic growth leading to increased land values in the areas as compared to the percentage growth in larger cities, and they can only benefit from the development of High-Speed Rail to the fullest if there is good and integrated last mile connectivity leading to attractive investments in economic activity.

Mumbai–Ahmedabad High-Speed Rail (MAHSR) corridor is a 508.17-km-long route having 12 stations, namely: Mumbai (Kurla Bandra Complex), Ahmedabad, Sabarmati, Vadodara, Thane, Anand/Nadiad, Surat, Bilimora, Bharuch, Virar, Boisar, and Vapi. The system specifications include an operational speed of 320 km/h, while the design speed stands at 350 km/h, running on a standard gauge of 1435 mm [62–66]. It is proposed to be operated on a 10-car configuration, and the train capacity is being 750 passengers [67].

4 Case Study

4.1 Overview of Mumbai–Ahmedabad High-Speed Rail (MAHSR) Corridor

Various pre-feasibility studies were conducted on the Mumbai–Ahmedabad High-Speed Rail (MAHSR) by RITES (India), Systra (France) in FY2009. Also, Ministry of Land, Infrastructure, Transport, and Tourism (MLIT) of Japan conducted its study in FY2012. On May 29, 2013, a joint statement to do a joint study on the MAHSR route was issued by Japan and India with an aim to improve connectivity between the two business centers. It included the overall background and purpose of the study, detailed analysis of regions targeted, about the organization of study operations. Collecting basic route information in the study area, looking at the administrative structure, population, and economic conditions like GDP and working population helped in analyzing the conditions and land use planning.

Mumbai–Ahmedabad High-Speed Rail (MAHSR) corridor is a 508.17-km-long route having 12 stations, namely: Mumbai (Kurla Bandra Complex), Ahmedabad, Sabarmati, Vadodara, Thane, Anand/Nadiad, Surat, Bilimora, Bharuch, Virar, Boisar, and Vapi. The system specifications include an operational speed of 320 km/h, while the design speed stands at 350 km/h, running on a standard gauge of 1435 mm. It is proposed to be operated on a 10-car configuration, and the train capacity is being 750 passengers [67–70, 72]. Figure 1a shows the route map of the Mumbai–Ahmedabad High-Speed Rail (MAHSR), from which it can be noticed that the high-speed corridor is built along the existing railway and highway route mostly aligned to the railway route. Figure 1b shows the population density of the sub-districts along the HSR route. Figure 1c shows the working population density of the sub-districts along the HSR route.

Maharashtra has 57,376,776 migrants from various states in India who migrate for various reasons like work or employment, business, education, and other reasons, but we will be focusing on these three aspects only for the purpose of our study. The major reason for migration from Gujarat to Maharashtra is for work and employment purpose accounting for about 18.82% of the total migrants from Gujarat as shown in Table 1 followed by 3.33% for business and 1.29% for educational purpose as depicted above.

There are three categories under which the railways can be classified: HSR, conventional intercity rail, and urban and suburban rail. Delhi Metro is an example of the suburban rail type which is aimed at transporting the passengers in a range of a few km. The conventional intercity rail is used for traveling between cities with distances between stations ranging in tens of km, and some examples of it are being the Rajdhani and Shatabdi Express trains in India. HSR is aimed at reaching out to farther distances in shorter amount of time having a maximum speed of about 300 km/h, with covering distances between 300 and 800 km on an average. Mumbai, the capital of Maharashtra, is the commercial and entertainment capital of India due to the presence of one of the largest film industries. It has a population of close to
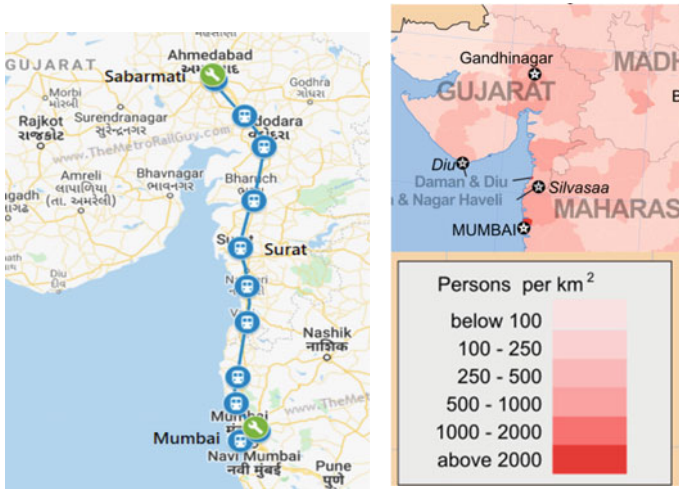
(a)

(b)
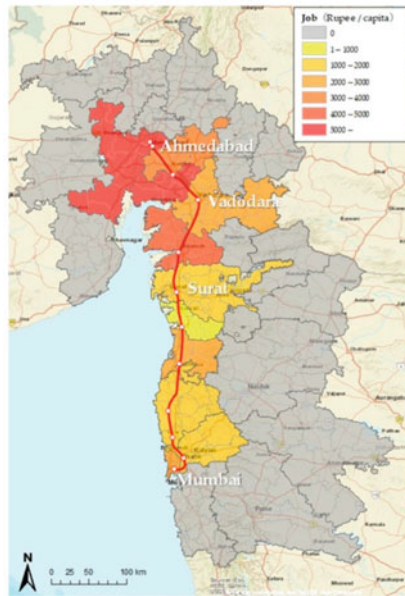
(c)

Fig. 1 **a** Location map of MAHSR; **b** population density map (middle); **c** working population map [67]

Table 1 Migrants from Gujarat to Maharashtra

	Migrants	Migrants from Gujarat	Migrants from Gujarat (% age)
Total	57,376,776	579,558	1.01
Work/employment	7,901,819	109,051	18.82
Business	382,033	19,289	3.33
Education	775,062	7499	1.29

12.5 million as per the census data collected in 2011. It has an area of 4355 km^2. Surat has a population of around 4 million as per the census data 2011 and is the second largest city in Gujarat lying as the midpoint of the MAHSR route.

Regression analysis is used for assessment and evaluation. It has a significant overlap in the field of machine learning. It is not related to population, such an observation is called outlier. Simply put, it is of immense value. An external problem is a problem because it often hinders the results we have achieved. When independent variables are interrelated, a variable is called a multicolonial. A variety of regression methods suggest that there should be no multicoloniality in the dataset. This is because it causes problems in the ranking variables based on their importance or it makes it difficult to select a very important independent variable. When the difference between the target variable and the independent variable is not constant, it is called heterosexuality. Example: The diversity of food consumption increases as one's income increases. A poor man always spends a steady amount of money instead of eating cheap food; the rich can sometimes buy cheap food and at other times eat expensive food. High-income people exhibit greater diversity of food consumption. When we use unnecessary descriptive variables, it makes it overly fit. Overfitting means that our algorithm works well in the training set but does not work well on the test set. This is also known as the High Variations' problem. When our algorithm works very poorly, it will not be able to set up the training set properly, which will truncate the data. This is also known as a high bias problem.

In India, MOR in December 2009 formulated the "Indian Railway Vision 2020" with a long-term vision for 2020. Vision is designed to address four national goals: geographically and socially comprehensive development; strengthen national unity; massive production of productive employment; and environmental sustainability. It plans to invest 14 trillion rupees (rupees) over the next ten years. In particular, the vision sets goals such as significantly increasing revenue, expanding network and transport capacity, increasing safety and environmental sustainability, and improving passenger services. It sets targets for business development in a variety of sectors, including traditional railways, HSR and rail freight, luggage, advertising, telecommunications, and passenger services. HSR operates at a maximum speed of 250–350 km/h with a vision to implement projects for at least four corridors by 2020 [20–35]. Apart from these, it also plans a number of ways to connect commercial centers, tourist destinations and pilgrimages. Destination, etc. The MOR is systematically studying the pre-feasibility of these routes [39].

According to the Environmental (Protection) Act, 1986, GoI's Environmental Impact Assessment Notification issued by the Ministry of Environment and Forests (MoEF) in New Delhi on September 14, 2006, railway and bridge construction projects are not required to maintain environmental impact. An evaluation (EIA) study was conducted for MAHSRC, including the preparation of an Environmental Management Plan (EMP) to mitigate adverse environmental impacts. The main objective of the EIA study was to manage the baseline data production of environmental characteristics to understand the current scenario of environmental parameters and identify the environmental impacts caused by the construction and operation of the proposed MAHSR corridor and related facilities (depots, railway stations and maintenance depots, etc.). It is proposed to start an EIA study. The aim of the study was to establish existing ones environmental conditions, assess the effects of high-speed train running, and related characteristics and prepare EMPs. An EIA report is required for a joint feasibility study for the said HSR. The EIA study was conducted according to the latest guidelines of the Japan International Cooperation Agency (JICA) on environmental and social issues. The project is proposed by the Government of India MoR. It is tentatively suggested for the detailed purpose that the RVNL/HSRC is a government agency to carry out the construction, operation, and maintenance [36–38, 40–44].

The planned route is at latitudes 19° and 23° north, extending from the western part of the state of Maharashtra and from the coast of the Arabian Sea west to the Western Ghats to the southeastern part of the state of Gujarat. The weather along the way raises warm temperatures and high humidity as it moves south with heavy rains from June to September due to monsoons. Near the proposed route from Mumbai to Thane, two important ecologically sensitive areas are SGNP and TWLS. In addition, as there are wetlands of mangrove forests at Thane Creek in Mumbai, it is planned to adopt a tunnel construction to prevent changes. Mumbai, which is located in the coastal region in the western part of the state of Maharashtra. According to the Climate Zone Map, Mumbai has a tropical monsoon climate. With the impact of the southwest monsoon, this is an area with high rainfall. The maximum temperature during the day does not change significantly throughout the year. It is usually around 30–35. On the other hand, the minimum temperature is in January. It is about 15. The minimum temperature during the monsoon season is 25. Temperature change is very high throughout the year. The monsoon season lasts from June to September. Most of the annual rainfall is concentrated during this period. Surat and Ahmedabad are in the state of Gujarat. According to the climate zone map, Surat along the coast has a tropical savanna climate and inland Ahmedabad has an arid steppe climate. Mumbai does not receive much rainfall during the monsoon season. However, both cities have high temperatures. The maximum temperature in Ahmedabad is above 40 in May. Also, due to the effect of southwest monsoons, the monsoon and dry seasons are very different like in Mumbai. Most of the annual rainfall is concentrated during the monsoon season from June to September.

There is in principle no restriction on participation from foreign capital direct investment. Most areas fall under the purview of the Reserve Bank of India, with

applications for automated licenses, with the exception of airports with foreign overseas participation, or nuclear and fixed assets prohibited for foreign capital. In January 2014, the Department of Industrial Policy and Promotion (DIPP) under the Ministry of Commerce and Industry announced a proposal to allow 100% FDI in railway network construction and maintenance. The proposal was approved and the government issued a notification in August 2014 to allow 100% FDI in rail infrastructure for FDI regulations. The DIPP policy has been amended to allow FDI in railway transport to allow private investment in railway infrastructure, including construction, operation, and maintenance of high-speed railway projects; suburban corridor projects by PPP; dedicated freight routes; rolling stock including train sets; locomotive construction and maintenance facilities; railway electrification and signaling systems; freight terminals and passenger terminals; infrastructure and rapid transportation systems in industrial parks for railway lines [73–76]. While private partnership based on the PRP model is already allowed in the railway MRT, it must comply with the country's FDI policy and industrial development and regulation law. The DIPP proposes to allow up to 100% FDI in high-speed railway networks and dedicated freight corridors. The policy was first approved in December 2012, where it stated that foreign direct investors could only participate in the expansion and modernization of the railway network. As mentioned above, for railway users and for regional and urban development, the location of an HSR station in a city is a very important issue. The location of an HSR station can be classified into two types, HSR for high standards independently of traditional railways and HSR using current conventional railways. In order to use the existing conventional railways, the following condition is required, and sufficient spare track capacity is required for the HSR on the conventional route and both HSR line. The line and the traditional line must be identical.

One of the basic features is that the operation method is closely related to the construction method and the role of the high-speed train. When the track capacity of a conventional line reaches its limit, the complete construction method of the new high-speed line is generally adopted to dramatically improve the track capacity and operating speed. Some flexibility can be achieved through measures that improve access. On the other hand, when the traditional line has extra capacity and requires higher operating speeds, the method of partially using the traditional lines or upgrading the traditional lines is often adopted. In the latter case, interoperability is required, while in the previous case, a high-speed service independent of the maintenance of conventional trains can be realized. When the traditional lines are partially used or the traditional routes are upgraded, these routes take the form of mixed transport by running freight trains, low-speed passenger trains, and high-speed trains. The traditional methods continue. Meanwhile, while adopting the complete construction method of the new high-speed line, a dedicated high-speed passenger rail line has been designed in many cases from a safety and efficiency point of view. In Europe, there are a few examples of high-speed lines designed for mixed track purposes. However, as the frequency of high-speed railway operation was limited under mixed traffic, many new high-speed lines were built as dedicated high-speed passenger lines. To set the maximum operating speed to 320 km/h to reduce travel time (maximum design speed for the future is 350 km/h). Since the maximum operating speed of

HSR is currently in the revenue service and is constant at 320 km/h in the world, the maximum operating speed of the project should be set at 320 km/h to reduce the scheduled time. Adopting 70% of the average passenger load factor to establish an operation plan. The average passenger load factor should be 70%, with the number of passengers fluctuating. For reference, passengers in Japan can usually book alternate train seats exclusively when setting up trains with an average passenger load factor of 70%. To set two types of stop models of the train. The different needs of travelers, in terms of different origin and destination, are a necessity to reduce travel time, and two types (fast train and each stop train) should be planned: The high-speed train only stops at major stations and each stop train stops at each station. Stations where "fast service trains" stop are determined. For special operation time zones and maintenance time zones, security activities are the first priority to ensure for HSR. Maintenance work for facilities should be done properly by completely separating operation time zone and maintenance time zone. Safeguarding safety operations and avoiding the confusion of operation problems, which can sometimes lead to serious accidents, it is recommended not to adopt two-way operations when the traffic density is too thick. The train operating time zone and maintenance time zone are as follows: Train operating time zone: 6:00–24:00 (0:00) and maintenance service time zone: 0:00–6:00. At that time, to assess how the demand for train fares had changed, three fares were fixed for high-speed railways: 1A class, 1.5 times and 1A class 2.0 times for existing railways. More than planes. After estimating the total fare revenue of the high-speed railways per case, the study team found that the fare revenue was higher if the 1A class was 1.5 times higher than the current railways. Therefore, a train operation plan is prepared based on the demand for train fares at the rate of 1.5 times per 1A category. The fastest train journey time between Mumbai and Ahmedabad is one hour and 59 min (less than two minutes), which is two minutes and two hours and seven minutes at Surat, Vadodara, and Ahmedabad stations. The train took two minutes at Ahmedabad station between Mumbai and Sabarmati. Each stop train between Mumbai and Sabarmati takes two hours and 58 min (less than three hours and two minutes). Train capacity is a very important factor in train operation planning. Based on the demand forecast, train capacity determines the number of trains. Train capacity severely affects the type of seats and the number of cars. The four types of seat arrangement that represent the Shinkansen case in Japan are first class (seat arrangement 1 + 2), occupational class (seat arrangement 2 + 2), and second class (seat arrangement) + introductory features and characteristics) and checked the comfort class (seat arrangement 3 + 3). To determine the number of trains, three cases, 6-, 10- and 16-car train configurations, were compared (number of trains in operation, maximum and frequency of train operations in off-peak hours), train capacity, views heard Stock costs and maintenance costs and MOR Related Experts in Receiving 16-car trains when starting a business involves a small number of train activities and, as a result, the time field in which only one train operates per hour varies widely. Due to the fact that high-frequency train operations in India are of great concern, the operation of 16-car trains does not meet this requirement. Therefore, 16-car train operation should not be recommended at an early stage.

High-speed railway track maintenance works will be completed in the time zone from 24:00 a.m. to 6:00 a.m. daily train operations. To provide fast track with various maintenance services, heavy handling machinery and material/machine transport cars run to the main line for the work site and return to the maintenance depot after maintenance services are completed. At the end of the work time zone, the new train Operation Time Zone Revenue Service will begin operating trains. This work time field involves the operation of the confirmation car to ensure that track maintenance services are completed. Distribution of track maintenance depots at intervals of 50–80 km with a view to a six-hour working time field. Track Maintenance Depot Track Maintenance Work Systematically arranges maneuverable cars, material/maintenance transport cars, car deployment workers, material/machine storage shed and maintenance car servicing sheds. Weighty and long track work article about rails treatment, basic specifications of 200-m-long welded rail for rails of this class, transported directly from iron mills to work site by railway lines in India. Therefore, a track maintenance depot will be set up where high-speed railways will cross or contact the existing railway line and prepare them with train receiving and sending tracks. In the case of road transport, eight pieces of 25-m-long train transported by road are welded to the track maintenance depot to produce a 200-m-long train. The 200-m-long train thus produced is sent to the construction site, again welded to a certain length and laid on the track. Compared to this method, track construction works can eliminate seven welding points per 200-m-long rail to lay rails transported by existing railway lines. This means that even seven weak points (welded points) per 200 m on the mainline track will be removed. High-speed railroads are five points close to the existing railway line or on the running track. These are Thane Station, Surat Station, Vadodara Station, Anand/Nadiad Station, and Sabarmati Rolling Stock Depot. At the Track Maintenance Depot associated with these stations, we lay the receiving/sending track of the train parallel to the existing railway line. Other track management depots are connected to Boiser station, Vapi station, and Bharuch station. In addition to these eight track maintenance depots, we will build certified car housing depots along with Bilimora station. Each track maintenance depot can be accessed to ground level via a down-gradient ramp 25 from the station branch corresponding to the station auxiliary track.

High-speed train reduces travel time between cities. It promotes the transfer of people traveling for business, tourism, and pilgrimages; in addition, it develops HSR capability by seamlessly connecting the HSR station and the area around the station with other modes of transport. There is so much hope to take advantage of. HSR will develop the station based on station and toad (transportation based development). The HSR station area is likely to be a hub for the activities of HSR passengers as well as other non-railway customers. There are three materials about station area development; urban planning around the station area: Some important points are mentioned and some insights with specific examples of station area development in the world are shown. Price Capture Model: High-level value extraction is estimated by station area development at some stations with the proposed station location. Non-Rail Business: The potential of non-railway business at the station will be discussed with a high level of assessment at the major proposed stations.

The main points for the development of HSR stations based on the TOD concept and passenger facilities for the proposed 12 stations are discussed in this chapter. As high revenue is expected from the station area development, the discussion of the price capture model for HSR from the station area development is a major consideration, which includes safe comfort for passengers, access and short-term, good relationship with traditional train, metro, and others. Transportation-mode HSR station, convenient station chowk, pedestrian facility (unobstructed, pedestrian deck and motivation signs), compatibility with urban and regional planning, compatibility with current urban and regional planning, approximately station area. Development (residential area to residential area) Increase HSR consumer through increased population and urbanization, regional development urban issue with HSR allocation and smart city concept), station area development and new draw of city. Benefits from station building development and station area development include railway operators (through railway land development), municipalities (by raising property taxes), commuters (by achieving their goal on station complex facilities), and businesses (by making profits through land development) and communities (through improved lifestyles). Commercial business development can be classified into three types such as trade which includes retail, restaurants, hotels, offices, and other ancillary facilities; social facilities which include convention halls, exhibition spaces, schools, medical, recreational, and cultural facilities, and residence consisting of apartments and residential buildings.

High-Speed Rail technology is one of the most sustainable means of transport when passenger transport is concerned. It not only caters to the environment but also leads to a transit-oriented development (TOD). An important aspect in the Urban Development and Planning, TOD integrates the transport ecosystem leading to intense connectivity of a range of means of public transport creating a symbiotic interaction between the urban residents and public transport systems. Over the years, it has been studied, and inferences from these studies have shown that public transport is beneficial over private transport not only in terms of a great level of aggregation but also up to a large extent which helps in reducing the negative impact on the natural ecosystem.

Transit-bound development is that exciting quick growing trend in making spirited, livable, property communities, additionally called TOD; it is the creation of compact, pedestrian-oriented, mixed-use communities targeted around top-quality train systems. This makes it attainable to measure a lower-stress life while not completely dependent on an automobile for quality and survival. Transit-bound development is regional designing, town betterment, residential district renewal. TOD is apace sweeping the state with the creation of exciting folks' places in town when town. The general public has embraced the idea across the state because it is the most fascinating places to measure, work, and play. Assets' developers have quickly followed to satisfy the high demand for quality urban places served by rail systems. Transit-bound development is additionally a significant resolution to the intense and growing issues of global climate change and international energy security by making dense communities that greatly cut back the necessity for driving and energy consumption. This sort of organization will cut back driving by up to eighty fifth.

Some factors driving the drive toward transit-oriented development square measure, apace growing, mind-numbing hold up nation-wide, growing antipathy for suburbia and fry-pit strip development, growing need for quality urban style, growing need for lifestyles off from traffic, changes in family structures, etc., growing national support for good growth, new focus of Federal policy. The parts of transit-bound development square measure, walk in a position style with pedestrian because the highest priority, train depot as outstanding feature of city center, public sq. fronting train depot, a regional node containing a combination of uses in shut proximity (office, residential, retail, civic), high density, district inside 10-min walking circle close train depot, collector support transit systems together with self-propelled vehicle, light rail, and buses, etc., designed to incorporate the simple use of bicycles and scooters as daily support transport, massive ride-in bicycle parking areas inside stations, bike share rental system and bike manner network integrated into stations, reduced and managed parking within 10-min walk circle city center/train depot and specialized retail at stations serving commuters and locals together with cafes, grocery, dry cleaners. The benefits of transit-bound development embody higher quality of life with higher places to measure, work, and play, larger quality with simple on the road, redoubled transit ridership, reduced hold up, automobile accidents and injuries, reduced unit disbursement on transportation, leading to more cost-effective housing, healthier style with additional walking, and fewer stress, higher, additional stable property values, redoubled pedestrian traffic and customers for space businesses, greatly reduced dependence on foreign oil, reduced pollution and environmental injury, reduced incentive to sprawl, redoubled incentive for compact development, more cost-effective than building roads and sprawl, and increased ability to keep up economic fight. Transit investment has double the economic profit to a town than will road investment. Transit will alter a town to use economic processes to extend densities close to stations, wherever most services square measure situated, therefore making additional economical sub-centers and minimizing sprawl. Transit allows a town to be additional corridor-oriented, creating it easier to produce infrastructure. Transit enhances the economic potency of a city; denser cities with less automobile use and additional transit use pay a lower proportion of their gross regional product or wealth on traveler transportation.

Mumbai, formerly Bombay, city, is capital of the state of Maharashtra, southwest India. It is the economic and commercial center of the country, and its main port is in the Arabian Sea. It was built on the site of an ancient settlement and originated from the local deity Parvati Mumbai, one of the major deities of the Union of Shiva, Hinduism, whose temple was once located in the southeast. Is in the section. Of the city. It was the English corruption of Bombay, Mumbai during the British colonial period, or locally known as Bombay ("Good Harbor") by the Portuguese. Although Bombay is still in common use, the name Mumbai was officially restored in 1995. Mumbai, the hub of the cotton textile industry in India, has grown into a very diverse manufacturing sector with an important aspect of information technology (IT). In addition, the city's commercial and financial institutions are strong and formal and Mumbai serves as the country's financial hub. However, this is one of the perennial problems of many large industrial cities: air and water pollution, standard housing,

and extensive areas of congestion. The final problem is exacerbated by the physical limitations of the city's island location. The city of Mumbai is located on a peninsula on the island of Bombay, a land of seven islands off the coast of the Konkan in western India. The island has been associated with drainage and reconstruction projects since the seventeenth century, as well as the construction of Bombay Island and the breaker. To the east of the island are the waters off the port of Mumbai (Bombay). The island of Bombay consists of inland plains, about a quarter of which are below sea level; the plain is lined with high hills parallel to the eastern and western hills. Kollaba Point, the headland built south of those rafts, protects the port of Mumbai from the open sea. The western peak ends at 180 feet (55 m) above sea level at Malabar Hill, making it one of the highest peaks in Mumbai. There is a shallow extension of the Back Bay between Colaba Point and Malabar Hill. The area known as the Palace, on a slightly stretched plain between the rear bay and the harbor, is the site of a seventeenth-century British fort (which is a bit rugged), in which the city grew further. The area is now mainly occupied by government and commercial offices. This land stretches from the Back Bay to the middle land to the north. The northern part of Mumbai is occupied by a large salt marsh. The natural beauty of Mumbai is unique from other cities in the region. Entering the port of Mumbai from the sea reveals a spectacular view around the Western Ghats mountain range. The island and the many small craft heavy harbors lined with white sails provide a safe place for ships to sail, especially when it touches the shore. The port is the largest of the Elephanta Islands and is famous for its eighth and ninth century Hindu cave temples.

Often referred to as the cultural capital of Gujarat, Calcutta may not have seen the colorful history of Vadodara like Bombay as well as the great imperial builders like Delhi. However, unlike these cities, its history begins somewhere in the Middle Ages. There is evidence that there is an old stone old man in several places within 10–20 km in the Mahi River valley. In the northeastern part of the present Vadodara, at the beginning of the Christian era, a small settlement developed on the right bank of the Vishwamitri River. It is called Ankotka (present-day Akota). The town of Ankotka flourished under the rule of Guptakot and Vallabhi. But in 600 AD, severe flood inhabitants had to leave the base and head east toward Ankotakka. It formed the nucleus of a new township called Vadapadka, which may be due to the abundance of banyan species, which are still very much present today. Eleventh century development of Vadodara a. The fort was built strong and neat, and therefore, considering the security angle, the residents of Nibi villages came and settled here. Then, many lakes were built. Over the next two centuries, the areas adjacent to the fort were also inhabited. Later, Vadodara lived during the Maratha period as indicated by coins and pottery. To the people of Vadodara today, its history begins with Sayajirao III. The identity of Vadodara is expressed through its holistic culture, Catholics, and common sense of perspective. The identity of Vadodara is stamped on a person and that person is Sayajirao III. You cannot speak without mentioning any aspect of this city. The identity of Vadodara is the contribution of Sayajirao. Vadodara was so developed during the reign of Sayajirao that it was the second largest princely state in the country after Nizam Hyderabad. He introduced several reforms in the state

of Vadodara such as power supply, automation of productive sectors, without co-operative movement and introduction of compulsory education and ban. Vadodara is now on the cultural, educational, and economic map of the country, largely due to Sayajirao III. Whatever the heritage of the city, it is the legacy of this great ruler that mined the character of his people. After a glorious life of 76 years of events, this great hero, adopted by the widow of Maharaja Khanderao at the age of 12, went for his worship in 1939. Vadodara saw the growth of all kinds of industries like medium and large scale. With great progress in the financial sector, the city has huge industrial complexes and government agencies like Gujarat Refinery, Indian Petrochemicals, Gujarat State Fertilizer, Heavy Water Project, Oil and Natural Gas Commission. Today, the city is located on the banks of the Vishwamitra River and is known as the cultural capital of Gujarat and a center of educational activities.

Cities reappear and disappear in the table of Indian civilization. Ahmedabad is a historic city founded in the wake of the rise of Islamic occupation that shook India. It was founded in 1411 AD. I was married to an aristocrat, Ahmad Shah, who rebelled against his lords over Delhi. The new rulers of Gujarat, anxious to establish their dominance in the physical sphere, had a manic program of construction activities in their new capital Ahmedabad. His model is the most influential Hindu architecture of the last centuries. One and a half centuries later, the result is the "Sultanate Architecture" of Ahmedabad, which is considered to be the highest point of world architectural heritage. The structure, along with the Jain, Swaminarayan, and Hindu temples in the city, is a true safari of monumental architecture that attracts beauty lovers to the city from all over the world. The construction and design of the walled city of Ahmedabad on the Sabarmati River are a continuation of Hindu building traditions in other ways. These "other ways" are the new stylistic elements brought in by the new rulers. The city is located close to the Solanki Commercial Center on the 371-km-long Sabarmati River and is 173 feet above sea level. It was a magnificent court seat, as evidenced by Tavernier, a French traveler who visited the city in the eighteenth century, who described it as "the largest city in India, the manufacturing headquarters, worse than Venice for great flaws, and some described gold objects were flying badly with birds and flowers". A treaty was brought to Ahmedabad during British rule in 1817. The British expressed a desire to encircle Ahmedabad. "The Commanding Effect" Sovereignty over it. The city of Ahmedabad relies heavily on its owner in the assessment of the country. During the First World War, the textile industry of Ahmedabad was given the status of "Manchester of India". The mills survived till the end of 1989. The growth of the textile industry in Ahmedabad was the Gujarati of pragmatism, innovation, and creative collaboration. After Mahatma Gandhi's return from South Africa in 1917, he ordered his own decision to stay in the city for thirteen years, historically ignoring the non-violent movement against colonial power, and his achievements in textiles made the nineteenth century Ahmedabad Mahajans great builders. He was instrumental in building companies such as IIM, NID, ATIRA, and CEPT in the mid-twentieth century buildings that attracted modern masters of world architecture such as Louis Kahn and Le Corbusier to the city in the 1950s. Of India, the city gives a 14% share of the total investment in all stock exchanges. Sardar Patel, a great associate of Mahatma Gandhi and a modern

Indian architect, was once the Mayor of Ahmedabad. Sardar's vision for the people living in Indian cities is like paradise for Indian urbanites, directing the movement for the future of this great city. Sabarmati is a city in Ahmedabad, India. Sabarmati is a developed and affluent region of western Ahmedabad. Rober Nagar, Dharmanagar, Jawahar Chowk, Kabir Chowk, Ranip, Kaligram, Motorra, Janata Nagar, Chandkheda, D-Cabin Sabarmati are the main areas. There is a very religious place to stay in Sabarmati. Most of the communities in Sabarmati live very peacefully. But, the largest population in the area is Hindu or Jain. There are many famous Jain temples in Sabarmati. There are a large number of good hotels, restaurants, and snack bars available. All urban facilities are available including bus stop, railway station, bank, post office, hospital. Contact with the highway and airport is part of the attraction for a better living space. The nearest international airport is 10 km away. Living areas with peaceful communities and availability of all modern resources make this place the best place to live.

Surat is a city in the western part of the Indian state of Gujarat. It has one of the highest growth rates due to migration. Surat is one of the cleanest cities in India and is also known by many other names like "The Silky City", "The Diamond City", "The Green City". It is a very powerful present and equals a different heritage of the past. It was the first city where the British came to India. The Dutch and Portuguese also established trading posts in Surat, the remains of which are still preserved in modern Surat. In the past, it was an excellent port, with ships from more than 84 countries anchored in its harbor at any time. To this day, the same tradition continues in Surat, which is practiced by people across the country for trade and employment. Surat has a practically zero unemployment rate, and it is very easy to get a job here due to the rapid growth of various industries in and around Surat. The origin of the city is 1500–1520 AD. During this period, it can be found in the old Hindu city of Suryapur, which was later inhabited by Sauvira Raja on the banks of the river Brigas or Tapi. In 1759, the British rulers took over the Mughals in the early twentieth century. The city is located on the Tapi River and has a coastline of 6 km along the Arabian Sea. For these reasons, the city emerged as an important trading center and enjoyed prosperity through maritime trade in the sixteenth, seventeenth, and eighteenth centuries. Surat became the most important trade link between India and many other countries and flourished until the rise of the port of Bombay in the seventeenth and eighteenth centuries. Surat is a prosperous center for shipbuilding. The entire masonry coast from the eight lands to the Dumas is exclusively for the construction of ships. After the rise of the port in Bombay, Surat's shipbuilding industry also declined. In the post-independence period, commercial activities in Surat as well as industrial activities (especially, textiles) increased significantly. The concentration of these activities in combination with residential activities has led to a significant expansion of city limits. Surat Mahal is one of the oldest sixteenth-century monuments in the city and has an important hashtag for its history. However, such a great fort built to provide adequate protection to the citizens of Surat from invader attacks seems to have forgotten the minds of the present generation. The King of Ahmedabad, Sultan Mahmud III (1538–1554), was furious with this series of destruction of Surat and ordered the building of a very strong palace named after

the Turkish soldier Safi Agha. Khudawand Khan. The palace was completed in 1546. After the conquest of Surat by Emperor Akbar (1573), the fort remained under the control of commandants appointed from Delhi until 1751, when it was captured by a direct admirer of the Mughal seat. The palace did not last long, as it was annexed by the English in 1759 to the rest of the city. Although practically independent in the past, the British nominated the palace under the Mughals. The token of this divided order has two flags from the palace walls, the English flag on the southwest side and the Moorish standards on the southeastern stronghold. The practice was followed in 1842, after the death of the last of the Nawabs of Surat, by the removal of the English navy from the masonry and the removal of the Moorish standard from the palace walls. However, in defense of any well-equipped enemy, they remained vacant for a long time, and the palace buildings were initially repaired, and by 1862, a small body of European and local soldiers had been captured. That year, unnecessarily, the power was lifted, and empty rooms were built to house the various offices connected with the Revenue and Police Departments, which have since occupied the Palace.

On August 15, 1947, British rule ended and India became independent. The new government merged the Imperial States into the Bombay State. Kheda District came into existence on 1/8/1949. Subsequently, some changes were made in some taluka villages and villages were identified for different talukas in the district from 15/10/1950. Kheda district consists of Khambhat, Petlad, Borsad, Anand, Nadiad, Matar, Mahemawad, Kapadwanj, Tasara, and Balashinor taluks. Since 1/10/97, the state government has formed six new districts and formed a separate district from Anand Kheda. Anand district, originally a part of Kheda district, was engraved with golden letters in the history of modern India due to the White Revolution and the development of the largest co-operative sector. Anand came into existence in 1997 itself. Hence, the history of Anand district is not so old, but it is a very extensive and rich heritage as part of "Charotar" (another name in use for Kheda district). Anand is also known as "Charotar" because it is a good land, fertile, and well-drained soil. The dialect spoken by the people who live here is also known as "Charotari". The land is fertile and green with vegetation, so it is pleasing to the eye and is also known as the Charotar Path. Although the whole area is prosperous and productive, parts of Khambhat taluka and Tarapur taluka are known as "bhal" areas, where the problem of agricultural productivity due to saltwater and seabed influence occurs. But, the wheat of the "Bhal" region is very famous because of its great quality. Anand is located in central Gujarat, Mahisagar district in the north, Gulf of Kambe (Khambhat) in the south, Panchmahal in the east, Vadodara district in the southeast, and Kheda district in the west. Anand is known as the dairy capital of India. It is famous for Amul Dairy and its dairy revolution. The city is home to the Gujarat Cooperative Milk Marketing Federation Limited (AMUL), the headquarters of the National Dairy Development Board of India, the renowned Business School-IRMA, and the Anand Agricultural University. Apart from this, other famous educational centers in the city are Vallab Vidyanagar and Karamsad, the educational suburbs of Anand, home to about 10,000 students from all over India.

Bharuch, also known as Broch, is located on the banks of the Narmada River near the Gulf of Khambat (Kambe) in the Arabian Sea. Bharuch is the most famous port in

ancient India, named after Periplus Maurice Erythroy (80 AD) and Ptolemy Barigaja. It also appears in the Hindu epic Mahabharata. The city was ruled by Kshatrapas in the second century and by the Gurjars in the seventh century. It was annexed by the Muslim kingdom of Gujarat and later brought back to the Mughal Empire in 1572. It has been ruled by the Marathas since 1685 and was captured by the British in 1782. After changing hands several times, it was handed over to the East India Company in 1803. Bharuch is a commercial and industrial center, along with the cotton industry for hand loom weaving and making of veins and glass. The city exports cotton, wheat, flakes, pulses, and firewood. It is served by rail and is on the national highway. Cotton, millet, rice, and wheat cultivations are the main economic activity in the surrounding area, having previously been cultivated along forests and salt piles along the coast.

Thane is one of the few industrially developed districts in the state of Maharashtra. Thane district is located north of the Konkan Division. It ranks third in the state in terms of population according to the 2011 census. The district covers an area of 4214 km^2. This is 1.37% in the state. The Sahyadri Mountains are bounded on the east and west by the Arabian Sea, on the north by the dense forest cover of the state of Gujarat and on the south by Mumbai. Developed industrial areas in Thane, Kalyan, Ulhasnagar, Ambernath, Bhiwandi taluka of the district and Mumbai are influenced by the modern culture of the city. It is 720 km off the coast of Maharashtra and less than 27 km off the coast of Thane district. The area of 7642 hectares is suitable for groundwater fishing. In addition to marine fishing, groundwater fishing also takes place. Mumbai has such a large market for fishermen, and there is also a huge demand for fish production from the Gulf countries. Thane district ranks third in the state in terms of industrial development. More than half of the economic and social development of the district is due to industrialization. Maharashtra Industrial Development Corporation has developed eight industrial estates. International markets such as Mumbai and friendly ports, communication facilities, and facilities provided by the government have enriched the industry in the district. There is a concentration of industries, especially in the southern and western parts of the district. The registered industries in the district mainly produce large quantities of chemicals and pharmaceuticals. In addition, medium and small manufacturers are making large quantities of plastic goods, iron goods, and powerloom clothing. After Ichalkaranji in Maharashtra, Bhiwandi's textile industry became famous for its textile industry. The Central Government Sponsored Ammunition and Weapons Manufacturing Plant is located at Ambernath. Due to increasing industrialization, skilled and unskilled workers have found large-scale employment. Although the mineral production in the district is not very high, there is a large-scale sand mining business for construction works in Mumra, Thane, and Ghodbandar.

Vapi in the Valsad region of Gujarat is probably the best example of the state developing. Vapi, one of the largest industrial hubs in Asia, makes a significant contribution to the Gujarat economy. However, due to this progress, increasing pollution in the state, picturesque scenic spots, nearby natural beaches, and vibrant local culture make this industrial city a surprisingly enjoyable tourist destination. Vapi on the banks of the Damanga River at the southern end of the state is also famous for its historical

heritage and magnificent ancient temples, which have great religious value and are of interest to history lovers and archaeologists alike. If you are going through Gujarat or going on a tour of Daman, staying in Vapi is absolutely enjoyable. The Daman-ganga River flows not only through Gujarat but also through Maharashtra, Daman, Diu, and Dadra and Nagar Haveli before finally meeting the Arabian Sea. There are many famous picnic spots along this river that flows through the city of Vapi, which is friendly with locals and tourists alike. GIDC Garden is a wonderful picnic spot in the city. If you are in Vapi, do not forget to visit this site. Daman Beach is very close to Vapi, so people from the city, as well as those from other areas, prefer to drive to spend the day. The beach is clean, and there are some huts where you can sit comfortably. It is definitely worth the drive. Vapi is also famous for the many temples that surround the city. The Mahalakshmi Temple and the Shiva Temple are probably the most famous and are visited by thousands of devotees every year. Chaneshwar Temple, dedicated to Lord Shiva, is an ancient temple located on a hill, which offers a mesmerizing view of the scenic environment. Local city buses in Vapi are a common way to transport locals. You can rent an auto rickshaw, which runs throughout the city. Private taxis or taxis can be hired and the best way to explore the city. Surat Airport handles about four flights a day. The leading airline brand that frequently travels to this airport is Air India. Apart from flying, Vapi can also be reached by train. Vapi is one of the most popular railway stations in Vapi. An average of 100 + trains pass through Vapi daily. The most popular routes from Surat to Vapi, Mumbai to Vapi, and Valsad to Vapi are 263, 238, and 201 trains a week respectively.

Boisar, being one of the largest industrial areas in Mumbai, was originally a part of Thane district before it became part of Palghar district. It is 85 km from the state capital Mumbai and 98 km from the Union Territory of Daman. The district is located in Palghar. Boisar is managed by the Palghar Municipal Council (PMC). Boiser hosts India's first nuclear power plant—Tarapur Atomic Power Station (TOPS). It is a railway station on the Western Railway Zone of the Indian Railways and the Mumbai Suburban Railway. The Mumbai–Ahmedabad High-Speed Rail corridor will stop at Boisar. Boisar is a popular weekend destination for tourists and locals alike due to its nearby beaches, forts, and lakes. Boisar was part of the Rashtrakuta dynasty that ruled the Deccan Plateau between the eighth and tenth centuries. There are a few forts near the city, namely Aswa Fort (11 km), Tarapur Fort (11 km [6.8 miles]), Kaladurg Fort (174 km [108 miles]), Shirgaon Fort (18 km [11 miles]), Mahim Fort (20 km [12 miles]), and Ashiri Fort (25 km [16 miles]) (Census, 2011).

The city of Bilimora is divided into 12 wards, for which elections are held every 5 years. According to a 2011 report released by Censor India, Bilimora Municipality has a population of 53,187, of which 27,325 are males and 25,862 are females. The population of children aged 0–6 years is 4757, which is 8.94% of the total population of Bilimora (M). In the municipality of Bilimora, the female ratio is 946 against the state average of 999. Also, the child ratio in Bilimora is about 879 as compared to the state of Gujarat. About 890 Bilimora city literacy is 89.24% higher than the state average of 78.03%. Male literacy is 92.55%, while female literacy is 85.77%. The municipality of Bilimora governs a total of 11,822 households that provide basic amenities such as water and sewerage. The municipality also has the

power to build roads within its limits and to tax the property that falls within its jurisdiction. Virar is the city well connected to Mumbai by the Western Railway and the Mumbai–Ahmedabad National Highway. The city is connected to Navi Mumbai, Thane, Bhiwandi, Kalyan, and Panvel by the Vasi–Diva railway line. The city of Vasai-Virar has significant development potential due to its proximity to Vasai Murai. Vasai-Virar City Municipal Corporation (VVCMC) was established on July 3, 2009. Vasai-Virar Corporation is among the 19 declines.

5   Data Collection and Data Analysis

Based on the evidence collected on various HSR routes around the world, the impact of introduction of HSR has led to heterogeneous results as explained in Sect. 2 have been found. Using the same fundamentals, a predictive model using regression analysis will be used to study the impact of the introduction of the Mumbai–Ahmedabad High-Speed Rail (MAHSR) corridor on the stations along the route for the year 2025. The research framework will be used as given Fig. 2.

Regression analysis is widely used in determining trends and forecasting in a way that it quantifies the relationship between two variables that may provide a logical conclusion and have a connection such that it shows the dependence of one variable on the other independent variable. There are various types of regression models categorized under linear and nonlinear models, such as exponential, polynomial, and logarithmic models which are used to obtain scatter plots and equations, useful in predicting values. Regression helps to determine the factors that have an influence on other factors. Regression models are made up of two types of variables, namely dependent variables and independent variables. Dependent variables are the values that need to be predicted with the change of the other variables. Independent variables are the ones that have an influence on the dependent variables. For example, in our case, the independent variable in predicting the population dynamics is year and the
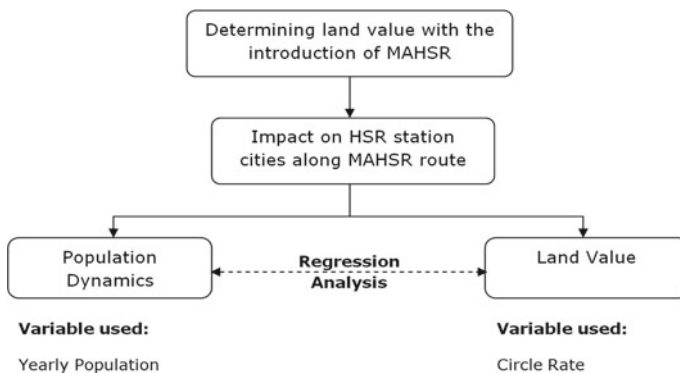
Fig. 2 Research framework

dependent variable is the yearly population of the cities that are being studied. The other analysis looks into studying the effect of population dynamics on land value, the independent variable is yearly population, and the dependent variable is being the circle rate of the city having HSR station along the MAHSR route. Regression analysis is used for assessment and evaluation. It has a significant overlap in the field of machine learning. It is not related to population, and such an observation is called outlier. Simply put, it is of immense value. An external problem is a problem because it often hinders the results we have achieved. When independent variables are interrelated, a variable is called a multicolor. A variety of regression methods suggest that there should be no multicoloniality in the dataset. This is because it causes problems in the ranking variables based on their importance or it makes it difficult to select a very important independent variable. When the difference between the target variable and the independent variable is not constant, it is called hetero-sexuality. Example: The diversity of food consumption increases as one's income increases. A poor man always spends a steady amount of money instead of eating cheap food; the rich can sometimes buy cheap food and at other times eat expensive food. High-income people exhibit greater diversity of food consumption. When we use unnecessary descriptive variables, it makes it overly fit. Overfitting means that our algorithm works well in the training set but does not work well on the test set. This is also known as the High Variations' problem. When our algorithm works very poorly, it will not be able to set up the training set properly, which will truncate the data. This is also known as a high bias problem. To determine the value of land after the introduction of HSR line, population dynamics and land value will be studied with yearly population and circle rate as their variables, respectively.

5.1 Data Collection on the Population Dynamics Along MAHSR

Population data till 2020 for each station city are collected in this section which will be analyzed in the further Sect. 5.2 to predict the population in 2025.

Figure 3 shows the population data collected for the HSR station cities along the route till the year 2020 depicting the trend of growth of population. Table 2 shows the population in 2020, density in the station city along with the working population density range as per Fig. 1c.

Mumbai and Surat show the highest population and density with a high working population followed by Ahmedabad and Thane, whereas Anand and Vadodara have a fair population density, while Bharuch has the lowest out of all the other station cities mentioned.

In Mumbai, the station is located in Bandra Kulra Complex at the underground level. Ahmedabad has its HSR station that connects to the existing Ahmedabad railway station. The Sabarmati HSR station is recommended considering road access to the station. It is situated in Ahmedabad on the bans of river Sabarmati with a
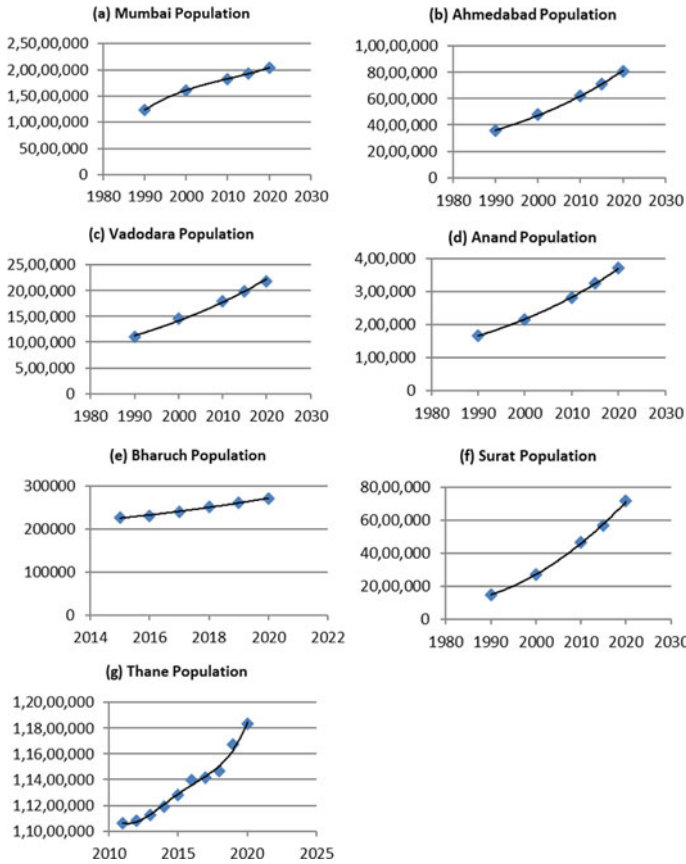
Fig. 3 Population data collection till the year 2020: **a** Mumbai, **b** Ahmedabad, **c** Vadodara, **d** Anand, **e** Bharuch, **f** Surat, **g** Thane

Table 2 Population and density data collection till the year 2020

Station area	Population in 2020	Density in 2020 (persons per sq. km)	Working population density (persons per sq. km) range as per Fig. 1c in 2020
Mumbai	20,411,274	20,000	10,001–25,000
Ahmedabad	8,059,441	9900	5001–10,000
Vadodara	2,189,973	551	501–750
Anand	371,559	711	501–750
Bharuch	271,779	238	101–250
Surat	7,184,590	14,000	10,001–25,000
Thane	11,834,886	1157	1001–2500

population of 73,669 as per the data in 2020 which is around 0.9% of the total population of Ahmedabad. Vadodara has its HSR station which connects to the existing Vadodara railway station similar to that of Ahmedabad. In Anand, the station is located in the National Highway No. 8 between Anand and Nadiad. The Bharuch HSR station is located near State Highway No. 6 at suburb on the west. In Surat, the HSR station is located near National Highway No. 6 at suburb on the east. Thane has its HSR station that connects to existing railway line. The Virar HSR station is located in the vacant green field between mountains on east side of the city. It is a city in Maharashtra under the Thane district, and the population as per the census 2011 is 1,222,390 with a density of 3900 persons per sq. km. having around 36.75% working population.

The Bilimora HSR station is located near State Highway No.15 at suburb on the east. It is a municipality city in the Navsari district in Gujarat with a population of 53,187 as per census data in 2011. About 19,750 which is around 37.13% out of the total population constituted the working population involved in business activities, job, service, cultivation, and labor activities. ("Bilimora Municipality City Population Census 2011–2021 | Gujarat", 2011) The Boisar HSR station is located in the vacant green field at a little distance from Boisar Road toward the east. It has a population of 36,151 as per census 2011 and a density of 4100/km^2. Out of the total population, 14,372 is the working population. (Suburban et al. 2011) The Vapi HSR station is located in Near State Highway No. 185 at suburb on the southeast. The city population accounts for 163,630 as per census 2011 showing around 8.65%yearly population growth as per the estimates for 2021 being 374,965. About 67,289 of the total population is the working population as per 2011.

5.2 Data Analysis of the Population Dynamics Along MAHSR

The data collected for population in Sect. 5.1 as shown in Fig. 3 have been used to predict the values for the year 2025 which is the proposed year for the operations to start along the HSR route.

It can be noticed that cities with lower population density show higher average yearly increase in population as can be seen in the case of Bharuch which has the smallest population in 2020 as per Table 3 which shows highest average yearly growth as it has a higher scope for accommodating industries and people with urbanization. Sabarmati and Virar lying in Ahmedabad and Thane, respectively, account for similar trends shown by the later two. The HSR stations in Bilimora and Boisar are proposed to be near the green fields showing that the places have a very small working population, while Vapi is showing a growing population showing potential for industrialization and urbanization to a greater extent.

Table 3 Summarized table for population dynamics with regression model formula and value of R^2

Station area	Value of R^2	Average yearly increase in population (%)	Population in 2025	Type of regression model used	Regression model equation
Mumbai	0.999	1.04	21,452,454	Polynomial (order 3)	$y = 260.7x^3 - 2E + 06x^2 + 3E + 09x - 2E + 12$
Ahmedabad	0.998	2.42	9,610,699	Exponential	$y = 1E - 17e0.027x$
Vadodara	0.991	2.09	2,370,845	Exponential	$y = 2E - 14e0.022x$
Anand	0.999	2.50	422,435	Exponential	$y = 9E - 19e0.026x$
Bharuch	0.996	3.72	322,758	Polynomial (order 2)	$y = 482.9x^2 - 2E + 06x + 2E + 09$
Surat	0.999	3.65	8,328,909	Polynomial (order 2)	$y = 3265x^2 - 1E + 07x + 1E + 10$
Thane	0.991	0.99	12,438,584	Polynomial (order 4)	$y = 518.0x^4 - 4E + 06x^3 + 1E + 10x^2 - 2E + 13x + 9E + 15$

5.3 Data Analysis on the Effect of Population Dynamics on Land Price Along MAHSR

This section is aimed at establishing a relationship and studying the effect of population dynamics on land price by plotting the yearly population on the *x*-axis and the annual average circle rate on the *y*-axis as depicted in Fig. 4.

Figure 4 shows the data collected to show the effect of population dynamics on land price till the year 2020. It depicts the growth trends of circle rate per year with the yearly increase in population as the demand for the land increases with the growth of population leading to increased land value.

Table 4 shows the summary of the regression models used for each HSR station area for Mumbai, Ahmedabad, Vadodara, Anand, Bharuch, Surat, and Thane. The high value of R^2 suggests that there is a correlation between population dynamics and land value. The coefficient of determination, R^2 being very close to 1 in all the predictive regression models above, shows that there is a good model fit to the real values.

Mumbai which is a city with high level of urbanization has to the unmatched level of population with the insufficient transportation system to cater to the over flowing population. Due to increasing population and migration into the city, there has been
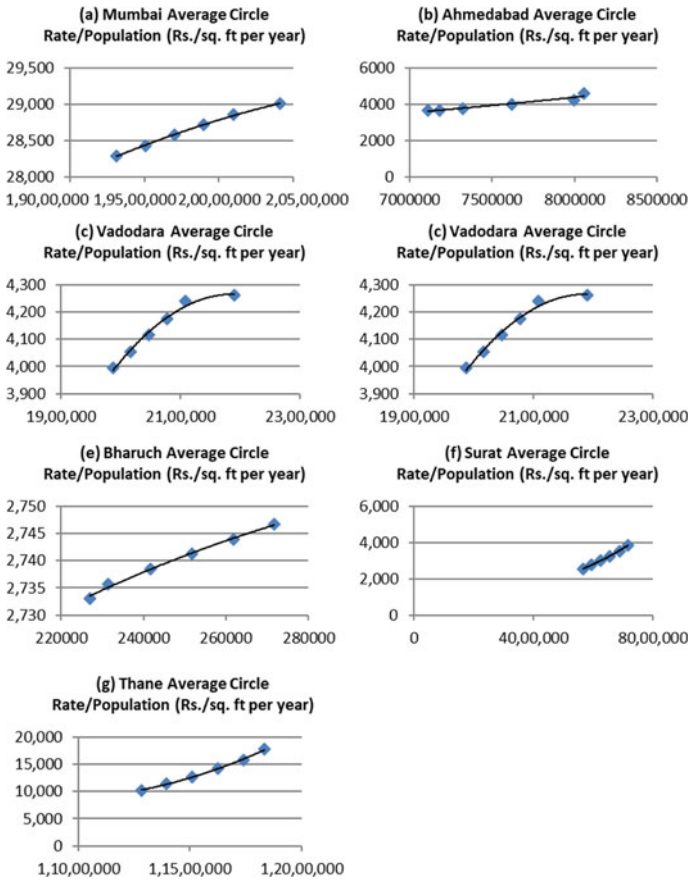
Fig. 4 Data collected to show the effect of population dynamics land price till the year 2020

an increasing demand to property near the transport facilities for better accessibility, hence leading to a greater land value. As seen from the evidence from cities with HSR around the world, there is a shift noticed with the introduction of High-Speed Rail to the nearing places which have higher possibility of urbanization. There is potential of employment opportunities in the less developed nearing places like Boisar and Bilimora due to reduced time of travel and increased accessibility. Similarly, other densely populated cities like Ahmedabad, Surat would see a shift in population to the nearing hubs for industrial development like Vapi.

Table 4 Summarized table for the effect of population on land value with regression model formula and value of R^2

Station area	Regression model used	Value of R^2	Average yearly increase in land value with population (%)	Land value (Rs.) in 2025
Mumbai	*Polynomial (order 2);* $y = -2E - 10x^2 + 0.006x - 45,581$ $R^2 = 0.998$	0.998	0.55	29,824
Ahmedabad	*Exponential;* $y = 771.5e2E - 07x$	0.934	4.14	5437
Vadodara	*Polynomial (order 2);* $y = -7E - 09x^2 + 0.030x - 28,643$	0.988	1.43	4590
Anand	*Exponential;* $y = 967.3e3E - 06x$	0.999	3.10	4015
Bharuch	*Polynomial (order 2);* $y = -1E - 09x^2 + 0.001x + 2583$	0.993	0.1	2758
Surat	*Exponential;* $y = 550.1e3E - 07x$	0.999	8.56	5816
Thane	*Polynomial (order 2);* $y = 9E - 09x^2 - 0.203x + 1E + 06$	0.998	11.57	30,617

6 Results and Discussion

This section discusses about the effect of yearly population growth on average yearly circle growth from the data collected and analyzed in Sect. 5 taking into consideration the qualitative factors like last mile accessibility and location to predict the effect on land values along the city having HSR stations along the route in 2025.

Table 5 shows that there is heterogeneous effect on land value growth in cities with proposed HSR station. Mumbai being a densely populated city shows slower growth in population around 1.04% and land value, i.e., 0.55% as it is mostly an urbanized region, the demand will fall for property along the city as with the introduction of HSR, and there will be a tendency for people to move to other nearing cities like Boisar and Bilimora which has a higher scope of industrialization and urbanization. Very high population in Mumbai will lead to decrease in land values, and as a result of improved accessibility, the demand for property will decrease as an effect of negative externalities. Surat and Ahmedabad with yearly population growth of 3.65% and 2.42%, respectively, are showing fairly high land value growth of 8.56% and 4.14%, respectively, as the level of urbanization has not reached its peak but is still in the developing stage. Once they are urbanized to a large extent which is quite expected in the coming 5 years as can be seen with the rapid increase in growth rate of land values in Surat and Ahmedabad, it will also show a shift of property demand

Table 5 Summarized table for the yearly population and average yearly land value growth

Station area	Average yearly increase in population (%)	Average yearly increase in land value with population (%)	Density in 2020 (persons per sq. km)	Population in 2025	Land value (Rs.) in 2025
Mumbai	1.04	0.55	20,000	21,452,454	29,824
Ahmedabad	2.42	4.14	9900	9,610,699	5437
Vadodara	2.09	1.43	551	2,370,845	4590
Anand	2.50	3.10	711	422,435	4015
Bharuch	3.72	0.1	238	322,758	2758
Surat	3.65	8.56	14,000	8,328,909	5816
Thane	0.99	11.57	1157	12,438,584	30,617

in nearing smaller areas like Vapi which has a higher scope for urbanization with the introduction of HSR along the route. Thane although shows a slow yearly growth rate in population, i.e., 0.99% has an average yearly land value growth rate of 11. 57%, as a result of fair density of 1157 showing that is it going under rapid urbanization. Bharuch shows a high yearly growth rate in population, i.e., 3.72% accounts for a minute 0.1% increase rate in average yearly land value growth showing that there is a high potential for urbanization leading to growth in land value in 2025. Vadodara and Anand show a yearly growth rate in population of 2.09% and 2.50%, respectively, and their average yearly land values show 1.43% and 3.10% growth, respectively, having moderate density which indicate that the two station cities will experience minute fluctuations in the land value growth after the introduction of the HSR line as the amount of urbanization is balanced with the population growth rate. With the heterogeneous effect of introduction of the HSR line along the route, the next part, i.e., Sect. 8 takes in view of the various land use developments as a part of research recommendation to gain the most advantages out of the development of this transport system in India.

7 Research Recommendations

High-Speed Rail in other countries where implemented has been a major boost in their economy due to the transit-oriented development seen alongside the development of High-Speed Rail. There is an essential need of the following recommendations that are mentioned below alongside the implementation of High-Speed Rail in India:

1. India should consider developing and implementing its own High-Speed Rail technology in the upcoming projects in order to cater to the infrastructural needs specific to the particular region/area of development with the study of land use pattern along the route.

2. Sustainable development along the HSR route would lead to a better environmental condition which is essential for any system and ecosystem to sustain in the long run.
3. As studied from this research, there is a scope of industrial development in the smaller cities having HSR stations in order to spread the population to maintain a balance and reduce the burden on a particular piece of land. Therefore, land use pattern planning is of utmost importance with the introduction of High-Speed Rail in order to get the maximum socioeconomic benefits out of it.

It has been very evident that the countries around the world has seen a lot of positive effect with the advent of the High-Speed Rail starting from trade to economy to industrial development, transit-oriented development, and anything that a transport infrastructure and system could offer to the mankind. It has been a huge success with its in the countries where it has been developed and led to the use of sustainable development not only with the rise of its energy efficiency methods and use of renewable energy but also contributed a lot to the policy development. The increasing population of any city leads to a huge set of issues when it comes to population growth beyond a certain limit leading to all kinds of problems like traffic congestion, all kinds of pollution like air, water, land, and noise. This is due to densely population regions in a certain area. It is caused as a result of urban sprawl with the increase in development and setup of industries which open the market with a lot of employment opportunities. This leads to clustering up with regions being highly congested and the nearing places being left as vacant lands due to underutilization. When it comes to predicting land values, this study is meant to initiate the planning process of developing cities, industrial and urban hubs in a sustainable manner to allow the High-Speed Rail project a success in a country like India which is still on the development phase. It is not far that the population would become so large that it would become even more challenging to mitigate such issues related to urban sprawl ultimately leading to putting huge burden on the environment and the ecosystem, the reason which is responsible for rapid climate change and sufferings to the mankind to frequent natural calamities and disasters. Urban planning must go hand in hand with the development of such transport systems like the High-Speed Rail project that act as a natural catalyst in transit-oriented development to sustain its technology in the long run. Like Japan built its HSR system on a totally separate gauge apart from the conventional rail line, European countries decided to run the HSR system on the existing lines, and India must consider and develop technologies that cater to the needs of its surroundings. It is highly appreciated when we learn a technology from the ones that have already been tested and tried, but it is another thing to advance its technology that caters to the specific area of implementation as it would not only lead to a better durability of the technology in the long run, but the local design, planning would not just lead to higher employability but also reduced overall costs employed in engaging experts from the places where it has been developed. It is equally important to develop the other infrastructural essentials like bridges, tunnels, stations, electrification, etc., by involving people in the country who have a deep knowledge about the construction

and its operations. It is as important as developing the train and rake system of the HSR transport system.

8 Conclusion

As concluded from the study, there is a heterogeneous impact of the introduction of HSR line along a route. The major takeaways as depicted from the discussion in Sect. 6 show that cities with high population and density show smaller growth in land prices, i.e., 0.55% as in the case of Mumbai. The negative externalities like noise, pollution, and congestion in highly populated cities like Mumbai, Ahmedabad, Thane, and Surat would lead to a fall in the land prices around the crowded areas as more industrial and employment opportunities are created in the less urbanized areas like Bharuch, Bilimora, Boisar, Virar, and Vapi as summarized in Table 5 and discussed in Sect. 6. The immediate effect as observed from the heterogeneous effect of the introduction High-Speed Rail in a route leads to a balance in the population ecosystem. This is due to the spread of population over a large region than creating two extremes where, one place is suffocating being overcrowded and the other left as vacant barren lands. The places with an intermediate population density like Vadodara and Anand will experience very little change in land prices but will have an increased economic development with the increase in trade as a result of being connecting hubs for the rest of the High-Speed Rail route as depicted in Sect. 6.

India is a vast country with rapid increase in population. India, in fact, needs to consider an implementation of High-Speed Rail as quickly as possible. Due to its increasing population, the availability of land will become a major problem for implementing the HSR transport infrastructure in the near future. It would become much more challenging to plan a sustainable development of land. High-Speed Rail as seen from the evidences from other countries is the solution to not only having positive economic impact with the growth of industries an employment opportunity but also have shown major positive impacts on the climatic conditions around places in the world due to the increased of public transport due to its transit-oriented development leading to reduced carbon emissions.

This paper can be taken as a base to study all other routes of High-Speed Rail that are proposed in India to do a predictive analysis of land value in order to determine the present status of urban and regional plannings employed in a particular route and area of study. It has been noticed that data for places that are fairly developed and urbanized having a huge population and density are always under study for regional planning, but the nearing areas which have a lot of potential for growth and development are kept under the cover which needs to be unleashed as we are advancing toward problems caused due to over population on one hand and underutilization of smaller nearing areas on the other hand. This is the time and High-Speed Rail technology has been proved to be effective in a way such that it takes of a bundle of problems related to ecosystem imbalance and economic opportunities with the development of one transportation system that establishes a baseline for land use planning catering

not only to the urban regions but also the rural regions creating a balance between the two. The High-Speed Rail technology is a need of the hour in order for India to match the world standards in its economy, at the very same time creating a future that is sustainable in the long run.

References

1. Sharma, S.K., Lee, J., Jang, H.-L.: Mathematical modeling and simulation of suspended equipment impact on car body modes. Machines **10**, 192 (2022). https://doi.org/10.3390/machines10030192

2. Vishwakarma, P.N., Mishra, P., Sharma, S.K.: Formulation of semi-active suspension system and controls in rail vehicle. SSRN Electron. J. (2022). https://doi.org/10.2139/ssrn.4159616

3. Vishwakarma, P.N., Mishra, P., Sharma, S.K.: Characterization of a magnetorheological fluid damper a review. Mater. Today Proc. **56**, 2988–2994 (2022). https://doi.org/10.1016/j.matpr.2021.11.143

4. Sharma, S.K., Sharma, R.C., Lee, J., Jang, H.-L.: Numerical and experimental analysis of DVA on the flexible-rigid rail vehicle carbody resonant vibration. Sensors **22**, 1922 (2022). https://doi.org/10.3390/s22051922

5. Sharma, S.K., Mohapatra, S., Sharma, R.C., Alturjman, S., Altrjman, C., Mostarda, L., Stephan, T.: Retrofitting existing buildings to improve energy performance. Sustainability **14**, 666 (2022). https://doi.org/10.3390/su14020666

6. Sharma, R.C., Palli, S., Sharma, S.K.: Ride analysis of railway vehicle considering rigidity and flexibility of the carbody. J. Chinese Inst. Eng. **46**, 355–366 (2023). https://doi.org/10.1080/02533839.2023.2194918

7. Sharma, S.K., Sharma, R.C., Lee, J.: In situ and experimental analysis of longitudinal load on carbody fatigue life using nonlinear damage accumulation. Int. J. Damage Mech. **31**, 605–622 (2022). https://doi.org/10.1177/10567895211046043

8. Sharma, R.C., Sharma, S.K.: Ride analysis of road surface-three-wheeled vehicle-human subject interactions subjected to random excitation. SAE Int. J. Commer. Veh. **15** (2022). https://doi.org/10.4271/02-15-03-0017

9. Sharma, S.K., Lee, J.: Crashworthiness analysis for structural stability and dynamics. Int. J. Struct. Stab. Dyn. **21**, 2150039 (2021). https://doi.org/10.1142/S0219455421500395

10. Wu, Q., Cole, C., Spiryagin, M., Chang, C., Wei, W., Ursulyak, L., Shvets, A., Murtaza, M.A., Mirza, I.M., Zhelieznov, К., Mohammadi, S., Serajian, H., Schick, B., Berg, M., Sharma, R.C., Aboubakr, A., Sharma, S.K., Melzi, S., Di Gialleonardo, E., Bosso, N., Zampieri, N., Magelli, M., Ion, C.C., Routcliffe, I., Pudovikov, O., Menaker, G., Mo, J., Luo, S., Ghafourian, A., Serajian, R., Santos, A.A., Teodoro, Í.P., Eckert, J.J., Pugi, L., Shabana, A., Cantone, L.: Freight train air brake models. Int. J. Rail Transp. 1–49 (2021). https://doi.org/10.1080/23248378.2021.2006808

11. Sharma, S.K., Sharma, R.C., Lee, J.: Effect of rail vehicle-track coupled dynamics on fatigue failure of coil spring in a suspension system. Appl. Sci. **11**, 2650 (2021). https://doi.org/10.3390/app11062650

12. Mohapatra, S., Mohanty, D., Mohapatra, S., Sharma, S., Dikshit, S., Kohli, I., Samantaray, D.P., Kumar, R., Kathpalia, M.: Biomedical application of polymeric biomaterial: polyhydroxybutyrate. In: Bioresource Utilization and Management: Applications in Therapeutics, Biofuels, Agriculture, and Environmental Science. pp. 1–14. CRC Press (2021). https://doi.org/10.21203/rs.3.rs-1491519/v1

13. Bhardawaj, S., Sharma, R.C., Sharma, S.K., Sharma, N.: On the planning and construction of railway curved track. Int. J. Veh. Struct. Syst. **13**, 151–159 (2021). https://doi.org/10.4273/ijvss.13.2.04

14. Sharma, R.C., Sharma, S., Sharma, N., Sharma, S.K.: Linear and nonlinear analysis of ride and stability of a three-wheeled vehicle subjected to random and bump inputs using bond graph and Simulink methodology. SAE Int. J. Commer. Veh. **14** (2021). https://doi.org/10.4271/02-15-01-0001

15. Sharma, R.C., Sharma, S., Sharma, S.K., Sharma, N., Singh, G.: Analysis of bio-dynamic model of seated human subject and optimization of the passenger ride comfort for three-wheel vehicle using random search technique. Proc. Inst. Mech. Eng. Part K J. Multi-body Dyn. **235**, 106–121 (2021). https://doi.org/10.1177/1464419320983711

16. Choi, S., Lee, J., Sharma, S.K.: A study on the performance evaluation of hydraulic tank injectors. In: Advances in Engineering Design: Select Proceedings of FLAME 2020, pp. 183–190. Springer Singapore (2021). https://doi.org/10.1007/978-981-33-4684-0_19

17. Lee, J., Han, J., Sharma, S.K.: Structural analysis on the separated and integrated differential gear case for the weight reduction. In: Joshi, P., Gupta, S.S., Shukla, A.K., Gautam, S.S. (eds.) Advances in Engineering Design. Lecture Notes in Mechanical Engineering, pp. 175–181 (2021). https://doi.org/10.1007/978-981-33-4684-0_18

18. Sharma, S.K., Sharma, R.C.: Multi-objective design optimization of locomotive nose. In: SAE Technical Paper, pp. 1–10 (2021). https://doi.org/10.4271/2021-01-5053

19. Sharma, R.C., Palli, S., Sharma, N., Sharma, S.K.: Ride behaviour of a four-wheel vehicle using H infinity semi-active suspension control under deterministic and random inputs. Int. J. Veh. Struct. Syst. **13**, 234–237 (2021). https://doi.org/10.4273/ijvss.13.2.18

20. Sharma, S.K., Sharma, R.C., Sharma, N.: Combined multi-body-system and finite element analysis of a rail locomotive crashworthiness. Int. J. Veh. Struct. Syst. **12**, 428–435 (2020). https://doi.org/10.4273/ijvss.12.4.15

21. Sharma, R.C., Sharma, S.K., Palli, S.: Linear and non-linear stability analysis of a constrained railway Wheel Axle. Int. J. Veh. Struct. Syst. **12**, 128–133 (2020). https://doi.org/10.4273/ijvss.12.2.04

22. Palli, S., Sharma, R.C., Sharma, S.K., Chintada, V.B.: On methods used for setting the curve for railway tracks. J. Crit. Rev. **7**, 241–246 (2020)

23. Mohapatra, S., Pattnaik, S., Maity, S., Mohapatra, S., Sharma, S., Akhtar, J., Pati, S., Samantaray, D.P., Varma, A.: Comparative analysis of PHAs production by Bacillus megaterium OUAT 016 under submerged and solid-state fermentation. Saudi J. Biol. Sci. **27**, 1242–1250 (2020). https://doi.org/10.1016/j.sjbs.2020.02.001

24. Sharma, R.C., Sharma, S.K., Sharma, N., Sharma, S.: Analysis of ride and stability of an ICF railway coach. Int. J. Veh. Noise Vib. **16**, 127 (2020). https://doi.org/10.1504/IJVNV.2020.117820

25. Sharma, S.K., Phan, H., Lee, J.: An application study on road surface monitoring using DTW based image processing and ultrasonic sensors. Appl. Sci. **10**, 4490 (2020). https://doi.org/10.3390/app10134490

26. Sharma, R.C., Sharma, S., Sharma, S.K., Sharma, N.: Analysis of generalized force and its influence on ride and stability of railway vehicle. Noise Vib. Worldw. **51**, 95–109 (2020). https://doi.org/10.1177/0957456520923125

27. Lee, J., Sharma, S.K.: Numerical investigation of critical speed analysis of high-speed rail vehicle. 한국정밀공학회 학술발표대회 논문집 (Korean Soc. Precis. Eng. **696** (2020)

28. Sharma, S.K., Lee, J.: Finite element analysis of a fishplate rail joint in extreme environment condition. Int. J. Veh. Struct. Syst. **12**, 503–506 (2020). https://doi.org/10.4273/ijvss.12.5.03

29. Bhardawaj, S., Sharma, R., Sharma, S.: Ride analysis of track-vehicle-human body interaction subjected to random excitation. J. Chinese Soc. Mech. Eng. **41**, 237–236 (2020). https://doi.org/10.29979/JCSME

30. Bhardawaj, S., Sharma, R.C., Sharma, S.K.: Development in the modeling of rail vehicle system for the analysis of lateral stability. Mater. Today Proc. **25**, 610–619 (2020). https://doi.org/10.1016/j.matpr.2019.07.376

31. Bhardawaj, S., Sharma, R.C., Sharma, S.K.: Analysis of frontal car crash characteristics using ANSYS. Mater. Today Proc. **25**, 898–902 (2020). https://doi.org/10.1016/j.matpr.2019.12.358

32. Sharma, S., Sharma, R.C., Sharma, S.K., Sharma, N., Palli, S., Bhardawaj, S.: Vibration Isolation of the quarter car model of road vehicle system using dynamic vibration absorber. Int. J. Veh. Struct. Syst. **12**, 513–516 (2020). https://doi.org/10.4273/ijvss.12.5.05

33. Acharya, A., Gahlaut, U., Sharma, K., Sharma, S.K., Vishwakarma, P.N., Phanden, R.K.: Crashworthiness analysis of a thin-walled structure in the frontal part of automotive chassis. Int. J. Veh. Struct. Syst. **12**, 517–520 (2020). https://doi.org/10.4273/ijvss.12.5.06

34. Bhardawaj, S., Sharma, R.C., Sharma, S.K.: Development of multibody dynamical using MR damper based semi-active bio-inspired chaotic fruit fly and fuzzy logic hybrid suspension control for rail vehicle system. Proc. Inst. Mech. Eng. Part K J. Multi-body Dyn. **234**, 723–744 (2020). https://doi.org/10.1177/1464419320953685

35. Sharma, S.K., Lee, J.: Design and development of smart semi active suspension for nonlinear rail vehicle vibration reduction. Int. J. Struct. Stab. Dyn. **20**, 2050120 (2020). https://doi.org/10.1142/S0219455420501205

36. Sharma, S.K.: Multibody analysis of longitudinal train dynamics on the passenger ride performance due to brake application. Proc. Inst. Mech. Eng. Part K J. Multi-body Dyn. **233**, 266–279 (2019). https://doi.org/10.1177/1464419318788775.

37. Goyal, S., Anand, C.S., Sharma, S.K., Sharma, R.C.: Crashworthiness analysis of foam filled star shape polygon of thin-walled structure. Thin-Walled Struct. **144**, 106312 (2019). https://doi.org/10.1016/j.tws.2019.106312

38. Sharma, S.K., Sharma, R.C.: Pothole detection and warning system for Indian roads. In: Advances in Interdisciplinary Engineering, pp. 511–519 (2019). https://doi.org/10.1007/978-981-13-6577-5_48

39. Goswami, B., Rathi, A., Sayeed, S., Das, P., Sharma, R.C., Sharma, S.K.: Optimization design for aerodynamic elements of indian locomotive of passenger train. In: Advances in Engineering Design, pp. 663–673. Lecture Notes in Mechanical Engineering. Springer, Singapore (2019). https://doi.org/10.1007/978-981-13-6469-3_61

40. Bhardawaj, S., Chandmal Sharma, R., Kumar Sharma, S.: Development and advancement in the wheel-rail rolling contact mechanics. IOP Conf. Ser. Mater. Sci. Eng. **691**, 012034 (2019). https://doi.org/10.1088/1757-899X/691/1/012034

41. Choppara, R.K., Sharma, R.C., Sharma, S.K., Gupta, T.: Aero dynamic cross wind analysis of locomotive. In: IOP Conference Series: Materials Science and Engineering. p. 12035. IOP Publishing (2019)

42. Sinha, A.K., Sengupta, A., Gandhi, H., Bansal, P., Agarwal, K.M., Sharma, S.K., Sharma, R.C., Sharma, S.K.: Performance enhancement of an all-terrain vehicle by optimizing steering, powertrain and brakes. In: Advances in Engineering Design, pp. 207–215 (2019). https://doi.org/10.1007/978-981-13-6469-3_19

43. Sharma, S.K., Saini, U., Kumar, A.: Semi-active control to reduce lateral vibration of passenger rail vehicle using disturbance rejection and continuous state damper controllers. J. Vib. Eng. Technol. **7**, 117–129 (2019). https://doi.org/10.1007/s42417-019-00088-2

44. Bhardawaj, S., Chandmal Sharma, R., Kumar Sharma, S.: A survey of railway track modelling. Int. J. Veh. Struct. Syst. **11**, 508–518 (2019). https://doi.org/10.4273/ijvss.11.5.08

45. Sharma, R.C., Palli, S., Sharma, S.K., Roy, M.: Modernization of railway track with composite sleepers. Int. J. Veh. Struct. Syst. **9**, 321–329 (2018)

46. Sharma, R.C., Sharma, S.K., Palli, S.: Rail vehicle modelling and simulation using Lagrangian method. Int. J. Veh. Struct. Syst. **10**, 188–194 (2018). https://doi.org/10.4273/ijvss.10.3.07

47. Palli, S., Koona, R., Sharma, S.K., Sharma, R.C.: A review on dynamic analysis of rail vehicle coach. Int. J. Veh. Struct. Syst. **10**, 204–211 (2018). https://doi.org/10.4273/ijvss.10.3.10

48. Sharma, S.K., Sharma, R.C.: An investigation of a locomotive structural crashworthiness using finite element simulation. SAE Int. J. Commer. Veh. **11**, 235–244 (2018). https://doi.org/10.4271/02-11-04-0019

49. Sharma, S.K., Sharma, R.C.: Simulation of quarter-car model with magnetorheological dampers for ride quality improvement. Int. J. Veh. Struct. Syst. **10**, 169–173 (2018). https://doi.org/10.4273/ijvss.10.3.03

50. Sharma, S.K., Kumar, A.: Impact of longitudinal train dynamics on train operations: a simulation-based study. J. Vib. Eng. Technol. **6**, 197–203 (2018). https://doi.org/10.1007/s42417-018-0033-4

51. Sharma, R.C., Sharma, S.K.: Sensitivity analysis of three-wheel vehicle's suspension parameters influencing ride behavior. Noise Vib. Worldw. **49**, 272–280 (2018). https://doi.org/10.1177/0957456518796846

52. Sharma, S.K., Kumar, A.: Ride comfort of a higher speed rail vehicle using a magnetorheological suspension system. Proc. Inst. Mech. Eng. Part K J. Multi-body Dyn. **232**, 32–48 (2018). https://doi.org/10.1177/1464419317706873

53. Sharma, S.K., Kumar, A.: Disturbance rejection and force-tracking controller of nonlinear lateral vibrations in passenger rail vehicle using magnetorheological fluid damper. J. Intell. Mater. Syst. Struct. **29**, 279–297 (2018). https://doi.org/10.1177/1045389X17721051

54. Sharma, S.K., Kumar, A.: Impact of electric locomotive traction of the passenger vehicle ride quality in longitudinal train dynamics in the context of Indian railways. Mech. Ind. **18**, 222 (2017). https://doi.org/10.1051/meca/2016047

55. Sharma, S.K., Kumar, A.: Ride performance of a high speed rail vehicle using controlled semi active suspension system. Smart Mater. Struct. **26**, 055026 (2017). https://doi.org/10.1088/1361-665X/aa68f7

56. Sharma, S.K., Kumar, A.: Dynamics analysis of wheel rail contact using FEA. Procedia Eng. **144**, 1119–1128 (2016). https://doi.org/10.1016/j.proeng.2016.05.076

57. Sharma, S.K., Chaturvedi, S.: Jerk analysis in rail vehicle dynamics. Perspect. Sci. **8**, 648–650 (2016). https://doi.org/10.1016/j.pisc.2016.06.047

58. Kulkarni, D., Sharma, S.K., Kumar, A.: Finite element analysis of a fishplate rail joint due to wheel impact. In: International Conference on Advances in Dynamics, Vibration and Control (ICADVC-2016) NIT Durgapur, India 25–27 February 2016. National Institute of Technology Durgapur, Durgapur, India (2016)

59. Sharma, S.K., Sharma, R.C., Kumar, A., Palli, S.: Challenges in rail vehicle-track modeling and simulation. Int. J. Veh. Struct. Syst. **7**, 1–9 (2015). https://doi.org/10.4273/ijvss.7.1.01

60. Sharma, S.K., Kumar, A., Sharma, R.C.: Challenges in railway vehicle modeling and simulations. In: International Conference on Newest Drift in Mechanical Engineering (ICNDME-14), 20–21 December, M. M. University, Mullana, India, pp. 453–459. Maharishi Markandeshwar University, Mullana—Ambala (2014)

61. Sharma, S.K., Kumar, A.: A comparative study of Indian and Worldwide railways. Int. J. Mech. Eng. Robot. Res. **1**, 114–120 (2014)

62. Sharma, S.K.: Zero energy building envelope components: a review. Int. J. Eng. Res. Appl. **3**, 662–675 (2013)

63. Sharma, S.K., Lavania, S.: An autonomous metro: design and execution. In: Futuristic trends in Mechanical and Industrial Engineering. pp. 1–8. JECRC UDML College of Engineering, Jaipur (2013)

64. Sharma, S.K., Lavania, S.: Green manufacturing and green supply chain management in India a review. In: Futuristic trends in Mechanical and Industrial Engineering, pp. 1–8. JECRC UDML College of Engineering (2013)

65. Sharma, S.K., Lavania, S.: Skin effect in high speed VLSI on-chip interconnects. In: International Conference on VLSI, Communication and Networks, V-CAN, pp. 1–8. Institute of Engineering and Technology, Alwar (2011)

66. Lavania, S., Sharma, S.K.: An explicit approach to compare crosstalk noise and delay in VLSI RLC interconnect modeled with skin effect with step and ramp input. J. VLSI Des. Tools Technol. **1**, 1–8 (2011)

67. JICA & Ministry of Railways: Joint Feasibility Study for Mumbai—Ahmedabad High Speed Railway Corridor. Nhsrcl, p. 1 (2015)

68. Sharma, R.C., Palli, S., Jha, A.K., Bhardawaj, S., Sharma, S.K.: Vibration And Ride Comfort Analysis of Railway Vehicle System Subjected to Deterministic Inputs. resmilitaris. **12**, 1345–1355 (2022).

69. Sharma, R.C., Gopala Rao, L.V.V., Sharma, S.K., Palli, S., Satyanarayana, V.S.V.: Analysis of Lateral Stability and Ride of an Indian Railway Constrained Dual-Axle Bogie Frame. SAE Int. J. Commer. Veh. **16**, 02-16-02–0014 (2022). https://doi.org/10.4271/02-16-02-0014

70. Lu, X., Tang, Y., Ke, S.: Does the construction and operation of high-speed rail improve urban land use efficiency? Evid. China Land. **10**, 303 (2021). https://doi.org/10.3390/land10030303

71. Sharma, S.K., Kumar, A.: The Impact of a rigid-flexible system on the ride quality of passenger bogies using a flexible carbody. In: Pombo, J. (ed.) Proceedings of the Third International Conference on Railway Technology: Research, Development and Maintenance, Stirlingshire, UK. p. 87. Civil-Comp Press, 2016, Stirlingshire, UK (2016). https://doi.org/10.4203/ccp.110.87

72. Arief, A., Yudono, A., Akil, A., Ramli, I., Rahim, A.: Determining of the suitable location for the development of coastal transit oriented development. J. Urban Environ. Eng. **12**, 210–218 (2018). https://doi.org/10.4090/juee.2018.v12n2.210218

73. Chen, H., Hou, L., Zhang, G. (Kevin), Moon, S.: Development of BIM, IoT and AR/VR technologies for fire safety and upskilling. Autom. Constr. **125**, 103631 (2021). https://doi.org/10.1016/j.autcon.2021.103631

74. Kumar, U., Kasvekar, R., Sharma, S.K., Upadhyay, R.K.: Wear of Wheels and Axle in Locomotive and Measures Taken by Indian Railway. In: Advances in Engine Tribology. pp. 77–96. Springer (2022). https://doi.org/10.1007/978-981-16-8337-4_5

75. Sharma, S.K., Sharma, R.C., Choi, Y., Lee, J.: Experimental and Mathematical Study of Flexible–Rigid Rail Vehicle Riding Comfort and Safety. Appl. Sci. **13**, 5252 (2023). https://doi.org/10.3390/app13095252

76. Sharma, R.C., Palli, S., Gopala Rao, L.V.V., Duppala, A., Sharma, S.K.: Four-Wheel Vehicle Response under Bump, Pothole, Harmonic, and Random Excitations Using Bond Graph/Simulink Technique. SAE Int. J. Commer. Veh. **16**, 02-16-02–0008 (2022). https://doi.org/10.4271/02-16-02-0008

Comparative Study of Regenerative Braking at Different Gradients for Indian Railways WAP-7 Locomotive Incorporating a Flywheel Model

Subhadeep Kuila, Sudhanshu Yadav, Mohd Avesh, and Rakesh Chandmal Sharma

Abstract This chapter discusses a novel mathematical model for estimating the regenerative braking effectiveness of Indian locomotives equipped with the regenerative braking system. It is proven on Indian rails for a WAP-7 locomotive. The necessity for an additional energy recovery mechanism in the locomotive mechanical model is discussed in this study. The present energy reliance of AC-powered Indian locomotives has been examined. To research the electrical energy flow and electric machinery in an AC locomotive, the essential components of a modern electric rail vehicle, a WAP-7 locomotive, were chosen. The phenomena of energy recovery while braking has been explained using regenerative energy generation and electrical braking of an AC locomotive. To better comprehend the mathematical modelling of an AC locomotive, a traditional mechanical model based on the WAP-7 locomotive was used. The new model has been simulated on Shatabdi Express, train no. 12010 running from Ahmedabad Junction to Mumbai Central. The effect of gradient on the recovered energy has been calculated and compared with five levels of gradients, viz. 1 in 400,300,200,150 and 100. Simulation of the mathematical model has been carried out using Python in Microsoft Visual Studio. The simulation results have been discussed with the flywheel models and the energy efficiency achieved.

Keywords FBESS · Flywheel · Mathematical model · Regenerative braking

S. Kuila · S. Yadav
School of Engineering and Applied Sciences, National Rail and Transportation Institute, Vadodara, India

M. Avesh
Star Saidham Services Solutions, Doiwala, Dehradun, India

R. C. Sharma (✉)
Mechanical Engineering Department, Graphic Era (Deemed to Be University), Dehradun, India
e-mail: rcsharmaiitr@gmail.com

1 Introduction

Railways are one of the most ecologically beneficial modes of transportation. It's an important strategy for meeting expanding transportation demands in an environmentally concerned economy [1–8]. The rail sector in India continues to consume a lot of energy. With a growing population and more energy use, the need for train services will continue to rise, as will energy consumption [9]. The energy wasted as trains arrive at rail terminals is an obvious additional source of energy that may be utilized to minimize demand on electricity generation facilities and enhance overall grid efficiency in big metropolitan areas [10–13]. The energy wasted as trains arrive at rail terminals is an obvious additional source of energy that may be utilized to minimize demand on electricity generation facilities and enhance overall grid efficiency in big metropolitan areas. Our civilization wastes a staggering amount of energy every day [14]. The causes range from inefficient systems in residences, such as single-pane windows, to essential but inelegant systems on practically every method of transportation, such as friction brakes [15, 16].

Regenerative braking is a hypothesis that catches the energy squandered when automobiles use their brakes to slow down and gives a practical solution to use otherwise wasted energy. The overall efficiency of the electrical grid may be improved by using wasted energy to raise energy supply to the grid without incurring additional production costs. By employing electrical generators positioned on railway rails at proper locations to produce the deceleration forces necessary for braking, otherwise squandered braking power may be successfully and cheaply collected and used to replenish the neighbouring electrical grid.

2 Current Scenario of Regenerative Braking in Indian Railways

The Indian Railways have paid special attention to energy conservation and efficient usage [17–20]. Regenerative braking is a feature of electric traction that transforms the train's energy in motion to electric energy and returns it to the feeder services when the railway stops. This function has been successfully implemented in the WAG-9, WAP-7 and WAP-5 locomotive classes, with savings of up to 20%, and on all new electrical multiple units (EMU), with savings of up to 30%. This feature not only saves energy, but also increases the locomotive's availability for driving trains, making electric traction more cost-effective [21–25] (Fig. 1).

The regeneration and traction values of three-phase electric rolling stock utilized by Indian Railways in WAG-9, WAP-5, WAP-7 and EMUs are shown in the diagram above. It can be observed that EMUs' regeneration capacities are more important than those of the other groups [26–30]. While it is commendable that Indian Railways has achieved a regeneration savings of more than 20% on locomotive classes WAG-9
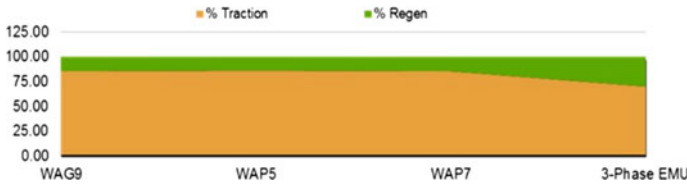
Fig. 1 Regeneration values of three-phase electric rolling stock of Indian Railways

and WAP-5, it is equally critical to improve regeneration efficiency in these classes of locomotives to compensate for energy losses [31–34].

2.1 Braking of a WAP-7 Locomotive

There are two types of braking in traction systems: dynamic (electric) braking and conventional friction braking. When a traction motor is transferred to a generator for dynamic braking, the generated current is used for regenerative braking [35–38]. Heavy-haul diesel-electric locomotives operating on routes with large downgrades benefit from this braking [39–41]. When the train is decelerated using regenerative braking, the current in the electric motors is reversed [42–44].

The hydraulic mechanism drives the braking system of a conventional friction brake. A main, or master, cylinder is filled with fluid and connected to a secondary, or slave, cylinder [45–47]. When you depress the brake pedal, a piston in the master cylinder depresses, sending fluid down the circuit and into the slave cylinders at each wheel, which push the pistons to effectively apply the brakes [48–50]. With advances like disc brakes, floating and multi-piston callipers, and power brakes, this system has evolved over time, making braking more effective and pleasant for the driver, especially with today's engines' higher power outputs [35] (Fig. 2).
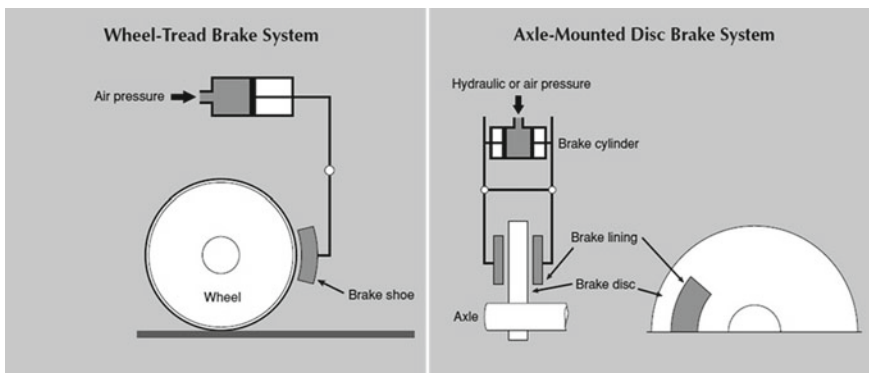
Fig. 2 Conventional friction braking of a WAP-7 locomotive

If we obtain energy back from the traction motor in regenerative braking on a WAP-7 locomotive, it operates as a generator, creating electrical energy from the kinetic energy when braked [51–55]. As a result, when regenerative braking is used, an induction motor becomes an induction generator. When the slip becomes negative, that is, when the slip is less than 0, the motor operates as an induction generator, and when the slip is more than 0, the motor activates its regenerative braking capabilities [56–60]. The gadget is affected by the motor traction capabilities.

$$slip = \frac{N_S - N_R}{N_S} \qquad (1)$$

N_S is synchronous speed and N_R is speed of rotor.

Slip > 0, $N_S > N_R$: Induction Motor.

Slip < 0, $N_S < N_R$: Induction Generator.

When the brakes are used, the N_S is lowered to the point where it is less than the N_R value. As a result, the motor functions as a generator, producing electricity from inertia-induced mechanical shaft movement. Because NS is dependent on the frequency of the alternating current supplied to the motor, it may be changed [61–64]. When braking is required, the slip might be modified to make it smaller than 0.

We could reduce the NS or synchronous speed by lowering the frequency of the AC supply, but due to the inertia obtained by spinning, the NR or rotor speed would not [65–68]. This is how the NS, or slip, is adjusted to make the motor operate like a generator. To adjust the frequency of the AC supplied to the motor, we utilize variable frequency drives (VFD). The frequency and voltage of an electric motor's power supply are controlled using a variable frequency drive (VFD) [69–72].

The motor's torque becomes negative as soon as the slip becomes negative, reversing the direction of applied torque. The motor's torque tries to correct itself by moving from negative to positive, but when the amount of torque approaches 0, i.e. zero torque, the supply of current to the motor is shut off, forcing the motor to halt. This regeneration mechanism provides us with surplus energy as a form of energy conservation (Fig. 3).

A: Normal Operating Point

B: Synchronous speed for situation 1

C: Synchronous speed for situation 2

D: Torque of motor at situation 2.

Point A is the normal operating point, while point B (N_{S1}) is the synchronous speed for a particular frequency, as shown in the graph above. The torque required to drive a constant load is represented by the TL curve. The rotor speed remains constant when the synchronous speed is altered from point B (N_{S1}) to point C (N_{S2}) through a VFD (N_{R1}). The motor's torque became negative at that time (point D). The motor would now attempt to stabilize its torque such that it could leap from point D to point C and back to point E. Even so, as the motor torque reaches point C, we would turn off the power.
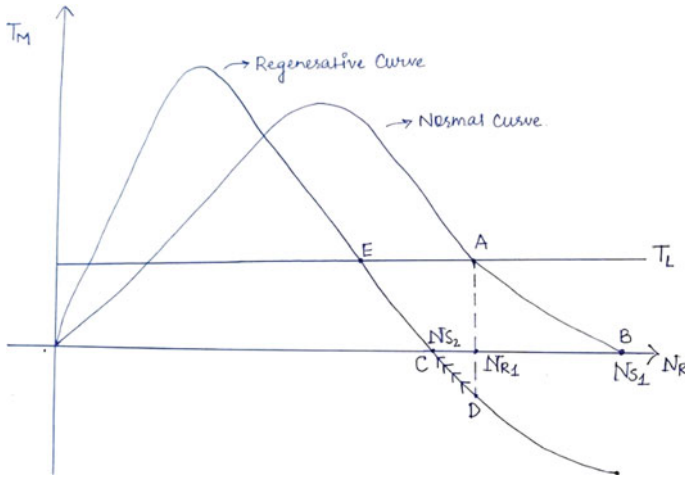
Fig. 3 Torque and speed characteristics of an induction motor

3 Mathematical Modelling of WAP-7 Locomotive

The equations of motion are used in the mathematical model for the WAP-7 loco-motive produced in this study. The three primary operational forces on the train's body are tractive effort, track resistance force (F_{res}) and gradient force (F_{grad}). As a result of the balance of these forces in the track's direction, the train accelerates and decelerates.

3.1 Equations Governing Train Dynamics

Newton's third law of motion governs the motion of trains to big extent. The mass of the engines, the tare mass of the coaches and the mass of the shipment/passenger all contribute to the train's effective mass. If all the carriages have the same payload, the train's effective mass will be:

$$M_{eff} = M_{loco} + N_{carr.} \times \left(M_{tare}^{carr.} + M_{payload}\right) \tag{2}$$

$$a = \frac{d^2x}{dt^2} = \frac{F_{traction} - F_{friction} - F_{gradient}}{M_{train}} \tag{3}$$

3.2 *Tractive Effort*

Tractive effort refers to the net force exerted by locomotive parallel to the direction of movement. The tractive effort is limited by motor current restrictions and mechanical constraints. The starting effort, continuous traction effort and brake effort numbers are taken from the WAP-7 locomotive's official documentation.

3.3 *Track Resistance*

Resistance for the train is calculated using Davis equation as follows:

$$F_{res} = D_A + D_B \cdot v + D_C \cdot v^2 \tag{4}$$

3.4 *Force Due to Gradient*

An extra force, $F_{grad,}$ is included in the calculations for track portions with a gradient in slope. One can get the following results by using geometrical arguments.

$$F_{grad} = M_{train} \times g \sin\theta \tag{5}$$

Value of the gradient is denoted by θ.

3.5 *Train Parameters*

The WAP-7 locomotive will be the subject of our research, and we will use the Shatabdi Express on the ADI-MMCT (Ahmedabad Jn—Mumbai Central) line. Because it is one of the fastest convoys on one of the busiest sectors, being the reasons for this choice. The data that was used may be seen in the Table 1.

4 Drive Cycle and Energy Estimation

A driving cycle is necessary to estimate the train's energy usage and the potential energy savings from adding a flywheel energy storage device. This is crucial since the efficiency of a hybrid power train is highly dependent on the duty cycle as well as route parameters such as stop spacing, gradient profile and vehicle types.

Table 1 WAP-7 locomotive physical parameters

Name	Description	Unit	Value
M_{loco}	Mass of the locomotive	kg	123,000
$M_{carriage}$	Mass of the individual carriage	kg	45,000
$M_{payload}$	Mass of payload in a carriage	kg	
$N_{carriage}$	Number of carriages		18
S	Surface area of locomotive	m^2	13.4
F_{start}	Starting force by the locomotive	kN	322.4
P_{train}	Power of the locomotive	kW	4560
V_{max}	Maximum velocity of the locomotive	m/s	50
F_{br}	Braking effort of the locomotive	kN	18,600
P_{max}	Maximum power of locomotive	kW	4740

Table 2 Route data for simulation (drive cycle)

S. no.	Station	Waiting time (sec)	Travel time (sec)	Distance (m)
1	Ahmedabad	0	2040	45,000
2	Nadiad	120	1020	19,000
3	Anand	120	1800	35,000
4	Vadodara	300	2820	71,000
5	Bharuch	120	2760	58,000
6	Surat	300	3840	93,000
7	Vapi	120	5220	140,000
8	Borivali	180	3420	30,000

We recreated the driving cycle in simulation using data from the Shatabdi Express route between Ahmedabad and Mumbai. The distances and time of the reconstructed driving cycle were evaluated and validated against erail.in statistics. The input for the driving cycle is shown in Table 2, which should be read from left to right.

Even though the track's gradient data is omitted, the model can handle gradients, allowing for the illustration of broad dependencies on uniform slopes.

4.1 Energy Estimations

Most important data for this study is the power consumption by the train during the whole journey. It is determined using the following equation:

$$\text{Power} = F_{\text{Traction}} \times v \tag{6}$$

The energy consumption during the traction will be calculated by using:

$$E_{\text{traction}} = \int P_{\text{traction}} dt \qquad (7)$$

The energy recovered during the braking of train will be calculated using:

$$E_{\text{braking}} = \int P_{\text{braking}} dt \qquad (8)$$

4.2 Calculating Efficiencies

We may utilize the entire energy consumed by the train in traction to determine the energy derived from the substation using equation.

$$E_{\text{trac}}^{\text{Ac}} = \frac{E_{\text{trac}}}{\eta_1} \qquad (9)$$

$E_{\text{trac}}^{\text{Ac}}$ is the total energy consumed from the substation, E_{trac} is the traction energy obtained from Eq. 7. η_1 is the induction motor's efficiency. The gross braking energy created throughout the driving cycles is also calculated using simulation. We can use the following equation to calculate the net amount of energy arriving at the flywheel.

$$E_{\text{brake}}^{\text{Dc}} = E_{\text{brake}} \times \eta_1 \qquad (10)$$

Recovered energy is equal to the multiplication of energy stored in flywheel with flywheel's efficiency

$$E_{\text{FESS}} = E_{\text{brake}}^{\text{DC}} \times \eta_2 \qquad (11)$$

In Eq. (10), $E_{\text{brake}}^{\text{DC}}$ is the energy reaching the flywheel energy storage system (FESS). Multiplied with efficiency of the FESS (η_2), we obtain E_{FESS} that is the energy stored in the FESS. Since the energy must again pass through the induction motor to reach the wheels of the train, the energy recovered is equal to the energy collected by the FESS multiplied by η_1.

$$E_{\text{recoverd}} = E_{\text{FESS}} \times \eta_1 \qquad (12)$$

We also calculate the efficiency gain, which is defined as the ratio of energy recovered to energy wasted during the journey. In addition to the energy recovery efficiency value, which is defined as the ratio of energy recovered to braking energy (14).

$$\varepsilon = \frac{E_{\text{recovered}}}{E_{\text{trac}}^{\text{AC}}} \tag{13}$$

$$\epsilon = \frac{E_{\text{recovered}}}{E_{\text{braking}}} \tag{14}$$

5 Results and Discussion

A numerical model was constructed in Python that included all of the concepts outlined above. After considering the route profile, train specifications and other limitations, the driving cycle is calculated. Every segment of track uses the velocity step method. The distance travelled and needed braking distance are calculated via continuous computing. It starts with calculating the force necessary to overcome friction and other resistances for each velocity step. After that it calculates the resulting acceleration, the velocity and acceleration are also updated. Following that, it calculates the braking distance and time necessary to stop this train, as well as the time for which the train will travel at a constant speed. The distance covered in each of the three stages (accelerating, constant speed and braking) is summed. This method is repeated until the sum of the distances matches the section's prescribed length. After the drive cycle is formed, all time-dependent kinematic variables and forces are measured and the energy consumption is evaluated.

5.1 Velocity Step Method for Determining the Driving Cycle

The velocity step method uses the distance and time spans given in Table 1 as input. The acceleration is determined by the user-defined parameters like maximum power capacity of the locomotive. The deacceleration is taken as a constant value to reduce complex calculations, and it is set to a value satisfying all the safety and comfort parameters. The time is gradually increased in a step-like manner to obtain the change in velocity ΔV. Then final velocity, distance travelled and time spent are updated as shown in Eq. (15).

$$
\begin{aligned}
V_{i+1} &= V_i + \Delta V \\
t_{i+1} &= t_i + \Delta t \\
X_{i+1} &= X_i + (V_i + 0.5\Delta V)\Delta t
\end{aligned}
\tag{15}
$$

Here V_i, t_i, X_i are the velocity, time and distance at the current step, respectively, while $V_{i+1} t_{i+1}, X_{i+1}$ are associated with the next steps. Since time is increased in constant step, the value of acceleration is needed to be determined for every next step. Following are the parameters on which the acceleration is determined.

Table 3 Allowed gradients for trains in Indian Railways

Type of gradient	Characteristics or values
Ruling gradient for plains	0.5% to 0.67%
Ruling gradient for hilly regions	0.67% to 1.0%
Gradient in station yards	in 400 to 1 in 1000 is allowed

Maximum allowed acceleration ($\hat{a}$): The acceleration (a) must be less than the maximum allowed acceleration on the section. The acceleration is dependent on the traction effort which is limited by the power capacity of the motor. Safety and comfort parameters are also kept in mind. Rate of change of acceleration or jolt must be restricted for the safety and comfort of the passengers.

After increasing time by a definite step, power consumption on the current velocity is determined by multiplying the constant traction force and then compared to the maximum power limit. The minimum of both powers is selected, and the corresponding force is taken as the final tractive effort. After obtaining tractive force acceleration is obtained and is made sure to be in the limits. The velocity for the next step is determined, the time spent and distance travelled during this step are updated.

Parallelly the braking distance along with the braking time for the updated velocity is computed. Subtracting the sum of time travelled and the braking time from the total journey time we obtain the time travelled at constant speed. On obtaining the value of constant speed journey time, we also get the distance travelled at a constant speed. The sum of all the three distances (travelled, braking and at constant speed) is compared with the journey distance. If the sum of distances is equal to or more than journey distance, then further acceleration is not required, else further acceleration is needed.

Value for gradient is taken at random from between the maximum and minimum allowed gradient. The value of gradient for the various scenarios is given in the Table 3:

5.2 Velocity–Time Curve

Graphs given below are the velocity time graphs for trainset of 18 LHB II AC coaches with WAP-7 locomotive. Value of gradient for operation is set at zero in (a) and at 1 in 150 (0.67%) in (b). The graph (a) is for the zero gradient and graph (b) is for the 1 in 150 (0.67%) gradients. The maximum value observed for the velocity in plot (a) is 28.72 m/s (103.3 km/h), but in plot (b) it only reaches till 28 m/s (100.8 km/h). The decrease in maximum velocity attained for the whole route is barely noticeable. Whereas in certain sections of the route the difference is quite clear. For example, maximum velocity attained in second section of the route (highlighted in orange), the reduction in peak velocity is quite significant. If we examine it closely, we can see that the travel time at a constant speed in the second section (highlighted in orange) is higher in plot (b) compared to plot (a) (Fig. 4).

Table 4 Results obtained for the various gradients for rack of 18 LHB II AC coaches

Gradient	Train Composition	$E_{traction}$ (MWh)	$E^{AC}_{traction}$ (MWh)	$E_{braking}$ (MWh)	E^{DC}_{brake} (MWh)	E_{FESS} (MWh)	$E_{recovered}$ (MWh)	ε	ϵ
0%	WAP-7 loco; 18 LHB II AC Full load	4660	5295	2304	2028	1825	1606	0.30	0.70
	WAP-7 loco; 18 LHB II AC half load	4500	5114	2199	1935	1742	1533	0.30	0.70
1 in 400 (0.25%)	WAP-7 loco; 18 LHB II AC Full load	5840	6636	2137	1881	1693	1489	0.22	0.70
	WAP-7 loco; 18 LHB II AC half load	5640	6409	2042	1797	1617	1423	0.22	0.70
1 in 300 (0.33%)	WAP-7 loco; 18 LHB II AC Full load	6320	7182	2111	1858	1672	1471	0.20	0.70
	WAP-7 loco; 18 LHB II AC half load	6080	6909	2016	1774	1597	1405	0.20	0.70
1 in 200 (0.5%)	WAP-7 loco; 18 LHB II AC Full load	7250	8239	2058	1811	1630	1434	0.17	0.70
	WAP-7 loco; 18 LHB II AC half load	6990	7943	1978	1741	1567	1379	0.17	0.70

(continued)

Table 4 (continued)

Gradient	Train Composition	$E_{traction}$ (MWh)	$E^{AC}_{traction}$ (MWh)	$E_{braking}$ (MWh)	E^{DC}_{brake} (MWh)	E_{FESS} (MWh)	$E_{recovered}$ (MWh)	ε	ϵ
1 in 150 (0.67%)	WAP-7 loco; 18 LHB II AC Full load	8390	9534	2049	1803	1623	1428	0.15	0.70
	WAP-7 loco; 18 LHB II AC half load	8020	9114	1959	1724	1552	1365	0.15	0.70
1 in 100 (1%)	WAP-7 loco; 18 LHB II AC Full load	10,990	12,489	2049	1803	1623	1428	0.11	0.70
	WAP-7 loco; 18 LHB II AC half load	10,430	11,852	1951	1717	1545	1360	0.11	0.70
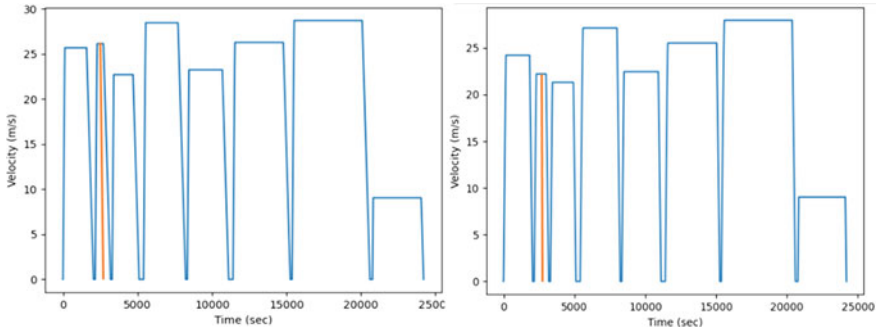
Fig. 4 Velocity time graphs for trainset of 18 LHB II AC coaches with WAP-7 locomotive
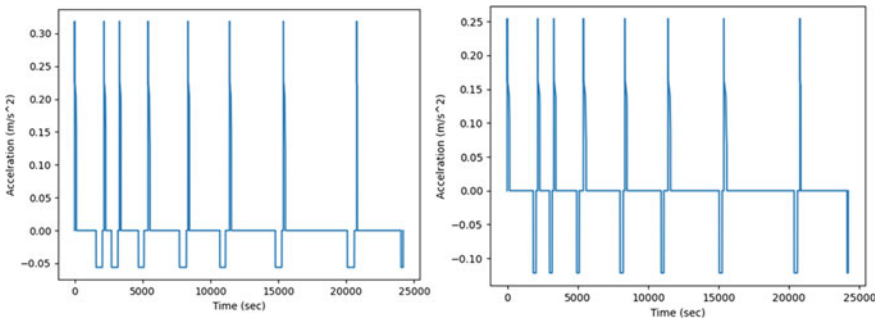
Fig. 5 Acceleration time graphs for trainset of 18 LHB II AC coaches with WAP-7 locomotive

5.3 Acceleration-Time Curve

In Fig. 5, (a) is acceleration–time plot is for zero gradient, while the (b) is for 1 in 150 (0.67%) gradients. We can clearly see the effect of uphill gradient on the peak acceleration and deacceleration values. Value for the maximum acceleration is reduced from 0.31 m/s2 to 0.25 m/s2. While the value of deacceleration has increased from 0.05 m/s2 to 0.12 m/s^2.

5.4 Power–Time Curve

Peak power attained for zero gradient 4.79 megawatts and for 1 in 150 gradient the value is 4.78 megawatts. As stated above in Eq. (8) Power = $F_{\text{Traction}} \times v$, both cases achieve the maximum traction force theoretical possible. Difference appears due to slight decrease in peak velocity of the system in 1 in 150 gradients. Whereas the difference in the braking power is much more noticeable as it increased from 1.54 megawatts to 3.24 megawatts. This is also due to the increased gravitational force.
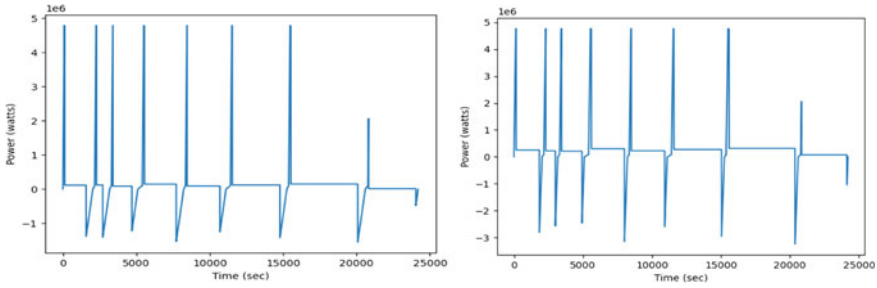
Fig. 6 Power time graphs for trainset of 18 LHB II AC coaches with WAP-7 locomotive

In the following Fig. 6, power–time plot is shown, (a) for zero gradient, while the (b) is for 1 in 150 (0.67%) gradients.

5.5 Traction Energy–Time Curve

In Fig. 7, plot (a) is cumulative traction energy plot for zero gradient, while the (b) is for 1 in 150 (0.67%) gradients. Final value noted for the case of zero gradient is 4.65×10^9 W-hrs. On the other hand for 1 in 150 gradient, this value is noted at 8.39×10^9 W-hrs. This rise is because of the extra work done to counter the resistive force of gravity. The pattern for traction energy through the journey depicted by both curves is the same. The increased consumption of traction energy for the gradient is observed from the start. In plot, *a* energy consumed in first 5000 s is noted to be 1.35×10^9 W-hrs, while in plot *b* the traction energy consumption for the first 5000 s is 2.12×10^9 W-hrs. Similarly, the consumption of energy for the whole trip is higher in case of the gradient.
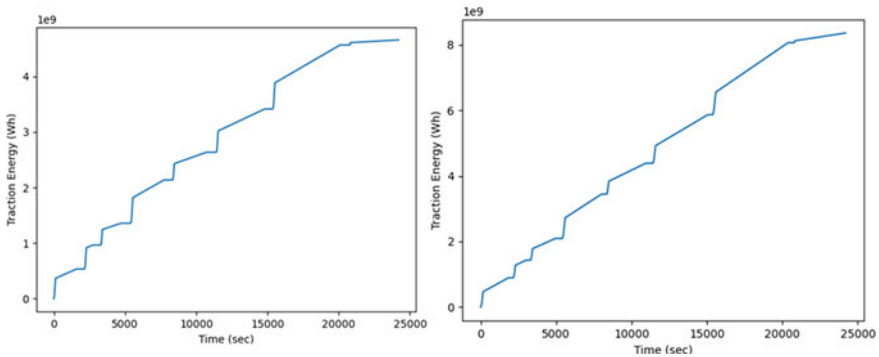
Fig. 7 Traction energy time graphs for trainset of 18 LHB II AC coaches with WAP-7 locomotive
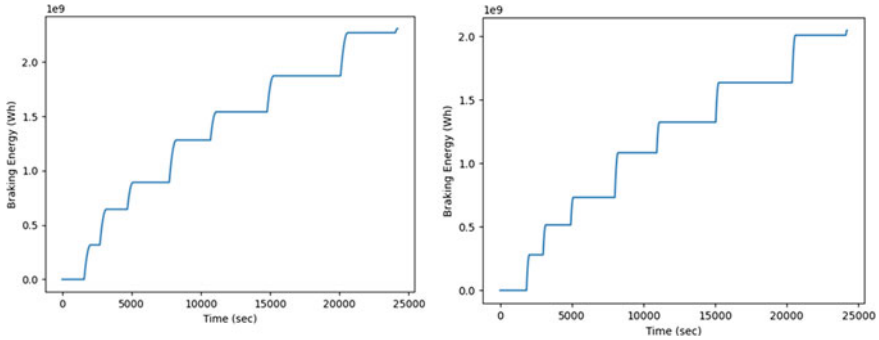
Fig. 8 Braking energy time graphs for trainset of 18 LHB II AC coaches with WAP-7 locomotive

5.6 Braking Energy–Time Curve

In Fig. 8, part (a) is cumulative braking energy plot for zero gradient, while the (b) is for 1 in 150 (0.67%) gradients. Final value noted for the case of zero gradient is 2.304×10^9 W-hrs. On the other hand for 1 in 150 gradient, this value is noted at 2.049×10^9 W-hrs. A slight reduction in final braking energy is noticed. However, the pattern for braking energy through the journey depicted by both curves is the same.

5.7 Energy Comparison of WAP-7 Running with and Without FESS

In Fig. 9, part (a) is comparative plot of train with fess to without fess at zero gradient, while the (b) is for 1 in 150 (0.67%) gradient.
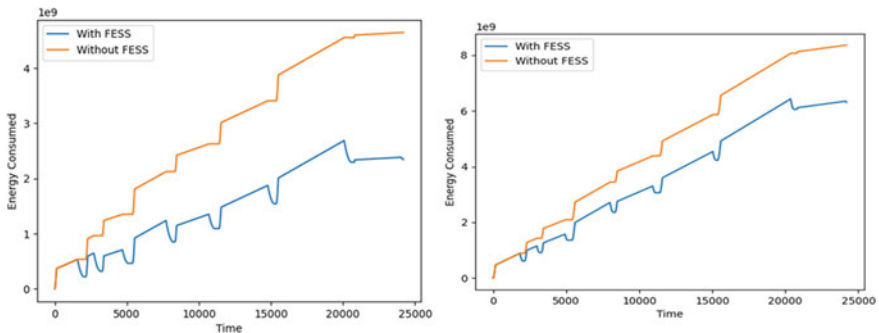
Fig. 9 Energy comparison of WAP-7 running with and without FESS

Pattern visible in both the cases (a) & (b) is very similar to one another. However, the gap between the orange and blue curves in (a) appears to be larger than in (b). In case of zero gradient, the energy consumption without FESS (orange curve) reached value of 4.65×10^6 kWh. If FESS was used in the same scenario (blue curve), the energy consumed falls to 2.36×10^6 kWh giving the savings of 2.29×10^6 kWh. For gradient of 0.67%, the orange curve reaches the value of 8.39×10^6 kWh, whereas the blue curve provides the value of 6.30×10^6 kWh. So, using FESS with 0.67% gradient will provide us with 2.09×10^6 kWh of savings.

5.8   Effect of Various Gradients

This section will discuss the results obtained for the various values of gradient for a train set of 18 LHB II AC coaches. The value for the efficiency of induction motor (η_1) is taken as 0.88 and the value of flywheel efficiency (η_2) as 0.90. The value of $E_{traction}$ or energy consumed increases as we increase the gradient, but $E_{braking}$ or braking energy reduces. This is because the train is climbing uphill, this requires higher energy to move against the gravity but takes less energy to stop. The ratio of energy consumed to energy recovered ε falls from 0.30 at zero gradient to 0.11 at 1% gradient. As given in Table 4, range of allowed gradient for ruling plain is 0.5–0.67%. For the maximum gradient allowed on a ruling plain that is 0.67% value of energy recovered is 1.428×10^9 watthours. If we increase the gradient even more, which is to 1%, the maximum allowed gradient for the hilly regions. The recovered energy is 1.359×10^9 watthours. If we compare the magnitude of this recovered energy, it's not much less than that of a 0% gradient. But the percentage recovered on the amount spent for traction has reduced significantly. For 0% gradient, the energy recovered was 30.32% for full loaded and 29.97% for half loaded, whereas for 1% gradient it reduced to mere 11.43% for full loaded and 11.47% for half loaded.

6   Conclusions

The results show that utilizing the FESS can save a significant amount of energy. The predicted energy savings vary based on the track, cargo, train number and FESS type. The net recovered energy ranges from 29 to 31% of the total energy consumed. With increasing gradient, the energy savings from a flywheel decreased due to less requirement of braking on up-terrain. The recovered energy with increasing terrain ranged from 22% at 1 in 400 to 11% at 1 in 100 gradients. The feasibility of a FESS for decreasing energy usage in passenger rail transportation systems is confirmed in this study. The technique and results can be applied to various rail routes, even if the results were achieved for a specific route.

References

1. Sharma, S.K., Lavania, S.: Skin effect in high speed VLSI on-chip interconnects. In: International Conference on VLSI, Communication & Networks, V-CAN, pp. 1–8. Institute of Engineering & Technology, Alwar (2011)
2. Lavania, S., Sharma, S.K.: An explicit approach to compare crosstalk noise and delay in VLSI RLC interconnect modeled with skin effect with step and ramp input. J. VLSI Des. Tools Technol. **1**, 1–8 (2011)
3. Sharma, S.K.: Zero energy building envelope components: A review. Int. J. Eng. Res. Appl. **3**, 662–675 (2013)
4. Sharma, S.K., Lavania, S.: An autonomous metro: Design and execution. In: Futuristic Trends in Mechanical and Industrial Engineering, pp. 1–8. JECRC UDML College of Engineering, Jaipur (2013)
5. Sharma, S.K., Lavania, S.: Green manufacturing and green supply chain management in India A Review. In: Futuristic Trends in Mechanical and Industrial Engineering, pp. 1–8. JECRC UDML College of Engineering (2013)
6. Sharma, S.K., Kumar, A., Sharma, R.C.: Challenges in railway vehicle modeling and simulations. In: International Conference on Newest Drift in Mechanical Engineering (ICNDME-14), December 20–21, M. M. University, Mullana, India, pp. 453–459. Maharishi Markandeshwar University, Mullana—Ambala (2014)
7. Sharma, S.K., Kumar, A.: A comparative study of Indian and Worldwide railways. Int. J. Mech. Eng. Robot. Res. **1**, 114–120 (2014)
8. Sharma, S.K., Sharma, R.C., Kumar, A., Palli, S.: Challenges in rail vehicle-track modeling and simulation. Int. J. Veh. Struct. Syst. **7**, 1–9 (2015). https://doi.org/10.4273/ijvss.7.1.01
9. Sharma, S.K., Sharma, R.C., Choi, Y., Lee, J.: Experimental and mathematical study of flexible–rigid rail vehicle riding comfort and safety. Appl. Sci. **13**, 5252 (2023). https://doi.org/10.3390/app13095252
10. Sharma, S.K., Kumar, A.: Dynamics analysis of wheel rail contact using FEA. Procedia Eng. **144**, 1119–1128 (2016). https://doi.org/10.1016/j.proeng.2016.05.076
11. Sharma, S.K., Kumar, A.: The Impact of a rigid-flexible system on the ride quality of passenger bogies using a flexible carbody. In: Pombo, J. (ed.) Proceedings of the Third International Conference on Railway Technology: Research, Development and Maintenance, Stirlingshire, UK, p. 87. Civil-Comp Press, Stirlingshire, UK (2016). https://doi.org/10.4203/ccp.110.87
12. Sharma, S.K., Chaturvedi, S.: Jerk analysis in rail vehicle dynamics. Perspect. Sci. **8**, 648–650 (2016). https://doi.org/10.1016/j.pisc.2016.06.047
13. Kulkarni, D., Sharma, S.K., Kumar, A.: Finite element analysis of a fishplate rail joint due to wheel impact. In: International Conference on Advances in Dynamics, Vibration and Control (ICADVC-2016) NIT Durgapur, India February 25–27. National Institute of Technology Durgapur, Durgapur, India (2016)
14. Sharma, R.C., Palli, S., Sharma, S.K.: Ride analysis of railway vehicle considering rigidity and flexibility of the carbody. J. Chinese Inst. Eng. **46**, 355–366 (2023). https://doi.org/10.1080/02533839.2023.2194918
15. Sharma, S.K., Kumar, A.: Impact of electric locomotive traction of the passenger vehicle Ride quality in longitudinal train dynamics in the context of Indian railways. Mech. Ind. **18**, 222 (2017). https://doi.org/10.1051/meca/2016047
16. Sharma, S.K., Kumar, A.: Ride performance of a high speed rail vehicle using controlled semi active suspension system. Smart Mater. Struct. **26**, 055026 (2017). https://doi.org/10.1088/1361-665X/aa68f7
17. Sharma, R.C., Palli, S., Sharma, S.K., Roy, M.: Modernization of railway track with composite sleepers. Int. J. Veh. Struct. Syst. **9**, 321–329 (2018)
18. Sharma, R.C., Sharma, S.K., Palli, S.: Rail vehicle modelling and simulation using Lagrangian method. Int. J. Veh. Struct. Syst. **10**, 188–194 (2018). https://doi.org/10.4273/ijvss.10.3.07
19. Palli, S., Koona, R., Sharma, S.K., Sharma, R.C.: A review on dynamic analysis of rail vehicle coach. Int. J. Veh. Struct. Syst. **10**, 204–211 (2018). https://doi.org/10.4273/ijvss.10.3.10

20. Sharma, S.K., Sharma, R.C.: An investigation of a locomotive structural crashworthiness using finite element simulation. SAE Int. J. Commer. Veh. **11**, 235–244 (2018). https://doi.org/10.4271/02-11-04-0019

21. Sharma, S.K., Sharma, R.C.: Simulation of quarter-car model with magnetorheological dampers for ride quality improvement. Int. J. Veh. Struct. Syst. **10**, 169–173 (2018). https://doi.org/10.4273/ijvss.10.3.03

22. Sharma, S.K., Kumar, A.: Impact of longitudinal train dynamics on train operations: a simulation-based study. J. Vib. Eng. Technol. **6**, 197–203 (2018). https://doi.org/10.1007/s42417-018-0033-4

23. Sharma, R.C., Sharma, S.K.: Sensitivity analysis of three-wheel vehicle's suspension parameters influencing ride behavior. Noise Vib. Worldw. **49**, 272–280 (2018). https://doi.org/10.1177/0957456518796846

24. Sharma, S.K., Kumar, A.: Ride comfort of a higher speed rail vehicle using a magnetorheological suspension system. Proc. Inst. Mech. Eng. Part K J. Multi-body Dyn. 232, 32–48 (2018). https://doi.org/10.1177/1464419317706873

25. Sharma, S.K., Kumar, A.: Disturbance rejection and force-tracking controller of nonlinear lateral vibrations in passenger rail vehicle using magnetorheological fluid damper. J. Intell. Mater. Syst. Struct. **29**, 279–297 (2018). https://doi.org/10.1177/1045389X17721051

26. Sharma, S.K.: Multibody analysis of longitudinal train dynamics on the passenger ride performance due to brake application. Proc. Inst. Mech. Eng. Part K J. Multi-body Dyn. **233**, 266–279 (2019). https://doi.org/10.1177/1464419318788775

27. Goyal, S., Anand, C.S., Sharma, S.K., Sharma, R.C.: Crashworthiness analysis of foam filled star shape polygon of thin-walled structure. Thin-Walled Struct. **144**, 106312 (2019). https://doi.org/10.1016/j.tws.2019.106312

28. Sharma, S.K., Sharma, R.C.: Pothole detection and warning system for Indian roads. In: Advances in Interdisciplinary Engineering, pp. 511–519 (2019). https://doi.org/10.1007/978-981-13-6577-5_48

29. Goswami, B., Rathi, A., Sayeed, S., Das, P., Sharma, R.C., Sharma, S.K.: Optimization design for aerodynamic elements of Indian locomotive of passenger train. In: Advances in Engineering Design, pp. 663–673. Lecture Notes in Mechanical Engineering. Springer, Singapore (2019). https://doi.org/10.1007/978-981-13-6469-3_61

30. Bhardawaj, S., Chandmal Sharma, R., Kumar Sharma, S.: Development and advancement in the wheel-rail rolling contact mechanics. IOP Conf. Ser. Mater. Sci. Eng. **691**, 012034 (2019). https://doi.org/10.1088/1757-899X/691/1/012034

31. Choppara, R.K., Sharma, R.C., Sharma, S.K., Gupta, T.: Aero dynamic cross wind analysis of locomotive. In: IOP Conference Series: Materials Science and Engineering, p. 12035. IOP Publishing (2019)

32. Sinha, A.K., Sengupta, A., Gandhi, H., Bansal, P., Agarwal, K.M., Sharma, S.K., Sharma, R.C., Sharma, S.K.: Performance enhancement of an all-terrain vehicle by optimizing steering, powertrain and brakes. In: Advances in Engineering Design, pp. 207–215 (2019). https://doi.org/10.1007/978-981-13-6469-3_19

33. Sharma, S.K., Saini, U., Kumar, A.: Semi-active control to reduce lateral vibration of passenger rail vehicle using disturbance rejection and continuous state damper controllers. J. Vib. Eng. Technol. **7**, 117–129 (2019). https://doi.org/10.1007/s42417-019-00088-2

34. Bhardawaj, S., Chandmal Sharma, R., Kumar Sharma, S.: A survey of railway track modelling. Int. J. Veh. Struct. Syst. **11**, 508–518 (2019). https://doi.org/10.4273/ijvss.11.5.08

35. Sharma, S.K., Sharma, R.C., Sharma, N.: Combined multi-body-system and finite element analysis of a rail locomotive crashworthiness. Int. J. Veh. Struct. Syst. **12**, 428–435 (2020). https://doi.org/10.4273/ijvss.12.4.15

36. Sharma, R.C., Sharma, S.K., Palli, S.: Linear and non-linear stability analysis of a constrained railway wheelaxle. Int. J. Veh. Struct. Syst. **12**, 128–133 (2020). https://doi.org/10.4273/ijvss.12.2.04

37. Palli, S., Sharma, R.C., Sharma, S.K., Chintada, V.B.: On methods used for setting the curve for railway tracks. J. Crit. Rev. **7**, 241–246 (2020)

38. Mohapatra, S., Pattnaik, S., Maity, S., Mohapatra, S., Sharma, S., Akhtar, J., Pati, S., Samantaray, D.P., Varma, A.: Comparative analysis of PHAs production by Bacillus megaterium OUAT 016 under submerged and solid-state fermentation. Saudi J. Biol. Sci. **27**, 1242–1250 (2020). https://doi.org/10.1016/j.sjbs.2020.02.001

39. Sharma, R.C., Sharma, S.K., Sharma, N., Sharma, S.: Analysis of ride and stability of an ICF railway coach. Int. J. Veh. Noise Vib. **16**, 127 (2020). https://doi.org/10.1504/IJVNV.2020.117820

40. Sharma, S.K., Phan, H., Lee, J.: An application study on road surface monitoring using DTW based image processing and ultrasonic sensors. Appl. Sci. **10**, 4490 (2020). https://doi.org/10.3390/app10134490

41. Sharma, R.C., Sharma, S., Sharma, S.K., Sharma, N.: Analysis of generalized force and its influence on ride and stability of railway vehicle. Noise Vib. Worldw. **51**, 95–109 (2020). https://doi.org/10.1177/0957456520923125

42. Lee, J., Sharma, S.K.: Numerical investigation of critical speed analysis of high-speed rail vehicle. 한국정밀공학회 학술발표대회 논문집 (Korean Soc. Precis. Eng. 696 (2020)

43. Sharma, S.K., Lee, J.: Finite element analysis of a fishplate rail joint in extreme environment condition. Int. J. Veh. Struct. Syst. **12**, 503–506 (2020). https://doi.org/10.4273/ijvss.12.5.03

44. Bhardawaj, S., Sharma, R., Sharma, S.: Ride analysis of track-vehicle-human body interaction subjected to random excitation. J. Chinese Soc. Mech. Eng. **41**, 237–236 (2020). https://doi.org/10.29979/JCSME

45. Bhardawaj, S., Sharma, R.C., Sharma, S.K.: Development in the modeling of rail vehicle system for the analysis of lateral stability. Mater. Today Proc. **25**, 610–619 (2020). https://doi.org/10.1016/j.matpr.2019.07.376

46. Bhardawaj, S., Sharma, R.C., Sharma, S.K.: Analysis of frontal car crash characteristics using ANSYS. Mater. Today Proc. **25**, 898–902 (2020). https://doi.org/10.1016/j.matpr.2019.12.358

47. Sharma, S., Sharma, R.C., Sharma, S.K., Sharma, N., Palli, S., Bhardawaj, S.: Vibration isolation of the quarter car model of road vehicle system using dynamic vibration absorber. Int. J. Veh. Struct. Syst. **12**, 513–516 (2020). https://doi.org/10.4273/ijvss.12.5.05

48. Acharya, A., Gahlaut, U., Sharma, K., Sharma, S.K., Vishwakarma, P.N., Phanden, R.K.: Crashworthiness analysis of a thin-walled structure in the frontal part of automotive chassis. Int. J. Veh. Struct. Syst. **12**, 517–520 (2020). https://doi.org/10.4273/ijvss.12.5.06

49. Bhardawaj, S., Sharma, R.C., Sharma, S.K.: Development of multibody dynamical using MR damper based semi-active bio-inspired chaotic fruit fly and fuzzy logic hybrid suspension control for rail vehicle system. Proc. Inst. Mech. Eng. Part K J. Multi-body Dyn. **234**, 723–744 (2020). https://doi.org/10.1177/1464419320953685

50. Sharma, S.K., Lee, J.: Design and development of smart semi active suspension for nonlinear rail vehicle vibration reduction. Int. J. Struct. Stab. Dyn. **20**, 2050120 (2020). https://doi.org/10.1142/S0219455420501205

51. Sharma, S.K., Lee, J.: Crashworthiness analysis for structural stability and dynamics. Int. J. Struct. Stab. Dyn. **21**, 2150039 (2021). https://doi.org/10.1142/S0219455421500395

52. Wu, Q., Cole, C., Spiryagin, M., Chang, C., Wei, W., Ursulyak, L., Shvets, A., Murtaza, M.A., Mirza, I.M., Zhelieznov, К., Mohammadi, S., Serajian, H., Schick, B., Berg, M., Sharma, R.C., Aboubkr, A., Sharma, S.K., Melzi, S., Di Gialleonardo, E., Bosso, N., Zampieri, N., Magelli, M., Ion, C.C., Routcliffe, I., Pudovikov, O., Menaker, G., Mo, J., Luo, S., Ghafourian, A., Serajian, R., Santos, A.A., Teodoro, Í.P., Eckert, J.J., Pugi, L., Shabana, A., Cantone, L.: Freight train air brake models. Int. J. Rail Transp. 1–49 (2021). https://doi.org/10.1080/23248378.2021.2006808

53. Sharma, S.K., Sharma, R.C., Lee, J.: Effect of rail vehicle-track coupled dynamics on fatigue failure of coil spring in a suspension system. Appl. Sci. **11**, 2650 (2021). https://doi.org/10.3390/app11062650

54. Mohapatra, S., Mohanty, D., Mohapatra, S., Sharma, S., Dikshit, S., Kohli, I., Samantaray, D.P., Kumar, R., Kathpalia, M.: Biomedical Application of polymeric biomaterial: polyhydroxybutyrate. In: Bioresource Utilization and Management: Applications in Therapeutics, Biofuels, Agriculture, and Environmental Science, pp. 1–14. CRC Press (2021). https://doi.org/10.21203/rs.3.rs-1491519/v1

55. Bhardawaj, S., Sharma, R.C., Sharma, S.K., Sharma, N.: On the planning and construction of railway curved track. Int. J. Veh. Struct. Syst. **13**, 151–159 (2021). https://doi.org/10.4273/ijvss.13.2.04

56. Sharma, R.C., Sharma, S., Sharma, N., Sharma, S.K.: Linear and nonlinear analysis of ride and stability of a three-wheeled vehicle subjected to random and bump inputs using bond graph and simulink methodology. SAE Int. J. Commer. Veh. **14**, 02–15–01–0001 (2021). https://doi.org/10.4271/02-15-01-0001

57. Sharma, R.C., Sharma, S., Sharma, S.K., Sharma, N., Singh, G.: Analysis of bio-dynamic model of seated human subject and optimization of the passenger ride comfort for three-wheel vehicle using random search technique. Proc. Inst. Mech. Eng. Part K J. Multi-body Dyn. **235**, 106–121 (2021). https://doi.org/10.1177/1464419320983711

58. Choi, S., Lee, J., Sharma, S.K.: A study on the performance evaluation of hydraulic tank injectors. In: Advances in Engineering Design: Select Proceedings of FLAME 2020, pp. 183–190. Springer Singapore (2021). https://doi.org/10.1007/978-981-33-4684-0_19

59. Lee, J., Han, J., Sharma, S.K.: Structural analysis on the separated and integrated differential gear case for the weight reduction. In: Joshi, P., Gupta, S.S., Shukla, A.K., and Gautam, S.S. (eds.) Advances in Engineering Design. Lecture Notes in Mechanical Engineering, pp. 175–181 (2021). https://doi.org/10.1007/978-981-33-4684-0_18

60. Sharma, S.K., Sharma, R.C.: Multi-objective design optimization of locomotive nose. In: SAE Technical Paper, pp. 1–10 (2021). https://doi.org/10.4271/2021-01-5053

61. Sharma, R.C., Palli, S., Sharma, N., Sharma, S.K.: Ride behaviour of a four-wheel vehicle using h infinity semi-active suspension control under deterministic and random inputs. Int. J. Veh. Struct. Syst. **13**, 234–237 (2021). https://doi.org/10.4273/ijvss.13.2.18

62. Sharma, S.K., Lee, J., Jang, H.-L.: Mathematical modeling and simulation of suspended equipment impact on car body modes. Machines. **10**, 192 (2022). https://doi.org/10.3390/machines10030192

63. Vishwakarma, P.N., Mishra, P., Sharma, S.K.: Formulation of semi-active suspension system and controls in rail vehicle. SSRN Electron. J. (2022). https://doi.org/10.2139/ssrn.4159616

64. Vishwakarma, P.N., Mishra, P., Sharma, S.K.: Characterization of a magnetorheological fluid damper a review. Mater. Today Proc. **56**, 2988–2994 (2022). https://doi.org/10.1016/j.matpr.2021.11.143

65. Sharma, S.K., Sharma, R.C., Lee, J., Jang, H.-L.: Numerical and experimental analysis of dva on the flexible-rigid rail vehicle carbody resonant vibration. Sensors. **22**, 1922 (2022). https://doi.org/10.3390/s22051922

66. Sharma, S.K., Mohapatra, S., Sharma, R.C., Alturjman, S., Altrjman, C., Mostarda, L., Stephan, T.: Retrofitting existing buildings to improve energy performance. Sustainability. **14**, 666 (2022). https://doi.org/10.3390/su14020666

67. Sharma, S.K., Sharma, R.C., Lee, J.: In situ and experimental analysis of longitudinal load on carbody fatigue life using nonlinear damage accumulation. Int. J. Damage Mech. **31**, 605–622 (2022). https://doi.org/10.1177/10567895211046043

68. Sharma, R.C., Sharma, S.K.: Ride Analysis of Road Surface-Three-Wheeled Vehicle-Human Subject Interactions Subjected to Random Excitation. SAE Int. J. Commer. Veh. **15**, 02–15–03–0017 (2022). https://doi.org/10.4271/02-15-03-0017.

69. Gong, D., Zhou, J., Sun, W.: On the resonant vibration of a flexible railway car body and its suppression with a dynamic vibration absorber. J. Vib. Control. **19**, 649–657 (2013). https://doi.org/10.1177/1077546312437435

70. Shi, H., Luo, R., Wu, P., Zeng, J., Guo, J.: Application of DVA theory in vibration reduction of carbody with suspended equipment for high-speed EMU. Sci. China Technol. Sci. **57**, 1425–1438 (2014). https://doi.org/10.1007/s11431-014-5558-5

71. Gong, D., Zhou, J., Sun, W., Sun, Y., Xia, Z.: Method of multi-mode vibration control for the carbody of high-speed electric multiple unit trains. J. Sound Vib. **409**, 94–111 (2017). https://doi.org/10.1016/j.jsv.2017.05.010

72. Guo, J., Shi, H., Luo, R., Wu, P.: Parametric analysis of the car body suspended equipment for railway vehicles vibration reduction. IEEE Access. **7**, 88116–88125 (2019). https://doi.org/10.1109/ACCESS.2019.2918777

Multibody Model of Freight Railcars Interaction in a Train

Angela Shvets

Abstract A modern railway train is a complex mechanical system, the movement of which is determined by mechanical, dynamic, electrical, and thermodynamic processes. It is necessary to consider analytical models of varying degrees of complexity of their oscillations and interaction with the railway track to solve numerous problems regarding the dynamics of rail vehicles. Often there is a need to take into account the longitudinal forces transmitted to the railcar from neighboring railcars, as well as their components in the vertical and horizontal transverse directions. These forces can be obtained from the solution of the train dynamics problem and then used to study the dynamics of a single railcar. However, in a number of papers, analytical models appear in which the problems of train dynamics and spatial oscillations of a railcar are combined together. When combining the problems solved in the dynamics of the train and the spatial oscillations of a single railcar, the studied rail vehicle is considered according to the full design scheme and neighboring ones according to the simplified one. The spatial oscillations of a train of freight railcars moving along a section of the track with vertical and horizontal irregularities are described in the presented analytical model.

Keywords Freight railcar · Longitudinal forces · Train dynamics · Forces in automatic couplers

1 Introduction

A modern railway train is a complex mechanical system, the movement of which is determined by mechanical, dynamic, electrical, thermodynamic processes, features of devices, and properties of forces that cause acceleration or deceleration of the train, vibrations of its individual elements (locomotives, railcars, and cargos in them) and determining the relationship of their movement, as well as the strength and stability of the system as a whole [1–5].

S. K. Sharma et al. (eds.), *Transportation Energy and Dynamics*, Energy, Environment, and Sustainability, https://doi.org/10.1007/978-981-99-2150-8_10

Longitudinal forces of a quasi-static or shock nature (with a quasi-static component) can be dangerous for traffic safety. It is the presence of longitudinal quasi-static compressive forces (lasting up to 2 s) that lead to the derailment of the rolling stock. This fact has been repeatedly proven by theoretical studies and technical expertise. The unloading and loading of the wheels of one wheelset, moving along the outer and inner rails, take place at the same time. Such forces, under certain conditions, can cause railcars to be squeezed out (extrude) from the train [6–8].

Analysis of numerous studies on analytical modeling in solving problems of train dynamics demonstrates the multiplicity and diversity of the studied aspects [9–11]. Numerical experiments, as well as simulations that use digital twins associated with train dynamics' evaluation with the usage of analytical models, require constant improvement [10, 12, 13]. Along with the development and improvement of the analytical model of the train, the model of oscillations of an individual railcar while moving at a constant speed developed and became more complicated [14–16], air brake models [17], the model of operation of friction draft gears [18], as well as the representation of the railway track and turnouts in the analytical model of the movement of vehicles [19–22].

2   Methodology

2.1   Model of Spatial Oscillations of a Single Railcar

The rolling stock is a mechanical system in which the number of degrees of freedom depends on the design of the body support on the bogies, the number of axles, the design of the axle boxes, and the method of transferring the traction force. The design scheme of a real structure should, if possible, fully reflect the properties of the subject under study. In railcars, the stiffness of the body, wheelsets, and bogie frames is very high. The same cannot be said about their elastic suspension elements (i.e., the stiffness is comparably very low). Railcars, when one studies spatial vibrations, can be viewed as mechanical systems which consist of absolutely rigid bodies; these bodies are interconnected by elastic and rigid bonds [23–26].

The movement of railcars on three-piece bogies of the basic model is considered. The disadvantage of such running gears is that the side frames are not rigidly connected to each other by bolster beam and spring sets. Therefore, longitudinal lozenging of side frames relative to each other occurs in it. Their value is determined by the gaps in the axle boxes and the magnitude of the horizontal deformation of the springs. As a result of the lozenging of side frames, the intensity of the bogie hunting increases, this worsens the smooth running of the railcar.

The freight railcar is considered a mechanical system of eleven solid bodies (a railcar body, two bolsters, four side frames, and four wheelsets). The connections between them can be characterized as elastic and dissipative. The railcar has a double suspension and spacers that installed between the axle boxes and side frames of

Table 1 Elements of a freight railcar and their movements

System bodies	Displacement					
	Linear along the axes			Angle relative to axes		
	X	Y	Z	X	Y	Z
Body	x	y	z	θ	φ	ψ
Bolsters	x_i	y_i	z_i	θ_i	φ_i	ψ_i
Side frames	x_{fij}	y_{fij}	z_{fij}	θ_{fij}	φ_{fij}	ψ_{fij}
Wheel sets	x_{kim}	y_{kim}	z_{kim}	θ_{kim}	φ_{kim}	ψ_{kim}
Rails	–	y_{pimj}	z_{pimj}	–	–	–

the bogie. The designation of the displacements of the bodies of the considered mechanical system is given in Table 1.

In Table 1, henceforth x, y, z denote the body center of mass displacements along the corresponding axes, and θ, φ, ψ—denote the body rotation angles relative to principal central axes of inertia; the analogous bolster displacements are marked by index i (i = 1, 2–a number of a bogie), side-frame displacements—by index fij (j = 1—the left side, j = 2 the right side of a railcar), wheel set displacements—by index kim (m = 1, 2—a number of a wheel set in the bogie), rail displacements at the points of contact with wheels—by index pimj (the displacements of rail lines are assumed only in two directions—along the axes Y and Z). Wheel displacements are marked by index imj [13, 25].

The schematic view of a freight railcar and positive directions for displacements, as well as rotation angles, are shown in Fig. 1.

The following connections are established between the bodies of a mechanical system [12, 13, 24]:
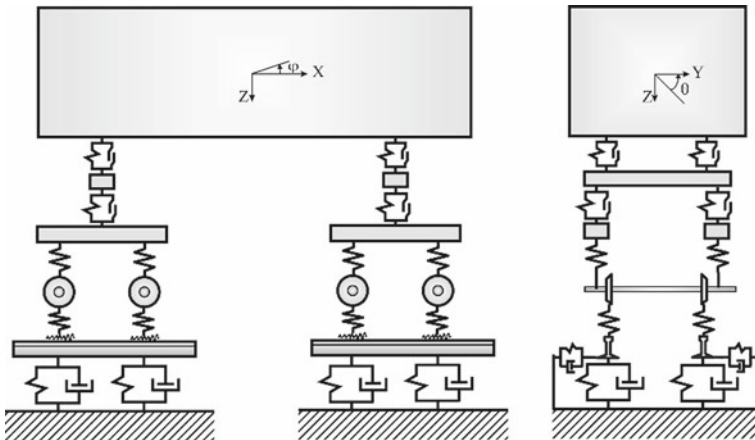
Fig. 1 Schematic view of a freight railcar

- Body and bolster. The gap between the central plate and the heel is neglected, which means there are no translational movements. The same goes for the pitching of these bodies. Hunting and rolling of the bolster, independent of the corresponding body oscillations, can take place.
- Bolster and side frame. It is assumed that there are elastic connections present. As a result, the relative translational and angular movements in the horizontal plane (hunting) of these bodies can occur.
- Side frame and wheelset. It is assumed that there are also connections present that make relative translational and angular movements in the horizontal plane (hunting) of these bodies possible.

Pseudosliding forces that arise when a wheel contacts a rail, taking into account physical and geometric nonlinearities, are determined according to Carter's theory. We accept that there is no rolling of a side frame ($\theta_{\text{fij}} = 0$). With respect to the Y-axis, the angles of wheelset rotation are determined without taking into account the wheel crippage [27]:

$$\varphi_{\text{kim}} = \frac{x_{\text{kim}}}{r}. \tag{1}$$

Here r average wheel rolling circle radius. At the point of contact between the wheelset and the rail, deformations always occur, causing the sliding mode of movement of the wheelset. However, since real deformations and their speeds are small, the actual dependences between the angles of rotation of wheelsets and their translational displacements are close to dependence (1).

Constraint equations based on the introduced assumptions about the relative displacements of the body and bolsters:

$$x_{\text{i}} = x + h \cdot \varphi, \tag{2}$$

$$y_{\text{i}} = y - (-1)^{\text{i}} \cdot \ell \cdot \psi - h \cdot \theta, \tag{3}$$

$$z_{\text{i}} = z + (-1)^{\text{i}} \cdot \ell \cdot \varphi, \tag{4}$$

$$\varphi_{\text{i}} = \varphi. \tag{5}$$

We accept that all wheels' movement is steady. In this case, rails' vertical displacements are equal to:

$$x_{\text{imj}} = x_{\text{kim}} - (-1)^{\text{j}} \cdot b_2 \cdot \psi_{\text{kim}}, \tag{6}$$

$$y_{\text{imj}} = y_{\text{kim}} - r_{\text{imj}} \cdot \theta_{\text{kim}} - y_{\text{pimj}} - \eta_{\text{himj}}, (\text{i, m, j} = 1, 2). \tag{7}$$

$$z_{\text{pimj}} = z_{\text{imj}} + \Delta r_{\text{imj}} - \eta_{\text{vimj}} = z_{\text{kim}} + (-1)^{\text{j}} \cdot b_2 \cdot \theta_{\text{kim}} + \Delta r_{\text{imj}} - \eta_{\text{vimj}}. \quad (8)$$

Here x_{imj}, z_{imj}, y_{imj} respectively are longitudinal, vertical, and horizontal wheel displacements relative to rails; y_{pimj}—rail displacement; η_{vimj}, η_{himj} are current ordinates of vertical and horizontal irregularities; 2ℓ is a railcar base; h is the height of a railcar body center of mass above the plane of bolster resting on elastic elements; r_{imj} is the imj-th wheel rolling circle radius; $2b_2$ is the distance between wheel rolling circles; $\Delta r_{\text{imj}} = f(y_{\text{imj}})$ are wheel rolling circle radius changes:

$$\Delta r_{\text{imj}} = (-1)^{\text{j}} \mu_0 y_{\text{imj}} + \alpha_1 \left[(-1)^{\text{j}} y_{\text{imj}} - \delta\right]^3 \sigma_0 \left[(-1)^{\text{j}} y_{\text{imj}} - \delta\right]. \quad (9)$$

Here μ_0 is a wheel tread surface conicity, $\alpha_1 = 6 \cdot 10^4$ is a coefficient obtained by approximating the nonlinear part of the wheel rolling profile by a cubic parabola, and σ_0 is the Heaviside step function. Entering parameter r_{imj} will allow exploration of various degrees of the running gear wheels' wear [27].

With horizontal transverse movements of the wheels relative to the rails, the radii of the rolling circles of the wheels Δr_{imj} and the tangents of the angles $(tg\alpha_{\text{imj}})$ of inclination of the rolling surface of the wheels to the horizontal change, which depend on the displacements y_{imj}. They can be determined approximately by analytical expressions or set based on calculations of the real profile of the wheel tread surface and the profile of the rail head:

$$tg\alpha_{\text{imj}} = \frac{d}{dy_{\text{imj}}}(\Delta r_{\text{imj}}) = (-1)^{\text{j}} \mu_0 + 3\alpha_1 \left[(-1)^{\text{j}} y_{\text{imj}} - \delta\right]^2 \sigma_0 \left[(-1)^{\text{j}} y_{\text{imj}} - \delta\right]. \quad (10)$$

The degree of freedom of the mechanical system is determined depending on the number of bodies in the system (11 bodies) and their possible displacements (6 displacements, Table 1), the possibility of mutual displacement of wheels (8 wheels), and rails (2 displacements, Table 1) and the number connections imposed on the system ((1)–(8) and $\theta_{\text{fij}} = 0$). The number of bonds increases by the number of bodies they are superimposed on. Twenty-four coupling equations have been derived according to the given assumptions. The system has $11 \cdot 6 + 8 \cdot 2 - 24 = 58$ degrees of freedom: $q_1 = z$, $q_2 = \varphi$, $q_3 = \theta$, $q_4 = y$, $q_5 = \psi$, $q_n = \theta_i$ ($n = 6, 7$), $q_n = \psi_i$ ($n = 8, 9$), $q_n = \psi_{\text{sfij}}$ ($n = 10 \div 13$), $q_n = y_{\text{sfij}}$ ($n = 14 \div 17$), $q_n = z_{\text{sfij}}$ ($n = 18 \div 21$), $q_n = \varphi_{\text{sfij}}$ ($n = 22 \div 25$), $q_n = \psi_{\text{kim}}$ ($n = 26 \div 29$), $q_n = y_{\text{kim}}$ ($n = 30 \div 33$), $q_n = z_{\text{kim}}$ ($n = 34 \div 37$), $q_n = \theta_{\text{kim}}$ ($n = 38 \div 41$), $q_n = y_{\text{pimj}}$ ($n = 42 \div 49$), $q_n = x_{\text{sfij}}$ ($n = 50 \div 53$), $q_n = x_{\text{kim}}$ ($n = 54 \div 57$), $q_{58} = x$ [13].

As a system of generalized coordinates, linear and angular body displacements are taken. Generalized coordinates are used for expressing relative body displacements as follows:

- body—bolsters: during hunting (yaw) $\Delta\psi_i = \psi - \psi_i$ ($i = 1, 2$); during rolling $\Delta\theta_i = \theta - \theta_i$ ($i = 1, 2$);
- bolsters—side frames in longitudinal, lateral, vertical directions, and hunting (yaw), respectively:

$$\Delta_{cxij} = x + h \cdot \varphi - (-1)^j \cdot b \cdot \psi_i - x_{fij}, \tag{11}$$

$$\Delta_{cyij} = y - (-1)^i \cdot \ell \cdot \psi - h\theta - y_{fij}, \tag{12}$$

$$\Delta_{czij} = z + (-1)^i \cdot \ell \cdot \varphi + (-1)^j \cdot b \cdot \theta_i - z_{fij}, \tag{13}$$

$$\Delta_{c\psi ij} = \psi_i - \psi_{fij}, (i, j = 1, 2), \tag{14}$$

where $2b$ is the distance in lateral direction between the axles of spring assemblies;

- side frames—wheel sets in longitudinal, lateral, vertical directions, and hunting (yaw), respectively:

$$\Delta_{fximj} = x_{fij} - x_{kim} + (-1)^j \cdot b_1 \cdot \psi_{kim}, \tag{15}$$

$$\Delta_{fyimj} = y_{fij} - y_{kim} - (-1)^m \cdot \ell_1 \cdot \psi_{fij}, \tag{16}$$

$$\Delta_{fzimj} = z_{fij} - z_{kim} + (-1)^m \cdot \ell_1 \cdot \varphi_{fij} - (-1)^j \cdot b_1 \cdot \theta_{kim}, \tag{17}$$

$$\Delta_{f\psi imj} = \psi_{fij} - \psi_{kim}, (i, m, j = 1, 2) \tag{18}$$

where $2\ell_1$ is a bogie base, $2b_1$ is the distance in lateral direction between the axles of axle boxes;

- wheels—rails in longitudinal and lateral directions are determined as in (6), (7).

In the track plane, there are wheels crippage on rails in longitudinal (ε_x) and horizontal (ε_y) directions taking place. It is expressed as:

$$\varepsilon_{ximj} = -\left[(-1)^j \cdot b_2 \cdot \frac{\dot{\psi}_{kim}}{v} + \frac{\Delta r_{imj}}{r_{imj}} \right], \tag{19}$$

$$\varepsilon_{yimj} = \frac{1}{v} \left[\dot{y}_{kim} - \dot{y}_{pimj} - r_{imj} \cdot \dot{\theta}_{kim} \right] - \psi_{kim}. \tag{20}$$

The tangent frictional forces T_{ximj} and T_{yimj} were determined from these wheel crippage:

$$T_{ximj} = -F_{ximj} \cdot \varepsilon_{ximj}, \ T_{yimj} = -F_{yimj} \cdot \varepsilon_{yimj} \tag{21}$$

F_{ximj} is the coefficient of pseudosliding in the directions along the *x*-axis. F_{yimj} is the coefficient of pseudosliding in the directions along the *y*-axis across the axis of the track. The coefficients of pseudosliding are determined by the dependence [27]:

$$F_{\text{ximj}} = F_{\text{yimj}} = \frac{f_{\text{imj}}}{\sqrt{1 + h_{\text{imj}}^2 \cdot \varepsilon_{\text{imj}}^2}}; \quad h_{imj} = \frac{f_{\text{imj}}}{P_{\text{imj}} \cdot f_{\text{T}}}, \tag{22}$$

The total relative slippage of the wheel on the rails is:

$$\varepsilon_{\text{imj}}^2 = \varepsilon_{\text{ximj}}^2 + \varepsilon_{\text{yimj}}^2, \tag{23}$$

Where f_{T} coefficient of friction of the wheel on the rail, the coefficient f_{imj} depending on the total wheel pressure on rail P_{imj} is determined as in [24, 25] in such a way:

$$f_{\text{imj}} = 235 \cdot P_{\text{imj}} - 2.4 \cdot P_{\text{imj}}^2 + 0.01 \cdot P_{\text{imj}}^3, \tag{24}$$

$$P_{\text{imj}} = P_{\text{st}} + S_{\text{pzimj}}. \tag{25}$$

Here P_{st} is static pressure of the wheel on the rail. In Eq. (25), the interaction forces S_{pzimj} are equal to:

$$S_{\text{pzimj}} = a_{\text{pz}} \cdot \ddot{z}_{\text{pimj}} + \chi \cdot k_z \cdot \dot{z}_{\text{pimj}} + k_z \cdot z_{\text{pimj}}, \tag{26}$$

$$S_{\text{pyimj}} = a_{\text{py}} \cdot \ddot{y}_{\text{pimj}} + \chi \cdot k_y \cdot \dot{y}_{\text{pimj}} + k_y \cdot y_{\text{pimj}}, \tag{27}$$

where a_{pz}, a_{py}, k_z, k_y are the given track parameters (inertial and quasi-elastic coefficients); χ is a coefficient characterizing the dissipation in the base.

The Lagrange equation of the second kind is used for compiling the differential equations for the system oscillation:

$$\frac{d}{dt}\left(\frac{\partial T}{\partial \dot{q}_n}\right) - \frac{\partial T}{\partial q_n} + \frac{\partial P}{\partial q_n} + \frac{\partial R}{\partial \dot{q}_n} = Q_n + F_n, \tag{28}$$

where T, P—are kinetic and potential energies of the system; R—system energy dissipation function; q_n—generalized coordinates; Q_n—the corresponding generalized forces, which are the sum of the interaction forces between the wheel and the rail and the forces acting in the connections between the railcars during the train motion; F_{n}—external traction or braking forces; n—number of freedom degrees.

The forces S acting between the railcar bodies having similar indices were determined from the relative motions (11)–(18). Differential equations of spatial oscillations of a «railcar – track» system are presented by the following expressions [27]:

$$m \cdot \ddot{x} + m_{\text{bl}} \cdot (\ddot{x}_1 + \ddot{x}_2) + \sum_{i=1}^{2} \sum_{j=1}^{2} S_{\text{cxij}} = 0, \tag{29}$$

$$m \cdot \ddot{y} + m_{\text{bl}} \cdot (\ddot{y}_1 + \ddot{y}_2) + \sum_{i=1}^{2} \sum_{j=1}^{2} S_{\text{cyij}} = 0, \tag{30}$$

$$m \cdot \ddot{z} + m_{\text{bl}} \cdot (\ddot{z}_1 + \ddot{z}_2) + \sum_{i=1}^{2} \sum_{j=1}^{2} S_{\text{czij}} - (m + 2m_{\text{bl}}) \cdot g = 0, \tag{31}$$

$$I_{\text{x}} \cdot \ddot{\theta} + \sum_{i=1}^{2} M_i - 2M_\theta - m_{\text{bl}} \cdot (\ddot{y}_1 + \ddot{y}_2) \cdot h + \\ b_3 \cdot \sum_{i=1}^{2} \sum_{j=1}^{2} (-1)^{\text{j}} \cdot S_{\text{cij}} - h \cdot \sum_{i=1}^{2} \sum_{j=1}^{2} S_{\text{cyij}} = 0, \tag{32}$$

$$I_{\text{y}} \cdot \ddot{\varphi} + I_{\text{ybl}} \cdot (\ddot{\varphi}_1 + \ddot{\varphi}_2) + m_{\text{bl}} \cdot (\ddot{z}_2 - \ddot{z}_1) \cdot \ell + h \cdot \sum_{i=1}^{2} \sum_{j=1}^{2} S_{\text{cxij}} + \\ \ell \cdot \sum_{i=1}^{2} \sum_{j=1}^{2} (-1)^{\text{i}} S_{\text{czij}} + m_{\text{bl}} \cdot (\ddot{x}_1 + \ddot{x}_2) \cdot h = 0, \tag{33}$$

$$I_{\text{z}} \cdot \ddot{\psi} + m_{\text{bl}} \cdot (\ddot{y}_1 - \ddot{y}_2) \cdot \ell - \ell \cdot \sum_{i=1}^{2} \sum_{j=1}^{2} (-1)^{\text{i}} S_{\text{cyij}} + \\ \sum_{i=1}^{2} S_{\psi \text{i}} + b_3 f. \sum_{i=1}^{2} \sum_{j=1}^{2} S_{\text{ij}} \cdot sign \dot{\Delta}_{\psi \text{i}} = 0, \tag{34}$$

$$I_{\text{xbl}} \cdot \ddot{\theta}_{\text{i}} - M_i - b_3 \cdot \sum_{j=1}^{2} (-1)^{\text{j}} \cdot S_{\text{cij}} + b \cdot \sum_{j=1}^{2} (-1)^{\text{j}} \cdot S_{\text{czij}} = 0, \tag{35}$$

$$I_{\text{zbl}} \cdot \ddot{\psi}_{\text{i}} + \sum_{j=1}^{2} S_{\text{c}\psi \text{ij}} - b \cdot \sum_{j=1}^{2} (-1)^{\text{j}} S_{\text{cxij}} - S_{\psi \text{i}} - b_3 f. \sum_{j=1}^{2} S_{\text{ij}} \cdot sign \dot{\Delta}_{\psi \text{i}} = 0, \tag{36}$$

$$m_{\text{f}} \cdot \ddot{x}_{\text{fij}} - S_{\text{cxij}} + \sum_{m=1}^{2} S_{\text{fximj}} = 0, \tag{37}$$

$$m_{\text{f}} \cdot \ddot{y}_{\text{fij}} - S_{\text{cyij}} + \sum_{m=1}^{2} S_{\text{fyimj}} = 0, \tag{38}$$

$$m_{\text{f}} \cdot \ddot{z}_{\text{fij}} - S_{\text{czij}} + \sum_{m=1}^{2} S_{\text{fzimj}} - m_{\text{f}} \cdot g = 0, \tag{39}$$

$$I_{\text{yf}} \cdot \ddot{\varphi}_{\text{fij}} + \ell_1 \cdot \sum_{m=1}^{2} (-1)^{\text{m}} S_{\text{fzimj}} = 0, \tag{40}$$

$$I_{\text{zf}} \cdot \ddot{\psi}_{\text{fij}} - S_{c\psi ij} - \ell_1 \cdot \sum_{m=1}^{2} S_{\text{fyimj}} + \sum_{m=1}^{2} S_{f\psi imj} = 0, \tag{41}$$

$$\left(m_{\text{k}} + \frac{I_{\text{xk}}}{r^2} \right) \cdot \ddot{x}_{\text{kim}} - \sum_{j=1}^{2} \left(T_{\text{ximj}} + S_{\text{fximj}} \right) = 0, \tag{42}$$

$$m_{\text{k}} \cdot \ddot{y}_{\text{kim}} - \sum_{j=1}^{2} \left(T_{\text{yimj}} + S_{\text{fyimj}} \right) + \sum_{j=1}^{2} f'\left(y_{\text{imj}} \right) \cdot S_{\text{pzimj}} = 0, \tag{43}$$

$$m_{\text{k}} \cdot \ddot{z}_{\text{kim}} - \sum_{j=1}^{2} S_{\text{fzimj}} + \sum_{j=1}^{2} S_{\text{pzimj}} - m_{\text{k}} \cdot g = 0, \tag{44}$$

$$I_{\text{xk}} \cdot \ddot{\theta}_{\text{kim}} - b_1 \cdot \sum_{j=1}^{2} (-1)^{\text{j}} \cdot S_{\text{fzimj}}$$
$$+ \sum_{j=1}^{2} \left[(-1)^{\text{j}} b_2 - r_{\text{imj}} \cdot f'\left(y_{\text{imj}} \right) \right] \cdot S_{\text{pzimj}} + \sum_{j=1}^{2} r_{\text{imj}} \cdot T_{\text{yimj}} = 0, \tag{45}$$

$$I_{\text{zk}} \cdot \ddot{\psi}_{\text{kim}} + b_1 \cdot \sum_{j=1}^{2} (-1)^{\text{j}} \cdot S_{\text{fximj}} - \sum_{j=1}^{2} S_{f\psi imj} + b_2 \cdot \sum_{j=1}^{2} (-1)^{\text{j}} \cdot T_{\text{ximj}} = 0, \tag{46}$$

$$m_{\text{p}} \cdot \ddot{y}_{\text{pimj}} + T_{\text{yimj}} + S_{\text{pyimj}} - f'\left(y_{\text{imj}} \right) \cdot S_{\text{pzimj}} = 0, \ (i, \ m, \ j = 1, \ 2), \tag{47}$$

where $2b_3$ is the distance between the side bearing of one bogie in the transverse direction; m, m_{bl}, m_{f}, m_{k}, m_{p}—respectively, masses of the body, bolster, side frame, wheelset, and linear mass of the rail; I_{x}, I_{y}, I_{z}—moments of inertia of the body relative to the main central axes; I_{xbl}, I_{zbl}—moments of inertia of bolsters relative to the main central axes; I_{yf}, I_{zf}—moments of inertia of the side frames relative to the main central axes; I_{xk}, I_{zk}—moments of inertia of the wheelset relative to the main central axes.

The following forces act on the bolsters, corresponding to the relative displacements of the bolsters and side frames [26, 27]:

$$S_{\text{csij}} = k_{\text{cs}} \cdot \Delta_{\text{csij}} + \beta_{\text{cs}} \cdot \dot{\Delta}_{\text{csij}} + F_{\text{cs}} \cdot sign\,\dot{\Delta}_{\text{csij}}, \ (s = x, y, z, \psi), \tag{48}$$

where k_{cs} is the stiffness of the spring set of the central suspension of the bogie when bending (k_{cx}, k_{cy}), compressed (k_{cz}), and twisting ($k_{c\psi}$); β_{cs}—coefficients of viscous

friction of the corresponding dampers (if viscous friction dampers are present); F_{cs}—amplitude values of the dry friction forces of the corresponding dampers. Displacements (Δ_{csij}) are determined by dependencies (11)–(14).

The forces that arise between the side frames and wheelsets are determined by the following expressions:

$$S_{fsimj} = k_{fs} \cdot \Delta_{fsimj} + \beta_{fs} \cdot \dot{\Delta}_{fsimj} + F_{fs} \cdot sign \dot{\Delta}_{fsimj}, \ (s = x, y, z, \psi), \qquad (49)$$

where k_{fs} is the rigidity of sets of springs of axle box suspension stage in bending (k_{fx}, k_{fy}), compressed (k_{fz}), and twisting ($k_{f\psi}$); β_{fs}—coefficients of viscous friction of the corresponding dampers (if viscous friction dampers are present); F_{fs}—amplitude values of the dry friction forces of the corresponding dampers. Displacements (Δ_{fsimj}) are determined by dependencies (15)–(18).

When the bogie hunting is relative to the body in the plane of support of the heel, the moment of dry friction forces acts on the thrust bearing ($S_{\psi i}$). When the body rolls on the heel, a moment arises that overturns the body (M_θ) and a recovery moment (M_i). When the body rolls relative to the bolster, there are moments caused by forces in the side bearings acting on the body and the bolster (S_{cij}) [28]:

$$S_{\psi i} = S_\psi \cdot sign \Delta_{\psi i}, \qquad (50)$$

$$M_\theta = \frac{m \cdot g}{2} - h \cdot \theta, M_i = \frac{m \cdot g}{2} \cdot d_i, \ (i = 1, 2), \qquad (51)$$

where S_ψ—amplitude value of the moment. The shoulder (d_i) will be considered to change linearly as the body roll relative to the bolster increases from zero to its maximum value, equal to $d/2$ when the heel is on the edge [28].

With standard side bearings, initially, there is a gap between them (Δ_0), after removal of which shock forces arise. If we assume that during the lateral rolling of the body relative to the bolster, the heel slips along the center plate, then the distance between the bearings is determined as follows [28]:

$$\Delta_{cij} = \Delta \theta_i \cdot b_3, \ (i,j = 1, 2), \qquad (52)$$

Analytically expression for forces S_{cij} with standard side bearings:

$$S_{cij} = k_c \cdot \left[(-1)^j \cdot \Delta_{cij} - \Delta_0 \right] \cdot \sigma_0 \cdot \left[(-1)^j \cdot \Delta_{cij} - \Delta_0 \right], \qquad (53)$$

where $k_{ck} = tg\alpha_0$ is the contact stiffness between side bearings.

The movement of the railcar along the straight section of the track is described by the system of differential Eqs. (29)–(47). In the case of movement along a curved section of the railway track, it is necessary to use the coordinates in the stationary system [27]:

$$q^a = q + q^e, \qquad (54)$$

Here q and q^e are coordinates in relative and transferable motion. The coordinate q^e and its derivatives are determined by a curve equation. The coordinates q^e are functions depending on the parameters of the curve and the railway track traversed by the center of mass of the corresponding rigid body of coupled railcars.

Additions in expressions for relative horizontal lateral displacement appear:

$$\Delta_{\text{fyimj}} = y_{\text{fij}} - y_{\text{kim}} - (-1)^{\text{m}} \cdot \ell_1 \cdot \psi_{\text{fij}} - \frac{k_{\text{o}}}{2} \ell_1^2, \tag{55}$$

$$\Delta_{\text{cyij}} = y - (-1)^{\text{i}} \cdot \ell \cdot \psi - h \cdot \theta - y_{\text{fij}} - \frac{k_{\text{o}}}{2} \ell^2. \tag{56}$$

Here k_{o} is the curvature of a curve. The expressions for the longitudinal wheel crippages on rails (7) are also subject to change [27]:

$$\varepsilon_{\text{ximj}} = -\left[(-1)^{\text{j}} \cdot b_2 \cdot \frac{\dot{\psi}_{\text{kim}}}{v} + \frac{\Delta\, r_{\text{imj}}}{r_{\text{imj}}} (-1)^{\text{j}} \cdot b_2 \cdot k_{\text{o}} \right]. \tag{57}$$

Centrifugal forces on curves appear in the equations of lateral play of all bodies. These are terms with second-time derivatives.

It was noted in the work [27] that since the biggest side wear appears with a two-point contact, then considered of the second phase of the contact after the clearance in the gauge is taken up, i.e., after the fulfillment of conditions:

$$\Delta y^{\text{h}}_{\text{wpimj}} = (-1)^{\text{j}} \big(y_{\text{kim}} - (r_{\text{imj}} + \Delta r_{\text{fl}}) \cdot \theta_{\text{kim}} - y_{\text{pimj}} - \eta_{\text{himj}} - (-1)^{\text{j}} \cdot \delta \big) \geqslant 0, \tag{58}$$

where Δr_{fl} is the increment of wheel radius from a middle rolling circle to a flange; δ is half a railway gauge.

According to Carter's theory, it is assumed that pseudosliding forces also occur on the side surface of the flange. They are summed up with the corresponding forces on the tread. The vertical wheel pressure on rail is redistributed from tread (index «w») on a flange (index «fl») with increasing the wheel pressure on rail. The wheel-rail contact in the horizontal plane is modeled by a linear spring. The tread wear is determined according to the expression [27]:

$$W_{\text{wimj}} = \sqrt{\left(T_{\text{ximj}} \cdot \varepsilon_{\text{ximj}} \right)^2 + \left(T_{\text{yimj}} \cdot \varepsilon_{\text{yimj}} \right)^2}, \tag{59}$$

that is essentially the linear work of friction forces. The wear of the flange surface is defined as:

$$W_{\text{flimj}} = \sqrt{\left(T^{\text{fl}}_{\text{ximj}} \cdot \varepsilon^{\text{fl}}_{\text{ximj}} \right)^2 + \left(\frac{T^{\text{fl}}_{\text{yimj}} \cdot \varepsilon^{\text{fl}}_{\text{yimj}}}{\cos^2 \alpha_{\text{fl}}} \right)^2}, \tag{60}$$

where α_{fl} is the angle between side surface of the wheel flange and horizontal plane.

2.2 Model of Spatial Oscillations of a Railcar According to a Simplified Scheme

In this study, we consider the possibility of using an analytical model that describes the spatial oscillations of a specific group of railcars in a train (Fig. 2). One rail carriage is considered according to the complete design scheme, and the design schemes of neighboring cars, depending on the problem formulation, are simplified as the distance from the central carriage in both directions increases [28, 29].

Railcars adjacent to the central one are presented as systems with 12 degrees of freedom. The last coupled railcars are considered according to an even more simplified scheme—these railcars are systems with 6 degrees of freedom.

In the study of spatial oscillations of railcars considered according to a simplified calculation scheme, the following assumptions were introduced. It is assumed that the railcars have a single-stage spring suspension; each of them consists of eleven solid bodies: a body, two bolsters, four side frames, and four wheelsets. The scheme of the bogie frame is assumed to be hinged, which makes it possible to take into account the "lozenging" of the side frames. The track under the railcars is considered absolutely rigid in the vertical direction and elastic in the horizontal transverse direction. Consequently, the number of generalized coordinates is reduced, which simplifies the integration process. This approach is not mandatory. The presented multibody model of the rolling stock can be used in other models of the interaction of wheels with the railway track structure (rails, sleepers, ballast, and subgrade). The latter assumption, combined with the assumption that the rail deflection rate in the expressions for the transverse friction forces can be neglected, does not affect the number of degrees of freedom (i.e., the number does not increase).

It is assumed that the following movements are possible between the railcar bodies [28]:

- body—bolster: there are no relative movements, with the exception of the hunting of the bolster, which coincides with the hunting of the wheelsets of the bogies;
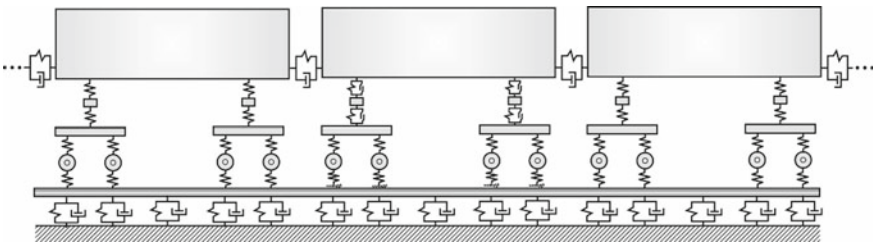
Fig.2 Scheme of the coupling of freight railcars as part of a train

- bolster—side frame: relative translational (along the Y- and Z-axes) and angular (when hunting) movements of these bodies are possible;
- side frame—wheelset: only one angular (when hunting) movement of these bodies relative to each other is possible.

  Constraint equations (for one of the railcars):
- based on the above assumptions about the relative movements of the body and bolsters, the equations of relations correspond to (2)–(5) and the roll of the bolsters $\theta_i = \theta$;
- we neglect the longitudinal gaps between the bolsters and the side frames, therefore:

$$x_{fij} = x_i - (-1)^j \cdot b \cdot \psi_{kij}, \tag{61}$$

- lateral motion and hunting of the side frames of one bogie coincide with each other:

$$y_{fi1} = y_{fi2}, \ \psi_{fi1} = \psi_{fi2}, \tag{62}$$

- displacement of the side frames along the z-axis and rotation around the y-axis depends only on the vertical irregularities of the rails:

$$z_{fij} = \frac{1}{2} \sum_{m=1}^{2} \eta_{vimj}, \ \varphi_{fij} = \frac{1}{2\ell_1}\left(\eta_{vi2j} - \eta_{vi1j}\right), \tag{63}$$

- there is no lateral rolling of the side frames $\theta_{fij} = 0$,
- the translational displacement of the wheelsets coincides with the translational displacement of the body $x_{kij} = x$;
- lateral motion of wheelsets depends on the lateral motion and hunting of the side frames:

$$y_{kim} = y_{fi} - (-1)^m \cdot \ell_1 \cdot \psi_{fi}, \tag{64}$$

- the angles of rotation of the wheelsets relative to the horizontal transverse axis Y will be determined without taking into account the crippage of the wheels (1);
- the hunting of the wheelsets coincides with the hunting of the corresponding bolster:

$$\psi_{ki1} = \psi_{ki2} = \psi_i, \tag{65}$$

- vertical movement and rolling of wheelsets depend on the vertical irregularities of the rail threads:

$$z_{kim} = \frac{1}{2} \sum_{j=1}^{2} \eta_{vimj}, \ \theta_{kim} = \frac{1}{2b_2}(\eta_{vim1} - \eta_{vim2}). \tag{66}$$

For railcars with 11·6-54=12 freedom degrees, the following values are taken as gen-eralized coordinates: $q_1^p = x^p$, $q_2^p = z^p$, $q_3^p = \varphi^p$, $q_4^p = \theta^p$, $q_5^p = y^p$, $q_6^p = \psi^p$, $q_k^p = \psi_{ki}^p$ (k = 7, 8), $q_k^p = \psi_{sfi}^p$ (k = 9, 10), $q_k^p = y_{sfi}^p$ (k = 11, 12), where i = 1, 2—is the bogie number; p = 1, − 1—is the railcar number in a coupling.

To compile differential equations of vehicle oscillations, expressions for the relative displacements of all bodies of the system are used:

- body—bolster when hunting:

$$\Delta_{\psi i} = \psi - \psi_{ki}, \tag{67}$$

- bolster—side frame in vertical, horizontal transverse directions and hunting:

$$\Delta_{cyi} = y - (-1)^i \cdot \ell \cdot \psi - h\theta - y_{fi}, \tag{68}$$

$$\Delta_{czi} = z + (-1)^i \cdot \ell \cdot \varphi + (-1)^j \cdot b \cdot \theta - z_{fij}, \tag{69}$$

$$\Delta_{c\psi ij} = \psi_i - \psi_{fi}, (i, j = 1, 2), \tag{70}$$

- side frame—wheelset when hunting:

$$\Delta_{f\psi i} = \psi_{fij} - \psi_{kim}, \tag{71}$$

- wheelset—rail in longitudinal, transverse, and vertical directions:

$$x_{ij} = x - (-1)^j \cdot b_2 \cdot \psi_{ki}, \tag{72}$$

$$y_{imj} = y_{ki} - y_{pimj} - \eta_{himj}, (i, m, j = 1, 2). \tag{73}$$

$$z_{imj} = \eta_{vimj}, \tag{74}$$

The crippage of the wheels on the rails, in this case, takes the following form:

$$\varepsilon_{ximj} = -\left[(-1)^j \cdot b_2 \cdot \frac{\dot{\psi}_{kim}}{v} + \frac{\Delta r_{imj}}{r}\right], \tag{75}$$

$$\varepsilon_{yimj} = \frac{1}{v}\left[\dot{y}_{fi} - (-1)^m \psi_{fi}\right] - \psi_{ki}. \tag{76}$$

Differential equations of oscillations of a railcar ($p = 1, - 1$) with the usage of the d'Alembert principle [28]:

$$\left(m_{car} + 4\frac{I_{xk}}{r^2}\right) \cdot \ddot{x} + 2m_{bl}h \cdot \ddot{\varphi} - \sum_{i=1}^{2}\sum_{m=1}^{2}\sum_{j=1}^{2} T_{ximj} = 0, \tag{77}$$

$$(m + 2m_{bl}) \cdot \ddot{y} + \sum_{i=1}^{2}\sum_{j=1}^{2} S_{cyij} = 0, \tag{78}$$

$$(m + 2m_{bl}) \cdot \ddot{z} + \sum_{i=1}^{2}\sum_{j=1}^{2} S_{czij} - (m + 2m_{bl}) \cdot g = 0, \tag{79}$$

$$\left(I_x + 2m_{bl} \cdot h^2 + 2I_{xbl}\right) \cdot \ddot{\theta} - h \cdot \sum_{i=1}^{2}\sum_{j=1}^{2} S_{cyij} + $$
$$b \cdot \sum_{i=1}^{2}\sum_{j=1}^{2} (-1)^{j} \cdot S_{czij} = 0, \tag{80}$$

$$\left(I_y + 2m_{bl} \cdot \ell^2 + 2m_{bl} \cdot h^2 + 4m_f \cdot h^2 + 2I_{ybl}\right) \cdot \ddot{\varphi} + $$
$$2m_{bl} \cdot h \cdot \ddot{x} + \ell \cdot \sum_{i=1}^{2}\sum_{j=1}^{2} (-1)^{i} \cdot S_{czij} = 0, \tag{81}$$

$$\left(I_z + 2m_{bl} \cdot \ell^2\right) \cdot \ddot{\psi} - \ell \cdot \sum_{i=1}^{2}\sum_{j=1}^{2} (-1)^{i} S_{cyij} + \sum_{i=1}^{2} S_{\psi i} = 0, \tag{82}$$

$$2(m_f + m_k) \cdot \ddot{y}_{fi} - \sum_{j=1}^{2} S_{cyij} - \sum_{m=1}^{2}\sum_{j=1}^{2} \left(T_{yimj} - P_{imj} tg\alpha_{imj}\right) = 0, \tag{83}$$

$$2\left(I_{zf} + m_k\ell_1^2\right) \cdot \ddot{\psi}_{fi} - \sum_{j=1}^{2} S_{c\psi ij} + \sum_{m=1}^{2}\sum_{j=1}^{2} S_{f\psi imj} + $$
$$\ell_1 \cdot \sum_{m=1}^{2}\sum_{j=1}^{2} (-1)^{m}\left(T_{yimj} - P_{imj} tg\alpha_{imj}\right) = 0, \tag{84}$$

$$\left(I_{zbl} + m_f b^2 + 2I_{zk}\right) \cdot \ddot{\psi}_{ki} - S_{\psi i} + \sum_{j=1}^{2} S_{c\psi ij} - \sum_{m=1}^{2}\sum_{j=1}^{2} S_{f\psi imj} $$
$$+ b_2 \cdot \sum_{m=1}^{2}\sum_{j=1}^{2} (-1)^{j} \cdot T_{ximj} = 0, \tag{85}$$

$$m + 2m_{bl} + 4m_f + 4m_k = m_{car}, \tag{86}$$

In the end railcars of the coupling, only body oscillations are taken into account: $q_1^p = x^p$, $q_2^p = z^p$, $q_3^p = \varphi^p$, $q_4^p = y^p$, $q_5^p = \theta^p$, $q_6^p = \psi^p$, where $p = 2, -2$ is the railcar number in a coupling. In the design schemes describing the oscillations of these railcars, the side frame lozenging is retained as the main characteristic of the freight car bogies.

In the study of spatial oscillations of railcars considered according to a simplified calculation scheme ($p = 2, -2$), the equations of relations based on the introduced assumptions about the relative displacements of the body and bolsters correspond to (2)–(5), and the roll of the bolsters $\theta_i = \theta$. Compressions Δ_{czij} and horizontal transversal Δ_{cyij} mutual displacements of the body and bogies to determine the forces acting in the spring sets of these railcars are determined by the dependencies (68)–(69), where y_{fij}, z_{fij}—horizontal transverse and vertical displacements of the side frames of the bogies under the spring sets, determined by the horizontal transverse displacements of the wheelsets and the vertical movements of the wheels [29]:

$$y_{fi1} = y_{fi2} = \frac{y_{ki1} + y_{ki2}}{2}, \; z_{fij} = \frac{z_{i1j} + z_{i2j}}{2}. \tag{87}$$

Displacements of wheelsets are determined from dependencies:

$$y_{kim} = \frac{\eta_{him1} + \eta_{him2}}{2}, z_{kim} = \frac{\eta_{vim1} + \eta_{vim2}}{2}, \theta_{kim} = \frac{\eta_{vim2} - \eta_{vim1}}{2b_2}. \tag{88}$$

The translational displacement of the wheels coincides with the translational displacement of the body $x_{imj} = x$, and the vertical displacements of the wheels are equal to the vertical irregularities of track $z_{imj} = \eta_{vimj}$. . Forces (48) act on the railcar bodies, corresponding to relative displacements at s = y, z. Differential equations for the oscillations of these railcars [29]:

$$m \cdot \ddot{x} = 0, \tag{89}$$

$$m \cdot \ddot{y} + \sum_{i=1}^{2}\sum_{j=1}^{2} S_{cyij} = 0, \tag{90}$$

$$m \cdot \ddot{z} + \sum_{i=1}^{2}\sum_{j=1}^{2} S_{czij} - m \cdot g = 0, \tag{91}$$

$$I_x \cdot \ddot{\theta} - h \cdot \sum_{i=1}^{2}\sum_{j=1}^{2} S_{cyij} + b \cdot \sum_{i=1}^{2}\sum_{j=1}^{2} (-1)^j \cdot S_{czij} = 0, \tag{92}$$

$$I_y \cdot \ddot{\varphi} + \ell \cdot \sum_{i=1}^{2}\sum_{j=1}^{2} (-1)^i \cdot S_{czij} = 0, \tag{93}$$

$$I_z \cdot \ddot{\psi} - \ell \cdot \sum_{i=1}^{2} \sum_{j=1}^{2} (-1)^i S_{cyij} = 0, \tag{94}$$

2.3 Forces of Interaction Between Railcars

Let's consider connections between railcars. We assume that there are relative displacements of neighboring railcars in the longitudinal Δ_x, horizontal transverse Δ_y, vertical Δ_z and angular (relative to the longitudinal axis—Δ_θ) directions. In Fig. 3 depicts the "first" railcar and the forces applied to it from the side of the "second", located in front in the direction of the train, and the "central" one, located behind [30, 31].

Expressions for relative displacements between railcars where $p = -2 \div 2$ is the railcar number in a coupling:

$$\Delta_x^{p+1;p} = x^p + h_a \cdot \varphi^p - x^{p+1} - h_a \cdot \varphi^{p+1}, \tag{95}$$

$$\Delta_y^{p+1;p} = y^{p+1} - (L - \ell_o) \cdot \psi^{p+1} - h_a \cdot \theta^{p+1} - y^p - (L - \ell_o) \cdot \psi^p + h_a \cdot \theta^p, \tag{96}$$
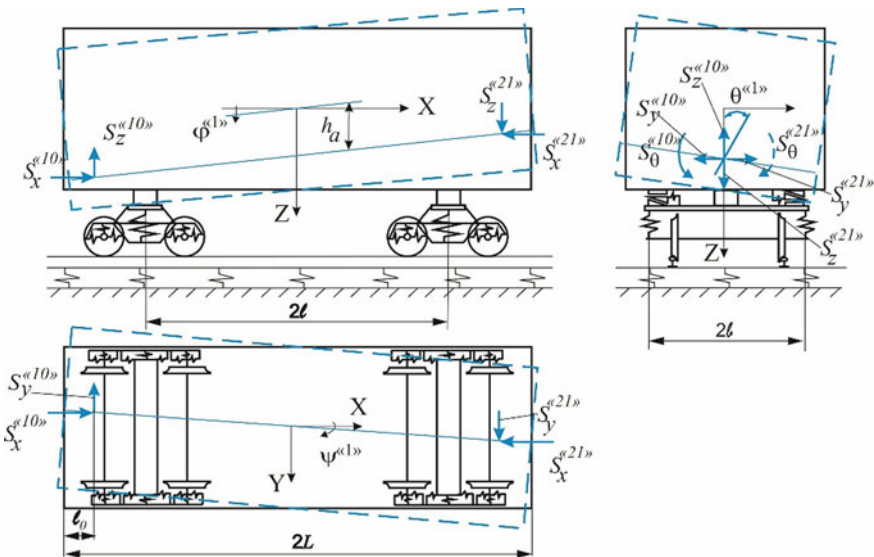

Fig. 3 Scheme of the forces acting in the connections between the railcars during the movement of the train

$$\Delta_z^{p+1;p} = z^{p+1} + (L - \ell_o) \cdot \varphi^{p+1} - z^p + (L - \ell_o) \cdot \varphi^p, \qquad (97)$$

$$\Delta_\theta^{p+1;p} = \theta^{p+1} - \theta^p, \qquad (98)$$

where $2L$—the distance between axles of automatic couplers of one railcar in the longitudinal direction; h_a—the vertical distance between the longitudinal axis of the automatic coupler and the center of mass of the body; ℓ_o—distance from the center of the coupler hitch wedge to the socket support surface. Only the angular displacements of the railcar are considered, assuming that the angles θ, φ, and ψ are small enough and their sines are equal to the angles themselves.

Relative displacements Δ_s $(s = x, y, z, \theta)$ are used to determine the forces acting between the railcars (Fig. 3). Longitudinal forces S_x are determined as described in work [2, 30] and depend on the type of draft gear. Horizontal transverse S_y, vertical S_z forces and moments S_θ, operating between the railcars are determined by the dependencies given in [1, 2, 30]. Only longitudinal forces ($S_x^h(t)$ and $S_x^e(t)$) are acting on the outermost railcars from the side of the discarded part of the train.

Horizontal transverse and vertical forces in an automatic coupler depend not only on the relative movements of the railcars and the rate of change of these movements but also on the longitudinal forces in the automatic coupler. To determine the longitudinal force in the draft gear of the automatic coupler, we will use the existing mathematical model described in the works [31, 32].

Figure 4 makes it possible to determine the vertical component of the longitudinal force in the automatic coupling (for the horizontal transverse component—the dependence is exactly the same) according to the dependence [32]:

$$S_s = \begin{cases} 0, \text{ if } S_x < S_0 \text{ and } \dfrac{\Delta_s}{2} \leqslant \Delta_0^s, \\[2mm] \left[k_{as}\Delta_s + \beta_{as}\dot{\Delta}_s \right] \dfrac{\ell_o}{2\ell_a} + S_s^*, \text{ if } S_x \geqslant S_0 \text{ and } \dfrac{\Delta_s \ell_o}{2\ell_a} < \Delta_a^s, \\[2mm] \left[k_{as}\dot{\Delta}_a^s + k_{as}^*\left(|\Delta_s| - \Delta_a^s\right) sign\Delta_s + \beta_{as}^*\dot{\Delta}_s \right] \dfrac{\ell_o}{2\ell_a} + S_s^*, \text{ if } \dfrac{\Delta_s \ell_o}{2\ell_a} \geqslant \Delta_a^s, \end{cases}$$
$$(99)$$

where Δ_0^s and Δ_a^s $(s = y, z, \theta)$—relative displacements at which the slipping of automatic couplers in the engagement contour stops (Δ_0^s) and there is an ultimate compression of the springs supporting the centering beam (Δ_a^s); ℓ_a—distance from the vertical axis of the coupler head to the wedge; α_s—the angle of rotation of the shank of the automatic coupler with a relative movement of the railcars by the value Δ_s; S_0—maximum longitudinal force at which slippage of automatic couplers still occurs in the engagement contour ($S_0 = 20$ kN); k_{as}, β_{as}—stiffness and coefficient of viscous friction of springs imitating elastic inserts; k_{as}^*, β_{as}^*—stiffness and coefficient of friction characterizing the compliance and energy dissipation of the body structure. The longitudinal force S_x component is defined as follows:
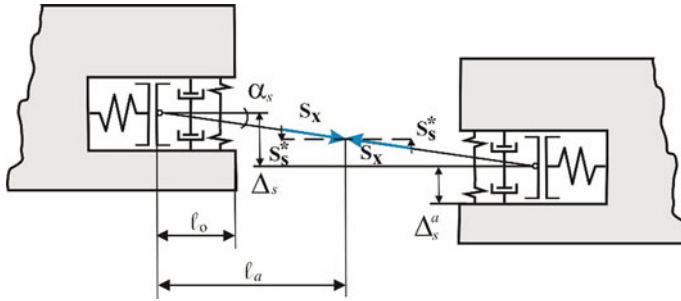
Fig.4 Schematic view of automatic couplers for railcars with bodies in the form of a chain of solid bodies

$$S_s^* = S_x \sin \alpha_s = S_x \frac{\Delta_s}{2\ell_a}, \quad S_\theta^* = 0. \tag{100}$$

Figure 3 shows the initial (solid line) and arbitrary (dashed line) positions for the railcar under study. Let us determine the additives to the generalized forces $(Q_s^n; s = x, y, z, \theta, \varphi, \psi; \ p = -2, -1, 0, 1, 2)$ included in the right-hand sides of the differential equations describing the vibrations of the bodies of the railcars under consideration. The generalized forces included in the equations of the railcar with the number $p = 2$ [28, 29]:

$$Q_x^p = S_x^{p;p-1} - S_x^h(t); \quad Q_y^p = -S_y^{p;p-1}; \quad Q_z^p = -S_z^{p;p-1}, \tag{101}$$

$$Q_\theta^p = h_a \cdot \left[S_y^{p;p-1} + \theta^p \cdot S_z^{p;p-1} \right] - S_\theta^{p;p-1}, \tag{102}$$

$$Q_\varphi^p = -h_a \cdot \left(S_x^h(t) - S_x^{p;p-1} \right) - (L - \ell_o)\left[S_z^{p;p-1} - \varphi^p \cdot \left(S_x^h(t) + S_x^{p;p-1} \right) \right], \tag{103}$$

$$Q_\psi^p = (L - \ell_o)\left[S_y^{p;p-1} + \psi^p \cdot \left(S_x^h(t) + S_x^{p;p-1} \right) \right], \tag{104}$$

The generalized forces included in the equations of the railcar with the number $p = -1, 0, 1$:

$$Q_x^p = S_x^{p;p-1} - S_x^{p+1;p}; \quad Q_y^p = S_y^{p+1;p} - S_y^{p;p-1}; \quad Q_z^p = S_z^{p+1;p} - S_z^{p;p-1}, \tag{105}$$

$$Q_\theta^p = -h_a \cdot \left[S_y^{p+1;p} - S_y^{p;p-1} + \theta^p \cdot \left(S_z^{p+1;p} - S_z^{p;p-1} \right) \right] + S_\theta^{p+1;p} - S_\theta^{p;p-1}, \tag{106}$$

$$Q_\varphi^p = -h_a \cdot \left(S_x^{p+1;p} - S_x^{p;p-1} \right) - (L - \ell_o)\left[S_z^{p+1;p} + S_z^{p;p-1} + \varphi^p \cdot \left(S_x^{p+1;p} + S_x^{p;p-1} \right) \right], \tag{107}$$

$$Q_\psi^p = (L - \ell_o)\Big[S_y^{p+1;p} + S_y^{p;p-1} + \psi^p \cdot \big(S_x^{p+1;p} + S_x^{p;p-1}\big)\Big], \qquad (108)$$

The generalized forces included in the equations of the railcar with the number $p = -2$:

$$Q_x^p = S_x^e(t) - S_x^{p+1;p}; \quad Q_y^p = -S_y^{p+1;p}; \quad Q_z^p = -S_z^{p+1;p}, \qquad (109)$$

$$Q_\theta^p = h_a \cdot \Big[S_y^{p+1;p} + \theta^p \cdot S_z^{p+1;p}\Big] - S_\theta^{p+1;p}, \qquad (110)$$

$$Q_\varphi^p = -h_a \cdot \big(S_x^{p+1;p} - S_x^e(t)\big) - (L - \ell_o)\Big[S_z^{p+1;p} - \varphi^p \cdot \big(S_x^e(t) + S_x^{p+1;p}\big)\Big], \qquad (111)$$

$$Q_\psi^p = (L - \ell_o)\Big[S_y^{p+1;p} + \psi^p \cdot \big(S_x^e(t) + S_x^{p+1;p}\big)\Big]. \qquad (112)$$

2.4   Spatial Oscillations of Railcars in a Train

Solving the problem of train dynamics (LTD) makes it possible to determine the longitudinal force acting on the first and the last railcar of the coupling from the side of the thrown-away parts of the train (Figs. 3 and 4) at any time. The longitudinal force that can occur at any moment is determined from the solution of the problem of the train's longitudinal dynamics. The longitudinal forces causing tension are considered positive. The forces occurring in the draft gears of the automatic couplers are determined according to the works [1, 2, 30, 31].

Spatial oscillations of the train are considered as a chain of rigid bodies connected to each other, representing the movement of the railcar bodies in the train. The forces acting on the body of the i-th railcar from the automatic couplers depend on the movement of the railcars and the features of the draft gears, which are equipped with adjacent railcars. The dependence S_{xi} on the total deformations q_{fi} of draft gears and other elements of the coupling of railcars is assumed to be known. Longitudinal forces in automatic couplers are determined in this case as follows [30, 33]:

$$S_{xi} = \begin{cases} [S_\Delta + k_k(|q_f| - \Delta)] \cdot sign q_f + \beta \cdot \dot{q}_f, & \text{if } |q_f| \geqslant \Delta, \\ \min\,[S_\ell(|q_f|)], \ S_{kp}(|q_f|) \cdot sign q_f, & \text{if } q_f \dot{q}_f \geqslant 0, \\ \max\,\big[S_p(|q_f|)\big], \ S_{kp}(|q_f|) \cdot sign q_f, & \text{if } q_f \dot{q}_f < 0, \end{cases} \qquad (113)$$

$$S_{kp}(|q_f|) = |S(t - h_t)| + k_k(|q_f| - \tilde{q}_f) + \beta \cdot \big(\dot{q}_f - \dot{\tilde{q}}_f\big), \qquad (114)$$

$$\tilde{q}_f = q_f(t - h_t), \quad \dot{\tilde{q}}_f = \dot{q}_f(t - h_t), \qquad (115)$$

where h_t—step of integration; $S_\ell(|q_f|)$—the dependence of the force on the elonga-tion of the connection of railcars under loading, if $q_f < \Delta$; Δ—full (maximum possible) extension of coupled couplers; S_Δ—the force corresponding to this elongation; $S_p(|q_f|)$—dependence of force on elongation during unloading [1, 2].

The canonical differential equations of the spatial motion of a train along a path that is curvilinear in plan and profile, after substituting the corresponding quantities into the Lagrange equations of the second kind and performing the transformations necessary to eliminate dynamic connections, can be represented as [30, 33]:

$$\dot{v}_{xi} = \frac{F_{1i} + F_{2i} + m_{gi} g \cdot i(x_i) + S_{xi} - S_{x,i+1}}{m_{\mu i}}, \tag{116}$$

$$\dot{q}_i = v_{x,i-1} - v_{xi} + h_{o,i-1} \cdot \omega_{y,i-1} - h_{ai} \cdot \omega_{yi}, \tag{117}$$

$$\dot{v}_{yi} = \frac{m_i g \cdot \theta_\varepsilon(x_i) - m_i \cdot \psi_{\varepsilon x}(x_i) v_{xi}^2 -}{m_i}, \tag{118}$$

$$\dot{v}_{zi} = \frac{m_i g - m_i \cdot \varphi_{\varepsilon x}(x_i) v_{xi}^2 - \left(m_i / m_{\mu i}\right) h_{ri} \theta_{\varepsilon x}(x_i) \left(Q_{xi} + m_{gi} g \cdot i(x_i)\right) + Q_{zi}}{m_i}, \tag{119}$$

$$\dot{x}_i = v_{xi}, \ \dot{y}_i = v_{yi}, \ \dot{z}_i = v_{zi}, \tag{120}$$

$$\dot{\omega}_{xi} = \frac{\left(I_{xi} / m_{\mu i}\right) \theta_{\varepsilon x}(x_i) \cdot \left(m_{gi} g \cdot i(x_i) + Q_{xi}\right) + Q_{\theta i}}{I_{xi}}, \tag{121}$$

$$\dot{\omega}_{yi} = \frac{\left(m_i / m_{\mu i}\right) h_i \left(m_{gi} g \cdot i(x_i) + Q_{xi}\right) + m_i g h_i \cdot \left(i(x_i) + \varphi_i\right) + Q_{\varphi i}}{I_{yi} + m_i h_i^2}, \tag{122}$$

$$\dot{\omega}_{zi} = \frac{-\left(I_{zi} / m_{\mu i}\right) \cdot \psi_{\varepsilon x}(x_i) \left(Q_{xi} + m_{gi} g \cdot i(x_i)\right) + Q_{\psi i}}{I_{zi}}, \tag{123}$$

$$\dot{\theta}_i = \omega_{xi}, \ \dot{\varphi}_i = \omega_{yi}, \ \dot{\psi}_i = \omega_{zi}, \ i = \overline{1, n}, \tag{124}$$

$$\theta_{\varepsilon x}(x_i) = \frac{1}{\ell_p}, \ \psi_{\varepsilon x}(x_i) = \frac{1}{R_y}, \ \varphi_{\varepsilon x}(x_i) = \frac{1}{R_z}, \tag{125}$$

where $v_{xi}. \ v_{yi}, \ v_{zi}$—projections of the velocities of the centers of mass of bodies on the axes of the moving coordinate system; $\omega_{xi}, \omega_{yi}, \omega_{zi}$—angular speeds of rotation of the body relative to the axes x, y, and z; $\dot{q}_i$—relative displacements of adjacent ends of railcars in the longitudinal direction; $i(x_i) = \varphi_\varepsilon(x_i)$—the slope of the path,

taken as a positive value in the direction of movement; $\theta_\varepsilon(x_i)$, $\psi_\varepsilon(x_i)$, $\varphi_\varepsilon(x_i)$—angles of rotation of the center of mass of the railcar body relative to the fixed reference system; R_y and R_z—respectively, the radii of the curves of the railway track in the plan and the radii of the conjugation of sections of the longitudinal profile of the track; ℓ_p—length of the transition section of the curve; m_{gi}—the gravitational mass of the railcar (body, two bogies); m_i—the weight of the body of the i-th railcar; $m_{\mu i}$—reduced railcar mass (body, two bogies); S_{xi} and $S_{x,i+1}$—the longitudinal force acting in the i-th automatic coupler; F_{1i} and F_{2i}—external traction or braking forces; h_{oi}—a distance of the automatic coupler axle from the bearing surface of the body plates; h_{ri}—distance from the center of mass of the body to the plane touching the rail heads. Q_{xi}, Q_{yi}, Q_{zi}, $Q_{\varphi i}$, $Q_{\psi i}$, $Q_{\theta i}$—generalized non-potential forces acting on the i-th carriage of the train, with the exception of gravity. This includes spring suspension reactions, moments of friction forces during relative rotations around the z-axis of the body and bogies, longitudinal and transverse forces, and moments acting on the body from automatic couplings, traction, and braking forces.

The position of the center of mass of the i-th vehicle along the track is determined with an error equal to the deformation of the train [30]:

$$x_t = -\frac{1}{2} \sum_{\vartheta=2}^{i} (L_{\vartheta-1} + L_\vartheta) + x_1. \tag{126}$$

Dependence allows not to integrate additional (n−1) differential equations; L_ϑ— length of the ϑ-th vehicle along the axes of coupling of automatic couplers, x_1— position of the first vehicle, which is determined by integrating the equations of its motion.

The values of longitudinal forces S_{xi} are determined by the characteristic of draft gears and depend on the value of relative longitudinal displacements q_i and the relative velocity $\dot{q}_i$ of the neighboring carriages, which are defined as follows [1, 2]:

$$q_i = x_i - x_{i+1}, \quad \dot{q}_i = v_i - v_{i+1}. \tag{127}$$

In case the automatic coupler is equipped with the same center coupler draft gears, we use the method described in the works [1, 10] to determine the longitudinal forces. If the automatic coupler includes the gears with different characteristics, the longitudinal force is determined from the following condition [1, 2]:

$$\begin{cases} S_{xi}^f = S_{xi}^r = S_{xi}, \\ q_i^f + q_i^r = q_i \end{cases}, \tag{128}$$

where S_i^f and S_i^r—are the values of longitudinal forces in the front and rear draft gears, correspondingly; q_i^f and q_i^r—are the deformations of the corresponding draft gears.

3 Summary

A multibody model of spatial oscillations of a freight railcar is described for modeling spatial oscillations on an elastic-viscous and inertial railway track, which arise as a result of its movement along vertical and horizontal irregularities. A multibody model, both of a single railcar and a couple of several rail vehicles, can be inserted anywhere along the length of the train. The solution of the differential equations presented, which describe the movement of railcars in the form of forces and moments that arise in the automatic couplers of railcars, can also be used for another analytical model of the interaction of wheels with rails.

The main theoretical provisions of the multibody model of the interaction of freight railcars as part of a train can be used to solve problems about the influence of a promising rolling stock on the dynamics of a train, as well as in current research in the field of train traffic safety, which are impossible without analytical modeling.

References

1. Blokhin, Y.P., Manashkin, L.A.: Train dynamics (unsteady longitudinal oscillations). Transport, Moscow (1982)
2. Blokhin, Y.P., Manashkin, L.A., Stambler, Y.L.: Calculations and tests of heavy trains. Transport, Moscow (1986)
3. Manashkin, L.A., Granovskaya, N.P.: Mathematical model of the train for the study of the loading of the car. Interuniversity Collection of Scientific Papers DIIT **232**(31), 24–28 (1984)
4. Blokhin, E.P., Khachapuridze, N.M., Polyakov, V.A.: On the construction of a mathematical model of train movement along a path of arbitrary shape. Problems of Dynamics and Strength of Railway Rolling Stock **220**(28), 3–14 (1981)
5. Dybeł, K., Kampczyk, A.: Sensitivity of geometric parameters in the sustainability development of continuous welded rail. Acta Technica Jaurinensis (2022). https://doi.org/10.14513/actate chjaur.00663
6. Shvets, A.O.: Gondola cars dynamics from the action of longitudinal forces. Sci. Trans. Progr. **6**(84), 142–155 (2019). https://doi.org/10.15802/stp2019/195821
7. Shvets, A.O., Shatunov, O.V., Dovhaniuk, S.S., Muradian, L.A., Pularyia, A.L., Kalashnik, V.: Coefficient of stability against lift by longitudinal forces of freight cars in trains. In: IOP Conference Series: Materials Science and Engineering, pp. 1–10, 15th Intern. Sci. and Techn. Conf. "Problems of the railway transport mechanics" (PRTM 2020), Dnipro, Ukraine (2020). https://doi.org/10.1088/1757-899X/985/1/012025
8. Cole, C., Spiryagin, M., Wu, Q., Sun, Y.Q.: Modeling, simulation and applications of longitudinal train dynamics. Veh. Syst. Dyn. **55**(10), 1498–1571 (2017). https://doi.org/10.1080/004 23114.2017.1330484
9. Zh., Qi, Zh., Huang, Kong, X.: Simulation of longitudinal dynamics of long freight trains in positioning operations. Veh. Syst. Dyn. **50**(9), 1409–1433 (2012). https://doi.org/10.1080/004 23114.2012.661063
10. Wu, Q., Spiryagin, M., Cole, C.: Longitudinal train dynamics: an overview. Veh. Syst. Dyn. **54**(12), 1688–1714 (2016). https://doi.org/10.1080/00423114.2016.1228988
11. Qi, Zh.G., Huang, Zh., Kong, X.: Simulation of longitudinal dynamics of long freight trains in positioning operations. Veh. Syst. Dyn **50**(9), 1409–1433 (2012). https://doi.org/10.1080/004 23114.2012.661063

12. Zhang, H., Zhang, C., Lin, F., Wang, X., Fu, G.: Research on simulation calculation of the safety of tight-lock coupler curve coupling. Symmetry **13**(11), 1–25 (2021). https://doi.org/10.3390/sym13111997
13. Wu, Q., Spiryagin, M., Cole, C.: Longitudinal train dynamics: an overview. Veh. Syst. Dyn. **54**(12), 1688–1714 (2016). https://doi.org/10.1080/00423114.2016.1228988
14. Wu, Q., Cole, C., Spiryagin, M.: Assessing wagon pack sizes in longitudinal train dynamics simulations. Aust. J. Mech. Eng. **18**(3), 277–287 (2020). https://doi.org/10.1080/14484846.2018.1512440
15. Shvets, A.O.: Dynamic interaction of a freight car body and a three-piece bogie during axle load increase. Vehicle System Dynamics, published online: 2021–07–07. https://doi.org/10.1080/00423114.2021.1942930
16. Shvets, A.O.: Analysis of the dynamics of freight cars with lateral displacement of the front bogie. Adv. Math. Models Appl. **6**(1), 45–58 (2021)
17. Shvets, A.O., Bolotov, O.M., Percevoj, A.K., Ghlukhov, V.V., Bolotov, O.O., Saparova, L.S.: Research of dynamic indicators and influence of different types of rolling stock on railway track. In: IOP Conference Series: Materials Science and Engineering, pp. 1–10, 15th Intern. Sci. and Techn. Conf. "Problems of the railway transport mechanics" (PRTM 2020), Dnipro, Ukraine (2020). https://doi.org/10.1088/1757-899X/985/1/012014
18. Wu, H.: Effects of wheel and rail profiles on vehicle performance. Veh. Syst. Dyn. **44**(1), 541–550 (2006). https://doi.org/10.1080/00423110600875393
19. Wu, Q., Cole, C., Spiryagin, M., Chang, Ch., Wei, W., Ursulyak, L., Shvets, A., Murtaza, M.A., Mirza , I.M., Zhelieznov, K., Mohammadi, S., Serajian, H., Schick, B., Berg, M., Sharma, R.Ch., Aboubakr, A., Sharma, S.K., Melzi, S., Di Gialleonardo, E., Bosso, N., Zampieri, N., Magelli, M., Crăciun, C.I., Routcliffe, I., Pudovikov, O., Menaker, G., Mo, J., Luo, Sh., Ghafourian, A., Serajian, R., Santos, A.A., Teodoro, Í.P., Eckert, J.J., Pugi, L., Shabana. A., Cantone, L.: Freight train air brake models. Int. J. Rail Transport. (2021). https://doi.org/10.1080/23248378.2021.2006808
20. Manashkin, L., Myamlin, S., Prikhodko, V.: Oscillation dampers and shock absorbers in railway vehicles (mathematical models). Dnipropetrovsk National University of Railway Transport named after Academician V. Lazaryan, Dnipropetrovsk (2009). DOI: https://doi.org/10.15802/978-966-348-121-0
21. Kurhan, D.: Determination of load for quasi-static calculations of railway track stress-strain state. Acta Technica Jaurinensis **9**(1), 83–96 (2016). https://doi.org/10.14513/actatechjaur.v9.n1.400
22. Kurhan, M., Kurhan, D., Husak, M., Hmelevska, N.: Increasing the efficiency of the railway operation in the specialization of directions for freight and passenger transportation. Acta Polytechnica Hungarica **19**(3), 231–244 (2022)
23. Kurhan, D., Fischer, S.: Modeling of the dynamic rail deflection using elastic wave propagation. J. Appl. Comput. Mech. **8**(1), 379–387 (2022). https://doi.org/10.22055/JACM.2021.38826.3290
24. Kovalchuk, V., Sysyn, M., Gerber, U., Nabochenko, O., Zarour, J., Dehne, S.: Experimental investigation of the influence of train velocity and travel direction on the dynamic behavior of stiff common crossings. Facta Univesitatis: Series Mechanical Engineering **17**(3), 345–356 (2019). https://doi.org/10.22190/FUME190514042K
25. Lazaryan, V.A.: Vehicle Dynamics: Selected Works. Publisher "Naukova dumka", Kiev (1985).
26. Danovich, V.D.: Spatial Cars Oscillations in Inertia Track. Dnepropetrovsk Institute of Railway Transport Engineering, Dnepropetrovsk (1981)
27. Blokhin, E.P., Danovich, V.D., Morozov, N.I.: Mathematical model of spatial oscillations of a four-axle rail vehicle. Dnepropetrovsk Institute of Railway Engineers, Dnepropetrovsk (1986)
28. Shvets, A.O.: Dynamic indicators influencing design solution for modernization of the freight rolling stock. FME Trans. **49**(3), 673–683 (2021). https://doi.org/10.5937/fme2103673S
29. Blokhin, E.P., Pshinko, O.M., Danovich, V.D., Korotenko, M.L.: Effect of the state of car running gears and railway track on wheel and rail wear. In: Railway Bogies and Running Gears: Proceedings of the 4th International Conference, pp. 313–323. Budapest (1998).

30. Blokhin, E.P., Danovich, V.D., Morozov, N.I.: Mathematical model of spatial oscillations of a train of cars as part of a train moving along a straight section of the track. Dynamics, strength and reliability of railway rolling stock **252**(34), 4–19 (1987)
31. Danovich, V.D., Malysheva, A.A. Mathematical model of spatial oscillations of the coupling of five cars moving along a rectilinear section of the track. Transport. Stress loading and durability of a rolling stock 1, 62–69 (1998)
32. Pshinko, A.N.: On the mathematical model of train movement in solving the problem of wear of wheels and rails. Transport. Stress loading and durability of a rolling stock 1, 29–46 (1998)
33. Khachapuridze, N.M., Khoroshmanenko, P.G.: Mathematical modeling of oscillations of train cars in the longitudinal vertical plane (including bending) under transient conditions of train movement. Dynamics, loading and reliability of the rolling stock **234**(32), 17–29 (1985)
34. Manashkin, L.A., Granovskaya, N.I., Zhakovsky, A.D., Kalenichenko, E.A.: Mathematical model for studying the loading of the center plate of a freight car during vibrations in the vertical-longitudinal plane. Dynamic loading of railway rolling stock **256**(35), 59–69 (1988)
35. Manashkin, L.A., Granovskaya, N.I.: Differential equations of spatial oscillations of a train. Transport mechanics: train weight, speed, traffic safety **2**, 15–25 (1994)

Sustainable Energy and Environment

Sustainable Energy via Thermochemical and Biochemical Conversion of Biomass Wastes for Biofuel Production

Abiodun Oluwatosin Adeoye, Olayide Samuel Lawal, Rukayat Oluwatobiloba Quadri, Dosu Malomo, Muhammed Toyyib Aliyu, Gyang Emmanuel Dang, Emmanuel Oghenero Emojevu, Musa Joshua Maikato, Mohammed Giwa Yahaya, Oluyemisi Omotayo Omonije, Victor Great Edidem, Yakubu Khartum Abubakar, Onyeka Francis Offor, Ezeaku Henry Sochima, Boniface Eche Peter, and Baba Nwunuji Hikon

Abstract Environmental pollution is one of the major disadvantages of fossil fuel and their derivatives, but alternative energy resources have performed better in this area. A well-known example within these alternative energy sources that can increase total available energy for human's consumption is biomass, and it has been proven to be the most important renewable energy source. Its benefits include reduced emission, ease of growth (agricultural materials), more available when compared

A. O. Adeoye (✉) · O. S. Lawal · R. O. Quadri · D. Malomo
Department of Chemistry, Federal University Oye-Ekiti, Oye, Ekiti State, Nigeria
e-mail: bioken2017@gmail.com

M. T. Aliyu
Department of Chemical Engineering, Ahmadu Bello University Zaria, Zaria, Nigeria

G. E. Dang
Department of Electrical and Electronic Engineering, Abubakar Tafawa Balewa University, Bauchi, Nigeria

E. O. Emojevu
Department of Chemistry, University of Benin, Benin, Nigeria

M. J. Maikato
Department of Mechanical Engineering, Ahmadu Bello University Zaria, Zaria, Nigeria

M. G. Yahaya · V. G. Edidem
Department of Mechanical Engineering, Federal University of Technology Minna, Minna, Nigeria

O. O. Omonije
Department of Biochemistry, Federal University of Technology Minna, Minna, Nigeria

Y. K. Abubakar
Department of Mechanical Engineering, Federal Polytechnic Idah, Idah, Nigeria

O. F. Offor
Department of Pure and Industrial Chemistry, University of PortHarcourt, PortHarcourt, Nigeria

E. H. Sochima
Department of Metallurgical and Materials Engineering, University of Nigeria Nsukka, Nsukka, Nigeria

to non-renewable sources of energy and can be directly used by local methods. Biomass wastes heating is a major energy generation process. Processes that use heat on biomass wastes to generate energy are termed thermochemical conversion processes. The use of wood that store chemical energy in cooking is as far back as the creation of the world. Thermochemical conversion of biomass releases products which are extremely best when compared with other renewable energy source finding usefulness in automobile, power, chemical, production, and biomaterials industries. Pyrolysis is a heating process whereby carbon-based matter (organic material) such as lignocellulosic agricultural waste is heated to 450 °C and above in a non-O_2 atmosphere, e.g., N_2 atmosphere. Oxygen or air supports biomass combustion to generate heat, steam, and electricity. Gasification occurs at > 650 °C; it is a method of converting biomass waste into energy with the sole purpose of generating syngas useful for combustion, heating, and electricity generation. Liquefaction is a method of converting coal/biomass to petroleum through series of chemical reactions. Bio-oil, syngas, and char are useful products with stored chemical energy obtained from via thermochemical conversion. Biochemical conversion of biomass refers to the gradual and continuous release of biofuel from biomass waste through the activity of microorganisms and enzymes. Thermal and biochemical conversions are suitable processes to tap unused energy in largely available lignocellulosic biomass wastes to reduce reliance on the use of non-renewable fossil fuels as source of energy.

Keywords Biomass · Pyrolysis · Combustion · Liquefaction · Alternative energy

Abbreviation

GHG   Greenhouse gases
FC   Fixed carbon
AC   Ash content
VM   Volatile matter
BTL   Biomass to liquid
HHV   Higher heating value
NMOCs   Non-methane organic molecules in anaerobic circumstances (NMOCs)
MC   Moisture content
HTG   Hydrothermal gasification
HTL   Hydrothermal liquefaction

B. E. Peter
Department of Pure & Applied Chemistry, Usmanu Danfodiyo University, Sokoto, Nigeria

B. N. Hikon
Department of Chemical Sciences, Federal University Wukari, Wukari, Taraba State, Nigeria

1 Introduction

1.1 Need for Alternative Energy

The modern world's ability to function without energy, primarily in the form of fossil fuels derived from the mining of coal, natural gas, and crude oil sources, appears to be a highly and practically impossible phenomenon. Fossil fuel has stood out as a significant source of world energy directly or via its wide range of derivatives [1]. Crude oil today is the primary energy source for the automobile/transportation industry, and this natural oil has served as more than 90% good source of other organic compounds [2]. Some of the crude oil that we are exploring now took millions of years and 107 years cycle to form, which brought about setting limitations to the exploration of crude oil to the world market because it is a limited, scarce, and non-renewable resource [3]. The output of fossil fuel follows Hubbert Curve, i.e., as the output increases, stabilizes, and then with time, decreases continuously [4]. All global oil output rises at the onset, then peaks, and later part falls constantly. According to various forecasts, crude oil which is a fossil fuel will begin to decline in the next 20 years to more than a century [5]. As the modern world relies on energy, demand for fossil fuel, majorly crude oil, is increasing, but its reserves are depleting as each day passes. As of 2014, [6] reported the daily consumption of crude oil stood at approximately 92 million barrels. By 2030, it was statistically projected to surge to the approximated value of 116 million barrels/day. This is an essential need, but we are not expected to keep exploring and consuming an entire planet's worth of oil [1].

Nonetheless, technical advances offer some hope for replacing less abundant crude oil with unconventional energy, e.g., shale oil, oil sands, and ultra-heavy oils. However, as everyone is aware, they are limited resources that will eventually be depleted. Furthermore, these oil extraction and utilization technologies can negatively impact the environment. Using fossil fuel for energy involves combustion, which releases toxic gases (CO_2, N_2O, light hydrocarbons) into the atmosphere. In developing countries, activities that cut across domestic, industrial, and transportation burn fuel, but in particular, the transportation industry accounted for the most significant amount of greenhouse gases (GHG) [7].

The world population is increasing due to increased medical accessibility and the discovery of curable drugs for life-threatening diseases. In order to support this population boom, there is need for industrialization as done in Japan, China, and India. Gains of industrialization are tremendous but with reported increase in energy demand according to [3]. As a result, fossil supplies would rapidly deplete, and GHG emissions would rise. In addition, the ecosystem is endangered by the exploration of and burning of fossil fuels and products formed from it (derivatives). Domestic or industrial **w**aste materials produced from petrochemicals includes: (rubber and plastics) are now commonly thrown into the sea in areas non-strict environmental protection laws making aquatic region unsafe for aquatic animals since they can

feed on them. These environmental pollutants (rubber and plastics wastes) have slow biodegradation rate hence could last hundreds of years in the deep oceans.

An energy shift from fossil fuel could be historically traced to "first-generation" biorefineries which used edible crops rich in carbohydrates and sugar, such as corn, wheat, sugar cane, and beets, as feedstocks for the production of biofuel [8, 9]. The most common fuel generated from the food crops listed as natural sugar source is ethanol, which not only provides energy but also serves as chemical additives. However, because these food crops are predominantly used for food and feed, their utilization in this context would compete for feedstock, fresh water, and fertile agricultural area for the food and feed sectors [10–12]. With these demerits, using food crops in first-generation biorefineries is a debate discussed under politics, environmental consequences, and ethical concerns [11]. Furthermore, these food crops are seasonal; therefore, the possibility of availability throughout the year is an issue to ponder. Additionally, the season's availability is influenced by the agricultural technique and the soil's organic/inorganic richness, and its conversion requires a significant quantity of energy [1]. Although these food crops serve as a good source of alternative energy(biofuel), their use as a feedstock in biorefinery concept raises critical questions as listed below (i–ii) that beg for answers:

Can it produce sufficient crops without affecting our fundamental needs?
Are conversion technologies effective and easily implemented?

Non-edible parts of biomass constitute waste, i.e., lignocellulose biomass such as wood waste, agro-residues (e.g., rice husk, sugar bagasse, cocoa pod, maize stover, grasses, and municipal solid wastes) have recently attracted several research studies [13]. Lignocellulose materials, like first-generation biorefinery feedstocks, have a high concentration of sugars (polysaccharides) with potential application in the biorefinery industry [8] and [14]. As a result, the constraints of first-generation biorefineries can be eliminated or reduced by using non-edible feedstocks (lignocellulose biomass wastes), and the process of converting these biomass wastes into biofuel is termed "second-generation" biorefinery [1] and [14]. There are currently few second-generation commercial biorefineries (dedicated to producing bio-oil), e.g., Borregaard in Norway that uses Nordic wood.

1.2 Biomass

Biomass is an organic material which has carbon, hydrogen, and oxygen as its principal elemental composition and some other trace amounts of nitrogen, sulfur, and minerals [15, 16]. In its wet form, the renewable resource (plant) manufactures its food through photosynthesis, where solar energy is trapped by chlorophyll and stored as chemical energy in the biomass. Biomass is an extensive term for a diverse range of plants, their derivative resources, and biodegradable waste. It also expands to all biological material, its residues, and dead biomass.

Crops and residues can be obtained from food processing companies, poultry, wood waste from the sawmill, municipal solid wastes, sewage sludge, trees, energy crops (water weeds, rushes, water, hyacinth, algae, seaweeds). Aquatic plants are also valuable biomass feedstock. Biomass wastes can be obtained from sorghum, maize, sugarcane, and rice. All crop residues have stored chemical energy that might fits as an alternative energy source, depending on its dry mass per unit of land (hectares). Increased output reduces the demand for land thereby reducing the cost of producing biomass energy.

Among all current renewable sources (solar, wind, hydro, tidal, and geothermal), biomass stands out as the only sustainable carbon carrier. It has been identified as an important source in the global transition to carbon–neutral energy [17]. Biomass accounts for around 10% of global energy use [18]. It includes photosynthesis-produced organic compounds such as hemicellulose, cellulose, lignin, moisture, extractives, and traces of various inorganic elements. Animal waste and sewage sludge are degradable biomasses from animals and microorganisms [19]. The composition of biomass is not fixed but determined by many factors such as biological origin [16]. Biomass is abundant as waste in various forms, including urban solid waste, wood residue, forest residue, agricultural waste, and industrial waste, making its acquisition more convenient, cost-effective, and environmentally friendly [15] and [20]. When biomass waste is left unmanaged in its huge mass, it constitutes an environmental nuisance. More than 75% of biomass utilized for energy generation comes from agro-wastes [21]. Agro-remnants are crop residues that would typically be discarded. If the residues are not combustible, they are usually burned or dumped in landfills.

The global energy potential of biomass is immense. The terrestrial standing biomass carbon on the globe was estimated to be 100 times the yearly world energy consumption. The forest biomass and its residues account for between 80 and 90% of total biomass carbon [22]. In terms of annual net energy output, marine biomass carbon (which has the lowest natural abundance) is predicted to outnumber forest biomass carbon [23]. The only renewable carbon source that can be converted into useable char, bio-oil, and volatile gaseous fuels, as well as high-value compounds, is biomass. The use of woody biomass and its residues as the oldest energy source cannot be disputed and still stand as the most used in developing and underdeveloped countries as a source of heat for cooking or charcoal production. It still serves the same purpose of heating. However, the direct combustion of these woody biomass contributes to a more hazardous environment via the release of CO_2 (a significant gas in GHG), SO_2, and NOx (mix with moisture to form acid rain), and ash which makes such an environment becomes dusty. Compared to fossil combustion, biomass burning emits much less hazardous pollutants [24].

Forest residues, i.e., wood and its dust (sawdust), contribute about 64% of biomass energy, about 24% of biomass energy is possible with municipal solid waste, and 5% each is contributed by agricultural and landfill gases [24].

The general classification of biomass energy is:

Traditional biomass.
Modern biomass.

In developing and emerging countries, traditional biomass is the commonest used, comprising fuelwood, animal wastes, sugarcane bagasse, charcoal, and plant residues.

The concept of modern biomass is extended to wood and its wastes, agricultural residues, domestic and industrial wastes, and biofuels (biogas from animal wastes, energy crops, and so on), and it is widely employed to replace traditional energy sources [24].

1.3 Lignocellulosic Biomass as a Source of Renewable Energy

Lignocellulose biomass stood as the largest source of renewable carbon as it is expected that its production will be between at a minimum of 10 billion dry tons/yr and maximum of 50 billion dry tons/yr [25, 26] and then will assume that production of lignocellulosic biomass from energy crops and agricultural waste is a viable renewable source for transportation fuels and bio-based goods.

In simple terms, lignocellulosic biomass is composed of three major components of biomass: hemicellulose, cellulose, and lignin. They are preferred as feedstock biomass due to their abundance, renewable nature, low cost, and higher energy content in dried form [27]. According to [28], the per energy growth rate of lignocellulosic biomass is 30–240 barrels of oil equivalent hectare-^{1} yr-^{1}.

Lignocellulose biomass feedstock includes: agricultural resources and their wastes, crop and its residues, forestry resources and wastes, carbon-rich domestic and industrial wastes, and animal waste.

Agricultural produce stood as the primary source of Nigerians' revenue before the discovery of oil and gas, accounting for almost half of her GDP and 75% of export [29]. Had the trend of farming continued, there would not be an issue of food shortage, and agro-waste from this source would have been easily diverted as a source of energy. Currently, the world is being driven by progressive usage of limited reserves of non-renewable fossil fuel resources which has adverse climatic repercussions [20]. Geologists and geophysicists are always charged with a continuous search for new oil fields, but lots of oil fields discovered are non-economical to be explored. Scientists must look for alternative energy sources to create energy balance, security, and sustainability.

A bio-based economy is built on the sustainable production of food, feed, chemicals, fuel, materials, and plant energy. It is impossible to store these energy sources (wind, water, solar energy, and nuclear) as a liquid fuel. Some selected thermochemical conversion techniques can be used to obtain liquid products useful as biofuels to serve the same function as oil in automobile engines. This means the successful use of bio-oil as an industrial raw material will significantly depend on biomass processing processes [20]. The adoption of biomass remains the only alternative to replace fossil fuels for transportation or automobile industry [20].

Photosynthesis is a process that uses solar energy to produce sugar, starch, and structural polysaccharides which are viable carbohydrates used to produce biofuel. Bio-C_2H_5OH, a suitable biofuel, is obtainable from these carbohydrates via biochemical extraction process and fermentation [30]. Since structural polysaccharides are the most predominant carbohydrates and integral components of plants' cell walls, they account for most plant biomass. However, since they can be converted into biofuel more easily than cell wall polysaccharides, soluble sugars and starch currently make up the majority of the production of bioethanol [9]. For example, the secondary cell wall of a plant is a strong, shielding biological structure that offers stability and resistance to deterioration. This is a result of its primary components which include the structural polysaccharides carbohydrate cellulose and hemicellulose as well as the phenolic polymer lignin, interlinking to create a strong matrix [31]. Plant biomass that contains cell walls, or lignocellulose, can be converted into bioethanol, but first, the cell wall structure needs to be treated to make it more pliable. This procedure combines thermal energy, mechanical pressure, and chemicals to break down the crosslinks between the major components of the cell wall and increase the exposure of the polysaccharides to enzymatic hydrolysis [32]. Hydrolysis is necessary to separate cellulose and hemicellulose into their monomeric sugar components. After that, by fermenting these components, bioethanol can be produced [30]. Although structural polysaccharides are rarely or never utilized in food and feed applications, they are the most widely used carbon source in the large-scale generation of biofuels [32].

Nigeria is a tropical area with a vast land mass covered in trees. A vast amount of residue, including bark, sawdust, and mill chips, is produced when these trees are felled and made into boards. They are made up of wood processing waste and scrap that cannot be used to make new wood, such as wood particles/dust, veneer rejects, veneer log cores, edgings, slabs, trimmings, and other wood wastes from carpentry and joinery. Biomass wastes from rice, cassava, sorghum, maize, millet, and bailey all contribute to the supply of lignocellulose in the form of residues from farming processes. Maize is typically grown for its grain, where the plant's leaf and stem parts are used (referred to as stover). There is huge energy harvest possibility when considering the overall collection of residues based on worldwide harvest and average residue production per hectare. The lack of technical know-how in most of Africa countries has made lots of useful forest residues untapped as biomass energy.

2 Biomass Chemistry

Organic and inorganic components, as well as water, make up biomass [33]. The chemical structure and essential organic constitutents of biomass determine the appropriate technologies for converting it into fuels and chemicals [30]. Biomass comprises three primary categories of naturally occurring polymeric components in dry mass. These carbon-based polymers are [30]:

i.   Cellulose (approximately 50%),
ii. Hemicellulose: its value is between 10–30% in forests, and for herbaceous biomass, it stood at 10–40%.
iii. Lignin: this made up 20–40% of woods resources and stood at 10–40% in herbaceous biomass.

The amount of cellulose, lignin, and hemicellulose in biomass largely depends on the species, as stated above, and these variations are primarily noticed with hardwoods and softwoods. Of the three major components, cellulose and hemicellulose are in higher proportion in hardwood than softwood. Table 1 showed a comparison of compositions [30] and [34].

Proximate and ultimate analyses are used to determine the principal organic constituents of biomass (cellulose, hemicelluloses, and lignin) and the percentage elemental composition of biomass [19]. Ultimate analysis of biomass showed biomass contains largely carbon (30–60%), followed by oxygen (30–40%), hydrogen has about (5–6%), and other elements including S, N, and Cl make up < 1% of the biomass. Biomass elemental composition is listed in decreasing order of abundance as; C > O > H > N > Ca > K > Si > Mg > Al [19].

The common inorganic components in biomass are: alkali metal compounds (K, Ca, Na, Si, P, Mg, and Cl in herbaceous biomass). However, the amounts of these inorganic compounds differ, and it depends on the biomass species; wood (< 1%), herbaceous biomass (15%), and agroforestry residues (25%) [35].

Extractives from biomass are majorly smaller organic molecules and some other giant molecules such as acids, protein, and salt. Plant stems, foliage, and barks contain equivalent amounts of the significant classes of food, ash, hydrocarbons, and other substances [35].

Carbohydrates are organic polyhydroxy molecules having the elemental formula $(CH_2O)_n$. They contain a homogeneous carbon content of about 40%, which is significantly lower than that of hydrocarbons. They have exceptional physicochemical qualities due to their oxygenation, which enhances conversion and utilization. Monosaccharides, disaccharides, oligosaccharides, and polysaccharides are the four

Table 1 Composition distribution in biomass

Wood type	Cellulose (%)	Hemicellulose (%)	Lignin (%)	Extractive (%)
Softwood	40–44	25–29	25–31	1–5
Hardwood	43–47	25–35	16–24	2–8

forms of carbohydrates. Starch and sugar are the primarily used feedstocks in first-generation refineries, while cellulose and hemicellulose stood as the feedstock in the second-generation refinery [36]. Of the three major biomass components, cellulose and hemicellulose are carbohydrates, while lignin is non-carbohydrate [37, 38].

2.1 Chemistry of Biomass Components

The production of biofuel from any biomass depends on its three major components: cellulose, hemicelluloses, and lignin. These components stood as a fixed base for the production of fuels and other chemical additives. However, lignocellulose biomass can generally be woody substrates and agricultural residues. In lignocellulosic biomass, cellulose and hemicelluloses are the two carbohydrate polymers that make a more significant percentage of the material. At the same time, the third principal component (lignin) is a non-carbohydrate but complex aromatic compound that is highly branched [39]. Apart from the fact that the variation of these components depends on plant specie type, other factors such as soil, age, and growth stage contribute to their variation [40].

In the order of abundance (%), the three significant components of biomass followed the order cellulose > hemicellulose > lignin [41]. The high content of cellulose and lignin is recorded in woody biomass, while soft tissue plants such as grasses are low in lignin but significantly high in hemicellulose [25].

Lignocellulosic biomass has cell wall extractives (proteins, pectin), macro- and micronutrients inform inorganic compounds, ashes, and the three major components. However, these have little effect on the buildup of the lignocellulose structure. The existence of lignin, hemicelluloses, pectin, and other plant cell wall components, as well as their spatial interlinks with cellulose, is hypothesized to have resulted in a plant cell wall with a robust and compact structure (Fig. 1) (physical barriers) that is resistant to microbial degradation [25].

Fig. 1 Arrangement of major components of biomass
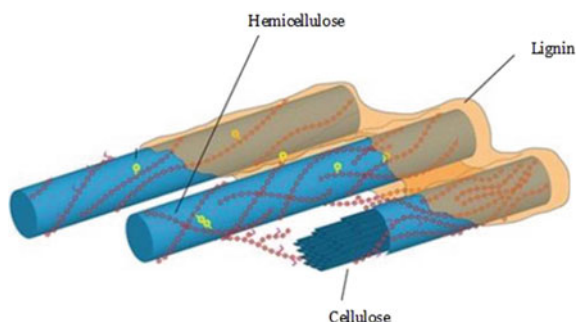
2.2 The Structural Properties of Lignocellulose

2.2.1 Cellulose

Cellulose is a polysaccharide with a molecular weight of 162.1406 g/mol represented in Fig. 2. Celloboise, an oligomar of two $C_6H_{12}O_6$ units linked together by fourteen glycosidic bond units. The cellulose polymer(s) $(C_6H_{10}O_5)n$ has about 100 to 20,000 (14) linked D-$C_6H_{12}O_6$ molecules. Lignocellulose has the parallel linking of about 36 cellulose molecules via bonds and forces (hydrogen and van der Waal's) to form a non-amorphous structure with straight, stable supramolecular fibers of great tensile strength and limited openness. The basic fibrils are subsequently linked to other biomass components such as pectin, hemicelluloses, and lignin (Fig. 1). Cellulose microfibrils are little cellulose bundles that give plants mechanical strength and chemical stability. Some cellulose microfibrils are regularly joined to produce macro-fibrils [35].
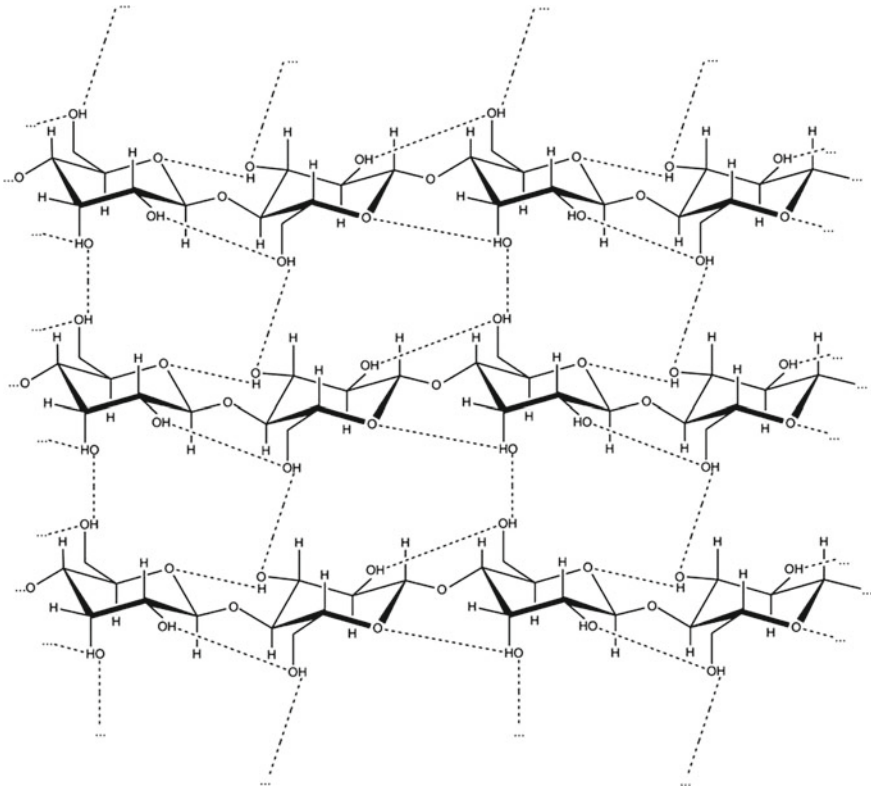
Fig. 2 Structure of cellulose

Cellulose has some degree of crystallinity, degrades less, and is typically insoluble in H_2O and common organic solvents. It is important to note that cellulose contains soluble, easily degradable, amorphous/non-ordered components. Many cellulose characteristics, however, are typically governed by its degree of polymerization.

2.2.2 Hemicellulose

After cellulose, hemicellulose (a polysaccharide grouping) is the second most significant carbohydrate component of lignocelluloses [41]. Hemicelluloses are heterogeneous short-chain linear and branching sugar polymers comprised of five different sugars, which are listed in (i–v) [25]; Fig. 3.

L-Arabinose ($C_5H_{10}O_5$)
D-Galactose ($C_6H_{12}O_6$)
D-Glucose ($C_6H_{12}O_6$)
D-Mannose ($C_6H_{12}O_6$)
D-Xylose ($C_5H_{10}O_5$).

The pentose (C5) sugars are: L-arabinose and D-xylose, while the others are hexose (C6) sugars. Xylan is the commonest hemicellulose family sugar, with examples listed in (i–vi). There are possibilities for minute amount of these sugars [42].

L-Rhamnose
L-Fucose
4-O-methyl glucuronic
Organic acids like acetic
Ferulic acid
Galacturonic.

Its sugar acetyl groups were replaced temporarily by –OH groups. However, the 1, 4-linked -D-hexosyl residues that make up most of the hemicellulose's backbone also occasionally include hexose(C6) sugars, pentose (C5) sugars, and uronic acids [25]. Unlike cellulose, hemicellulose's composition and structure vary depending on the source (such as the type of side chains and glycosidic linkages) [43]. Homopolymers, which are repeating units of a single sugar, include xylans, mannans, and glucans. Heteropolymers, on the other hand, are mixtures of various sugars, including arabino-galactan, arabinoxylans, arabinoglucuronoxylans, galactoglucomannans, glucomannans, glucomannans, glucomannans, and glucom. For instance, agricultural waste, O-acetyl-4-O-methylglucuronoxylans, and O-acetylgalactoglucomannan are utilized to create hardwood hemicellulose [44]. Due to their short-chain branching structure and acetyl groups attached to the polymer chains, hemicelluloses, unlike cellulose, lack crystallinity [42]. Its degree of polymerization ranges of minimum (70) to maximum (200) suggests that it is an amorphous polymer that degrades quickly [45].
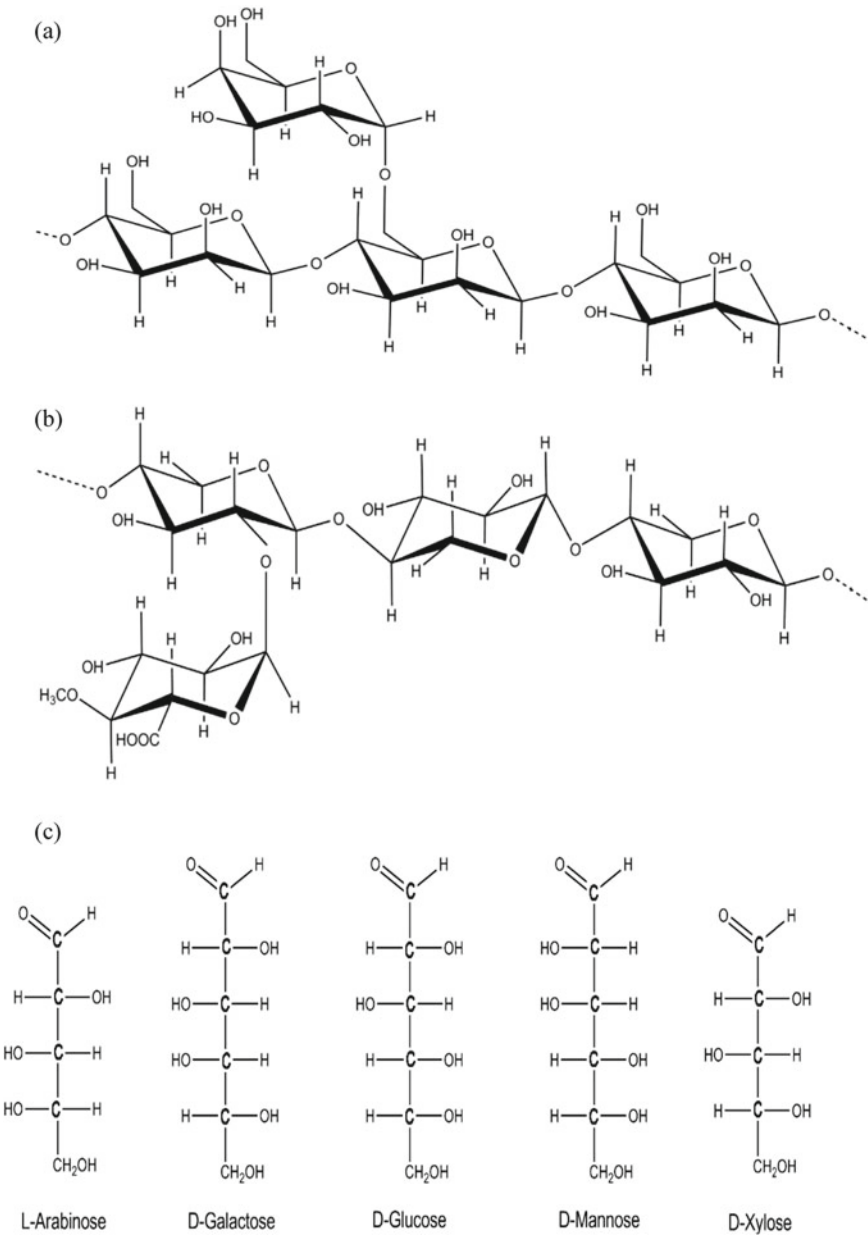
Fig. 3 Hemicellulose (**a**) represents galactomannan, (**b**) represents glucuronoxylan, (**c**) represents sugar monosaccharides

2.2.3　Lignin

After carbohydrates, lignin stood as the second-most available component of ligno-cellulose biomass on earth and the primary source of natural aromatic polymers [46]. The primary building units of lignin, an amorphous and highly branched rigid polymer, are three phenylpropane units. These three components, p-coumaryl alcohol, coniferyl alcohol, and sinapyl alcohol, combine to form a random sequence of p-hydroxyphenyl (H-lignin), guaiacol (G-lignin), and syringyl (S-lignin) subunits [47]. Depending on the lignocellulose source, different H, G, and S-lignin composi-tions exist [48]. Herbaceous plants have high concentrations of all three lignins—G, S, and H—in various ratios, whereas hardwood lignins are largely composed of G and S monolignols with very little H. The G units make up the majority of the lignins in softwood, with H units making up the remaining fraction [43]. Lignin strengthens the cell wall by filling in the gaps between the two other major components of biomass (cellulose and hemicelluloses) and other cell wall components and acting as a cell, fiber, and vessel binding material [49]. Additionally, it has impact on how water, minerals, and metabolites are transported [39]. The development of lignocellulose's complex structure, the formation of plant cells, and the defense of plants against disease and insect attack all depend on it [42]. Although some bacteria and fungi may break down lignin, it can survive for a very long time [50].

2.2.4　Other Constituents

Proteins, ashes, extractives (including terpenoids, steroids, lipids, waxes, and phenolic compounds), and pectin, which is composed of neutral sugar side chains and acidic sugar backbones, are also present in the lignocellulose cell walls (often galacturonic acid) [51]. The homogalacturonan, rhamnogalacturonan, and xylogalac-turonan subclasses make up the highly branching, complex heterogeneous polysac-charides known as pectins [52]. Their cross-linking influences plant morphogen-esis and wall porosity and supports cell adhesion and wall hydration [51]. There are several uses for extractives; some safeguard plants, others act as precursors for certain compounds, and many others have unclear benefits [53].

2.3　Lignin, Cellulose, and Hemicellulose Interactions Chemical

The cellulose macro- and microfibrils embedded in lignin serve as the structural core (skeleton) of lignocellulose, whereas hemicelluloses are scattered between them

Table 2 Overview of significant connections between and among the three lignocellulose components

Linkage	Interpolymer	Interpolymer
ROR bond (Ether)	Lignin, (hemi)cellulose	Cellulose-lignin, hemicellulose-lignin
C–C	Lignin	NI
H- bond	Cellulose	Cellulose-hemicellulose, hemicellulose-lignin, cellulose-lignin
RCOOR bond (Ester)	Hemicellulose	Hemicellulose-lignin

NI: Not identified.

(Fig. 1). The crucial four interpolymers (between various components) and inter-polymer (inside specific components) linkages that exist between these three components are ROR (ether), ester (RCOOR), carbon–carbon (C–C), and hydrogen bonds, as shown in Table 2 [45] and [54].

Ether (ROR) and H-bonds are the primary chemical bonds that hold cellulose polymers together. The glycosidic bonds in cellulose are comparable to ether bonds that bind 2-C atoms to an oxygen molecule [55]. The two –OH groups on various cellulose polymer chains interact to produce H- bonds. A number of the character-istics of natural cellulose, including its crystallinity, are thought to be caused by the hydrogen bonds between cellulose threads [56]. Similar to cellulose, hemicelluloses are connected mainly by either type of linkages. Several ester (carboxyl) groups are present instead of hydrogen bonds [45]. The C–C bonds make up 30% of the intrapolymer linkages between lignin monomer units, and ether bonds make up 70% of those linkages [45]. They can be found within and/or between the carbon atoms in allylic and aryl compounds [57]. Cellulose, hemicellulose, and lignin are joined by hydrogen via interpolymer bonds [54]. Hemicellulose and lignin are linked by ester (RCOOR) bonds, ether and ester bridges make up the majority of lignin and polysaccharide complexes. Although ether groups between lignin and the polysac-charides are known to exist, it is yet unknown if they also occur between lignin and cellulose or hemicellulose [45].

3   Role of Biomass in Energy Generation

3.1   *Biomass Energy*

The technologies applied to derive energy from biomass are: thermochemical and biochemical pathways. These two listed approaches are helpful in the transformation of lignocellulose biomass resources into three essential energy products: Biomass gasification has unique application since it is very promising for producing renewable chemicals and generating electricity in turbines or internal combustion engines [58].

Gasification of biomass is simply the use of a gasifier, which is a machine that uses a programed mechanism involving heat (700 °C), steam, and O_2 to convert biomass into useful products such as syngas, biochar, biofuel, heat, power, and fertilizer without the use of combustion. The sustainable use of biomass for producing energy and chemicals depends on understanding its physicochemical properties. The variety and variations among biomass species are determined by chemical composition, MC, AC, and the presence of inorganic materials. Metals (Mn, Na, Al, Mg, K, Ca, Fe), metalloid (Si), and non-metals (Cl, S, N, H, O, and C) make up the majority of the components in biomass [59]. These elements are found in biomass in varying percentages.

Unlike fossil fuels, which have a high energy density, biomass has a low thermal efficiency. Low bulk density (typically 8.0×10^1–1.0×10^2 kgm^{-3} for agricultural straws and grasses and 1.5×10^2–2.0×10^2 kgm^{-3} for woody biomass) contributes to the low energy content of biomass in its original form [60]. Raw biomass is more expensive to handle, store, and transport than fossil fuels. Therefore, improving the biomass's handling, storage, and transport qualities are crucial for biomass's most efficient and productive valorization. Biomass is primarily converted via thermal and biochemical technologies to obtain improved biomass properties/products suitable for energy and lessen drawbacks associated with the use of biomass for energy purposes [61]. Fossil fuel serves as a better fuel when compared to bio-oil because bio-oil has low calorific values, a high percentage of moisture and oxygen, low energy density, high volatile matter, high density because of the presence of oxygenates, pH less than 5 (acidic), highly viscous and corrosive due to its water content attack on metallic engine and degradation with an increase in storage days [33].

3.2 Biofuels

Biofuel is an organic fuel derived from either live or dead carbon-based material. High-quality ethanol is produced from these sources using biomass conversion processes. This biomass conversion produces biofuels, which can be solid, liquid, or gaseous fuels. Biofuels include, among other things (a–c): **A. Solid biofuel:** Pelletized wood, briquettes, chips of wood, firewood; **B. Fluid biofuel:** Biodiesel, a bioethanol bioalcohols, **C. Gaseous biofuel:** Biogas \Syngas.

3.3 Biofuel from a Few Familiar Biomass Sources

3.3.1 Cassava

Cassava-Based Fuel: "Biomass" refers to all chemical energy sources that can be generated by converting plant and animal components into solid, liquid, and gaseous forms. To provide thermal energy for uses like cooking, propulsion, or the creation

of electricity, these fuels can be burned alone or in conjunction with traditional fossil fuels.

Ethanol is a biomass fuel type. By fermenting starchy substances like cassava and sugarcane, ethanol, a liquid fuel, can be produced. Other biomass fuel sources include biogas obtained from waste and rotting plant and animal matter in landfills or biogas digesters [62]. This part exclusively takes into account liquid biomass fuels, primarily ethanol.

Because cassava is commonly cultivated in Nigeria hence its preference for the production of C_2H_5OH. Government initiatives like the one that required cassava to be included in flour during the Obasanjo administration should have encouraged farmers to increase their cassava production in recent years. Most C_2H_5OH produced in Nigeria is made from petrochemicals, which has the unfavorable effect of taxing the country's petroleum reserves even more. So it is more than appropriate to adopt an alternative like cassava. This would have the desired result of creating employment in the rural areas where cassava is cultivated and lowering the dependence on petroleum components for ethanol synthesis. The lesson is that initiatives to support a biofuel sector of this kind must be pursued along with actions to ensure it does not affect the nation's food supply. Undoubtedly, these measures will involve educating farmers about the importance of giving food crop cultivation equal attention in the face of a cassava boom and subsidizing food crop production by providing farmers access to seedlings, farming equipment, fertilizer, financing, and other resources to make growing food crops simple.

3.3.2 Sugarcane

A perennial grass, sugarcane (saccharin spp.) grows well in tropical and subtropical climates. It needs an environment free from frost and with enough moisture during the growing season. Sugarcane uses chemical energy that it stores inside the plant to transform sunlight into energy as it grows. Approximately, one-third of the plant's stored energy is found in each of the following primary parts (a–c) below:

a. Juice, which contains sucrose and is found inside sugarcane stalks, is used to produce ethanol and sugar.
b. Bagasse: A ton of sugarcane yields 270 kilos of this dry, fibrous by-product after being crushed.
c. Straw: The stalks of sugarcane leaves and tips.

Removing sugarcane bagasse in Nigeria is majorly via burning, and its straws are also usually burned to ward off snakes and other potentially deadly creatures. A third of the energy in sugarcane is destroyed via this procedure. Additionally, it has been found that burning the sugarcane field before harvesting is where the great bulk of emissions originate. According to experts, experts, straw, and bagasse can be burned together in high-efficiency boilers to provide up to 11,500 MW of bioelectricity [63]. Bagasse, a significant waste product, particularly during the dry season, offers a range of potential power output from 1000 to 9000 MW, depending

on the technology employed [63]. A significant source of both sugar and ethanol is juice. A biofuel known as bioethanol is increasingly frequently made from ethanol. The most crucial benefit of bioethanol for the environment is that it has the potential to be carbon neutral throughout its lifecycle, which means that the carbon dioxide (CO_2) released during production will be balanced by the amount absorbed from the atmosphere during usage. This guarantees a decrease in dangerous emissions and air pollution. Ethanol from sugarcane reduces greenhouse gas emissions by at least 60% compared to gasoline.

3.3.3 Husk of Rice

Rice husk is a typical agricultural by-product. Rice is one of the agricultural products designated for expansion by the Federal Government of Nigeria to diversify the country's current crude oil economy. In Nigeria, rice is a staple food, and if local production is expanded, this will lead to a rise in rice-processing wastes, including rice husk and straw. Igbinmo, Ebonyi, Isu, Kano, Ifon, Abeokuta, Jigawa, Cross-Rivers, and Sokoto are among towns that produce rice husk. In places, the number of dumps made of rice husks is rising alarmingly. Due to the impending environmental risks, deterioration, and pollution, it poses to people and the environment, disposing of and evacuating the rice dumps is urgently necessary. Most communities seek to dispose of rice husks by setting fire to the rice husk dumps, but a modest pile of rice husks takes months to burn to ashes. Even after being reduced to ashes, it still blights the neighborhoods, particularly during the rainy season. Air pollution and ash buildup are the results of burning rice husk dumps. Consequently, there is a pressing need to remove the rice dumps from these areas.

Rice husk, the main waste of the rice-processing industry, is one potential biomass-based energy source for generating electricity. With a calorific value of 3259 kcal/kg, rice husk is a renewable fuel source [64]. It is possible to produce electricity from rice husks using a gasifier and a modified internal combustion engine that drives a generator. Rice husk can be converted into fuel gas in a gasifier at high temperatures and in an atmosphere with just 1% oxygen. The generated clean gas (syngas) can be used right away in a gas-powered plant to generate electricity for local use as well as the powering of the rice mill. Rice husk power plants' by-product, rice husk ash, can be used in the cement and steel industries. It also increases the diversity and security of the electricity supply, is more environmentally friendly, creates more opportunities for local people to find work, and is a better way to dispose of agricultural waste.

3.3.4 Maize

Because it is the largest crop in the world in terms of overall acreage, maize is expected to be important in the development and widespread commercialization of cellulosic fuels [65]. Maize must be bred to function as a dual-purpose crop, demonstrating excellent grain production and quality features, high stem-biomass yield, and

Table 3 Biomass in bio-refinery

Biofuel	Description	Examples
First-generation biofuel	Made from raw materials that compete with those used in the food and feed industries	(i) Bioethanol from crops such as sugar beet, sugar cane, and starch (corn and wheat) (ii) Rapeseed, sunflower, soyabean, palm, and leftover food oil-based biodiesel biogas generated from starch
Second-generation biofuels	Produced from waste residues or non-food crops (energy crops)	(i) Biogas from leftovers and garbage (ii) Lignocellulosic material-based biofuel from energy crops, biofuel
Third-generation biofuel	From aquatic microorganisms, such as algae	(i) Biodiesel from algae (ii) Green hydrogen
Fourth-generation biofuels	Biofuels based on cultivation with high solar efficiency	(i) Technology that produces no carbon (ii) Future-day technology

higher processing amenability, in order to achieve this. The study [66] demonstrated that grain yield, agronomic fitness, and stover quality were not mutually exclusive breeding objectives and came to the conclusion that current maize breeding efforts might incorporate stover traits beneficial to the cellulosic ethanol sector without using foreign germplasm. With a wealth of genetic and agronomic resources, maize can be developed into a dual crop with the appropriate biomass quality characteristics and a significant amount of stover output. Given that it is widely produced, utilized as a feed crop, and generates enormous amounts of lignocellulosic wastes, maize is perhaps the most suitable model crop in the research of biomass quality. As shown in Table 3, maize and its waste can be used in biorefineries to generate electricity. Therefore, the main goals of research into maize bioenergy are to analyze and understand biomass recalcitrance as well as to specifically alter the composition of cell walls.

4 Chemistry of Biomass Conversion to Energy

4.1 The Use of Biomass

Lignocellulosic biomass is a significant organic embodiment of many components in which the major components are (hemicellulose, cellulose, and lignin); the carbohydrates components are (sugars, cellulose, and hemicellulose) and non-carbohydrate (lignin), with the presence H_2O, polysaccharides (starch, protein), fatty acids, oils, extractives, HC, AC, and other substances [34] and [67], in contrast to carbohydrates,

which make up < 30%, and lipids (oil), which make up < 10% of a biomass species, cellulose, lignin, and hemicellulose make up the majority of a biomass species. Lignin and the other two primary components of biomass term (carbohydrates) are typically recognized as lignocellulosic biomass [67].

Lignocellulosic biomass is a class of energy crops with distinct physicochemical properties (ultimate and proximate) or constituents (cellulose and hemicellulose) that are used as feedstock in second-generation refineries [36]. These compositions make biomass suitable for energy generation via thermochemical or biochemical conversion, and these factors are taken into account when selecting the appropriate conversion technologies for any biomass waste [68]. Biomass wastes have a high concentration of organic elements such as cellulose, hemicellulose, and lignin, as well as traces of other organic compounds or polymers, which are known to be a reservoir of solar converted to chemical energy [69]. Biomass contents vary; they can be converted to energy materials (bio-oil fuels, chemicals), and the selection of biomass depends on the required end products [70]. Bio-oil rich in lipids are frequently turned into biodiesel via the process of esterification (transesterification) with CH_3OH or C_2H_5OH, in contrast to carbohydrates (starchy and sugary components) which are typically converted through biological fermentation into C_2H_5OH. Naturally, lipids, proteins, and lignin are produced from sugars during photosynthesis. Long-chain hydrocarbon fatty acids with high calorific value contents are frequently produced when consumed by cyclic carbohydrates (glucose) [67]. As an alternative, solid biomass is commonly turned into syngas ($CO + H_2$), which, when subjected to Fischer–Tropsch (FT) process, produces liquid fuels and other chemicals. This process, however, requires several labor-intensive processes, energy, and financial investment. Direct liquefaction, often known as "biomass to liquid (BTL)," provides a more dependable and simple conversion of biomass leftovers to liquid. Numerous thermal and thermocatalytic BTL approaches are constantly being developed [67]. The choice of any biomass material for the generation of energy source is influenced by factors such as moisture content (MC), higher heating value (HHV), fixed carbon (FC), volatile matter (VM), ash slagging, and fouling indices via its group I metal content, and its cellulose/lignin ratio [37].

4.2 Criteria for Selecting Biomass

4.2.1 Ultimate and Proximate

There are two types of physicochemical parameters for determining the viability of any biomass waste as a source of biofuel. Proximate parameters commonly used are moisture content (%), volatile matter content (%), fixed carbon (%), and ash (%), while ultimate parameters are C, H, N, and S percentages.

MC Approximate Parameters

The moisture content of the same species of biomass varies greatly, making it an undesirable property of biomass for use in thermal conversion processes. Moisture content affects gross calorific value, combustion efficiency, and combustion temperature directly [16]. Sawdust moisture content (7.62%) is one of the factors that determined its HHV of 16.01 MJ/Kg, which is within the desirable range of 10% MC [15].

Ash Content (AC)

Ash is a residue that results from the thermal breakdown of organic and inorganic constituents of biomass waste. Higher ash content indicates higher carbon content, which favors gas yields. It is not a desirable property of a biofuel because depending on the elemental composition of ash, its constituents' catalytic influences thermal decomposition, slagging, fouling, and sintering.

Fixed Carbon (FC)

The fixed carbon fraction of a biomass is the carbon that exists in an uncombined state, that is, it is not chemically bonded to another element. FC produces biochar in a thermochemical conversion process of biomass, such as combustion, which is then burned in the reactor. A higher FC value is a property of herbaceous biomass wastes that favors combustion properties [71]. The expected FC range in such a waste is 7–20% [16].

$$FC = 100 - (\%\ MC\ +\ \%\ VM\ +\ \%\ Ash) \tag{1}$$

Volatile Matter (VM)

Volatile matter refers to the fraction of biomass that can escape and disappear from the reactor chamber during thermochemical conversion. Oxides of carbon (CO and CO_2), hydrogen gas, moisture, light hydrocarbons (CH_4), and tars are a few examples [24] and [71]. %VM is high in all biomasses, but values vary depending on the chemical composition of the biomass and range from 75 to 90% [16].

4.2.2 Gross Calorific Value (GCV)

The gross calorific value is a measurement of the chemical energy stored in biomass using an oxygen bomb calorimeter or a mathematical computation, as shown in Eq. (2). Equation (2) can be used to calculate the HHV or gross calorific value of

biomass [16].

$$\text{HHV}\left(\frac{\text{MJ}}{\text{kg}}\right) = {}^{3491}/_{10000} \times (C) + 1.1783(H)$$
$$+ 0.105(S) - 0.1034(O) - 0.015(N) - 0.0211(Ash)$$

(2)

4.2.3 Ultimate Parameters

The basic elements in biomass are C, H, N, and O. During the combustion process, the C component of biomass reacts with atmospheric oxygen to produce CO_2 and H_2O, a process known as an exothermic reaction. Equation (2) is a mathematical expression used to calculate HHV which demonstrated that these elements have a positive impact on biomass HHV and the combustion process itself.

Carbon is the most important element in thermochemical conversion processes; the higher its value, the higher the heating value of such biomass [15]. A very low percentage of hydrogen in biomass indicates a problem because it exists together with carbon to determine the heating value of biomass [15].

For a biomass waste not dried at 105 °C prior to CHNS analysis, Eq. (3) applies

$$O_2 = 100\% - (\%\,C + \%\,H + \%\,N + \%\,S + \%\,M + \%\,AC)$$

(3)

Oven dried biomass waste before its ultimate analysis, Eq. (4) applies

$$O_2 = 100\% - (\%\,C + \%\,H + \%\,N + \%\,S + \%\,AC)$$

(4)

The best biomass conversion methods (technically easy, cheap, and high yielding) must be selected for any biomass due to the nature of the polymers in lignocellulosic biomass to get fuels and chemicals.

Biomass is found worldwide, is highly abundant, and is renewable, which has sparked a growing interest in and driven current attempts to produce organic compounds with this diversity of biomass, with the sole aim of sugar conversions to value-added chemicals, e.g., ethanol. Hexoses, mainly glucose and D-fructose, are the best biomass sugar feedstock to use as chemical precursors or intermediaries [29].

5 Catalysis in the Conversion of Biomass

Biomass processing has historically used organic catalysis (also known as enzymatic catalysis). However, inorganic catalysis, utilized to transform unprocessed biomass feedstock into valuable products, is more economically efficient [67]. Due to their

higher capacity for molecular deoxygenation through various chemical processes, acid catalysis is commonly used in biomass valorization [72]

In converting biomass into alternative fuel and other chemical additives, catalysts are essential for either accelerating or improving the conversion products (liquids or gases). However, their properties and mechanism routes differ depending on the technology conversion employed.

5.1 Heterogeneous and Homogeneous Catalysis

Heterogeneous catalyst is largely employed as a crucial agent in the conversion of fossil fuels into fuels, power, and chemicals. Given the entirely different chemical make-up of these heterogeneous catalysts, their function in the digestion of biomass is still unknown. In recent years, zeolites have demonstrated tremendous progress for use in biomass valorization, particularly in converting lignocellulosic biomass into fuels and chemicals [73]. Catalyzing processes including dehydration, esterification, decarboxylation, and acylation play a crucial part in transforming oxygenates into hydrocarbons. Thus, it has been discovered that using zeolite catalysts in biomass processing is a feasible alternative technique for transporting fuels and chemicals [73]. However, a significant problem in the field of biochemicals is the discovery of innovative catalytic pathways for the selective, efficient, and direct conversion of biomass feedstock to manufacture specific compounds [74]. Both homogeneous and heterogeneous catalysts are typically used to catalyze the transesterification process for biodiesel production.

The chemical catalysts used in transesterification are classified as homogeneous or heterogeneous. Examples of homogeneous catalysts include potassium hydroxide (KOH), sodium hydroxide (NaOH), and sodium methoxide (CH_3ONa). NaOH is preferable to KOH because it dissolves quickly in solvents such as methanol (CH_3OH). It also has some intrinsic properties such as high purity and low cost when compared to KOH [75, 76]. The examples given above, in their concentrated/strong form, can help improve the quality of biodiesel production during transesterification.

When compared to homogeneous catalysis, heterogeneous catalysts are typically solid acid or solid alkali catalysts that improve transesterification by lowering costs and pollutant release [77]. Heterogeneous catalysts have several advantages, including low cost, ease of recovery after use, and reusability. Li/ CaO, $CaCO_3$ rock, MgO/KOH, modified zeolites, anionic clays (hydrotalcite), Eni Slurry Technology (EST-4), and Na/NaOH/-Al_2O_3 are some examples of excellent heterogeneous catalysts used in transesterification reactions [78]. Solid acid catalysts promote both esterification and transesterification in the production of biodiesel from oils high in free fatty acid (FFA). K_2CO_3/Al_2O_3, SrO, CaO, MgO, KNO_3/Al_2O_3, [79], Li/CaO, KF/ZnO, basic hydrotalcite of Mg/Al, Li/Al, anion exchange resins, and base zeolites are some of the solid-base catalysts used in transesterification [80].

In a recent study [81], heterogeneous catalysts (acid or base) examples were reported and their applications in lab-scale biodiesel production. These include:

i. Derivatives and oxides of Group I metals, e.g., (KOH), sodium hydroxide (NaOH), and sodium methoxide (CH$_3$ONa)
ii. Derivatives and oxides of transition metals
iii. Group II metal oxides and their derivatives; BeO, MgO, CaO, SrO, BaO and RaO.MgO and SrO
iv. Products, metal oxides, and composites; Li/CaO, KF/ZnO, basic hydrotalcite of Mg/Al, Li/Al
v. Sulfur dioxides
vi. Ion exchange resins
vii. Catalyst for carbon-based composites
viii. Catalysts made of biological enzymes
ix. Composite catalysts made of boron.
x. Catalyst made from waste products.

Depending on the number and strength of active acid or main sites, they are extremely active, selective, and water-tolerant [81]. However, the production paths for biodiesel and bioethanol limit the use of heterogeneous catalysts in those processes (i.e., it favors the application of homogeneous bases in the fermentation of sugars and transesterification).

Heterogeneous catalyzed biodiesel production has emerged as a preferred route because it is environmentally friendly, requires no water washing, and product separation is much easier, and thus has a significant positive impact on the production of better biofuels (high energy density and fuel property compatibility). There are various important heterogeneous catalysts that have found use in pyrolysis, gasification, and catalytic upgrading of aqueous phase sugar processing, hydrotreatment of vegetable oils, and related feedstocks [74]. In this case, heterogeneous catalysts are pertinent, i.e., they are used appropriately and serve the required purposes.

Additionally, catalyst aids formation of gasification products. They increase conversion effectiveness, enhance gas quality, and lower tar content. Common gasification catalysts include dolomite, alkaline metal oxides, and oxides based on nickel. The importance of Fe, Co, ruthenium, and K catalysts in the FT synthesis of biofuel in liquid from biosyngas is well documented [30]. The effectiveness of various catalysts varies, though, and the choice of one depends on the desired end product and the catalyst's characteristics and reaction routes [30]. Catalysis has emerged as a key step to producing renewable chemical energy in recent years. Catalyst function has been demonstrated by the production of furan derivatives from biomass sugar in recent years, which have been used as alternatives to chemicals derived from crude oil or as building blocks for the synthesis of new products such as composite materials, metal casting, degrease metal, macrocyclic ligands, resins, agrochemicals, pharmaceuticals, liquid fuels, or solvents [29] and [82]. The commercialization of processes in which catalysts are used for biomass conversion to functional chemical additives has not been actualized. However, research is still going on in this area to improve these catalysts' selectivity and conversion efficiencies.

Furthermore, with recent improved research in the area of green chemistry, the choice of catalyst to be selected in biomass conversion should be the one that is cheap,

recoverable, and eco-friendly. Also, multipurpose catalysts derived from natural sources should be prioritized in catalytic chemistry. As a result, many reaction steps can be carried out in a single reactor without the need for pricey intermediary separation procedures. And also, the efficient recovery and separation of the desired products and the recycling of catalysts are crucial to catalytic research in general and biomass catalytic conversion. These, however, are complicated by the insufficient knowledge of the structure–property relationships of catalysts and the precise mechanisms underlying biomass conversion reactions, as well as the process compositions, catalyst optimization, and development, particularly for industrial scale production [29].

5.2   Technologies for Converting Biomass

Energy generation and environmental remediation were the two primary goals of biomass conversion technology. The toxic effect of released gases from the combustion of fossil fuels prompted the search for a low-cost and environmentally friendly alternative to energy generation. The use of readily available large biomass waste that constitute a nuisance to the environment is one approach that meets two objectives (energy generation and achieving of an environment cleaner and safer to live).

The two basic mechanisms for digesting biomass are biochemical and thermochemical reactions. Thermochemical pathways are frequently more efficient than biological routes due to their faster reaction times and greater capacity to break down the organic components of biomass [33]. The bulk density, MC, particle size, and intermittent availability of biomass conversion feedstock can all vary substantially. As a result, modern industrial technologies and fossil fuels are usually coupled so that in the case of a disruption in biomass supply, the fossil fuel serves these purposes (preheating, drying, and fuel supply maintenance) [83].

Different techniques are used to convert biomass into various energy sources. The quantity, kind, biofuel product, feedstock qualities, economic situations, legislation, and environmental requirements all play a role in selecting an appropriate conversion procedure [71]. The feedstock's desired energy form and accessibility are two important factors.

Biomass conversion into fuels, additive chemicals, and thermal energy materials is governed by three important processes. There are three types of chemical reactions: biochemical, thermochemical, and physicochemical. There are four main processing possibilities in the thermochemical pathway, which are outlined in (i–iv):

Combustion
Gasification
Pyrolysis
Liquefaction.

While the biochemical pathway consists of two primary processes (i–ii):

Anaerobic digestion
Fermentation.

The physicochemical route consists primarily of extraction followed by esterification, whereby oils are obtained from the hydrocarbons [70].

The listed biomass conversion methods are suitable for producing energy in the form of chemical/fuel, heat, and electrical sources. These processes can generate liquefied fuel (transport fuels), biochar, and gaseous fuels (H_2, biogas, producer gas). The bioconversion of biomass predominantly yields biofuels, which are roughly categorized into four types and include bioalcohols, biodimethyl ether, syngas (bio-CH_4), FT fuels, and hydrogen (Table 2) [84]. Burning biomass to generate heat and power, converting it to gas-like fuels (CH_4, H_2, and CO), or turning it into liquid fuels are the three main ways to use biomass (biofuels). Currently, biomass energy accounts for about 4% of all energy utilized globally, compared to 12% from coal, 15% from gas, and 14% from electricity [34].

Simple sugars, lipids, starches, and vegetable oils are the primary raw materials used to make first-generation biofuels with commercialized methods. The second-generation biofuels, made mostly from lignocellulose biomass such as non-feed crops, forest leftovers, and household, agricultural, and industrial wastes, were developed in response to the debate between food and energy. The second-generation biofuels still need a lot of arable lands to grow the feedstock crops while having resolved the contentious food versus fuel dilemma faced by the first-generation biofuels. Consequently, food development is hindered, and a dispute similar to that around first-generation biofuels is implicitly imposed.

As described in Table 3, the third-generation biofuels that use algae and seaweed are grown on barren ground, marshy terrain, and sea waters overcome these concerns. These innovations are still being developed. The conceptual stage of the fourth-generation biofuel technology is still ongoing. They are designed to be made using technologies that successfully convert biomass into fuel, consuming more CO_2 during production than is created during usage or burning. As a result, these biofuels would be crucial in reducing gases responsible for global warming, which would help to mitigate climate change. They are produced by genetically modified algae, a carbon-negative energy source, with improved hydrocarbon yields, which results in the creation of an artificial carbon sink [84].

The majority of second-generation biofuels are produced utilizing biothermochemical methods from lignocellulosic sources. The procedure's first thermochemical processes include gasification and/or pyrolysis, which are then followed by gas conditioning, cleaning, and FT synthesis to produce synthetic liquid fuels. According to the biochemical process, the cellulose and hemicellulose components of biomass are first broken down enzymatically into their unique sugars, which are then fermented to make bio-C_2H_5OH. Despite having a lower likelihood of being commercialized than the previous technology, this has a significant future cost reduction potential [81]. While biological processing works with lower efficiencies and

extremely slow reaction times (days, weeks, etc.) and is unable to completely break-down the majority of organic compounds in biomass, such as lignin, thermochemical processes work with higher efficiencies and faster reaction times and can completely decompose a lot of the organic compounds in biomass [70]. The pyrolysis, gasification, and hydrothermal processing of biomass are the three current thermochemical conversion pathways for producing fuels and chemicals discussed in the next section.

6 Thermochemical Conversion

Techniques commonly used to convert biomass or their wastes into higher calorific value fuel by increasing the energy density of the biomass, lowering its oxygen content, adding weight to the resulting hydrocarbon fuel, and creating carbon–carbon bonds are termed thermochemical conversion [84]. In addition to immediately generating sustainable energy from biomass, these processes yield more practical, portable, and energy-dense forms of energy carriers (-OH fuel, synthetic gases, light hydrocarbon, and so on) while preserving controlled temperatures and oxygen conditions [83]. They are influenced by the selected biomass feedstock, its ultimate properties, proximate properties, and the process operating parameters, and these factors are determining factors in thermo-converted product distribution and quality [35]. The end products of biomass thermochemical processing are typically categorized as the volatile and non-volatile fractions. The gases, vapor, and tar make up the volatile fraction while char or residual ash makes up the non-volatile component [30], and they usually take the form of the three states of matter with par or equivalent ecological and industrial significance [69].

Biomass can be thermochemically converted via processes listed below (i–v) and Fig. 5:

Combustion
Gasification
Pyrolysis
Torrefaction
Liquefaction

Pyrolysis begins with any type of thermochemical conversion. These techniques liberate the energy store organic chemical energy in biomass by turning it into solid (charcoal), liquid (bio-oils), or gaseous fuels (synthetic gas) via pyrolysis, gasification, or liquefaction, as well as direct heat via combustion or co-firing. The most profitable of the listed thermochemical conversion processes is the one with the greatest potential for future advancement, producing higher yield intermediate energy carriers such as liquid or gaseous intermediate energy carriers [70]. Gasification is the most successful and economical method for producing bioenergy from lignocellulose biomass [84].

Variations in these processes' operational parameters, such as heating rate in °C/min, vapor residence time, reactor configuration, cause these processes to occur.

Biomass waste pyrolysis products exist in three states of matter: solid (biochar), liquid (pyro-oil), and gas (syn gas). The distribution of these products is determined by the feedstock used, pretreatment techniques, and pyrolyzer operating conditions. In most cases, fast pyrolysis techniques are used to achieve a maximum yield of bio-oil, which operates at a high heating rate (i.e., 1000 °C/s) suitable for achieving 60–70 wt% bio-oil, 15–25 wt% biochar, and 10–15 wt% syngas [85]. At lower heating rates and slower pyrolysis rates, all products (biochar/oil/gas) are capable of providing energy to sustain and drive the pyrolysis process.

A heated sand medium in an oxygen-deprived system quickly heats the biomass waste to the target pyrolysis temperature (450 °C -500 °C) to produce biochar, bio-oil, gas, vapors, and aerosol that exit the reactor via the conveying fluiding gas stream in a fluidized bed pyrolyzer.

A vacuum pyrolyzer is made up of stacked heated circular plates. A vacuum pump maintains a vacuum, which lowers the boiling point of gas products and prevents adverse chemical reactions. The top plate is around 200 °C, while the bottom is around 400 °C. Scrappers transport biomass from the top plate to successive lower plates. While moving across the plates, the biomass is dried and pyrolyzed. In this pyrolyzer, no carrier gas is required. When the biomass reaches the lowest plate, only char remains. The heating rate is relatively slow here, and vapor residence time in the pyrolysis zone is short. As a result, the liquid yield in this process is relatively low, ranging from 35 to 50% on dry feed, with a high char yield.

The longer the vapor residence time in a pyrolyzer, the more bio-oil is formed from the biomass.

Biochar, a solid by-product of pyrolysis, is widely used in soil management techniques to sequester carbon. Flue gas and syngas, which can be burned to provide heat and electricity or used as a feedstock for FT synthesis, are the primary products of the gasification process [35]. Only the production of liquid fuels under high pyrolysis pressure in various solvents like H_2O, CH_3COCH_3, CH_3OH, or their mixes is the focus of the liquefaction process (hydrothermal) [19]. The structural components of biomass (cellulose, hemicellulose, and lignin) thermally depolymerize and decompose, producing chemicals in the form of liquids, gases, and residual solid charcoal. Numerous compounds, including benzene, ethanol, isobutanol, methanol, 3-Pentanol, Butan-1-ol, 2-methylbutan-1-ol, and ethanol are present in bio-oil [15]. The process heating rate and temperature significantly impact these compounds' chemical make-up. Syngas (H_2 & CO), CH_3OH, dimethyl ether, C_2H_5OH, mixed alcohols, C1-C4 gases, hydrocarbons, FT liquids, styrenes, oxygenates, C_6H_5OH, cyclohexane, biphenyls, substituted C_6H_5OH, cresols, catechols, eugenols, resorcinols, syrinols, guaiacols, etc. are obtainable from biomass thermochemically converted.

6.1 Pyrolysis

In a system deprived of oxygen, thermal degradation of biomass is termed pyrolysis, which occurs at a temperature range of 350–450 °C to produce char, pyrolytic oil,

and non-condensable gas [33]. The variation in the distribution of pyrolysis products depends mainly on the process temperatures, residence times, and particle size distribution. Because of the composition of biomass, pyrolysis is a complex reaction. To achieve fast pyrolysis, it is critical to use a small but not extremely small particle size of biomass in order to achieve a kinetically controlled system at particle size of < 1 mm and low heating rates. Maximum yield of bio-oil can be achieved in fast pyrolysis with biomass particle size of < 1 mm. The higher the temperature, the faster the biomass composition is broken down to yield bio-oil and gas. At low temperatures (slow pyrolysis), a large amount of char is produced; as temperature rises, the char degrades further to produce bio-oil; and at higher temperatures (550 °C–650 °C), gas yield is significantly enhanced. Higher vapor residence time in the pyrolytic chamber favors higher gas yields. It means gas production is principally favored at higher temperatures and extended vapor (hot) residence times. The need for high-quality and large quantity bio-oil is favored by a short residence time, and lower temperature < 550 °C while temperature below 350 °C favors the large generation of charcoal [15]. The process condition or the modified process conditions determines how much of these three essential products are generated via pyrolysis [70]. This method produces fuels with high fuel-to-feed ratios, making it the most effective method for converting biomass. Additionally, the CV of biofuel products is optimized using thermal and catalytic processes. In comparison to other thermochemical conversion processes, pyrolysis offers a broader perspective and prospects for biomass valorization, which involves adding value to biomass wastes such as starch wastes, rice husk, corn husk, algae, grass, municipal waste, animal wastes, and so on by converting them to an energy source or biofuel and is roughly divided into two groups (i–ii): fast, slow, which are based on the operating circumstances [35]. In all practical thermochemical biomass conversion processes, pyrolysis is a key factor in reactor design, reaction kinetics, and the determination of product distribution, characteristics, and composition [30]

The four main pyrolysis-based processes (i–iv):

Slow pyrolysis and syngas upgrading
Fast pyrolysis and hydroprocessing
Catalytic pyrolysis and hydroprocessing

Hydropyrolysis and hydroprocessing, which are generally to provide transport fuels [86]. The combined hydrocracking and hydrotreating procedures are referred to as hydroprocessing. The quantity, kinds, and quality of the produced products are strictly controlled by the chemical make-up of selected biomass feedstock and the pyrolysis temperature [69]. The initial breakdown of the solid biomass species during pyrolysis results in char, light gases, and secondary tar, as well as the secondary reactions of the condensable volatile organic compounds. Pyrolysis of biomass in a thermogravimetric analyzer runs to the highest temperature of 700 °C, but most metallic components of this biomass degrades at higher temperatures, and also combustion and gasification occur at higher temperatures as compared to pyrolysis. Additionally, it happens at lower pressures (0.1×10^6–0.5×10^6 Pa) as opposed to hydrothermal liquefaction, which occurs at pressures between 10 and 25 MPa [35]. A key factor

in determining the distribution of pyrolysis products is temperature. Most of the products are made between 352 °C and 452 °C. As pyrolysis temperature increases, the breakdown of heavy molecules in the liquid and remaining solid enriches the gaseous portion with lighter molecules. High T (°C), a high heating rate (°C/min), and a short residence T(s) result in high liquid production. A long residence time, a moderate heating rate, and low temperatures encourage char formation. The production of charcoal is reduced as the temperature rises. High temperatures, a prolonged gas residence time, and a rapid heating rate are used to produce fuel gases [30].

The biomass components are typically thermally cracked into gases and vapor using heat from the outside, which leads to a vast spectrum of products [70]. Many variables influence performance, product kinds, distribution, and quality of biomass pyrolysis. Particle shrinkage and moisture content are a couple of them, as well as reactor design, catalysts, additives, and physicochemical characteristics like thermal conductivity and emissivity, permeability and density, specific heat capacity, and heat of reaction. Therefore, the variation in the parameters listed above will determine the outcome of any pyrolysis type [35]. The high interest in pyrolysis is due to its technological versatility, operational adaptability, and suitability for a wide range of biomass streams and products [70].

The pyrolysis technique is characterized by short hot vapor residence in 2 s, a high heating rate, and an overall rapid reaction time. It occurs at moderate temperatures of roughly 500 °C. The biomass is rapidly broken down into vapor, aerosols, biochar-coal, and gas. The process is best suited to obtain dark brown liquid bio-oil after condensing the syngas [70]. The process produces a lower amount of biochar when compared with slow pyrolysis [33]. Small particle size is also needed to achieve fast pyrolysis because the pyrolyzer is designed to remove any remaining vapor to avoid coming in contact with the hot feedstock particles again.

The following reactor types (i–iv) can be used for fast pyrolysis [35]:

Fluidized bed reactors
Ablative reactors
Vacuum reactors..
Stirred or moving bed reactors.

The acceptability of fast pyrolysis is due to its tremendous economic benefits. It produces liquids that can be utilized as energy carriers, fuels for transportation, and fuels for storage and energy. In this type of pyrolysis, about 60–70 w% pyrolytic oil, 15–25 w% biochar, and 10–20 w% non-condensable gases are produced. To optimize pyrolytic oil obtained from bio-oil, it is necessary to have conditions such as: low T (°C) high heating rate (°C/min), and short gas residence T(s), while high temperature, long residence time, and low heating rate are necessary to increase gas output [30]. However, rapid heating and quenching cause intermediate pyrolysis liquid to condense before its heavier elements break down into gaseous products [30] and [69].

The following are the salient characteristics of fast pyrolysis for pyrolytic oil products (high yields):

Biomass sieve to a diameter < 5 mm for quick volatilization and rapid heating.

A brief (2 s) vapor residence duration to reduce subsequent reactions.

For maximum liquid yields, a regulated reaction temperature of about 500 °C.

For biomass to ignite quickly, its moisture level must be < 10 w%, as all of the water from the feed's pyrolysis processes settles in the liquid phase with the feed.

Heating and heat transfer rates should be highly rapid at the interface of biomass particle reactions. Due to its poor thermal conductivity, this requires biomass that has been processed to a fineness of less than 3 mm. The rate-limiting phase in this process is the particle heating rate.

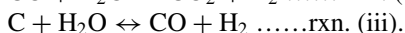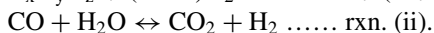Quick removal of char to reduce vapor cracking.

The production of bio-oil through the quick cooling of pyrolysis vapor and aerosols.

Mass and heat transfer processes, pyrolysis kinetics, and phase transition phenomena are critical since fast pyrolysis for liquids happens in a matter of seconds.

The ability to predict the maximum pyrolytic capacity of a pyrolyzer and feedstock used is known as mass transfer, and the ability to predict the temperature/exit temperature to achieve this is known as heat transfer. It is critical to subject biomass to thermogravimetric analysis at various heating rates in order to confirm the thermal degradation pattern. The results of this analysis can be used in kinetic analysis to obtain useful parameters such as activation energy value (Ea), free energy G of the pyrolysis process, and so on. Understanding the thermal degradation pattern of biomass will reveal the state changes (solid–liquid–gas). Because fast pyrolysis is intended to produce a large amount of high-quality bio-oil, temperature data is critical. Thus, it is crucial in this process to quickly raise the reacting biomass particles to the ideal process temperature and reduce their exposure to lower temperatures (for the generation of charcoal) and higher temperatures (for thermal cracking) [70]. Fluidized bed reactors are primarily used to do this. For fast pyrolysis, reactors with bubbling fluidized beds, circulating fluidized beds, ablative flows, entrained flows, spinning cones, and vacuum reactors are frequently utilized [33].

Fast pyrolysis has the tendency to produce H_2 gas through steam reforming and water–gas shift processes. Study [87] used steam reforming of biomass pyrolysis oil to produce hydrogen (H_2). They carried out a steam reforming experiment on a bench-scale fluidized bed unit. The tubular reactor was heated electrically from the outside. 250 g of catalyst were loaded into the reactor. The researchers used Su d-C11-NK Chemie's catalyst commonly used for naphtha reforming and other four laboratory formulations catalyst which contains Ni, K, Ca, and Mg supported on alumina. These catalysts were first activated in an H_2/N_2 environment at 850 °C for about 2 h prior to the reforming reaction. Superheated steam, which is also a reactant in the reforming process, was used to fluidize the catalyst. Pyro-oil was loaded at the rate of 84 g/h through a temperature-controlled injection nozzle and sprayed as very fine droplets on the catalyst. A cyclone and a hot-gas filter were used to collect fine catalyst particles and possibly char generated in the reactor. The fluidized bed unit was incorporated with two heat exchangers for condensing the excess steam and obtained condensate weight was constantly monitored. A mass flow meter and a dry test meter were used to measure the outlet gas flow rate. Infrared spectrometer and a microgas chromatograph were used to measure the concentrations of hydrogen gas

(H_2), carbon oxides (CO_2 & CO), light hydrocarbons (CH_4), ethane ($CH_2 = CH_2$), and N_2 in the reformed gas. For all the catalysts, H_2 gas volume percentage in the product gas was around 70 vol.%, and the yield was 70–80% of the stoichiometric potential. The reaction sequence is as described in reactions (i-iii) below[87]:

$C_xH_yO_z + (x - z)H_2O \rightarrow xCO + (x + \frac{y}{2} - z)H_2$ ……. rxn.(i).

$CO + H_2O \leftrightarrow CO_2 + H_2$ …… rxn. (ii).

$C + H_2O \leftrightarrow CO + H_2$ ……rxn. (iii).
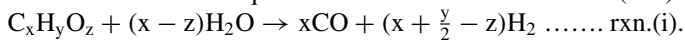
The processes entail the conversion of CH_4, straightforward aromatics, various hydrocarbon vapors (C_2-C_5), and others that are primarily converted into H_2 gas. Generally speaking, steam reforming turns hydrocarbons into CO and H_2, and the CO then reacts with water to create H_2 and CO_2 [33]. Although it has been commercialized for the manufacturing of chemicals, the technology is still being worked on for the generation of liquid fuels. Lab-scale fast pyrolysis techniques have higher energy efficiency and comparatively lower capital cost than other thermochemical conversion methods [30]. Lab scale has small-scale size pyrolyzer reactor, hence heat transfer is effective throughout the reactor, and the smaller size dictates lower cost when compared to industrial pyrolyzer. The drawbacks of lab-scale fast pyrolysis are that the samples must be heated at high rates (around 200 °C/min), necessitating the use of high energy heating elements, and the small reactor size can only accommodate a limited amount of feedstock, resulting in a low bio-oil yield. An external energy is required to achieve fast pyrolysis which means the process itself is an endothermic reaction. The external heat supply degrades polymers (hemicellose, cellulose, and lignin) at different temperature.

Liquids and gases are by-products of slow and intermediate pyrolysis, which focuses on the production of biochar. The process is characterized by longer vapor residence time and greater particle sizes compared to fast pyrolysis, and it takes place at low temperatures with mild heating. It is a well-known process that frequently occurs in the conventional charcoal kiln between 277 and 677 °C [69]. The most often used slow pyrolysis technologies include agitated (i–iv) [35]:

Drum kilns
Huge retorts (continuous or batch)
Rotary kilns
Screw pyrolyzers.

Slow pyrolysis is frequently used to decrease the amount of waste that needs to be disposed of and to lessen the adverse environmental effects of waste. Additionally, pyrolysis has been utilized for centuries to produce charcoal; nevertheless, it wasn't until recently (within the past 35 years) that rapid pyrolysis for the creation of liquids was created [70]. The petroleum equivalent of bio-oil is produced by the flash pyrolysis process, which runs at temperatures between 777 and 1027 °C and has a yield efficiency of up to 70%. Along with producing pyrolytic water, this procedure also has significant drawbacks. This bio-crude oil can be utilized as refined fuels for the production of heat and electricity or directly as fuel in boilers, motors, and turbines [69].

6.1.1   Energy Application of Pyrolysis Products

. The production of solid (char), liquid (tar), and gaseous products by the pyrolysis of biomass is a well-known process that can replace or provide an alternate energy source to fossil fuels. The liquids can either be catalytically transformed into liquid transport fuels or used directly as liquid fuels for boilers, diesel engines, and gas turbines to generate heat and power. Through catalytic cracking and hydrogenation, its oxygen content may need to be reduced and its alkalis content eliminated for other applications [30] and [69]. It mainly produces volatile materials or flue gas that is high in carbon. The flue gas is typically utilized to produce hydrocarbons, solvents (acetone, methanol), and power. Chemicals like CH_3COOH and levoglucosan, which can be converted into motor fuel or burned to produce energy, are abundant in the bio-oil component. The char could be used as activated carbon in industrial applications, slurry fuel, or soil enrichment agents [35].

In all thermochemical conversion processes, pyrolysis is crucial to determine reaction kinetics, reactor design, and the assessment of product distribution, composition, and characteristics [69].

6.1.2   Biomass Pyrolysis Oil

Pyrolysis oil is dark brown in color, a mixture of complex compounds with unknown quantification of the exact chemical composition. Its components are organic classes: hydrocarbon, aldehyde, aromatic, organic acids, ethanol, methanol, C_6H_5OH, anhydrosugars such as levoglucosan, pyrolytic lignin (a guaiacyl- and a syringyl-based fragment of the original polymeric lignin), and a limited amount of H_2O make up the majority of their chemical make-up (about 25%). Two distinct phases make up the pyrolysis liquid (i-ii) [30]:

An aqueous phase which is majorly organo–oxygen compounds of low molecular weight,

e.g., (higher CH_3OH, CH_3COOH, and acetone ratios).

ii. A non-aqueous phase that is primarily made up of high-molecular-weight insoluble organics called tar or bio-oil (aromatics).

A liquid mixture of oxygenated molecules with carboxyl, carbonyl, and phenolic groups makes up the bio-oil component of the pyrolysis products. Its chemical and physical composition differs significantly from that of fuels obtained from petroleum. Still, bio-oil is highly similar to the original biomass, making it difficult for pyrolytic oils to use as a substitute for fossil fuels. The chemical constituents of bio-oil are the same as those of the biomass from which it was derived [15]. The high water content of bio-oil content must be reduced before it could be suitable as engine fuel.

Components distribution in pyrolytic oil (i–vi):

About 20–25% H_2O
25–30% H_2O-insoluble pyrolytic lignin
5–12% organic acids

5–10% anhydrosugars

5–10% of non-polar hydrocarbons

10–25% oxygenated compounds.

Their low energy density is due to the water content of bio-oils, which decreases the flame temperatures of the oil, results in ignition problems, probable injection problems, and early oil evaporation during preheating. They are very polar and readily absorb over 35% water, in contrast to non-polar, insoluble petroleum oils. They also have a low heating value of 16 MJ/kg as opposed to 43 MJ/kg for ordinary diesel fuel because of their oxygenated nature and water content. The oils' pH range of 2.5–3.0 contributes to their mildly acidic nature. Additionally, compared to their petroleum equivalents, oxygenated bio-oils have significantly higher kinetic viscosities and densities [30].

Pyrolytic oils are typically used as fuel for boilers and turbines to produce heat energy and electricity. Through thermal or catalytic cracking, they can also be upgraded into transport fuels, or they can be used to produce useful chemicals and organic solvents. Bio-oils' low volatility, high viscosity, corrosiveness, and coking have, however, limited their applicability thus far.

Bio-oil does not dry off easily (low volatility); if directly used as engine fuel, large residue of carbon will be left in the ignition part of the engine.

One of the properties of fluid is viscosity, and for pyrolytic oil, its kinematic viscosity is the parameter usually measured at 40 °C. There is tendency for bio-oil viscosity to change during storage because of phase separation of its components (water and oil). Based on standard, bio-oil that could be use as fuel should have maximum viscosity is 125 cSt (or mm^2/s) (ASTM D7544) while the standard viscosity of pure biodiesel is between 1.9–6.0 cSt (B100 and ASTM D6751). The composition of is bio-oil complex which depends on its source [15], i.e., the biomass and its water content which is responsible for variation in bio-oil viscosity. Addition of alcohol, e.g., small amount of CH_3OH, will decrease the rate of viscosity increase during storage.

Bio-oil derived from biomass pyrolysis was extremely corrosive to carbon steel and 214 Cr - 1 Mo steel, and some of the bio-oils corroded 409 stainless steels significantly. X-ray diffraction (XRD) analysis was used to identify compounds formed on the surface of the corroded carbon steel and 214 Cr - 1 Mo steel, which confirmed a hydrated form of iron formate. The study confirmed that formic acid is a significant corrodent in bio-oils, but it is almost certainly not the only corroding species, as evidenced by the lack of a direct correlation between formic acid concentration and measured corrosion rates [88].

SS410 alloy specimens were immersed in pyro-oil containing varying concentrations of four –COOH compound. Corrosion exposures revealed a linear relationship between the amount of formic acid added to the bio-oil and the amount of SS410 mass loss, indicating that formic acid is the most aggressive of the four acids tested [89].

Coking of bio-oil occurs during thermal cracking; coke has higher oxygen content than raw bio-oil and appears spongy [90].

Levoglucosan, furfural, HCOOH, guaiacol, cyclopentanone, CH_3COOH, methoxyphenyl, CH_3OH, CH_3COCH_3, C_6H_5OH, and their alkylated phenol are a few examples of these. The following chemical groups, as well as the minimum and maximum weights of the compounds that might probably be produced from fast pyrolysis oils, are listed in the study [30]): acids, ketones, aldehydes, aromatics, etc. that are organic.

6.1.3 Types of Pyrolysis

i   Slow pyrolysis is a thermochemical reaction typically occurring at 400 °C or lower. The three pyrolytic products are all used, although biochar is the most frequent. If some charcoal or oil is burned together with the pyrolytic gas, the heating process can be continuous and self-sufficient. This will give the reaction all the energy it needs to move forward. The heating process is often sluggish and low-rate, releasing gases with very little bio-oil. There is excellent potential for slow pyrolysis to produce biochar [16]. Due to a few process limitations, slow pyrolysis is not the best method for creating high-quality bio-oil. Data from Nigerian forestry and wood processing show that as of 2010, biomass wastes from solid and dust from logging, sawmilling, plywood, and particle board manufacturing totaled 65,753,628 m^3 [65]. This might have been converted into charcoal through slow pyrolysis, providing clean energy for factories and peasants' boilers.

ii. Fast pyrolysis: This method is typically used at 500 °C and a heating rate of 1,000 °C/s [16]. In a compartment with low oxygen levels, the pyrolyzer elevates the temperature of the biological materials to a high level. It occurs at a quick heating rate, which causes a substantial heat transfer to produce vapor with a short residence period, swiftly cooling and yielding a sizable volume of bio-oil [23]. The pyrolyzer uses this method to produce syngas, continuously burned to keep the system temperature constant. Fast pyrolysis can produce 15 to 25% char, 60 to 70% of pyrolytic liquid, and only 10–15% of pyrolytic gases; however, this mostly depends on the feedstock. Production of pyrolytic liquid for use as fuels, specialty compounds, and industrial chemicals has been a prominent application of fast pyrolysis technology. Agricultural waste, widely available in Nigeria, can also be used to extract bio-oil, the main by-product of this process, and transform it into biofuel. According to a study by [91], Nigerian maize cobs have an excellent potential for producing bio-oil, which may be used to generate electricity.

iii Flash pyrolysis, a procedure that can create up to 75% of the bio-oil produced, can be used to produce the gas, bio-oil and char [24]. The biomass is rapidly devolatilized in an oxygen-free chamber with a gas residence time of < 1 s, a suitable high heating rate, and reactor temperatures in the range 450 °C–1000 °C [92]. Although this method generates a lot of bio-oil, it has significant techno-logical restrictions. Flash pyrolysis has some technological limitations which include: poor thermal stability, char formed has catalytic properties that activate

the bio-oil to produce a more viscous bio-oil that sometimes contains some solid residues.

The produced pyrolysis oil has low heat stability, tendency for iron rustiness, incorporation of particles in the oil, produced char acts as catalyst reducing oil lubricating value over time, production of alkali in bio-oil, etc. [93].

iv. Vacuum pyrolysis: In a vacuum, this form of pyrolysis occurs at lower pressure. Vacuum pyrolysis was first carried out in 1914 [94]. By removing the primary volatile products from the heated part of the pyrolyzer chamber, this type of pyrolysis slows down the breakdown processes that come after [95]. According to [96], inhibiting the cracking process and recondensation lowers gas production.

v. Catalytic pyrolysis: This process, which produces primarily liquid that can be utilized as fuel or valuable compounds, occurs in an oxygen-deficient environment at moderate temperatures (about 500 °C), a high heating rate, and a brief residence period. This strategy has the best possibility of resolving the problems with polymerization, corrosion, low heat stability, and high viscosity that liquid pyrolysis products have. Additionally, it facilitates the handling and transportation of these liquid items [30]. A catalyst's effects during a pyrolysis process can include cracking reactions and upgrading biomass products, depending closely on the catalyst type and reactor design. Pyrolysis vapor is catalytically broken over a range of catalysts to create a variety of liquid and gaseous fuels. By reducing the oxygenates in a particular pyrolysis oil with the help of zeolites catalysts, the energy content of the oil is decreased [35]. In addition to promoting the synthesis of high-value products (hydrocarbons) that can raise the value of bioheating oil, catalysts are frequently employed to reduce oil viscosity, minimize the corrosiveness of bio-oil (by reducing carboxylic acid formation), and ultimately. Catalysts alter the pyrolysis procedure as illustrated below [35]:

i. Might cause a significant decrease in the temperatures at which biomass constituents decompose.

ii. Affect reaction networks as well as multifunctional phenols, which are precursors to polymerization and are used to stabilize bio-oil (deoxygenation).

iii. There is a chance that CO, CO_2, and H_2O will be emitted during the decarboxylation, decarbonization, and dehydration reactions.

iv. Promote coke production through dehydration procedures (mostly due to the very acidic catalysts).

6.2 Gasification

In the presence of gasifying agents like O_2, air, steam, CO_2, or their mixtures as well as impurities like nitrogen, sulfur, tars, and alkali compounds, the gasification process transforms carbonaceous materials (coal, petroleum coke, biomass, etc.) into combustible gases (CO, H_2, CO_2, CH_4, etc.) and trace amounts of light hydrocarbons

[33]; [86] and [97]. Syngas is the ultimate by-product after the production of bio-oil, an intermediate. In conjunction with a catalytic or chemical upgrading facility, the conversion unit frequently transforms syngas and bio-oil into usable biofuels and chemicals [84]). The process of partially oxidizing biomass at high temperatures to produce mostly gaseous products with very little tar and ash is known as "biomass gasification. "According to the gasifying agent, the gasification process is typically split into groups: steam, air, airstream, steam-oxygen, oxygen-enriched air, etc. [30]. Temperature increases favor gas production. Recently, advanced gasification techniques have been used for plasma gasification [61] and [70] and supercritical water gasification to break down biomass into primarily H_2, CO, and CO_2.

Hydrodynamics, or how the gasifying agent interacts with the solid fuel, operating circumstances (temperature, pressure, etc.), and the gasifying chemicals used by different biomass gasifiers all differ (air, oxygen, or steam).

Common types of gasifiers.

Entrained flow.

Fluidized bed.

Fixed-bed (updraft, downdraft, or cross draft).

The fixed-bed gasifiers are the most appropriate of these gasifiers [33] and [61]. The type of fuel, its properties (such as moisture content, particle size, density, ash content, and toxicity), how oxygen is delivered, and the type of combustion bed all affect how these gasifiers are constructed [69]. Supercritical water gasification (SCWG) is a highly effective method for converting high moisture biomass materials like algae, manure, olive mill water, sludge, etc. into H_2 (with little tar) [84].

6.3 Biomass Gasification Mechanism

Depending on the process temperature, this technology converts organic feedstock (solid fuel or liquid) into gases. Syngas is a gaseous mixture primarily made up of CO, H_2, CH_4, and CO_2 with traces of tar and ash at temperatures above 1200 °C and below that. The effectiveness of the process and subsequent end-use are adversely affected by potential gasification by-products including tar and ash [70].

When the carbon in the feedstock material is partially oxidized in the presence of gasifying carriers (air, oxygen, steam, or CO_2), char is created. Char is a mixture of ash and unconverted carbon [59]. The inert component of the processed biomass is called char, which is the unconverted organic fraction. Producer gas, also referred to as syngas, is a gaseous mixture of nitrogen, light hydrocarbons (ethane, propane), heavy hydrocarbons (tar), methane (CH_4), carbon monoxide (CO), carbon dioxide (CO_2), and hydrogen (H_2). It condenses at temperatures between 250 and 300 degrees Celsius. Some of the contaminants include tar, particulate matter, alkalis, halides, sulfur, hydrogen sulfide (H_2S), chloridric acid (HCl), and inert gases like nitrogen (N_2). The amounts of each component, as well as ash and unconverted carbon, are influenced by the kind of biomass used as feedstock, the gasifying agent, and the gasification process operating parameters [14, 69, 84].

Table 4 Typical gasification reactions

Reaction	Calorific value (Kj/mol)
$2C + O_{2(g)} \leftrightarrow 2CO_{(g)}$	+ 246.4
$2C + O_{2(g)} \leftrightarrow CO_{2(g)}$	+ 408.8
$CH_{4(g)} + H_2O_{(l)} \leftrightarrow CO_{(g)} + 3H_{2(g)}$	−206
$CH_{4(g)} + 2H_2O_{(l)} \leftrightarrow CO_{2(g)} + 4H_{2(g)}$	−165
$C + CO_{2(g)} \leftrightarrow 2CO_{(g)}$	−172
$C + H_2O_{(l)} \leftrightarrow CO + H_2O_{(l)}$	−131

The basic example of biomass gasification is lignocellulosic biomass, which when burned in an oxygen environment produces CO, CO_2, H_2, CH_4, light hydrocarbons, tar, charcoal, ash, H_2S, NH_3, and trace species [84, 30]. The many chemical reactions that take place during biomass gasification are listed in Table 4 [97].

Based on temperature ranges and reaction chemistry, the entire gasification process is separated into primary, secondary, and tertiary reaction stages. At temperatures lower than 500 °C, biomass is first converted into oxygenated vapor and liquid species with water and CO_2. At temperatures between 700 and 850 °C, the initial moisture and liquid species react to create CO, H_2, CO_2, water vapor, phenols, gaseous olefins, and aromatics. The tar is made up of mixed oxygenates, phenolic esters, alkylphenols, heterocyclic esters, and PAHs. Processes like methanation, steam reforming, cracking, and water–gas shift also take place in addition to the tars and residual gases. At temperatures between 850 °C and 1000 °C, the tertiary reactions result in liquid tar, water vapor, PAHs, CO, H_2, and CO_2 [84].

To achieve optimum gasification, it is necessary to effectively control the process requirements for the biomass feedstock's homogeneity, bulk density, moisture and ash content, particle size, and energy content [70]. The woody biomass is first dried at temperatures above 200 °C before being gasified. Char and vapor are created early in the pyrolysis process. The char and vapor are oxidized by the oxygen in this atmosphere, releasing pollutants such as sulfur, tar, NH_3, and others as a gaseous mixture of CO, H_2, CO, and H_2O [70]. The energy required for the biomass oxidation step is frequently supplied by an allo-thermal technique (energy from an external source) as well as an auto-thermal procedure (internal heating of the gasifier by partial combustion) [61]. The process of gasification is entirely endothermic. The process of converting biomass into gas involves the following crucial techniques [97]:

Exchange of air (exothermic): This is necessary to generate the thermal energy that the endothermic processes (as a whole) require and to maintain the system's required operating temperature. In the absence of oxygen, the fuel only partially oxidizes while maintaining the stoichiometric ratio.

Dried (endothermic): In this instance, the feedstock's moisture content evaporates and directly impacts heat production.

Around 150 °C is the temperature at which this process is completed.

i. Pyrolysis (endothermic): The breakdown of cellulose, hemicelluloses, and lignin occurs in biomass species between 250 and 700 °C, resulting in the generation of light molecules such as solids (char), liquids (tars), and gases (CO, H_2, CO_2, and light hydrocarbons) [30, 97]. Heat transfer, series reactions, and product diffusions are examples of process phenomena. At low temperatures, the reaction's kinetics is rate-limiting, but at high temperatures, the process is controlled by heat transfer or product diffusion.

ii. Decrease (endothermic): Here, char and other remnants from the earlier steps are reduced through a series of reactions to create the final syngas [97]. Full-scale biomass gasification typically takes place between 800 °C and 1100 °C, while systems requiring oxygen for the gasification stage usually operate between 500 °C and 1600 °C [59]. The reduction temperatures influence the final qualities of the syngas constituents and the solid residue. The gasification pathway offers the best potential for incorporating flexible primary fuel input concepts and product mix ideas that could achieve zero or even negative carbon emissions [83]. The method improves the use of biomass and uses gas turbine technology to generate biomass electricity more effectively and at lower investment costs. Because the gas turbine's waste gases are collected and used to generate steam for the steam turbine, combined-cycle gas turbine systems can reach higher efficiencies of up to 50% [24].

Almost all hydrocarbon molecules, including C_2H_5OH, CH_3OH, transport fuels, dimethyl ether (DME), methane, and high-value compounds, can be created from syngas after it has been treated. Using the Fischer–Tropsch process, catalyzed by transition metal-based catalysts (cobalt or iron) at a higher temperature, syngas can also be upgraded into biomethane for injection into the gas grid or transformed into synthetic diesel. Separated hydrogen can be used to power both fuel cells and batteries in electric vehicles. However, the final end-use of the syngas is significantly influenced by end demand and plant scale [70]. Hydrocarbon waxes and long-chain alkanes are also produced when the clean syngas is processed by the Fischer–Tropsch method over a cobalt, platinum, or iron catalyst [86]. These products need upgrading and purification, but doing so consumes a lot of energy, is expensive, and necessitates further research and development to make them more effective for use on a large scale [70].

Catalysts are needed for the production of gasification products. They increase conversion effectiveness, enhance gas quality, and lower tar content. Common gasification catalysts include dolomite, alkaline metal oxides, olivine, and Ni-based oxides. It is well known that the Fischer–Tropsch process converts syngas into liquid fuels like diesel and hydrocarbons using iron, cobalt, ruthenium, and potassium catalysts. However, while selecting a catalyst, the intended end product should be considered in addition to the catalyst's characteristics and the reaction pathways [30]. For partial tar oxidations, catalytic steam reforming, and the catalytic upgrading of the gasification products into liquid biofuels, dolomite- or Ni-based catalysts are widely utilized in gasifiers. This is frequently carried out after a successful gas cleaning and composition modification [70].

6.4 Pretreatments and Feedstock for Gasification

Cellulose, hemicellulose, lignin, and protein breakdowns for the softwood, hardwood, and straw gasifiable biomass feedstocks are provided in Table 5 [59]. Saccharides that polymerize into long strands are the biomass fibers (cellulose and hemicellulose). Lignin, phenolic polymers that link fibers and are essential for maintaining the structural rigidity of proteins, serves as the binding agent between the fibers. The majority of proteins are produced by herbaceous plants [59]. These energy sources can be divided into the following groups: Biomass blends, wood, leftovers, animal and human waste, contaminated and industrial waste, waste biomass, and agricultural and horticultural waste are only a few examples [84].

The goal of biomass pretreatment is that biomass feedstock must be consistent in size, composition, and moisture content (25–30wt%) for the gasification process to function correctly. Torrefaction and hydrothermal upgrading (HTU) are the two non-drying pretreatment techniques for gasification [59]. Torrefaction increases the potential for gasification of biomass by reducing moisture, hydrogen, and oxygenated molecules at temperatures between 200 °C and 300 °C in an inert environment without oxygen. It might increase the biomass's ability to withstand moisture and improve its heating value as a form of mild pyrolysis. The biomass feedstock's high moisture content and solid fibrous structure are lost during this process, increasing the material's energy density. Pelletization and torsion can both occur at the same time [59] and [84]. Bio-crude is produced by hydrothermal upgrading (HTU), which breaks down biomass using water as a solvent. The procedure is typically carried out in two steps: first, the biomass feed is treated in water at pressures of approximately 30 bars and temperatures of 200 °C to 300 °C, and then the biomass (bio-crude) is converted at pressures of 120–180 bar and temperatures of 300 °C to 350 °C for a variable time of 5 to 10 min. The resulting bio-crude contains a range of hydrocarbons that can be used to make chemicals, a fuel that is synthetically made to resemble diesel, or as a co-fuel in coal-fired power plants [33].

Table 5 Biomass feedstocks for gasification

Supply sector	Example
Forestry	Wood chips, wood blocks, and willow
Agriculture	Herbaceous plants such as miscanthus, reed canary grass, giant reed, oilseeds for methyl esters such as rapeseed and sunflower, and sugar plants such as maize and wheat for ethanol production
Industry	Straw, wet and dry manure, industrial waste wood, sawdust from sawmills, fibrous vegetable waste from paper manufacturers, and pruning of fruit trees and vineyards
Waste	Grass and pruning remnants from parks and gardens, organic elements of municipal solid trash, biodegradable garbage buried in landfills, landfill gas, and sewage sludge

6.5   By-products of Biomass Gasification

The type and composition of the fuel, the gasifying medium or gasifier design, the temperature, the operating pressure, the moisture content of the fuel, and the method of contact between the reactants (biomass fuel and gasifying agent) within the gasifier all affect the precise components of the products produced by biomass gasification. Therefore, it is impossible to ascertain the precise composition of the gas produced by biomass [30]. The highest quantities of tar and dust in hardwood, lowest levels of char in softwood biomass, and highest levels of hydrogen are produced by straw [59]. The characteristics of the feedstock, such as its moisture content, ash content, volatile matter, char, organic contents, thermal conductivity, and inorganic elements, have a considerable impact on gasification [61]. By-products of gasification may be solid or gaseous, frequently divided into a gas and a condensable phase. Less than one weight percent of char is present in the solid phase (ash), composed of inert feedstock components and unreacted char. Char is acceptable for direct industrial application because it contains more carbon than 76%. The gas phase in the gas/vapor phase (syngas) is constituted of an incondensable gaseous mixture of CO, H_2, CO_2, CH_4, light hydrocarbons, and some C2-C4 hydrocarbons as well as a negligible amount of NH_3, H_2S, and HCl, depending on the make-up of the feedstock. They can be burned to produce heat or power or used to produce chemicals, hydrogen, or liquid transportation fuels. Syngas' dry mass basis generation can range from 1–3 Nm^3/kg, and its low heating value (LHV) can range from 4 to 15 MJ/Nm^3.

In gasification, products formed are bio-oil, gas, and tar, but gas has the highest percentage. Table 6 presents a physicochemical comparison of pyro-oil and diesel fuel, and Table 7 presents tar classes [59].

Table 6 Physicochemical comparison of pyro-oil and diesel fuel

Physical Properties	Bio-oil	Diesel Fuel
MC	20–30 wt.%	0.1wt.%
pH	2.0–2.5	
Density	1.2 kgm^{-3}	0.94 kgm^{-3}
Ultimate Analysis (wt%)		
C	55–58	85
H	5–7	11
O	35–40	1
N	0–0.2	0.3
Ash	0–0.2	0.1
Gross CV	16–19 $MJKg^{-1}$	40 $MJKg^{-1}$
Viscosity	40–100 cp	180 cp
Biochar (wt.%)	0.1 -0.5	1.0
Vacuum distillation residue	Up to 50 wt.%	One wt.%

Table 7 Classes of tar

Tar Type	Type Name	Peculiarity	Characteristics Compounds
1	GC-undetected	Very heavy tars that are not GC detectable	calculated by deducting the total gravimetric tar from the GC- detectable tar fraction
2	Heterocyclic aromatics	Tars with heteroatoms and other highly insoluble in water substances	Phenol, dibenzo phenol, pyridine, phenol, cresol, quinolone, and isoquinoline
3	Light aromatics (1 ring)	typically thin, single-ring hydrocarbons that don't have any issues with condensability or solubility	Xylene, styrene, toluene, and ethylbenzene
4	Light PAH compounds (2–3 rings)	compounds with 2 and 3 rings condense at low temperatures even when their concentration is relatively low	Fluorine, anthracene, indene, naphthalene, biphenyl, acenaphthene, and phenanthrene
5	Heavy PAH compound (4–7 rings)	These compounds, which have more than three rings, condense at high temperatures and low concentrations	Coronene, pyrene, chrysene, perylene, fluoranthene, and pyrene

The rate of the process of synthesizing gaseous fuels from biomass is governed by the rate-limiting phase known as char gasification [59]. Bituminous oil is believed to exist as the condensable phase (tar), composed of various chemical components.

The European Board of Standardization refers to all organic chemicals present in syngas with established analysis methodologies as "tar" (a complex mixture of condensable hydrocarbons), with the exception of the gaseous hydrocarbons C1-C6. The tar composition is greatly influenced by the gasification procedure, the operating circumstances, and the biomass feedstock. They are normally grouped into five major classes based on their molecular weights (Table 7) [59]. Tar is a by-product of the pyrolysis process and is degraded and recombined during the gasification stage. Depending on how they form, they are separated into three groups: primary, secondary, and tertiary tars. The primary tars are formed immediately during the pyrolysis cycle and are dependent on the biomass intake. Due to the high oxygen concentration of cellulose and hemicellulose as feedstock, primary tars made of oxygenated chemicals (carbon acids, aldehydes, alcohols, ketones, etc.) are produced from these materials. Aromatic compounds, especially bi- and tri-functional substituted phenols (xylenol, cresol, etc.), are the main by-products of lignin pyrolysis [59].

The oxidation cycle results in the production of secondary tars. At temperatures above 500 °C and in the presence of an oxidant such air, oxygen, or steam, their

manufacture involves the rearrangement reactions (dehydration, decarbonylation, and decarboxylation) of primary tars [59]. They include dioxin, furan, pyridine, thiophene, and other hetero- and mono-alkylated aromatics. Tertiary tars, often referred to as recombination or high-temperature tars, are produced at temperatures higher than 800 °C. They mostly consist of polynuclear aromatic hydrocarbons (PAH), such as phenanthrene, benzene, pyrene, and benzopyrene, as well as aromatics. Instead of during biomass gasification, tertiary tars are frequently created following the recombination and degradation of primary tars in the syngas reduction environment. They also do not live with primary tars; rather, they only emerge as secondary tars once all primary tars have been changed [59].

6.6   Upgrading Methods for Bio-oil

Bio-oil made from biomass is not suitable for use directly in engines due to its abnormally high moisture content, low energy density, and lack of a free-flowing physical form. Because of this, bio-oil needs to be cleaned and improved in order to increase its fuel efficiency, remove impurities, and increase its energy density [98]. Table 6 compares the differences between pyrolysis oil and diesel fuel [73].

Its major characteristics include bioviscosity, acidity, thermal instability, and a substantial proportion of oxygenated molecules. It can be difficult to produce high-quality bio-oil that perfectly replaces fossil fuels. To solve this issue, the bioquality oil must be raised in the manufacturing facility before total production or through product enhancement [30]. The three main procedures for converting bio-oil into high-quality transportation fuels are zeolite upgrading, hydrodeoxygenation using a hydrotreating catalyst (alumina supported sulfided CoMo or NiMo), and emulsion formation with diesel fuel. Char and bio-oil can also be combined with steam reforming to produce syngas or H_2 [30]. Bio-oil needs to be enhanced to improve its quality and purity because it is commonly generated with impurities. Physical, chemical, or catalytic methods can be used [70].

Integrated catalytic pyrolysis or decoupled liquid phase hydrodeoxygenation are two methods for catalytic bio-oil upgrading, which is the complete deoxygenation of the bio-oil and conventional refining. A partial upgrade into intermediate products compatible with refinery streams is additionally suggested to take advantage of the traditional refinery's substantial scale economies of scale and breadth of experience. The three fundamental ways of upgrading through refinery integration are gasification to syngas followed by synthesizing alcohols or hydrocarbons, in situ or ex situ catalytic vapor cracking, and hydrodeoxygenation [70].

To form saturated C–C bonds by removing oxygen, bio-oil is treated with high-pressure hydrogen at moderate temperatures (302 °C–602 °C) in the presence of heterogeneous catalysts, increasing the fuel's energy content and stability. When hydrotreating industrial feedstocks, sulfided $CoMo/Al_2O_3$ and $NiMo/Al_2O_3$ are frequently used [30]. A hydrogen supply, a temperature of around 400 °C, and a pressure of about 20 MPa are needed. Because of the phenols in bio-oil, complete

deoxygenation is frequently difficult. A naphtha-like by-product of full hydrodeoxygenation needs traditional refining to produce conventional transport fuels like gasoline. The estimated comparable output from biomass is 25 w%, or around 55% in terms of energy, without the addition of hydrogen. The yields are reduced to roughly 33% in energy and 15% in weight when hydrogen from biomass gasification is added [70].

Hydrogen must come from sustainable and renewable sources. It is possible to create H_2 locally by electrolyzing water, gasifying biomass, converting CO to H_2, and removing the H_2, steam-forming bio-oil, or the aqueous phase of a phase-separated product to H_2, converting CO to H_2 and removing the H_2, and more.

Given the high expenses of delivering and storing H_2, external supplies are improbable [70]. Zeolite cracking/upgrading, which removes oxygen primarily as CO_2 with a trace quantity of CO from catalyst coking, takes place in a closed system at pyrolysis temperatures between 352 °C and 502 °C and standard atmospheric pressure. The oil's thermal stability is enhanced as a result. It is estimated that the procedure will produce aromatics at a rate of about 18%. The chemical industry highly emphasizes the manufacture of aromatics, a crucial primary chemical [70].

Because the pyrolysis oil's negative side effects prevent direct use, it is frequently enhanced by being transformed into gasoline using zeolites (crystalline microporous aluminosilicate materials). This method generates hydrocarbons and by-products such as coke, water, and COx by forcing oil vapors over the catalyst at temperatures between 300 and 500 degrees Celsius. The impacts of unprocessed biocoking oil are eliminated by coke production (on the zeolites). Depending on the kind of organic component being treated, the catalyst extracts CO_2, CO, or H_2O [19]. Zeolite cracking of bio-oil is particularly advantageous because it does not require H_2, operates under atmospheric pressure, significantly lowers operating costs, and occurs at temperatures equivalent to those needed to produce bio-oil. The ZSM-5 zeolite catalysts transform oxygenated oil into mixtures of hydrocarbons ranging from C1 to C10 using their potent acidity, high activity, and shape selectivity. This method's primary limitations are its simple coking, poor yield (14–22.5%), and brief catalyst life [30].

The temperature range required for catalytic steam reforming over a nickel catalyst is 752 °C to 852 °C. The following technique has two steps reactions. (1 and 2), the shift response being one of them [30].

$Pyro-oil + H_2O \rightarrow CO + H_2$ (Reaction 1) $CO + H_2O \rightarrow CO_2 + H_2$ (Reaction 2)

6.7 Syngas Processing

Tar, particulate debris, nitrogen (NH_3, HCN), alkali, halides, sulfur (H_2S, COS), and trace elements are common contaminants in synthetic gas. These pollutants are leading causes of gasifier blockage, corrosion, and catalyst deactivation. Biofuels, chemicals, and electricity generation use synthetic gas as raw material. As a result,

Fischer–Tropsch synthesis, the production of biomethanol, the use of fuel cells, and other processes require syngas.

Syngas is typically used to generate biohydrogen (at a rate of 25%), NH_3 (at a rate of 50%), and other processes such as the production of biomethanol and FT.

The methods used to clean syngas are frequently divided into two groups based on the temperatures at which its constituent elements condense. Some of these pollutants are covered along with the techniques employed to purify them [84].

Flue gases and unwanted by-products like ashes and tar (the gasification bottleneck) are the principal by-products of biomass gasification used to produce electricity. The latter is typically discarded despite having significant chemical and fuel potential.

Recently, efforts have been made to valorize this biomass gasification waste into liquid fuels and chemicals due to the complicated nature of gasification tar, which contains hundreds of chemical components and has a significant potential for soil contamination when released into the environment untreated [58].

However, tar treatment, removal, or conversion severely impedes the development and use of biomass-derived gas (poor efficiency, fouling tendency, plugging pipes and tubes, operational problems, etc.). End pipe tar syngas cleanup, in-bed catalytic tar reforming, and in-bed thermal tar cracking technologies are a few techniques that are frequently employed [59]. By encouraging the transformation of tar into useable combustible gases through processes like steam reforming, thermal cracking, dry reforming, hydrocracking, water–gas shift reactions, and hydroforming, catalysts play a critical role in increasing reaction rates at low temperatures. They could serve as feedstock or bed materials [33].

Right now, the primary goal of biomass gasification is to produce fuel gases with low- or medium heating values for use in internal combustion engines that produce power.

Less emphasis has been given to gasification in the literature than to manufacturing liquid chemicals or transportation fuels. Gasification provides a great deal of flexibility and efficiency to value biomass. To promote future technologies, gasification systems and procedures must be complex, affordable, and highly effective. To increase process efficiency, boost gas quality and purity, lower investment costs, and improve the technology's performance in the future, additional research and development into biomass gasification are necessary. Fundamental conditions for attaining these include high-temperature gas cleaning, catalytic conditioning, and the development of novel catalysts, sorbents, and high-temperature filter media.

6.8   *Hydrothermal Conversion of Biomass*

Since hydrothermal energy was adopted as a high potential energy source, biomass hydrothermal conversion has attracted much interest. There was initially a lot of focus on selecting the proper solvent and especially on high temperature and pressure processing materials due to the lack of knowledge on chemical solubility and how

it affects the process as a whole [99]. It is a fantastic way of converting biomass with high energy and moisture content into a range of products, such as a solid (biochar), a liquid (bio-oil), or a gas (hydrogen, methane, etc.) [38]. This procedure involves heating organic wastes or aqueous biomass slurries at higher pressures and low to moderate temperatures to produce a high-density energy carrier or liquid product in the presence of a catalyst [24]. Subcritical and supercritical water is used as the processing medium whole [99]. The primary processing conditions are high pressures (4–22 MPa) and temperatures between 250 and 374 °C. Compared to other thermochemical processes, this technology's low temperatures, low tar production, and excellent energy efficiency are the critical reasons for the recent spike in interest [37] and [98]. Due to their high ash and moisture contents, manures, food wastes, anaerobic digestate, sewage sludge, aquatic biomass (micro and macroalgae), and municipal wastes are some examples of acceptable feedstock. The solid content of the slurries may reach 30% by weight [70].

In the four primary hydrothermal processing steps of carbonization, aqueous phase reforming (APR), liquefaction, and gasification, water functions as a reactant, solvent, and catalyst [70]. At pressures between 20 and 40 bar and temperatures between 180 °C and 250 °C, the mildest type of carbonization, known as hydrothermal carbonization (HTC), produces hydro-char, a solid with properties like those of low-rank coal. This process, which is influenced by temperature and residence time, allows for the reduction of the oxygen and hydrogen contents of the biomass feedstock through dehydration and decarboxylation processes [100].

Hydrothermal liquefaction (HTL) produces liquid bio-crude at pressures of up to 180 bar and temperatures of between 250 °C and 375 °C, which can subsequently be enhanced by catalytic hydrotreatment into a variety of distillate petroleum-derived products.

Hydrothermal gasification (HTG) or supercritical water gasification (SCWG) occurs at pressures larger than 200 bar and temperatures greater than 375 °C to create syngas, CO_2, CH_4, and C1-C4 hydrocarbon gases such C_2H_4 and C_3H_6 [38]. By-products, including char, tar, and microscopic bio-oil, are produced at low temperatures. At temperatures between 220 °C and 250 °C and pressures between 1.5 and 5 MPa, the aqueous phase reforming, a subset of HTG, generates H_2 syngas, alkanes, and a variety of biobased chemical products, including fibers and plastic compounds [99].

These processes utilize wet biomass without any initial dewatering, have high conversion rates, can collect, store, and sequester carbon, create a wide range of chemicals and fuels in the gaseous, liquid, or solid phases, and most importantly, capture, store, and sequester carbon [99]. Hydrothermal biomass processing has several drawbacks and benefits [37, 38]. Hydrothermal liquefaction (HTL) is a hydrothermal treatment used to create bio-oil. It is more energy-efficient than thermal processes (pyrolysis, gasification and combustion). A suitable biomass for pyrolysis and gasification must have a water content of less than 10%; otherwise, drying must be performed prior to use [101, 102]. Because HTL has a low oxygen content, upgrading bio-oil obtained through this process requires less hydrogen [37]. If HTL is implemented industrially, it is expected to result in a direct and continuous supply

of biomass wastes for effective valorization [103]. HTL technology implementation on an industrial scale is prone to operational issues. Corrosion of metallic parts by water in bio-oil, high operating costs, easy deactivation and sintering of catalyst, plugging due to solid deposition, corrosion, pumpability of feedstock, and safety process due to high pressure and temperature. For instance, managing large-scale separation and extraction operations involves managerial issues, more expensive and advanced reactors, extensive water handling equipment, etc. The hydrothermal processing of biomass is based on the critical water point (374 °C and 22.1 MPa), which determines both the subcritical and supercritical water conditions. Biomass constituents like cellulose and lignin are insoluble in water at ambient temperature but soluble in supercritical water (high-temperature water). When biomass is broken down hydrothermally, the water-soluble component disperses into the water at around 100 °C, and hydrolysis occurs above 150 °C. The solid biomass is transformed into a slurry at about 200 °C and 1 MPa, and liquefaction takes place at about 300 °C and 10 MPa, producing oily products. By altering the process variables, such as temperature, reactor pressure, reaction duration, and catalyst presence, biomass is converted here into solid (biochar), liquid (bio-oil), and gaseous products [37]. Supercritical water oxidation removes harmful compounds (pollutants) from biological and organic waste and power generation cycles. Understanding biomass hydrothermal processing and the many degradation processes require a thorough knowledge of water properties under hydrothermal conditions (subcritical and supercritical). At higher temperatures, water has a low dielectric constant. Non-polar compounds are therefore insoluble in water at room temperature, but in supercritical conditions, they are excellent solvents for non-polar substances [37].

6.8.1   Hydrothermal Liquefaction (HTL)

Hydrothermal liquefaction of biomass wastes has been extensively researched as a source of useful chemicals that could serve as biofuel obtained at moderate temperatures and high pressures sufficient to keep water in the liquid phase [99]. A technology that has promise for producing high-quality bio-oil from biomass is hydrothermal liquefaction. This process does not need the energy to dry biomass because it entails only wet feedstocks/high moisture content directly from the field. This does away with the necessity for energy-intensive feedstock drying, which is required in thermochemical processes such as torrefaction, combustion, gasification, and pyrolysis [104]. HTL produces liquid bio-crude with a high calorific value and aqueous, gaseous, and solid phase by-products in H_2O at high pressures (10×10^6 –25×10^6 Pa) at moderate temperatures of around 280–370 °C [38]. This comprises several intricate reactions that result in products with high energy densities and an improved heat recovery mechanism. Two main feedstock groups defined the process mechanism. These are the wet feedstocks (algal biomass), which are made up of essential ingredients such as lipids, proteins, carbohydrates, and algaenans, and the dry feedstocks (lignocellulose biomass), which are composed of cellulose, hemicellulose, and lignin constituents [98].

Along with bio-crude, a variety of compounds can be obtained by HTL. Monoaromatic compounds, fatty acids, alkenes, alkanes, polyaromatic compounds, nitrogenous, and other oxygenated chemicals make up most of these, as described in detail by [98]. HTL concepts are highlighted in this section, including the process principles, the elemental make-up of bio-crude, the different types of feedstocks, the energy efficiency of the process, as well as its future potential.

HTL produces four distinct product phases, which are (i–iv) [104]:

Bio-oil
Light molecular weight gases (CO_2 and trace amounts of CH_4, CO, and H_2)
Biochar
Water vapor rich in carbon

Process parameters that affect HTL (i–x):

Temperature (T)
Pressure (P)
Biomass waste composition
Residence time
Heating rate
Water ratio
Catalyst
Particle size
Solvent density and type
Reaction media.

As mentioned in a study, these factors significantly impact bio-oil output [105]. The transformation of crude bio-oil to high-quality liquid biofuel can be achieved via chemical additives upgrade, catalytic upgrade, and physical process (ultrasonication, distillation, extraction, solvent addition, or separation. The need for energy to dry the wet biomass does not arise in this process. Its uniqueness is that it uses water, making it an eco-friendly method that runs at lower and is slightly energy-efficient [19]. The products of these processes are characterized by high reduced H_2O content, a lower amount of oxygenated compounds, and higher yields which give it a gross calorific value comparable to that of pyrolytic/gasification oil but higher compared to fossil fuels. The drawback is that it requires high pressure, making such equipment expensive to run large-scale or industrial processing [104].

The reduced content of oxygen and high calorific value of bio-oil obtained from HTL is mainly due to dehydration and decarboxylation reactions which converted oxygen to H_2O and CO_2, respectively [105]. This process can reduce biomass oxygen from 40 wt.% to about 10 wt.% [99]. According to [104], bio-oil yield can also be enhanced via temperature increase before bio-oil cracking and repolymerization reactions leading to a reverse trend. And also, bio-oil products can be improved by adding residence time in the 5–30 min range. However, if the reaction time is prolonged, lighter gases and char are produced in the cracking and polymerization reactions, which reduce the bio-oil yield. There are documented techniques for bio-oil components separation and extraction, chemical composition using CHNS elemental

analyzer, nuclear magnetic resonance (NMR) spectroscopy, and high-performance liquid chromatography (HPLC) [37].

The HTL process primarily transforms biomass into bio-oil, a fuel that can replace fossil fuels. However, this procedure faces difficulties under intense pressure, leading to severe economic problems. Organic fertilizer for agriculture, CO_2, and nutrients used to grow and photosynthesize algae in culture. Wastewater that can be recycled to require less processed water is all by-products from the HTL of algal biomass. This process is hugely energy-efficient since it creates between 85 and 90% of the energy it needs and only consumes 10% to 15% of the energy from the feedstock. Additionally, with minor upgrading, the resulting bio-crude may be used economically because it is similar to its petroleum equivalents [98]. If employed appropriately, all the by-products mentioned above could aid HTL in resolving its financial problems. Additional study to improve the mechanisms and parameters of the process is still needed to overcome the disadvantages of HTL and successfully commercialize the procedure.

Water is kept in the liquid phase throughout the operation by operating at or above its saturation point, which significantly reduces the enthalpy change caused by the latent heat of vaporization of water [70]. There has been a lot of interest in compressed hot water as a green reaction medium in recent years. It is currently widely used in a variety of fields, including waste treatment, inorganic and organic material synthesis, polymer recycling, biomass energy recovery, waste resource recovery, and others [99]. Subcritical processes are those that occur below the critical point of water. During the supercritical process, which occurs above the critical water point (274 °C and 22.1 MPa), the properties of water are in the liquid and gas phases. Water can act as a catalyst, a solvent, or a reactant at times. When the dielectric constant of insoluble organic compounds decreases, they become more soluble. Furthermore, because of the high diffusion coefficient, reaction rates increased as water viscosity decreased [104].

In recent years, considerable effort has been made toward using biomass and its derivatives to produce liquid fuels. This study area covers pyrolysis, gasification of biomass, HTL of lignocellulose, and strategies for upgrading bio-crude. The petro-chemical sector has excellent hopes and goals for synthesizing fuels, fine chemicals, and raw materials because of the choice of biomass.

The HTL has recently received a lot of attention as one of the promising approaches for dry and wet biomass [98], as well as for converting biomass into fuels and chemicals. Currently, various pyrolysis and gasification techniques are used to produce fuels (biofuels) and chemicals, primarily from dry biomass feedstocks (dry wood). Despite the enormous potential of wet biomass feedstocks, as demonstrated by documentation [98], little interest or effort has been put into developing the HTL method for wet biomass valorization. Because of their high photosynthetic efficiency, rapid development, high biomass production, and lack of reliance on arable land, microalgae are recognized as a superior fuel and chemical source through wet biomass processing. To improve the performance, prospects, and applicability of this technology, particularly

for wet biomass, as well as to ensure HTL's financial viability, the best process feedstocks and operational conditions must be selected, as well as the current parameters and process mechanisms optimized (Figs. 6a and 6b).

6.9 Dry Biomass HTL

The complex routes shown in Fig. 4 are used to produce bio-crude in a continuous or batch reactor. The feedstock is pretreated to reduce particle size, remove impurities, and create a stable slurry that can be easily pumped. After the HTL process, which takes about 15 min at 350 °C and 150 bar pressure, a gaseous mixture of CO_2, bio-crude, solid trash, and traces of the aqueous phase (water) is formed as a result of phase separation. The HTL unit can use this gaseous mixture again to produce more bio-oil or use less process water. The other water stream is subjected to anaerobic or catalytic hydrothermal gasification, which produces hydrogen- or methane-rich syngas. The presence of phenols and furfurals, on the other hand, limits the anaerobic treatment process.

Because it contains less moisture and oxygen, the resulting bio-crude can be used directly or upgraded for commercial use through additional hydrotreatment. This technique uses relatively little energy because the hydrothermal gasifier can be operated effectively and efficiently with the overall heat generated [98].

6.10 HTL for Wet Biomass

Because it does not require pretreatment and has an HTL that is quite close to that of dry biomass, wet/algae biomass has a significant potential for nutrient recycling. Figure 5 provides a schematic representation of wet biomass hydrothermal processing.

In this process, the algae biomass feed from an algal culture is first dewatered to create a feed slurry with about 20% solids, which is then pumped into the HTL unit to create bio-crude and is then further hydrotreated to produce refined hydrocarbon fuels. The process is made more economically and sustainably feasible by the aqueous phase's production of CO2 and nutrients that are then used to cultivate algae [98].

6.11 Mechanism of HTL

A dehydrogenation process, a dehydration process, a decarboxylation process, and a deoxygenation process are all methods of breaking down the components of biomass feedstock into smaller molecules after hydrolysis has broken down the biomass feedstock into smaller pieces after the hydrolysis process has broken down the biomass
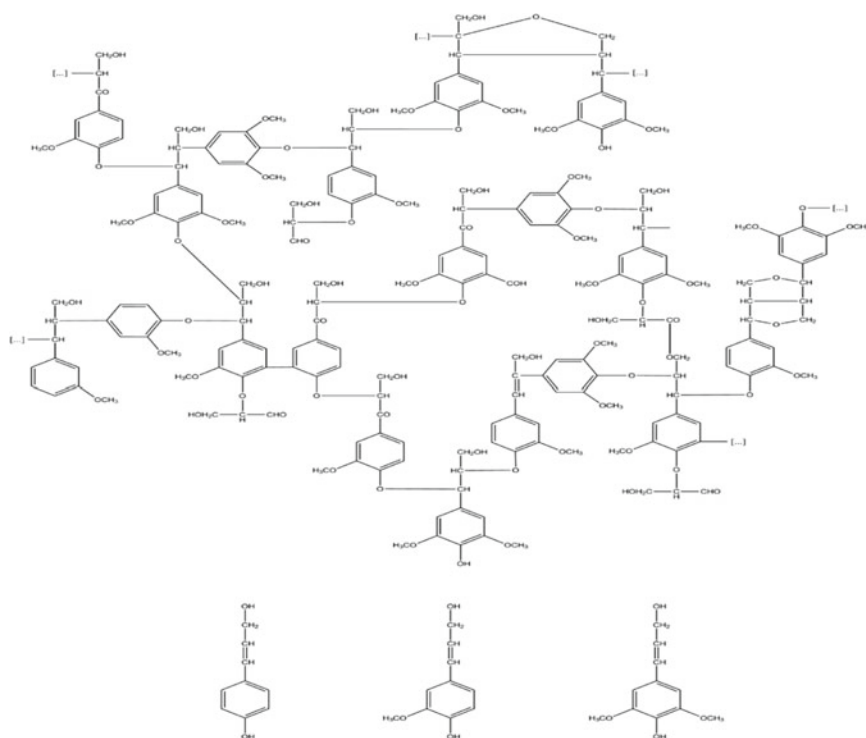
Fig. 4 Three main precursors of monolignol, (**a**) p-coumaryl alcohol, (**b**) coniferyl alcohol, (**c**) sinapyl alcohol, are shown in a schematic of lignin
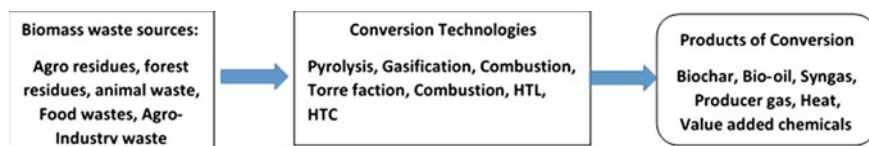
Fig. 5 Biomass waste thermochemical conversion processes

feedstock into smaller molecules. Aldehydes, phenols, acids, ketones, alcohols, and esters are a few complex chemicals that can be made by repolymerizing lighter molecules [98]. HTL begins with the solvolysis of the biomass in micellar forms, followed by the disintegration of the biomass's primary polymeric components (cellulose, hemicellulose, and lignin), and is finally completed by the thermal depolymerization of those components into smaller fractions [38]. The precise mechanism of HTL is currently unknown. Depolymerization is a step in the process; decomposition and recombination reactions come before it. To create simpler monomers, such as glucose and other products like acetic acid, furfural, and aldehyde compounds, the biomass must first be broken down and depolymerized into highly reactive
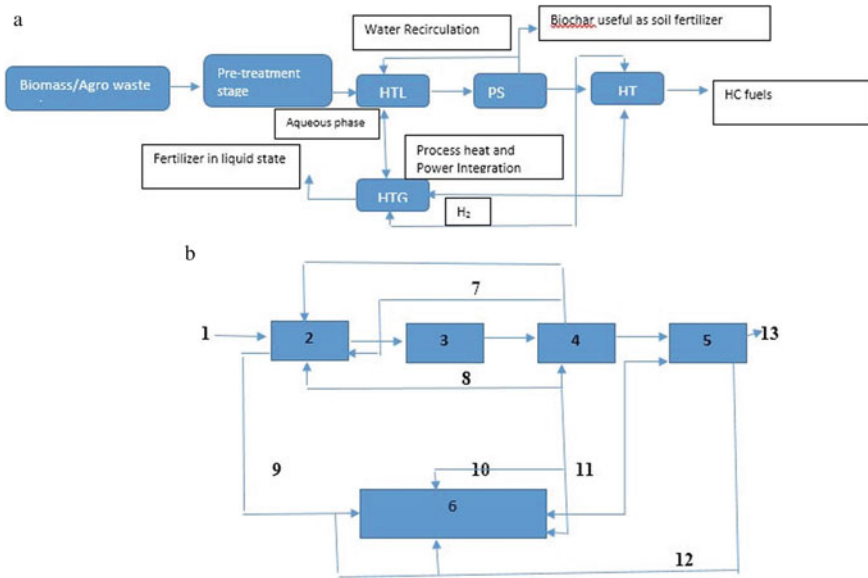
Fig. 6a **a** Consecutive pathway for lignocellulose biomass HTL [98], **b** Consecutive pathway for wet biomass HTL [98]:**1**. Water and nutrients **2**. Algae cultivation **3**. H_2O removal **4**. Hydrothermal liquefaction **5**. Hydrotreating **6**. Catalytic hydrothermal gasification **7**. Carbon (iv) oxide **8**. Solid particle recycle **9**. Nutrient and CO_2 **10**. Aqueous phase **11**. Process heat and power integration **12**. H_2 gas **13**. Hydrocarbon fuels
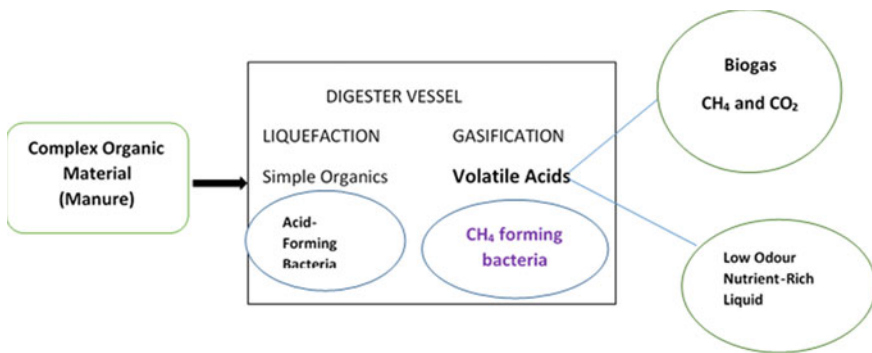
Fig. 7 Procedure for anaerobic digestion

lighter molecules (water-soluble oligomers) [38]. This repolymerization results in the production of bio-crude, gas, and solids.

The complexity of the biomass affects the mechanism and reaction chemistry as well as essential process factors such as residence time, temperature, process
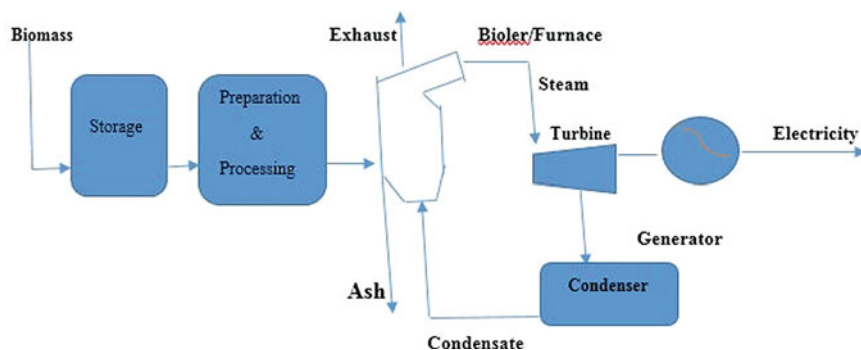
Fig. 8 Schematic representation of direct combustion/ steam turbine system

breakdown, Condensation, and polymerization of the constituents [98]. Temperature, pressure, particle size, and resection durations affect how much bio-oil may be produced using HTL [38].

The polymeric components of biomass are successively dissolved during biomass depolymerization, thanks to their physicochemical properties. The process temperature and pressure change the long-chain structure of the polymer, and the presence of water recycles the energy content of the organic components [98]. The biomass monomers are disassembled by cleavage, deamination, decarboxylation, and dehydration. Dehydration results in the loss of water molecules, decarboxylation results in the loss of carbon dioxide, and deamination results in the removal of the amino acid content. The polymers are hydrolyzed into polar monomers and oligomers by removing oxygen from biomass through the decarboxylation and dehydration processes as CO_2 and H_2O, respectively. When applied under high heat and pressure, water causes the hydrogen-bonded cellulose structure to split into glucose monomers. Compared to glucose, fructose is subject to greater isomerization, hydrolysis, reverse-aldol breakdown, dehydration, recombination, and rearrangement reactions. These reactions result in various products, such as furfural, polar organic molecules, phenols, organic acids, and glycolaldehyde, which are highly water-soluble [98]. The breakdown and deoxygenation reactions, among others, are the main processes that lead to the bio-crude, which is made of acids, aldehydes, and aromatics [105].

The repolymerization and recombination step result from the system's absence of hydrogen compounds. Free radicals, which are reactive by-products of earlier processes, have a propensity to repolymerize or recombine to generate heavier char molecules, which are notorious for producing coke when they are present in significant quantities [106, 107]. However, if there is sufficient hydrogen in the organic mixture during the liquefaction process, stable weight species will be produced by capping the free radicals with hydrogen molecules [98].

6.12 Catalytic Hydrothermal Liquefaction

Homogeneous and heterogeneous catalysts boost bio-oil production, lower biochar production, and raise conversion efficiency. Homogeneous catalysts (alkali salts, with the K salts being more active than the Na salts) such as $KHCO_3$, KOH, K_2CO_3, and $NaOH$, enable water–gas shift reactions by facilitating ester formation via decarboxylation reaction between biomass hydroxyl groups and the formate ions in the alkali carbonates, followed by dehydration, deoxygenation, decarboxylation, and dehydration of micellar-like fragments Condensation, polymerization, and cyclization processes are then used in a cycle to create the final products. This group of catalysts favored inhibiting the formation of unstable and unsaturated molecules during dehydration processes (with high pH), enhancing the yield and properties of bio-crude, and minimizing solid yields [108–110].

The disadvantage of this method is that the catalyst recovery process costs a lot of money, uses a lot of energy, and requires a lot of capital [38].

Although heterogeneous catalysts are most typically used in HTG, incorporating a catalyst into the HTL process has been done in a select few instances to improve the quality of the bio-crude produced from lignocellulose biomass. Magnesium oxide, nickel oxide, manganese oxide, zinc oxide, cerium oxide, lauryl oxide, and other catalysts have been used [38]. The scarcity of Pt, Ni, and Pd stimulates the use of the above-mentioned heterogeneous catalyst.

Using CsOH and RbOH (very potent bases), the first catalytic hydrothermal liquefaction of wood biomass was conducted [37]. It was discovered that these potent bases, like other base catalysts, considerably boost oil yields by inhibiting char formation and creating mainly phenolic and benzenediol derivatives.

7 The Biochemical Transformation of Biomass

The biochemical conversion of biomass refers to the gradual and continuous release of biofuel from biomass waste through the activity of microorganisms and enzymes. Lignocellulosic biomass, which can produce chemicals, fuels, and other materials with energy value, is being adopted progressively as a renewable and alternative energy source to fossil fuels. Lignocellulose, which contains cellulose and hemicellulose, is primarily composed of sugars. Due to the difficulty in accessing this biomass polysaccharides content and the stiff and compacted assembly of plant cell walls, the synthesis of fermentable sugars has become constrained. Thus, using thermochemical pretreatment and an acid catalyst to overcome these challenging barriers, plant cell walls are frequently physically or chemically broken. After pretreatment, enzymatic hydrolysis is the preferred approach for creating sugars that microbial biocatalysts can later ferment to yield liquid fuels (such as C_2H_5OH). The release of inhibitory compounds, such as furfural, 5-hydroxymethyl furfural, C_6H_5OH, and aliphatic acids, is increased when biomass is pretreated with acid. These chemicals

have a considerable effect on both enzymatic hydrolysis and microbial fermentation. When Avicel cellulose and acid-treated spruce wood hydrolysate were mixed, the efficiency of enzymatic hydrolysis was discovered to be 63% lower than when Avicel was hydrolyzed in aqueous citrate buffer. The acid hydrolysates could seldom ever be fermented, either. As a result, the problems that come with lignocellulose conversion can be avoided by using less resistant feedstocks or by developing efficient pretreatment techniques that simultaneously yield high sugar yields and don't produce inhibitory by-products.

7.1 Technologies for Biochemical Conversion

The techniques for biochemical conversion include: anaerobic digestion (also known as biomethanation); ethanol fermentation. The recycling of waste such as poultry waste is usually done via anaerobic digestion. Anaerobic digestion can be done industrially. It is a fermentation process that converts organic waste into biogas, mainly composed of CH_4 (about 60%) and CO_2 (about 40%), comparable to landfill gas.

Anaerobic means a biological process taking in the absence of oxygen in which bacteria act as a catalyst in breaking down organic matter into biodegradable forms to produce biogas rich in CH_4 and CO_2 with some trace amounts of H_2S. This process takes place naturally.

In this method, biomass is fermented anaerobically without oxygen to produce biogas (also known as gobar gas) from cow dung, human waste, and other organic waste with high moisture content. Two distinct metabolic bacterial species carry out two degrees of fermentation.

The organic material undergoes the first hydrolysis to produce fatty acids, alcohols, sugars, H_2, and CO_2. Bacteria that produce methane transform the result of the first stage into CH_4 and CO_2 between 30 and 55 °C. The residual sludge is transformed into enriched fertilizer in a digester, a sealed tank used for fermentation (Fig. 7).

An anaerobic digestion facility can produce biogas and digestate, which can be processed further or utilized to make secondary goods. In addition to being a fuel for electricity and heat production, biogas can also be used for transportation. Biogas can also be enhanced and applied to gas distribution systems. The characteristics of anaerobic digestion were given in Table 8.

Digestate may be further processed to produce alcohol and a fibrous substance. Fiber, a bulky substance with little nutritional value that may be composted can be employed as a soil improver or a low-level fertilizer. The liquor preserves a significant portion of the nutrients and can be used as liquid fertilizer.

(ii) Ethanol fermentation.

Ethanol can be produced by dissolving sugar-containing biomass into sugar molecules like glucose ($C_6H_{12}O_6$) and sucrose ($C_{12}H_{22}O_{11}$), such as sugarcane, and sweet cassava sorghum, beet, potato, corn, and grapes.

Table 8 Characteristics of anaerobic digestion

Characteristics	Anaerobic
Reaction in Anaerobic digestion	$C_6H_{12}O_6 \rightarrow CO_2 + 3CH_4$
Energy produced in KJ/mol. glucose	-393
C balance	95% $\rightarrow CO_2 + CH_4$ (= biogas)5% $\rightarrow biomass$
Energy balance	90% retained in CH_4 5% $\rightarrow biomass$ 5% $\rightarrow heat generated$
Biomass production	Slow growth of biomass

The biological fermentation of ethanol involves turning sugar into ethanol and CO_2 as part of the process.

Nowadays, gasoline is blended with ethanol, which serves as the primary alcohol fuel.

7.2 Biogas

"Biogas" refers to any gas produced when organic material decomposes anaerobically. It falls under the category of renewable energy. It may be produced using locally available raw materials such as recyclable rubbish and is environmentally friendly. Manure, sewage, municipal trash, green waste, and crops that have undergone anaerobic fermentation are among the sources of biogas.

A fuel gas called biogas has a CH_4 content of 65% and a CO_2 content of 35%. It is a renewable energy source made from biomass. Biogas is categorized based on its chemical composition and resulting physical characteristics. Nevertheless, "biogas" refers to various gases created from specific treatment processes, starting with various organic wastes from multiple enterprises, animal or domestic waste, etc.

7.3 Power Generation Based on Biogas

There are three methods for doing this (i–iii):

Landfill
Direct method
Gasification.

i. Direct action.

For years, wood, by-products, and other solids were the only commercially feasible choices for producing electricity. The technique involves burning biomass

directly in a boiler connected to a steam turbine, which produces steam from the hot gases through a heat exchanger and generates electricity from the steam through a steam turbine (Fig. 8).

Burning fuel in the boiler produces steam, which powers a turbine or generator to produce electricity. The steam is then condensed into liquid in the condenser by cooling water circulating the tubes. The condensed water can be heated once more to create steam by being returned to the boiler.

Heat and power combined.

Combining heat and power (CHP), also known as cogeneration or distributed generation, generates heat and electricity simultaneously from a single fuel source, frequently natural gas.

Biogas cogeneration.

Renewable raw materials and the production of biogas anaerobic fermentation of organic material in a fermenter yields biogas. Between 45 and 70% of this gas is made of CH_4. After burning, almost the same amount of CO_2 the substrates absorbed during growth is released. Cogeneration plants reduce the emissions that would otherwise be produced when burning fossil fuels by converting biogas into electricity.

An electric generator, a gas turbine, steam turbine, or combustion engine is a typical component of CHP systems. In addition to the electric generator, a waste heat exchanger is built. This device uses the heat or exhaust gas recovered from the generator to produce steam or hot water.

ii. Gasification as a Process.

The steps taken in gasification facilities are depicted in the image below. To ensure that the provided solid biomass fuel has the appropriate fuel parameters (particle size, water content), it must be modified (fuel conditioning and handling). The gasification process uses the cleaned fuel to create raw product gas. The gas quality of the raw material is required for further use. The washed product gas is employed in various procedures to produce fuel, heat, and power.

iii. Landfill.

Landfill gas is primarily CH_4 and CO_2, with trace amounts of N_2, O_2, H_2S, and non-methane organic molecules in anaerobic circumstances (NMOCs). The amount of organic waste and moisture in a landfill is linearly related to the volume of landfill gas produced by bacterial decomposition. Gas can be extracted from landfills by drilling vertical wells into the trash connected by underground pipelines and "capping" a portion of the dump with clay. The gas is collected by vacuum compressors and then transported to a blower/flare station, where it is either fed to the electricity-generating plant or flared. Methane is converted into the less dangerous gas carbon dioxide during combustion. Even if stopping the process now reduces methane gas emissions, it does not utilize the heat energy generated during the conversion. After being gathered, the gas will be piped to a power plant, which will be burned to power engine generator sets.

Burning fuel in the boiler produces steam, which powers a turbine or generator to produce electricity. The steam is then condensed back into liquid form in

the condenser by cooling water being circulated around the condenser tubes. The condensed water can be heated once more to create steam by being returned to the boiler.

Contribution Abiodun Oluwatosin Adeoye **(Conceptualization, write-up, resource research, data presentation, and editing of manuscript).**

Olayide Samuel Lawal **(Supervision, Design, and Conceptualization).**

Rukayat Oluwatobiloba Quadri **(Resource research and editing of manuscript).**

Dosu Malomo **(Resource research and Editing).**

Muhammed Toyyibb Aliyu, Gyang Emmanuel Dang, Emmanuel Oghenero Emojevu, Musa Joshua Maikato, Mohammed Giwa Yahaya, Oluyemisi Omotayo Omonije, Victor Great Edidem, Yakubu Khartum Abubakar, Onyeka Francis Offor, Ezeaku Henry Sochima, Boniface Eche Peter, Baba Nwunuji Hikon **(Resource research).**

References

1. Cherubini, F.: The biorefinery concept: Using biomass instead of oil for producing energy and chemicals. Energy Convers. Manage. **51**(7), 1412–1421 (2010)
2. Witcoff, H.A., Reuben, B.G.: Industrial Organic Chemicals, John Wiley & Sons, (1996)
3. Clark, H.J., Deswarte, E.I.F.: The Biorefinery Concept–An Integrated Approach. John Wiley & Sons (2008)
4. Hubbert: Historical studies in the natural sciences **44**(1), pp. 37–79. ISSN 1939–1811, electronic ISSN 1939–182X (1956)
5. Mousdale, D. M.: Biofuels: biotechnology, chemistry, and Sustainable development. CRC Press, pp. 328, USA, (2008)
6. Energy Information Administration (EIA), Annual Energy Outlook (2016)
7. Szulczyk, K.R.: Which is a better transportation fuel—butanol or ethanol? Int. J. Energy Environ. **1**(1), (2010)
8. Fernando, S., Adhikari, S., Chandrapal, C., Murali, N.: Biorefineries: Current status, challenges, and future direction. Energy Fuels **20**, 1727–1737 (2006)
9. Naik, S.N., Goud, V.V., Rout, P.K., Dalai, A.K.: Production of first and second generation biofuels: A comprehensive review. Renew. Sustain. Energy Rev. **14**, 578–597 (2010)
10. Zilberman, D., Hochman, G., Rajagopal, D., Sexton, S., Timilsina, G.: The impact of biofuels on commodity food prices: Assessment of findings. Am. J. Agr. Econ. **95**(2), 275–281 (2013)
11. Thompson, P.B.: The agricultural ethics of biofuels: the food vs. fuel debate. Agriculture. **2**, 339–358 (2012)
12. Rosillo-Calle, F.: Food versus fuel: toward a new paradigm—The need for a holistic approach. ISRN Renew. Energy (2012)
13. Cheng, S., Zhu, S.: Lignocellulosic feedstock biorefinery—the future of the chemical and energy industry. BioResources **4**(2), 456–457 (2009)
14. Menon, V., Rao, M.: Trends in bioconversion of lignocellulose: Biofuels, platform chemicals & biorefinery concept. Prog. Energy Combust. Sci. **38**(4), 522–550 (2012)
15. Adeoye, A.O., Quadri, R.O., Lawal, O.S.: Physicochemical assessment, pyrolysis and thermal characterization of Albizia Zygia Tree Sawdust. Int. J. Nanotechnol. Nanomed. **7**(1), 91–99 (2022)
16. Adeoye, A.O., Quadri, R.O., Lawal, O.S.: Biomass pyrolysis in the context of Nigeria's oil and gas: An overview. Int. J. Ambient Energy (In press) (2023)

17. Sharma, S.K., Lee, J.: Design and Development of Smart Semi Active Suspension for Nonlinear Rail Vehicle Vibration Reduction. Int. J. Struct. Stab. Dyn. 20, 2050120 (2020). https://doi.org/10.1142/S0219455420501205

18. Bhardawaj, S., Sharma, R.C., Sharma, S.K.: Development of multibody dynamical using MR damper based semi-active bio-inspired chaotic fruit fly and fuzzy logic hybrid suspension control for rail vehicle system. Proc. Inst. Mech. Eng. Part K J. Multi-body Dyn. 234, 723–744 (2020). https://doi.org/10.1177/1464419320953685

19. Liu, H., Ma, M., Xie, X.: New materials from solid residues for investigation the mechanism of biomass hydrothermal liquefaction. Ind. Crops Prod. 108, 63–71 (2017).https://doi.org/10.1016/j.indcrop.2017.06.026

20. Adeoye, A.O., Quadri, R.O., Lawal, O.S.: Channeling biomass waste as an alternative industrial and domestic energy with pollution effects mitigation in Nigeria: An overview. Int. J. Nanotechnol. Nanomed. **7**(1), 78–90 (2022)

21. Saleem, M.: Possibility of utilizing agriculture biomass as a renewable and sustainable future energy source. Heliyon **4**8(2), e08905 (2022). https://doi.org/10.1016/j.heliyon.2022.e08905. PMID:35198772;PMCID:PMC8841379

22. Houghton R.A. Biomass. Encyclopedia of Ecology. pp. 448–453 (2008)

23. Chen, H., Wang L.: Technologies for biochemical conversion of biomass. Elsevier Inc., (2017)

24. Demirbas, A.: Biomass resource facilities and biomass conversion processing for fuels and chemicals. Energy Convers. Manage. 42, 1357–1378 (2001).https://doi.org/10.1016/S0196-8904(00)00137-0

25. Zhao, X., Zhang, L., Liu, D.: Biomass recalcitrance. Part I: the chemical compositions and physical structures affecting the enzymatic hydrolysis of lignocellulose. Biofuels, Bioproducts and Biorefining **6**(4), 465–482 (2012a)

26. Sánchez, Ó.J., Cardona, C.A.: Trends in biotechnological production of fuel ethanol from different feedstocks. Biores. Technol. **99**(13), 5270–5295 (2008)

27. Vaibhav, D., Thallada, B.A.: Comprehensive review on the pyrolysis of lignocellulosic biomass. Renew. Energ. **129**, 695–716 (2018)

28. Huber, G.W., Iborra, S., Corma, A.: Synthesis of transportation fuels from biomass: chemistry, catalyst, and engineering. Chem. Revol. **106**, 4044–4098 (2006)

29. Tong, X., Ma, Y., Li Y.: Biomass into chemicals: Conversion of sugars to furan derivatives by catalytic processes", Appl. Catal. A Gen **385** (1–2), 1–13, (2010). https://doi.org/10.1016/j.apcata.2010.06.049

30. Balat, M., Balat, M., Kırtay, E., Balat, H.: Main routes for the thermo-conversion of biomass into fuels and chemicals. Part 1 : Pyrolysis systems, Energy Convers. Manage. **50**(12), 3147–3157, (2009). https://doi.org/10.1016/j.enconman.2009.08.014

31. Himmel, M.E., Ding, S.Y., Johnson, D.K., Adney, W.S., Nimlos M.R., Brady, J.W., Foust, T.D.: Biomass recalcitrance: engineering plants and enzymes for biofuels production. Science. 315 (2007)

32. Mosier, N., Wyman, C., Dale, B.: Elander, R., Lee, Y.Y., Holtzapple, M., Ladisch, M. Features of promising technologies for pretreatment of lignocellulosic biomass. Bioresource Technol. **96**, 673–686 (2005)

33. Adeoye, A.O., Quadri, R.O., Lawal, O.S.: Assessment of biofuel potential of tenera palm kernel shell via fixed bed pyrolysis and thermal characterization, Results in Surfaces and Interfaces. **9**(1), 100091(2022). https://doi.org/10.1016/j.rsurfi.2022.100091

34. Demirbas, A.: Biorefineries: For biomass upgrading facilities. Springer (2010).https://doi.org/10.1007/978-1-84882-721-9

35. Sharma, A., Pareek, V., Zhang D.: Biomass pyrolysis—A review of modelling, process parameters and catalytic studies. Renew. Sustain. Energy Rev. **50**, 1081–1096, (2015). https://doi.org/10.1016/j.rser.2015.04.193

36. Hayes, D.J.M.: Biomass composition and its relevance to biorefining. In The Role of Catalysis for the Sustainable Production of Biofuels and Bio-chemicals, pp. 27–65. Elsevier B.V. (2013)

37. Tekin, K., Karagoz, S., Bektaş, S.: A review of hydrothermal biomass processing. Renew. Sustain. Energy Rev. **40**, 673–687, (2014). https://doi.org/10.1016/j.rser.2014.07.216

38. Kumar, M., Oyedun, A.O., Kumar A.: A Review on the Current Status of Various Hydrothermal Technologies on Biomass Feedstock (2017)
39. Sharma, S.K., Phan, H., Lee, J.: An Application Study on Road Surface Monitoring Using DTW Based Image Processing and Ultrasonic Sensors. Appl. Sci. 10, 4490 (2020). https://doi.org/10.3390/app10134490
40. Pauly, M., Keegstra, K.: Plant cell wall polymers as precursors for biofuels. Curr Opin Plant Biol. **13**, 305–312 (2010)
41. Saha, B.C.: Hemicellulose bioconversion. J. Ind. Microbiol. Biotechnol.. **30**(5), 279–291
42. Mussatto, S.I., Teixeira, J.A.: Lignocellulose as raw material in fermentation processes. In: A. Méndez-Vilas, A. (ed.) Applied Microbiology and Microbial Biotechnology. Formatex, pp. 897–907 (2010)
43. Chundawat, S.P.S., Beckham, G.T., Himmel, M.E. Dale, B,E.: Deconstruction of ligno-cellulosic biomass to fuels and chemicals. Annu. Rev. Chem. Biomol. Eng. **2**(6), 1–6.25 (2011)
44. Peng, F., Ren, J.L., Xu, F., Sun, R.C.: Chemicals from hemicelluloses: A review. In: Zhu, J.Y., Zhang, X., Pan, X. (eds.) Sustainable Production of Fuels, Chemicals, and Fibers from Forest Biomass. ACS Symposium Series, pp. 219–259. Washington DC, USA (2011)
45. Harmsen, P.F.H., Huijgen, W.J.J., Bermúdez López, L.M., Bakker, R.R.C.: Literature Review of Physical and Chemical Pretreatment Processes for Lignocellulosic Biomass. Energy Research Centre of Netherlands (ECN) (2010)
46. Ragauskas, A.J, Beckham, G.T., Biddy, M.J., Chandra, R., Chen, F., Davis, M.F., Davison, B.H., Dixon, R.A., Gilna, P., Keller, M., Langan, P., Naskar, A.K., Saddler, J.N., Tschaplinski, T.J., Tuskan, G.A., Wyman, C.E.: Lignin valorization: improving lignin processing in the biorefinery. Science **344** (6185) (2014)
47. Ralph, J., Lundquist, K., Brunow, G., Lu, F., Kim, H., Schatz, P.F., Marita, J.M., Hatfield, R.D., Ralph, S.A., Christensen, J.H., Boerjan, W.: Lignins: Natural polymers from oxidative coupling of 4-hydroxyphenylpropanoids. Phytochem. Rev. **3**, 29–60 (2004)
48. Guo, F., Shi, W., Sun, W., Li, X., Wang, F., Zhao, J., Qu, Y.: Differences in the adsorption of enzymes onto lignins from diverse types of lignocellulosic biomass and the underlying mechanism. Biotechnol. Biofuel. **7**(38) (2014)
49. Sticklen, M.B.: Plant genetic engineering for biofuel production: towards affordable cellulosic ethanol. Nat. Rev. Genet. **9**, 433–443 (2008)
50. Bugg, T.D.H., Ahmad, M., Hardiman, E.M., Singh, R.: The emerging role for bacteria in lignin degradation and bio-product formation. Curr. Opin. Biotechnol. **22**, 394–400 (2011)
51. Xiao, C., Anderson, C.T.: Roles of pectin in biomass yield and processing for biofuels. Front Plant Science **4**(67) (2013)
52. Caffall, K.H., Mohnen, D.: The structure, function, and biosynthesis of plant cell wall pectic polysaccharides. Carbohyd. Res. **344**, 1879–1900 (2009)
53. Rowell, R.M., Pettersen, R., Tshabalala, M.A.: Cell wall chemistry. In: Rowell, R.M. (ed.) Handbook of Wood Chemistry and Wood Composites, Second Edition. CRC Press, pp. 33–72 (2012)
54. Faulon, J., Carlson, G.A., Hatcher, P.G.: A three-dimensional model for lignocellulose from gymnospermous wood. Org. Geochem. **21**(12), 1169–1179 (1994)
55. Sharma, R.C., Sharma, S., Sharma, S.K., Sharma, N.: Analysis of generalized force and its influence on ride and stability of railway vehicle. Noise Vib. Worldw. **51**, 95–109 (2020). https://doi.org/10.1177/0957456520923125
56. Poletto, M., Ornaghi Júnior, H.L., Zattera, A.J.: Native cellulose: Structure, characterization and thermal properties. Materials **7**, 6105–6119 (2014)
57. Adler, E.: Lignin chemistry-past, present and future. Wood Sci. Technol. **11**, 169–218 (1977)
58. Laksmono, N., Paraschiv, M., Loubar, K., Tazerout M.: Biodiesel production from biomass gasification tar *via* thermal/ catalytic cracking. Fuel Process. Technol. **106**, 776–783 (2013). https://doi.org/10.1016/j.fuproc.2012.10.016
59. Molino A., Chianese S., Musmarra D.: Biomass gasification technology : The state of the art overview. J. Energy Chem. **25**(1), 10–25, (2016). https://doi.org/10.1016/j.jechem.2015.11.005

60. Mani, S., Tabil, L.G., Sokhansanj, S.: Specific energy requirement for compacting corn stover. Bioresource Technol. **97**(12), 1420–1426 (2006). https://doi.org/10.1016/j.biortech.2005.06.01918:58

61. Baruah, D., Baruah, D.C.: Modeling of biomass gasification: A review. Renew. Sustain. Energy Rev. **39**, 806–815 (2014). https://doi.org/10.1016/j.rser.2014.07.129

62. Sambo, A.S.: Renewable energy electricity in Nigeria: The way forward. In: The Renewable Electricity Policy Conference 2016, pp. 11–12, Abuja (2006)

63. Heinimö, J., Junginger, M.: Production and trading of biomass for energy—An overview of the global status. Biomass Bioenerg. **33**(9), 1310–1320 (2009). https://doi.org/10.1016/j.biombioe.2009.05.017

64. Awulu, J.O., Omale, P.A., Ameh, J.A.: Comparative analysis of calorific values of selected Agricultural wastes. Nigerian J. Technol. (NIJOTECH) **37**(4), 1141–1146 (2018)

65. FAOSTAT. FAO statistics division, http://www.faostats.fao.org. Accessed 31/08/2022

66. Lewis, M.L., Robenzon, J., Hans-Joachim N., Bernardo, R..: Potential for Simultaneous Improvement of Corn Grain Yield and Stover Quality for Cellulosic Ethanol. Crop Science (2010). 50. https://doi.org/10.2135/cropsci2009.03.0148.

67. O'Connor, P.: A general introduction to biomass utilization possibilities. In: The Role of Catalysis for the Sustainable Production of Bio-fuels and Bio-chemicals, pp. 1–25. Elsevier (2013)

68. Adeoye, A.O., Quadri, R.O., Lawal, O.S.: Fixed-bed pyrolysis and thermal analyses of pressed oil palm fruit fibre as potential source of alternative energy. FUOYE J. Innov. Sci. Technol. (In press) (2022)

69. Panwar, N.L., Kothari, R., Tyagi, V.V.: Thermo chemical conversion of biomass—Eco-friendly energy routes. Renew. Sustain. Energy Rev. **16**(4),1801–1816 (2012). https://doi.org/10.1016/j.rser.2012.01.024

70. Adams, P., Bridgwater, T., Lea-Langton, A., Ross A., Watson, I.: Biomass conversion technologies. In: Greenhouse Gas Balance of Bioenergy Systems. 1st Edition, pp. 107–139. Elsevier Inc. (2018). https://doi.org/10.1016/B978-0-08-101036-5.00008-2

71. Vassilev, S.V., Baxter, D., Vassileva, C.G.: An overview of the behaviour of biomass during combustion: Part I. Phase-mineral transformations of organic and inorganic matter. Fuel **112**, 391–449 (2013)

72. Bhardawaj, S., Sharma, R., Sharma, S.: Ride Analysis of Track-Vehicle-Human Body Interaction Subjected to Random Excitation. J. Chinese Soc. Mech. Eng. 41, 237–236 (2020). https://doi.org/10.29979/JCSME.

73. Taarning, E., Osmundsen, C.M., Yang, X., Voss, B., Andersen, I., Christensen C.H.: Zeolite-catalyzed biomass conversion to fuels and chemicals. Energy Environ. Sci. **4**, 793–804 (2011). https://doi.org/10.1039/C004518G

74. Serrano-Ruiz, J.C., Luque, R., and Clark, J.H.: The Role of heterogeneous catalysis in the biorefinery of the future. In: The Role of Catalysis for the Sustainable Production of Bio-fuels and Biochemicals, pp. 557–576. Elsevier B.V. (2013)

75. Fukuda, H., Kondo, A., Noda, H.: Biodiesel fuel production by transesterification of oils. J. Biosci. Bioeng. **92**, 405–416 (2001)

76. Renganathan, S.V., Narashimhan, S.L., Muthukumar, K.: An overview of enzymatic production of biodiesel. Bioresour. Technol. **99**, 3975–3981 (2008)

77. Xie, W., Huang, X., Li, H.: Soybean oil methyl esters preparation using NaX zeolites loaded with KOH as a heterogeneous catalyst. Bioresour. Technol. **98**, 936–939 (2007)

78. İlgen, O., Akin, A.N.: Development of alumina supported alkaline catalysts used for biodiesel production. Turk J Chem. **33**, 281–287 (2009)

79. Gama, P.E., Lachter, E.R., Gil, R.: Characterization and catalytic activity of K_2CO_3/Al_2O_3 in the transesterification of sunflower oil in conventional and microwave heating. Quim Nova **38**, 185–190 (2015)

80. Vyas, A.P., Verma, J.L., Subrahmanyan, N.: A review on FAME production processes. Fuel **89**, 1–9 (2010)

81. Chouhan, A.P.S., Sarma, A.K.: Modern heterogeneous catalysts for biodiesel production: A comprehensive review. Renew. Sustain. Energy Rev. **15**(9),4378–4399 (2011).https://doi.org/10.1016/j.rser.2011.07.112

82. Hu, L., Lin, L., Wu Z., Zhou S., Liu S.: Recent advances in catalytic transformation of biomass-derived 5-hydroxymethylfurfural into the innovative fuels and chemicals. Renew. Sustain. Energy Rev. **74**, 230–257 (2017). https://doi.org/10.1016/j.rser.2017.02.042

83. Sharma, S., Meena, R., Sharma, A., Goyal P. Biomass conversion technologies for renewable energy and fuels: A review Note, IOSR J. Mech. Civ. Eng. **11**(2), 28–35 (2014). https://doi.org/10.9790/1684-11232835

84. Sikarwar, V.S., Zhao, M., Fennell, P.S., Shab, N., Anthony E.J. Progress in biofuel production from gasification. Pror. Energy Combust. Sci. **61**, 89–248 (2017). https://doi.org/10.1016/j.pecs.2017.04.001

85. Rolando, Z., Krister, S., Emilia, B.: Rapid pyrolysis of agricultural residues at high temperature. Biomass and Bioenergy. **23**, 357–366. https://doi.org/10.1016/S0961-9534(02)00061-2

86. Brown T.R.: A techno-economic review of thermochemical cellulosic biofuel pathways. Bioresour. Technol. (2014). [PMID: 25266684]

87. Czernik, S., Evans, R., French, R.: Hydrogen from biomass-production by steam reforming of biomass pyrolysis oil. Catal. Today **129**, 265–268 (2007)

88. Keiser, J. R., Warrington, G. L., Lewis, S. A., Connatser, R. M., Jun, J., Qu, J., Lee, K., Brady, M. P.: Corrosion and Chemical Characterization of Bio-Oils from Biomass with Varying Ash and Moisture Contents. USA (2021)

89. Sulejmanovic, D., Keiser, J.R., Su, Y., Kass, M.D., Jack, R., Ferrell, J.R., Mariefel, V., Olarte, M.V., Wade, J.E., Jun, J.: Effect of Carboxylic Acids on Corrosion of Type 410 Stainless Steel in Pyrolysis Bio-Oil. Sustainability. **14**(18), 11743 (2022). https://doi.org/10.3390/su141811743

90. Hu, X.Z., Zhanming, G., Mortaza, Z., Shu, L., Jason, C.-H., Zhe, W.Y.: Coke formation during thermal treatment of bio-oil. Energy Fuels XXXX (2020). https://doi.org/10.1021/acs.energyfuels.0c01323

91. Bamgboye, A.I., Oniya. O.: Pyrolytic conversion of corn cobs to medium grade fuels and chemical preservatives. The Federal University of Technology Journal of Engineering and Environmental Technolog. **3**(2), 50–53 (2003)

92. Jahirul, M.I., Rasul M.: Recent developments in biomass pyrolysis for bio-Fuel production, its potential for commercial applications. In: Recent Researches in Environmental and Geological Sciences, pp. 256–265 (2012)

93. Cornelissen, T., Yperman, Y., Reggers, G., Schreurs, S., Carleer, R.: Flash co-pyrolysis of biomass with polylactic acid. Part 1: influence on bio-oil yield and heating value. Fuel **87**, 1031–1041 (2008)

94. de Jongh, W.A.: Possible applications for vacuum pyrolysis in the processing of waste materials. Stellenbosch; SU (Thesis-M.Sc.) (2001)

95. Kong, S.H., Lam, S.S., Yek, P.N.Y., Liew, R.K., Ma, N.L.: Self- purging microwave pyrolysis: an innovative approach to convert oil palm shell into carbon-rich biochar for methylene blue adsorption. J. Chem. Technol. Biotechnol. **94**(5), 1397–1405 (2019)

96. Goyal, H.B., Seal D., Saxena. R.C. Bio-fuels from thermochemical conversion of renewable resources: a review. Renew. Sustain. Energy Rev. **12** 504–517 (2008)

97. Damartzis, T., Zabaniotou, A.: Thermochemical conversion of biomass to second-generation biofuels through integrated process design—A review. Renew. Sustain. Energy Rev. **15**(1), 366–378 (2011). https://doi.org/10.1016/j.rser.2010.08.003

98. Gollakota, A.R.K., Kishore, N., Gu S.: A review on hydrothermal liquefaction of biomass. Renew. Sustain. Energy Rev. 1–15, (2017)

99. Hrncic, M.K., Kravanja, G., Knez, Z.: Hydrothermal treatment of biomass for energy and chemicals. Energy 1–11 (2016)

100. Wang, T., Zhai, Y., Zhu, Y., Li, C., Zeng, G.: A review of the hydrothermal carbonization of biomass waste for hydrochar formation: Process conditions, fundamentals, and physicochemical properties. Renew. Sustain. Energy Rev. **90**, 223–247 (2018)

101. Yaashikaa, P.R., Kumar, P.S., Varjani, S., Saravanan, A.: A critical review on the biochar production techniques, characterization, stability and applications for circular bioeconomy. Biotechnology Reports. **28**: e00570 (2020). https://doi.org/10.1016/j.btre.2020.e00570

102. Lepage, T., Kammoun, M., Schmetz, Q., Richel, A.: Biomass-to-hydrogen: a review of main routes production, processes evaluation and techno-economical assessment. Biomass Bioenergy **144** 105920 (2021). https://doi.org/10.1016/j.biombioe.2020.105920

103. Ozdenkci, K., De Blasio, C., Muddassar, H.R.: A novel biorefinery integration concept for lignocellulosic biomass. Energy Convers. Manage. 149, 974–987 (2017). https://doi.org/10.1016/j.enconman.2017.04.034

104. De Caprariis, B., De Filippis, P., Petrullo, A., Scarsella M.: Hydrothermal liquefaction of biomass : Influence of temperature and biomass composition on the bio-oil production. Fuel **208**, 618–625 (2017). https://doi.org/10.1016/j.fuel.2017.07.054

105. Akhtar, J., Aishah, N., Amin S.: A review on process conditions for optimum bio-oil yield in hydrothermal liquefaction of biomass. Renew. Sustain. Energy Rev. **15**(3), 1615–1624 (2011). https://doi.org/10.1016/j.rser.2010.11.054]

106. Sharma, S.K., Sharma, R.C., Sharma, N.: Combined Multi-Body-System and Finite Element Analysis of a Rail Locomotive Crashworthiness. Int. J. Veh. Struct. Syst. **12** (2020). https://doi.org/10.4273/ijvss.12.4.15

107. Bhardawaj, S., Sharma, R.C., Sharma, S.K.: Development in the modeling of rail vehicle system for the analysis of lateral stability. Mater. Today Proc. **25**, 610–619 (2020). https://doi.org/10.1016/j.matpr.2019.07.376

108. Sharma, R.C., Sharma, S., Sharma, S.K., Sharma, N., Singh, G.: Analysis of bio-dynamic model of seated human subject and optimization of the passenger ride comfort for three-wheel vehicle using random search technique. Proc. Inst. Mech. Eng. Part K J. Multi-body Dyn. **235**, 106–121 (2021). https://doi.org/10.1177/1464419320983711

109. Sharma, S.K., Sharma, R.C., Lee, J.: Effect of Rail Vehicle–Track Coupled Dynamics on Fatigue Failure of Coil Spring in a Suspension System. Appl. Sci. **11**, 2650 (2021). https://doi.org/10.3390/app11062650

110. Sharma, S.K., Sharma, R.C.: Pothole Detection and Warning System for Indian Roads. In: Advances in Interdisciplinary Engineering. pp. 511–519 (2019). https://doi.org/10.1007/978-981-13-6577-5_48

Process Management in Green Manufacturing

Srihari Palli , **Sivasankara Raju Rallabandi** , **Sreeramulu Dowluru** , **Azad Duppala** , **Venkatesh Muddada** , **Pavankumar Rejeti** , **and Raghuveer Dontikurti**

Abstract Manufacturing process management signifies a massive stage in the pursuit to connect product design with production digitally, so as to enhance information quality and decrease the time-to-market. In this era of virtualization where product and process data are transferred across sectors electronically manufacturing process management (MPM) is making huge strides in sending out the right product with the manufacturer's major focus on eliminating all kinds of waste in the plant without compromising on the quality. The main advantage of MPM is that it betters the production efficiencies resulting from more firmly designed and managed processes. MPM applications deliver analytical and data administration abilities needed by organizations to transfer to mixed model production systems to diminish work-in-process (WIP) or in-process-inventory (IPI), complete products inventory, and progress whole product quality and manufacturing sensitivity. The present amount of earth resources human beings are using is not justifiable, and it will disturb the environment in numerous ways. Manufacturing is a huge resource-consuming activity, it is significant to contemplate sustainability at all stages of product life cycle which are being made. Life cycle investigation is a recognized technique to find the ecological effect of the manufacturing. So as to include ecological necessities into manufacturing practices a totally different means of thought process needs to be employed by the investigators. Sustainable or green manufacturing is today attainable goal and various zones within manufacturing are profited through this. The current article is aimed at discussing how the advancements of traditional manufacturing techniques have improved and also the takeover of modern manufacturing methods and their processes management to reduce waste, scrap, etc., and contributing toward environmental sustainability.

Keywords Sustainability · Manufacturing process management · Product life cycle · Green manufacturing

S. Palli (✉) · S. R. Rallabandi · S. Dowluru · A. Duppala · V. Muddada · P. Rejeti · R. Dontikurti
Department of Mechanical Engineering, Aditya Institute of Technology and Management, Tekkali, Andhra Pradesh 532201, India
e-mail: srihari.palli@gmail.com

1 Introduction

Over the past 70 years, human beings had consumed more resources compared to the previous history. During the years 1950–2020, global metals production grew approximately 8 times, oil ingesting 10 times, and natural gas usage more than fifteen times. Resources are presently mined annually in a total amount of 60 billion tons, which is nearly 50% more than it was just 30 years ago. The circular economy estimates that 100.6 billion tons of materials are consumed worldwide each year. The degree of enervation of the metals, though, is debatable, with some researchers signifying that the existing stock of a choice of metals will drain out in a span of 50 years or even lesser than that [1–3].

It is absolutely true that this amount of utilizing natural resources is not at all sustainable, and if the next generations to relish the similar kind of atmosphere and resources, then there should be an immediate focus by all humans. The damaging results of our consumption and its concluding effects on the mankind are inevitable. This entire theory indicates that precisely forecasting upcoming worldwide metallic supply needs a thorough comprehension of mineral sources. Manufacturing is considered to be a very good source of consumption process, and hence, it has become vital to contemplate sustainability in entire number of stages of the life cycle of the products that are produced [4, 5].

The influx of non-traditional manufacturing processes such as ultrasonic machining, abrasive jet machining, electrodischarge machining, electrochemical machining, and plasma arc machining focus on reducing the scrap, accurate material removal rate (MRR) with quality product delivery. Additive manufacturing (AM) processes like 3D printing, fused deposition modeling (FDM), laminated object manufacturing (LOM), and selective laser sintering (SLS) specifically concentrated on metal/material deposition techniques and are thereby drastically reducing unnecessary raw material blank usage. AM methods proving to be worthy manufacturing processes for the upcoming decades, especially in terms saving materials for the future and are contributing heavily to sustainable/green manufacturing. Since AM uses the powder metallurgical and molten metal as material and is carried out straight from CAD design it often saves lot of material and almost eliminates scrap, thereby contributing to green manufacturing. With the advent of lean and agile methodologies coupled with technologies, the process management of the sustainability is growing leaps and bounds delivering magical results. Today, it is possible to achieve sustainable manufacturing, which has positive effects across several manufacturing-related industries. The goal of the research is to use less energy during manufacturing processes and practices and more ecologically friendly materials [6–8].

The challenge of globalization today is to meet the steadily growing demand for consumer goods and capital while also making sure that the social, environmental, and economic aspects of human life continue to grow in a way that is sustainable. Sustainability-focused industrial value development is necessary to meet this challenge. The transition to the fourth stage of industrialization, or "Industry 4.0," is

currently influencing how value is created in the early industrialized nations. Significant opportunities are presented by this development for the implementation of sustainable manufacturing. Based on current advancements in research and application, this article will give a state-of-the-art evaluation of Industry 4.0. The next section will give an overview of the various opportunities for sustainable production in Industry 4.0 [1, 9].

The primary domains shared by the manufacturing industry and the study issues for green/sustainable manufacturing are thus broadly categorized as follows: product design for sustainability; sustainable manufacturing processes; and sustainable manufacturing systems.

2 Product Design for Sustainability

Traditional product design processes cost between 5 and 7% of the total cost of the product, whereas early design decisions secure 70–80% of the total cost. We can also surmise that the sustainability of the product is significantly influenced by the early choices taken. Therefore, in light of the limited knowledge available at the early stages of the design process, it is essential that the designers use specialized techniques to evaluate the environmental impact. LCA has been regarded as a tool for determining a product's sustainability over the course of its life, as was previously said. Design for environment is the practice of including environmental factors in the engineering design of products and processes (DFE). LCA is one of the assessment tools used in DFE during the design and manufacturing of a component or product. As LCA assesses the impact of the product and its manufacturing processes and the goal of DFE is to minimize the effect of the product, and processes on environment LCA and DFE are often combined. It is employed to create environmentally friendly goods and procedures while upholding industry standards for performance, cost, and quality. Several design tools are currently available for this purpose. According to ISO-TR 14062, there are about 30 instruments that can be used for this. Other design tools have also become accessible since then. The majority of them rely on LCA, quality function deployment (QFD), or checklists [10] deliver.

The checklists have the benefit of being simple to use and very practical at the beginning of the design process. However, they depend greatly on the understanding and preferences of the designer and are highly subjective. It takes a great deal of expertise and experience to use these technologies properly. As a result, there won't be uniformity across designers in terms of the results of using these checklists [11]. The benefits of applying QFD, LCA, and checklists include:

- designate requirements of spoken and unspoken customer;
- identify and transform customer needs into technical specifications;
- manufacture and deliver a quality product or service by concentrating all staff toward customer satisfaction;
- channelize efforts and skills of any industry from project start to end;

- enhance customer satisfaction;
- improve product quality.

Traditionally, QFD has been used to translate customer requirements into engineering specifications by comparing them to those of competitors' products. The QFD is modified by including the product's environmental effects, and if new customer needs arise over the product's life cycle, a set of eco-design tools may be developed. The voice of the customer for the environment is described in the QFD for the environment (QFDE) in the form of reduced material usage, ease of transport and storage, ease of processing and assembly, ease of processing and assembly, less energy consumption, etc. Finding out the engineering specifications for the setting is recommended. This includes things like the weight, volume, number of parts, materials, dirtiness risk, hardness, physical lifetime, etc. After that, a functional study determines how traditional and environmental hot spots are related to engineering qualities (including structure or components). A significant drawback of these QFD-based tools is the fact that the creation of correlation coefficients among changing environments, quality, and project requirements is entirely up to the designers and that these correlations are frequently built on knowledge from the conventional environ practice of engineering without having taken life cycle into account (similar to traditional QFD). Among these are the establishment of environmentally friendly quality functions, the building of a House of Ecology, and the implementation of QFD for the environment. The collecting of customer and environmental demands, as well as the establishment of relationships between those needs and quality attributes, are frequent first steps in the application of these strategies. The following stage is to do a functional analysis to identify the relationships between the environmental aspects and the engineering needs (including the structure or components) and to provide sustainable engineering requirements from the viewpoint of the environment. Building connections between engineering requirements and environmental needs is completely the responsibility of the designers. Typically, these correlations don't consider the complete life cycle because they are based on information from the traditional discipline of environmental engineering. As previously said, LCA is the most widely used tool for assessing a product's or process's environmental footprint. But the problem with LCA is that it needs a lot of data to be conducted, and thus it can't be employed early in the design phase. Since there won't be any information from earlier generations of items available, this is more challenging for a completely new design. Therefore, efforts must be made to ensure that a streamlined or simplified LCA is created for the initial stages of product design. Allocating environmental impacts across functions is a different approach that has been used to evaluate the sustainability of concepts produced during the early stages of design. There are several computer-aided technologies that are available that may be used to determine the environmental authenticity of the product design once the product concept has been determined.

3 Sustainable Manufacturing Processes

An enterprise's manufacturing process consumes a substantial quantity of resources and generates a substantial number of pollutants and trash, resulting in environmental contamination. They are categorized into the following groups in order to lessen the negative effects of manufacturing operations on the environment:

Optimize the environmental performance of the existing processes.

- Machining process optimization
- Optimum tool path generation using environment variable
- Optimizing for minimum energy usage
- Cutting fluids
- Machine tool chatter.

3.1 Sustainable Cutting Fluid Workbench

Cutting fluids are frequently used in metal working processes to eliminate and minimize the heat produced during the machining operations. Cutting fluid use considerably raises tool life while lowering machining costs and improving machining quality. There is a vast variety of cutting fluids made of both organic and inorganic ingredients. However, the widespread use of cutting fluids has a number of negative consequences on the environment, forcing modern industry to pay more attention to this issue. There are strict standards in place to limit the mist and vapor produced during the machining procedures since they are dangerous to the operator. Numerous occurrences of skin cancer have been brought on by direct contact with cutting fluids. The used cutting fluids must be recycled or disposed of in a way that doesn't harm the environment due to strict environmental regulations. Depending on the type of cutting fluid used, this necessitates extra spending on recycling and disposal operations [10, 12–14].

According to Klocke and Eisenblatter [15], 350,000 tons of cutting fluids were reportedly handled and ultimately disposed of in Germany alone in 1994. The price of buying and getting rid of coolant is almost one billion German Marks. In the German automobile sector, cutting fluid expenses are reported to be between 7 and 17% of component manufacturing costs, compared to tool prices, which are stated to be between 2 and 4%. These costs also include monitoring, maintenance, health precautions, and absenteeism. As a result, research that can lower the expenses of cutting fluids by lowering the cost of their disposal or lowering the volume consumed is currently receiving more attention.

Due to the high cost of machining, the potentially harmful effects on the environment and the potential health risks to operators, scientists are investigating alternatives to the use of cutting fluids, such as minimum quantity lubrication (MQL) or similar dry cutting conditions. Although water-soluble fluids have also been used in specific applications, plain oil is often the fluid used in MQL. Tiny amounts of these

fluids are delivered to the tool and/or machining spot. The so-called airless systems involve a pump that delivers oil to the tool in a series of quick, precisely measured drops. Air could also be used for this. Mist application is the process of atomizing the lubricant with air in the nozzle to create incredibly small droplets. However, they came to the conclusion that wet machining was still better for tool life and that dry cutting was only really useful for shallow cuts [16, 17].

Vegetable oil-based alternative cutting fluids are biodegradable and regenerative. The heat generated at the workpiece/cutter interface with petroleum-based cutting fluids frequently results in a mist, which poses a risk to machine operators due to the fluid's low flash point (about 215 °C). Due to their large molecular weight and high flash point of roughly 315 °C, soybean-based cutting fluids greatly reduce the likelihood of mist creation in machining processes. Also, the high film strength of these soy-based cutting fluids helps to reduce heat and tool wear by reducing friction between the cutting tool and the workpiece. Despite the fact that bio-based cutting fluids have been available for some time, most companies do not employ them [10, 18]. Only a few studies on bio-based cutting fluids have been published in the literature. Belluco and DeChiffre's [19] study was mostly about drilling into AISI 316L is an austenitic stainless steel with specially made oils that included rapeseed oil, ester oil, sulfur, and phosphor. Compared to mineral oil-based drilling solutions, bio-based fluids performed better in terms of tool life, chip breaking, tool wear, and cutting forces, has shown by the results of the trials. Similarly, the research by Rao et al. suggests that using cutting fluids based on soybeans has advantages for performance enhancement that are comparable to or greater than those of petroleum-based fluids [20]. As a result, it will strengthen its reputation as a green-cutting fluid because it lacks any toxic ingredients that would make disposal more difficult and expensive.

When making decisions about machining to consider when choosing the cutting fluid (C), quality (Q), and cost are usually the most important objective factors. However, they have a greater influence on the environment (E) due to green manufacturing (GM). In a multi-object decision-making model for the selection of cutting fluid for GM, Tan et al. combined consideration of the objects of quality (Q), cost (C), and environmental impact (E). A cutting fluid cost calculation model has been put forth by Hubbard et al. to address the environmental standards. The following expenses have been included in the overall cost of the machining. The following are included in the overall cost of cutting fluid:

- Maintenance of the cutting fluid, the cost of additives, and any associated labor costs.
- The price of cosmetic fluid, the price of volumetric cutting fluid loss from evaporation, leakage, etc.
- Waste-cutting fluid disposal and system flushing costs must also be factored in.
- According to their findings, the model takes into account the environmental price tag adequately.

3.2 Formulations of Vegetable-Based Cutting Fluid

In association with chemistry, chemical technology and/or agricultural department identify an appropriate formulation of vegetable-based cutting fluid. The oils that were tried in the literature are: blended with rapeseed oil, ester oil and sulfur and phosphor additives, soybean-based oil, coconut oil, etc. The requirement to be looked at is good ability for lubrication, high flash point, high viscosity, and high-temperature viscosity stability in these formulations. Avoid the use of EP additives as these are harmful to the environment. The points to be considered are biodegradability, renewable, low cost, and easy availability.

3.3 Evaluation of Cutting Fluid Standard Approach

The use cutting fluid for a given application depends upon the availability of application data. With the development of new cutting fluids, it is also important to develop application data to the user so that the decision to use it for a given application will become easy on the part of the user. To facilitate this, it is necessary to develop some standardized cutting fluid tests so that the cutting fluids can be easily compared.

3.4 MQL—Mist Application Process

Using the above procedure conduct experiments on different engineering work material to develop application data to compare MQL and flooding techniques with a view to establish the conditions under which flooding is useful and when MQL would be relevant.

3.5 Cutting Fluid Cost Model

Compared to petroleum-based alternatives, vegetable-based cutting fluids are widely acknowledged to be more expensive. To defend the use of cutting fluids made from plants, you need to think about how much they cost over their whole life. The numerous expenses that will be spent over the entire cutting fluid life cycle must be determined for this reason. Create a realistic cutting fluid cost model by identifying every cost incurred over the course of the product's life.

3.6 Optimization of Machining Process Utilizing Cutting Fluid

Based on the above lifecycle cutting fluid cost model, develop a decision support system for selecting optimum cutting process parameters for any machining operation. The objective function should include the life cycle costs of the tools and cutting fluids so that all the environmental aspects will be covered.

4 Sustainable Manufacturing Systems

An increase in industrial production systems' digitalization over the past few years has led to an intelligent, networked, and decentralized manufacturing. The term "Industry 4.0" or "The fourth industrial revolution" is widely used to describe this new organizational level. The main goal of Industry 4.0 is to fully integrate commercial and technological processes through the use of cutting-edge technology. This will make it possible for manufacturing to be flexible, efficient, sustainable, and always affordable. Manufacturing companies need to maximize their return on investment while minimizing their environmental impact. They must also establish an ideal workplace that prioritizes collaboration, education, and competency growth [9, 21].

The objective of sustain manufacturing for automation is to increase the industrial sector's capability for resource-efficient and sustainable production from 2016 to 2030.

- Focusing on emissions reductions, the phase-out of particularly dangerous compounds, increased resources and energy efficiency, renewability and recyclability, and improved environmental performance, new or improved technologies, goods, and services are being developed.
- Making use of emerging digital and even other technology to facilitate the shift to a circular economy free of fossil fuels.
- Supporting business models for the circular economy.
- Making sure that laws and other governance structures encourage or make it easier for production that is resource-efficient, ecologically friendly and has a steady access to raw materials.

4.1 Green Supply Chain Management (GSCM)

To make it more significant, feel free to add or remove anything. Because of globalization, a finished product can now be made up of parts that come from practically wherever in the world. Following assembly, the item is sent for distribution before being delivered to the customer. As a result, efforts to realize sustainable products must consider manufacturing activities at the process, factory, and supply chain

levels. The supply chain may be responsible for 25% of all production expenses, which means it probably also adds to environmental expenses. The main goal of conventional supply chain management strategies is to satisfy consumer needs by making the most effective use of resources, such as labor, inventory, and delivery capacity.

Therefore, shorter industrial process chains are required for GSCM, especially for geographically well-localized portions of life cycles and those that lessen the environmental impact of products. Academic and business interest in GSCM has significantly increased recently as a result of the growing environmental sustainability issues. As a result, the reuse issue can also be seen from a logistical standpoint. In contrast to the conventional supply chain management strategy, a sustainable supply chain should be planned to minimize its financial and environmental costs. Implementing GSCM practices encompasses green purchasing, integrated life cycle management supply chains that go from supplier to manufacturer to consumer, and then closing the loop using reverse logistics. The Sustainability Consortium, which unites academic institutions, corporations, NGOs, and governmental groups to create a sustainable product index for consumer goods, was supported by Wal-Mart. One of the main goals is to construct life cycle inventories and analyses for thousands of items that are produced and utilized globally using technologies that are based on science.

Customers' willingness and capacity to return goods are simply one aspect of the issue; another is the existence of a well-organized reverse supply chain. The two main approaches to the problem of reverse logistics are independent and integrated. The forward supply chain and the reverse supply chain are thought to function independently of one another in an autonomous method. An integrated strategy, on the other hand, takes them all into account, including their relationships.

The major goal of this research is to develop linear multi-objective programming models that can optimize forward and reverse logistics operations in a specific green supply chain. A closed-loop manufacturing system that oversees a reverse logistics network is preferred. The product's whole environmental impact should be taken into account in collaboration with the suppliers, distributors, customers, recycling businesses, and waste-processing organizations. Several elements that could be used in the model development include:

- Carbon footprint of suppliers, distributors, transporters, and any others involved in the supply chain
- Modularization of products
- Product reuse
- Product remanufacturing
- Cannibalization of sales of new products by remanufactured products
- Product recycling.

4.2 Links Between Industry 4.0 and Sustainable Manufacturing

Digitalization and sustainability are broad challenges that have an impact on every step of the industrial process. Indeed, both approaches provide a synthesis of methods, including engineering for disassembly, reprocessing, and recycling as part of a management system; reverse supply for a circular economy; "lean and green management" for resource utilization; sustainable design that lessens risks to workers and consumers; and the elimination of harmful elements in production processes [9].

Reduced waste, energy consumption, and excess output; increased productivity, resource efficiency, and adaptability (e.g., big data for preventive analytics and rapid system reconfiguration in production); increased usage of big data. Industry 4.0 is expected to make sustainability better by getting stakeholders involved and getting them to work together (e.g., closed-loop producer and consumer interconnect machines, data management, and production processes).

More and more machines and equipment are being networked using cyber-physical systems. The industrial industry is employing more and more computerization to keep up with the increasing output demands. Smart production systems are flexible, use resources efficiently, are easy to use, and can include customers and business partners in the process of creating value. In-depth expertise and continuing relationships with consumers, suppliers, and other types of stakeholders are required due to the large number of product varieties, short product life cycles, and complicated procedures at every level of the hierarchy. Given the effects of globalization and rising competitive pressure, efficient resource usage is crucial.

Industry 4.0 may encourage value generation in all facets of sustainability, claim Stock and Seliger [22]. They highlight opportunities for growth in the industry by considering things like (1) the proliferation of smart data-driven business models that yield novel devices; (2) closed-loop product standardization and industry symbiosis that constructs value networks; (3) CPS-using tools for digitally enhancing small and medium-sized enterprises; (4) ICT-enabled trainings and competency development; (5) CPS-using programs (like games and individual incentives) to foster positive behavioral change.

Each product is a distinct system that is developing around an integrated data solution, according to Stark et al. [23]. Thus, an implemented solution might have both direct and indirect effects on the various systems comprising the sustainability dimensions. The relationships between a solution's effects and its primary and secondary impacts are known as causal relations. Other types of interactions between sustainability systems include volume and scale drivers, latency and timely length constraints, and direct and indirect effects that are influenced by a solution's volume and scale of distribution (between effects and impacts). When analyzing the research, only the causal connections between the variables will be taken into consideration (Fig. 1).

Sustainable Manufacturing in Industry 4.0

Technological Pillars*	Scope of Sustainable Manufacturing**	Industry 4.0 and SM ***	Sustainability Dynamics Model****
1. Autonomous robots 2. Simulation 3. Horizontal and vertical system integration 4. The industrial IoT 5. Cybersecurity 6. The cloud 7. Additive Manufacturing 8. Augmented reality 9. Big data and analytics	1. Manufacturing Technologies 2. Product lifecycles 3. Value creation networks 4. Global manufacturing impacts	1. Business Model 2. Value Creation Network 3. Equipment 4. Human Factor 5. Organization of Smart Factories 6. Sustainable Manufacturing Processes 7. Product Development	1. Direct effects on Environmental dimension 2. Direct effects on Social dimension 3. Direct effects on Economical dimension 4. Indirect effects on Environmental dimension 5. Indirect effects on Social dimension 6. Indirect effects on Economical dimension

Industry 4.0 Principles ***
Digitization and integration of vertical and horizontal value chains
Digitization of product and service offerings
Digital business models and customer access

Fig. 1 Framework concepts for the scientific report [9]

4.3 The Economic and Social Effects of Smart Manufacturing

The term "smart factory" describes a factory with a digitalized environment, whereby machines and devices have the capability to automate and optimize processes. It is one of the essential elements of Industry 4.0, and every nation is making an effort to transition over by mobilizing its resources. Due to globalization and ongoing market competitiveness based on client needs, the majority of businesses began their path toward smart factories in an effort to maintain their position as the industry's top rivals. The transition from a traditional manufacturing to a smart factory produced a wide range of social and economic effects [24].

The production, service, and consumer markets are all places where the consequences of the smart factory's influence on the economy can be observed and felt. A "smart factory" is one that uses intelligent machinery, such as robots, workpieces, and machines with machine intelligence, in its manufacturing operations. This intelligence manufacturing enhances operations and yields the final products known as smart products by virtue of their ability to self-organize and self-adapt. Customers are also pleased with the items thanks to clever production because they are of high quality, distinctively designed, and produced quickly.

In terms of society, smart factories show how they affect the labor market, workplace safety, and labor legislation. A factory automates and self-improves when a company uses smart manufacturing. This alters the labor market since fewer people with lower skill levels are required as more activities and responsibilities are taken on

by smart gadgets. More skilled individuals will be needed to manage the functionality of the smart devices, though. Additionally, smart factories increase opportunities for employment, education, and professional advancement, which lower the unemployment rate. The transformation of the facility into a smart factory has resulted in an additional risk to workers' safety. To ensure the upholding of civil rights and the strengthening of labor laws, as well as the elimination of workspace [25].

The four categories such as data, compute capabilities and network; analytics and intelligence; interpersonal behavior; and digital-to-physical conversion are created from the same group of technologies. These four divisions which are seen to be essential for digitization lead to the grouping of similar technologies that are discussed in the local literature. The key technologies required to completely execute Industry 4.0 are listed in Fig. 2. Technologies must satisfy needs derived from operations within current architectures. These specifications are important to ensure system connectivity, flexibility, and dependability. Greater robustness and compliance with top quality in research, planning, production, operations, and logistics processes will be delivered by Industry 4.0 [25]. Notable firms which have adapted Industry 4.0 in their march for sustainability include:

- Aveva's Vision AI Assistant which is an image categorization-based analytic tool which empowers manufacturer to use visuals from prevailing general-purpose cameras and translate them into accessible information.
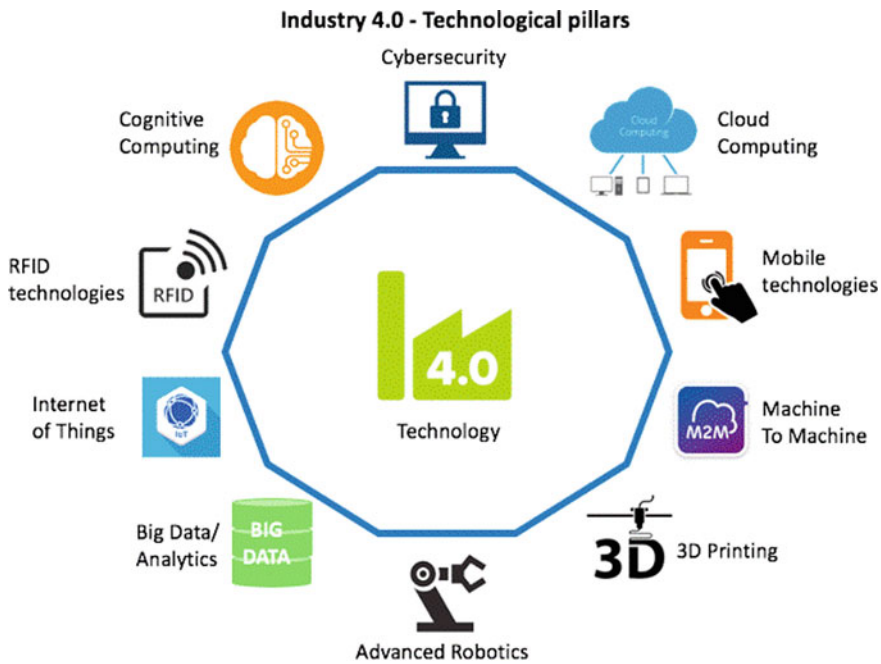
Fig. 2 Technology foundations for Industry 4.0 [26]

- Volvo Group, producing trucks, buses, construction equipment, and power solutions for marine and industrial applications, have begun using a measure to transform its IT architecture by integrating its PLM and CAD platforms to assist improved leverage of product data over the value chain.
- Siemens Digital Industries Software through it's Xcelerator portfolio is propelling metamorphosis to authorize digital enterprise where engineering, manufacturing, and electronics design industries of all sizes create and leverage digital twins to drive restructuring.
- AI-based Refinery tool developed by Beyond Limits, Google Cloud customized by Siam Cement Company, Digital transformation tools developed by Emerson pneumatic valves, and Malaysian airlines.

5   Other Factors for Green Manufacturing

The concepts of Design for Manufacturability (DFM), Design for Assembly (DFA), and Design for Environment (DFE) allow for the efficient use of resources and minimize environmental effects, respectively. This is accomplished by reducing or sacrificing the number of components, the number of procedures, the assembly process, the manufacturing time, the quantity of materials used, etc. [27–29]. Because of numerous catastrophic failures, there has been an increase in human awareness of environmental safety throughout the world [30–40]. Various approaches used in DFE are essentially listed below:

- Recycling and reuse of materials
- Minimization of waste
- Process waste minimization
- Easy for Disassembly
- Avoid the use of harmful material
- Avoid danger to industry workers and customers
- Recycling of packaging material
- Noise reduction from product.

Designers began to create environmentally friendly things that were more eco-friendly. As a result, the terms "Green design" and "Eco-design" have emerged. While Green design particularly aimed on the environmental impact, Eco-design addressed how a product will affect the environment over its lifetime. As they create things, designers now have a greater obligation to consider the local and global implications of their choices in terms of sustainability.

6 Discussion

Digital transformation with sustainability is serving consumer product maker's advance the much-needed agility and resilience in the after pandemic scenario.

The product manufacturers can:

- Advance cross-functional supply chain prominence.
- Generate a digital thread which studies, analyzes, and passes data across processes.
- Install cutting-edge production planning and scheduling techniques.
- Generate production plans which are viable to perform on the basis of practical situations prevailing in the plants.
- Provide the perceptibility, transparency, and traceability to end-customers and regulators on demand and supply.
- Influence and control process information with prognostic and rigid AI for constant output, asset dependency, and eco-sustainability optimization.

7 Conclusion

Based on the discussions, green design and manufacturing is the rise of trust needed in mechanical design services. The important thing here is, various countries, and organizations have already initiated working toward. Smart manufacturing integrated with green concepts deliver several positive effects both in economical and social features comprising of process efficiency, labor safety, condensed production cost, manufacturing agility, environmental sustainability and quality enhancement. It is a required tendency for human beings to keep their association with sustainable growth. This practice of green manufacturing and design will support in preventing barriers of sustainability and endorse ecological shield to reduce usage and improve efficiency.

References

1. Wang, S., Wan, J., Li, D., Zhang, C.: Implementing smart factory of Industrie 4.0: an outlook. Int. J. Distrib. Sens. Netw. 1–10 (2016)
2. Davies, B.: The future of the manufacturing system. Prod. Eng. **50**, 233 (1971)
3. Beier, G., Niehoff, S., Xue, B.: More sustainability in industry through industrial internet of things? Appl. Sci. (Switzerland). **8**, 219–223 (2018)
4. Sharma, R.C., Sharma, S., Sharma, S.K., Sharma, N., Singh, G.: Analysis of bio-dynamic model of seated human subject and optimization of the passenger ride comfort for three-wheel vehicle using random search technique. Proc. Inst. Mech. Eng. Part K J. Multi-body Dyn. **235**, 106–121 (2021). https://doi.org/10.1177/1464419320983711
5. Bhardawaj, S., Sharma, R.C., Sharma, S.K.: Analysis of frontal car crash characteristics using ANSYS. Mater. Today Proc. **25**, 898–902 (2020). https://doi.org/10.1016/j.matpr.2019.12.358

6. Pattnaik, S., Dash, D., Mohapatra, S., Pattnaik, M., Marandi, A.K., Das, S., Samantaray, D.P.: Improvement of rice plant productivity by native Cr (VI) reducing and plant growth promoting soil bacteria *Enterobacter cloacae*. Chemosphere **240**, 124895 (2020)

7. Agrahari, R., Sarraf, G., Joshi, N.C., Mohapatra, S., Varma, A.: Insight of biopolymers and applications of polyhydroxyalkanoates. In: Microbial Polymers, pp. 177–191. Springer, Singapore (2021)

8. Sahoo, N., Pattnaik, S., Pattnaik, M., Mohapatra, S.: Methane emission and strategies for mitigation in livestock. Environ. Agric. Microbiol Appl Sustain. 257 (2021)

9. Machado, C.G., Winroth, M.P., Ribeiro da Silva, E.H.D.: Sustainable manufacturing in Industry 4.0: an emerging research agenda. Int J Prod Res. 58, 1462–1484 (2020).

10. Rao, P.N.: Sustainable manufacturing—principles, applications and directions. In: Twenty-Eighth National Conventions of Production Engineers on "Advancements in Production and Operations Management" organized by Rajasthan State Centre, pp. 24–36. The Institution of Engineers (India) (2013)

11. Sharma, R.C., Palli, S., Sharma, N., Sharma, S.K.: Ride behaviour of a four-wheel vehicle using h infinity semi-active suspension control under deterministic and random inputs. Int. J. Veh. Struct. Syst. **13**, 234–237 (2021)

12. Siva Sankar Raju, R., Srinivasa Rao, G., Muralidhara Rao, M.: Optimization of machinability properties on aluminium metal matrix composite prepared by in- situ ceramic mixture using coconut shell ash—Taguchi approach. Int. J. Concep. Mech. Civ. Eng. **3**, 17–21 (2015)

13. Hossain, I., Velkin, V.I., Shcheklein, S.E.: Experimental study in reduction of two phase flow induced vibration. MATEC Web Conf. **211**, 16001 (2018). https://doi.org/10.1051/matecconf/201821116001

14. Waydande, R., Ghatge, D.: Performance evaluation of different types of cutting fluids in the machining of hardened steel—a review. Int. J. Mech. Prod. Eng. **4**, 34–39 (2016)

15. Klocke, F., Eisenblätter, G.: Dry cutting. CIRP Annals **46**, 519–526 (1997)

16. Davim, J.P., Sreejith, P.S., Silva, J.: Turning of brasses using minimum quantity of lubricant (MQL) and flooded lubricant conditions. Mater. Manuf. Process. **22**, 45–50 (2007)

17. Dhar, N.R., Kamruzzaman, M., Ahmed, M.: Effect of minimum quantity lubrication (MQL) on tool wear and surface roughness in turning AISI-4340 steel. J. Mater. Process. Technol. **172**, 299–304 (2006)

18. Mitra, B.C.: Environment friendly composite materials: biocomposites and green composites. Def. Sci. J. **64**, 244–261 (2014)

19. Belluco, W., Chiffre, L.: Surface integrity and part accuracy in reaming and tapping stainless steel with new vegetable based cutting oils. Tribol. Int. **35**, 865–870 (2002)

20. Sharma, S.K., Kumar, A.: The impact of a rigid-flexible system on the ride quality of passenger bogies using a flexible carbody. In: Proceedings of the Third International Conference on Railway Technology: Research Development and Maintenance Stirlingshire UK 5-8 April 2016 Cagliari Sardinia Italy. Stirling-shire UK: Civil-Comp Press. p. 87 (2016). https://doi.org/10.4203/ccp.110.87

21. Hossain, I., Velkin, V.I., Shcheklein, S.E.: The study of passive vibration dampers in pipelines using piv-methodology for single phase flow. In: WIT Transactions on Ecology and the Environment. pp. 565–570 (2017). https://doi.org/10.2495/ESUS170521

22. Stock, T., Seliger, G.: Opportunities of sustainable manufacturing in Industry 4.0. Proc. CIRP 536–541 (2016)

23. Bhardawaj, S., Sharma, R.C., Sharma, S.K.: Development in the modeling of rail vehicle system for the analysis of lateral stability. Mater. Today Proc. 25, 610–619 (2020). https://doi.org/10.1016/j.matpr.2019.07.376.

24. Waibel, M.W., Steenkamp, L.P., Moloko, N., Oosthuizen, G.A.: Investigating the effects of smart production systems on sustainability elements. Proc. Manuf. **8**, 731–737 (2017)

25. Edwards, B., Gray, M., Hunter, B.: The social and economic impacts of drought. Aust. J. Soc. Issues **54**, 22–31 (2019)

26. Puskás, E., Bohács, G.: Physical internet—a novel application area for Industry 4.0. Int. J. Eng. Manage. Sci. **4**, 152–161 (2019)

27. Siva Sankara Raju, R., D, A., Thimothy, P.: Determination of stress and deformations analysIs on LPG steel cylinder. Int. J. Eng. Res. Appl. (IJERA) **3**, 733–737 (2013)
28. Sharma, R.C., Palli, S., Koona, R.: Stress and vibrational analysis of an Indian Railway RCF bogie. Int. J. Veh. Struct. Syst. **9**, 296–302 (2017)
29. Palli, S., Koona, R., Sharma, R.C., Muddada, V.: Dynamic analysis of Indian railway integral coach factory bogie. Int. J. Veh. Struct. Syst. **7**, 16–20 (2015)
30. Sharma, S.K., Kumar, A.: The Impact of a rigid-flexible system on the ride quality of passenger bogies using a flexible carbody. In: Pombo, J. (ed.) Proceedings of the Third International Conference on Railway Technology: Research, Development and Maintenance, Stirlingshire, UK, p. 87. Civil-Comp Press, Stirlingshire, UK (2016). https://doi.org/10.4203/ccp.110.87
31. Sharma, S.K., Sharma, R.C.: Pothole detection and warning system for Indian roads. In: Advances in Interdisciplinary Engineering, pp. 511–519 (2019). https://doi.org/10.1007/978-981-13-6577-5_48
32. Goswami, B., Rathi, A., Sayeed, S., Das, P., Sharma, R.C., Sharma, S.K.: Optimization design for aerodynamic elements of Indian locomotive of passenger train. In: Advances in Engineering Design. Lecture Notes in Mechanical Engineering, pp. 663–673. Springer, Singapore (2019). https://doi.org/10.1007/978-981-13-6469-3_61
33. Bhardawaj, S., Chandmal Sharma, R., Kumar Sharma, S.: Development and advancement in the wheel-rail rolling contact mechanics. IOP Conf. Ser. Mater. Sci. Eng. **691**, 012034 (2019). https://doi.org/10.1088/1757-899X/691/1/012034
34. Choppara, R.K., Sharma, R.C., Sharma, S.K., Gupta, T.: Aero dynamic cross wind analysis of locomotive. In: IOP Conference Series: Materials Science and Engineering, pp. 12035. IOP Publishing (2019)
35. Sinha, A.K., Sengupta, A., Gandhi, H., Bansal, P., Agarwal, K.M., Sharma, S.K., Sharma, R.C., Sharma, S.K.: Performance enhancement of an all-terrain vehicle by optimizing steering, powertrain and brakes. In: Advances in Engineering Design, pp. 207–215 (2019). https://doi.org/10.1007/978-981-13-6469-3_19
36. Bhardawaj, S., Chandmal Sharma, R., Kumar Sharma, S.: A survey of railway track modelling. Int. J. Veh. Struct. Syst. **11**, 508–518 (2019). https://doi.org/10.4273/ijvss.11.5.08
37. Sharma, S.K., Sharma, R.C., Sharma, N.: Combined multi-body-system and finite element analysis of a rail locomotive crashworthiness. Int. J. Veh. Struct. Syst. **12**, 428–435 (2020). https://doi.org/10.4273/ijvss.12.4.15
38. Sharma, R.C., Sharma, S.K., Palli, S.: Linear and non-linear stability analysis of a constrained railway wheelaxle. Int. J. Veh. Struct. Syst. **12**, 128–133 (2020). https://doi.org/10.4273/ijvss.12.2.04
39. Palli, S., Sharma, R.C., Sharma, S.K., Chintada, V.B.: On methods used for setting the curve for railway tracks. J. Crit. Rev. **7**, 241–246 (2020)
40. Sharma, S.K., Sharma, R.C., Choi, Y., Lee, J.: Experimental and mathematical study of flexible–rigid rail vehicle riding comfort and safety. Appl. Sci. **13**, 5252 (2023). https://doi.org/10.3390/app13095252

Heavy Metals Contaminants Threat to Environment: It's Possible Treatment

Pankaj Malviya, Anil Kumar Verma, Amit Kumar Chaurasia ⓘ **, Hemant Parmar, Lokendra Singh Thakur** ⓘ **, Prashant Kumbhkar, and Palak Shah**

Abstract Heavy metals usually exist in the crust of the earth. It has certain compositions in the localities which result in the structural disparity with the surrounding concentrations. It has traced on the amount of the respect to the living organisms that are related to the metabolic activities. The highly soluble ways to meet the extremely toxic yet perilous contaminants of the eater have included the activities where the metals are released into the environment. They are leached into the underground waters along with the depositing the aquifers. The surface water might run out of the potential contaminants for the environmental metals. Heavy metals have potential contaminants for environment has to make the trophic transfer in food chains take place. The heavy metals dependency has added on the relative oxidation state where physiological bio-toxic effects can enter to the world. The toxic compounds such as arsenic, cadmium, lead have altered the productive functioning of the bio-reactions. This has led to the production of the mutagenic, carcinogenic, and genotoxic effects to the occurrence and allocation in the heavy metals. The impact of the environment has added on the toxicological measures in the environment. The study further focused on the occurrence and allocation of heavy metals along with the possible eco-friendly remedies in the environment.

Keywords Heavy metals · Contamination · Environment · Toxicity · Remediation's

P. Malviya · P. Shah
Department of Chemical Engineering, Indore Institute of Science and Technology, Indore, India

A. K. Verma
Department of Chemical Engineering, Assam Energy Institute, Sivasagar, India

A. K. Chaurasia
Amity Institute of Biotechnology, Amity University Uttar Pradesh, Noida, India

H. Parmar
Department of Mechanical Engineering, Ujjain Engineering College, Ujjain, India

L. S. Thakur (✉) · P. Kumbhkar
Department of Chemical Engineering, Ujjain Engineering College, Ujjain, India
e-mail: lokendrast@gmail.com

1 Introduction

The term environment is referred to the surroundings where the human exists. It has made the atmospheric conditions more evident. The microorganisms, plants, and animals have the life to make the part of the combination on the physical, chemical, and aesthetic and cultural properties [1]. It has added on the foregoing conditions which influence the human behavior and well-being. It has analyzed the biosphere conditions where living organism's harbors. It remarks on the ways to find the interactive chain to the non-living environment conditions. This can last on the industrialization and globalization of the impaired pristine environment [2]. The components might comprise of the holistic functioning of the environment with intrinsic values.

Pollution has added contaminations through detrimental impact on the environment. The substances or energy have provided the deleterious effects on the living resources which would bring the human health hazards [3]. This has also created hindrance to the environmental activities and impaired on the quality of the environment with the reduction of amenities [4]. The contamination on the other hand has preserved to the elevated concentrations and natural background levels in the area. The environmental pollution has added undesirable and unwanted change in the characteristics of air, water, and soil [5]. The pollution has somehow added chemical energy such as noise, light, and heat to the substances that are focusing on synergies or naturally occurring contaminations [6].

Heavy metals are metallic elements that have relatively high density and metalloids set with atomic density greater than 5 g/cm^3. The environmentally stable yet non-biodegradable practices tend to manage the plants and animals causing different chronic effects on the human health has added on the details affecting the environment [7]. The heavy metals cannot be degraded or destroyed but have persistent with the natural constituents where the entire body system might provide the water, food, and air through the bio-accumulation over a period of time [8]. The natural processes that are adding on the geological deposits of lead, arsenic, and other heavy metal might dissolve in the water. This can potentially degrade the level of the drinking water.

The study reveals on the applications and strategies that can be advantageous for environmental balance. Furthermore, it will also focus on the existence of the heavy metals in the environment with the great concern as there is a high level of toxicity and susceptible carcinogenic effects [9]. The heavy metals are likely to include the metals such as lead, copper, zinc, copper, and cadmium along with the other pollutants with the living organisms [10]. There are different diseases which can be lower in concentrations but due to extensive contamination of the aqueous waste streams from several industrial activities such as electroplating, chemical, mining, tanneries, and painting have been addressing to the agricultural sources where fertilizers are widely used [11].

The heavy metals if consumed in the small proportion by the human than its necessitate the body level but if consumed in higher proportion, then it is toxic [12]. Henceforth, it reveals that toxicity of the heavy metals is becoming a great threat to

our health and environment. It has been reported that metals such cobalt, copper and chromium and iron and magnesium, manganese, molybdenum, and nickel-based biochemical and physiological functions [13]. Heavy metals have a trace of the elements to which the concentrations might focus on the environmental matrices. This can focus on the physical factors such as temperature, phase association along with the adsorption and physiological adaptation with important role play. The requirement of the biochemical and physical aspects has deemed to manage the hazardous pollutants in the natural environment along with the toxicity and rapidity and bio-accumulation problems [14]. The elements direct on the oxidative stress-related factors such as copper is the best example that presents a cross-linking of collagen.

1.1 Sources of Heavy Metals

The environmental front has received heavy metals from both natural and anthropogenic sources that percolates on the layers of the earth. The volcanic eruptions, weathering of rocks, windblown dust particles, and aerosols have naturally influenced the source of heavy metals [15]. It has remarked on the inorganic and organic fertilizers, pesticides, and fungicides. The anthropogenic sources have added municipal waste and organic manure along with the atmospheric pollution where the metals are found in various heavy metal sources in the environment [16]. Some of the listed sources are arsenic, cadmium, chromium, copper, lead, manganese, mercury, nickel, and zinc as shown in Table 1.

The environment has been severely contaminated with the toxic metals. This has also included the olivine, augite, sedimentary measures such as minerals and rocks in the sufficient quantity of metals. The extraction through the ores and contribution in

Heavy metals	Sources in the environment
Arsenic (As)	Pesticides, metal smelters
Cadmium (Cd)	Welding, electroplating, fertilizers, nuclear fission plant
Chromium (Cr)	Mining, electroplating, tannery industries
Copper (Cu)	Pesticide, mining, and electroplating
Lead (Pb)	Paint, automobile, emission, mining, burning of coal
Manganese (Mn)	Fuel addition, leachate generation, acid mine drainage
Mercury (Hg)	Paper industries, batteries, and pesticides
Nickel (Ni)	Zinc base casting, battery industries, and electroplating
Zinc (Zn)	Refineries, brass manufacture, immersion of painted idols

Table 1 Sources of heavy metals in environment [2, 7, 17]

the metal has added a pure extraction of the forms [18]. The deeds of electroplating, mining, smelting, pesticides, and fertilizers discharge as well as bio-solids and municipal sewage and paint industries have become more significant with things [19]. The prevalence of the heavy metals adds on the terrestrial and aquatic bodies to meet with the attributes in the environment. Heavy metals have environment pollutants which led to toxicity, persistence in the environment, and bio-accumulative nature of the sources. It has influenced the human health and also affected the trophic transfer of the Cr, Ni, Cu, Pb, Zn, Cd, Hg, and As elements in the aquatic and terrestrial food chain/webs. It is important to assess and monitor the concentration so that the impact on the human health and environment can be minimized [20]. The operations that are directed must lead to the non-stop soil contamination because of the regular practices around the field. The manufacturing of the various products is important and so its applications where transport of the metals takes place with effective hindrance to benefit in the environment.

Industries have turned out to be the primary responsible conditions where the environment might have extensive applications of Cr contaminants in the environment. The electroplating and paint industries would contribute on Pb-based contaminations to the environment. The use of the fertilizers and fungicides in the activities takes place with the metal pollution solutions. The significant growth in the health progression of plants and concentration excess of metals would affect the resources of the environment to wider extent.

1.2 Arsenic (As)

Arsenic mainly belonging to VA group has mineral in the various forms most commonly presented form is As_2O_3. This exists in the oxidized state where the lethal and expansively existing forms of metal affect the salts. The predominant features of the coloring agents in the textiles, toy-making industry, and other have affected the environment. Arsenic is used in the insecticides and rat killing to protect the timber and termites. However, it is also present in the ashes from coal combustion. It provides the elemental change in the simplest organic compound like AsH_3 (Arsine) that relates to the extremely reducing environment [21]. The dimethyl arsine and compounds would generate on the methylation with extremely dangerous and toxic pattern in nature.

The compounds of arsenic that are converted are more poisonous and are responsible for inducing the carcinogenesis. It provides the circulatory measures with the problems where the presence of As (Arsenic) in drinking water is more permissible to the clinico-pathological diseases. The enzymes that are involved might associate As (Arsenic) with oxidative phosphorylation and resulting in the variety of the high concentrations of As in the matter. It has provided by the permissible limit for severe issues. This can provide the main mechanisms with the associated uncoupling oxidative groups with the interaction in the proteins and enzymes to the substitute P in the variety of biochemical reactions.

1.3 Cadmium (Cd)

Cadmium has provided different sources of the by-product of Zn refining. It has constituted on the prevalence of the source of Cd contamination in the environment. The applicable sources have added on numerous industrial preferences. The electroplating, stabilizing agent, and vending machine of the soft drinks are some of the areas which provide corrosion-free aspects to the content with the higher amounts. Electroplating is the process of deposition of the metallic film on the seed metal layer. It represents the deposition of salt of metal on cathode when the aqueous solution is undertaken.

Stabilizers commonly used the sodium alginate and sodium carboxymethyl cellulose to manage the thickness of the gel to the required consistency in the food. However, the soft drinks and polysaccharides carbohydrates give rise to the waste generation. Therefore, the stabilizing agent helps in accomplishing the recarbonation with several acids using CO_2.

Cd has been the most hazardous and noxious metal where the agency might relate to the ranking of the ATSDR which is agency for toxic substance and disease registry. The human and animals that are severely contaminated with the extensive exposure to the factories are result of the working areas in the substitution of Zn by Cd. This might cause the disruption in the metabolic activities to the wider extent.

The deficiencies that are caused by the cadmium have resulted the oxidative stress that relates to the carcinogenic and mutagenic nature of the health. The toxicity level of the heavy metal has remarked toward the oxidative stress and nutritive values in the inhibitory effects. The deficiencies have remark on the responsible renal and hepatic damages caused due to the severe health complications.

1.4 Chromium (Cr)

Chromium has been identified as the only element in the VIB group which is not in the pure form in the environment. It has been mainly composite of the sediments and rocks along with the ores that are mainly made of the compounds of chromites. This can commonly present the water, soil, and air and food products range.

There are different forms of the divalent to hexavalent sources that make the things more stable yet relevant to the human exposures and toxicity. The implications of the pollutants and carcinogens have led to death many times. This can be subjected to the process where leather tanning, metal refining, pharmaceutical drugs, and other have set out the parameters for the environment concern. Unlike the mobility, solubility, toxicity, and bioavailability, the Cr (VI) has been more stable and cellular from the permeable point of time. This can generate the sulfate transport system with the denaturation and nucleic acids and protein to meet the trivalent substances. The primary bound to the organic matters might represent the water and soil environment to the better handling. The soil changes have brought microbial diversity and reduced

the growth and metabolic activities. It might disturb on the accumulation of food chain with the critical health issues where the nasal irritation is impaired.

The trivalent preferences have set out the vital range for the humans where the effects result the cancer mutations and abnormalities in the humans and animals. The soil change has represented the accumulation of the food chain to which critical health factors that meet on the genotoxic abnormalities. Chromium compounds have several intermediates to the chromosome aberration in the replication of the DNA and damage for forming the protein-based complexes.

1.5   Lead (Pb)

Lead has bluish-gray metal color where the natural occurrence to the component of the sulfides has managed the concentration between 10 and 30 mg/kg. It can regulate on the hair dyes, paints, sindoor, and exhausting activities. The road transports and vehicles have related the non-ferrous metals with the noticeable contribution in the pollution of the water. The soil sources can provide the lead (Pb) in form of the ionic, hydroxide, oxide, and oxyanion forms within the environment. The Pb (VI) has tended to cause the covalency and strong oxidants with the industrial exposure. The highly poisonous act has uptake the severe illness as evident one. The modifications in the Pb toxicity and alterations in the cell have provided the enzymatic reactions, physiological processes, and protein folding too much bivalent cations. The presence of the high quantity has produced the species that result in the damage of the plant growth in the better processes and suppress to results.

1.6   Mercury (Hg)

Mercury (Hg) is silver white transition which belongs to d-block and period 6 tables. It is often used as scientific tools where equipments such as thermometers and barometers have taken process to next level. The electrochemical process has provided the chlorine manufacturing and electrodes in alkali industry to meet with the practices in the environment. However, the production of caustic soda has led to the antifungal agents involvement for wood processing and solvent enacting to the precious metals.

The hazardous metal range usually exists and forms the alkylated form of the basic requirement of the nature. The redox potentiality and pH system might be accountable in handling the diverse toxicity and bioavailability. However, it exceeds poisonous and gastrointestinal toxicity, nephrotoxicity to major extent. The structure of the tertiary and quaternary function of the cell has increased the MDA due to Hg complexes. It has affected the kidney, lungs, and liver along with the microtubule destructions in the sulfhydryl groups.

1.7 Nickel (Ni)

Nickel (Ni) has lustrous yet slight golden tinge that makes it ductile and hard. The primary consumption of Ni has categorized it in the oral form which is highly contaminated. The borderline metal has bind to different metabolic reactions in the permissible limits. The cumulative toxin might add on the higher concentration and industrial exposure to make it more toxic. The implicated form of the embryo has approached on the atmospheric conditions to which the increased applications. The humans can engross on the tobacco, smoke and detergents and coins. The plasma from chelating actions adds on the hemodialysis with the residues of nickel.

2 Literature Review

Barakat et al. [22] have added on the innovative process along with the treatment of industrial wastewater of the heavy metals. It has involved the better technologies through which the treatment standards and reduction of toxicity takes place. It has recently developed the processes such as adsorption on new adsorbents, membrane filtration, and photocatalysis. It has provided range of the operating conditions where pH treatment and performance can be taken place. Photocatalysis is one of the attractive solutions to degrade the organic pollutants by using photocatalysts in the treatment of wastewater. It allows both spontaneous and non-spontaneous reactions to optimize the whole process. It helps in the advanced oxidation processes with the improvement in the drawbacks caused such as high cost, hydroxyl radical, and incomplete mineralization to overcome the challenges of the wastewater treatments.

The photocatalytic ones are turned out to be cheap and degrading in the organic pollutants. The conventional process and lime precipitation have found one to be most effective in the treatment of inorganic effluent yet metal concentrated activity. The technical selection of method depends on the local conditions.

Tytla et al. [23] aimed on the study of the pollution and ecological risks caused due to heavy metals. It has added the extensive use of the coupled plasma optical spectrometry and chemical speciation, cold vapor atomic absorption spectrometry (CVAAS). It has sequentially added on the risk factors where the individual contamination might result in the risk assessment and processing the dominant metals like Zn and Cu by anaerobic digestion and dehydration. The permissible standard limits to the heavy metals have indicated on the values compared to the moderate level practices. The results that are obtained might present the secondary pollution of soils with heavy metals and raising the health risks characterized with high metal content.

Mishra et al. [24] have focused on different types of pollutants in the dumpsites of the developing countries. It has certainly set an incomplete combustion of the waste that has adverse effect on the environment. The municipal dumpsite is a low-cost technique to decontaminate the heavy metals pollutants. However, the biochars have been considered to treat the mixture of organic and cellulosic waste that derives

the heavy metals and organic contaminants in the water. This can utilize pyrolytic temperature through which grinding of the surface areas has exploited the adsorptive medium for the remediation and treatment in the regions.

Sall et al. [24] identified that heavy metals are polluting water and major origin is human as they burn fossil fuels and gases of vehicles and other incineration of solid and liquid wastes. The heavy metals occurring in the natural form, i.e., spring activity, volcanoes, and other, have caused toxicity to human life as living beings have created threat to the aquatic life. Therefore, the evident technique that has been found to reduce the level of pollution of natural water and work on the toxicity is the synthesizing and characterization method organic polymers. It can help in the removal of heavy metals from the environment. It has been reviewed that the electrochemical synthesis of the heavy metals has added CoPs as the good approach to remove the heavy metals from waters. With the rapid development of industrialization, the removal of the heavy metal ion of wastewater has discharged the industrial sewage to which the environment and water ecosystem can be undertaken. It has helped in the investigation of performance of removing Pb and Cu from the wastewater through saturated adsorption capacities. It has added on the higher porous materials with the excessive adsorbents and showcasing adsorption kinetics.

Rahman [25] has focused on the chemical pollutants which create anthropogenic imbalances in the environment and raising the threat to the life. This might pose multiple heavy metals and their types where the imperative yet safe way to attractive scheme for remediation takes place. It has applied the conventional techniques where concomitant treatment solutions fail to meet various parameters. However, the microorganisms technique can be considered significant for the bioremediation of the chemical pollutants. It can also use for heavy metals resistant and adding industrial applications to it.

Yadav et al. [26] represented the ubiquitous environmental contamination by the industries. It has concern over the health hazards caused by the heavy metals on the human. The organic pollutants degraded the environmental conditions through toxic elements and their effects. This can be a serious threat to ecosystem in upcoming years. Therefore, the implementation of the bioremediation and phytoremediation cleanup technologies might add a range of expansion and limitation to the restored environment in the clean form.

Qureshi et al. [27] reported on the effects of irrigation and treatment of wastewater on accumulation of heavy metals in the soil and food. It has created a mess of health hazard where consumption of food is evaluated. It can add on higher concentration of iron and tracing out the metal levels with the trends of dietary intakes. The recorded levels of the food plants who take low quantity of heavy metals are insignificant. Therefore, it is necessary to identify the properties and overcome the risk of appropriate crops and metal contamination.

Suman et al. [27] represented heavy metal pollution as serious threat to environment and human health. It has characterized the heavy metals as the chemically degraded material. It can detoxify on the residues and removal of the soil from the matrix. The phytoremediation is the application which can help in restoration of

the polluted environment and adding green alternative to the society. The considerable advantages that are taken place might provide good acceptance for the method of the physical and chemical activities. The possible follow-up process of biomass and phytoextraction strategies has added on the multiple variant and high biomass production and potentially generated areas in the environment.

Rajendran et al. [28] review focused on the general status of the heavy metal contamination in the environment. It has been processed with the geological problems and political issues surrounding the immobilization of the metal in the environment. The challenges include a molecular and genetic mechanism which allows the microbes to be managed by the plants and overcome heavy metal tolerance. The utilization of the phytoextraction and biological methods has been proven to be practically the best treatment method. This can add on the better possibilities which occur at different stages of remediation in the study.

3   Methodology

To manifest the importance of the heavy metals affecting the environmental conditions can be overcome by using various methods that researchers have been using. One of the primarily applicable techniques is physical separation. It includes discrete particles or metal-bearing particles along with the hydrodynamic form of the classification, mechanical screening, and magnetic separation. The attributes of the scrubbing and efficiency of the physical separation have influenced the properties of the heavy metals on the particle surface. This can help in removing the Fe & Ca, heavy metals from the chemical process.

Other than this, the chemical precipitation has heavy metal removal with the help of simple operations. This has changed the solutions and metal ions to major levels as pH, temperature, concentration initial, charge of ion are all considered to be part of technique. It can target of the pH range from 8 to 11. Coagulation and flocculation mechanism are other measurement criteria through which electrostatic interaction between pollutants takes place. However, the removal of heavy metals basically provides the particle size and discrete size for collisions and interactions. The separation of the particles can add on applications of chemical and transfer of toxic compounds in the solid phase with major drawbacks.

Electrolysis is also a recovery technology for environmental measures in the removal of heavy metals from wastewater stream. This can be aqueous metal-bearing solution with the insoluble anode. This can present the weak acidic and other electrodeposited materials to the treatment methods. An attempt to stabilize sludge from groundwater treatment through electrokinetic method is electrode stabilization. It predominantly treats the sludge samples containing ferrous oxide that is placed in fabricated electro-osmotic cells and directly applied current through end samples via copper electrodes. The samples are subjected to have positive effect after certain days of treatment with variation in the load imposed and voltage applied to the samples.

Electrode stabilization has categorized the reduced sludge production with no chemical use. It has also eased the operations by in situ management of the metal species in the water. This can change aqueous solution to solid waste disposal without recovering metal.

One of the promising processes of the removal of heavy metal ion from water involves the bonding of metals and firstly adding special bonding agent and then separating them by separation process. The filtration stage involves the hybrid process of floatation where membrane separation while overcoming the limitation. The feasibility of powdered synthetic zeolites as bonding agents.

Membrane filtration is also drawing attention for the treatment of heavy metals but it requires various types of membrane. One of the kinds is ultrafiltration which helps in separating heavy metals from the inorganic solutions. It has been dependent on the characteristics of membrane. However, the metal concentration has ranged to some advantages that are required to drive lower yet small space requirements in the packed densities.

Reverse osmosis (RO) is another method that utilizes pressure force to separate the solute from one side and allow the pure form of the semi-permeable membrane. It can be dense and occurs in the diffusive manner. The efficiency has been dependent on the concentration, pressure, and water flux rate where the polymer matrix occurs.

In the current study, the biological method has been focused on the treatment of the wastewater as it involves the removal of the heavy metals in the better yet eliminated way. The pollutants from wastewater can be settled solid in the solution. It requires activated sludge, trickling filters, and stabilization ponds to be treated properly. This can set out the aeration and agitation ways where the organic materials breakdown can help in decomposition of the organic waste. In most researches, the suspended growth might represent the sludge process with the growing aeration to the relatively inefficient yet biological methods to rely upon. The biosorption is the method that can be used to remove heavy metals from wastewater. Gradually, the process consists of the adsorption and precipitation reactions. It has added on the low-cost adsorbents derived from the waste.

The industrial effluent has recently focused on the bioremediation and phytoremediation process which can transit the metal ion. The heavy metals removal from the environment sources has various input loads and rapid processes. It can outweigh by the number of drawbacks and high operational costs, high-energy consumption. The studies have added on the biological techniques as the suitable one for the treatment of the heavy metals linkages.

4 Discussion

4.1 Influence on Heavy Metals Make Toxic Impact on the Environment

The contamination of the metal has heavily invested in the toxic traits of soils, sediments, groundwater, air, and natural water in the environment. The pathways that are demonstrated with the several exposures might route on the inhalation and dermal contact of the diet within environment (Table 2).

The metals have been lethal and hazardous when the organic substances are interfered. This has added excessive depositions or accumulations to the metalloids which are harmful in activities. The natural environment gets severely contaminated with the direct or indirect exposures. The productive and fertility-based contamination address that heavy metal has contaminated the environment through dangerous toxicological risks and human problems.

Table 2 Toxic metals and its hazardous impact on environment [25–29]

Metals	Applications	Hazards
Cr	Tanning, paints	Cancer, hair loss
Hg	Coal vinyl chlorides, thermometers, electrical batteries	Depression, fatigue, drowsiness, tremors
Pb	Plastic, gasoline, auto exhaust, pipe	Neurotoxic and cardiovascular
Cd	Fertilizers, plastic, pigments	Carcinogenic, kidney damage
Ni	Electroplating	Itching, genotoxic, fertility effect
Zn	Fertilizers	Vomiting, renal damage, cramps
As	Pesticides, herbicides	Cellular processes are affected ATP synthesis

Table 3 Values and limit of heavy metals (mg/L) in drinking water [26, 28, 30, 31]

Metals	WHO 2022	IS (IS10500.2012)
Pb	0.01	0.01
As	0.01	0.01
Hg	0.06	0.001
Cd	0.003	0.003
Ba	1.3	0.7
Cr	0.05	0.05
Ni	0.07	0.02
Cu	2	0.05
Zn	-	5
Mn	0.08	0.1

It is highly evident that the level of the Cr, Pb, Hg, Ni needs to be under 1 mg/L (Table 3) as it can contaminate the water source-to-higher ratio. The permissible limit has somehow managed the concentration level of the groundwater and surface water through it. The local minerals are somehow managed to provide high level of Hg in the groundwater. Water in a solvent and dissolves minerals from rocks with which it comes in contact. While in the case of Hg, it would taste flat. This is the most common dissolved mineral substance constituents that typically exceeds minerals to 1000 mg/L. It would provide slightly saline and sometimes used in the areas of the less mineralized water. As per the study by [32, 33], the Hg elevates the concentration from groundwater atmospheric deposition with strong hydraulic gradients.

4.2   Influence of Heavy Metals on Human

Heavy metals are highly influencing the health of the human in different way. The dietary limits of the metals in the different forms are subjected but it showcases various toxicological effects in the documented way. Heavy metal-induced toxicity and carcinogenicity in many mechanistic ways. The dietary consumption of groundwater includes supplementation of certain nuts in rats, neurochemical aberrations have stabilized. In the current research by [34], the dietary shortages might decrease heavy metal intoxication but if it is in abundance, then it includes cytokines, tumor necrosis factor-α, and other neuronal death. The heavy metals have changed the food quality and affected the cultivated areas of the soils with the change in the food quality. The effects of the safety and occurrence of excess concentration arises and causing the risk to kidney and liver. Furthermore, it has led to many toxicity problems such as nervous breakdown, leukemia, and other mental complications.

The ecological transmission of heavy metals has set out the quality of the pollutants of the food, air, and water supply in the better surrounding range. It is directly proportional to the damages cause to the population in the specific manner. The pollution caused due to the terrestrial and aquatic ecosystem with toxic metal is concern for environment as well as public health. It has been found that the heavy metals occurring in the water have a high atomic weight and density at least 5 times greater than that of water. The committees that are listed to manage those damages are focusing on the different heavy metals concentrations involvement in daily activities. For example, Agency for Toxic Substances and Disease Registry (ASTDR) has focused on Cd to be most toxic substance which affects metabolic rates of the human body by creating calcium deficiency. This can result in the bone fractures and cartilage disease.

On the other hand, the lead (Pb) has been entering the human body via respiratory tract and reaches out to the gastrointestinal part of the body. It results in the damage to the protein complexes in the blood and accumulates insoluble phosphate form that affects each part of the body system, i.e., urinary, nervous, genetic, and reproductive systems.

A trace of Ni, Cu, Zn has turned out to be more crucial where enzymatic activities have added higher quantity to the metals causing destruction in the injuries. The direct exposures are the result of the industries not looking toward the health of the workers. Therefore, the nickel enters their respiratory system and leading to cancer and other dangerous and toxic symptoms. This may include itching of nose, skin, and nasal septum damage.

4.3   Influence of Heavy Metals on Plants

Metal has showcased detrimental impact on the development years and growth of plants in the environments. This has presented some acute toxic symptoms and chronic capacity of metal to get contaminated. The pigmentation and enzymes involvement have considered their damage to the disrupting practices and exhibit on the imbalance and nutritive values to the plants in the environment.

The mobilization and transportation of the nutrients are disturbed with the Cd inhabitation through photosynthesis. Cadmium (Cd) has an unessential trace element in plants which is ubiquitous in the environment. This is adding activities such as disposal of urban refuse and smelting and metal manufacturing along with the applications of synthetic phosphate fertilizers in the environment and carcinogenic to human health. The Cd inhibition has added on the translocation and toxicity of Cd in plants help in increasing oxidative damage and disrupt the plant metabolism and inhibits the disciplinary action in the strategies. It showed that Cd and Zn reduce catalytic activities in the enzymes measures. It adversely affects the root and shoots growth of the plant in the environment. The direct involvement of the Cr complexes has noxiously polluted the seed germination and damage to the plant growth with different actions. The activity and transport surge have reduced the growth process of the plants and leading to affect the plants in the environment. Essential and non-essential heavy metals have generally produced the low biomass accumulation, inhibition of growth and photosynthesis along with altered water balance and nutrients that have toxic effects on plants which ultimately result in plant death.

4.4   Influence of Heavy Metals on Soil

Human activities have been in demand as they degrade and deteriorate the quality of the soil, air, water in the environment. It is unnecessary but regular use of the metals in the industry has development a toxicity level that affects the environment. The metals that are found might be smaller in concentration but giving rise to the risks of soil contamination as pesticides, compost, mines, smelting, and other processes take place. The heavy metals have been one way added difficulty to remediate on the harmful yet farming ways that are considered to the serious ecological damage and change. Thus, the wastewater from tannery and transportation of the vehicles and

other high quantity contain metals has open areas for direct disposal. The accumulation in the soil and plants, aquatic life has disrupted the ecological balance which tamed the soil in the highly dangerous way. This can negatively result in the species richness and diversity of plants spoilage.

4.5 Possible Treatment Ways for Heavy Metals in the Environment

The variant forms of heavy metals involved in the environment contamination have given rise to major threats that world is facing today. It has involved surface water contamination, air contamination with toxic metals, organic and inorganic pollutants. A persistent ratio of breaking the toxic forms of the contamination and forming the non-toxic environment would require several years as well as long-lasting effects of it on the ecosystem.

As per the current environmental conditions, the development of the new technologies has emphasized on the destruction of pollutant. The remediated nature to the destruction of the environment requires conventional approaches rather than prevailing on the entry in the food chain of the environment. The most effective treatment measures that took place are:

4.5.1 Bioremediation

Bioremediation is the process through which microorganisms have to detoxify the contaminants in the soil and other environment. It has included degrading, removing, changing, and immobilizing or detoxifying various chemical and physical activities of bacteria and plants. It helps in cleaning up of the water sources and creating the healthier soil along with improving the water and air quality around the globe. This has facilitated remediation of environmental impacts without damaging delicate ecosystem.

There are technologies that specialize microbe culture that added bioaugmentation to enhance biodegradation in groundwater. Few examples of bioremediation are phytoremediaton, bioventing, bioleaching, landfarming, composting, rhizofiltration and biostimulation and mycoremediation.

It has been viable alternative where the cost convention has added on physicochemical methods for metal decontamination. The process might naturally occur with microorganisms' range of converting the toxic substances with less or nontoxic compounds. The involvement of the environmental safety practices has remediated the contaminated sites through managing different factors. The eco-friendly yet primary measures to the waste material management involve bacteria, plants, fungi, and other to transferred ratio.

There are various factors which remarks pH, soil type, and temperature as well as nutrient amendments to major influence. The bioremediation process has added ability to detoxifying the inorganic pollutants. It has utilized the metals which takes adsorption, ex situ and contaminants in the remarkable way. The direct contact with the microorganisms can be controlled by dissolving the contaminants and using it as substrates in comparison with the cleaning up methods of the soil.

A reliable knowledge of physiochemical properties and heavy metal concentrations can be attained. This might limit the adverse impact on the ecosystem as they lend carefully in the soil management. Other than this, metals are not destroyed but can be transformed into a stable form by biotransformation. It includes the biosorption, biomineralization, bioleaching, and intracellular accumulation of the metals. The microbes that are adding several implications to the environment and heavy metals can be treated as environmental change in day-to-day life. This has represented the metal-resistant bacteria which are less toxic yet helping other to tolerate and uptake the ions in such a way that methylation, reduction, and oxidation can be taken place through survival limit.

The extreme morphological changes have exhibited the texture, opacity, and margin appearance of heavy metals in the environmental conditions. The phenomenon has added on the phase variation results that are exposing on the environmental stress. In terms of managing the enzymatic functions and bacterial growth, some heavy metals are necessary but it requires mechanisms to uptake the drawn cells. This can be quick and unspecific to the driven case of chemiosmotic gradients and ATP hydrolysis process. With this substrate-specific energy, they can be more efficient and raise the mechanism influx of wider variety of the heavy metals. This has accumulated yet higher concentrated cell-membrane inside the cell so it can control the toxic effects.

4.5.2 Phytoremediation

Phytoremediation is a conventional technology but is costly to implement. However, it helps in clearing out the disturbances caused in the environment and other damages. With this method, the plant-based development of the environment can take place. It involves the green plants and their associated microbiota to overcome the contaminated soil and groundwater. Phytoremediation is a bioremediation process which include various types of the plants to remove transfer, stabilize, and destroy contaminants in the soil and groundwater.

The effective use of concept of the phytoremediation has helped in removing the heavy metals from the compounds that propound on the soil and plants that can be actually implemented. For developing countries, this is eco-friendly technique through which aesthetic and cost-effectiveness approach can be viable, especially for India. This is yet to become commercial despite of its potentiality. Henceforth, the dependence of the mechanism of remediation has involved the phytoextraction and phytofiltration along with phytostabilization, phytovolatilization, and phytodegradation take place. It has added on the metal ions to accumulate on the aerial parts of
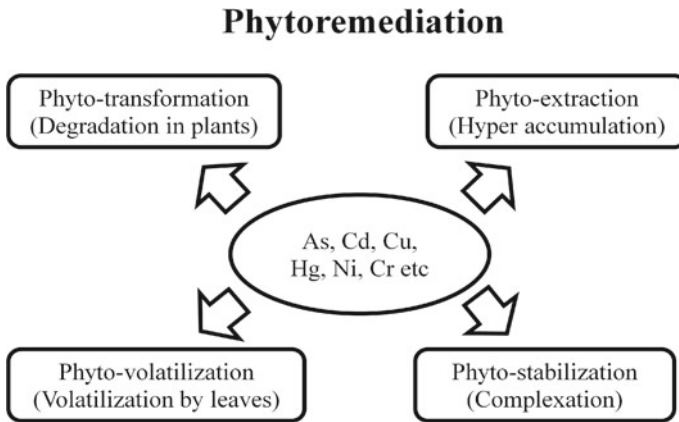
Phytoremediation

Fig. 1 Phytoremediation process to remove toxic metals [2, 28, 29, 33]

the plants. It can be disposed of the recovering environment conditions by burning the metals (Fig. 1).

The removal of metals from wastes has stabilized the pollutants from soil and added privilege to root out the stored form of the rhizosphere and rendering on the harmless yet preventive way through plant root [35]. The pollutants such as Hg require phytovolatilization so that they can degrade the organic pollutants. There are several researchers who have invested in the hyper-accumulation of the heavy metals. Among them, the extraction of the metals from the soil and water has resulted in adopting phytoextraction so that the contaminated Cr, Cu, Zn, and other heavy metals take place with hydroponic solutions.

For the analysis, the mathematical model using the nonlinear convection reaction diffusion partial differential equation with Michaelis–Menten coupling terms in order to stimulate the evolution of heavy metal levels in a domain of shallow water. It considers the concentration of generic heavy metal in water, concentration of heavy metal deposited in algae, concentration of algae in water and height averaged in water column and defining state variables to the problem.

5 Conclusion

Pollution caused by heavy metals is a major threat to the environment. It has also concerned with the major setback with the bio-accumulation and biomagnifications of available heavy metals. The heavy metal cannot be degraded into any harmless by-product through any physical, chemical, and biological means to transform the less toxic means of the plants and microbes. The advancement in the technologies has hold a safety and healthy place for keeping the environment green and clean

through bioremediation/phytoremediation. This has remarked on the future technical limitations where things need to be addressed with the development of the phase regarding the technical limitations. The metal-resistant microorganisms and hyperaccumulator plants remain to be discovered with the microbial diversity. This can be future prospects for the metal accumulating in the areas and surviving the metal-contaminated environment.

With the potential influence on human, plants and animal's health, the contamination of the heavy metals in the environment has been a great concern. It has been challenging that soil and water around the industrial plant have described the technologies that were needed with the precious natural resource and biological diversity. The application of the recovery of the metals from waste streams has gained a lot of attention. Therefore, it has remarked toward the cost-effective and eco-friendly solutions with technological processes, i.e., phytoremediation, bioremediation, and other promising approach for addressing the future of the environmental concerns.

References

1. Chaurasia, A.K., Mohapatra, S., Shankar, R., Thakur, L.S.: (1AD) Technologies for the clean and renewable energy production for the sustainable environment, pp. 141–178. https://services.igi-global.com/resolvedoi/resolve.aspx?doi=104018/978-1-7998-9810-8.ch007. https://doi.org/10.4018/978-1-7998-9810-8.CH007
2. Singh Thakur, L., Parmar, H., Kumar Varma, A., et al.: Removal of manganese from synthetic wastewater by *Vetiveria zizanioides*. Mater. Today Proc. 8–11 (2022). https://doi.org/10.1016/j.matpr.2022.08.395
3. Chaurasia, A.K., Shankar, R., Mondal, P.: Effects of nickle, nickle-cobalt and nickle-cobalt-phosphorus nanocatalysts for enhancing biohydrogen production in microbial electrolysis cells using paper industry wastewater. J. Environ. Manage. **298**, 113542 (2021). https://doi.org/10.1016/j.jenvman.2021.113542
4. Sharma, S.K., Phan, H., Lee, J.: An application study on road surface monitoring using DTW based image processing and ultrasonic sensors. Appl. Sci. **10**, 4490 (2020). https://doi.org/10.3390/APP10134490
5. Chaurasia, A.K., Mondal, P.: Enhancing biohydrogen production from sugar industry wastewater using Ni, Ni–Co and Ni–Co–P electrodeposits as cathodes in microbial electrolysis cells. Chemosphere 286. https://doi.org/10.1016/j.chemosphere.2021.131728
6. Kadier, A., Chaurasia, A.K., Sapuan, S.M., et al.: Essential factors for performance improvement and the implementation of microbial electrolysis cells (MECs). In: Bioelectrochemical Systems, pp. 139–168. Springer, Singapore
7. Thakur, L.S., Mondal, P.: Techno-economic evaluation of simultaneous arsenic and fluoride removal from synthetic groundwater by electrocoagulation process: optimization through response surface methodology. New pub Balaban **57**, 28847–28863 (2016). https://doi.org/10.1080/19443994.2016.1186564
8. Thakur, L.S., Goyal, H., Mondal, P.: Simultaneous removal of arsenic and fluoride from synthetic solution through continuous electrocoagulation: operating cost and sludge utilization. J. Environ. Chem. Eng. **7**, 102829 (2019). https://doi.org/10.1016/J.JECE.2018.102829
9. Sharma, S.K.: Multibody analysis of longitudinal train dynamics on the passenger ride performance due to brake application. **233**, 266–279 (2018). https://doi.org/10.1177/1464419318788775

10. Sharma, S.K., Chandmal Sharma, R., Sharma, S.K., Sharma, R.C.: Simulation of quarter-car model with magnetorheological dampers for ride quality improvement. Int. J. Veh. Struct. Syst. **10**, 169–173 (2018). https://doi.org/10.4273/ijvss.10.3.03

11. Chaurasia, A.K., Goyal, H., Mondal, P.: Hydrogen gas production with Ni, Ni–Co and Ni–Co–P electrodeposits as potential cathode catalyst by microbial electrolysis cells. Int. J. Hydrogen Energy **45**, 18250–18265 (2020). https://doi.org/10.1016/j.ijhydene.2019.07.175

12. Kachroo, H., Chaurasia, A.K., Chaurasia, S.K., Yadav, V.K.: Sustainable clean energy production from the bio-electrochemical process using cathode as nanocatalyst. Handb. Green Sustain. Nanotechnol. 1–30 (2022). https://doi.org/10.1007/978-3-030-69023-6_58-1

13. Sharma, S.K., Kumar, A.: Ride comfort of a higher speed rail vehicle using a magnetorheological suspension system. **232**, 32–48 (2017). https://doi.org/10.1177/1464419317706873

14. Rani, M., Shanker, U., Chaurasia, A.K.: Catalytic potential of laccase immobilized on transition metal oxides nanomaterials: degradation of alizarin red S dye. J. Environ. Chem. Eng. (2017). https://doi.org/10.1016/j.jece.2017.05.026

15. Sharma, S.K., Kumar, A.: Disturbance rejection and force-tracking controller of nonlinear lateral vibrations in passenger rail vehicle using magnetorheological fluid damper. **29**, 279–297 (2017). https://doi.org/10.1177/1045389X17721051

16. Chaurasia, A.K., Siwach, P., Shankar, R., Mondal, P.: Effect of pre-treatment on mesophilic anaerobic co-digestion of fruit, food and vegetable waste. Clean Technol. Environ. Policy (2021). https://doi.org/10.1007/s10098-021-02218-5

17. Mitra, S., Thakur, L.S., Rathore, V.K., Mondal, P.: Removal of Pb(II) and Cr(VI) by laterite soil from synthetic waste water: single and bi-component adsorption approach. New pub Balaban **57**, 18406–18416 (2015). https://doi.org/10.1080/19443994.2015.1088806

18. Sharma, S.K., Chaturvedi, S.: Jerk analysis in rail vehicle dynamics. Perspect. Sci. **8**, 648–650 (2016). https://doi.org/10.1016/J.PISC.2016.06.047

19. Chaurasia, A.K., Mondal, P.: Hydrogen production from waste and renewable resources, 22–46 (2021). https://doi.org/10.4018/978-1-7998-4945-2.ch002

20. Thakur, L.S., Mondal, P.: Simultaneous arsenic and fluoride removal from synthetic and real groundwater by electrocoagulation process: parametric and cost evaluation. J. Environ. Manage. **190**, 102–112 (2017). https://doi.org/10.1016/J.JENVMAN.2016.12.053

21. Mohapatra, S., Pandey, N., Dey, S., et al.: Production of biodegradable polymers (PHAs) by soil microbes utilizing waste materials as carbon source. Front. Soil Environ. Microbiol. 237–246 (2020). https://doi.org/10.1201/9780429485794-25

22. Barakat, M.A.: New trends in removing heavy metals from industrial wastewater. Arab. J. Chem. **4**, 361–377 (2011). https://doi.org/10.1016/J.ARABJC.2010.07.019

23. Tytła, M.: Assessment of heavy metal pollution and potential ecological risk in sewage sludge from municipal wastewater treatment plant located in the most industrialized region in Poland—case study. Int. J. Environ. Res. Public Health **16** (2019). https://doi.org/10.3390/IJERPH16132430

24. Mishra, S., Bharagava, R.N., More, N., et al.: Heavy metal contamination: an alarming threat to environment and human health. Environ. Biotechnol. Sustain. Futur. 103–125 (2019). https://doi.org/10.1007/978-981-10-7284-0_5

25. Rahman, Z.: An overview on heavy metal resistant microorganisms for simultaneous treatment of multiple chemical pollutants at co-contaminated sites, and their multipurpose application. J. Hazard Mater. 396 (2020). https://doi.org/10.1016/J.JHAZMAT.2020.122682

26. Yadav, A., Chowdhary, P., Kaithwas, G., Bharagava, R.N.: Toxic metals in the environment : threats on ecosystem and bioremediation approaches. Handb. Met. Interact. Bioremediation 128–141 (2017). https://doi.org/10.1201/9781315153353-11

27. Qureshi, A.S., Hussain, M.I., Ismail, S., Khan, Q.M.: Evaluating heavy metal accumulation and potential health risks in vegetables irrigated with treated wastewater. Chemosphere **163**, 54–61 (2016). https://doi.org/10.1016/J.CHEMOSPHERE.2016.07.073

28. Rajendran, S., Priya, T.A.K., Khoo, K.S., et al.: A critical review on various remediation approaches for heavy metal contaminants removal from contaminated soils. Chemosphere **287** (2022). https://doi.org/10.1016/J.CHEMOSPHERE.2021.132369

29. Singh, V., Thakur, L., Mondal, P.: Removal of lead and chromium from synthetic wastewater using *Vetiveria zizanioides*. CLEAN – Soil. Clean—Soil, Air, Water **43**, 538–543 (2015). https://doi.org/10.1002/CLEN.201300578

30. Adegoke, K.A., Adesina, O.O., Okon-Akan, O.A., et al.: Sawdust-biomass based materials for sequestration of organic and inorganic pollutants and potential for engineering applications. Curr. Res. Green Sustain. Chem. **5**, 100274 (2022). https://doi.org/10.1016/J.CRGSC.2022.100274

31. Shankar, R., Pathak, N., Chaurasia, A.K., et al.: Energy production through microbial fuel cells. Sustain. Util. Nat. Resour. 354–380 (2017). https://doi.org/10.1201/9781315153292

32. Sall, M.L., Diaw, A.K.D., Gningue-Sall, D., et al.: Toxic heavy metals: impact on the environment and human health, and treatment with conducting organic polymers, a review. Environ. Sci. Pollut. Res. Int. **27**, 29927–29942 (2020). https://doi.org/10.1007/S11356-020-09354-3

33. Suman, J., Uhlik, O., Viktorova, J., Macek, T.: Phytoextraction of heavy metals: a promising tool for clean-up of polluted environment? Front. Plant Sci. **871**, 1476 (2018). https://doi.org/10.3389/FPLS.2018.01476/BIBTEX

34. Anjum, M., Miandad, R., Waqas, M., et al.: Remediation of wastewater using various nano-materials. Arab. J. Chem. **12**, 4897–4919 (2019). https://doi.org/10.1016/j.arabjc.2016.10.004

35. Mondal, P., Kumari, P., Singh, J., et al.: Oil from algae. Sustain. Util. Nat. Resour. 214–253 (2017). https://doi.org/10.1201/9781315153292

Operational Greenhouse Gas Emissions of Air, Rail, Road, and Sea Transport Modes in Life Cycle Perspective

Levent Bilgili

Abstract Transport takes place on four main elements: Air, rail, road, and sea. The question of which of these four elements is more environmentally friendly is a subject that has been studied frequently. In order to give a full answer to such a question, all modes of transport (including vehicles of transport) must be comprehensively examined from a life cycle perspective. In this study, the CO_2eq, which is identified as the greenhouse gas impact of different greenhouse gases is measured from the CO_2 unit, emissions of the four modes of transport in the case of carrying 1 tkm of unit load, which means the transport of 1 t of cargo at a distance of 1 km, were calculated. The first reason for choosing only CO_2eq emissions is that the method used calculates only CO_2eq emissions, while the second reason is that global warming is the most important environmental impact category for different transport modes. Calculations were made according to the Intergovernmental Panel for Climate Change (IPCC) method, which considers only CO_2eq emissions and thus can be accepted more accurate than other methods, and life cycle approach and the effects were measured at 20-, 100-, and 500-year periods, which are called individualistic, hierarchist, and egalitarian, respectively. Accordingly, maritime transport is the most environmentally friendly mode of transport in all three periods, and air transport has the largest share in greenhouse gas production. The main aim of the study is to draw attention to the life cycle perspective in the calculation of greenhouse gas emissions and to compare the short-, medium- and long-term effects of transportation modes both with themselves and with each other.

Keywords Life cycle assessment · Transport modes · Greenhouse gas

L. Bilgili (✉)
Department of Naval Architecture, Maritime Faculty, Bandirma Onyedi Eylul University, Bandirma, Balikesir 10200, Türkiye
e-mail: lbilgili@bandirma.edu.tr

1 Introduction

Global energy demand is in a steady increase trend depending on the increasing population, growing trade volume, and developing economies. According to the 2017 data of the International Energy Agency (IEA), the global primary energy demand was 13.792 Mtoe and the energy demand of the transportation modes (road-rail-air-sea) for the same period was 3.985 Mtoe, which corresponds 28.89% of the total global energy consumption [1]. According to the current data of the IEA, it is seen that transportation modes are responsible approximately for 23% of the carbon dioxide (CO_2) generated via fuel combustion between 1990 and 2017 [2]. According to the data obtained from the 2020 records of the European Energy Agency (EEA), the contributions of various sectors to the production of other air pollutants except carbon dioxide are shown in Fig. 1.

Carbon monoxide (CO), non-methane volatile organic compounds (NMVOC), nitrogen oxides (NO_x), particulate matter (PM_{10} and $PM_{2.5}$), and sulfur oxides (SO_x) are presented in Fig. 1. As it can be seen in Fig. 1, transportation sector produces less emissions compared to non-transport sectors.

CO_2 production, which is an important greenhouse gas (GHG), is generally used to determine the environmental impacts of the transport mode and to compare transport modes in terms of environmental performance. In order for a realistic comparison, the amount of CO_2 per ton-kilometer (tkm) is used because of the need for a single comparable unit to compare the environmental performances of transport modes, which include very different cargo capacities, on different routes. Thus, a comparison can be realized independent of the carrying capacity, route and other potential variables of the transport mode. This unit, determined as CO_2/tkm, is also called CO_2 efficiency.

The CO_2 efficiency values of the four main transport modes are found as 139.85, 52.92, 1061 and 18.89 g CO_2/tkm for road, rail, air and sea, respectively [4]. This ranking has been verified by other studies [5–12].

These values indicated that while sea transport has the highest environmental performance, air transport has the lowest performance. On the other hand, the emission estimation in the transport phase alone cannot provide sufficient information
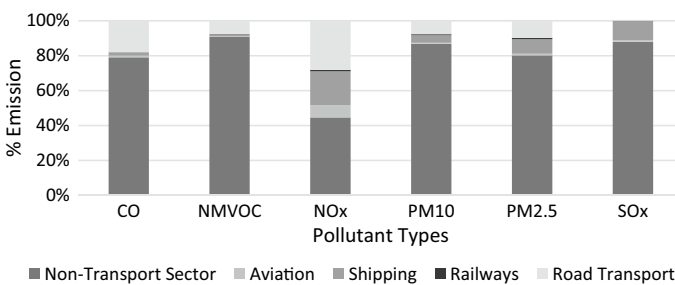

Fig. 1 Contribution of the various sectors to the main air pollutants [3]

to compare the modes in all aspects and to decide which one has superior environmental performance. Therefore, with a holistic perspective, emissions produced per one tkm unit should also be analyzed using the Life Cycle Assessment (LCA) method. Besides, in the LCA perspective, the production and maintenance processes of different transport vehicles must be considered. In this way, a more realistic comparison can be made by calculating the total environmental impacts that occur during transportation, production, and maintenance processes. Since LCA can evaluate a product as a whole with all of its life cycle phases, it has a great success in determining and explaining what kind of errors or deficiencies there are in sub-processes and thus, the practitioner can focus on the correct point.

In this study, the answer to the question of whether sea transport is really the most environmentally friendly mode of transportation was sought with the LCA method. The main purpose of asking this question is to discuss the importance of emission reduction issue, on which many studies have been published, and to open a way for organizations such as International Maritime Organization (IMO) for developing more comprehensive and exact regulations. For this purpose, the real environmental effects of transport modes have been examined from a holistic perspective, considering the emissions per one tkm unit in road, rail, air and sea transport. In addition, the production, and maintenance processes of one transport vehicle are included for once in the calculations.

1.1 Literature Review

Numerous studies have been conducted on emissions from different transport modes and examining these modes by LCA method. In this section, important ones of these studies are reviewed and summarized in Table 1, which includes only the environmental impacts and LCA of transport modes studied separately. Comparative studies are presented in the next paragraph.

Reference [31] compared the potential mitigation of CO_2 emissions in case of switching domestic travel from short-haul air transport to high-speed rail transport. The study was established on a life cycle perspective and it was concluded that annual life cycle CO_2 emissions would decrease by 18% when compared to the air mode in the target year 2056. The authors also indicated that substitution of high-speed rail for short-haul air travel would be successful in the long term. Reference [32] also compared air and high-speed rail transport in terms of environmental impacts. The authors resulted that the environmental friendliness of rail transport, which seems more comparing with air transport, strongly depends on the energy sources used to generate the electricity. Reference [33] investigated the road and rail transport GHG emissions between Hamburg, Germany and Bratislava, Slovakia. It was concluded that although the routes have similar distances (approximately 1000 km), rail transport produces much less CO_2eq emissions. Reference [34] concluded that the CO_2eq emissions of national average of all bus travel is more than the average of all rail travel during 1990–2014 per pkm. On the other hand, it was also concluded that

Table 1 The summary of the previous studies for transport modes' emissions and LCA calculations

Mode	Reference	Scope
Air	[13]	The impact of anticipated technologies on reducing CO_2 emissions from air transport
	[14]	The impact of bio-jet fuels on emission reduction
	[15]	LCA of air transport, including airport construction, aircraft construction, fuel production, and aircraft emissions
	[16]	Investigation on the impacts of German air traffic on climate change
Rail	[17]	LCA of Shanghai metro system
	[18]	Investigation on high-speed rail transport between the cities of Beijing and Shanghai in China
	[19]	Sustainability assessment of Hong Kong urban rail system
	[20]	The analysis for energy use and environmental emissions of high-speed rail transport in China
	[21]	LCA of China's high-speed rail systems
	[22]	Environmental analysis and LCA of German high-speed rail system
	[23]	LCA of Portuguese high-speed rail system
	[24]	Impact of high-speed rail system on climate change
Road	[25]	Life cycle energy demand and GHG emissions of future road transport in China
	[26]	LCA of road transport
Sea	[27]	LCA of material efficiency to reduce CO_2 emissions
	[28]	LCA of ship hull maintenance
	[29]	LCA of a ship
	[30]	LCA of different power systems

although average CO_2eq emissions of urban bus was higher than average urban electric rail until 2010, due to the changes in energy sources, electric rail systems produce less CO_2eq after 2010. Reference [35] applied a case study including a road-only and intermodal road-rail route and compared the amounts of various air pollutants. According to the results, it was concluded that the intermodal operations would reduce emissions by up to 77.4% and cheaper up to 80%., parking and insurance of the infrastructure and the total energy production. Reference [36] reviewed the previous studies on the GHG's of air, road, and rail transport in life cycle perspective. The authors indicated that CO_2eq emissions occurs much higher during operation phase in all transportation modes. Reference [37] compared the CO_2 emissions per pkm of high-speed, road, and air transport. The results showed that while high-speed rail transport produce 11.0 g CO_2/pkm, road and air transport is responsible for 151.6 g CO_2/pkm and 164 g CO_2/pkm, respectively. Reference [38] investigated the CO_2/$ for air and sea transport modes and for three different scenarios. According to the results, sea transport is much more efficient in both environmental and economic perspectives. Reference [39] compared the environmental impacts and externalities

of rail, road, and inland water transport in Belgium. The results show that while road transport has the worst values in climate change, photochemical oxidant formation, particulate matter formation, damages to human health, ecosystem diversity and resource availability, rail transport has the best values in the same issues. Similarly, rail transport has also the best values for external costs.

The study revolves around the research question of whether the sea transport is really the most environmentally friendly mode of transport in terms of climate change, but also includes a general comparison of life cycle of all modes of transport.

2 Materials and Methods

LCA is an innovative approach to examine the environmental impacts of all processes occurred in whole life cycle, which is called as cradle-to-grave (from raw material to disposal) or cradle-to-cradle (from raw material to another raw material, i.e., recycling) of a product or service (or product system as identified in LCA terminology). At the end of a product's lifespan, it can be disposed by various methods or recovered through recycling or reuse. LCA calculations cover all phases of a product system and connects each other. Since the LCA examines the product system as a whole, it follows a different path from traditional approaches that divide the same system into parts and evaluate them separately. According to the LCA concept, the product system is a whole and any process affects any other. LCA accepts systems as a whole, consisting of different subsystems that are examined individually, and both calculations and interpretations are made according to this approach. Accordingly, if a product system is examined in four main subsystems such as production, transportation, consumption, and disposal, LCA tries to find the effect of each subsystem on the other and the whole by considering all of them in a single calculation and evaluation. In doing so, it is seen that the total effect is also present. In the LCA approach, subsystems are only auxiliary elements and the main result is the final holistic value. Therefore, a holistic perspective dominates the LCA approach.

LCA approach started to be used by some manufacturers for the first time in the 1970s, and its area of use has expanded considerably after the standardization process in the 2000s. LCA is currently used by a large number of manufacturers and service providers to assess the overall environmental impact of product systems. LCA works with the support of databases in which a large amount of data from different sources is processed and the environmental impacts of various products or services are labeled. In this way, it is possible to calculate the environmental impact of the product or service whose environmental impact will be examined. LCA allows the processing of new data as well as using data from previous studies. The main difference of LCA from traditional approaches is that it allows to examine the product or service holistically instead of a single process. In this way, it can be determined which stage of the product system has the most environmental impact and appropriate measures can be taken.

LCA is basically based on the concept of sustainability. Sustainability can be defined as "Ensuring that future generations reach the same amount of resources without restricting the access of today's generation to resources" [40]. LCA plays a very important role in ensuring sustainability, which is one of the most important and popular issues of today. Thanks to LCA calculations, the total environmental impact created by the product system over the entire life cycle can be calculated. This data allows quantitative measurement of improvements in processes. Another advantage of the LCA is that it can be applied to all products and services and that it allows the evaluation of different product systems together and holistically. Traditional approaches have several limitations in the study of complex systems. The environmental effects of a large system, which consists of subsystems intricately feeding each other, cannot be evaluated from a single point of view as if it consists of only a whole, one system. LCA provides the opportunity to first disassemble the subsystems or different systems that make up a system and then combine their effects holistically. By LCA, it is possible to compare different product systems with the same goal and to calculate which one is more environmentally friendly, just as in this study. In this way, the attention of producers, consumers, and policy makers is drawn to environmental awareness, which is the desired point, and the necessary measures are taken and it is aimed to protect the resources in the most appropriate way.

There are many package programs to make LCA calculations correctly. In this study, 9.3.0.2 version of SimaPro package program, which was developed by PRé Sustainability, and Ecoinvent database were used. IPCC 2021 was preferred among the methods defined in the program.

The damage assessment values are represented in three time periods, short, medium, and long. Short-term (20 years) is also called as individualistic (I), and it is the most optimistic approach, in which it is assumed that many major problems can be avoided in the near future. Medium-term (100 years) is also called as hierarchist (H), and it is generally accepted as the default model. The last one, long-term (1000 years) is also called as egalitarian (E) is based on a pessimistic and precautionary point of view, in which it is assumed that the problems may be increased [41].

3   Results and Conclusions

The results are presented in Table 2.

GWP is a unit in which the greenhouse gas impact of different greenhouse gases is measured from the CO_2 unit. As seen in Table 2, air, rail, road, and sea transport produce 0.88, 0.052, 0.093, and 0.0095 kg of CO_2eq GHGs, respectively, in the short-term period of 20 years. These values tend to decrease with time, and this can be shown as the effect of greenhouse gases decreases as the duration of their stay in the atmosphere increases. CO_2eq/tkm (or CO_2eq/pkm) is also called CO_2 efficiency and it is a unit used to understand the impacts of a transportation vehicle, i.e., its environmental efficiency. The lower this value, the higher the environmental

Table 2 The results for Global Warming Potential (GWP) values of different transport modes (kg CO_2eq)

Mode	Mode	GWP20	GWP100	GWP500
Fossil	Air	0.88	0.76	0.75
	Rail	0.052	0.048	0.047
	Road	0.093	0.089	0.087
	Sea	0.0095	0.0093	0.0091

efficiency. Vehicles have a lower efficiency value by traveling shorter distances in the same time in heavy traffic conditions. Therefore, values in urban areas are usually higher. In rural areas, it can be concluded that efficiency is higher since the distance covered in the same time period generally increases.

Table 2 also allows comparison of transport modes. In return for 1 tkm of freight transport, the most emissions are produced in air transport by far. Road transport comes second, railway transport comes third, and maritime transport seems to be the mode of transport that produces the lowest emissions.

When these values, which were given as per unit load and distance, are evaluated in terms of the total load carried, the importance of maritime transportation becomes even more evident. Since the average ship has a much larger capacity than all other modes of transportation, maritime transport is the most logical choice both economically and environmentally. On the other hand, the values presented in Table 2 are given only for freight transportation and the processes such as manufacturing, maintenance/repair, and end-of-life of the vehicles were not taken into consideration. Accordingly, since the ship is the largest vehicle of transportation, maritime transport may fall further behind in terms of environmental performance. The material and energy consumed in the production and routine maintenance of a ship is higher than that of other vehicles. However, considering the overall cumulative performance, maritime transport has always been more environmentally friendly and will remain so for a very long time.

On the other hand, it should be noted that the environmental efficiency of the electrically powered high-speed train (and other electrically powered vehicles) is closely related to the electricity generation process. For this reason, it is an expected result that the environmental efficiency of these vehicles will increase if the electrical energy produced from alternative sources is used more widely. It is foreseen that the amount of energy produced by utilizing hydro, thermal, wave or tidal energy will increase in the future, and in parallel, electric vehicles will be more environmentally friendly.

Since the greatest advantage of maritime transport compared to rail and road transport is that it can continue in places where land ends, it would not make economic sense to compare these transport modes. Airplanes can reach wherever ships reach and even beyond. However, the size of the amount of fuel that airplanes have to spend in order to take off and the constraints on their carrying capacity are the

biggest obstacles for these vehicles to compete with ships. Emerging technologies may find a solution to these constraints, but there is still time.

References

1. IEA: Key world energy statistics (2019)
2. IEA: IEA data and statistics. https://www.iea.org/data-and-statistics
3. EEA: EEA transport emissions. https://www.eea.europa.eu/data-and-maps/indicators/transport-emissions-of-air-pollutants-8/transport-emissions-of-air-pollutants-8
4. Buhaug, Ø., Corbett, J.J., Endresen, O., Eyring, V., Faber, J., Hanayama, S., Lee, D.S., Lindstad, H., Markowska, A.Z., Mjelde, A., Nelissen, D., Nilsen, J., Pålsson, C., Winebrake, J.J., Wu, W., Yoshida, K.: Second IMO GHG study. London (2009)
5. Abadie, L.M., Goicoechea, N., Galarraga, I.: Adapting the shipping sector to stricter emissions regulations: fuel switching or installing a scrubber? Transp. Res. Part D Transp. Environ. **57**, 237–250 (2017). https://doi.org/10.1016/j.trd.2017.09.017
6. Cristea, A., Hummels, D., Puzzello, L., Avetisyan, M.: Trade and the greenhouse gas emissions from international freight transport. J. Environ. Econ. Manage. **65**, 153–173 (2013). https://doi.org/10.1016/j.jeem.2012.06.002
7. Fan, Y.V., Perry, S., Klemeš, J.J., Lee, C.T.: A review on air emissions assessment: transportation. J. Clean. Prod. **194**, 673–684 (2018). https://doi.org/10.1016/j.jclepro.2018.05.151
8. Haglind, F.: A review on the use of gas and steam turbine combined cycles as prime movers for large ships. Part III: fuels and emissions. Energy Convers. Manag. **49**, 3476–3482 (2008). https://doi.org/10.1016/j.enconman.2008.08.003
9. Harald, M.H., Fridell, E.: When is short sea shipping environmentally competitive? In: Oosthuizen, J. (ed.) Environmental Health—Emerging Issues and Practice (2012)
10. Jehanno, A., Palmer, D., James, C.: High speed and rail sustainability (2011)
11. Psaraftis, H.N., Kontovas, C.A.: CO_2 emission statistics for the world commercial fleet. WMU J. Marit. Aff. **8**, 1–25 (2009). https://doi.org/10.1007/BF03195150
12. Svindland, M., Hjelle, H.M.: The comparative CO_2 efficiency of short sea container transport. Transp. Res. Part D Transp. Environ. **77**, 11–20 (2019). https://doi.org/10.1016/j.trd.2019.08.025
13. Chèze, B., Chevallier, J., Gastineau, P.: Will technological progress be sufficient to stabilize CO_2 emissions from air transport in the mid-term? Transp. Res. Part D Transp. Environ. **18**, 91–96 (2013). https://doi.org/10.1016/j.trd.2012.08.008
14. Wise, M., Muratori, M., Kyle, P.: Biojet fuels and emissions mitigation in aviation: an integrated assessment modeling analysis. Transp. Res. Part D Transp. Environ. **52**, 244–253 (2017). https://doi.org/10.1016/j.trd.2017.03.006
15. Cox, B., Jemiolo, W., Mutel, C.: Life cycle assessment of air transportation and the Swiss commercial air transport fleet. Transp. Res. Part D Transp. Environ. **58**, 1–13 (2018). https://doi.org/10.1016/j.trd.2017.10.017
16. Hepting, M., Pak, H., Grimme, W., Dahlmann, K., Jung, M., Wilken, D.: Climate impact of German air traffic: a scenario approach. Transp. Res. Part D Transp. Environ. **85**, 102467 (2020). https://doi.org/10.1016/j.trd.2020.102467
17. Li, Y., He, Q., Luo, X., Zhang, Y., Dong, L.: Calculation of life-cycle greenhouse gas emissions of urban rail transit systems: a case study of Shanghai Metro. Resour. Conserv. Recycl. **128**, 451–457 (2018). https://doi.org/10.1016/j.resconrec.2016.03.007

18. Yue, Y., Wang, T., Liang, S., Yang, J., Hou, P., Qu, S., Zhou, J., Jia, X., Wang, H., Xu, M.: Life cycle assessment of high speed rail in China. Transp. Res. Part D Transp. Environ. **41**, 367–376 (2015). https://doi.org/10.1016/j.trd.2015.10.005

19. To, W.M., Lee, P.K.C., Yu, B.T.W.: Sustainability assessment of an urban rail system—the case of Hong Kong. J. Clean. Prod. **253** (2020). https://doi.org/10.1016/j.jclepro.2020.119961

20. Chang, Y., Lei, S., Teng, J., Zhang, J., Zhang, L., Xu, X.: The energy use and environmental emissions of high-speed rail transportation in China: a bottom-up modeling. Energy **182**, 1193–1201 (2019). https://doi.org/10.1016/j.energy.2019.06.120

21. Yue, Y.: Life cycle assessment of China's high speed rail systems (2013)

22. Von Rozycki, C., Koeser, H., Schwarz, H.: Ecology profile of the German high-speed rail passenger transport system. ICE. Int. J. Life Cycle Assess. **8**, 83–91 (2003). https://doi.org/10.1007/bf02978431

23. Jones, H., Moura, F., Domingos, T.: Life cycle assessment of high-speed rail: a case study in Portugal. Int. J. Life Cycle Assess. **22**, 410–422 (2017). https://doi.org/10.1007/s11367-016-1177-7

24. Åkerman, J.: The role of high-speed rail in mitigating climate change—the Swedish case Europabanan from a life cycle perspective. Transp. Res. Part D Transp. Environ. **16**, 208–217 (2011). https://doi.org/10.1016/j.trd.2010.12.004

25. Ou, X., Zhang, X., Chang, S.: Scenario analysis on alternative fuel/vehicle for China's future road transport: life-cycle energy demand and GHG emissions. Energy Policy **38**, 3943–3956 (2010). https://doi.org/10.1016/j.enpol.2010.03.018

26. Eriksson, E., Blinge, M., Lövgren, G.: Life cycle assessment of the road transport sector. Sci. Total Environ. **189–190**, 69–76 (1996). https://doi.org/10.1016/0048-9697(96)05192-3

27. Gilbert, P., Wilson, P., Walsh, C., Hodgson, P.: The role of material efficiency to reduce CO_2 emissions during ship manufacture: a life cycle approach. Mar. Policy. **75**, 227–237 (2017). https://doi.org/10.1016/j.marpol.2016.04.003

28. Wang, H., Oguz, E., Jeong, B., Zhou, P.: Life cycle cost and environmental impact analysis of ship hull maintenance strategies for a short route hybrid ferry. Ocean Eng. **161**, 20–28 (2018). https://doi.org/10.1016/j.oceaneng.2018.04.084

29. Chatzinikolaou, S.D., Ventikos, N.P.: Holistic framework for studying ship air emissions in a life cycle perspective. Ocean Eng. **110**, 113–122 (2015). https://doi.org/10.1016/j.oceaneng.2015.05.042

30. Perčić, M., Ančić, I., Vladimir, N.: Life-cycle cost assessments of different power system configurations to reduce the carbon footprint in the Croatian short-sea shipping sector. Renew. Sustain. Energy Rev. **131** (2020). https://doi.org/10.1016/j.rser.2020.110028

31. Robertson, S.: The potential mitigation of CO_2 emissions via modal substitution of high-speed rail for short-haul air travel from a life cycle perspective—an Australian case study. Transp. Res. Part D Transp. Environ. **46**, 365–380 (2016). https://doi.org/10.1016/j.trd.2016.04.015

32. D'Alfonso, T., Jiang, C., Bracaglia, V.: Air transport and high-speed rail competition: environmental implications and mitigation strategies. Transp. Res. Part A Policy Pract. **92**, 261–276 (2016). https://doi.org/10.1016/j.tra.2016.06.009

33. Kirschstein, T., Meisel, F.: GHG-emission models for assessing the eco-friendliness of road and rail freight transports. Transp. Res. Part B Methodol. **73**, 13–33 (2015). https://doi.org/10.1016/j.trb.2014.12.004

34. Mulley, C., Hensher, D.A., Cosgrove, D.: Is rail cleaner and greener than bus? Transp. Res. Part D Transp. Environ. **51**, 14–28 (2017). https://doi.org/10.1016/j.trd.2016.12.004

35. Pinto, J.T. de M., Mistage, O., Bilotta, P., Helmers, E.: Road-rail intermodal freight transport as a strategy for climate change mitigation. Environ. Dev. **25**, 100–110 (2018). https://doi.org/10.1016/j.envdev.2017.07.005

36. Trevisan, L., Bordignon, M.: Screening life cycle assessment to compare CO_2 and Greenhouse Gases emissions of air, road, and rail transport: an exploratory study. Proc. CIRP **90**, 303–309 (2020). https://doi.org/10.1016/j.procir.2020.01.100

37. Baron, T., Martinetti, G., Pépion, D.: High Speed Rail and Sustainability. Background Report: Methodology and Results of Carbon Footprint Analysis. (2011)

38. Avetisyan, M.: Impacts of global carbon pricing on international trade, modal choice and emissions from international transport. Energy Econ. **76**, 532–548 (2018). https://doi.org/10.1016/j.eneco.2018.10.020

39. Merchan, A.L., Léonard, A., Limbourg, S., Mostert, M.: Life cycle externalities versus external costs: the case of inland freight transport in Belgium. Transp. Res. Part D Transp. Environ. **67**, 576–595 (2019). https://doi.org/10.1016/j.trd.2019.01.017

40. Hauschild, M.Z., Rosenbaum, R.K., Olsen, S.I. (eds.): Springer, Cham, Switzerland (2018)

41. Huijbregts, M., Steinmann, Z.J.N., Elshout, P.M.F.M., Stam, G., Verones, F., Vieira, M.D.M., Zijp, M., van Zelm, R.: ReCiPe 2016: a harmonized life cycle impact assessment method at midpoint and endpoint level: Report I-Characterization (2016)

Materials and Design

Mobile Aerial Ropeways Based on Autonomous Self-Propelled Chassis: Designs and Operation

Alexander V. Lagerev and **Igor A. Lagerev**

Abstract Single-span mobile aerial ropeways, formed by two autonomous self-propelled units connected by a single rope system on the basis of wheeled chassis of high load capacity and cross-country ability, are a promising type of transport equipment for the sustainable development of hard-to-reach territories that do not have the necessary transport and logistics infrastructure. They can also be effectively used for rapid deployment during transport operations in the foci of natural or man-made disasters. The chapter presents the main promising types of structural design of autonomous units (with a central, end and remote locations of the end tower; with lifting of the end tower by means of a hydraulic cylinder, folding rod and two-stage installation) and options for placing multi-axle wheeled chassis on the bearing frame of the main technological equipment of the ropeway for various installation options and fixing in the working position of the end tower. The principles of operation of these units at the stage of deployment from the transport position to the working position and the stage of regular operation are described. A comparative analysis of the functional advantages of the considered types of autonomous units is carried out. The chapter will be of interest to researchers and production specialists in the field of design and operation of transport rope systems.

Keywords Mobile ropeway · Wheeled chassis · Terminal unit · Designs

1 Introduction

Currently, quite often there is a need for operational implementation within a relatively short time interval of various transport and logistics activities, which are subject to strict requirements on the timing of the start of their implementation, in difficult natural and social conditions–in hard-to-reach or ecologically vulnerable territories (in nature reserves, mountain, tropical or arctic ecosystems, etc.), in the absence of the necessary transport infrastructure, unfavorable natural relief (in mountainous,

A. V. Lagerev (✉) · I. A. Lagerev
Academician I G Petrovskii Bryansk State University, Bryansk 241036, Russia
e-mail: avl-bstu@yandex.ru

hilly, forest, swampy or river territories, etc.), in areas of destruction in natural or man-made disasters, during military conflicts, etc.

A promising direction for the effective solution of this problem may be the creation of rapidly deployable mobile aerial ropeways, the mobility of which is ensured by the placement of the necessary technological rope equipment on autonomous self-propelled special multi-axle basic wheeled or tracked chassis of increased cross-country ability and carrying capacity–mobile transport and reloading rope units [1].

Also, aerial rope transport fits well into the "Smart City" concept, since together with traditional ground modes of transport, it is able to provide the most important property of a smart city–"smart mobility" [2, 3]. "Smart mobility" is a key component of the "Smart City", as it ensures the effective implementation of such important principles as the ability to get to all areas of the city in the shortest possible time and with a guaranteed arrival time, the availability of a stable, innovative and safe transport system (primarily public transport system), and the availability of information transport infrastructure. The logical way to overcome the problems associated with the use of ground public transport is to move to another high-altitude level. The transfer of traffic flows to the urban aboveground space remains a promising, but little-developed direction for improving the transport infrastructure of modern cities. Technically, this can be implemented with the help of rope transport technologies, including mobile ropeways.

However, at present, there is a shortage of such specialized transport and reloading rope systems for the practical implementation of the tasks of using rope technologies with the aboveground movement of goods or passengers. For the successful creation of modern competitive samples of mobile ropeways formed by mobile transport and overloading rope units and having high technical, economic, and environmental characteristics, it is necessary to develop promising designs of such units based on self-propelled chassis and the necessary technological equipment, including the rope system and the mechanisms and supporting metal structures that serve it.

2 Structural and Functional Schemes and Operation Principles of a Mobile Ropeways

A typical design of a mobile ropeway formed by two terminal units connected by a single rope system on the basis of self-propelled wheeled chassis of high cross-country ability and carrying capacity is shown in Fig. 1. It includes typical structural and functional elements specified in Table 1.

Figure 2 shows a structural and functional scheme of a mobile ropeway corresponding to the typical design in Fig. 1. This figure also shows external structural elements that are not part of the structure of a mobile ropeway but have a significant direct impact on the operation of its structural and functional elements [4]. These elements are listed in Table 2.
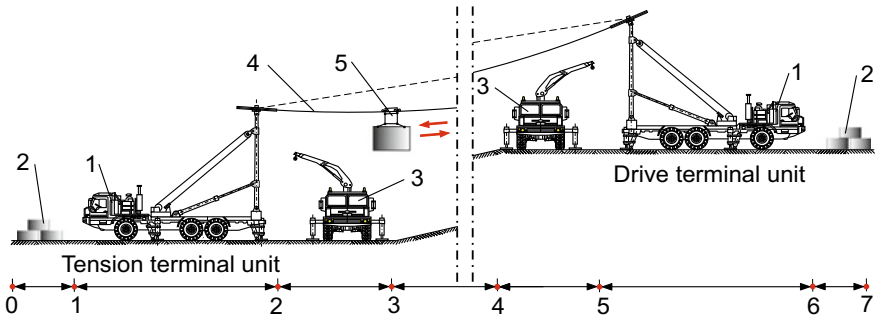
Fig. 1 Typical design of a mobile ropeway based on self-propelled terminal units (*1*–self-propelled chassis, *2*–transported cargo, *3*–crane manipulator, *4*–carrying traction rope, *5*–load handling fixture)

Table 1 Structural and functional elements of a mobile ropeway

Designation	Name of the element	Element function
E_{rs}	Carrying-traction rope system with coupled load handling fixture	Suspension and transportation of various cargoes or passengers
E_{dtu}	Drive terminal unit	Provides the movement of carrying-traction ropes together with transported cargoes or passengers
E_{ttu}	Tension terminal unit	Provides the required technological tension of carrying-traction ropes
E_{pp}	Power plant	Provides the operation of the drives of the mechanisms of the drive and tension terminal units
E_{sc}	Self-propelled chassis (or trailers, semi-trailers)	Placement of the main technological equipment of the drive and tension terminal units
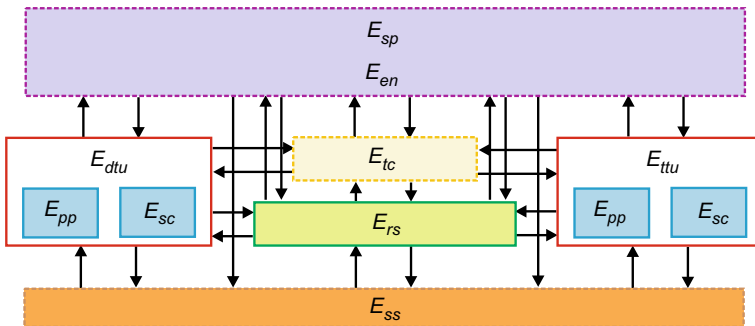
Fig. 2 Structural and functional scheme of a mobile ropeway based on autonomous self-propelled chassis

Table 2 External structural elements

Designation	Name of the element	Element function
E_{tc}	Transported cargo	Provides force loading of technological equipment of terminal units
E_{ss}	Supporting surface	Provides placement and anchoring of terminal units
E_{en}	Environment	Has a negative impact on the technological equipment of terminal units
E_{sp}	Special processes of natural or man-made nature	Lead to abnormal or emergency operation of functional and structural elements of the mobile ropeway

A typical mobile ropeway is formed using a machine kit, which includes two autonomous terminal units (E_{dtu} and E_{ttu}) based on self-propelled wheeled chassis with high load capacity and cross-country ability 1, united by a common rope system 4 (E_{rs}). Terminal units are located on the ground at the terminal points of the mobile ropeway route (sections 1–2 and 5–6 in Fig. 1). Specialized main technological equipment, which is mounted on the load-bearing frame of the self-propelled chassis of each terminal unit, allows for the pendulum movement of cargoes (E_{tc}) along the ropeway route (section 3–4) between loading and unloading points (sections 2–3 and 4–5). First, the transported cargoes 2 are delivered to the storage area (sections 0–1 and 6–7) in the immediate vicinity of the terminal points of the mobile ropeway route. Then, with the help of loading and unloading machines, mechanisms, or devices of various types (for example, mobile crane-manipulators 3, loaders, conveyors, etc.), they are suspended from the carrying-traction rope 4 using load handling fixtures 5 of various designs depending on the type of cargo. During operation, one of the terminal unit performs the functions of a drive terminal unit (E_{dtu}) and ensures the pendulum movement of the carrying-traction rope with the transported cargo. The second terminal unit performs the functions of a tension terminal unit (E_{ttu}) and ensures the optimal tension of the carrying-traction rope, depending on the length of the route, the height difference between the terminal points of the route, and the weight of the cargo.

Figure 3 shows the structural and functional schemes of the drive (E_{dtu}) and tension (E_{ttu}) terminal units, which detail the main technological equipment included in their structure, which is necessary for the operation of the mobile ropeway. They include the structural and functional elements listed in Table 3.

Design options for self-propelled terminal units corresponding to these structural and functional schemes are discussed later in this article; however, they have similar design and operational features.

As a self-propelled chassis, it is advisable to use special self-propelled wheeled chassis for tractors of high cross-country ability and carrying capacity. Such chassis civilian, military, and multi-purpose produced by a number of countries, including Germany, Italy, China, Russia, France, Sweden, Belarus, the USA, Japan [1]. As an example, Fig. 4 shows a general view of such a 4-axis self-propelled chassis. The main
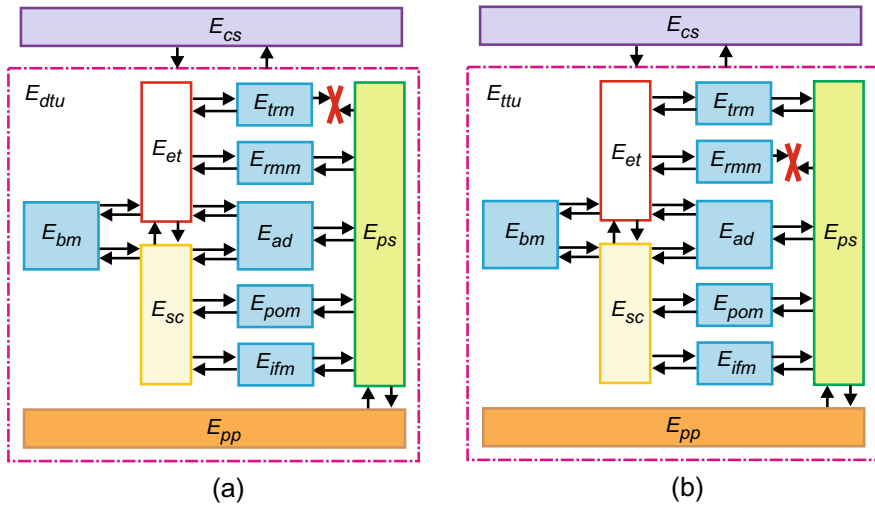
Fig. 3 Structural and functional schemes of the drive terminal unit (**a**) and tension terminal unit (**b**)

technological equipment of the mobile ropeway is placed on its open load-bearing frame. Taking into account the existing regulatory restrictions on the dimension of motor transport in height $[H_{max}]$ and width $[B_{max}]$ when driving on general-purpose roads, the main technological equipment in the transport position can be located only within the zone shown in Fig. 4. The use of a chassis with a number of wheel axles from 4 to 8 allows them to install end towers with a length of 8–20 m [1] in order to increase the length of the mobile ropeway.

For all design options for end stations, the following elements are installed on the self-propelled chassis load-bearing frame (E_{sc}):

- the main supporting structure for the rope system of the mobile ropeway—the end tower (E_{et});
- lifting hydraulic cylinder of the mechanism for installing and fixing the end tower in the working position (E_{ifm});
- external brake device of the brake mechanism (E_{bm});
- carrying-traction rope tension mechanism (E_{trm}).

The end tower is mounted either directly on the chassis load-bearing frame or on a turning platform that is hinged to the load-bearing frame. A rope pulley is fixed on the top of the end tower, under it are placed the carrying-traction rope movement mechanism (E_{rmm}) and the rope pulley spatial orientation mechanism (E_{pom}). The end tower and the lifting hydraulic cylinder, as well as the end tower and the carrying-traction rope tension mechanism are kinematically connected to each other and to the load-bearing frame by means of cylindrical hinges.

To the place of deployment of the ropeway, both terminal units move independently with the help of a standard internal combustion engine of a self-propelled

Table 3 Structural and functional elements of a terminal unit

Designation	Name of the element	Element function
E_{et}	End tower	Provides high-altitude location of the rope system and transported cargo or passengers
E_{ifm}	Mechanism of installing and fixing of the end tower in the working position	Provides lifting of the end tower from the transport position to the working position and its fixation in the working position
E_{rmm}	Carrying-traction rope movement mechanism	Provides pendulum movement of transported cargoes
E_{pom}	Rope pulley spatial orientation mechanism	Provides mutual parallelism of the longitudinal axes of the pulley groove and the rope, taking into account the natural sagging of the rope under load during operation
E_{trm}	Carrying-traction rope tension mechanism	Provides optimal tension of the carrying-traction rope during the operation of the mobile ropeway
E_{bm}	Brake mechanism	Protects the end tower from self-overturning when it is lifted from the transport position to the working position
E_{ad}	Additional devices, mechanisms and systems	Provide the specific design features of the main technological equipment of the mobile ropeway (for example, the mechanism of rope or rope-hydraulic fixation of the end tower, the articulated rod of the mechanism of installing and fixing of the end tower in the working position, the end tower pre-lift mechanism, the device for anchoring the end tower, etc.)
E_{cs}	Control system	Provides regular operation and monitoring of all parts, devices, and mechanisms of the main technological equipment of the ropeway
E_{ps}	Pamping system	Provides the operation of all hydraulic drives and devices of the mobile ropeway
E_{pp}	Power plant	Provides the operation of the drives of the mechanisms of the drive and tension terminal units
E_{sc}	Self-propelled chassis (or trailers, semi-trailers)	Placement of the main technological equipment of the drive and tension terminal units

Fig. 4 General view of a 4-axle wheeled chassis with an open load-bearing frame (*1*–driver's cab, *2*–load-bearing frame, *3*–wheel axle, *4*–area of possible placement of the main technological equipment of the mobile ropeway)

wheeled chassis, using, if possible, general-purpose roads or moving in off-road conditions. At this time, the end towers are in a transport position (close to horizontal) within the area of possible placement of the main technological equipment of the mobile ropeway (Fig. 4). At the location, each terminal unit is oriented in such a way that the longitudinal axis of the self-propelled chassis coincides with the longitudinal axis of the ropeway. To ensure overall stability under conditions of significant horizontal overturning loads from the tension force of the carrying-traction ropes and transported cargoes, self-propelled chassis are mounted on outriggers and fixed to the ground with additional anchor devices.

When the rod of the lifting hydraulic cylinder is extended, the end tower turns in a vertical plane relative to the cylindrical hinge connecting it to the load-bearing frame and occupies the required working position (close to vertical). For terminal units with an outrigger location of the end tower, turning relative to the cylindrical hinge connecting the load-bearing frame to the turning platform first leads to the lowering of the platform to the ground. Then further turning relative to the cylindrical hinge connecting the end tower to the turning platform moves the tower to the working position.

When operating a mobile ropeway, the end tower in the working position can be held by a lifting hydraulic cylinder, a power pulley block, or a folding rod.

To coordinate the mutual inclination of the rope pulleys of the mating terminal units, which is caused by the natural sagging of the carrying-traction rope and the location of the terminal units at different heights, a hydraulic rope pulley spatial orientation mechanism (E_{pom}) is used.

The necessary optimal tension of the carrying-traction rope is created by the tension mechanism (E_{trm}) of one of the terminal units with the help of a power pulley block and a tension winch included in its design.

3 Promising Design Variants of Terminal Units, their Classification

Design variants of self-propelled terminal units and their modifications are determined based on the following parameters adopted in their design:

(1) a design variant of the chassis on which the technological equipment is placed;
(2) a design variant of the end tower location in the working position;
(3) a variant for fixing the end tower in the working position;
(4) a variant for using additional technological devices;
(5) the length of the end tower.

The classification of possible design variants of self-propelled terminal units corresponding to these parameters is given in Table 4.

The full designation of the terminal unit design variant consists of the designations of the classification features in the sequence indicated in Table 4. For example, the designation Kc2m-4/12 corresponds to a terminal unit that has a terminal location of the end tower, a mechanism for installing and fixing the end tower in the working position with two parallel and synchronously operating lifting hydraulic cylinders of the same size, a mechanical braking device to prevent the end tower from self-overloading, a four-axle wheel chassis and a 12 m long end tower.

Several different modifications of promising design options for terminal units based on self-propelled wheeled chassis are shown in Fig. 5 [5–8].

The following designations of structural elements are used in Fig. 5: 1– end tower, 2–lifting hydraulic cylinder for installing and fixing the tower, 3–rope pulley, 4–carrying-traction rope, 5–rope winch, 6–holding rope, 7–brake hydraulic cylinder, 8–folding rod, 9–auxiliary lifting hydraulic cylinder, 10–power pulley block, as well as characteristic points of the structure: A is the hinge for attaching the lifting hydraulic cylinder to the chassis overframe structure; B is the hinge for attaching the end tower to the chassis overframe structure; C is the hinge for attaching the end tower and the main lifting hydraulic cylinder or the upper mating part of the folding rod; D is the hinge for attaching the end tower to the turning platform; E is the attachment point of the holding rope on the winch; F is the attachment point of the holding rope to the end tower; G is the hinge contact of the brake hydraulic cylinder with the end tower; H is the hinge for attaching the brake hydraulic cylinder to the chassis overframe structure; J is the hinge for attaching the mating parts of the folding rod; K is the hinge for attaching the lower mating part of the folding rod to the chassis overframe structure; L is the hinge for attaching the auxiliary hydraulic cylinder to the chassis overframe structure; M is the hinge for attaching the end tower and the auxiliary hydraulic cylinder.

Table 5 shows the possible design modifications of the terminal units that can be manufactured.

Table 4 Classification of design variants of self-propelled terminal units

Signs of classification	Construction description	Designation
Location of the end tower	Terminal location with support on the chassis load-bearing frame	K
	Central location with support on the chassis load-bearing frame	C
	Remote location with support on the ground	B
Structural design of the mechanism of installing and fixing of the end tower in the working position	Hydraulic fixation with the help of lifting hydraulic cylinders, which has the configuration options: – with single lifting hydraulic cylinder – with twin parallel mounted and synchronously operating hydraulic cylinders of the same size	c1 c2
	Rope fixation, which has the configuration options: – with a single lifting hydraulic cylinder and a single-branch holding rope – with a single lifting hydraulic cylinder and a two-branch holding rope – with twin parallel mounted and synchronously operating hydraulic cylinders of the same size and a single-branch holding rope – with twin parallel mounted and synchronously operating hydraulic cylinders of the same size and a two-branch holding rope	k11 k12 k21 k22
	Combined rope-hydraulic fixation, which has the configuration options: – with a single lifting hydraulic cylinder and a single-branch holding rope – with a single lifting hydraulic cylinder and a two-branch holding rope – with twin parallel mounted and synchronously operating hydraulic cylinders of the same size and a single-branch holding rope - with twin parallel mounted and synchronously operating hydraulic cylinders of the same size and a two-branch holding rope	x11 x12 x21 x22

Table 4 (continued)

Signs of classification	Construction description	Designation
	Rod fixation, which has the configuration options: – with a single folding rod and a single lifting hydraulic cylinder – with two folding rods and twin parallel mounted and synchronously operating lifting hydraulic cylinders of the same size	y1 y2
	Rod fixation with combined two-stage installation of the end tower, which has the configuration options: – with single folding rod, single main and auxiliary hydraulic cylinders – with twin folding rods, twin parallel mounted and synchronously operating main lifting hydraulic cylinders of the same size and a single auxiliary hydraulic cylinder - with twin folding rods, twin parallel mounted and synchronously operating main and auxiliary lifting hydraulic cylinders of the same size	o1 o2 o3
The design of the braking device to prevent the end tower from self-overturning	Mechanical braking device	m
	Hydraulic braking device	p
Number of chassis axles	Multi-axle wheeled chassis with a total number of axles n	n
Length of the end tower	The distance from the hinge of the end tower attachment to the place of attachment of the rope pulley h (in m)	h

4 Design and Operation Principles of Typical Modifications of Terminal Units

In this section, the designs and principles of operation several typical design modifications of terminal units are considered in detail. Naturally, the modifications considered do not exhaust the entire set of possible modifications of the terminal units (Table 5). However, the analysis of the considered modifications gives a complete picture of the design and principles of operation any other terminal units, which is characterized by an arbitrary combination of design parameters given in Table 4.
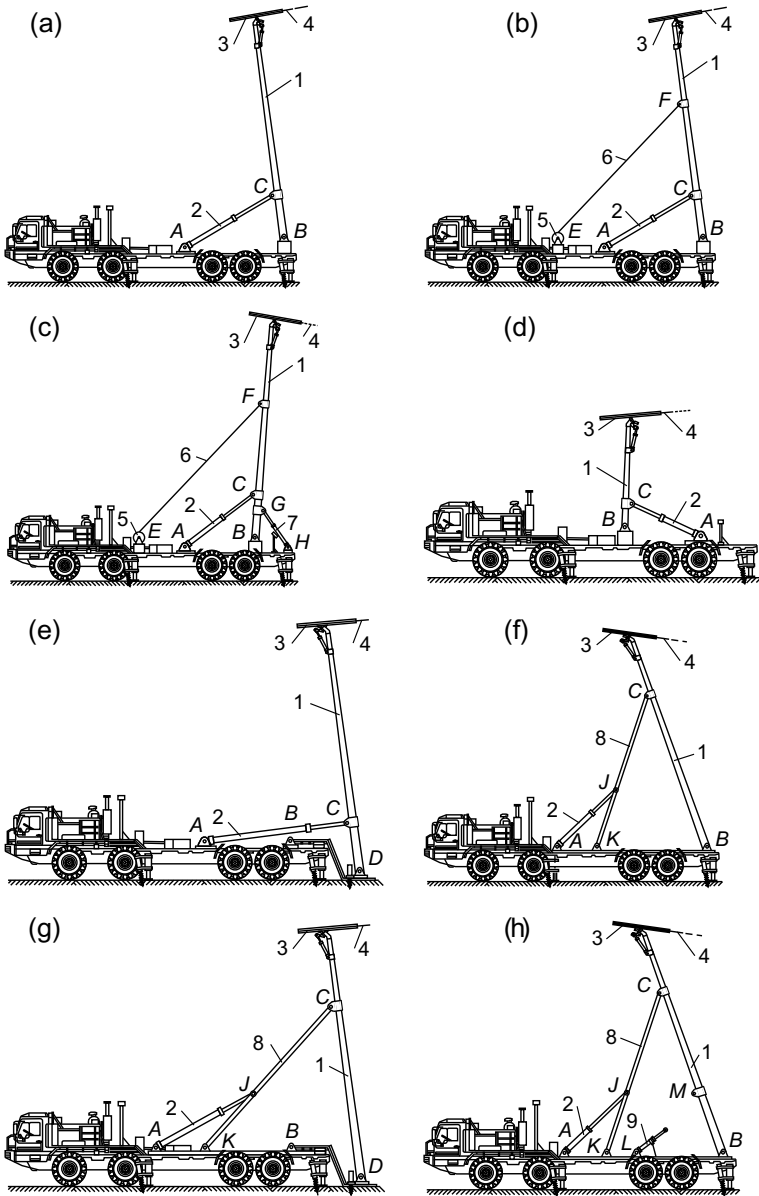
Fig. 5 Modifications of design variants for terminal units Kc2m-4/12 (**a**), Kk1m-4/12 (**b**), Kk2p-4/12 (**c**), Cc1m-4/8 (**d**), Bc2m-4/14 (**e**), Ky2-4/12 (**f**), By2-4/15 (**g**), Ko2-4/12 (**h**)

Table 5 Possible design modifications of terminal units

Modification	Design variant of the terminal unit		
	K	C	B
c	+	+	+
k	+	−	+
x	+	−	+
y	+	+	+
o	+	−	−
m	+	+	+
p	+	+	+

4.1 Terminal Units of Types Cc1-n/h Cc2-n/h

General view of terminal units of Cc1-n/h and Cc2-n/h types (i.e., having a central location and hydraulic fixation of the end tower with a length of h (m) in the working position using single or twin parallel mounted and synchronously operating lifting hydraulic cylinders of the same size, a mechanical or hydraulic braking device, and a n-axis chassis) shown in Figs. 6 and 7 (Patent RU 200827 [5]).

The numerical designations in Figs. 6, 7 and 8 correspond to the following elements: 1–overframe structure, 2–load-bearing frame, 3–self-propelled wheel chassis, 4–end tower, 5–rod, 6–lifting hydraulic cylinder, 7–frame, 8–semi-axle, 9–profiled lug, 10–rotary hydraulic cylinder, 11–rope pulley, 12–carrying-traction rope, 13–hydraulic motor, 14–gearbox, 15–transport rack, 16–outrigger, 17–additional anchor device, 18–safety cover.

The main technological equipment and supporting metal structures (Table 3) necessary for the operation of the mobile ropeway are placed on the overframe structure 1, which is attached to the load-bearing frame 2 of the self-propelled wheeled chassis 3. With the help of a cylindrical hinge B, an end tower 4 is attached to the overframe structure in its central part. The hinge B allows the end tower to make a rotary movement at an angle α of no more than 120° in a vertical plane coinciding with the longitudinal axis of the chassis. The rod 5 of the lifting hydraulic cylinder 6 is attached to the lower part of the end tower with the help of a cylindrical hinge C, and the housing itself is attached to the overframe structure with the help of a cylindrical hinge A. In the design of the terminal unit, it is possible to use a single lifting hydraulic cylinder or twin parallel mounted and synchronously operating hydraulic cylinders of the same size (Fig. 7). The use of two lifting hydraulic cylinders has an important advantage, since it is possible to use hydraulic cylinders of smaller diameter (approximately 1.4 times smaller than the diameter of a single hydraulic cylinder). To do this, a flow divider is included in the design of the hydraulic drive, which provides a throttle method for synchronizing the operation of two lifting hydraulic cylinders (synchronization of the start time and the speed of the rods).

The rope pulley spatial orientation mechanism and the actuating elements of the carrying-traction rope movement mechanism are attached to the end tower top part
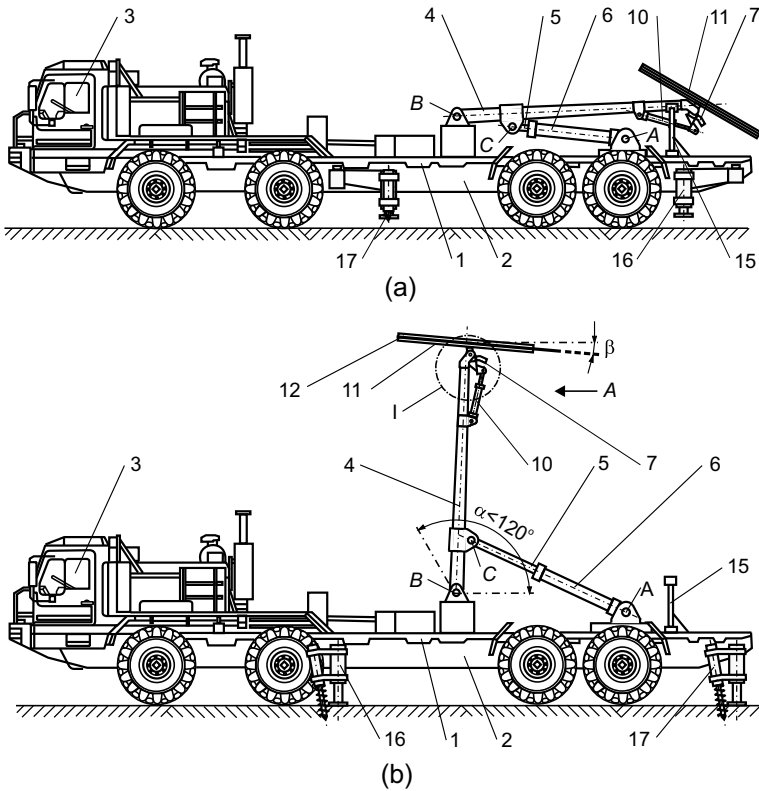
Fig. 6 General side view of the terminal units of types Cc1-4/h and Cc2-4/h in the transport position (**a**) and working position (**b**)

(element I in Fig. 6). One of the variants of the general appearance of the end tower in the area of its top is shown in Fig. 8. The structural elements of the carrying-traction rope movement mechanism are fixed on the frame 7. The frame has the ability to turn in a vertical plane relative to the semi-axes 8, fixed with the help of lugs 9 on the end tower metal structure. This turning is provided by moving the rod of the rotary hydraulic cylinder 10 of the rope pulley spatial orientation mechanism. This makes it possible to coordinate the angular position of the groove plane of the rope pulley 11 and the longitudinal axis of the carrying-traction rope 12, which is experiencing sagging under the influence of its own weight, the weight of the transported cargo, and the rope tension force [9–11]. The frame is fixed to the actuating elements of the carrying-traction rope movement mechanism, including a hydraulic motor or pump-motor 13 of axial piston or radial piston type, worm or planetary gearbox 14 and rope pulley. A carrying-traction rope is located in the profiled groove of the rope pulley.

When the self-propelled terminal unit moves to the installation place of the mobile ropeway, the end tower is in the transport position (as shown in Fig. 6). In order to prevent the failure of its metal structure due to the movement of the unit on an
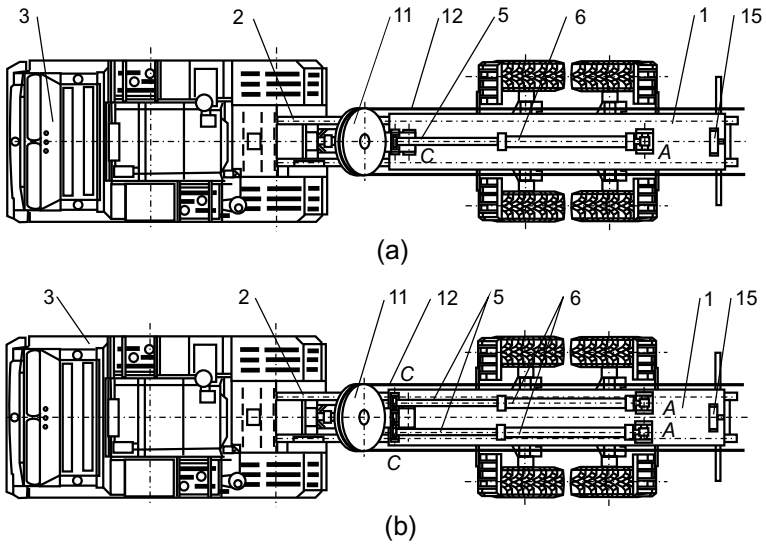
Fig. 7 General top view of the terminal stations of types Cc1-4/h and Cc2-4/h with a single lifting hydraulic cylinder (**a**) and with twin lifting hydraulic cylinders (**b**) in working position
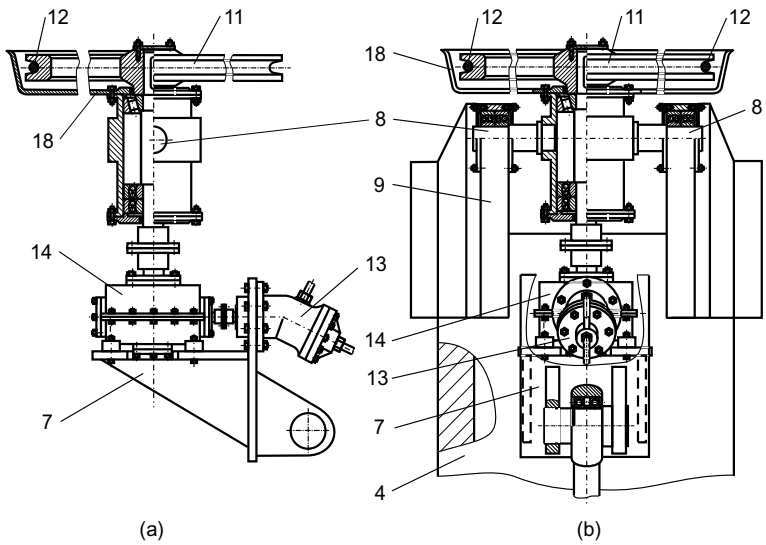
Fig. 8 General side view (**a**) and view A on Fig. 6 (**b**) the end tower top of the terminal unit

uneven surface, in the transport position, the end tower is supported and fixed on the transport rack 15. At the destination, the terminal unit is oriented in such a way that the longitudinal axis of the mobile chassis coincides with the longitudinal axis of the ropeway being mounted. To ensure overall stability under conditions of significant horizontal overturning loads from the tension force of the carrying-traction rope and the transported cargo, the self-propelled terminal unit is placed on outriggers 16, which are fixed in the ground with additional anchor devices 17. As outriggers and additional anchor devices, well-known designs can be used, which are used, for example, for mobile boom cranes [12, 13]).

The installation of the end tower is carried out in two stages due to the need to coordinate the relative position of the rope pulleys of the mating self-propelled terminal units when they are combined into a single rope transport system using a common carrying-traction rope.

At the first stage of installation, which is preliminary in nature, a looped carrying-traction rope is placed in the rope pulley groove. The safety cover 18 ensures reliable fixation of the rope, eliminating the possibility of its jumping off the rope pulley during further movement of the end tower from the transport to the working position. When the rod of the lifting hydraulic cylinder is extended, the end tower is pre-turned by approximately the required angle α (Fig. 6). The value of the required angle α is determined by the mutual altitude position on the terrain of self-propelled terminal units (Fig. 1) in accordance with the recommendations [1]. If the adjacent self-propelled terminal units is located higher, then the angle α should not be more than 90°; otherwise, the angle α should be at least 90°. In this case, the rope pulley spatial orientation mechanism located near the end tower top has minimal overall dimensions due to the small required stroke of the rotary cylinder rod. The value of the required angle α is determined by the mutual altitude position on the terrain of self-propelled terminal units (Fig. 1). If the adjacent self-propelled terminal unit is located higher, then (as a rule) the angle α should be at least 90°; otherwise, the angle α should be no more than 90 degrees. Further, when the rod of the rotary hydraulic cylinder of the rope pulley spatial orientation mechanism is extended, the frame of this mechanism, together with the rope pulley, is pre-turned around the semi-axes relative to the longitudinal axis of the end tower by approximately the required angle β. This angle is determined based on the need to match the angles of inclination to the horizon of the rope pulley plane and the longitudinal axis of the carrying-traction rope when installing both self-propelled terminal units in the working position.

At the second stage of the installation of the end tower, which is of an adjustment nature, as a result of an additional (corrective) extension of the rod of the lifting hydraulic cylinder, the end tower turns within a few degrees, which leads to the final value of the required angle α. The corrective turning of the end tower allows you to create a working tension of the carrying-traction rope. Further, by means of additional (corrective) movement (direct or return) of the rod of the rotary hydraulic cylinder, the frame of this mechanism together with the rope pulley is additionally turned relative to the longitudinal axis of the end tower by several degrees, which leads to obtaining the final value of the required angle of the rope pulley inclination β. The corrective turning of the rope pulley ensures precise alignment of the longitudinal

axis of the carrying-traction rope and the rope pulley plane. This eliminates the increased wear of the profiled pulley groove and the rope itself, increases the service life of the elements of the mobile ropeway, and the safety of its operation. During the ropeway operation, there is a periodic change in the amount of rope sagging due to changes in rope tension under conditions of variable operational load. This requires periodic changes in the angle β in order to maintain the alignment of the longitudinal axis of the rope and the plane of the rope pulley. It is performed automatically. For this purpose, during operation, the directional control valve of the rope pulley spatial orientation mechanism is installed in a position in which the opposite ends of the hydraulic cylinder are connected to each other. When the position of the rope axis and the pulley plane mismatch, a pressure force arises from the strained rope on the side surface of the pulley groove and the pulley rotates to the required additional angle due to the free flow of the working fluid between the head end and rod end of the hydraulic cylinder.

The requirement to turn the end tower by an angle α not exceeding 120°, together with the requirement to turn the rope pulley plane by an angle not exceeding 90°, allows you to provide an inclination angle β of the axis of the carrying-traction rope with respect to the horizon in the range of up to 60°. This makes it possible to use self-propelled terminal units for various types of terrain of the earth's surface, including in mountainous conditions with a significant difference in the heights of the locations of the terminal units.

4.2 Terminal Units of Types Kk11-n/h, Kk12-n/h, Kk21-n/h and Kk22-n/h

General view of the terminal units of the types Kk11-n/h, Kk12-n/h, Kk21-n/h and Kk22-n/h (i.e., having a terminal location and rope fixation of the end tower with a length of h (m) in the working position using a single-branch or two-branch holding rope, single or twin parallel mounted and synchronously working lifting hydraulic cylinders of the same size, a mechanical or hydraulic braking device and an n-axis chassis) shown in Figs. 9 and 10.

The numerical designations in Figs. 9 and 10 correspond to the designations of structural elements in Figs. 6, 7 and 8. Additional designations: 19–holding rope, 20–hinge attachment of the holding rope, 21–rope winch.

The technical task solved with the help of rope fixation of the end tower is to limit the functions of lifting hydraulic cylinders: their single task is to lift the end tower from the initial transport position to the required working position. The task of fixing the end tower during the mobile ropeway operation is excluded. The fixation of the end tower during the mobile ropeway operation is provided only by a holding rope, which perceives the entire operational load from the tension of the carrying-traction rope, the weight of the rope itself and the transported cargo, wind load, and inertia forces. This significantly reduces the weight and size characteristics of the lifting
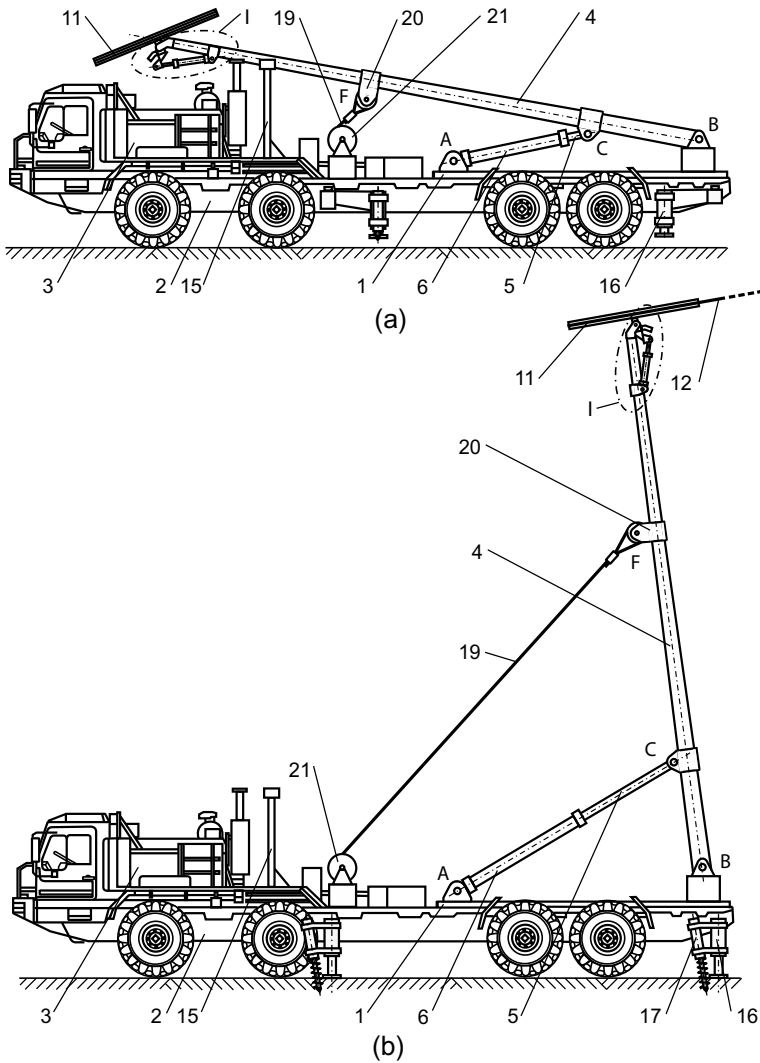
Fig. 9 General side view of the terminal units of types Kk11-4/h and Kk21-4/h with rope fixation of the end tower and a single-branch holding rope in the transport position (**a**) and working position (**b**)

hydraulic cylinders and the pumping unit power of the self-propelled terminal unit due to the reduction of operational loads that the lifting hydraulic cylinders must overcome. This also allows to reduce the support reactions in the supporting metal structure of the chassis, since the use of a holding rope allows to significantly increase the arm of the rope tension force, which perceives operational loads, to reduce the
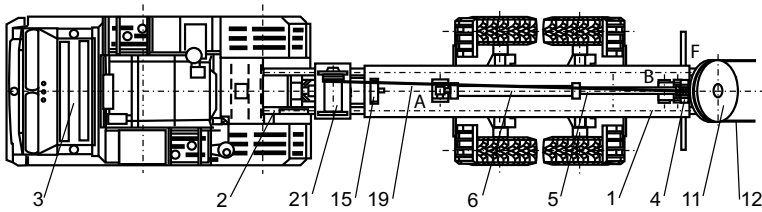
Fig. 10 General top view of the terminal units of types Kk11-4/h and Kk21-4/h with a single lifting hydraulic cylinder in working position

magnitude of the this force, the magnitude of the support reactions and the local loading of the overframe structure and the load-bearing frame of the chassis.

The design of a self-propelled terminal units with a rope fixation of the end tower for structural variants K and C is in many ways similar to the design of a self-propelled terminal units of variants K and C with hydraulic fixation of the end tower (Figs. 6, 7 and 8). However, the design additionally uses elements such as a holding rope 19, a hinge assembly 20 for attaching the holding rope to the end tower 4, and a rope winch 21 with an electric drum rotation drive. The hinge *F* is located at the maximum distance from the cylindrical hinge *B*, which provides fastening of the lower part of the end tower to the overframe structure. This ensures the maximum arm of the axial force in the holding rope and, consequently, the minimum value of this force and the minimum diameter of the holding rope. To reduce the range of materials and products used, it is advisable to choose the same brands of carrying and traction steel ropes as the brand of the holding rope that are used for rope systems of stationary and mobile cargo and passenger ropeways or lifting equipment [14, 15].

The sequence of actions of the maintenance personnel in preparation for the operation of the terminal unit with rope fixation of the end tower differs slightly from the sequence of actions of the personnel in relation to the terminal unit with hydraulic fixation. At the stage of installing the end tower in the working position, the drum of the rope winch rotates freely, providing the necessary increase in the length of the holding rope. When the end tower reaches the required working position, the extension of the rod of the lifting hydraulic cylinder stops, and the tower in this position is held by the hydraulic cylinder until the end of the preliminary hitching of the carrying-traction rope to the rope pulleys of the connected terminal units. Next, the length of the holding ropes of both terminal units is synchronously reduced, and then, after disconnecting the lifting hydraulic cylinders, the carrying-traction rope is tensioned to the required value.

4.3   Terminal Units of Types By1-n/h and By2-n/h

General view of terminal units of types By1-n/h and By2-n/h (i.e., having a remote location and a rod fixation of the end tower with a length of *h* (m) in the working

position using single or twin parallel mounted and synchronously operating folding rods and an *n*-axis chassis) shown in Figs. 11 and 12 (Patents RU 204003 and 204005 [6, 7]).

The numerical designations in Figs. 11 and 12 correspond to the designations of structural elements in Figs. 6, 7 and 8. Additional designations: 22–support plate, 23–Z-shaped rotary platform, 24–anchor device, 25–lower part of the rod, 26–upper part of the rod, 27–blocking plate.

The technical task, which is solved with the help of the rod fixation of the end tower, is to reduce the weight and overall characteristics of lifting hydraulic cylinders by reducing their required length and stroke of the rod, as well as their release from the additional function of holding the end tower in the required working position
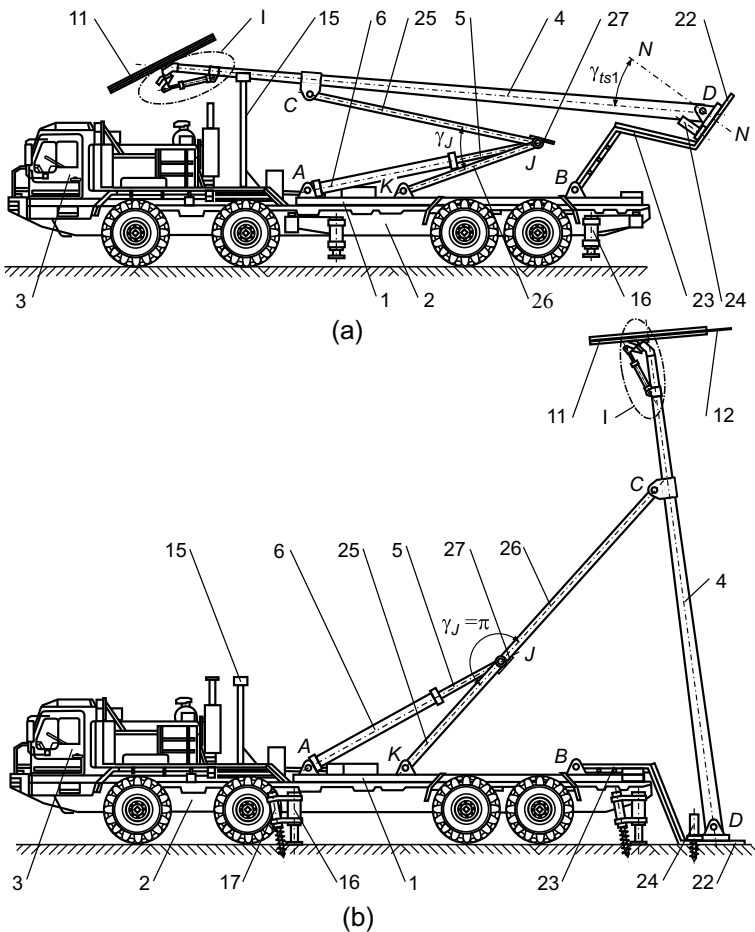
Fig. 11 General side view of the terminal units of types By1-n/h and By2-n/h with a rod fixation and a remote location of the end tower in the transport position (**a**) and the working position (**b**)
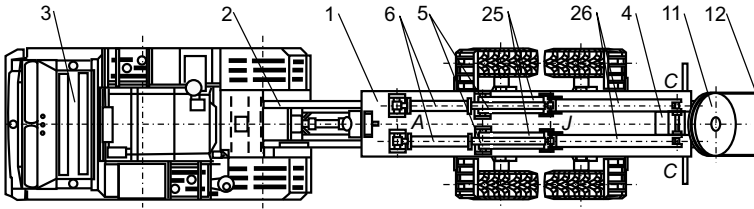
Fig. 12 General top view of the terminal units of types By1-n/h and By2-n/h with twin folding rods in the working position

during the operation of the mobile ropeway. According to data [1], to install the end tower in the working position using a folding rod, the stroke of the lifting hydraulic cylinder rod is required from 7 to 10 times less than when installed directly by the lifting hydraulic cylinder (for design variants K and C—from 4 to 8 times less). This allows the use of lifting hydraulic cylinders in the same number of times shorter length and, as a result, significantly less weight. The fixation of the end tower in the working position is provided only by an articulated folding rod. During the operation of a mobile ropeway, it perceives the entire operational load from the tension of the carrying-traction rope, the weight of the rope itself and the transported cargo, wind load, and inertia forces. Therefore, the use of a folding rod makes it possible to significantly increase the arm of the axial tensile force in the rod and, as a result, reduce the magnitude of this force and the magnitude of the support reactions and local loading of the overframe structure and the chassis load-bearing frame.

The technical task, which is solved with the help of the remote location of the end tower, is to unload the supporting structure of the self-propelled chassis of the terminal units from the effects of significant support reactions occurring in the attachment node of the end tower during the operation of the mobile ropeway, and to reduce the weight and overall characteristics of the overframe structure. This is explained by the fact that in the working position of the end tower, the acting support reactions are perceived not by the metal structure of the chassis, but by the ground surface through the support plate. At the same time, the magnitude of the support reactions in comparison with the location of the end tower on the chassis load-bearing frame also decreases. According to the data [1, 16], such a decrease can reach up to two times.

When the end tower is located remotely, the cylindrical hinge D of its attachment unit to the self-propelled chassis is located not on the overframe structure 1 (as in the design variants K and C), but on the support plate 22 of the Z-shaped rotary platform 23. The rotary platform is attached to the overframe structure by means of a cylindrical hinge B. Also, anchor devices 24 are additionally installed on the support plate. Thus, the end tower can make two rotary movements in a vertical plane coinciding with the longitudinal axis of the terminal unit: firstly, as a whole together with the rotary platform relative to the hinge B, and secondly, independently relative to the hinge D. In the transport position (Fig. 11a), the end tower is inclined by a certain angle γ_{ts1} relative to the normal N–N to the support plate. The angle

γ_{ts1} is determined in the process of finding the optimal layout of the terminal station [1], based on the provision of regulatory requirements for the permissible vertical dimension of vehicles on general-purpose highways. In this position, the end tower is rigidly fixed using a detachable locking connection.

The folding rod consists of a lower part 25 and an upper part 26 connected by a cylindrical hinge J. The lower part of the rod is attached to the overframe structure by means of a cylindrical hinge K located between the hinges A and B. The upper part of the rod is attached to the end tower 4 by means of a cylindrical hinge C. The rod 5 of the lifting hydraulic cylinder 6 is connected to the hinge J. In the transport position of the end tower, the angle of crossing of the lower and upper parts of the folding rod γ_J (Fig. 11) is minimal. With the return movement of the lifting cylinder rod, this angle increases, which leads to a rotary movement of the end tower. The working position of the end tower corresponds to the value of the angle $\gamma_J = \pi$. To exclude an emergency situation ($\gamma_J > \pi$), a blocking plate 27 is used, equipped with a limit switch for the hydraulic drive pump of the mechanism of installing and fixing of the end tower in the working position.

The sequence of actions of the service personnel when moving the terminal unit to its location and when oriented along the longitudinal axis of the mobile ropeway is similar to those previously discussed in Sects. 4.1 and 4.2. The transfer of the end tower from the initial transport position to the required working position is performed in two stages.

At the first stage, the rod of the lifting hydraulic cylinder performs a return movement, i.e., it is drawn into the housing interior. The rod moves the cylindrical hinge J towards the cab of the terminal unit in the longitudinal vertical plane. The hinge J performs a complex plane-parallel movement–rectilinear along the longitudinal axis of the lifting hydraulic cylinder and rotary relative to its own. In this case, the angle γ_J increases. The lower part of the rod acts on the upper part, forcing it to move upwards, while simultaneously turning relative to the axis of the hinge J in the longitudinal vertical plane in the opposite direction from the terminal unit cab. The upper part of the rod acts on the end tower at the point of attachment of the cylindrical hinge C, forcing the tower to turn in the longitudinal vertical plane. Since the end tower is rigidly fixed on a Z-shaped rotary platform by means of a locking connection, the specified turning is performed relative to the cylindrical hinge B, and the rotary platform also participates in it. The first stage of the installation of the end tower is completed when the support plate of the rotary platform is lowered to the ground surface. If necessary, the ground surface for the support plate can be pre-prepared by leveling it, ramming, strengthening. To ensure good adhesion of the support plate to the ground under conditions of significant horizontal and vertical support reactions from the end tower, the support plate is fixed to the ground surface using anchoring devices installed on it. After opening the locking connection, the second stage of installing the end tower in the working position begins.

At the second stage, the rod of the lifting hydraulic cylinder continues to make a return movement. In this case, the end tower turns relative to the plane of the support plate (relative to the cylindrical hinge D) until it occupies the required working position. The working position of the end tower is achieved when the longitudinal

axes of both parts of the folding rod are aligned. At this moment, the movement of the rod stops due to the operation of the limit switch mounted on the blocking plate, which leads to the shutdown of the hydraulic drive pump of the mechanism of installing and fixing of the end tower in the working position.

Upon completion of the mobile ropeway operation, the transfer of the end tower from the working position to the transport position is performed in reverse order, and the rod of the lifting hydraulic cylinder performs a direct movement (extension).

4.4   Units of Types By1-n/h and By2-n/h

General view of the terminal units of types Ko1-n/h, Ko2-n/h and Ko3-n/h (i.e., having a terminal position and a rod fixation of the end tower with a length of h (m) in the working position with its combined two-stage installation using single or twin parallel mounted and synchronously working folding rods, single or twin main and auxiliary lifting hydraulic cylinders, and an n-axis chassis) shown in Figs. 13 and 14 (Patent RU 206299 [8]).

The numerical designations in Figs. 13 and 14 correspond to the designations of structural elements in Figs. 6, 7, 8, 10 and 11. Additional designations: 28–auxiliary lifting hydraulic cylinder, 29–rod of auxiliary lifting hydraulic cylinder, 30–fixing rod.

According to researches [1, 16, 17], at the moment of the beginning of the end tower turning, the lifting hydraulic cylinder of the mechanism of installing and fixing of the end tower in the working position should develop maximum traction. This is due to the fact that the moment of resistance relative to the hinge B, created by the total weight of the rope pulley, the metal structure of the end tower and the mechanisms installed on it, has the maximum value. At the same time, the lifting moment relative to the hinge B, created by the lifting hydraulic cylinder, has a minimum value, since the lifting force acting on the end tower, transmitted by the hydraulic cylinder rod through the hinge C, is located at a small angle to the longitudinal axis of the end tower. With further turning, the value of force that needs to be created by the hydraulic cylinder decreases quickly enough. Therefore, the value of force created by the lifting hydraulic cylinder at the initial stage of turning the end tower may be an order of magnitude greater than the force that should be applied to the end tower at the final stage of its turning to the working position. This is typical for all design variants of terminal units, but is especially evident when using a folding rod. However, design calculations of the weight and overall characteristics of the lifting hydraulic cylinders and the power of the hydraulic system pump, as well as strength and dynamic calculations of the supporting metal structures are performed based on the maximum load that occurs during the installation of the end tower in the working position. Therefore, the technical task aimed at solving the two-stage installation of the end tower with the help of an auxiliary lifting hydraulic cylinder is to reduce the maximum traction force at the initial stage of the end tower turning and, as a consequence, reduce the weight, overall and energy characteristics of the hydraulic

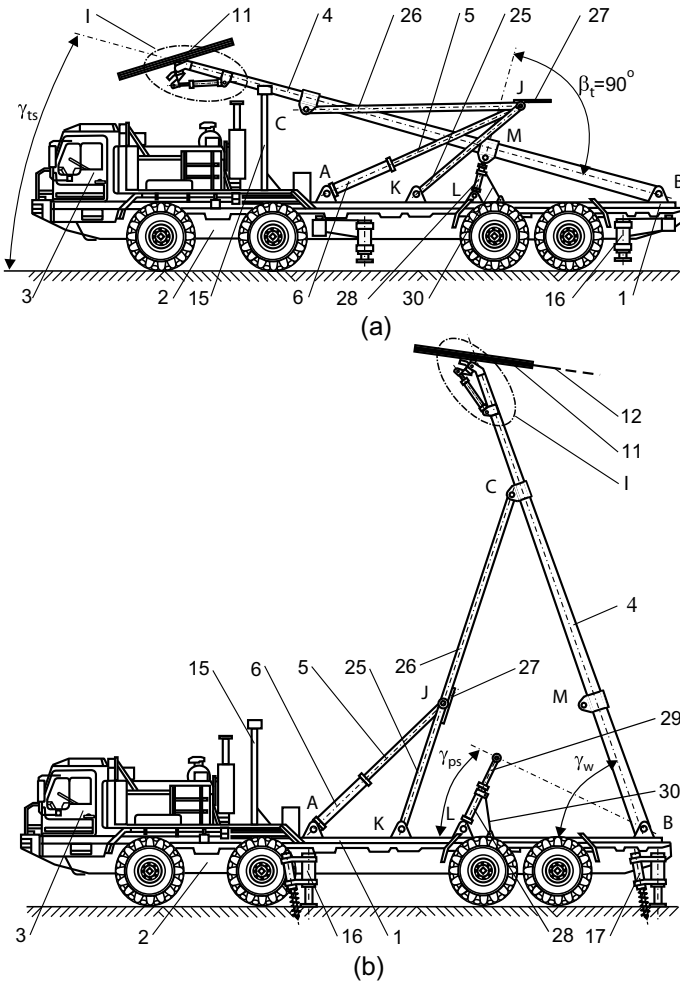**Fig. 13** General side view of the terminal units of types Ko1-n/h, Ko2-n/h and Ko3-n/h with a rod fixation and the terminal position of the end tower with its two-stage installation in the transport position (**a**) and working position (**b**)
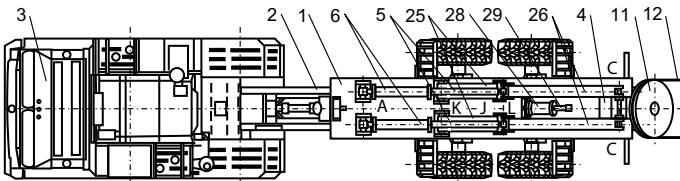
Fig. 14 General top view of the terminal unit of type Ko2-n/h with twin main and single auxiliary lifting hydraulic cylinders in the working position

drive, reduce the support reactions and stresses in the supporting metal structures of the terminal units.

To implement the procedure of combined two-stage installation of the end tower 4, an auxiliary lifting hydraulic cylinder 28 is additionally installed, which provides the initial turning of the end tower relative to the hinge B. With the help of a cylindrical hinge L located between the hinges A and B, the housing of the auxiliary hydraulic cylinder is attached to the overframe structure 1 of the self-propelled chassis 3. The hinge L provides their movable (turning) connection. With the help of a cylindrical hinge M located between the hinges B and C, the rod of the auxiliary hydraulic cylinder and the end tower are also conjugated by a turning connection. In the transport position of the end tower, the longitudinal axes of the end tower and the auxiliary lifting hydraulic cylinder are perpendicular, i.e., they form the maximum possible angle $\beta_t = \pi/2$ (Fig. 13a). To do this, the following condition must be met when designing: the distance l_{BM} between the centers of the hinges B and M and the distance l_{BL} between the centers of the hinges B and L should be related by the ratio [1]

$$l_{\mathrm{BM}} \approx l_{\mathrm{BL}} \cos \gamma_{\mathrm{ts}}, \tag{1}$$

where γ_{ts} is the inclination angle of the end tower in the transport position (Fig. 13a).

The sequence of actions of the service personnel when moving the terminal unit to its location and when oriented along the longitudinal axis of the mobile ropeway is similar to those previously discussed in Sects. 4.1–4.3. The installation of the end support from the initial transport position to the required working position is performed in two stages.

During the first stage, the end tower is turning from the initial transport position, which is characterized by the inclination angle γ_{ts}, to an intermediate position, which is characterized by the inclination angle γ_{ps} (Fig. 13a). The end tower turning to an intermediate position is performed by an auxiliary lifting hydraulic cylinder by extending its rod 29. At this time, the main lifting hydraulic cylinder 6 is disconnected from the hydraulic system, as a result of which its rod 5, the cylindrical hinge J and both parts 25 and 26 of the folding rod move freely following the turning of the end tower, with which they are kinematically connected by means of a cylindrical hinge C. The extension of the rod of the auxiliary lifting hydraulic cylinder ends when the required preliminary inclination angle of the end tower γ_{ps} is reached, after which the auxiliary hydraulic cylinder is disconnected from the hydraulic system. The maximum stroke of the auxiliary hydraulic cylinder rod is limited by its length, since it is possible to place a hydraulic cylinder of a sufficiently limited length in the space under the end tower in the transport position. Therefore, the preliminary inclination angle is $\gamma_{ps} \sim (1\ldots2)\,\gamma_{ts}$, i.e., it turns out to be significantly less than the angle γ_w required to install the end tower in the working position (Fig. 13b). Therefore, with further end tower turning, the mandatory use of the main lifting hydraulic cylinder is required. Before the start of the second stage, the rod of the auxiliary hydraulic cylinder is disconnected from the end tower by opening the cylindrical hinge M.

In such an inclined position, the auxiliary hydraulic cylinder is held by means of a fixing rod 30.

During the second stage, the end tower turning to the working position is performed by the main lifting hydraulic cylinder. The changes occurring in this case in the spatial position of the end tower and the folding rod are similar to those discussed in Sect. 4.3.

Upon completion of the operation of the mobile ropeway, the end tower turning from the working position to the transport position is performed in reverse order in two stages. First, the rod of the main lifting hydraulic cylinder performs a reverse movement until the end tower reaches an intermediate position with an inclination angle γ_{ps}. In this position, the main lifting hydraulic cylinder is disconnected from the hydraulic system, and the cylindrical hinge M is closed. Further end tower turning is performed due to the return movement of the rod of the auxiliary lifting hydraulic cylinder.

5 Conclusion

In this chapter, promising design variants for terminal units are considered, as well as possible variants for placing the main technological equipment of the rope system and mechanisms that ensure its operation on the basis of self-propelled multi-axle wheeled chassis of high load capacity and cross-country ability have the necessary technical characteristics that ensure the creation of single-span mobile ropeways on terrain with difficult terrain or under unfavorable operating conditions and in conditions of lack of time to carry out mantling or dismantling operations.

Design modifications of self-propelled terminal units are distinguished by a different combination of possible variants for the location of the end tower on the load-bearing frame of the wheeled chassis and variants for installing and fixing the end tower in the working position. Each such modification has its own technical advantages and disadvantages in comparison with other possible design variants of terminal units, as a result of which it has a certain area of its preferential use. Taking into account this circumstance allows the designer in the process of designing terminal units to choose not only sufficiently universal design variants, but also, if necessary, to focus on the specific operating conditions of mobile ropeways.

References

1. Lagerev, A.V., Lagerev, I.A., Tarichko, V.I.: Structures and Design Fundamentals of Mobile Transporting and Overloading Rope Facilities. RISO BGU, Bryansk, Russia (2020)

2. PAS 183:2017 Smart cities—Guide to establishing a decision-making framework for sharing data and information services. BSI (2017)
3. Panfilov, A.V., Korotkiy, A.A, Panfilova, E.A., Lagerev, I.A.: Development of transport infrastructure of urban mobility based on cable metro technology. IOP Conf. Series: Materials Sci. and Eng. **786**, 012067 (2020)
4. Lagerev, A.V., Lagerev, I.A.: A general approach to the creation of digital twins of mobile ropeways based on mobile transport and reloading rope units. Nauchno-tekhnicheskiy vestnik Bryanskogo gosudarstvennogo universiteta **1**, 38–60 (2022)
5. Lagerev, A.V., Lagerev, I.A., Tarichko, V.I.: Self-propelled terminal station of the mobile ropeway. Patent RU No. 200827, Filed 12 May 2020 (2020)
6. Lagerev, A.V., Lagerev, I.A., Tarichko, V.I.: Self-propelled terminal station of the mobile ropeway. Patent RU No. 204003, Filed 08 Dec 2020 (2021)
7. Lagerev, A.V., Lagerev, I.A., Tarichko, V.I.: Self-propelled terminal station of the mobile ropeway. Patent RU No. 204005, Filed 16 Dec 2020 (2021).
8. Lagerev, A.V., Lagerev, I.A., Tarichko, V.I.: Self-propelled terminal station of the mobile ropeway. Patent RU No. 206299, Filed 04 Apr 2021 (2021)
9. Bryja, D., Knawa, M.: Computational model of an inclined aerial ropeway and numerical method for analyzing nonlinear cable-car interaction. Comput. Struct. **89**, 1895–1905 (2011)
10. Qin, J., Qiao, L., Chen, J., Wan, J., Jiang, M., Hu, Ch.: Analysis of the working cable system of single-span circulating ropeway. In: MATEC Web of Conferences, vol. 136, p. 02003 (2017)
11. Lagerev, A.V., Lagerev, I.A.: Designing supporting structures of passenger ropeways of minimum cost based on modular intermediate towers of discretely variable height. Urban Rail Transit **6**(4), 265–277 (2020)
12. Duerr, D.: Mobile Crane Support Handbook, 5th edn. Levare Press Inc., Houston, USA (2019)
13. Lagerev, I.A., Lagerev, A.V., Tarichko, V.I.: Modeling the swing of mobile loader cranes with anchor outriggers when operating on weak soils. In: E3S Web of Conference, vol. 326, p. 00011 (2021)
14. Costello, G.A.: Theory of Wire Rope, 2nd edn. Springer, New York, USA (1997)
15. Feyrer, K.: Wire Ropes. Tension, Endurance, Reliability, 2nd edn. Springer-Verlag, Berlin, Heidelberg, Germany (2015)
16. Lagerev, A.V., Lagerev, I.A., Tarichko, V.I.: Kinematic and force analysis of the end tower positioning mechanism at mobile ropeway. In: Radionov, A.A., Gasiyarov, V.R. (eds.) The 7th International Conference on Industrial Engineering, 2021, pp. 394–404. Springer, Cham. (2022)
17. Lagerev, A.V., Tarichko, V.I., Lagerev, I.A.: Placement of technological equipment on the basic chassis of the mobile transportation and reloading rope complex. Nauchno-tekhnicheskiy vestnik Bryanskogo gosudarstvennogo universiteta **3**, 388–403 (2020)

Design and Analysis of Turbocharger Turbine Wheel Using Composite Materials

Duppatla Rambabu, Srihari Palli, D. Bhanuchandra Rao, Duppala Azad, B. A. Ranganath, and Ismail Hossain

Abstract The primary purpose of this research is to investigate the analysis of a turbocharger turbine wheel with the goal of optimising its design and its use of materials. The static, computational fluid dynamics (CFD), and thermal analyses of the turbine blades that make up the turbine phase of a turbocharger are the focus of this work. The blades are responsible for extracting strength from the high-temperature and high-strain gas that was created with the assistance of the combustor. Most of the time, the turbocharger is the element that limits the turbine's potential. In order for turbine blades to thrive in this harsh environment, it is common practise to make use of uncommon materials such as special alloys and a wide variety of innovative cooling technologies. Some of these ways include inner air channels, boundary layer cooling, and thermal barrier coatings. In this project, a turbine blade is developed and modelled using the 3D modelling programme CREO, and then analysed using the software ANSYS 14.5. To improve the effectiveness of the cooling, the base of the blade has been redesigned to accommodate the new configuration. The selection of materials is of the utmost significance since the design of turbomachinery is notoriously complicated, and the efficiency of the machine is inextricably linked to the performance of its constituent parts. In this research, two distinct types of fluid flow conditions, namely laminar and turbulent flow, are taken into consideration for both the original models and the modified versions of those models. The optimisation process involves experimenting with several types of materials, such as chromium steel, titanium alloy, and nickel alloy, on the turbine blades for both designs. This is done by doing coupled field analysis (static and thermal).

D. Rambabu · S. Palli (✉) · D. B. Rao · D. Azad
Department of Mechanical Engineering, Aditya Institute of Technology and Management, Tekkali, Andhra Pradesh, India
e-mail: srihari.palli@gmail.com

B. A. Ranganath
Department of Mechanical Engineering, MVGR College of Engineering, Vizianagaram, Andhra Pradesh, India

I. Hossain
School of Natural Sciences and Mathematics, Ural Federal University, Yekaterinburg 620000, Russia

1 Introduction

A turbocharger, sometimes known simply as a turbo, is a turbine-driven forced induction device that boosts the power and efficiency of an internal combustion engine by pushing more air into the combustion chamber [1–7]. This gain in output above that of a naturally aspirated engine is the consequence of the fact that the turbine is able to drive more air, and correspondingly more fuel, into the combustion chamber than atmospheric pressure alone can [8–12]. The use of turbocharging may either enhance the amount of power produced for a given capacity or enable a lower displacement engine to be used, hence improving fuel economy [13–17]. The engine that was awarded "Engine of the Year 2011" was one that was installed in a Fiat 500 and was turbocharged by MHI [18]. This engine is 10% lighter than its predecessor, resulting in fuel savings of up to 30% while maintaining the same horsepower as a 1.4-l engine. Both the 1.4-l turbocharged engine and the 1.8-litre non-turbocharged engine that are offered in the 2013 Chevrolet Cruze are capable of producing the same amount of horsepower [19–21]. While high-pressure turbocharging is more suited for racing and driving on highways/motorways/freeways, low-pressure turbocharging is the best option for city driving [22–25]. An internal combustion engine's intake air pressure may be increased with the use of a device called a turbocharger, which is made up of a compressor wheel, an exhaust gas turbine wheel, and a solid shaft that is connected together [26–29]. Energy is extracted from the exhaust gas by the exhaust gas turbine, and this energy is then used to drive the compressor and overcome the effects of friction [30–34]. Compressors and turbine wheels of the radial flow type are used in the vast majority of applications that are related to automobiles [35–37]. In some applications, such as medium- and low-speed diesel engines, an axial flow turbine wheel may be used instead of a radial flow turbine to provide the necessary amount of power [38–41] (Fig. 1).

A turbocharger, sometimes known simply as a turbo, is a kind of air compressor that is used in the process of forcing air into an internal combustion engine [42–45]. A turbocharger, much like a supercharger, is designed to augment the volume of air that is sucked into the engine in order to generate an increased amount of force [46–49]. On the other hand, a turbocharger is distinct in that its compressor is driven by a turbine that is driven by the exhaust gases produced by the engine. Analyses of mechanical, thermal, and acoustical data are included into the overall design of these turbo machines, just as they are in the designs of the other turbo machines [50–53]. Engineers and researchers are still looking for methods to enhance their designs while maintaining a healthy balance between the requirements and the available resources [54–57].

There is a subset of turbotechnology known as turbochargers, and its primary function is to boost the power output of internal combustion engines [58–61]. This is
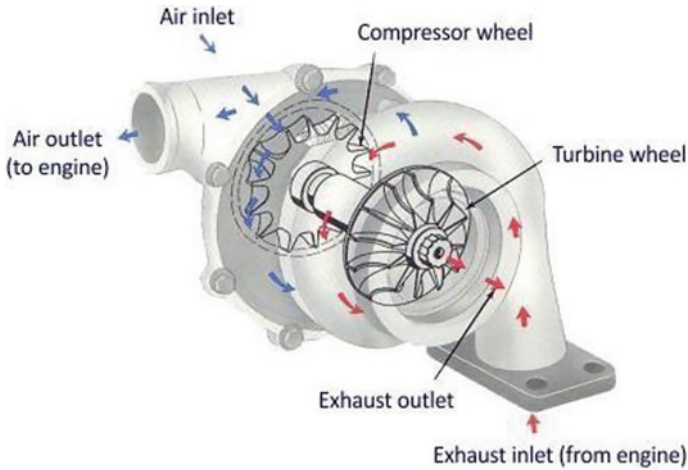
Fig. 1 Turbocharger with its parts

achieved by raising the pressure of the intake air, which in turn permits the combustion of a greater quantity of fuel. Rudolf Diesel and Gottlieb Daimler conducted research and experiments in the latter half of the 19th century on the effects of pre-compressing air on the power output and fuel economy of an engine [62–64]. Alfred Buchi, a Swiss engineer, developed the first exhaust gas turbocharger in 1925. He demonstrated a prototype that could improve the output of a diesel engine by a claimed 40%. During that time period, the concept of turbocharging did not have widespread support. However, over the course of the last several decades, it has evolved into a vital component of almost all diesel engines, with the exception of very small ones. Because of their restricted usage in gasoline engines, power output and fuel economy have both seen significant increases as a direct result [65–69].

Turbocharger is a unique product. It is difficult to manufacture the desired curvature angle at the curve intake inducer blades on turbochargers because of the sophisticated machining procedures that are required. This is one of the most significant issues with turbochargers. In order to live, it must have a pointed edge and considerable strength. Material selection is vital if you want the life of your turbocharger to be sustained. The turbocharger may take on a variety of characteristics depending on the material it is made of. At the tail end of the 1980s, turbocharging began to lose its competitive advantage; as a result, this innovation is only employed in a select few high-performance vehicles today [19–21, 70–72].

For example, Porsche is getting ready to construct a turbocharged version of its all-new 911 (which will be water-cooled), which will have increased performance. In Formula One, turbo engines were prohibited as well, with the purpose of lowering the overall performance of the vehicles (thereby making them safer too). Many people believe that this is a move in the wrong direction for Formula One, which is known for rethinking what the "future" of automotive technology would be like. It is possible to improve an engine's power by increasing either the cubic capacity of the engine

or the speed at which it operates. One further strategy involves providing it with more fuel. The supercharging technique, which is carried out by the turbocharger, is the answer to the problem. Increasing the amount of gasoline or diesel fuel that is injected during each cycle, on the other hand, will not bring about the desired results. In order for the engine to function properly, it is necessary for it to preserve the exact proportioning of the air to fuel mix. If this does not occur, the combustion process is incomplete, which leads to a significant rise in the rate of components that are not burnt and a decrease in the overall efficiency of the engine. Such repercussions would be completely incompatible with the requirements of the task at hand. Compressing the air in the cylinders is how the turbo achieves its primary function, which is to force more air into the engine while ensuring that the fuel-air ratio remains unchanged. This is the same as giving the engine a "virtual" cubic inch of displacement [70–72].

It has a capacity that is greater than the real cubic capacity it has. Simply explained, turbocharging is a method of boosting the output of the engine without expanding the size of the engine itself. The fundamental idea was straightforward and has previously been used in large diesel engines. It functions in this manner: when the machine is started, exhaust gases cause the turbine to spin, which in turn activates a compressor, which pressurizes the air. This compressed air from the turbocharger is then delivered via a duct to an air-cooled intercooler. The intercooler reduces the temperature of the intake charge, which in turn causes the density of the intake charge to rise. The air-cooled intercoolers take in air via different intakes, which is why turbocharged vehicles often have a few tiny scoops and louvres located on the hoods of the vehicles. When the intake air temperature is high or when the engine speed is low, modern turbo-diesel engines use a temperature-sensitive, motor-driven fan that increases airflow. This fan is only used when the engine speed is low. Using CREO software and a variety of various kinds of materials, the goal of this chapter is to build the impeller that goes inside of a turbocharger. In addition, the structural and thermal study of the impeller were carried out so that its qualities could be evaluated. Then, the outcome is compared to determine which use of the impeller is the most effective usage.

2 Modelling of Turbine Wheel

The measurements of the diesel engine turbocharger impeller were utilised in this inquiry. These parameters were acquired from an actual diesel engine turbocharger. Following the measurement of the dimensions, a 3D model is developed with the help of the CREO programme. The modelling is carried out in CREO parametric, and Fig. 2a, b displays the models that were considered as well as the models that were changed. The possibility of there being an error in the geometrical file is investigated in great detail by examining the overlapping facets, the redundant geometrical data, and the vertex-to-vertex rule that governs the relationships between the facets. Once the geometrical inaccuracy has been verified, the newly generated solid model is subjected to an examination of its mass property calculations, including its mass,
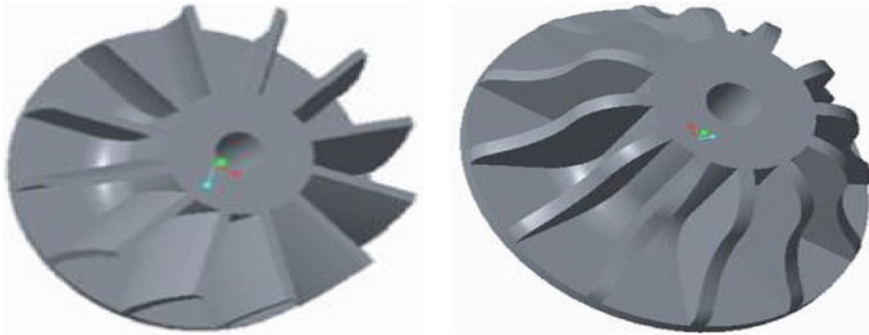
Fig. 2 Difference between **a** considered model and **b** modified model

volume, and density [19–21]. After carefully examining the mass property calculations, the 3D models that have been developed are converted to a standard file format. This is done in order to permit the simple transfer of data across different vendor applications and to communicate product information.

3 Materials and methods

Figure 3 shows the flowchart of this chapter. The model is created in 3D modelling software and transferred into the ANSYS analysis software. Then the meshing is created and validated. The simulation is performed with the different material and evaluated by comparing alternative materials [21].

3.1 Materials

Static, computational fluid dynamics, and thermal analysis are performed on the turbine wheel using chromium steel, titanium alloy, and nickel alloy. The results analysed are deformation, stress, strain, heat transfer coefficient, mass flow rate, heat
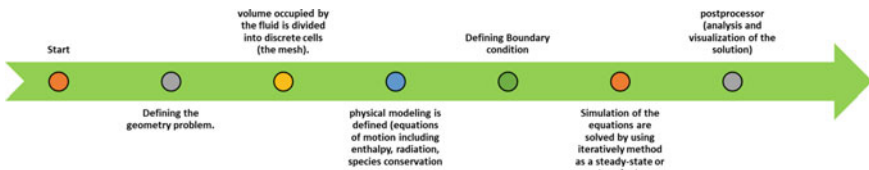
Fig. 3. Flowchart of the chapter

Table 1 Material properties of the different material [20, 70]

Materials	Density (kg/m³)	Young's modulus (GPa)	Poisson's ratio	Thermal conductivity (w/m-k)
Chromium steel	7150	245	0.2	60.5
Titanium alloy	4420	110	0.31	21.9
Nickel alloy	8908	150	0.26	70.1

flow rate, and heat flux [19, 70]. Table 1 shows the material property of different materials used in the analysis.

3.2 Meshing

The finite element analysis was performed separately on each of the three materials that were anticipated to be present. Both the static structural analysis as well as the thermal analysis were completed. The ANSYS version 14.5 software was used for the whole of both studies. Figure 4 shows the model of the impeller after it has been imported into ANSYS version 14.5 and meshing has been performed. After that, the loaded impeller is hexahedrally subdivided into the meshes by employing components of that shape. This is done to assure correct results.
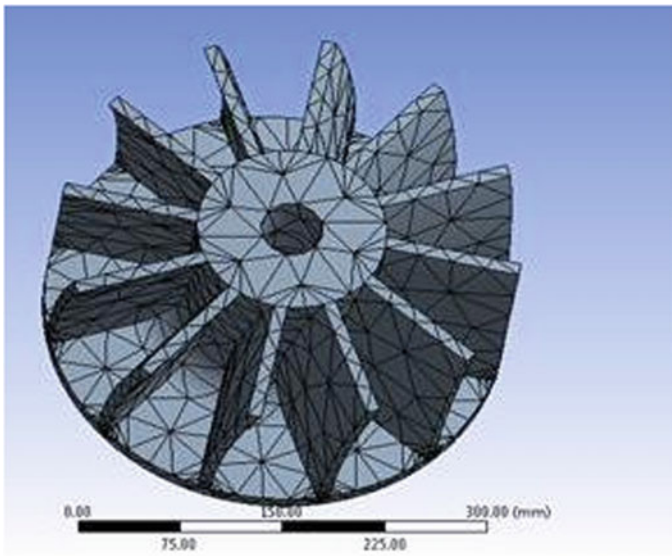
Fig. 4. Meshed model

In all of these approaches, the same basic procedure is followed. Static analysis is used to determine the strength of turbocharger by using the stress, strain, and deformation values. The structure of the turbine wheel was modelled and treated as an orthotropic elastic plate simulated as elements. Using these elements, a car body steel structure could be simulated accurately. As a means of simulating the counterbalance present in the basic scenario, a mass unit was used. According to this investigation, the subspace technique coupled with a preconditioned conjugate gradient (PGC) solver is more desirable than the subspace method alone. This technique, which may also be referred to as power dynamics, is used for modelling massive systems with up to 1,000,000 degrees of freedom (DOF). To be more precise, the model consists of the following data:

Total Mass: 32,253 kg

Total Volume: 4.1391e+009 mm^3

Total number of Nodes: 598,273

Total number of Elements: 112,477

4 Results and Discussions

4.1 Static Analysis Results

The structural module, the impeller, is subjected to an analysis using the finite element technique. The findings of the flow field were collected, and then they were imported into the static structure module for analysis. While doing this, the influence of centrifugal force and beginning load was taken into consideration. It is entered into the stress analysis model in its capacity as the surface load of the propeller. On the basis of this information, the operating speed of the impeller was set at 21,500 rpm, and the results of the simulation were obtained under the heading of fluid-structure interaction.

When the impeller is rotating at a high speed, the equivalent force distribution is mostly in the top edge of the blade. This can be observed by looking at the findings of the study of the equivalent force performed on the impeller, which are shown in Figs. 5, 6 and 7. The portion of the blade that is closer to the edge is lower, and the area of the blade that experiences the greatest amount of stress is closer to its tip than its root. The spot on the O-type model that experiences the greatest amount of stress is on the windward side, close to the blade root. The improved blade eliminates the differential in stress that was previously present on the middle and lower lateral sides of the blade. Table 2 presents the average value of the highest stress measured at the upper end of the blade. However, the area of the blade that experiences the most stress is closer to its root or even at the point where the blade meets the disc. This component's structural strength is very great, putting it light years ahead of the

O-type component with the highest stress levels and the highest risk of deformation fracture.

The metal fatigue strength of the compressor impeller blade is decided by the stress that is placed on each component during the high-speed rotation. The structural strength of each component also plays a role in this determination. Even the vibration and distortion of the blades are directly impacted by the phenomenon. If the structural strength remains the same, then the failure probability decreases in direct proportion to the stress level. The fluid-structure interaction may be seen to induce a deformation that is more extreme as one moves away from the root of the blade. The most important area of the blade's deformation may be found in any of the three models from the

Fig. 5. Comparisons between considered and modified models of deformation
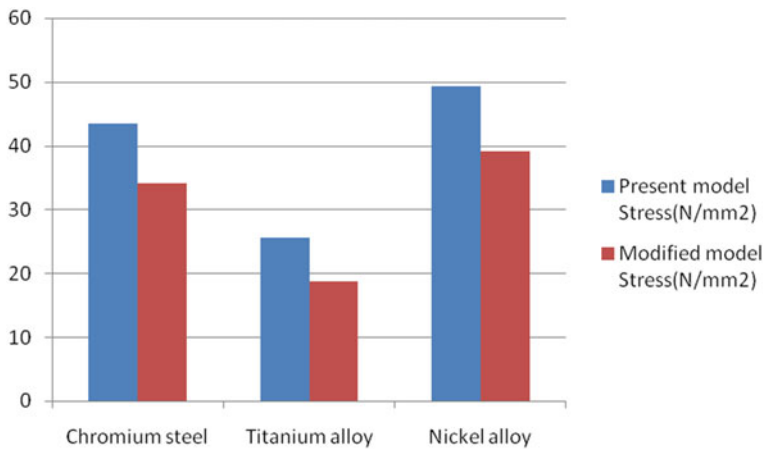
Fig. 6. Comparison between considered and modified models of stresses
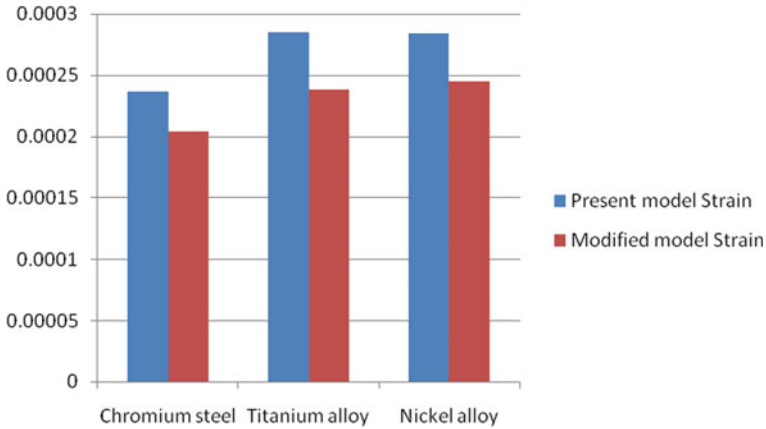
Fig. 7. Comparison between considered and modified models of strain

Table 2 Analysis with considered and modified geometry with different materials

Geometry	Material	Deformation (mm)	Stress (N/mm^2)	Strain
Considered	Chromium steel	0.054949	43.467	0.00023628
	Titanium alloy	0.066426	25.629	0.0002849
	Nickel alloy	0.065704	49.326	0.00028375
Modified	Chromium steel	0.010477	34.118	0.0002035
	Titanium alloy	0.011804	18.684	0.000238
	Nickel alloy	0.012666	39.117	0.00024479

top edge of the blade to the edge corner, with a maximum displacement of around 0.1 mm in this region.

The above-shown graphs clearly show the comparison among the structural properties between the three materials in the considered model and the modified model of turbine wheels. The titanium alloy seems to undergo moderate deformation and minimum stress compared to nickel alloy and chromium steel in the modified model compared to the considered model. Thus, the modified turbine wheel could withstand more stress if titanium alloy is used.

4.2 Analysis of CFD Results

As can be seen in Figs. 8, 9 and 10, the pressure is greatest on the lower edge of the blade, which is located close to the wheel, as well as on the windward edge of the upper edge. In contrast, the pressure on the curved surface located in the middle of the blade and close to the edge is significantly lower. Table 3 presents the information on

the windward side of the highest pressure. Because of the casting conditions and the blade's integrity, the structural strength can ensure that the blade can easily withstand tremendous pressure without deforming and vibrating. This is because the structural strength can ensure that the blade can easily withstand tremendous pressure at the lower edge of the blade near the wheel. On the side of the blade that faces towards the wind, the top edge, the relative degrees of freedom limitations are lower, making this area of the blade the most susceptible to deformation. As a consequence, increased fluid pressure will cause the blade to vibrate, surge, and eventually shatter. The area of the blade that is subjected to the highest pressure has been decreased, and the pressure gradient on the top edge of the blade, which is the area that is most prone to failure, has also been lowered to a very modest degree. According to the findings of the CFD study, the heat transfer rate and heat transfer coefficient are higher for the modified model in comparison to the model that was considered. On the other hand, the mass flow rate is lower for the modified model in comparison to the model that was considered. Therefore, the model with the modifications is superior than the model that was examined.

The comparison of the thermal characteristics of the three different materials that were taken into consideration and used in the updated models for heat flux can be seen in both Fig. 11 and Table 4. When compared to the considered model, the heat flux is greatest for titanium alloy as compared to nickel alloy and chromium steel in the modified model. Compare this to the considered model. Therefore, the model with the modification is superior.

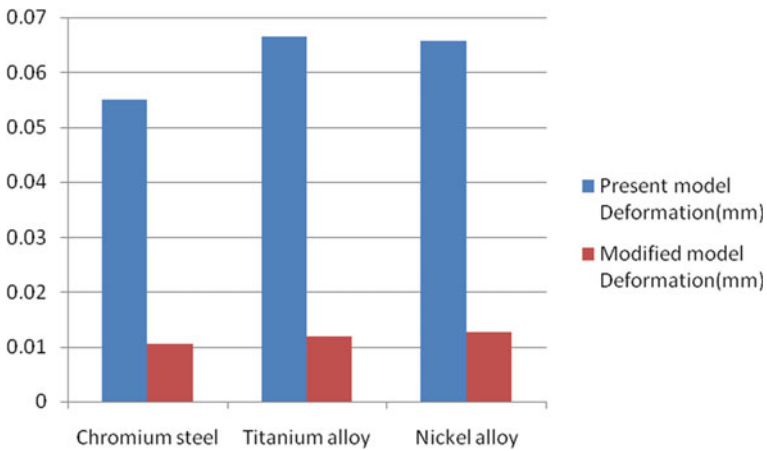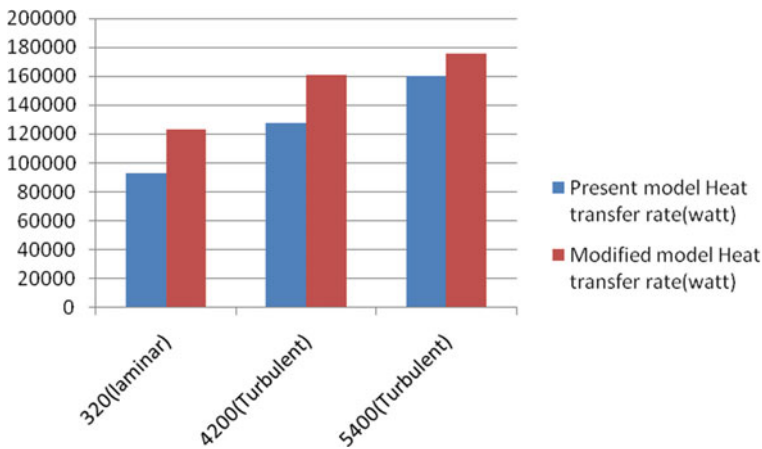**Fig. 8.** Comparison between considered and modified models of heat transfer coefficient
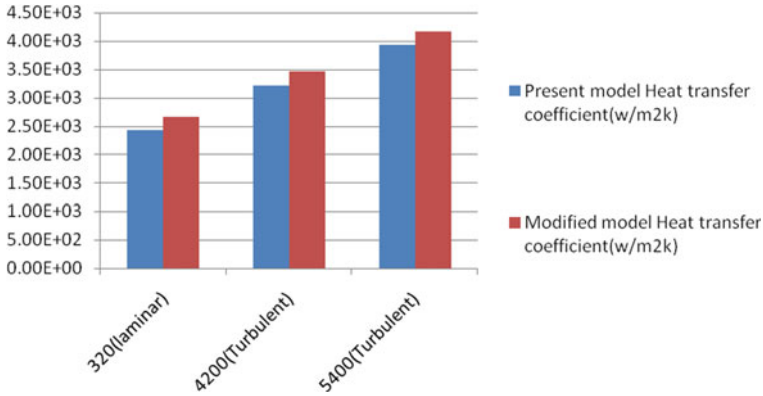
Fig. 9. Comparison between considered and modified models of mass flow rate
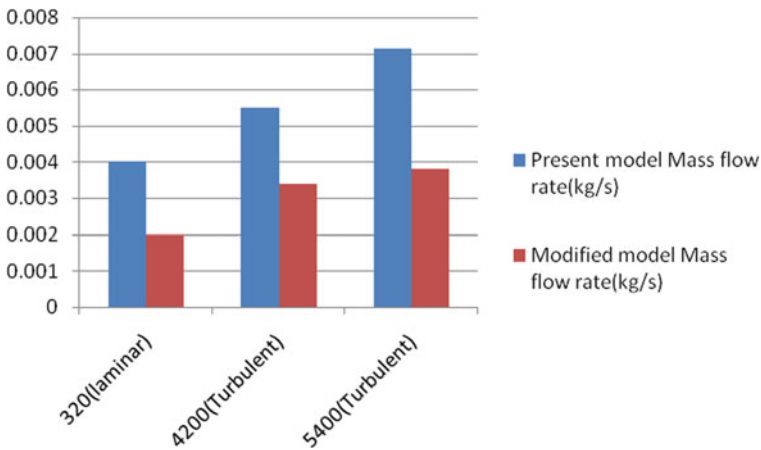
Fig. 10. Comparison between considered and modified models of heat transfer rate

5   Conclusions

The turbocharger turbine wheel is modelled in this chapter using the 3D modelling programme CREO, and the analysis is carried out using the ANSYS software. To improve the effectiveness of the cooling, the base of the blade has been redesigned to accommodate the new configuration. When compared to the model that was evaluated, the values for deformation, stress, and strain in the updated model are much lower. This can be seen by looking at the results of the static analysis. When the findings of the thermal study were compared, it was found that the modified model had a higher heat flow value than the model that was evaluated. According to the findings of the CFD study, the heat transfer rate and heat transfer coefficient are higher for the modified model in comparison to the model that was considered. On

Table 3 Computational fluid dynamics analysis at 1200k (temperature)

Geometry	Inlet velocity (m/s)	Pressure (Pa)	Velocity (m/s)	Heat transfer coefficient (w/m² k)	Mass flow rate (kg/s)	Heat transfer rate (watt)
Considered	320 (laminar)	174,000	832	2420	0.004	93,142
	4200 (turbulent)	176,000	1250	3210	0.0055	127,789
	5400 (turbulent)	307,000	1670	3930	0.00714	160,419
	320 (laminar)	209,000	1100	2660	0.002	123,244
Modified	4200 (turbulent)	410,000	1540	3460	0.0034	160,926
	5400 (turbulent)	676,000	1980	4170	0.0038	175,867
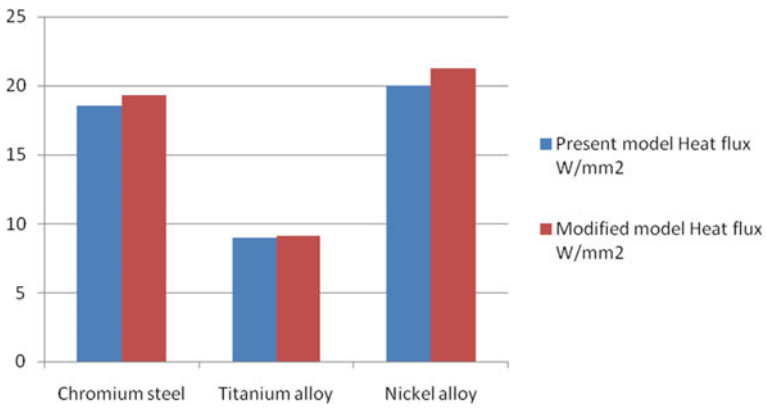
Fig. 11 Comparison between the considered and modified model of heat flux

Table 4 Thermal analysis

Geometry	Material	Temperature (K)		Heat flux
		Min	Max	W/mm²
Considered	Chromium steel	302.22	1203.4	18.5
	Titanium alloy	301.22	1203.6	8.966
	Nickel alloy	305.23	1203.4	20.012
	Chromium steel	306.63	1203.5	19.324
Modified	Titanium alloy	173.54	1203.1	9.1194
	Nickel alloy	308.12	1203.5	21.218

the other hand, the mass flow rate is lower for the modified model in comparison to the model that was considered. Based on the data presented above, it was found that a modified model for titanium alloy produced the least amount of stress while also producing a significant amount of deformation. Therefore, using titanium alloy, which has the best thermal characteristics out of the three materials studied for the considered and modified models, might allow the modified turbine wheel to endure much higher stress. When compared to nickel and chromium steel, the heat flux is greatest for titanium alloy in the modified model. Consequently, the model with the modifications is the superior option. According to the findings of the CFD analysis, the heat transfer coefficient as well as the heat transfer rate are higher for the redesigned model regardless of the velocity. According to the conclusion that can be drawn from the analysis of the preceding findings, titanium alloy is superior to both chromium steel and nickel alloy when it comes to modifying a model.

References

1. Sharma, S.K., Lee, J., Jang, H.-L.: Mathematical modeling and simulation of suspended equipment impact on car body modes. Machines **10**, 192 (2022). https://doi.org/10.3390/machines10030192

2. Vishwakarma, P.N., Mishra, P., Sharma, S.K.: Formulation of semi-active suspension system and controls in rail vehicle. SSRN Electron. J. (2022). https://doi.org/10.2139/ssrn.4159616

3. Vishwakarma, P.N., Mishra, P., Sharma, S.K.: Characterization of a magnetorheological fluid damper a review. Mater. Today Proc. **56**, 2988–2994 (2022). https://doi.org/10.1016/j.matpr.2021.11.143

4. Sharma, R.C., Sharma, S.K.: Ride analysis of road surface-three-wheeled vehicle-human subject interactions subjected to random excitation. SAE Int. J. Commer. Veh. **15**, 02-15–03-0017 (2022). https://doi.org/10.4271/02-15-03-0017

5. Sharma, S.K., Sharma, R.C., Lee, J., Jang, H.-L.: Numerical and experimental analysis of DVA on the flexible-rigid rail vehicle carbody resonant vibration. Sensors **22**, 1922 (2022). https://doi.org/10.3390/s22051922

6. Sharma, S.K., Mohapatra, S., Sharma, R.C., Alturjman, S., Altrjman, C., Mostarda, L., Stephan, T.: Retrofitting existing buildings to improve energy performance. Sustainability **14**, 666 (2022). https://doi.org/10.3390/su14020666

7. Sharma, S.K., Sharma, R.C., Lee, J.: In situ and experimental analysis of longitudinal load on carbody fatigue life using nonlinear damage accumulation. Int. J. Damage Mech. **31**, 605–622 (2022). https://doi.org/10.1177/10567895211046043

8. Sharma, S.K., Lee, J.: Crashworthiness analysis for structural stability and dynamics. Int. J. Struct. Stab. Dyn. **21**, 2150039 (2021). https://doi.org/10.1142/S0219455421500395

9. Wu, Q., Cole, C., Spiryagin, M., Chang, C., Wei, W., Ursulyak, L., Shvets, A., Murtaza, M.A., Mirza, I.M., Zhelieznov, К., Mohammadi, S., Serajian, H., Schick, B., Berg, M., Sharma, R.C., Aboubakr, A., Sharma, S.K., Melzi, S., Di Gialleonardo, E., Bosso, N., Zampieri, N., Magelli, M., Ion, C.C., Routcliffe, I., Pudovikov, O., Menaker, G., Mo, J., Luo, S., Ghafourian, A., Serajian, R., Santos, A.A., Teodoro, Í.P., Eckert, J.J., Pugi, L., Shabana, A., Cantone, L.:

Freight train air brake models. Int. J. Rail Transp. 1–49 (2021). https://doi.org/10.1080/232 48378.2021.2006808

10. Sharma, S.K., Sharma, R.C., Lee, J.: Effect of rail vehicle-track coupled dynamics on fatigue failure of coil spring in a suspension system. Appl. Sci. **11**, 2650 (2021). https://doi.org/10. 3390/app11062650

11. Mohapatra, S., Mohanty, D., Mohapatra, S., Sharma, S., Dikshit, S., Kohli, I., Samantaray, D.P., Kumar, R., Kathpalia, M.: Biomedical application of polymeric biomaterial: polyhydroxybutyrate. In: Bioresource Utilization and Management: Applications in Therapeutics, Biofuels, Agriculture, and Environmental Science, pp. 1–14. CRC Press (2021). https://doi. org/10.21203/rs.3.rs-1491519/v1

12. Bhardawaj, S., Sharma, R.C., Sharma, S.K., Sharma, N.: On the planning and construction of railway curved track. Int. J. Veh. Struct. Syst. **13**, 151–159 (2021). https://doi.org/10.4273/ ijvss.13.2.04

13. Sharma, R.C., Sharma, S., Sharma, N., Sharma, S.K.: Linear and nonlinear analysis of ride and stability of a three-wheeled vehicle subjected to random and bump inputs using bond graph and simulink methodology. SAE Int. J. Commer. Veh. **14**(02-15-01-0001) (2021). https://doi. org/10.4271/02-15-01-0001

14. Sharma, R.C., Sharma, S., Sharma, S.K., Sharma, N., Singh, G.: Analysis of bio-dynamic model of seated human subject and optimization of the passenger ride comfort for three-wheel vehicle using random search technique. Proc. Inst. Mech. Eng. Part K J. Multi-body Dyn. **235**, 106–121 (2021). https://doi.org/10.1177/1464419320983711

15. Choi, S., Lee, J., Sharma, S.K.: A study on the performance evaluation of hydraulic tank injectors. In: Advances in Engineering Design: Select Proceedings of FLAME 2020, pp. 183–190. Springer, Singapore (2021). https://doi.org/10.1007/978-981-33-4684-0_19

16. Lee, J., Han, J., Sharma, S.K.: Structural analysis on the separated and integrated differential gear case for the weight reduction. In: Joshi, P., Gupta, S.S., Shukla, A.K., and Gautam, S.S. (eds.) Advances in Engineering Design. Lecture Notes in Mechanical Engineering, pp. 175–181 (2021). https://doi.org/10.1007/978-981-33-4684-0_18

17. Sharma, S.K., Sharma, R.C.: Multi-objective design optimization of locomotive nose. In: SAE Technical Paper, pp. 1–10 (2021). https://doi.org/10.4271/2021-01-5053

18. Sharma, R.C., Palli, S., Sharma, N., Sharma, S.K.: Ride behaviour of a four-wheel vehicle using h infinity semi-active suspension control under deterministic and random inputs. Int. J. Veh. Struct. Syst. **13**, 234–237 (2021). https://doi.org/10.4273/ijvss.13.2.18

19. Li, M., Li, Y., Jiang, F., Hu, J.: An optimization of a turbocharger blade based on fluid-structure interaction. Processes. **10**, 1569 (2022). https://doi.org/10.3390/pr10081569

20. Andrearczyk, A., Bagiński, P., Klonowicz, P.: Numerical and experimental investigations of a turbocharger with a compressor wheel made of additively manufactured plastic. Int. J. Mech. Sci. **178**, 105613 (2020). https://doi.org/10.1016/j.ijmecsci.2020.105613

21. Liu, Z., Wang, R., Cao, F., Shi, P.: Dynamic behaviour analysis of turbocharger rotor-shaft system in thermal environment based on finite element method. Shock Vib. **2020**, 1–18 (2020). https://doi.org/10.1155/2020/8888504

22. Sharma, S.K., Sharma, R.C., Sharma, N.: Combined multi-body-system and finite element analysis of a rail locomotive crashworthiness. Int. J. Veh. Struct. Syst. **12**, 428–435 (2020). https://doi.org/10.4273/ijvss.12.4.15

23. Sharma, R.C., Sharma, S.K., Palli, S.: Linear and non-linear stability analysis of a constrained railway wheelaxle. Int. J. Veh. Struct. Syst. **12**, 128–133 (2020). https://doi.org/10.4273/ijvss. 12.2.04

24. Palli, S., Sharma, R.C., Sharma, S.K., Chintada, V.B.: On methods used for setting the curve for railway tracks. J. Crit. Rev. **7**, 241–246 (2020)

25. Mohapatra, S., Pattnaik, S., Maity, S., Mohapatra, S., Sharma, S., Akhtar, J., Pati, S., Samantaray, D.P., Varma, A.: Comparative analysis of PHAs production by Bacillus megaterium OUAT 016 under submerged and solid-state fermentation. Saudi J. Biol. Sci. **27**, 1242–1250 (2020). https://doi.org/10.1016/j.sjbs.2020.02.001

26. Sharma, R.C., Sharma, S.K., Sharma, N., Sharma, S.: Analysis of ride and stability of an ICF railway coach. Int. J. Veh. Noise Vib. **16**, 127 (2020). https://doi.org/10.1504/IJVNV.2020.117820

27. Sharma, S.K., Phan, H., Lee, J.: An application study on road surface monitoring using DTW based image processing and ultrasonic sensors. Appl. Sci. **10**, 4490 (2020). https://doi.org/10.3390/app10134490

28. Sharma, R.C., Sharma, S., Sharma, S.K., Sharma, N.: Analysis of generalized force and its influence on ride and stability of railway vehicle. Noise Vib. Worldw. **51**, 95–109 (2020). https://doi.org/10.1177/0957456520923125

29. Lee, J., Sharma, S.K.: Numerical investigation of critical speed analysis of high-speed rail vehicle. 한국정밀공학회 학술발표대회 논문집 (Korean Soc. Precis. Eng. **696** (2020)

30. Sharma, S.K., Lee, J.: Finite element analysis of a fishplate rail joint in extreme environment condition. Int. J. Veh. Struct. Syst. **12**, 503–506 (2020). https://doi.org/10.4273/ijvss.12.5.03

31. Bhardawaj, S., Sharma, R., Sharma, S.: Ride analysis of track-vehicle-human body interaction subjected to random excitation. J. Chinese Soc. Mech. Eng. **41**, 237–236 (2020). https://doi.org/10.29979/JCSME

32. Bhardawaj, S., Sharma, R.C., Sharma, S.K.: Development in the modeling of rail vehicle system for the analysis of lateral stability. Mater. Today Proc. **25**, 610–619 (2020). https://doi.org/10.1016/j.matpr.2019.07.376

33. Bhardawaj, S., Sharma, R.C., Sharma, S.K.: Analysis of frontal car crash characteristics using ANSYS. Mater. Today Proc. **25**, 898–902 (2020). https://doi.org/10.1016/j.matpr.2019.12.358

34. Sharma, S., Sharma, R.C., Sharma, S.K., Sharma, N., Palli, S., Bhardawaj, S.: Vibration isolation of the quarter car model of road vehicle system using dynamic vibration absorber. Int. J. Veh. Struct. Syst. **12**, 513–516 (2020). https://doi.org/10.4273/ijvss.12.5.05

35. Acharya, A., Gahlaut, U., Sharma, K., Sharma, S.K., Vishwakarma, P.N., Phanden, R.K.: Crashworthiness analysis of a thin-walled structure in the frontal part of automotive chassis. Int. J. Veh. Struct. Syst. **12**, 517–520 (2020). https://doi.org/10.4273/ijvss.12.5.06

36. Bhardawaj, S., Sharma, R.C., Sharma, S.K.: Development of multibody dynamical using MR damper based semi-active bio-inspired chaotic fruit fly and fuzzy logic hybrid suspension control for rail vehicle system. Proc. Inst. Mech. Eng. Part K J. Multi-body Dyn. **234**, 723–744 (2020). https://doi.org/10.1177/1464419320953685

37. Sharma, S.K., Lee, J.: Design and development of smart semi active suspension for nonlinear rail vehicle vibration reduction. Int. J. Struct. Stab. Dyn. **20**, 2050120 (2020). https://doi.org/10.1142/S0219455420501205

38. Sharma, S.K.: Multibody analysis of longitudinal train dynamics on the passenger ride performance due to brake application. Proc. Inst. Mech. Eng. Part K J. Multi-body Dyn. **233**, 266–279 (2019). https://doi.org/10.1177/1464419318788775

39. Goyal, S., Anand, C.S., Sharma, S.K., Sharma, R.C.: Crashworthiness analysis of foam filled star shape polygon of thin-walled structure. Thin-Walled Struct. **144**, 106312 (2019). https://doi.org/10.1016/j.tws.2019.106312

40. Sharma, S.K., Sharma, R.C.: Pothole detection and warning system for indian roads. In: Advances in Interdisciplinary Engineering, pp. 511–519 (2019). https://doi.org/10.1007/978-981-13-6577-5_48

41. Goswami, B., Rathi, A., Sayeed, S., Das, P., Sharma, R.C., Sharma, S.K.: Optimization design for aerodynamic elements of indian locomotive of passenger train. In: Advances in Engineering Design. Lecture Notes in Mechanical Engineering, pp. 663–673. Springer, Singapore (2019). https://doi.org/10.1007/978-981-13-6469-3_61

42. Bhardawaj, S., Chandmal Sharma, R., Kumar Sharma, S.: Development and advancement in the wheel-rail rolling contact mechanics. IOP Conf. Ser. Mater. Sci. Eng. **691**, 012034 (2019). https://doi.org/10.1088/1757-899X/691/1/012034

43. Choppara, R.K., Sharma, R.C., Sharma, S.K., Gupta, T.: Aero dynamic cross wind analysis of locomotive. In: IOP Conference Series: Materials Science and Engineering, p. 12035. IOP Publishing (2019)

44. Sinha, A.K., Sengupta, A., Gandhi, H., Bansal, P., Agarwal, K.M., Sharma, S.K., Sharma, R.C., Sharma, S.K.: Performance enhancement of an all-terrain vehicle by optimizing steering, powertrain and brakes. In: Advances in Engineering Design, pp. 207–215 (2019). https://doi.org/10.1007/978-981-13-6469-3_19

45. Sharma, S.K., Saini, U., Kumar, A.: Semi-active control to reduce lateral vibration of passenger rail vehicle using disturbance rejection and continuous state damper controllers. J. Vib. Eng. Technol. **7**, 117–129 (2019). https://doi.org/10.1007/s42417-019-00088-2

46. Bhardawaj, S., Chandmal Sharma, R., Kumar Sharma, S.: A survey of railway track modelling. Int. J. Veh. Struct. Syst. **11**, 508–518 (2019). https://doi.org/10.4273/ijvss.11.5.08

47. Sharma, R.C., Palli, S., Sharma, S.K., Roy, M.: Modernization of railway track with composite sleepers. Int. J. Veh. Struct. Syst. **9**, 321–329 (2018)

48. Sharma, R.C., Sharma, S.K., Palli, S.: Rail vehicle modelling and simulation using Lagrangian method. Int. J. Veh. Struct. Syst. **10**, 188–194 (2018). https://doi.org/10.4273/ijvss.10.3.07

49. Palli, S., Koona, R., Sharma, S.K., Sharma, R.C.: A review on dynamic analysis of rail vehicle coach. Int. J. Veh. Struct. Syst. **10**, 204–211 (2018). https://doi.org/10.4273/ijvss.10.3.10

50. Sharma, S.K., Sharma, R.C.: An investigation of a locomotive structural crashworthiness using finite element simulation. SAE Int. J. Commer. Veh. **11**, 235–244 (2018). https://doi.org/10.4271/02-11-04-0019

51. Sharma, S.K., Sharma, R.C.: Simulation of quarter-car model with magnetorheological dampers for ride quality improvement. Int. J. Veh. Struct. Syst. **10**, 169–173 (2018). https://doi.org/10.4273/ijvss.10.3.03

52. Sharma, S.K., Kumar, A.: Impact of longitudinal train dynamics on train operations: a simulation-based study. J. Vib. Eng. Technol. **6**, 197–203 (2018). https://doi.org/10.1007/s42417-018-0033-4

53. Sharma, R.C., Sharma, S.K.: Sensitivity analysis of three-wheel vehicle's suspension parameters influencing ride behavior. Noise Vib. Worldw. **49**, 272–280 (2018). https://doi.org/10.1177/0957456518796846

54. Sharma, S.K., Kumar, A.: Ride comfort of a higher speed rail vehicle using a magnetorheological suspension system. Proc. Inst. Mech. Eng. Part K J. Multi-body Dyn. **232**, 32–48 (2018). https://doi.org/10.1177/1464419317706873

55. Sharma, S.K., Kumar, A.: Disturbance rejection and force-tracking controller of nonlinear lateral vibrations in passenger rail vehicle using magnetorheological fluid damper. J. Intell. Mater. Syst. Struct. **29**, 279–297 (2018). https://doi.org/10.1177/1045389X17721051

56. Sharma, S.K., Kumar, A.: Impact of electric locomotive traction of the passenger vehicle Ride quality in longitudinal train dynamics in the context of Indian railways. Mech. Ind. **18**, 222 (2017). https://doi.org/10.1051/meca/2016047

57. Sharma, S.K., Kumar, A.: Ride performance of a high speed rail vehicle using controlled semi active suspension system. Smart Mater. Struct. **26**, 055026 (2017). https://doi.org/10.1088/1361-665X/aa68f7

58. Sharma, S.K., Kumar, A.: Dynamics analysis of wheel rail contact using FEA. Proc. Eng. **144**, 1119–1128 (2016). https://doi.org/10.1016/j.proeng.2016.05.076

59. Sharma, S.K., Kumar, A.: The Impact of a rigid-flexible system on the ride quality of passenger bogies using a flexible carbody. In: Pombo, J. (ed.) Proceedings of the Third International Conference on Railway Technology: Research, Development and Maintenance, Stirlingshire, UK, p. 87. Civil-Comp Press, Stirlingshire, UK (2016). https://doi.org/10.4203/ccp.110.87.

60. Sharma, S.K., Chaturvedi, S.: Jerk analysis in rail vehicle dynamics. Perspect. Sci. **8**, 648–650 (2016). https://doi.org/10.1016/j.pisc.2016.06.047

61. Kulkarni, D., Sharma, S.K., Kumar, A.: Finite element analysis of a fishplate rail joint due to wheel impact. In: International Conference on Advances in Dynamics, Vibration and Control (ICADVC-2016) NIT Durgapur, India, 25–27 Feb 2016. National Institute of Technology Durgapur, Durgapur, India (2016)

62. Sharma, S.K., Sharma, R.C., Kumar, A., Palli, S.: Challenges in rail vehicle-track modeling and simulation. Int. J. Veh. Struct. Syst. **7**, 1–9 (2015). https://doi.org/10.4273/ijvss.7.1.01

63. Sharma, S.K., Kumar, A., Sharma, R.C.: Challenges in railway vehicle modeling and simulations. In: International Conference on Newest Drift in Mechanical Engineering (ICNDME-14), 20–21 Dec, M. M. University, Mullana, India, pp. 453–459. Maharishi Markandeshwar University, Mullana, Ambala (2014)

64. Sharma, S.K., Kumar, A.: A comparative study of Indian and Worldwide railways. Int. J. Mech. Eng. Robot. Res. **1**, 114–120 (2014)

65. Sharma, S.K.: Zero energy building envelope components: a review. Int. J. Eng. Res. Appl. **3**, 662–675 (2013)

66. Sharma, S.K., Lavania, S.: An autonomous metro: design and execution. In: Futuristic trends in Mechanical and Industrial Engineering, pp. 1–8. JECRC UDML College of Engineering, Jaipur (2013)

67. Sharma, S.K., Lavania, S.: Green manufacturing and green supply chain management in India—a review. In: Futuristic trends in Mechanical and Industrial Engineering, pp. 1–8. JECRC UDML College of Engineering (2013)

68. Sharma, S.K., Lavania, S.: Skin effect in high speed VLSI on-chip interconnects. In: International Conference on VLSI, Communication & Networks, V-CAN, pp. 1–8. Institute of Engineering & Technology, Alwar (2011)

69. Lavania, S., Sharma, S.K.: An explicit approach to compare crosstalk noise and delay in VLSI RLC interconnect modeled with skin effect with step and ramp input. J. VLSI Des. Tools Technol. **1**, 1–8 (2011)

70. Hossain, I., Velkin, V.I., Shcheklein, S.E.: Experimental study in reduction of two phase flow induced vibration. MATEC Web Conf. **211**, 16001 (2018). https://doi.org/10.1051/matecconf/201821116001

71. Hossain, I., Velkin, V.I., Shcheklein, S.E.: The study of passive vibration dampers in pipelines using piv-methodology for single phase flow. In: WIT Transactions on Ecology and the Environment. **224**, 565–570 (2017). https://doi.org/10.2495/ESUS170521

72. Saravanan, U.: Design and analysis of turbochargers. Int. J. Eng. Res. **4**, 1–14 (2008)

Technology Driven Application

Deploying Machine Learning Algorithms for Predictive Maintenance of High-Value Assets of Indian Railways

Kumar Saurav, Mohd Avesh, Rakesh Chandmal Sharma, and Ismail Hossain

Abstract The process of maintenance is always considered to be a huge driver of costs in all industries. Depending on the industry, maintenance activities can account for 15–70% of the total production costs. Despite that, most of the industries still rely upon maintenance policies that are outdated and severely inefficient from a time and money point of view. In this context, the railway industry is no exception. Maintenance of high-value assets of Indian Railways is still done primarily through conventional maintenance practices. This causes the production time to go down and the overall quality of the components to deteriorate. On the other hand, there is ample research work being done to explore the details of several other maintenance policies. One of the most efficient and highly preferred maintenance policies is predictive maintenance. This study reviews existing literature on predictive maintenance and its implementation in the railway industry and identifies gaps and prospects for further research. The objective of this study is to begin with understanding the current maintenance policies used by Indian Railways, and then go about outlining the potential advantages of implementing predictive maintenance. To signify the importance of predictive maintenance, an analysis is performed over real-world data of rolling stock by training a machine learning model over the data and predicting the Remaining Useful Life of the components. The model is trained using a type of Recurrent Neural Network, known as Long Short-Term Memory networks. This training is carried out by a regression algorithm. Finally, the predictions from the model are plotted and

K. Saurav
School of Engineering and Applied Sciences, National Rail and Transportation Institute, Vadodara, India

M. Avesh (✉)
Star Saidham Services Solutions, Doiwala, Dehradun, India
e-mail: mail2avesh@gmail.com

R. C. Sharma
Mechanical Engineering Department, Graphic Era (Deemed to Be University), Dehradun, India

I. Hossain
School of Natural Sciences and Mathematics, Ural Federal University, Yekaterinburg 620000, Russia

401

compared with the actual data, to indicate the efficacy of the model. After interpreting the findings of the plot, it is concluded that such predictive maintenance systems could be installed in the rolling stock operated by the Indian Railways, as it would impact the overall availability and efficiency of the assets and boost the operations of the organization.

1   Introduction

Indian Railways is one of largest railway networks in the world. Serving as an employer for more than 1.2 million Indians, it serves as a backbone for the economy of India, which is one of the fastest growing economies in the world. Indian Railways has a railway network that spans over a length of more than 120,000 kms and is growing at a rapid pace [1–3]. On this huge network of railway tracks, Indian Railways operates nearly 10,000 locomotives, along with approximately 240,000 and 60,000 freight waggons and passenger coaches, respectively [4–6]. With the existence of such a vast network, there also comes the challenge of maintaining the assets that are a part of Indian Railways' inventory [1, 3–7]. Apart from the huge length of railway tracks that need to be constantly checked for all sorts of damages, there are also a huge number of other challenges associated with maintaining such a huge fleet of locomotives and coaches [7–9].

Most of the current maintenance practices used by Indian Railways are conventional in nature. Be it the maintenance of rolling stock, waggons or tracks, most of the maintenance processes involve a lot of manual inspection and manual labour, which in turn is time-intensive, resulting in significant downtimes [10–12]. Given the vast scale on which maintenance occurs at Indian Railways, even a little improvement in maintenance policies could bring about a huge improvement in the overall efficiency at which the entire operation takes place [13–15]. One of the most convenient ways of bringing about this change in the maintenance strategies of Indian Railways could be to deploy predictive maintenance on some of the high-value assets that are most critical to the performance and efficiency of the railways [16–18].

Predictive maintenance is also commonly referred to as condition-based maintenance. This maintenance strategy, based on the observations made, monitors the current condition of a machine and schedules maintenance activities [19–23]. Three distinct condition monitoring methods are feasible for predictive maintenance: monitoring on request, scheduled monitoring and continuous monitoring. Using predictive maintenance for railway machinery could help in pointing out defects before they even occur and tackle them before the occurrence of fatal errors that might hinder the productivity and effectiveness of the machinery [24–28]. For instance, predictive maintenance can result in increased efficiency by allowing the residual usable life
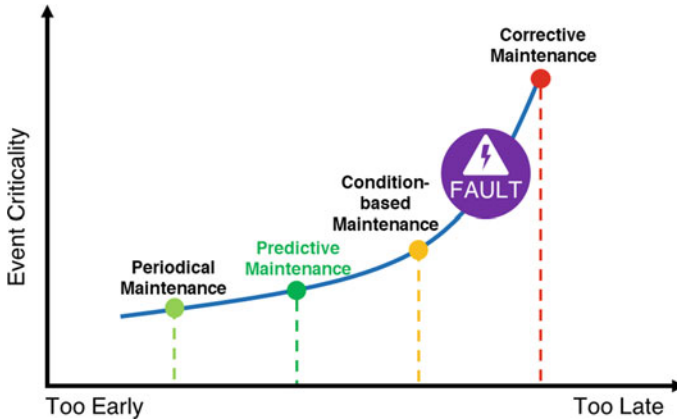
Fig. 1 Maintenance strategies represented in terms of event criticality and time

of the equipment to be calculated [29–31]. This method is based on condition moni-
toring, which is preferably carried out by sensors, allowing the appropriate system
parameters, such as vibration and temperature, to be constantly tracked [32–34].
Figure 1 illustrates several maintenance strategies, as and when they are implemented.

Using predictive maintenance on railway equipment can help in reducing mean
time to repair (MTTR), which refers to the amount of time that is needed to restore
the functionality of the machine by fully repairing it. Predictive maintenance can
also help increase the mean time between failures (MTBF), by helping reduce the
number of overall failures.

2 Machine Learning Models in Predictive Maintenance

When predictive maintenance systems are implemented, a lot of data is collected
by the means of data acquisition systems. Real-time data from sensors installed
on several components of the machinery is collected, which results in extremely
high volumes of data. To be able to use the predictive maintenance systems to their
fullest potential, these large volumes of data need to be analysed to draw insights
about the state of the machinery [35–37]. For the purpose of analysis of the data,
machine learning algorithms are used, which access and process these large datasets.
Supervised machine learning approaches learn from historic data that is provided,
and learn from them, in order to come up with predictions about the future, which
include details like failure occurrence or the Remaining Useful Life of the machine
[38–41]. As a result, it is fair to say, that machine learning algorithms can help the
decision makers immensely in the decision-making process, by clearly stating out
the need for a maintenance cycle, in advance.

When it comes to the types of machine learning models that can be deployed in predictive maintenance systems, it is important to narrow down the purpose of the predictive maintenance system, i.e. the kind of questions that need to be answered [42–45]. It is imperative for the policy-makers to come up with a comprehensive list of key issues that need to be solved by the predictive maintenance system [46–49]. In the case of railways, the most common issues that need to be solved are associated with the failures and the lifetime of the equipment. As a result, it is important to choose models that can perform these tasks. The two most important issues in the case of railways are.

2.1 Calculating Remaining Useful Life (RUL) of Equipment

To deal with these two key issues, the two approaches of machine learning that are used, respectively, are regression approach and classification approach. For calculating the RUL of an equipment using the regression approach, the basic requirement is to have static and historic data that can help train the model. The dataset will likely contain instances where there are failures in the system, and with the help of such datasets, it is possible to come up with models that clearly represent the machine's degradation process [50–54]. As a part of the regression model, only one type of "path to failure" is modelled. However, if the machine's architecture provides for the occurrence of more than one type of failures such that the behaviour of the machine preceding each one of them is different, it becomes important to come up with dedicated models for each one of them [55–58]. One of the most widely used regression models in the industry is the linear regression model, because of it being quick and easy to implement, and it also produces outputs that are easily interpretable. Regression models are preferably used in cases where the data is within a particular range, which generally is the case when data collection is done through sensors [59–62].

On the other hand, when it comes to implementing the classification approach to predict if a particular equipment is going to fail within a given time frame, it can often become a little challenging. It is to be noted that it is not very necessary to predict the lifetime of the equipment with an extremely high degree of accuracy. What is really important is that the decision makers should know if the machine is going to run into a damage anytime soon [63–66]. As a result, the overall problem is reduced to determining if the machine is about to fail within the next X days or cycles, or not. For this calculation as well, it is important that the model is provided with some sort of historical data with all the events and failures labelled, so that the model can be trained to predict the same. In this particular scenario of predicting if the machine fails in the next few cycles or not, classification models are much more suitable. The classification models can work with different types of machine failures as long as they are framed as a multi-class problem [67–71].

To summarize, both the previous approaches are aimed at modelling the features of the system against its degradation path. Predictive maintenance also implements multi-class classification as there can be multiple reasons why a machine can fail.

Multi-class classifications can also provide a few extra insights from the data. They can help predict two types of future outcomes: the range or period of time when the machine can undergo failure, and the probability of failure of the machine within that span of time. In addition to that, they can also predict the most probable root cause of a particular failure in the machine. All such information can be very valuable in coming up with a robust maintenance strategy for the machine.

2.2 High-Value Assets of the Indian Railways

When talking about the deployment of machine learning models in predictive maintenance of assets of Indian Railways, it is imperative to narrow down on a few key, critical, high-value assets, on which the analysis can be done:

Signalling Infrastructure: Indian Railways uses a host of signalling technologies to manage its vast network of trains. The most widely used methods of signalling that are used by Indian Railways are the Absolute Block Signalling and Automatic Block Signalling. Apart from this, the types of signal lights predominantly used are the two, three and four-aspect signal lights [72–74]. Nearly, 60,000 kms of India's rail network is covered by an optical fibre cable network. It has to be understood that since most of the rail network that Indian Railways has, is covered with proper signalling infrastructure, the amount of data collected by the signalling systems is huge and owing to its importance in the overall safety of train operations, it is very vital that these assets are maintained regularly to preserve their efficiency and productivity.

Rolling Stock: As stated earlier, rolling stock that comprises locomotives, passenger coaches and freight waggons is the most important asset of Indian Railways. Rolling stock can easily be said to be the whole and soul of Indian Railways. As of mid-2021, Indian Railways operates around 10,000 locomotives, 60,000 passenger coaches and 240,000 freight waggons. Given the large number of rolling stocks that operate, Indian Railways has established more than 150 large maintenance sheds, all over the country within the various railway zones, where routine maintenance activities take place. It is evident that rolling stock is the most capital-intensive asset of Indian Railways, consequently, making it the most critical asset. It is, hence, a very important step to optimize maintenance operations of rolling stock, as it can have a significant impact on their overall availability [75].

Railway Tracks: Indian Railways has railway tracks that cover more than 120,000 kms, as of mid-2021. Two-thirds of this network is single-line, and the remaining is double or multi-line. Most of the single-line rail network is non-electrified, while most of the multi-line network is electrified. With the existence of such a vast rail network, it becomes a very crucial task to maintain them. The railway tracks involve a lot of maintenance operations regarding the rails, sleepers and ballast. All these components need to be inspected at regular intervals for ensuring that they are safe enough for the regular plying of trains on them. Weather conditions, changing terrains and regular movement of trains cause the tracks to wear and tear, all of which must be

looked into, while maintaining them. As a result, maintenance operations of railway tracks are an equally vital part of train operations of Indian Railways.

While signalling systems, rolling stock and railways tracks are some of the most important groups of high-value assets of Indian Railways; there are a ton of other smaller machines and equipment that work in complete synchronization to make the entire organization run as smoothly as it runs. The railway industry is, undoubtedly, a machinery-driven industry and is heavily dependent on the state of machinery and its overall performance. However, for the sake of analysis in this paper, the asset that has been chosen to perform further mathematical modelling is rolling stock. It has been clearly mentioned that rolling stock is the backbone of the entire industry, and hence, it would make a lot of sense, if predictive maintenance practices were to be implemented on them, to start with. The later part of this paper will cover the analysis of machine learning models when deployed on data gathered from sensors installed on rolling stock, in order to perform predictive maintenance on them.

The current policy of maintenance of rolling stock in Indian Railways is predominantly based on manually inspecting them. This manual inspection is done either through trackside rolling-in examination or pit examination when the rolling stock is moving slowly or is completely stationary. It is true that most of the manual inspection is carried out by skilled employees, but it does lack an objective approach and relies a lot on the individual judgement of the inspector. However, Indian Railways plans to gradually instal Online Monitoring of Rolling Stock (OMRS) systems in its maintenance sheds, as a part of the Smart Yards Project.

2.3   Research Opportunities

Upon the analysis of several literature sources on predictive maintenance and its use in railways, there are a lot of gaps that can be used as a foundation for further research work. This section briefly outlines a few areas where research can be carried out, on the basis of the literature review done previously.

Current Scenario of Predictive Asset Management in Railways of Several Countries Across the Globe

The current maintenance practices of railways in a lot of countries include a manual inspection of the various parts of a railway system, which is a tedious and exhausting affair. In the case of assets like rolling stock, inspections are done by people, who are responsible for examining the rolling stock in stationary or slow-moving conditions. While all the inspections are done by skilled manpower, it does depend a lot on the individual judgement of the person. However, it is also seen that several railway organizations across the globe have started making a move towards the adoption of predictive maintenance systems. A great example of this move is that of Indian Railways. Indian Railways has taken up the Smart Yards Project that is aimed at automating railway yards that are responsible for the maintenance of rolling stock. This automation is supposed to be achieved by the use of Online Monitoring of

Rolling Stock (OMRS) systems. While this is a welcome step in the direction of boosting the productivity and efficiency of Indian Railways, there is still a long way to go, in terms of the different assets on which predictive maintenance can be implemented.

After the analysis of the state of maintenance policies of several railway organizations, there was very little literature describing the detailed process of asset management powered by predictive maintenance. This can be used as a potential area for research and several aspects of predictive maintenance and predictive asset management for railways, which could be highlighted. The current scenario of maintenance of several railway assets could be talked about, and a comparison with predictive maintenance could be made.

Assessment for Defining the Most Critical Railway Assets Which can Leverage Predictive Maintenance

As a follow-up on the state of affairs regarding the maintenance of assets in railway organizations across the globe, it is also practical to come up with a proper framework for deciding about the assets that can leverage the predictive maintenance technologies. While all assets would surely benefit from this, it is not possible to implement predictive maintenance methods on all high-value assets, at once. A set of categories can be defined, on the basis of which, a robust framework can be built, that decides the criticality of an asset and how beneficial predictive maintenance can be if implemented on it. Given the various factors that affect the level of use and consumption of resources by a particular asset, it is a good idea to take into account all such factors and see if implementing predictive maintenance can be of any benefit to the overall system in terms of reducing the cost and time of maintenance or boosting the efficiency and productivity of the asset. It is known that the setting up of predictive maintenance systems is an expensive process. This is the reason why an assessment should be done, for defining the most critical high-value railway assets that should make use of predictive maintenance on a priority basis. Since there is not much literature regarding the same, it can be treated as a prospective research ground and can be explained in much detail.

Machine Learning Models that can be used for Predictive Maintenance of These Assets

While it has been established that there is ample literature available regarding machine learning models for predictive maintenance, there is hardly any research done to highlight all such machine learning models that can be used to implement predictive maintenance on high-value assets owned by railway organizations of several countries. The OMRS systems, which are to be installed as a part of the Indian Railways Smart Yards Project in India, perform fault detection using image recognition algorithms that use deep neural networks. However, for other assets, the type of ML algorithms that need to be used for the implementation of predictive maintenance will be different and it is, hence, worthwhile for the development of other algorithms for the same. This can, hence, serve as a potential research area as a lot of different machine learning models that are being used in the predictive

maintenance systems, which can be scaled accordingly to work for the assets that are owned by railways of other countries.

3 Mathematical Modelling

3.1 Recurrent Neural Networks (RNNs) and Their Working

For the purpose of carrying out the analysis on the sensor data, a proper model has to be constructed that can be able to work with the data and draw information from it. The scope of this article covers the deployment of machine learning models on raw data. The machine learning model implemented in this article is the Long Short-Term Memory (LSTM) Neural Network. LSTM Networks are a type of Recurrent Neural Network (RNN). Hence, it is imperative to briefly understand the working of RNNs before talking about LSTM Networks.

RNNs add an extra functionality to a conventional neural network. A conventional neural network can only take a fixed vector as its input, which in turn, limits it from being useful in situations where the input is supposed to be in the form of a series. On the other hand, RNNs can accept series type inputs and also remember inferences from past data and influence further output on the basis of past information. This functionality of an RNN is extremely useful in the field of predictive maintenance, where trends are inferred from historic data in order to predict the future state of machinery. RNNs are capable of taking in multiple input vectors and the outputs are dependent upon the weights as well as the hidden state vector that represents the influence of previous inputs and outputs. As a result, a single input can produce multiple outputs based on previous data.

Owing to their internal memory, RNNs can process sequence of input data and are, hence, widely used for image and speech recognition tasks. As compared to a conventional neural network, where all inputs are independent of each other, inputs in RNNs are all related to each other.

Figure 2 illustrates what an RNN would look like, if unrolled. To start off, it takes x_o as input and yields h_0 as the output. The h_0 and x_1 together serve as the input for the next step, which yields h_1 as its output. The h_1 and x_2 are then served as input for the next step, and so on. In this fashion, the network remembers previous context while getting trained.

The current state can be formulated as

$$h_t = f(h_{t-1}, x_t) \tag{1}$$

On applying the activation function tanh, the current state can be formulated as

$$h_t = \tanh(W_{hh}h_{t-1} + W_{hx}x_t) \tag{2}$$
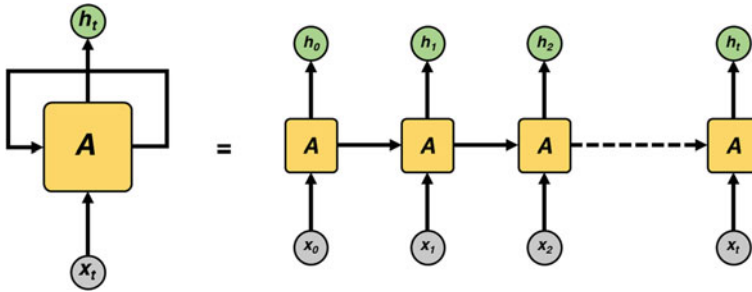
Fig. 2 Unrolled recurrent neural network

(W: weight, h: single hidden vector, W_{hh}: weight at previous hidden state, W_{hx}: weight at current input state, tanh: activation function).

Output of the network can be represented as

$$y_t = W_{hy}h_t \tag{3}$$

In summary, it can be said that RNNs are capable of modelling and working with data that is inputted in the form of a sequence, hence denoting that they are dependent on the outputs generated in the previous layers.

While RNNs do appear to have this advantage of remembering previous results, they cannot work with outputs that are not very recent. In certain cases, where there is a need to draw a reference from significantly old outputs, RNNs do not appear to be that useful. In the case of predictive maintenance of rolling stock, data acquired from the sensors is done very rapidly, and there are a lot of readings generated in a very short period of time. In such cases, we might need to look at older data to be able to predict a maintenance cycle for the machine. Since, it is the case of long-term dependency on historic data, RNNs might not be a very robust model to go through with. In such cases, a model that can remember long-term dependencies is required. One such model is the LSTM network that has been deployed in the analysis for this article.

3.2 Long Short-Term Memory (LSTM) Networks and Their Working

LSTMs, as discussed earlier, tackle the problem of long-term dependencies, owing to their design. While in a conventional RNN, the repeating unit has a very simple structure (as shown in Fig. 3), it is not the same for an LSTM network. It has four neural network layers, all interacting in a very special way.

Figure 4 illustrates what a typical LSTM network looks like. The most basic element of an LSTM is the cell state, represented by the horizontal line that runs

Fig. 3 Inner structure of a
cell in an RNN
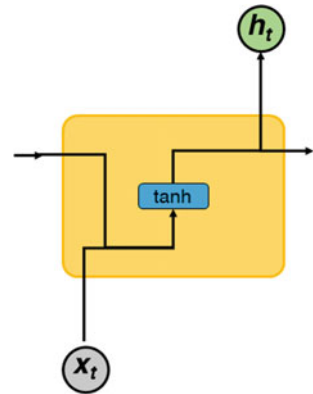
across the top of the cells. The cell state is analogous to a conveyor belt, as it runs
across the entire network, undergoing alterations and ensuring the flow of information
from one end to the other, as illustrated in Fig. 5.

LSTMs are also capable of appending or removing information from the cell
state, and this is done by regulating structures, known as gates. They are respon-
sible for allowing the inflow or outflow of information into the network, partially or
completely. These gates are made of a sigmoid layer, followed by a multiplication
operation. The task of this layer is deciding the level of influence of a component, by
allowing its entry into the network. This is achieved by the output generated by the
sigmoid layer, which lies between 0 and 1, where 0 stands for not letting anything
into the network, and 1 for allowing complete entry. A conventional LSTM houses
three such gates, hence, controlling the information flow in the cell state [2].

The first move inside the network is to finalize upon the amount of data that has
to be let go of, before making an input to a particular layer. This step is enabled by
the using the forget gate. This gate accepts h_{t-1} (output from previous layer) and x_t
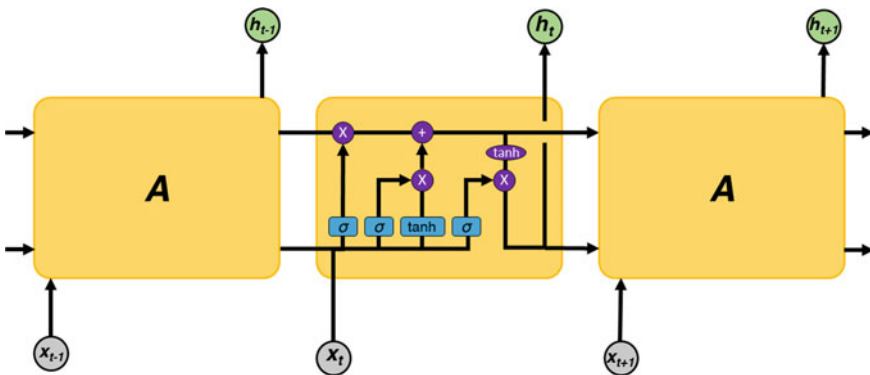
Fig. 4 Gates inside the recurrent unit of an LSTM

Fig. 5 Cell state
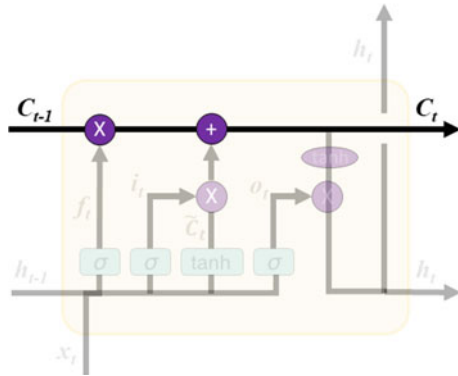
(input to current layer) as its inputs and yields a number between 1 and 0, for every number in the cell state C_{t-1}, signifying if all of the information has to be kept, or it has to be completely gotten rid of. This operation is illustrated in Fig. 6. The output of gate f_t can be formulated as

$$f_t = \sigma\left(W_f.[h_{t-1}, x_t] + b_f\right) \tag{4}$$

(f_t: output of the forget gate, W_f: weight of the forget gate, h_{t-1}: output from previous layer, x_t: input to the current layer, b_f: bias in the forget gate).

Having dealt with the forget gate, it is now imperative to come up with the new information that is supposed to be fed to the current cell state. This is done in two steps: input layer gate and the tanh layer gate. The input layer gate is another sigmoid layer responsible for deciding the values to be updated. Then, the tanh layer is used in creating a new vector $\tilde{C}_t$, followed by adding this vector to the cell state. Having created these two pieces of information, both the results are combined and the cell state value is updated. This combination of information is shown in Fig. 7. The output of the input layer gate i_t and the new vector $\tilde{C}_t$ can be formulated respectively as

Fig. 6 Forget gate
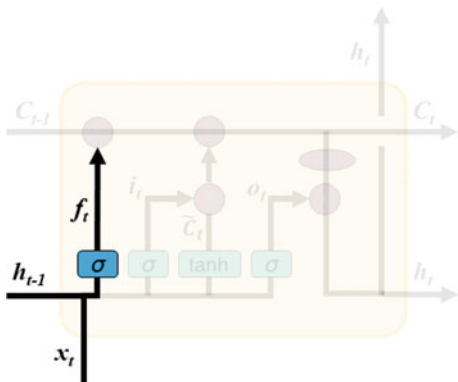
Fig. 7 Creating new pieces
of information to update the
cell state
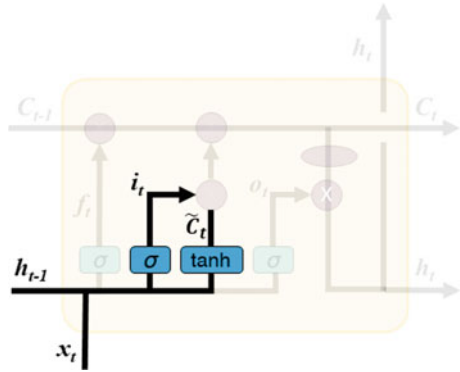
$$i_t = \sigma\left(W_i.\left[h_{t-1}, x_t\right] + b_i\right) \tag{5}$$

(i_t: output of the input gate, W_i: weight of the input gate, h_{t-1}: output from previous layer, x_t: input to the current layer, b_i: bias in the input gate).

$$\tilde{C}_t = \tanh\left(W_C.\left[h_{t-1}, x_t\right] + b_C\right) \tag{6}$$

($\tilde{C}_t$: new vector, W_C: weight of the layer, h_{t-1}: output from previous layer, x_t: input to the current layer, b_C: bias in the layer).

Now that the generation of new information is done, the next step involves the updating of cell state C_{t-1} to C_t. This is done by letting go data of the previous state and adding data from the current state, as illustrated in Fig. 8. This operation can be formulated as

$$C_t = \left(f_t * C_{t-1} + i_t * \tilde{C}_t\right) \tag{7}$$

Fig. 8 Updating the cell
state
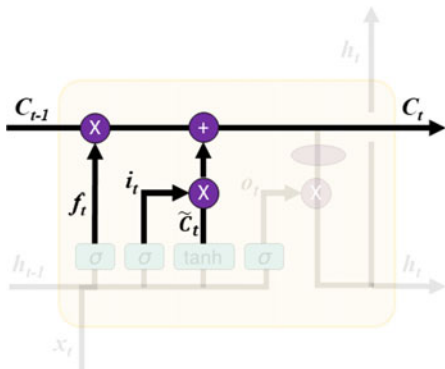
Fig. 9 Output generation
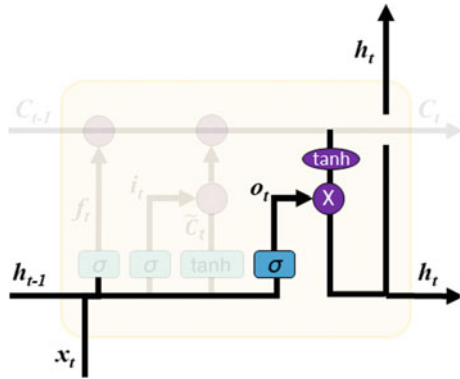
With the update of the cell state, the next step in the operation is to yield the final output of this cell. This final output is dependent upon the current cell state. This set of final operations involves generating an output o_t from another sigmoid layer through which h_{t-1} and x_t are passed, which can be formulated as

$$o_t = \sigma\left(W_o.\left[h_{t-1}, x_t\right] + b_o\right) \tag{8}$$

This is followed by filtering out a part of the current cell state by passing it through a tanh layer gate and combining or multiplying it with the previous sigmoid output, hence yielding the final output of the current cell, as illustrated in Fig. 9. The output h_t can be formulated as

$$h_t = o_t * \tanh(C_t) \tag{9}$$

4 Research Methodology

The previous section elucidates the functioning of LSTM networks and how they can be extremely helpful in dealing with problems that involve long-term dependencies. This section will deal with the actual analysis done by deploying an LSTM network over raw data in Python. This data is collected from sensors mounted on the actual machinery and then using it to predict the Remaining Useful Life of the machine, in terms of the number of cycles that it can still work for. Such a prediction can be extremely helpful in coming up with a robust maintenance schedule and planning maintenance activities beforehand in order to reduce downtime.

4.1 Data Pre-Processing

Dataset Summary: As mentioned earlier, the scope of analysis in this article is the predictive maintenance of rolling stock, due to their vitality in the railway industry. In order to carry out an analysis and come up with an optimized model, there should be a set of historic data that is gathered from sensors mounted on components of a well-functioning rolling stock. The data used in this analysis was sourced into a Python environment, from an open-source repository and was broken down into three smaller datasets and processed accordingly to suit the purpose of this analysis.

The three datasets used for the machine learning model are the training, testing and truth datasets, as illustrated in Figs. 10, 11 and 12. The training and the testing datasets are made up of multiple multivariate time series that have "cycle" as the unit of time. There are 25 sensors that take down readings for each and every cycle. There are 100 such components for which these readings are recorded, and each time series can be thought of as data generated from a different component of the rolling stock. All the readings also incorporate the type of operational setting at which the component runs and the dataset used accommodates three such settings. While the training and testing datasets follow the same general schema, the truth dataset contains the number of remaining working cycles of each of the 100 components. In the training dataset, all the components start functioning from an initial level of wear and after operating for a give number of cycles, they degrade to particular point, such that they stop working. This indicates that the last cycle of every time series is the point at which the particular component failed, or stopped working altogether.

Data Labelling: After describing the input data, the next step is to frame the entire case in the form of a question: *Given the historic data about the operation and failure of the rolling stock, can the next point of failure be predicted?*

This question can be reframed and then answered using a relevant machine learning model. The question can be modified as *For how many more cycles can the components in the rolling stock function, before failing*? In other words, the Remaining Useful Life (RUL) has to be calculated. As mentioned earlier, this can be

	id	cycle	setting1	setting2	setting3	s1	s2	s3	s4	s5	...	s16	s17	s18	s19	s20	s21	s22	s23	s24	s25
0	1	1	-0.0007	-0.0004	100	518.67	641.82	1589.70	1400.60	14.62	...	0.03	392	2388	100	39.06	23.4190	513.368431	44.53	2.78	7208.772058
1	1	2	0.0019	-0.0003	100	518.67	642.15	1591.82	1403.14	14.62	...	0.03	392	2388	100	39.00	23.4236	513.446916	45.08	2.78	7208.690109
2	1	3	-0.0043	0.0003	100	518.67	642.35	1587.99	1404.20	14.62	...	0.03	390	2388	100	38.95	23.3442	513.854125	44.64	2.78	7208.417976
3	1	4	0.0007	0.0000	100	518.67	642.35	1582.79	1401.87	14.62	...	0.03	392	2388	100	38.88	23.3739	513.122593	45.43	2.78	7208.011664
4	1	5	-0.0019	-0.0002	100	518.67	642.37	1582.85	1406.22	14.62	...	0.03	393	2388	100	38.90	23.4044	513.290138	44.94	2.78	7208.609278
...	...	...	...	...	...	...	...	...	...	...	...	...	...	...	...	...	...	...	...	...	...
20626	100	196	-0.0004	-0.0003	100	518.67	643.49	1597.98	1428.63	14.62	...	0.03	397	2388	100	38.49	22.9735	513.162253	45.45	2.78	7208.708021
20627	100	197	-0.0016	-0.0005	100	518.67	643.54	1604.50	1433.58	14.62	...	0.03	395	2388	100	38.30	23.1594	513.417661	44.86	2.78	7208.542430
20628	100	198	0.0004	0.0000	100	518.67	643.42	1602.46	1428.18	14.62	...	0.03	398	2388	100	38.44	22.9333	513.614172	45.08	2.78	7208.687075
20629	100	199	-0.0011	0.0003	100	518.67	643.23	1605.26	1426.53	14.62	...	0.03	395	2388	100	38.29	23.0640	513.338696	45.45	2.78	7208.961725
20630	100	200	-0.0032	-0.0005	100	518.67	643.85	1600.38	1432.14	14.62	...	0.03	396	2388	100	38.37	23.0522	513.541484	44.64	2.78	7208.600116

Fig. 10 Representation of the training dataset

	id	cycle	setting1	setting2	setting3	s1	s2	s3	s4	s5	...	s16	s17	s18	s19	s20	s21	s22	s23	s24	s25
0	1	1	0.0023	0.0003	100	518.67	643.02	1585.29	1398.21	14.62	...	0.03	392	2388	100	38.86	23.3735	513.282203	44.51	2.78	7208.098429
1	1	2	-0.0027	-0.0003	100	518.67	641.71	1588.45	1395.42	14.62	...	0.03	393	2388	100	39.02	23.3916	513.880391	45.40	2.78	7208.063564
2	1	3	0.0003	0.0001	100	518.67	642.46	1586.94	1401.34	14.62	...	0.03	393	2388	100	39.08	23.4166	513.592464	44.62	2.78	7208.012734
3	1	4	0.0042	0.0000	100	518.67	642.44	1584.12	1406.42	14.62	...	0.03	391	2388	100	39.00	23.3737	513.383942	44.78	2.78	7208.452399
4	1	5	0.0014	0.0000	100	518.67	642.51	1587.19	1401.92	14.62	...	0.03	390	2388	100	38.99	23.4130	513.723379	45.40	2.78	7208.027512
...	...	...	...	...	...	...	...	...	...	...	...	...	...	...	...	...	...	...	...	...	...
13091	100	194	0.0049	0.0000	100	518.67	643.24	1599.45	1415.79	14.62	...	0.03	394	2388	100	38.65	23.1974	513.130530	44.55	2.78	7208.370210
13092	100	195	-0.0011	-0.0001	100	518.67	643.22	1595.69	1422.05	14.62	...	0.03	395	2388	100	38.57	23.2771	513.548746	44.77	2.78	7208.047897
13093	100	196	-0.0006	-0.0003	100	518.67	643.44	1593.15	1406.82	14.62	...	0.03	395	2388	100	38.62	23.2051	513.631576	45.41	2.78	7208.786525
13094	100	197	-0.0038	0.0001	100	518.67	643.26	1594.99	1419.36	14.62	...	0.03	395	2388	100	38.66	23.2699	513.672740	44.67	2.78	7208.405240
13095	100	198	0.0013	0.0003	100	518.67	642.95	1601.62	1424.99	14.62	...	0.03	396	2388	100	38.70	23.1855	513.055729	44.54	2.78	7208.533415

Fig. 11 Representation of the testing dataset

Fig. 12 Representation of the truth dataset

	0
0	0
1	112
2	98
3	69
4	82
...	...
96	137
97	82
98	59
99	117
100	20

framed as a regression problem, i.e. a regression algorithm can be used to train the LSTM network.

Following the problem formulation, data labels for the training and testing data have to be generated, based on the truth dataset. Given that the aim of the problem is to evaluate the RUL, a data label for the same is generated in the training and testing dataset.

Feature Engineering: After data labelling, the last phase of the Data Pre-processing step is to generate features for training and testing the model. In this case, the features can be categorized into two groups: Raw and Aggregate.

Raw features are the data columns that are a part of the raw input. For this analysis, all the 25 sensor readings can be selected as the raw features. On the other hand, the moving average and the standard deviation of these sensor readings could be selected as the aggregate feature. However, creating the features manually requires domain expertise and reduces the reusability of the model. This is where the use of a deep learning model comes of immense use, as they are capable of extracting the right features from the data automatically and sparing the tedious task of engineering the features manually.

When LSTMs are deployed in time-series problems, it is crucial to decide upon a specific time window, or a suitable sequence length, for the model to refer back to and then generate features based on it. For instance, if the length of sequence was selected to be 10, then the model would refer to the last 10 sensor readings of all the 25 sensors and generate an aggregate feature by calculating the moving average or standard deviation for the particular sequence. Resultantly, if there lies a pattern in the sequence, the LSTM model would encode that, and incorporate it in the final calculation of the RUL. In this analysis, the LSTM model has been trained to generate features over 50 cycles.

Since an LSTM network is capable of dealing with long-term dependencies, it easily remembers readings from long-term sequences. This cannot be achieved with manual feature engineering.

4.2   Developing the LSTM Model

The selection of appropriate features is followed by the development of a proper LSTM network model that learns from the training dataset and evaluates the required results. The training, testing and evaluation phase of the model is realized in a Python environment. The training of the LSTM model is done using a regression approach, and several variations of the network are simulated in order to choose the best architecture for model prediction. The final model was capable of carrying out predictions with a great degree of accuracy. An approximate total of 33,000 rows of pre-processed experimental data, including the training, testing and truth data were involved in developing the LSTM model. The training dataset was used in training the model, and the testing data was the set on which the model was tested for accuracy, by checking the model's predicted results with that of the truth dataset that contained the actual data points from the ground.

The LSTM network, using the regression algorithm, gets trained during every epoch, while going through the training dataset. The model is trained with several LSTM variations with varying epochs, to come up with a model that is optimal enough, in terms of the error encountered in predicting the RUL. The major motivation behind comparing the values generated after running the model on the testing dataset with that of the truth dataset is to make sure that the model does not overfit the data. The concept of overfitting is that the model works accurately on the training set, but fails to draw strong patterns such that it is unable to generalize the results and predict values for datasets on which it was not trained.

The LSTM network is designed such that it has two hidden layers apart from the input and the output layers. The first layer has 100 units, while the second has 50 units. The final layer, i.e. the output layer has a single unit with linear activation, since the problem is based on regression. The design of the LSTM network is illustrated in Fig. 13. The inputs to the network that are represented as $x_1, x_2, \ldots x_n$ are nothing but the sensor readings for every cycle of a particular component. After being processed
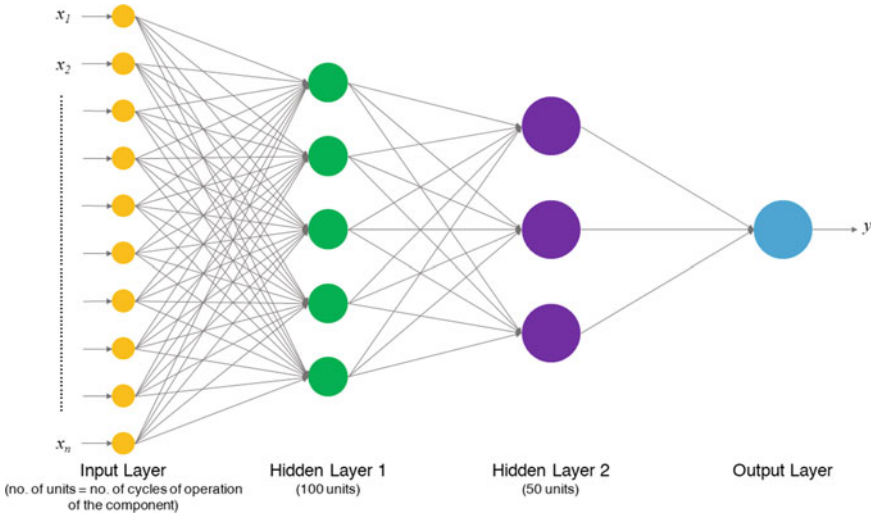
Fig. 13 Representation of the LSTM network designed for the analysis

by the two hidden layers, the output of the network y gives the predicted RUL of the component.

The designed model is supposed to predict the RUL of the component of the rolling stock to a high degree of accuracy and hence serve the purpose of the analysis. The number of hidden layers, as well as the number of nodes in them, is evaluated after running numerous simulations of the model.

5 Results

After simulating and choosing the right set of parameters for the LSTM model, the analysis is carried out over the datasets. The performance and precision of the model is dependent upon the design of the model, the parameters of the LSTM network and the linear regression activation function. While the actual set of parameters for the LSTM model was based on a set of simulations, it is imperative to check the performance of the final model as well. The accuracy of the model can be determined by checking how accurate the predicted values are, with respect to the actual values in the truth dataset. This accuracy can be evaluated calculating the Mean Absolute Error (MAE) value. MAE can be calculated using the following formula:

$$\text{MAE} = \frac{1}{n} \sum_{i=1}^{n} |x_i - x| \tag{10}$$

Table 1 Parameters of several LSTM networks before selecting the optimal network

No. of units in hidden layer 1	No. of units in hidden layer 2	Epochs	MAE	R^2
50	100	100	18.36	0.65
100	50	100	14.29	0.72
100	200	50	24.41	0.71

For training the LSTM model, a regression model was used. The regression model was chosen largely due to the nature of the problem statement, i.e. evaluating the RUL of the components. Given the lower value of MAE, the model can be trained, tested and evaluated quickly, resulting in saving a lot of precious time.

Apart from deciding the algorithm for training the model, several simulations were also carried out in terms of the number of units in the two hidden layers of the LSTM network and the number of epochs for training them. The parameters of a few LSTM networks that were a part of the simulation are illustrated in Table 1. Upon coming across an optimum value of MAE and R^2, the LSTM with 100 units in the first hidden layer and 50 units in the second layer was chosen, with 100 epochs for training the network.

When the LSTM network is run through the training and testing datasets, the accuracy and precision of results obtained are visualized clearly when the graphs of R^2 and MAE are plotted. Figures 14 and 15 represent the readings of R^2 and MAE alongside the epochs, respectively. As the model runs through the training dataset, it tries to fit using the regression algorithm. Having learnt from the training dataset, the model is then run through the testing dataset to gauge the level of fit that the regression model can achieve. Both the graphs of R^2 and MAE indicate that while running through the testing dataset, the model fits the data with a small consistent error, in the first 32–35 epochs, and starts to fluctuate a little in the later epochs, especially after 50 epochs, indicating slight occurrences of overfitting and underfitting. However, the final scores of R^2 and MAE are good enough, considering the size of the dataset and the simplicity of the model. This indicates that model, as a whole, performs well in predicting the required value, i.e. the Remaining Useful Life (RUL) of the components. The actual values from the truth dataset and the ones predicted by the model are plotted together in Fig. 16, and it can be seen that the predictions are reasonably accurate on a lot of occasions, which proves that the model performs well.

6   Discussion

The designed model in the above analysis is capable of predicting the RUL of the components of rolling stock, on the basis of the operational and failure data calculated over a period of time. The values of R^2 and MAE and the plots in Figs. 14, 15 and 16 are a proof that the model is reasonably accurate at carrying out its prediction.
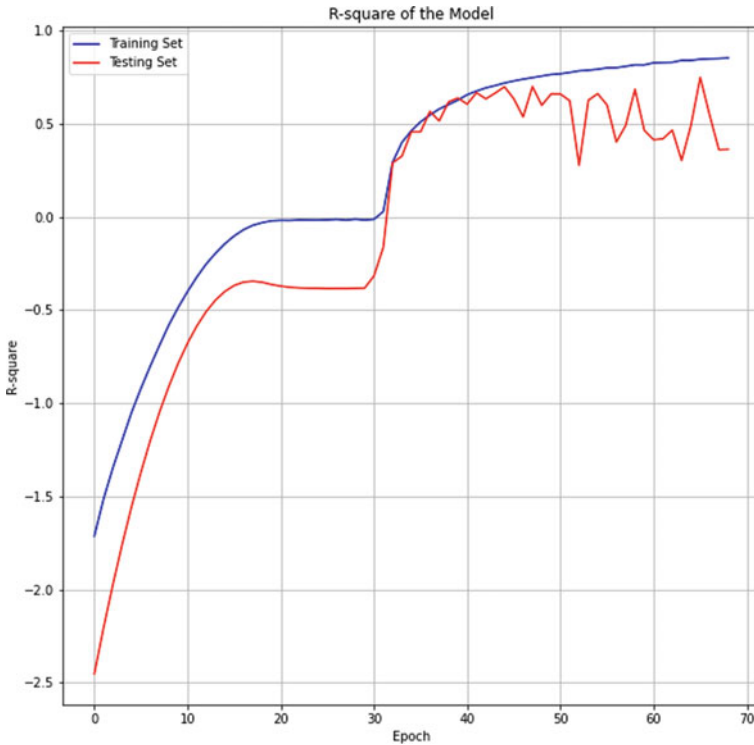
Fig. 14 Plot of R^2 of the model while training and testing the model

Such a task cannot be imagined to be done by a human at this level of precision. The model enables policy-makers to adopt the policy of predictive maintenance and avail the various advantages that it has over conventional policies of maintenance.

For components that are working fine for a long duration of time, it might get difficult for a conventional neural network to predict the number of cycles that the component would last for, as it would be a long-term dependency problem. However, an LSTM network efficiently tackles such dependencies and makes reasonably precise predictions. A model like this can be incorporated into predictive maintenance systems that can track the data collected by sensors mounted on the components of the machine and record the RUL of all the components of the machinery, so that a comprehensive schedule for carrying out maintenance activities can be laid out. Such a system will not only spare humans from performing tedious tasks like routine maintenance checks, but also reduce unnecessary downtimes of the assets. This, in turn, can have a phenomenal impact on the overall productivity and availability of the assets, especially for an organization as large as the Indian Railways.

It is known that Indian Railways operates a large number of rolling stocks. If such predictive maintenance systems were to be installed on the rolling stocks owned by
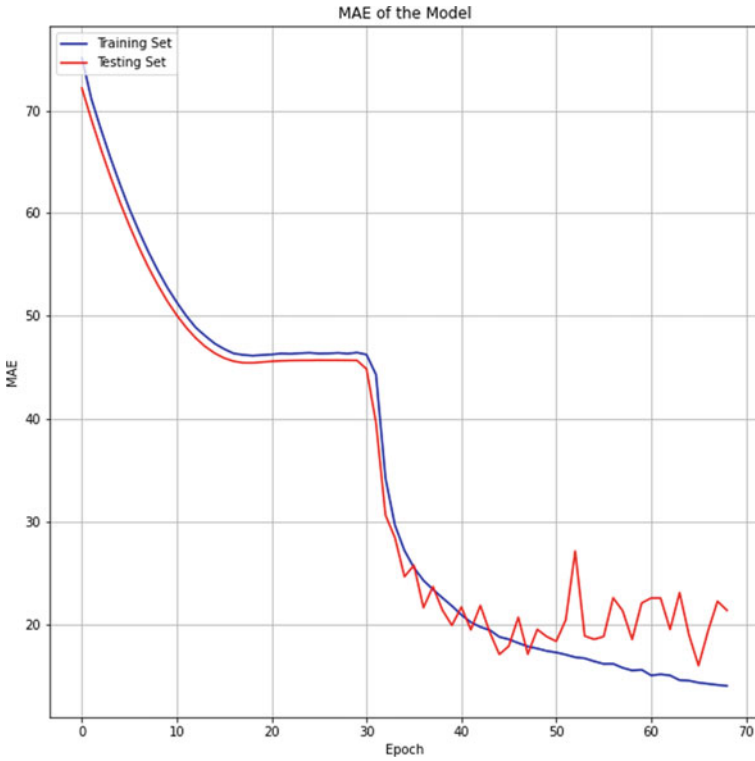
Fig. 15 Plot of MAE of the model while training and testing the model
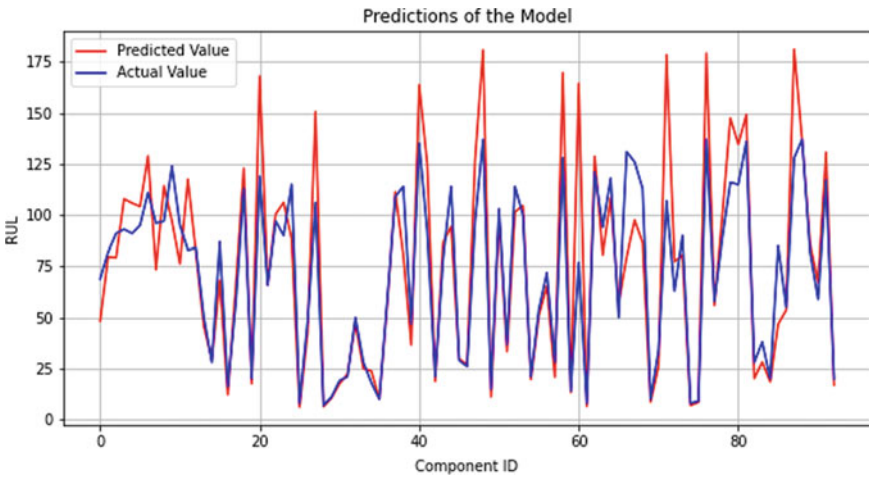
Fig. 16 Plot of the actual values and the values predicted by the model

Indian Railways, the overall impact on customer satisfaction as well as the revenue of the organization would be huge.

7 Conclusion

This study is a representation of a comprehensive analysis of the topic of predictive maintenance and the several machine learning and statistical models that can be used for implementing predictive maintenance on general machinery as well as railway machinery. Predictive maintenance can distinguish itself from conventional maintenance policies as it not only finds a defect in the component of the machine but also predicts when a failure might occur so that a maintenance cycle can be effectively scheduled. Reduced downtime, reduced costs, increased machine life and boosted productivity are the most promising advantages of deploying predictive maintenance.

After conducting an exhaustive review of existing literature on the deployment of predictive maintenance in the railway industry, research gaps were identified, and ground for further analysis was laid down. Following that, the study attempted to signify the importance of implementing predictive maintenance on one of the most crucial assets of Indian Railways, rolling stocks. This was done by training a Long Short-Term Memory (LSTM) network over a real-world dataset containing historic data of sensor readings on components of a rolling stock. The model was trained using a regression algorithm, such that it could predict the Remaining Useful Life (RUL) of the components of the rolling stock. The accuracy of the model was tested by the means of metrics like Mean Absolute Error (MAE) and R^2. Plots were also constructed to compare the actual values with the values predicted by the model.

The efficacy of the model makes it evident that such systems can be installed on rolling stock as well as other high-value assets of the Indian Railways and help boost the overall operations of the organization in an optimal fashion. The integration of predictive maintenance with machine learning can produce several positive results along with a reduction in costs. Another takeaway from the article is that with the increase in the availability of sensors and big data technologies, more responsive systems have come up which have the capability of supporting the maintenance decisions made, well in advance. Predictive maintenance can, undoubtedly, benefit a lot by leveraging big data technologies and machine learning algorithms.

References

1. Sharma, S.K., Lee, J., Jang, H.-L.: Mathematical modeling and simulation of suspended equipment impact on car body modes. Machines **10**, 192 (2022). https://doi.org/10.3390/machines10030192

2. Vishwakarma, P.N., Mishra, P., Sharma, S.K.: Formulation of semi-active suspension system and controls in rail vehicle. SSRN Electron. J. (2022). https://doi.org/10.2139/ssrn.4159616

3. Vishwakarma, P.N., Mishra, P., Sharma, S.K.: Characterization of a magnetorheological fluid damper a review. Mater. Today Proc. **56**, 2988–2994 (2022). https://doi.org/10.1016/j.matpr.2021.11.143

4. Sharma, S.K., Sharma, R.C., Lee, J., Jang, H.-L.: Numerical and experimental analysis of DVA on the flexible-rigid rail vehicle carbody resonant vibration. Sensors **22**, 1922 (2022). https://doi.org/10.3390/s22051922

5. Sharma, S.K., Mohapatra, S., Sharma, R.C., Alturjman, S., Altrjman, C., Mostarda, L., Stephan, T.: Retrofitting existing buildings to improve energy performance. Sustainability **14**, 666 (2022). https://doi.org/10.3390/su14020666

6. Sharma, S.K., Sharma, R.C., Lee, J.: In situ and experimental analysis of longitudinal load on carbody fatigue life using nonlinear damage accumulation. Int. J. Damage Mech. **31**, 605–622 (2022). https://doi.org/10.1177/10567895211046043

7. Sharma, R.C., Sharma, S.K.: Ride analysis of road surface-three-wheeled vehicle-human subject interactions subjected to random excitation. SAE Int. J. Commer. Veh. **15**, 02-15-03-0017 (2022). https://doi.org/10.4271/02-15-03-0017

8. Sharma, S.K., Lee, J.: Crashworthiness analysis for structural stability and dynamics. Int. J. Struct. Stab. Dyn. **21**, 2150039 (2021). https://doi.org/10.1142/S0219455421500395

9. Wu, Q., Cole, C., Spiryagin, M., Chang, C., Wei, W., Ursulyak, L., Shvets, A., Murtaza, M.A., Mirza, I.M., Zhelieznov, K., Mohammadi, S., Serajian, H., Schick, B., Berg, M., Sharma, R.C., Aboubakr, A., Sharma, S.K., Melzi, S., Di Gialleonardo, E., Bosso, N., Zampieri, N., Magelli, M., Ion, C.C., Routcliffe, I., Pudovikov, O., Menaker, G., Mo, J., Luo, S., Ghafourian, A., Serajian, R., Santos, A.A., Teodoro, Í.P., Eckert, J.J., Pugi, L., Shabana, A., Cantone, L.: Freight train air brake models. Int. J. Rail Transp. 1–49 (2021). https://doi.org/10.1080/23248378.2021.2006808

10. Sharma, S.K., Sharma, R.C., Lee, J.: Effect of rail vehicle-track coupled dynamics on fatigue failure of coil spring in a suspension system. Appl. Sci. **11**, 2650 (2021). https://doi.org/10.3390/app11062650

11. Mohapatra, S., Mohanty, D., Mohapatra, S., Sharma, S., Dikshit, S., Kohli, I., Samantaray, D.P., Kumar, R., Kathpalia, M.: Biomedical application of polymeric biomaterial: polyhydroxybutyrate. In: Bioresource Utilization and Management: Applications in Therapeutics, Biofuels, Agriculture, and Environmental Science, pp. 1–14. CRC Press (2021). https://doi.org/10.21203/rs.3.rs-1491519/v1

12. Bhardawaj, S., Sharma, R.C., Sharma, S.K., Sharma, N.: On the planning and construction of railway curved track. Int. J. Veh. Struct. Syst. **13**, 151–159 (2021). https://doi.org/10.4273/ijvss.13.2.04

13. Sharma, R.C., Sharma, S., Sharma, N., Sharma, S.K.: Linear and nonlinear analysis of ride and stability of a three-wheeled vehicle subjected to random and bump inputs using bond graph and simulink methodology. SAE Int. J. Commer. Veh. **14**, 02-15-01-0001 (2021). https://doi.org/10.4271/02-15-01-0001

14. Sharma, R.C., Sharma, S., Sharma, S.K., Sharma, N., Singh, G.: Analysis of bio-dynamic model of seated human subject and optimization of the passenger ride comfort for three-wheel vehicle using random search technique. Proc. Inst. Mech. Eng. Part K J. Multi-body Dyn. **235**, 106–121 (2021). https://doi.org/10.1177/1464419320983711

15. Choi, S., Lee, J., Sharma, S.K.: A study on the performance evaluation of hydraulic tank injectors. In: Advances in Engineering Design: Select Proceedings of FLAME 2020, pp. 183–190. Springer, Singapore (2021). https://doi.org/10.1007/978-981-33-4684-0_19

16. Lee, J., Han, J., Sharma, S.K.: Structural analysis on the separated and integrated differential gear case for the weight reduction. In: Joshi, P., Gupta, S.S., Shukla, A.K., Gautam, S.S. (eds.) Advances in Engineering Design. Lecture Notes in Mechanical Engineering, pp. 175–181 (2021). https://doi.org/10.1007/978-981-33-4684-0_18
17. Sharma, S.K., Sharma, R.C.: Multi-objective Design optimization of locomotive nose. In: SAE Technical Paper, pp. 1–10 (2021). https://doi.org/10.4271/2021-01-5053
18. Sharma, R.C., Palli, S., Sharma, N., Sharma, S.K.: Ride behaviour of a four-wheel vehicle using H infinity semi-active suspension control under deterministic and random inputs. Int. J. Veh. Struct. Syst. **13**, 234–237 (2021). https://doi.org/10.4273/ijvss.13.2.18
19. Sharma, S.K., Sharma, R.C., Sharma, N.: Combined multi-body-system and finite element analysis of a rail locomotive crashworthiness. Int. J. Veh. Struct. Syst. **12**, 428–435 (2020). https://doi.org/10.4273/ijvss.12.4.15
20. Sharma, R.C., Sharma, S.K., Palli, S.: Linear and non-linear stability analysis of a constrained railway wheelaxle. Int. J. Veh. Struct. Syst. **12**, 128–133 (2020). https://doi.org/10.4273/ijvss.12.2.04
21. Palli, S., Sharma, R.C., Sharma, S.K., Chintada, V.B.: On methods used for setting the curve for railway tracks. J. Crit. Rev. **7**, 241–246 (2020)
22. Mohapatra, S., Pattnaik, S., Maity, S., Mohapatra, S., Sharma, S., Akhtar, J., Pati, S., Samantaray, D.P., Varma, A.: Comparative analysis of PHAs production by Bacillus megaterium OUAT 016 under submerged and solid-state fermentation. Saudi J. Biol. Sci. **27**, 1242–1250 (2020). https://doi.org/10.1016/j.sjbs.2020.02.001
23. Sharma, R.C., Sharma, S.K., Sharma, N., Sharma, S.: Analysis of ride and stability of an ICF railway coach. Int. J. Veh. Noise Vib. **16**, 127 (2020). https://doi.org/10.1504/IJVNV.2020.117820
24. Sharma, S.K., Phan, H., Lee, J.: An Application study on road surface monitoring using DTW based image processing and ultrasonic sensors. Appl. Sci. **10**, 4490 (2020). https://doi.org/10.3390/app10134490
25. Sharma, R.C., Sharma, S., Sharma, S.K., Sharma, N.: Analysis of generalized force and its influence on ride and stability of railway vehicle. Noise Vib. Worldw. **51**, 95–109 (2020). https://doi.org/10.1177/0957456520923125
26. Lee, J., Sharma, S.K.: Numerical investigation of critical speed analysis of high-speed rail vehicle. 한국정밀공학회 학술발표대회 논문집 (Korean Soc. Precis. Eng. 696) (2020).
27. Sharma, S.K., Lee, J.: Finite element analysis of a fishplate rail joint in extreme environment condition. Int. J. Veh. Struct. Syst. **12**, 503–506 (2020). https://doi.org/10.4273/ijvss.12.5.03
28. Bhardawaj, S., Sharma, R., Sharma, S.: Ride analysis of track-vehicle-human body interaction subjected to random excitation. J. Chinese Soc. Mech. Eng. **41**, 237–236 (2020). https://doi.org/10.29979/JCSME
29. Bhardawaj, S., Sharma, R.C., Sharma, S.K.: Development in the modeling of rail vehicle system for the analysis of lateral stability. Mater. Today Proc. **25**, 610–619 (2020). https://doi.org/10.1016/j.matpr.2019.07.376
30. Bhardawaj, S., Sharma, R.C., Sharma, S.K.: Analysis of frontal car crash characteristics using ANSYS. Mater. Today Proc. **25**, 898–902 (2020). https://doi.org/10.1016/j.matpr.2019.12.358
31. Sharma, S., Sharma, R.C., Sharma, S.K., Sharma, N., Palli, S., Bhardawaj, S.: Vibration isolation of the quarter car model of road vehicle system using dynamic vibration absorber. Int. J. Veh. Struct. Syst. **12**, 513–516 (2020). https://doi.org/10.4273/ijvss.12.5.05
32. Acharya, A., Gahlaut, U., Sharma, K., Sharma, S.K., Vishwakarma, P.N., Phanden, R.K.: Crashworthiness analysis of a thin-walled structure in the frontal part of automotive chassis. Int. J. Veh. Struct. Syst. **12**, 517–520 (2020). https://doi.org/10.4273/ijvss.12.5.06
33. Bhardawaj, S., Sharma, R.C., Sharma, S.K.: Development of multibody dynamical using MR damper based semi-active bio-inspired chaotic fruit fly and fuzzy logic hybrid suspension control for rail vehicle system. Proc. Inst. Mech. Eng. Part K J. Multi-body Dyn. **234**, 723–744 (2020). https://doi.org/10.1177/1464419320953685
34. Sharma, S.K., Lee, J.: Design and development of smart semi active suspension for nonlinear rail vehicle vibration reduction. Int. J. Struct. Stab. Dyn. **20**, 2050120 (2020). https://doi.org/10.1142/S0219455420501205

35. Sharma, S.K.: Multibody analysis of longitudinal train dynamics on the passenger ride performance due to brake application. Proc. Inst. Mech. Eng. Part K J. Multi-body Dyn. **233**, 266–279 (2019). https://doi.org/10.1177/1464419318788775

36. Goyal, S., Anand, C.S., Sharma, S.K., Sharma, R.C.: Crashworthiness analysis of foam filled star shape polygon of thin-walled structure. Thin-Walled Struct. **144**, 106312 (2019). https://doi.org/10.1016/j.tws.2019.106312

37. Sharma, S.K., Sharma, R.C.: Pothole detection and warning system for Indian roads. In: Advances in Interdisciplinary Engineering, pp. 511–519 (2019). https://doi.org/10.1007/978-981-13-6577-5_48

38. Goswami, B., Rathi, A., Sayeed, S., Das, P., Sharma, R.C., Sharma, S.K.: Optimization design for aerodynamic elements of Indian locomotive of passenger train. In: Advances in Engineering Design, pp. 663–673. Lecture Notes in Mechanical Engineering. Springer, Singapore (2019). https://doi.org/10.1007/978-981-13-6469-3_61

39. Bhardawaj, S., Chandmal Sharma, R., Kumar Sharma, S.: Development and advancement in the wheel-rail rolling contact mechanics. IOP Conf. Ser. Mater. Sci. Eng. **691**, 012034 (2019). https://doi.org/10.1088/1757-899X/691/1/012034

40. Choppara, R.K., Sharma, R.C., Sharma, S.K., Gupta, T.: Aero dynamic cross wind analysis of locomotive. In: IOP Conference Series: Materials Science and Engineering, p. 12035. IOP Publishing (2019)

41. Sinha, A.K., Sengupta, A., Gandhi, H., Bansal, P., Agarwal, K.M., Sharma, S.K., Sharma, R.C., Sharma, S.K.: Performance enhancement of an all-terrain vehicle by optimizing steering, powertrain and brakes. In: Advances in Engineering Design, pp. 207–215 (2019). https://doi.org/10.1007/978-981-13-6469-3_19

42. Sharma, S.K., Saini, U., Kumar, A.: Semi-active control to reduce lateral vibration of passenger rail vehicle using disturbance rejection and continuous state damper controllers. J. Vib. Eng. Technol. **7**, 117–129 (2019). https://doi.org/10.1007/s42417-019-00088-2

43. Bhardawaj, S., Chandmal Sharma, R., Kumar Sharma, S.: A survey of railway track modelling. Int. J. Veh. Struct. Syst. **11**, 508–518 (2019). https://doi.org/10.4273/ijvss.11.5.08

44. Sharma, R.C., Palli, S., Sharma, S.K., Roy, M.: Modernization of railway track with composite sleepers. Int. J. Veh. Struct. Syst. **9**, 321–329 (2018)

45. Sharma, R.C., Sharma, S.K., Palli, S.: Rail vehicle modelling and simulation using Lagrangian method. Int. J. Veh. Struct. Syst. **10**, 188–194 (2018). https://doi.org/10.4273/ijvss.10.3.07

46. Palli, S., Koona, R., Sharma, S.K., Sharma, R.C.: A review on dynamic analysis of rail vehicle coach. Int. J. Veh. Struct. Syst. **10**, 204–211 (2018). https://doi.org/10.4273/ijvss.10.3.10

47. Sharma, S.K., Sharma, R.C.: An investigation of a locomotive structural crashworthiness using finite element simulation. SAE Int. J. Commer. Veh. **11**, 235–244 (2018). https://doi.org/10.4271/02-11-04-0019

48. Sharma, S.K., Sharma, R.C.: Simulation of quarter-car model with magnetorheological dampers for ride quality improvement. Int. J. Veh. Struct. Syst. **10**, 169–173 (2018). https://doi.org/10.4273/ijvss.10.3.03

49. Sharma, S.K., Kumar, A.: Impact of longitudinal train dynamics on train operations: a simulation-based study. J. Vib. Eng. Technol. **6**, 197–203 (2018). https://doi.org/10.1007/s42417-018-0033-4

50. Sharma, R.C., Sharma, S.K.: Sensitivity analysis of three-wheel vehicle's suspension parameters influencing ride behavior. Noise Vib. Worldw. **49**, 272–280 (2018). https://doi.org/10.1177/0957456518796846

51. Sharma, S.K., Kumar, A.: Ride comfort of a higher speed rail vehicle using a magnetorheological suspension system. Proc. Inst. Mech. Eng. Part K J. Multi-body Dyn. **232**, 32–48 (2018). https://doi.org/10.1177/1464419317706873

52. Sharma, S.K., Kumar, A.: Disturbance rejection and force-tracking controller of nonlinear lateral vibrations in passenger rail vehicle using magnetorheological fluid damper. J. Intell. Mater. Syst. Struct. **29**, 279–297 (2018). https://doi.org/10.1177/1045389X17721051

53. Sharma, S.K., Kumar, A.: Impact of electric locomotive traction of the passenger vehicle Ride quality in longitudinal train dynamics in the context of Indian railways. Mech. Ind. **18**, 222 (2017). https://doi.org/10.1051/meca/2016047

54. Sharma, S.K., Kumar, A.: Ride performance of a high speed rail vehicle using controlled semi active suspension system. Smart Mater. Struct. **26**, 055026 (2017). https://doi.org/10.1088/1361-665X/aa68f7

55. Sharma, S.K., Kumar, A.: Dynamics analysis of wheel rail contact using FEA. Procedia Eng. **144**, 1119–1128 (2016). https://doi.org/10.1016/j.proeng.2016.05.076

56. Sharma, S.K., Kumar, A.: The impact of a rigid-flexible system on the ride quality of passenger bogies using a flexible carbody. In: Pombo, J. (ed.) Proceedings of the Third International Conference on Railway Technology: Research, Development and Maintenance, Stirlingshire, UK, p. 87. Civil-Comp Press, Stirlingshire, UK (2016). https://doi.org/10.4203/ccp.110.87

57. Sharma, S.K., Chaturvedi, S.: Jerk analysis in rail vehicle dynamics. Perspect. Sci. **8**, 648–650 (2016). https://doi.org/10.1016/j.pisc.2016.06.047

58. Kulkarni, D., Sharma, S.K., Kumar, A.: Finite element analysis of a fishplate rail joint due to wheel impact. In: International Conference on Advances in Dynamics, Vibration and Control (ICADVC-2016) NIT Durgapur, India February 25–27, 2016. National Institute of Technology Durgapur, Durgapur, India (2016)

59. Sharma, S.K., Sharma, R.C., Kumar, A., Palli, S.: Challenges in rail vehicle-track modeling and simulation. Int. J. Veh. Struct. Syst. **7**, 1–9 (2015). https://doi.org/10.4273/ijvss.7.1.01

60. Sharma, S.K., Kumar, A., Sharma, R.C.: Challenges in railway vehicle modeling and simulations. In: International Conference on Newest Drift in Mechanical Engineering (ICNDME-14), December 20–21, M. M. University, Mullana, India, pp. 453–459. Maharishi Markandeshwar University, Mullana—Ambala (2014)

61. Sharma, S.K., Kumar, A.: A comparative study of Indian and Worldwide railways. Int. J. Mech. Eng. Robot. Res. **1**, 114–120 (2014)

62. Sharma, S.K.: Zero energy building envelope components: a review. Int. J. Eng. Res. Appl. **3**, 662–675 (2013)

63. Sharma, S.K., Lavania, S.: An autonomous metro: design and execution. In: Futuristic trends in Mechanical and Industrial Engineering, pp. 1–8. JECRC UDML College of Engineering, Jaipur (2013)

64. Sharma, S.K., Lavania, S.: Green manufacturing and green supply chain management in India a review. In: Futuristic Trends in Mechanical and Industrial Engineering, pp. 1–8. JECRC UDML College of Engineering (2013)

65. Sharma, S.K., Lavania, S.: Skin effect in high speed VLSI on-chip interconnects. In: International Conference on VLSI, Communication & Networks, V-CAN, pp. 1–8. Institute of Engineering & Technology, Alwar (2011)

66. Lavania, S., Sharma, S.K.: An explicit approach to compare crosstalk noise and delay in VLSI RLC interconnect modeled with skin effect with step and ramp input. J. VLSI Des. Tools Technol. **1**, 1–8 (2011)

67. Dao, D.K., Ngo, V., Phan, H., Pham, C.V., Lee, J., Bui, T.Q.: Rayleigh wave motions in an orthotropic half-space under time-harmonic loadings: a theoretical study. Appl. Math. Model. **87**, 171–179 (2020). https://doi.org/10.1016/j.apm.2020.06.006

68. Park, J., Lee, J., Le, Z., Cho, Y.: High-precision noncontact guided wave tomographic imaging of plate structures using a DHB algorithm. Appl. Sci. **10**, 4360 (2020). https://doi.org/10.3390/app10124360

69. Park, J., Lee, J., Min, J., Cho, Y.: Defects inspection in wires by nonlinear ultrasonic-guided wave generated by electromagnetic sensors. Appl. Sci. **10**, 4479 (2020). https://doi.org/10.3390/app10134479

70. Lee, J., Ngo, V., Phan, H., Nguyen, T., Dao, D.K., Cho, Y.: Scattering of surface waves by a three-dimensional cavity of arbitrary shape: analytical and experimental studies. Appl. Sci. **9**, 5459 (2019). https://doi.org/10.3390/app9245459

71. Park, J., Lee, J., Jeong, S.-G., Cho, Y.: A study on guided wave propagation in a long distance curved pipe. J. Mech. Sci. Technol. **33**, 4111–4117 (2019). https://doi.org/10.1007/s12206-019-0806-z

72. Rubió-Massegú, J., Palacios-Quiñonero, F., Rossell, J.M., Karimi, H.R.: A novel iterative linear matrix inequality design procedure for passive inter-substructure vibration control. Appl. Sci. **10**, 5859 (2020). https://doi.org/10.3390/app10175859

73. Sharma, S.K., Sharma, R.C., Choi, Y., Lee, J.: Experimental and mathematical study of flexible–rigid rail vehicle riding comfort and safety. Appl. Sci. **13**, 5252 (2023). https://doi.org/10.3390/app13095252

74. Palacios-Quiñonero, F., Rubió-Massegú, J., Rossell, J.M., Karimi, H.R.: Design of inerter-based multi-actuator systems for vibration control of adjacent structures. J. Franklin Inst. **356**, 7785–7809 (2019). https://doi.org/10.1016/j.jfranklin.2019.03.010

75. Shravanth Vasisht, M., Vashista, G.A., Srinivasan, J., Ramasesha, S.K.: Rail coaches with rooftop solar photovoltaic systems: a feasibility study. Energy **118**, 684–691 (2017). https://doi.org/10.1016/j.energy.2016.10.103

Developing and Validating a Verbal Alert Utility Scale for Intelligent Transportation Systems: To Address the Safety of Transportation Cyber-Physical Systems

A. Bhargavi

Abstract When cities across the world expand and people's mobility rises, so does the number of cars on the road. As a consequence, officials are facing an increasing number of problems in terms of road traffic control. As a result, there are more road chaos, more deaths, and waste. Despite the advancement of advanced traffic control systems and other vehicle-related technology, accidents remain a leading cause of death. As a result, a standard method for injury prevention must be created. For example, in most metropolitan environments, traffic congestion may be alleviated by route planning in real time. However, developing an efficient route planning algorithm to achieve globally optimal vehicle control remains a challenge, particularly when drivers' tastes are taken into account. Also, intelligent transportation systems (ITS) are an effective implementation of Cyber-Physical Systems (CPS) that enhance driving safety by advising drivers of hazards with alerts in advance. The efficacy of warnings must be assessed to facilitate ITS communication. This analysis aimed to create a scale to assess warning usefulness, or how effective a warning is at avoiding accidents in general. The Verbal Alert Utility Scale (VWUS) was validated in a virtual driving environment using a driving simulator. The VWUS had decent split-half reliability with a Spearman-Brown coefficient of 0.873, according to the reliability report. The significant prediction of safety benefits suggested by variables such as decreased kinetic energy and collision rate confirmed the predictive validity of VWUS in calculating the efficacy of verbal alerts. This scale is a better way to test the general effectiveness of verbal alerts in transmitting related dangers in intelligent transportation networks than doing experimental experiments. This scale can be used to enhance the nature of ITS alarms and thereby increasing transportation safety. The scale's uses in nonverbal alarm scenarios, as well as the new scale's shortcomings, are also discussed.

Keywords ITS · Spearman-Brown coefficient · Traffic · Control

A. Bhargavi (✉)
Prism Johnson Limited, Mumbai, India
e-mail: bhargaviaika1902@gmail.com

1 Introduction

The notion of a smart city is associated with a paradigm shift in which focus is being shifted toward concepts and technology initiatives that try to make cities smarter in order to improve the quality of life for people who work in them. For example, in 2010, the European Commission established what is now known as the European Initiative on Smart Cities. The regulation of the environment, construction, transportation, and the provision of energy are the four primary facets of community life that will be addressed by this project [1–5]. The growing number of traffic accidents is one of the most important problems that smart cities want to solve. These accidents have been brought on by an increase in the number of automobiles on the road, which has led to congestion [6, 7]. Accidents involving motor vehicles are one of the major causes of mortality in the USA, accounting for more than one hundred fatalities each and every day. According to the same report, there were more than 10 million people who were injured in 2007, which resulted in more than 43,000 deaths. In addition, insufficient traffic management technology is a significant contributor to injuries in the majority of nations throughout the globe [8–12]. Intelligent public transportation processes that are based on real-time data and that help drivers avoid congested areas and increase protection while simultaneously ensuring that cars run in an environmentally sustainable manner are referred to as "traffic management systems" [13–18]. The term "traffic management systems" refers to the processes that fall under this category. In recent years, academics from academic institutions as well as businesses have taken advantage of advances in wireless sensor technologies to improve existing traffic management networks and ensure their capacity to deal with the issues mentioned above in smart cities. These improvements have been made possible by taking advantage of recent advancements in wireless sensor technologies.

Pollution from vehicles is increasingly being recognized as one of the most significant challenges facing communities in the western USA. One of the most important repercussions of traffic jams is the fact that it takes longer for emergency services to arrive at the site of an accident, including firefighters, police officers, and ambulances, as well as other rescue and firefighting operations. This is an adverse scenario due to the fact that the welfare of the general public is dependent on the capacity of these services to respond to accidents in the most efficient and timely way that is practically possible [19–23]. Intelligent transit networks have not yet reached the point where they can address the issue of traffic congestion (ITSs). For example, Google Maps make use of pre-existing networking systems like Wi-Fi, GPS, and cellular networks to help users plan their routes and reduce the likelihood of being stuck in traffic. Nevertheless, not only are these systems expensive, but they also lack the responsiveness necessary to take prompt action in the event that a problem results from a collision on the road. These networks are the only ones that have access to real-time traffic data. As a consequence of this, it is essential for these emergency departments to have a system in place that can improve the adaptability of route routing in order to make it possible to obtain data in a more efficient manner and to

make use of real-time traffic data in order to reduce the number of instances of traffic jams.

To begin, emerging vehicular ad hoc networks, or VANETs, may be employed to offer an ITS infrastructure with expanded communications capabilities for the purpose of obtaining real-time traffic information in a more efficient and timely manner while also reducing associated costs. VANETs are able to handle both vehicle-to-roadside device (V2R) communications and vehicle-to-vehicle (V2V) communications, which enables real-time warnings to be transmitted from and to automobiles as well as roadside devices. After being gathered, this real-time information may be put to use for a variety of purposes, including route planning in individual cars [24], controlling the flow of traffic on highways, and localizing vehicles. Second, after data on real-time traffic is gathered, a variety of algorithms may be constructed with the intention of finding the routes that provide the most accessibility for each person. On the other hand, this might result in even additional congestion if the planning of the routes is not carried out in a methodical manner. Even though the vast majority of existing worldwide algorithms for route planning center their attention on network improvements, these algorithms often ignore driver expectations about journey durations and lengths. This is noteworthy, especially when one considers that choices about the re-planning of roads are driven more by the need to avoid traffic congestion and achieve traffic balance than by the investigation of routes that provide the greatest potential efficiency. Because of this, some drivers have the option of taking longer routes, despite the fact that doing so would result in greater charges. As a consequence of this, the design of algorithms may take into consideration both the decrease of the typical operating cost of a car as well as an increase in network traffic.

Warning is an extremely important part of the process of disseminating information about possible dangers, which is vital in order to reduce the number of accidents and deaths. There has been a perceptible rise in the number of studies on the coordination of road safety over the course of the last three decades [24]. This rise in the number of studies may be seen. Recent advancements in transportation CPS aim to provide a connected transportation environment between the cyber world (e.g., information, communication, and intelligence) and the physical world (e.g., sensors and actuators) and to provide integrated real-time information among multiple levels, including vehicle-to-vehicle communication, vehicle-to-infrastructures cooperation, and in-vehicle information communication, in order to improve driving safety. These developments were made in an effort to connect the cyber world with the physical world. These recent improvements were created in order to establish an environment for linked transportation between the physical world and the cyber world. The connection that is provided by the CPS makes it easier for drivers to get information about the current state of traffic while they are behind the wheel, and it provides them with more reaction time to alerts about potential dangers. This is in comparison with a traditional transportation setting, which makes it more difficult for drivers to get this information. The vast majority of research that has been carried out on intelligent transportation systems (ITS) has suggested developing algorithms to schedule alerts based on the usefulness of the alerts as a significant application of transportation

CPS. Due to the increasing amount of alerts that are being produced by ITS [19–23], it is becoming more crucial to do an analysis of the alert utilities during the design phase of the transportation CPS.

The term "warning utility" refers to the extent to which the manifestation of a warning contributes to an improvement in the functioning of a consumer. According to Shackel [24], the usefulness of a system may be seen as whether or not it is able to carry out the tasks that are necessary. According to the definition provided by Regan et al. [25], the idea of device efficacy is conceptually similar to that of utility. The authors Regan et al. provided an explanation of the ideas of effectiveness, usefulness, and simplicity of use [25]. According to the findings of their study, efficacy was defined as "the degree to which a person believes that using a particular system will improve his or her performance." Perceived utility was described as "the degree to which a person believes that using a particular system will be free of effort," and ease of use was characterized as "the degree to which a person believes that using a particular system will be painless." It was determined that usefulness and enjoyment were the two components that comprised acceptance [26–31, 31–36]. However, further study has shown that acceptance is contingent upon elements such as system effectiveness and societal impact. System acceptance has been defined as "the degree to which an individual desires to utilize a system and, when accessible, incorporates the system into his or her driving." Previous studies have shown that subjective evaluations of perceived usefulness may not always translate to an increase in driving efficiency while using the item in question. For instance, drivers may find it beneficial to get a message that is either too late or too early, despite the fact that it does not significantly increase driving safety. Because of this disparity, the results of our earlier study showed that alert utility could be a more powerful construct for evaluating projected objective benefits. In contrast to the ideas of usefulness and acceptability, the notion of utility places more of an emphasis on a user's capacity to get the most out of a given product than on the user's opinion of that product.

This investigation has an emphasis, first and foremost, on audible warnings, which are typical components of modern-day security systems. A benefit that auditory alarms have over other types of warnings is that the human ear, in contrast to the human sight, cannot be turned off. Studies have shown that the effectiveness of auditory warnings is much higher than that of spoken ones (e.g., Wogalter and Young). When humans are working in environments with high workload conditions, particularly high visual workload conditions, and/or when the operator needs to walk around a lot or when visual conditions are poor, auditory alerts may draw the human's attention regardless of where the human's attention is focused [37–41].

The most recent application of the scale has mostly focused on verbal auditory warnings because of how user-friendly they are. Users are able to easily perceive and differentiate verbal auditory alerts since they do not need any specialized teaching. As contrast to spoken auditory warnings, nonverbal auditory alerts need their contents to be comprehended, remembered, and heard at the same time that they sound. This presents a disadvantage over verbal auditory warnings. According to the findings of many pieces of research, humans are infamously bad at remembering and correctly processing nonverbal sensory cues. According to the findings of one

research, hospital staff members working in operating rooms and recovery rooms at teaching hospitals were unable to recall more than half of the alarms that were really being used at the facility. According to the findings of Patterson's study, individuals are able to remember the first few of a set of audio warnings nearly as rapidly as they can be provided; nevertheless, development slows once six or seven warnings have been learned. In addition, recognition of nonverbal auditory warnings in operational environments is likely to be poorer than in the laboratory because absolute recognition is lower than relative recognition. This is due to the fact that absolute recognition is measured in comparison to relative recognition. In a previous research, it was revealed that vocal alerts resulted in a quicker response time than nonverbal warnings, particularly in the event of complex road conditions [42–48]. This was one of the findings of the study. Note: Verbal notifications result in a lower accident rate than nonverbal messages do in intersection collision warning systems, according to research. This is especially true for drivers who are in their senior years. When it comes to matters of critical safety, there are many different recommendations on the use of vocal warnings. However, Noyes et al. [49] suggest that verbal warnings should be used in safety critical circumstances because drivers respond to verbal notifications more quickly and have a better chance of reacting correctly than they do to nonverbal warnings. The new ISO working draft suggests that verbal alerts should not be used for safety critical warnings because they take longer to present. Verbal auditory alerts, in general, may be utilized widely without needing any further education, making them perfect for transportation assistance program usage [50–53].

In order to accomplish successful communication in an Indian setting, the purpose of this chapter is to develop a scale for assessing the utility (efficacy) of verbal warnings in intelligent transportation systems. This will be done with the intention of achieving efficient communication. The efficiency of warnings is largely evaluated based on two criteria: the degree to which they are successful at attracting human attention, and the degree to which they are successful at providing viewers with data that are easy to grasp. A subjective evaluation will be used to choose the dimensions of the Verbal Warning Usefulness Scale (VWUS), which will include summarizing factors that have the potential to influence the determination of warning utility. After the construction of the measure, a split-half reliability study and a factor analysis were used in order to evaluate the reliability and composition of the scale, respectively, respectively, respectively, respectively. Following that, the predictive validity of the scale was examined using an experimental sample in a simulated environment. If the verbal warning utility score (VWUS) can be used to quantify the safety advantages supplied by alerts that have been developed, then the VWUS may be used to evaluate how effective warnings are in terms of enhancing driver safety. To measure the efficacy of verbal notifications in intelligent transportation networks, rather than undertaking behavioral experiments, a validated scale should be utilized instead.

2 Development of Scale: Method

Exploring pertinent variables to the definition being evaluated (i.e., workload), undertaking discretionary rating to select salient factors with a specific criterion.

2.1 Participants

One hundred and four people (72 males and 32 females) from Vadodara completed the exploratory questionnaire. Participants were contacted on a random basis. All had a valid driver's license and were residents of Vadodara. Participants' ages ranged from 18 to 69 years with an average age of 29.66 years (SD = 12.09). In terms of driving experience, the average years since obtaining a valid drivers' license were 11.11 years (SD = 11.47), while the average mileage was 9355.77 miles (SD = 7037.41).

2.2 Material

We looked at alert characteristics that may affect the efficacy of alerts because certain warning characteristics can interact to create a subjective warning value. To the best of our understanding, the following Fig. 1 shows the three categories of alert characteristics that can affect the effectiveness of the warning [1–4].

A questionnaire was used to investigate which significant things are subjectively equal to alarm usefulness. The participants were required to describe the association between each item's name and its description and the overall verbal alert usefulness (i.e., "a": subjectively identical, "b": associated, and "c": unrelated). The fact that an object is subjectively equal to the average verbal alert utility suggests that it may be used to reflect the utility of verbal alerts. When an object is linked to the total usefulness of verbal warnings, it means that it adds to the utility of verbal warnings. When an object is irrelevant to the general usefulness of verbal warnings that means it does not add to the utility of verbal warnings. "Representation of event urgency: How urgent is the event communicated by the warning?" is an example object [5–8].

2.3 Procedure

The city of Vadodara served as the location for the research project. Following the completion of a demographic questionnaire (which included questions about the participants' gender, age, and driving history, among other things), the discovery questionnaire was given to the participants. The participants were given the task

First category: hazard/task:

- Representation of Event Urgency: the degree to which an event's importance is reflected by an Alert
- Time to Display : The probability that an alert would appear at a convenient time;
- Number of Replications: the degree to which an alert can be distinguished from other alerts in the system;
- Distinctive Features: the degree to which a warning can be distinguished from other warnings in the system

Second category: important to the alarm itself:

- Modality : the way an alert is perceived.
- Loudness : a sensory sensation characterized by the ability to rank noises on a scale ranging from quiet to loud.
- Length of the warning: the number of terms in an alert.
- Voice Type: if a warning is spoken by a woman or a man.
- Voice quality : the degree to which an alarm can be recognized.
- Rate of speech: the number of words spoken in a given amount of time.

Third category: human learning function of verbal warnings:

- Alertness : the degree to which the user's focus is drawn
- Loss in Vigilance: the degree to which one's capacity to pay attention over extended stretches of time is harmed.
- Accuracy of understanding: the degree to which a person knows the danger in the presence of an alert.
- Familiarity : the degree to which a person is acquainted with an alert
- Annoyance : the degree to which an alert annoys a person.
- Likeness/preference: the degree to which a person likes the appearance of an alarm.
- Comfort: the degree to which an individual is at ease when reacting to a warning
- Trustworthy : The degree to which an individual believes an alert
- Reduced Workload : the amount of job that is reduced while an alarm is present.
- Forgetting : the probability of a warning being forgotten by an individual.

Fig. 1 Alert characteristics can affect the effectiveness of the warning

of visualizing a scenario in which they were forewarned about something that was going to take place and asked to describe what it was. Dangerous occurrences and help them increase the likelihood of colliding with other objects [54–58]. An example of the situation shown in Fig. 2 in which a warning device installed within the subject vehicle sounds an alarm to inform the driver to a potential threat caused by a hazard vehicle approaching from the left that has run a red light.

"A driver at your front-left is running the red light at the intersection," for example, is a sign. The participants were required to describe the association between each item's name and its description and the overall verbal alert usefulness (i.e., "a": subjectively identical, "b": associated, and "c": unrelated). The fact that an object is subjectively equal to the average verbal alert utility suggests that it may be used to reflect the utility of verbal alerts. When an object is linked to the total usefulness of verbal warnings, it means that it adds to the utility of verbal warnings. When an object is irrelevant to the general usefulness of verbal warnings that means it does not add to the utility of verbal warnings. "Representation of Event Urgency: How urgent is the event communicated by the warning?" is an example object.

Fig. 2 Example of the test scenario [59]

2.4 Results

We recorded three potential partnerships: those that were subjectively the same, those that were comparable, and those that were unrelated to the efficacy of vocal alerts. The frequency of each alliance is given in Table 1, which encompasses all twenty items. A chi-square goodness-of-fit test was carried out on each component in order to determine whether or not the frequency of connections that were subjectively comparable was marginally greater than the frequency of the other two relationships. The Bonferroni critical value was computed by dividing $p = 0.05$ by the number of tests (3), which resulted in a test needing to have a p 0.017 in order for it to be considered relevant. The Bonferroni correction was used for this calculation. Only the tests for the Representation of Event Urgency, Time to Display, Alertness, and Accuracy of Understanding displayed a slightly higher proportion of equivalency to alarm utility than the tests for being linked or irrelevant to warning utility in regard to that criterion. This was the case for all of the other tests as well. In the meanwhile, more than fifty percent of respondents believed that alarm usefulness was subjectively comparable to the following four factors: Representation of Event Urgency, Time to Display, Alertness, and Accuracy of Understanding (frequency of equivalent 52).

Finally, based on the findings of the aforementioned study, the Verbal Alert Utility Scale was determined to be the four most important objects (VWUS). The following are the meanings for the four items:

Table 1 Average rating for each component as well as the frequency of the three different types of connections that might exist between a given factor and the warning usefulness ($N = 104$) [59]

Items	Representation of event urgency	Time to display	No. of replications	Distinctive features	Warning modality
Equivalent	59	63	25	45	38
Related	38	33	57	46	40
Unrelated	7	8	22	13	26
x^2	25.62^{***}	34.74^{***}	4.04	4.62	0.48
Items	Loudness	Length of the warning	Voice type	Voice quality	Rate of speaking
Equivalent	43	37	14	34	38
Related	53	50	37	51	57
Unrelated	8	17	53	19	9
x^2	3.01	0.24	18.48^{***}	0.02	0.48
Items	Alertness	Loss of vigilance	Accuracy of understanding	Familiarity	Annoyance
Equivalent	62	31	52	24	21
Related	31	61	41	64	48
Unrelated	11	12	11	16	35
x^2	32.33^{***}	0.58	13.00^{***}	4.92	8.08^{*}
Items	Likeness	Comfort	Trust	Workload	Forgetting
Equivalent	19	23	41	25	32
Related	40	50	44	43	39
Unrelated	45	31	19	36	33
x^2	10.62^{*}	5.59	1.74	4.04	0.31

Note $^{*}p < 0.017$, $^{***}p < 0.001$. The p value of 0.017 was applied with Bonferroni correction for p value of 0.05

- I Representation of incident urgency (item 1): How effectively does the alarm express the event's urgency?
- When to display the message (item 2): When is the best moment to show the warning to users?
- Alertness (item 11): How effectively does the alarm alert consumers to the potentially harmful incident at the time they receive it?
- Accuracy of interpretation (item 13): How well does the alert assist consumers in comprehending the recent event?

3　Validation of Scale: New York Case Study

A study was done by The State University of New York (SUNY), Buffalo [7, 8], for the validation of a similar study. In a virtual driving exercise, an observational

analysis was performed to assess the association between VWUS scores and activity metrics in preventing future crashes, which would add support to VWUS' predictive validity. It was hypothesized that the VWUS scores established in this study would accurately predict human success in preventing a possible collision when auditory alarms were transmitted. The accident and impact avoidance were two behavioral measures included in the present research to quantify the efficacy of verbal alerts. The term "collision" was coded as a binary variable indicating whether a subject's automobile clashed with a danger vehicle (get collided: 1 and avoid collision: 0). The effect reduction caused by the alerts was specified by the subject's vehicle's decreased kinetic energy. We'll look at the decreased kinetic energy of a vehicle with unit mass since the mass of the vehicle will differ in practice.

3.1 Participants

Research was conducted at the State University of New York (SUNY), Buffalo, with a total of 32 participants (24 men and 8 females). The participants' ages varied from 18 to 26 years old, with a mean of 21.13 and a standard deviation of 2.54 years. The standard deviation of the total number of years after acquiring a new driver's license was 2.36 years, and the average distance was 8343.75 miles (standard deviation = 6438.0). Before participating in the experiment, each participant was needed to sign a paper indicating their informed permission, demonstrate normal or corrected-to-normal eyesight, and provide valid driver's licenses.

3.2 Apparatus

The driving objective was successfully completed with the help of a STISIM driving simulator. The driving simulator is comprised of a force input-capable Logitech Momo steering wheel, a power pedal, and a braking pedal. The highest amount of throttle that may be applied is 15.2°, and the direction that the throttle pedal should be in while it is idle is 38.2° (angle between the pedal surface and the ground). The greatest amount of brake input is 28.6 and the sting position of the brake pedal is at a degree angle of 60.1°. On a Dell Precision 490 workstation that also had a 256 MB PCIe × 16 nVidia graphics card, Sound Blaster X-Fi system, and Dell A225 sound system, the STISIM simulator was loaded (Precision 490, Dual Core Intel Xeon Processor 5130 2 GHz). The driving scenario was shown on an LCD display with a screen size of 27 inches and a resolution of 1920 by 1200 pixels.

3.3　Material

A ranking system and a weighting scale made up the VWUS (see Appendix 1). The rating scale included four items: "Representation of Event Urgency, Time to Display, Alertness, and Accuracy of Understanding," as well as a concern about the warning's overall usefulness. Participants were first asked to rate each element on a ten-point scale (e.g., "0": not at all to "9": incredibly well) to see how effective the alarm they heard in the trial was in helping them escape the danger. "How well did the alarm reflect the incident urgency?" is an example object. The participants were also questioned regarding the overall usefulness of the alert using the item, "In general, how helpful was the warning?" at the end of the rating scale.

A weighting scale was adopted in order to provide more precise scores. Two alternative causes of uncertainty in the ranking of verbal alert usefulness are accounted for by the weights derived from weighting scales. It contains variations in verbal warning utility definitions between subjects for the same warning, as well as differences in the origins of verbal warning usefulness between alerts. After completing the rating scales, participants were required to evaluate each pair of properties of the alert they had just scored and use the weighting scale to pick the one that added the most to the warning usefulness. Each dimension will receive three weighted scores after being compared to the other three dimensions ("0": contributes the least to the alert utility score and "1": contributes the most to the warning utility score). The sum of the three scores was used to determine the weighted score for each dimension. By combining the conducts of rating score and the weighted score of each dimension, the total score of alert utility was determined.

3.4　Experiment Design

In the present investigation, a single-factor within-subject technique was used, with lead time serving as the independent variable. During the experiment, a total of sixteen different phases of lead time were determined (0, 1, 1.5, 2, 2.5, 3, 3.5, 4, 4.5, 5, 6, 8, 10, 15, the 30, and 60 s). In the event that the drivers of the participating automobiles had a tendency to keep moving at their current relative position, speed, and acceleration, the lead period would have reflected the amount of time until their cars collided. The development of sophisticated transportation systems in modern times has made it feasible for drivers to be warned in advance of potential dangers, which is one reason why we create such a wide range for lead time.

Each participant is required to go through sixteen separate trials, each with a hazard that might result in a crash and an alarm. These trials all have sixteen different degrees of lead time. The sequence in which the 16 lead times and the 16 crash incidences were allocated was completely arbitrary. Figure 3 depicts a total of sixteen different accident scenarios, each of which comes with its own unique set of warnings. These

scenarios were devised and coded with the help of a driving simulator to represent the kinds of collisions that may occur in the real world.

During the experiment, the participants' line of sight to the looming danger was purposefully hidden so that they could only concentrate on the audible alert and find out about the coming collision at the very last second (i.e., they will not be able to see the hazard until the time when they cannot avoid the hazard successfully even with full braking when they confirm the hazard by vision). In this scenario, the behavioral measures unearthed the protective benefits offered by the warnings without clouding the participants' perception of the dangers. In the meanwhile, throughout the experiment, several alarm signals, such as news and weather forecasts, were chosen at random to see whether or not the participants would apply the brakes if a message came on the screen. As a consequence of this finding, we may draw the following conclusion: Drivers' responses to verbal warnings are determined by how well they understand the information conveyed in the warning. After then, the signals for alerts were purposefully created such that they wouldn't interfere with the alerts. They were operating as potential sources of distraction for drivers in actual traffic situations.

3.5 Procedure

Upon arriving at the laboratory, participants were given the instruction to first sign a paper indicating their informed permission and then complete a demographic questionnaire. During each trial, individuals would be given the opportunity to experience one potential crash scenario while simultaneously receiving a notice about it. They were instructed to complete the VWUS after each trial of the test block in order to evaluate the usefulness of the vocal warnings in aiding them in avoiding the subsequent crash event that occurred.

The participants were prepped for the experiment by completing a practice block before the experiment proper began. During this block, they were acquainted with the operation of the driving simulator as well as the driving climate. Participants were forced to drive a distance of four miles with two collision incidences (accompanied by accompanying voice warnings) and five non-warning messages blasted throughout the practice block. Participants were also expected to listen for and respond to five non-warning communications. They were warned that there will be crashes caused by verbal notifications, and they were instructed to make decisions based on their own prior expertise behind the wheel. Throughout the duration of the driving operation, the participants were given the instruction to stay in the inner lane, and this information was also broadcast over the radio. The scenario for the practice block was generated in the same manner as the scenario for the test block.

After completing the practice session, the participants moved on to the assessment block, which included a total of sixteen different runs over two lanes in a local environment (one in either direction). Before beginning the organized experiment, it was emphasized to each and every participant that they should move about in their chairs until they felt comfortable, and their feet were able to make full contact with
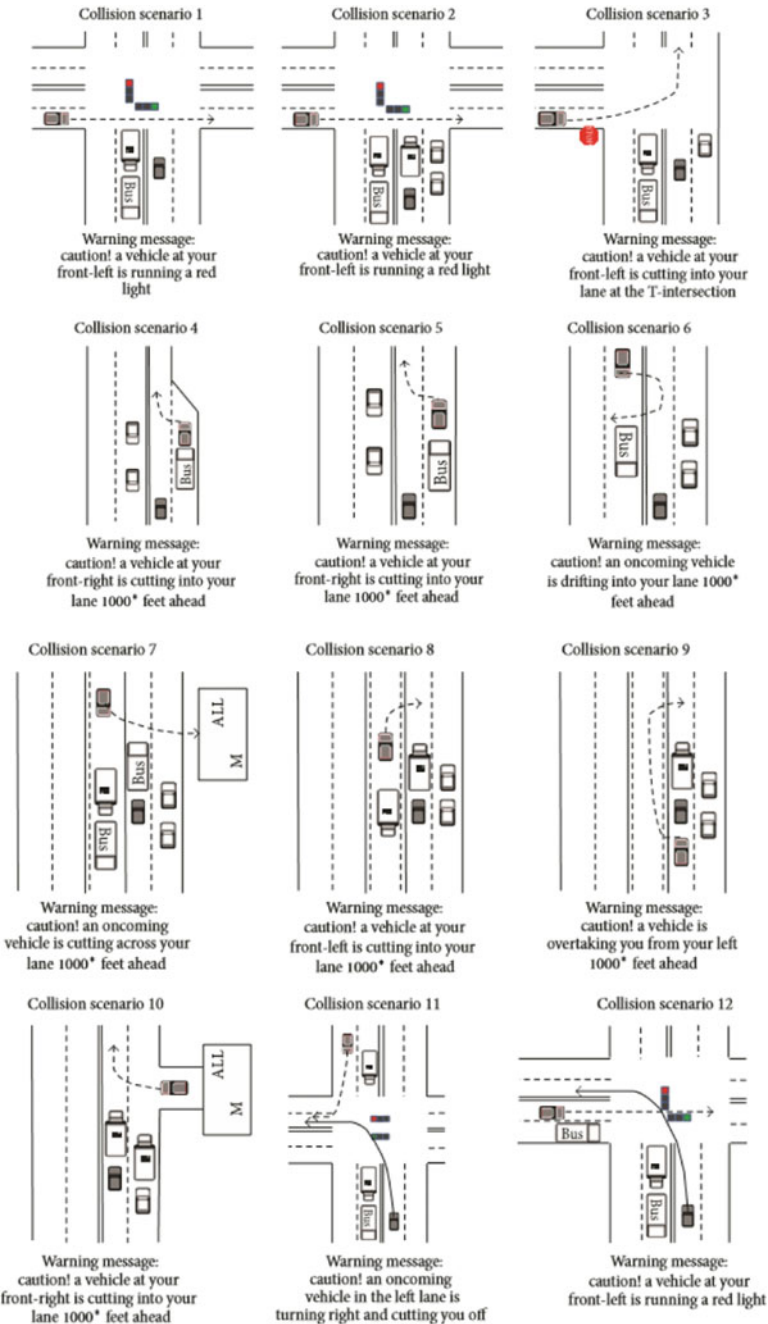
Fig. 3 Designed scenarios and verbal warnings for collision different condition [59]

Scenario 1
Attention! A vehicle from front-left is cutting into your lane at the T-intersection

Scenario 2
Attention! A vehicle from front-right is cutting into your lane 1000 feet ahead

Scenario 3
Attention! An oncoming vehicle in the left lane is turning right and cutting you off

Scenario 4
Attention! An oncoming vehicle is cutting across your lane at the intersection

	Other Vehicle		Subject vehicle track
	Hazard Vehicle		Hazard vehicle track (preprogrammed)
	Subject Vehicle		Other vehicle direction of movement

Fig. 3 (continued)

the pedal surface. Participants in the controlled experiment were instructed to follow all applicable traffic regulations and maintain a speed of 45 miles per hour for the duration of the study. They were allowed to slow down if their own speed was either lower than 40 miles per hour or higher than 50 miles per hour while there was no signal, switch, stop sign, or red light in the area.

4 Results and Discussion

We were given a total of 512 warnings for VWUS scores in total (32 participants × 16 alerts each). The informational data for the VWUS and the demographic factors are given in Table 2, along with the correlations between their total scores and variables such as age, gender, yearly mileage, and license year. The main criteria for establishing the usefulness of an alert were satisfied since the correlation coefficients between VWUS total scores and demographic variables were not relevant ($p > 0.05$),

Table 2 Mean and standard deviation for demographic measures and Spearman correlation coefficient [59]

Variables	Mean (SD)	Spearman's rho	p
Age (years)	21.13 (2.54)	− 0.01	0.99
Gender (proportion of male)	0.75	0.02	0.63
Annual millage (miles)	8343.75 (6437.95)	0.01	0.81
License year (years)	3.50 (2.36)	− 0.01	0.77
Reduced kinetic energy (J)	314.92 (152.09)	0.56	< 0.001
VWUS total score	5.88 (2.51)		

and they had low correlation coefficients (r 0.06) The greater the total VWUS ratings, the stronger the association is between the lower kinetic energy.

4.1 Split-Half Reliability

Due to the fact that the VWUS only had a single query for each item, we were unable to do an internal consistency check on the scale. In order to determine the reliability of the VWUS, a split-half reliability study was conducted with the 32 individuals who had previously completed the test during the experiment. The Spearman-Brown coefficient for the VWUS split-half dependability was 0.873, and the Cronbach's coefficients for each half were 0.762 and 0.777, respectively. In addition, the VWUS split-half reliability was excellent.

4.2 Factor Analysis

Factor analysis is a method of determining the relationship between two or the four VWUS objects that were subjected to a factor study of varimax rotation. The associations between objects are significant enough for the study, according to Bartlett's test of sphericity, $2(6) = 841.37$, $p.001$. An initial review was performed to obtain eigenvalues for each data variable. When combined, two components that each had an eigenvalue greater than 1.0 were able to explain 73.22% of the total variance in accordance with Kaiser's criterion. The two-factor extraction accounted for 73.22% of the variance despite communalities ranging from 0.51 to 0.97 and one-item cross-loadings. The communalities ranged from 0.60 to 0.84, and the one-factor extraction accounted for 41.51% of the variance, which is less than what was needed to explain the variation. The three-factor extraction accounted for 97.68% of the variance, which

Table 3 Loading values on items of VWUS [59]

Scale items	Factor 1	Factor 2
Time to display	− 0.84	− 0.51
Accuracy of understanding	0.75	
Representation of event urgency	0.6	
Alertness		0.97
Initial eigenvalues	1.66	1.27
Variance explained (%)	41.51	31.7

was determined by communalities that ranged from 0.51 to 0.97 and three-item cross-loadings. According to Osborne and Waters' factor extraction characteristics, the two-factor method was selected because it had the fewest item cross-loadings and had relatively larger variance. This led to the selection of the two-factor approach. Table 3 displays the initial eigenvalues as well as the variance that can be attributed to each component. In addition to this, a summary of the loading values for each item in the rotated factor matrix was supplied, with loading values that were less than 0.30 omitted. By doing an analysis of object loading on these characteristics, certain themes were determined based on the content of the items that were found among these factors. "Time to Display," "Representation of Event Urgency," and "Accuracy of Understanding" were the subcategories that fell under the umbrella of "Accuracy of Hazard Representation," the first dimension. The quality of Alertness was the second consideration in the equation.

4.3 Criterion Validity

Figure 4 demonstrated a statistically significant correlation between the VWUS total utility score (calculated by each item's rating and weighting scores in VWUS) and the overall utility score ($r = 0.851, p\ 0.001$) obtained directly from the studies. This correlation was demonstrated by a significant level of significance. When examining alert utility in general, it is claimed that the total utility score that was assessed using VWUS is a fair match for the overall utility score that was measured.

Because the normal distribution principle was violated, Spearman correlation coefficients were employed to indicate the intercorrelation between the scores of each component and the overall usefulness. This was done so as to account for the fact that normal distribution was not followed. As can be seen in Table 4, there was a significant correlation between the overall score for usefulness and the scores obtained for the variables "Accuracy of Hazard Representation" and "Alertness." There was not a significant impact from the interaction between the two variables (rs $= 0.07, p = 0.12$). According to the elements that make up the factor titled "Accuracy of Hazard Representation," the intercorrelation between the "Representation of Event Urgency" and "Time to Display" was found to be (rs $= − 0.35, p\ 0.01$) Accuracy of Understanding had a connection of (rs $= − 0.15, p\ 0.01$) with both Representation

Fig. 4 Correlation between the VWUS total scores and the overall utility scores (error bar: ± 1SE) [59]
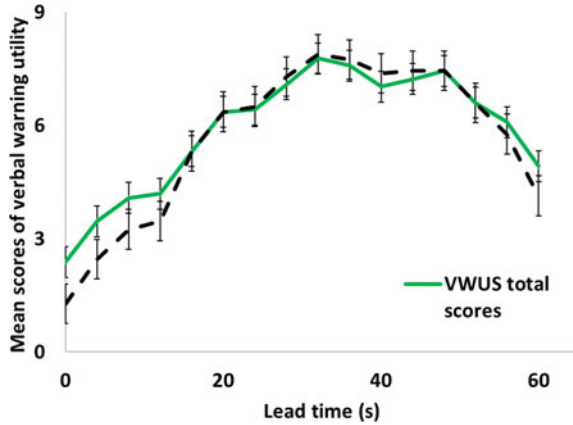
of Event Urgency and Time to Display having a correlation of (rs = − 0.45, p 0.01) with Accuracy of Understanding.

Two consecutive linear regression analyses were carried out to determine whether or not the VWUS was able to significantly predict the alarm's usefulness. The criterion validation measurements (i.e., reduced kinetic energy) acquired from the behavioral experiment were used for these analyses. It was believed that this particular behavioral assessment would provide a protective gain. The number of drivers who were involved in an accident as a percentage of the total number of drivers throughout each stage of the lead time was used to define the collision rate. At the same time, the user input their gender, age, and the year they received their license. Step 1; Step 2; VWUS total scores of each alarm ($N = 502$) or scores of two components (Accuracy of Hazard Representation and Alertness) were recorded at Step 3 in each research, respectively. Step 1; Step 2; Step 3; and the results of the first model are summarized in Table 5. This model used the VWUS total score to estimate the level of additional protection that is afforded to the user by spoken warnings.

The findings showed that the VWUS total value, which was determined using ranking scores and weighted scores for each parameter, predicted lower kinetic energy substantially ($t = 15.50$, $p < 0.001$). As drivers replied to alerts with higher VWUS total ratings, more kinetic energy was saved. The findings of the second model, which included ratings for two VWUS parameters, revealed that Hazard Representation precision substantially predicted decreased kinetic energy ($t = 2.36$,

Table 4 Intercorrelation of scores of VWUS factors and the overall utility [59]

Variables	1	2
Factor 1: Accuracy of hazard representation	—	
Factor 2: Alertness	0.07	—
Overall utility score	0.10[***]	0.86[***]

Note [***]$p < 0.01$

Table 5 Linear regression results for the prediction of reduced kinetic energy with VWUS scores [59]

Variables	R^2	F for change in R^2	B	SE	Beta	t
Model 1						
Gender			− 10.2	12.8	− 0	− 0.8
Age			− 6.46	2.47	− 0.1	− 2.62[*]
License obtaining year	0	2.72[*]	7.5	2.67	0.12	2.82[**]
Order of lead time			− 0.63	1.2	− 0	− 0.52
Scenario type			− 2.15	1.2	− 0.1	− 1.8
Lead time	0	2.35	0.01	0.01	0.08	2.09[*]
VWUS total score	0.4	240.33[***]	34.36	2.22	− 0.6	15.50[***]
Model 2						
Gender			− 4.09	15.4	− 0	− 0.27
Age			− 6.57	2.99	− 0.1	− 2.2[*]
License obtaining year	0	2.72[*]	8.79	3.23	0.14	2.72[*]
Order of lead time			1.17	1.44	0.04	0.81
Scenario type			− 3.67	1.44	− 0.1	− 2.55[*]
Lead time	0	2.25	0.01	0.01	0.03	0.77
Accuracy of Hazard Representation			− 72.4	30.7	− 0.3	0
Alertness	0.1	4.70[**]	− 41.1	31.2	− 0.1	− 1.32

Note [*]$p < 0.05$, [**]$p < 0.01$, and [***]$p < 0.001$

$p < 0.05$). According to the findings, the more accurately the alert represented the danger, the less kinetic energy was lost as a consequence of the braking reaction to the alerts. Both findings indicated that the VMUS could be used to predict the efficacy of verbal alerts. The VWUS was then put into a logistic regression study to see whether it could accurately forecast alarm usefulness using collision as a criteria validity test. Another example of the protection advantages provided by alerts was the accident (avoid a collision: 0 and collision: 1).

The first step required the input of gender, era, and license year; the second step required the input of an order of lead time, scenario form, and alert lead time; and the third step required the input of VWUS total scores for each warning ($N = 512$). Another research based on logistic regression was carried out, this time with the inputs at Step 3 consisting of the scores of two VWUS variables. The comparison of a constant-only model to a logistic regression model containing scores from two VWUS variables did not provide statistically significant results ($\times 2(8) = 12.53, p = 0.13$). Because of this, the only model that used VWUS total scores as predictors was the one that was distributed. The results of the logistic regression analysis together

Table 6 Logistic regression results for the prediction of collision in the VWUS scores [59]

	B	SE	Wald x^2	Exp (B)	995% CI for Exp (B)	
					Lower	Upper
Model 1						
Gender	− 0.19	0.27	0.47	0.83	0.49	1.41
Age	0.11	0.05	4.37*	1.11	1.01	1.23
License obtaining year	− 0.08	0.06	1.86	0.93	0.83	1.03
Order of treatment	− 0.02	0.03	0.35	0.99	0.94	1.04
Scenario type	− 0.04	0.03	2.6	0.96	0.91	1.01
Lead time	− 0.03	0.01	12.25***	0.97	0.96	0.99
VWUS total score	− 0.06	0.06	114.87***	0.54	0.48	0.6

Note $^*p < 0.05$, $^{***}p < 0.001$

with a review of the overall score on the VWUS are given in Table 6 for the purpose of assessing the protection advantages that are offered by verbal warnings.

The first logistic regression model was statistically important as compared to a constant-only model, meaning that the predictors as a group accurately predict the likelihood of collision ($x^2(8) = 15.62$, $p < 0.05$). A mild association between prediction and grouping was shown by Nagelkerke's R^2 of 0.50. The likelihood of a crash was correctly predicted 80 percent of the time. The Wald criteria revealed that the VWUS total score contributed significantly to prediction ($p.001$). Collisions were also forecast by age and alert lead period. Warnings with higher VWUS total ratings, in fact, greatly decreased the likelihood of a crash.

4.4   Scale Sensitivity

In order to establish the sensitivity of the scale, we compared two ANCOVA experiments in which the alert lead time served as the independent variable, the scenario form served as the covariate, and the scale scores and reduced kinetic energy served, respectively, as the dependent variables. After adjusting for the influence of scenario form, the findings showed that lead time had major key effects on scale scores (F(15, 490) = 21.68, p 0.001, partial $n2 = 0.41$) and decreased kinetic energy (F(15, 490) = 28.49, $p.001$, partial2 = 0.47). These results were discovered after the impact of scenario form was taken into account. As the lead time increases, there is a consistent upward trend in both the subjective usefulness of the alarm (i.e., the overall score on the VWUS) and the objective warning utility (i.e., the reduction in kinetic energy), as can be shown in Fig. 5.
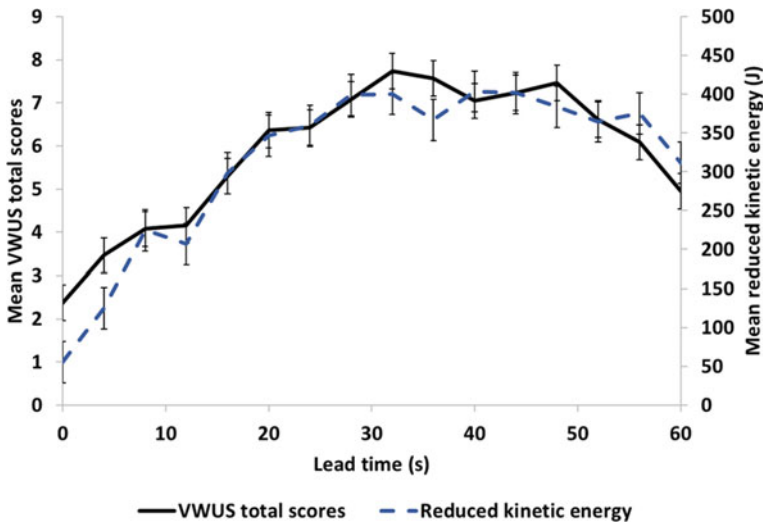
Fig. 5 Changes of VWUS total score and objective warning utility as a function of lead time (error bar: ± 1SE) [59]

There is a statistically significant difference (p 0.05) between the scale scores for warning utility and kinetic decreased energy for the following combinations of lead time levels:

• a lead time of 0 s and lead time levels ranging from 1 to 60 s; • a lead time of 1 s and lead time levels ranging from 2.5 to 60 s; • a lead time of 1.5 s and lead time levels ranging from 3 to 30 s; • a lead time of 1.5 s and lead time levels ranging from 3 to 30 s.

The main distinction in the post hoc experiments was that the scale ratings differed between lead times of the 60 s and lead times of 3–30 s, while the decreased energy differed between lead times of 60 s and lead times of 4–30 s.

5   Discussion

On the basis of our experience with the NASA-TLX development phase, we devised the VWUS in order to investigate the utility of the alert in general. The VWUS consisted of two components: the overall value, which was broken down into four subcategories and used as one component of the scale (these subcategories included Representation of Event Urgency, Time to Display, Alertness, and Accuracy of Understanding), and the weighting of these objects, which was accomplished by measuring them pair by pair based on the value that was perceived to be associated with each pair. According to the VWUS's liability report, the split-half efficiency of their vehicles was exceptional. Because each item in VWUS only had one rating

query, much as in NASA-TLX, we were unable to evaluate the accuracy of the system's internal ratings. On the other side, scales that include multiple questions for each dimension might cause the memory of the alert utility to degrade during the whole of the assessment process, which can lead to ratings that are less accurate and dependable. As a consequence of this, the Verbal Alert Utility Scale that was developed in the present research provides a distinct method to quantify warning effectiveness without creating an excessive amount of memory loss. This is because each rating inquiry in each dimension of the scale was included.

The results of a validation study that was carried out by the State University of New York at Buffalo demonstrated that VWUS was able to assess the effectiveness of an alert in terms of the quantitative protection advantages it offered. According to the results, a higher VWUS score revealed an alert with a greater utility, which had a better probability of minimizing the risk of potentially dangerous situations that may occur while driving activities were being carried out. In both linear and logistic regression investigations, it was shown that the VWUS total scale was a significant factor in determining the objective alert utility measures that were acquired from the experiment. These measurements included reduced kinetic energy and increased collision probability. To be more specific, a higher VWUS score indicated that the existence of the warning may result in a greater drop in kinetic energy and a reduced probability of collision, which implied that the warning was more helpful. Because the accuracy of Hazard Representation was the sole relevant predictor of alarm utility in the current validation experiment, the low R square value mentioned in the second linear regression model with two variables of VWUS as predictors may be due to the fact that this circumstance (see model 2 in Table 5). These results may have a number of potential explanations, one of which is that the independent variable used in the current validation experiment (lead time) was designed to place emphasis on the accuracy of threat representation. In light of the current discussion over alarm alertness levels, more confirmatory studies are necessary.

There has been a major rise in alarm architecture research in order to enhance the secure coordination of different devices utilizing verbal alerts. The topic of alert efficacy has drawn the interest of researchers in order to achieve a secure and successful interaction between human and machine activity. Previous research has shown that subjective assessments of approval and perceived utility do not necessarily correlate with improved driving efficiency when the device is. The scale built in the current study is based on previous work and aims to assess the efficacy of verbal alerts with a focus on driver results. The VWUS allows us to determine if the verbal alerts built into the framework are accurate in improving driver efficiency rather than relying on drivers' individual opinions on the warnings.

The present state of VWUS is focused mostly on verbal alerts. Since all of the measurements in the new edition of the scale are so large, it may even be used to test the effectiveness of nonverbal alarms. Visual alerts are often easier to recognize, hear, and recall than nonverbal warnings. Nonverbal alerts, on the other hand, take longer to reply than verbal warnings, making them a safer option whether the problem is urgent or if the person is prepared to use the alert device. Both forms of alerts may be selected in the system's notification architecture to alert humans to possible

dangers. The relevance of the scale extended to verbal alerts has also been shown in the ongoing validation trial. As a result, further research should be done to confirm its usefulness in evaluating the efficacy of nonverbal alerts in order to broaden its applicability. Meanwhile, the latest validation analysis suggests that the scale should be used to test transportation system alerts. Further, confirmation tests are needed to explore the associations between VWUS and human results in order to prevent the possible dangers of various alerts transmitting in different domains to generalize the testing capacity of VWUS.

A comparison of two ANCOVA experiments on scale scores and decreased kinetic energy was used to measure scale sensitivity. The VWUS scale was shown to be susceptible to improvements in alert efficacy with a 1 s lead time shift. If the lead period varies, changes in subjective alert usefulness (i.e., VWUS overall score) and analytical warning utility (i.e., Reduced Kinetic Energy) adopt a common trend. The sensitivity analysis revealed that the VWUS scale was vulnerable to variations in alert efficacy with as little as a 1 s difference in warning timing. Studies on alert timings found that a 1.5-s difference in nonverbal alerts and a 2.5-s difference in verbal warnings [59] are enough to improve drivers' crash avoidance results. In comparison with previous research, the current scale demonstrated sufficient response to improvements in alert efficacy.

6 Conclusion

Through this article, we developed a standardized technique for dealing with crashes in order to help cars navigate away from crowded places within an ITS. This method can be found in this chapter. First, we designed an accident response system that makes use of the cellular networks for public transit as well as VANETs. This system enables efficient real-time communication with a variety of vehicles, including hospitals, RSUs, and ambulances, as well as central servers. Following that, we propose an algorithm for real-time route planning with the objectives of maximizing the overall efficiency of space utilization and reducing the cost of travel by enabling cars to avoid navigating through busy sections of road. Last but not least, we have shown that the route planning algorithm that we suggested is effective. Finally, we have demonstrated that the algorithm for route planning that we suggest will reduce the amount of time it takes for ambulances to be notified of an accident and sent to the scene by avoiding congested road segments. This will, in turn, increase the likelihood that accident victims will be able to have their lives saved. Based on the findings of the validation study, the Verbal Alert Utility Scale (VWUS), which was developed as part of this investigation, was suggested as a practical instrument for evaluating the usefulness of verbal alerts. It exhibited acceptable levels of reliability and validity. When compared to earlier studies that depended on behavioral testing, the implementation of the scale enables a simpler evaluation of the usefulness of verbal warnings in intelligent transportation networks. This is because prior studies

focused on behavioral testing. Within the context of intelligent transportation, this scale may also be used to evaluate alert settings in order to improve communication.

References

1. Sharma, S.K., Sharma, R.C., Lee, J., Jang, H.-L.: Numerical and experimental analysis of DVA on the flexible-rigid rail vehicle carbody resonant vibration. Sensors **22**, 1922 (2022). https://doi.org/10.3390/s22051922
2. Sharma, S.K., Mohapatra, S., Sharma, R.C., Alturjman, S., Altrjman, C., Mostarda, L., Stephan, T.: Retrofitting existing buildings to improve energy performance. Sustainability **14**, 666 (2022). https://doi.org/10.3390/su14020666
3. Vishwakarma, P.N., Mishra, P., Sharma, S.K.: Characterization of a magnetorheological fluid damper a review. Mater. Today Proc. **56**, 2988–2994 (2022). https://doi.org/10.1016/j.matpr.2021.11.143
4. Vishwakarma, P.N., Mishra, P., Sharma, S.K.: Formulation of semi-active suspension system and controls in rail vehicle. SSRN Electron. J. (2022). https://doi.org/10.2139/ssrn.4159616
5. Sharma, R.C., Sharma, S.K.: Ride analysis of road surface-three-wheeled vehicle-human subject interactions subjected to random excitation. SAE Int. J. Commer. Veh. 15, 02-15-03-0017 (2022). https://doi.org/10.4271/02-15-03-0017
6. Sharma, S.K., Sharma, R.C., Lee, J.: In situ and experimental analysis of longitudinal load on carbody fatigue life using nonlinear damage accumulation. Int. J. DamageMech. **31**, 605–622 (2022). https://doi.org/10.1177/10567895211046043
7. Sharma, S.K., Lee, J., Jang, H.-L.: Mathematical modeling and simulation of suspended equipment impact on car body modes. Machines. **10**, 192 (2022). https://doi.org/10.3390/machines10030192
8. Sharma, S.K., Lee, J.: Crashworthiness analysis for structural stability and dynamics. Int. J. Struct. Stab. Dyn. **21**, 2150039 (2021). https://doi.org/10.1142/S0219455421500395
9. Bhardawaj, S., Sharma, R.C., Sharma, S.K., Sharma, N.: On the planning and construction of railway curved track. Int. J. Veh. Struct. Syst. **13**, 151–159 (2021). https://doi.org/10.4273/ijvss.13.2.04
10. Sharma, R.C., Palli, S., Sharma, N., Sharma, S.K.: Ride behaviour of a four- wheel vehicle using H infinity semi-active suspension control under deterministic and random inputs. Int. J. Veh. Struct. Syst. **13**, 234–237 (2021). https://doi.org/10.4273/ijvss.13.2.18
11. Choi, S., Lee, J., Sharma, S.K.: A study on the performance evaluation of hydraulic tank injectors. In: Advances in Engineering Design: Select Proceedings of FLAME 2020, pp. 183–190. Springer, Singapore (2021). https://doi.org/10.1007/978-981-33-4684-0_19
12. Lee, J., Han, J., Sharma, S.K.: Structural analysis on the separated and integrated differential gear case for the weight reduction. In: Joshi, P., Gupta, S.S., Shukla, A.K., Gautam, S.S. (eds.) Advances in Engineering Design. Lecture Notes in Mechanical Engineering, pp. 175–181 (2021). https://doi.org/10.1007/978-981-33-4684-0_18
13. Sharma, R.C., Sharma, S., Sharma, N., Sharma, S.K.: Linear and nonlinear analysis of ride and stability of a three-wheeled vehicle subjected to random and bump inputs using bond graph and simulink methodology. SAE Int. J. Commer. Veh. 14, 02-15-01-0001 (2021). https://doi.org/10.4271/02-15-01-0001
14. Mohapatra, S., Mohanty, D., Mohapatra, S., Sharma, S., Dikshit, S., Kohli, I., Samantaray, D.P., Kumar, R., Kathpalia, M.: Biomedical application of polymeric biomaterial: polyhydroxybutyrate. In: Bioresource Utilization and Management: Applications in Therapeutics, Biofuels, Agriculture, and Environmental Science, pp. 1–14. CRC Press (2021). https://doi.org/10.21203/rs.3.rs-1491519/v1
15. Sharma, S.K., Sharma, R.C.: Multi-objective design optimization of locomotive nose. In: SAE Technical Paper, pp. 1–10 (2021). https://doi.org/10.4271/2021-01-5053

16. Wu, Q., Cole, C., Spiryagin, M., Chang, C., Wei, W., Ursulyak, L., Shvets, A., Murtaza, M.A., Mirza, I.M., Zhelieznov, К., Mohammadi, S., Serajian, H., Schick, B., Berg, M., Sharma, R.C., Aboubakr, A., Sharma, S.K., Melzi, S., Di Gialleonardo, E., Bosso, N., Zampieri, N., Magelli, M., Ion, C.C., Routcliffe, I., Pudovikov, O., Menaker, G., Mo, J., Luo, S., Ghafourian, A., Serajian, R., Santos, A.A., Teodoro, Í.P., Eckert, J.J., Pugi, L., Shabana, A., Cantone, L.: Freight train air brake models. Int. J. Rail Transp. 1–49 (2021). https://doi.org/10.1080/232 48378.2021.2006808

17. Sharma, S.K., Sharma, R.C., Lee, J.: Effect of rail vehicle-track coupled dynamics on fatigue failure of coil spring in a suspension system. Appl. Sci. **11**, 2650 (2021). https://doi.org/10. 3390/app11062650

18. Sharma, R.C., Sharma, S., Sharma, S.K., Sharma, N., Singh, G.: Analysis of bio-dynamic model of seated human subject and optimization of the passenger ride comfort for three-wheel vehicle using random search technique. Proc. Inst. Mech. Eng. Part K J. Multi-body Dyn. **235**, 106–121 (2021). https://doi.org/10.1177/1464419320983711

19. Bhardawaj, S., Sharma, R.C., Sharma, S.K.: Development in the modeling of rail vehicle system for the analysis of lateral stability. Mater. Today Proc. **25**, 610–619 (2020). https://doi.org/10. 1016/j.matpr.2019.07.376

20. Lee, J., Sharma, S.K.: Numerical investigation of critical speed analysis of high-speed rail vehicle. 한국정밀공학회 학술발표대회 논문집 (Korean Soc. Precis. Eng. 696) (2020)

21. Mohapatra, S., Pattnaik, S., Maity, S., Mohapatra, S., Sharma, S., Akhtar, J., Pati, S., Samantaray, D.P., Varma, A.: Comparative analysis of PHAs production by Bacillus megaterium OUAT 016 under submerged and solid-state fermentation. Saudi J. Biol. Sci. **27**, 1242–1250 (2020). https://doi.org/10.1016/j.sjbs.2020.02.001

22. Palli, S., Sharma, R.C., Sharma, S.K., Chintada, V.B.: On methods used for setting the curve for railway tracks. J. Crit. Rev. **7**, 241–246 (2020)

23. Sharma, S.K., Lee, J.: Design and development of smart semi active suspension for nonlinear rail vehicle vibration reduction. Int. J. Struct. Stab. Dyn. **20**, 2050120 (2020). https://doi.org/ 10.1142/S0219455420501205

24. Leontiadis, I., Marfia, G., Mack, D., Pau, G., Mascolo, C., Gerla, M.: On the effectiveness of an opportunistic traffic management system for vehicular networks. IEEE Trans. Intell. Transp. Syst. **12**, 1537–1548 (2011). https://doi.org/10.1109/TITS.2011.2161469

25. Regan, M.A., Mitsopoulos, E., Haworth, N.L., Young, K.L.: Acceptability of in-vehicle intelligent transport systems to victorian car drivers. In: Medicine (2002)

26. Bhardawaj, S., Sharma, R., Sharma, S.: Ride analysis of track-vehicle- human body interaction subjected to random excitation. J. Chinese Soc. Mech. Eng. **41**, 237–236 (2020). https://doi. org/10.29979/JCSME

27. Bhardawaj, S., Sharma, R.C., Sharma, S.K.: Analysis of frontal car crash characteristics using ANSYS. Mater. Today Proc. **25**, 898–902 (2020). https://doi.org/10.1016/j.matpr.2019.12.358

28. Acharya, A., Gahlaut, U., Sharma, K., Sharma, S.K., Vishwakarma, P.N., Phanden, R.K.: Crashworthiness analysis of a thin-walled structure in the frontal part of automotive chassis. Int. J. Veh. Struct. Syst. **12**, 517–520 (2020). https://doi.org/10.4273/ijvss.12.5.06

29. Sharma, R.C., Sharma, S.K., Palli, S.: Linear and non-linear stability analysis of a constrained railway wheelaxle. Int. J. Veh. Struct. Syst. **12**, 128–133 (2020). https://doi.org/10.4273/ijvss. 12.2.04

30. Sharma, S., Sharma, R.C., Sharma, S.K., Sharma, N., Palli, S., Bhardawaj, S.: Vibration isolation of the quarter car model of road vehicle system using dynamic vibration absorber. Int. J. Veh. Struct. Syst. **12**, 513–516 (2020). https://doi.org/10.4273/ijvss.12.5.05

31. Bhardawaj, S., Sharma, R.C., Sharma, S.K.: Development of multibody dynamical using MR damper based semi-active bio-inspired chaotic fruit fly and fuzzy logic hybrid suspension control for rail vehicle system. Proc. Inst. Mech. Eng. Part K J. Multi-body Dyn. **234**, 723–744 (2020). https://doi.org/10.1177/1464419320953685

32. Sharma, R.C., Sharma, S., Sharma, S.K., Sharma, N.: Analysis of generalized force and its influence on ride and stability of railway vehicle. Noise Vib. Worldw. **51**, 95–109 (2020). https://doi.org/10.1177/0957456520923125

33. Sharma, S.K., Lee, J.: Finite element analysis of a fishplate rail joint in extreme environment condition. Int. J. Veh. Struct. Syst. **12**, 503–506 (2020). https://doi.org/10.4273/ijvss.12.5.03
34. Sharma, S.K., Phan, H., Lee, J.: An application study on road surface monitoring using DTW based image processing and ultrasonic sensors. Appl. Sci. **10**, 4490 (2020). https://doi.org/10.3390/app10134490
35. Sharma, R.C., Sharma, S.K., Sharma, N., Sharma, S.: Analysis of ride and stability of an ICF railway coach. Int. J. Veh. Noise Vib. **16**, 127 (2020). https://doi.org/10.1504/IJVNV.2020.117820
36. Sharma, S.K., Sharma, R.C., Sharma, N.: Combined multi-body-system and finite element analysis of a rail locomotive crashworthiness. Int. J. Veh. Struct. Syst. **12**, 428–435 (2020). https://doi.org/10.4273/ijvss.12.4.15
37. Goswami, B., Rathi, A., Sayeed, S., Das, P., Sharma, R.C., Sharma, S.K.: Optimization design for aerodynamic elements of Indian locomotive of passenger train. In: Advances in Engineering Design, pp. 663–673. Lecture Notes in Mechanical Engineering. Springer, Singapore (2019). https://doi.org/10.1007/978-981-13-6469-3_61
38. Choppara, R.K., Sharma, R.C., Sharma, S.K., Gupta, T.: Aero dynamic cross wind analysis of locomotive. In: IOP Conference Series: Materials Science and Engineering, p. 12035. IOP Publishing (2019).
39. Sharma, S.K.: Multibody analysis of longitudinal train dynamics on the passenger ride performance due to brake application. Proc. Inst. Mech. Eng. Part K J. Multi-body Dyn. **233**, 266–279 (2019). https://doi.org/10.1177/1464419318788775
40. Goyal, S., Anand, C.S., Sharma, S.K., Sharma, R.C.: Crashworthiness analysis of foam filled star shape polygon of thin-walled structure. Thin-Walled Struct. **144**, 106312 (2019). https://doi.org/10.1016/j.tws.2019.106312
41. Bhardawaj, S., Chandmal Sharma, R., Kumar Sharma, S.: Development and advancement in the wheel-rail rolling contact mechanics. IOP Conf. Ser. Mater. Sci. Eng. **691**, 012034 (2019). https://doi.org/10.1088/1757-899X/691/1/012034
42. Bhardawaj, S., Chandmal Sharma, R., Kumar Sharma, S.: A survey of railway track modelling. Int. J. Veh. Struct. Syst. **11**, 508–518 (2019). https://doi.org/10.4273/ijvss.11.5.08
43. Sharma, S.K., Saini, U., Kumar, A.: Semi-active control to reduce lateral vibration of passenger rail vehicle using disturbance rejection and continuous state damper controllers. J. Vib. Eng. Technol. **7**, 117–129 (2019). https://doi.org/10.1007/s42417-019-00088-2
44. Sinha, A.K., Sengupta, A., Gandhi, H., Bansal, P., Agarwal, K.M., Sharma, S.K., Sharma, R.C., Sharma, S.K.: Performance enhancement of an all-terrain vehicle by optimizing steering, powertrain and brakes. In: Advances in Engineering Design, pp. 207–215 (2019). https://doi.org/10.1007/978-981-13-6469-3_19
45. Sharma, S.K., Sharma, R.C.: Pothole detection and warning system for Indian roads. In: Advances in Interdisciplinary Engineering. pp. 511–519 (2019). https://doi.org/10.1007/978-981-13-6577-5_48.
46. Sharma, S.K., Kumar, A.: Ride comfort of a higher speed rail vehicle using a magnetorheological suspension system. Proc. Inst. Mech. Eng. Part K J. Multi- body Dyn. **232**, 32–48 (2018). https://doi.org/10.1177/1464419317706873
47. Palli, S., Koona, R., Sharma, S.K., Sharma, R.C.: A review on dynamic analysis of rail vehicle coach. Int. J. Veh. Struct. Syst. **10**, 204–211 (2018). https://doi.org/10.4273/ijvss.10.3.10
48. Sharma, R.C., Sharma, S.K., Palli, S.: Rail vehicle modelling and simulation using lagrangian method. Int. J. Veh. Struct. Syst. **10**, 188–194 (2018). https://doi.org/10.4273/ijvss.10.3.07
49. Noyes, J.M., Hellier, E., Edworthy, J.: Speech warnings: a review. Theor. Issues Ergon. Sci. **7**, 551–571 (2006). https://doi.org/10.1080/14639220600731123
50. Sharma, S.K., Kumar, A.: Impact of longitudinal train dynamics on train operations: a simulation-based study. J. Vib. Eng. Technol. **6**, 197–203 (2018). https://doi.org/10.1007/s42417-018-0033-4
51. Sharma, R.C., Sharma, S.K.: Sensitivity analysis of three-wheel vehicle's suspension parameters influencing ride behavior. Noise Vib. Worldw. **49**, 272–280 (2018). https://doi.org/10.1177/0957456518796846

52. Sharma, S.K., Kumar, A.: Impact of electric locomotive traction of the passenger vehicle Ride quality in longitudinal train dynamics in the context of Indian railways. Mech. Ind. **18**, 222 (2017). https://doi.org/10.1051/meca/2016047

53. Sharma, S.K., Kumar, A.: Ride performance of a high speed rail vehicle using controlled semi active suspension system. Smart Mater. Struct. **26**, 055026 (2017). https://doi.org/10.1088/1361-665X/aa68f7

54. Khalifa, M., Shaat, A., Ibrahim, S.: Optimum concrete filling ratio for partially filled noncompact steel tubes. Thin-Walled Struct. **134**, 159–173 (2019). https://doi.org/10.1016/j.tws.2018.10.011

55. Balaji, G., Annamalai, K.: Numerical investigation of honeycomb filled crash box for the effect of honeycomb's physical parameters on crashworthiness constants. Int. J. Crashworthiness. **24**, 184–198 (2019). https://doi.org/10.1080/13588265.2018.1424298

56. Wang, Z., Li, Z., Shi, C., Zhou, W.: Mechanical performance of vertex-based hierarchical vs square thin-walled multi-cell structure. Thin-Walled Struct. **134**, 102–110 (2019). https://doi.org/10.1016/j.tws.2018.09.017

57. Rabiee, A., Ghasemnejad, H.: Lightweight design to improve crushing behaviour of multi-stitched composite tubular structures under impact loading. Thin-WalledStruct. **135**, 109–122 (2019). https://doi.org/10.1016/j.tws.2018.11.002

58. Wang, S., Peng, Y., Wang, T., Che, Q., Xu, P.: Collision performance and multi-objective robust optimization of a combined multi-cell thin-walled structure for high speed train. Thin-Walled Struct. **135**, 341–355 (2019). https://doi.org/10.1016/j.tws.2018.10.044

59. Zhang, Y., Wu, C., Qiao, C., Sadek, A., Hulme, K.F.: Addressing the safety of transportation cyber-physical systems: development and validation of a verbal warning utility scale for intelligent transportation systems. Math. Probl. Eng. **2015**, 1–13 (2015). https://doi.org/10.1155/2015/126947

60. Laughery, K.R.: Safety communications: warnings. Appl. Ergon. **37**, 467–478 (2006). https://doi.org/10.1016/j.apergo.2006.04.020

61. Shackel, B.: Usability—context, framework, definition, design and evaluation. Interact. Comput. **21**, 339–346 (2009). https://doi.org/10.1016/j.intcom.2009.04.007

62. Sadiq, A.S., Khan, S., Ghafoor, K.Z., Guizani, M., Mirjalili, S.: Transmissionpower adaption scheme for improving IoV awareness exploiting: evaluation weighted matrix based on piggybacked information. Comput. Networks. **137**, 147–159 (2018). https://doi.org/10.1016/j.comnet.2018.03.019

63. Sharma, S.K., Sharma, R.C., Choi, Y., Lee, J.: Experimental and Mathematical Study of Flexible–Rigid Rail Vehicle Riding Comfort and Safety. Appl. Sci. **13**, 5252 (2023). https://doi.org/10.3390/app13095252

64. Sharma, R.C., Palli, S., Sharma, S.K.: Ride analysis of railway vehicle considering rigidity and flexibility of the carbody. J. Chinese Inst. Eng. **46**, 355–366 (2023). https://doi.org/10.1080/02533839.2023.2194918

Framework for Digital Supply Chains and Analysis of Impact of Challenges on Implementation of Digital Transformation

Karthik V. N. P. Perla and Rakesh Chandmal Sharma

Abstract Digital transformation in a supply chain can have far-reaching payoffs ensuring a smoother interface among all the stakeholders for seamless delivery. A Digital Supply Chain is an efficient way to leverage new methods to deal with changing customer expectations and importance of visibility across the supply chain. Recent literature discusses the importance of Digital Supply Chain and its applications. This paper aims at developing a framework for future research and practice. Interpretive structural modelling is used in this paper to create a hierarchical structural model that demonstrates the mutual dependency of the challenges in implementing digital transformation across supply chains. These challenges are graphically represented based on their driving force and dependency using cross-impact matrix multiplication applied to classification analysis.

Keywords Supply chain · Digital · Mobile · Company

1 Introduction

Personal computers, advanced television units, smartphones, and mobile devices have transformed how the exchange of information is possible. Technology has changed the way of communication between people and their interaction with the environment. New trends in the industry are being affected by the advancement of technology, and logistics and supply chain are no exception to that. Several operational activities like delivery of goods, production, and customer service are outsourced by firms to other companies. Traditional supply chains comprise physical assets and

K. V. N. P. Perla
Grasim Industries Limited, Mumbai, India

School of Engineering and Applied Sciences, National Rail and Transportation Institute, Vadodara, India

R. C. Sharma (✉)
Mechanical Engineering Department, Graphic Era (Deemed to be University), Dehradun, India
e-mail: rcsharmaiitr@gmail.com

facilities which are scattered geographically to maintain and form transportation networks between assets and facilities. A supply chain is usually defined as a series of interlinked activities which are planning, coordinating, and controlling products and services between the customers and suppliers [1–5].

Around 26 billion IoT environments are to become operational which would cause a disruptive transformation across the globe affecting industries, generating value, and increasing network efficiency. It is not impossible soon when people may even be able to dispatch fleets of vehicles with a handheld device. It would also be possible to find a particular container's contents with just a brief electronic glance [6].

Organizations have become more aware of such potential advancements and emphasize the importance of how the Digital Supply Chain (DSC) can add value to the business. Since organizations aim to hold control and develop their core functionalities, organizations should interact with the stakeholders such as dealers through DSC processes for manufacturing and delivering their products and services [7–12]. The potential of DSCs is yet to be realized despite that it has set the industry onto a path of change and innovation.

The relevance of DSC has been highlighted in recent literature, and many industrial researchers have discussed its implementations [9–13]. Determining all possible benefits of various DSC applications is a time-consuming process since the majority of the benefits are extracted from the multiple solutions that emerge from DSC applications, rather than the DSC itself. DSC integration can impact supply chains and logistics in a variety of ways, which are discussed throughout this paper. The study also considers DSC's consequences and inferences, as well as obstacles and success factors. This analysis of the literature aims to address the question, "How can the current value of digitalization be integrated into traditional existing supply chains?".

The answer to that question is a design of a framework that can be used in the detection, realization, and evaluation of benefits DSC can bring about. These discussions often include component similarities and differences, as well as their relationship to the problem statement, DSC technology implications and inferences, obstacles, and success factors [7, 8, 14–17]. A framework is required for the detection, realization, and assessment of DSC. Since critical organizational transformations and their management are often ignored or delayed, many benefits of digitization in supply chains remain undiscovered. Several approaches to evaluating possible DSC possibilities have been proposed by academic and industrial researchers, but little research has been done on how to construct a full conceptual or theoretical DSC system [18–23]. In this context, this research proposes a structure for capturing, presenting, and relating digitization in supply chains.

The key challenge of implementing and checking DSC is to define its essential stages, which is not only crucial for supply chains to handle and operate better, but also necessary for a standard supply chain to be digitized. The challenges mentioned in this article have an influence not only on the implementation of DSC, but also on one another. As a consequence, it is critical to examine how these barriers interact with one another. A detailed assessment of the impediments to DSC implementation, as

well as their interconnectedness, will provide decision-makers with critical information. The interpretative structural modelling approach is excellent for identifying and developing connections between variables. This study discusses the barriers to DSC based on current research and the perspectives of professionals from different businesses and academics. The interpretive structural modelling approach is then used to propose a systemic model that shows how they communicate, giving managers insights into how to prioritize their implementation efforts.

2 Literature Review

Although, in literature, there is no specific way to describe the concept of digital transformation. Some papers describe about specific technologies as an "organizational shift to big data analytics", while others focus on technology in general as the key factor of profound change.

> Digital Transformation is the result of change enabled by Information Technology which is aligned with the goals of the organization and is driven by a planned strategy. There is a cultural and technological shift due to this transformation while leveraging the technology which adds value-creating new business opportunities and models. It is generally a long-term process that requires a well-planned strategy and is implemented on a fundamental basis throughout the entire organization.

The term "digital transformation" refers not only to changes in technology but also to the effects of those changes on the enterprise as a whole. It causes "primary business activities to alter, as well as products and procedures, organizational structures, and management principles". People, culture, connectivity, and the entire industry are all affected by the changes brought about by digitization. Many of the innovations that affect digital transformation aren't brand new [24–28]. "Combinations of information, computation, communication, and networking technologies" are the focus of the innovation. Many academicians and professionals, on the other hand, see digitalization as having beneficial results [1, 4, 6, 29–34]. Professionals and academicians recognize the many advantages that result in increased revenue and efficiency as a result of new ways of creating value and interacting with consumers and suppliers. Furthermore, researchers believe that digital transformation has a positive impact because it stimulates job growth [35–39].

Despite the benefits of digital transformation, an increasing number of researchers is observing its negative consequences. Employees will be laid off in mostly low-order positions as a result of digital systems and increased use of industrial robots [40–44]. Additionally, threats to companies include cybersecurity threats and unregulated or erroneous data. The diverse landscape of interfaces and integration requirements is a challenge for businesses in all industries, i.e. railway, automobiles, etc. Nonetheless, there are strong aspirations for digital transformation. Researchers from various fields contribute to the ongoing evolution of digital transformation, its threats, and potential uses [45–48].

These possible drawbacks are summarized in the following segment:

- The period for the literature reviewed was from 2002 to 2017. Although the results are not exhaustive, the results are systematic since the results cover a large number of highly regarded scholarly journals.
- The DSC architecture depicted aims to deploy digitalization, technology deployment, and supply chain management integration. Further decomposition of the DSC model was left out because it is beyond the scope of this review.

In a DSC world, there aren't enough resources and technology to deal with supply chain issues [49–52]. Choices in the sense of a DSC necessitate innovative technologies that account for digitalization environments, such as the abundance of big data produced by Sensor Technology [53–58] and the Internet of Things [59–65]. Maintenance, efficiency [66–70], management of inventory [71–75], production planning [76, 77], and procurement [78–80] are only a few of the problems that will be impacted by digital transformation [81–85]. From both a managerial and technical perspective, there are many obstacles to digital transformation. There is a huge shift taking place across the world. Companies are on the verge of a DSC transformation competition [86–91]. Measurement of the entire supply chain's output may be fruitful in improving productivity. As a result, the DSC problems and issues discussed earlier in the report can be solved using success factors extracted from published literature about digital transformation.

3 Framework to Digitally Transform the Supply Chain

A framework is necessary to guide in developing a DSC that will enhance the efficiency compared to a tradition supply chain. There could be multiple and specific path of various industries and entities which depends on the objective or the reason why an organization wants to digitally transform its supply chain. The following sections discuss about a generalized and a basic structure for developing a DSC.

3.1 Pre-requisites

Successful supply chains have a strong vision and use structures and roadmaps to chart their course. The existing literature is divided into three stages, each with its sub-goals. This literature is then used to create a path, which paves the way for the digital transformation of a supply chain. Figure 1 depicts the path in a visual structure.

Supply chains are rapidly becoming an important part of decision-making and strategy development as a result of digital transformation. Organizations can use and improve DSC to supplement various aspects of their strategy and more efficiently target their unique needs in this way.

The problem of implementing and verifying a digitization framework in a traditional supply chain. As a result, the primary decomposition has been established.
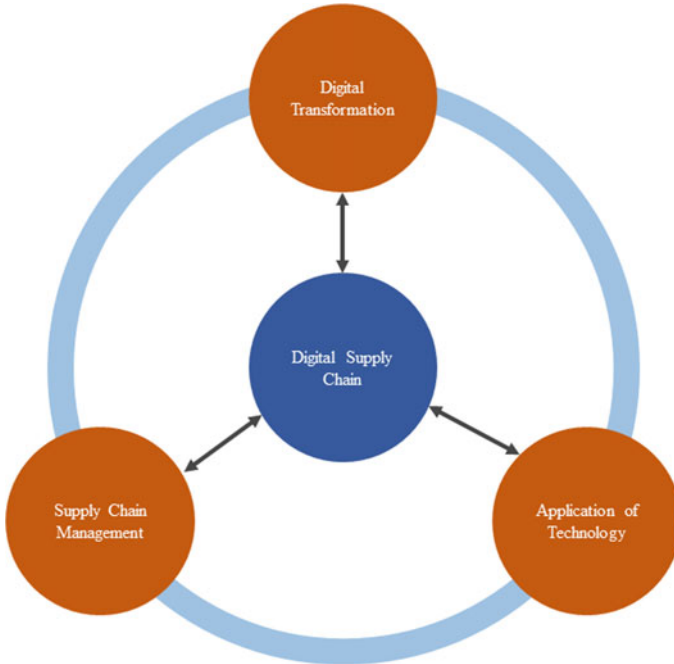
Fig. 1 Framework for development of DSC

Each supply chain will have its collection of digital transformation goals and priorities. The main desired digital assessment goals for supply chains also overlap the domains of digitalization, technology implementation, and supply chain management, which are critical steps for organizational alignment.

Most supply chain managers will be familiar with the basic DSC methodology after using this framework: evaluating the supply chain's current digitalization state, building a vision for technology adoption, and creating a supply chain management transition road map in a DSC context. The nature of technology integration in a conventional supply chain is the elaboration of these regions, their decompositions, and the creation of their structure.

3.2 Digitalization

Digitally transforming a supply chain does not necessitate the use of cutting-edge technology. It's all about aligning digital strategies with supply chain goals and implementing a digital approach to unlock the potential of existing tools and capabilities, resulting in improved results.
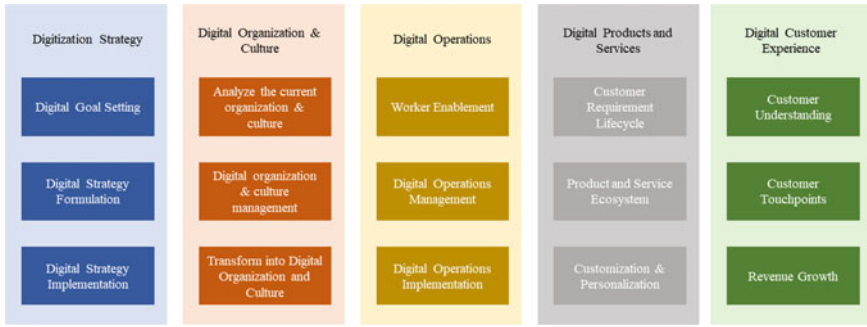
Fig. 2 Decomposed framework for the digitization of supply chain

Supply chains must have clarity about their digitization policies and concentrate on enhancing their digitalization capabilities. It is critical not only to survive but also to benefit from the digitization megatrend. Further breaking down the digitalization stage, which begins with the digitalization strategy, the first step is to create a digitalization strategy that outlines the organization's objectives and goals.

A successful digitalization process can be broken down into five distinct subgoals, each of which represents a stage in the digitization process. The goals are dependent on the efficient implementation of these methods. Figure 2 depicts the process for the digitalization of a supply chain.

The digitalization strategy is a critical move. If supply chains lack critical strategic tools, organizations would be primarily focused on resolving current issues. As a result, organizations are unable to provide consistent gains to their stakeholders. However, most supply chains lack a consistent digital strategy. Given that digital technology is rapidly intertwined into the very structure of most enterprises and institutions, this situation has created an unstable situation for many supply chains. New digital innovations offer a chance to improve how supply chains compete and lay the groundwork for outperforming competitors close and far.

Digitalization is divided into

- Digital Goal Setting is a crucial phase in the digitization process since it determines what the digital plan needs to accomplish and distinguishes what's important from what's meaningless or a diversion.
- The Digital Strategy Formulation process is the method of choosing the best-fitting target in realizing supply chains' objectives and thereby achieving their vision
- The Digital Strategy Implementation focuses on the whole supply chain, answering the questions of "how, where, where, and who" to achieve the desired aims and targets.

Digitalization has three more areas: Organizations and Culture, Operations, and Products and Services. Then customers, to improve service levels and the experience of the customer to know customers better. When all digital-thinking individuals and

organizations come together, they will achieve shared wisdom on digitalization. This is defined as Digital Organizations and Culture.

Consumers are being digitized these days and are demanding new digital goods and services every day. First and foremost, C-suite executives must comprehend and comprehend the concept of change. Digital managers and workers must be promoted by executives who identify their organizations' digital vision, mission, planning, and goals.

Organizational culture plays a significant role in its adaptability while transformation. If the existing culture opposes the change, the outcome would be a fragmented company, with one part moving forward and the other sticking to the conventional past, causing transition delays.

The first step is to evaluate the existing state of the organization and society in terms of digitalization. Following the completion of this study, digitalization must be controlled and completely converted into a DSC. Change happens at an incredible rate in today's digital world. To stay ahead of the competition, supply chains must examine and reconsider their organizational structure.

If businesses cannot keep up with and adapt quickly enough, businesses will lose to rivals. Implementing a digital organization strategy and initiating the digital evolution earlier rather than later, as well as developing a digital organizational framework are critical. Supply chains can build their digital vision, create new digital organizational models, and determine acquisition strategies for the required skill set of digitalization based on this foundation.

To achieve digital transformation, a few important things must happen. Advanced digital solutions, such as big data, cloud computing, and IoT or Sensor Technology, can help supply chain processes grow in a variety of ways. Big data, for example, can help in-bound logistics operate more smoothly by monitoring the exchange of goods and services; cloud computing can aid in the creation of standard business processing platforms, and mobile technology can allow people to work anywhere, and on any machine.

Digital operations stage: supply chains should be able to grow at the same rate as the rest of the organization and react more quickly to constant, immediate, and prompt changes. Worker Enablement is the personal virtualization of work. It differentiates the work process from the work site. Workers may now engage with clients or colleagues without meeting in person or visiting any places, thanks to the widespread use of email and other digital communication and collaboration technologies.

Digital Operations Management provides managers with greater knowledge of a particular product, area, and customers, allowing choices to be made based on real data rather than assumptions. It allows you to compare status across multiple areas and change capacities, allowing you to make smart decisions on how to handle and prioritize results. The implementation of a digital operations plan varies from the management of operations.

Structure and System Implementation and Track and Improve Implement Operations are two viewpoints on executing operations strategy. This creates a productive collection of operational strategies. Employees and operations management is not

the same as implementing operations. Digital activities have reached their conclusion. Almost every good supply chain has prioritized innovative digital products and services. Simultaneously, the presence of digitalization everywhere expands service design activities. This surge of new Services and Products has altered the pace and function of the consumer experience. Customer Requirement Lifecycle, Product & Service Ecosystem, and Customization & Personalization are all parts of this phase.

Digital goods and services fill the gap in long-term service experience and ultimately expand the lifespan of the customer relationship. The second feature is that digital services or goods are intertwined with other services and products to make them more viable. As a result, services and goods become a part of a larger set of services and brand interactions.

Personalization and customization are the foundations of new digitally enhanced goods and services. This allows for the delivery of exclusive experiences to the masses. It's not a guessing game when it comes to the Digital Customer Experience. Executives would only be able to build a DSC if executives understand the clients, their habits, personalities, and desires.

Digitally transforming the supply chain also requires changing the whole customer experience. Exploration of social media in understanding customer frustration and fulfilment, use of digital media for brand promotion, online community building to build client loyalty, development of products that enhance branding in lifestyle communities, structuring technical expertise to learn more about customers in-depth, using technology to improve communication during in-person sales are just a few examples of how this transformation is affecting customer experience.

Companies are beginning to take complete benefit of previous framework investments to gain a deep understanding of analytics-based market segments, consumer segments, relevant geographies, and socially educated information through customer understanding. Increasing revenues show how businesses are using technology to boost in-person sales conversations, improve predictive marketing, and optimize customer processes. Customer touchpoints are areas where digital initiatives, customer engagement, cross-channel coherence, and self-service can significantly improve an organization's services.

3.3 Technology Implementation

Since this target focuses on the efficient implementation acquired by the DSC efforts, the technology implementation process varies from the Digitization process. Technology enablers are used in this phase.

These core technologies, some of which are mature and others that are still in development, now serve as the fundamental building blocks for the modern supply chain ecosystem. Shortly, taking a holistic view of all of these enablers will help optimize market benefits and unlock new sources of value. Bringing technological transition into a company comes with its own set of challenges.

Supply chains must adopt the most cutting-edge creative technologies to maintain their competitive advantage and gain entry into new markets in a market that is constantly powered by technological enablers. The process of keeping supply chains updated is evolving, but it does take time. As a result, it divides into Management Process, Human-Technology Relationships, Technology Infrastructure Creation, and Technology Enablers. These objectives are the cornerstones of a successful technology implementation strategy. The decomposed architecture for the digital transformation of a supply chain also includes project management, as shown in Fig. 2.

During the transformation phase, any methodology should provide a thorough overview of which tasks must be completed and which equipment must be purchased. This advanced planning aids a supply chain in anticipating costs, avoiding delays, and minimizing work process disruptions caused by previous technologies. Teamwork may also be beneficial to employees during implementation and assessment.

Another objective of a successful technology delivery process is the human–technology partnership. People and technology are inextricably linked. Technology has evolved as a result of human evolution, allowing humans to become more adaptable. People need social connections to survive, and technology plays a major role in this. Human reliance on technology is increasing at a breakneck pace. The way humans communicate will be dominated by technology soon.

If the workforce is not adequately trained to operate and manage new resources, using novel technical means could be counterintuitive. As a result, adequate human and technological preparation and adaptation is a top priority. To be successful, the human–technology partnership should also involve intermediate objectives such as user training, engagement, and coordination.

About every new technology introduces a new range of threats as well as new forms of weaknesses. These considerations should be factored into the technology implementation process, which should outline the steps required to develop the infrastructure for the specific technology. The design of the infrastructure will also help identify the technical requirements and goals during the development process. The formation of technology infrastructure is particularly crucial for any supply chain seeking to take the next step in its digital transformation by taking the necessary measures. If a company wants to move beyond survival mode and move ahead towards being a large, profitable company, it will need to invest in technology infrastructure.

The final goal in the implementation process of technology is identifying the technology enablers. Enablers may be necessary to achieve the goals of the organization's plan, allow implementation within a reasonable timeframe, or find other means for the latest innovative niche, depending on the nature of the organization. Following the determination of desired requirements, the basic strategy for achieving the desired goals must be specified.

4   Framework and Methodology

This section gives a comprehensive description of a methodology for the analysis in Sect. 5 on the basement of obstacles affecting the implementation of digital transformation in a supply chain (Fig. 3).
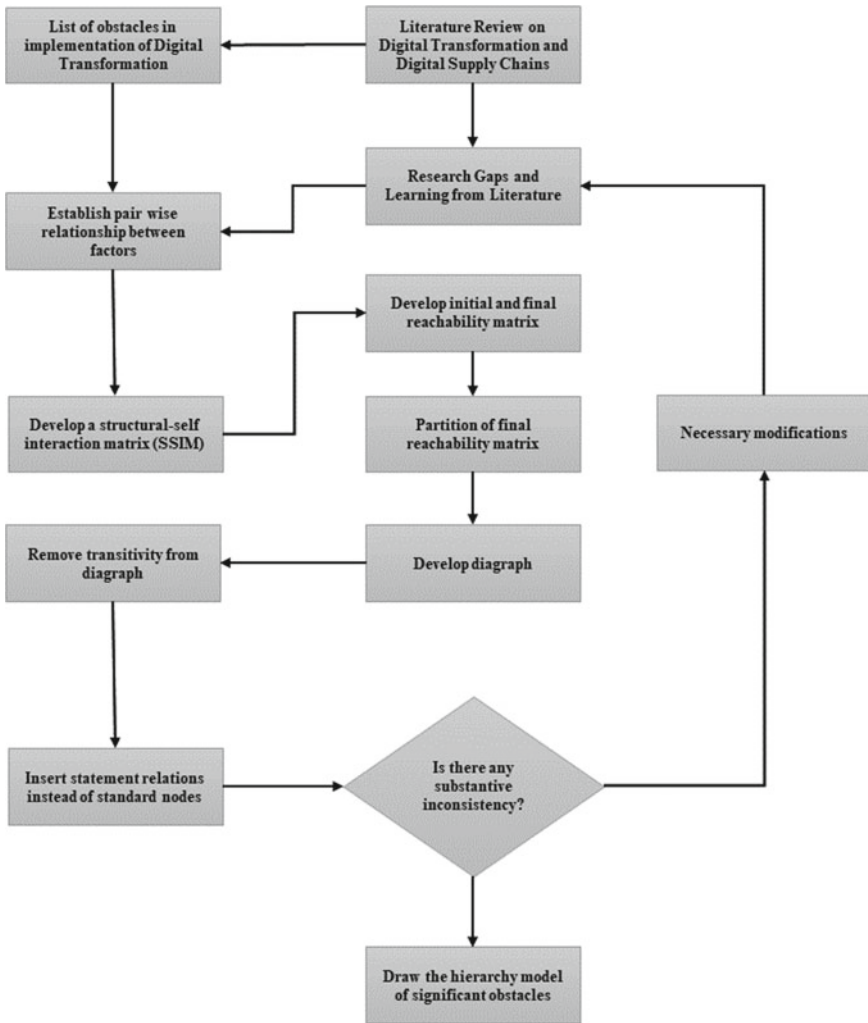
Fig. 3 Methodology for the analysis

5 Application of Interpretive Structural Modelling for the Obstacles of Digital Transformation of a Supply Chain

Step 1: The variables must be identified and defined.

The obstacles of the DSC are used as modelling elements in this analysis. Twelve obstacles have been established based on DSC's current literature and the opinions of experts from various industries and academia.

The 12 challenges selected from literature review are shown in Fig. 4.

Step 2: Understanding the background relationship between variables.

Following the selection of the obstacles, literature and its views are taken into account when deciding the contextual relationship of each pair. It is decided to use a contextual relationship of the form "influence" (e.g., obstacle i influences obstacle j). Four symbols reflect the path of relation between different obstacles i and j:

- "V" shows the direction of relation from i to j;
- "A" shows the direction of relation from j to i;
- "X" shows the bi-directional relation between i and j; and
- "O" shows i and j are not related.

Step 3: Formulation of a Structural Self-Interaction Matrix (SSIM).

The Structural Self-Interaction Matrix, which represents the pairwise relationship among the defined obstacles, is created after determining the contextual relationship between the obstacles. It is often discussed with experts in order to obtain their approval. Table 1 displays the SSIM.

Step 4: Creation of a reachability matrix.

Fig. 4 Challenges selected from literature review

Table 1 Structural self-interaction matrix

Obstacles	1	2	3	4	5	6	7	8	9	10	11	12
C1		V	V	O	O	O	O	X	O	V	V	O
C2			X	X	A	V	O	A	O	A	O	O
C3				V	V	V	O	A	O	X	O	O
C4					O	X	O	O	A	O	O	O
C5						O	V	A	O	A	A	O
C6							V	A	V	V	A	V
C7								A	A	O	A	O
C8									V	V	V	V
C9										V	A	V
C10											X	O
C11												O
C12												

This move entails creating an initial reachability matrix (Table 2) using Structural Self-Interaction Matrix (Table 1). All of the aspects of Structural Self-Interaction Matrix are replaced with binary digits to create the matrix (i.e. 1 and 0).

Table 3 contains the rules for this replacement. In this matrix, the transitivity rule is also tested, i.e. if "1st obstacle relates to 2nd obstacle" and "2nd obstacle relates to 3rd obstacle," "1st obstacle necessarily relates to 3rd obstacle". After applying the transitivity rules in the initial matrix (given in Table 4), the final matrix is formed.

Step 5: Partition levels are determined by partitioning the reachability matrix.

Table 2 Initial reachability matrix

Obstacles	1	2	3	4	5	6	7	8	9	10	11	12
C1	1	1	1	0	0	0	0	1	0	1	1	0
C2	0	1	1	1	0	1	0	0	0	0	0	0
C3	0	1	1	1	1	1	0	0	0	1	0	0
C4	0	1	0	1	0	1	0	0	0	0	0	0
C5	0	1	0	0	1	0	1	0	0	0	0	0
C6	0	0	0	1	0	1	1	0	1	1	0	1
C7	0	0	0	0	0	0	1	0	0	0	0	0
C8	1	1	1	0	1	1	1	1	1	1	1	1
C9	0	0	0	1	0	0	1	0	1	1	0	1
C10	0	1	1	0	1	0	0	0	0	1	1	0
C11	0	0	0	0	1	1	1	0	1	1	1	0
C12	0	0	0	0	0	0	0	0	0	0	0	1

Table 3 Transformation rule

If the (i, j)th element of SSIM is	Corresponding substitution in the initial matrix	
	(i, j)	(j, i)
V	1	0
A	0	1
X	1	1
O	0	0

The reachability and antecedent set of each obstacle are given in the final matrix. The reachability set of an obstacle is made up of the obstacle and the obstacles that are affected by it, while the antecedent set is made up of the obstacle and the obstacles that might affect it. Any column in the row of the obstacle under investigation is part of the reachability range.

The antecedent collection, on the other hand, contains any row with a "1" in the column of the obstacle under observation. The intersection set is then generated by combining the antecedent and reachability sets. At the first step, the obstacles for which the intersection and reachability sets match will be considered. In subsequent iterations, the obstacles that appear in the first stage are removed. Similarly, the level partition is repeated until each obstacle's level is determined as given in Table 5. In the hierarchical model, the first-level obstacles will take the top spot (Fig. 5).

Step 6: Constructing the digraph.

Using the partition levels and the final reachability matrix, the digraph is formed. The obstacles and relationships between them are represented by nodes and arrows, respectively. In digraph, only the transitive links whose meaning is critical are represented. Figure 6 shows a digraph with essential transitive relations.

Step 7: Creating a model focused on interpretive structural modelling.

By replacing the nodes with the perception of obstacles, an interpretive structural modelling for DSC obstacles is created. Figure 7 depicts the final interpretive structural modelling-based design for DSC obstacles.

6 Cross-Impact Matrix Multiplication Applied to Classification (MICMAC) Analysis

Because there are a lot of variables in a structure, there are two ways to look at how they interact: direct relationship analysis and indirect relationship analysis using matrix multiplication properties.

By evaluating the direct relationships in the final ISM, a direct relationship matrix "A" (Table 5) is obtained in direct relationship analysis. In this matrix, the transitive relationships are ignored, and the diagonal elements are set to zero. The motivating force of an obstacle is calculated by multiplying the number of "1" entries in the row

Table 4 Level partitioning of reachability matrix

Obstacles	Reachability set	Antecedent set	Intersection set	Level
Integration 1				
1	{1,2,3,4,5,6,7,8,9,10,11,12}	{1,8}	{1,8}	
2	{2,3,4,5,6,7,9,10,12}	{1,2,3,4,5,6,8,9,10,11}	{2,3,4,5,6,9,10}	
3	{2,3,4,5,6,7,9,10,11,12}	{1,2,3,4,5,6,8,9,10,11}	{2,3,4,5,6,9,10,11}	
4	{2,3,4,6,7,9,10,12}	{1,2,3,4,5,6,8,9,10,11}	{2,3,4,6,9,10}	
5	{2,3,4,5,6,7}	{1,2,3,5,6,8,9,10,11}	{2,3,5,6}	
6	{2,3,4,5,6,7,9,10,11,12}	{1,2,3,4,5,6,8,9,10,11}	{2,3,4,5,6,9,10,11}	
7	{7}	{1,2,3,4,5,6,7,8,9,10,11}	{7}	1
8	{1,2,3,4,5,6,7,8,9,10,11,12}	{1,8}	{1,8}	
9	{2,3,4,5,6,7,9,10,11,12}	{1,2,3,4,6,8,9,10,11}	{2,3,4,6,9,10,11}	
10	{2,3,4,5,6,7,9,10,11,12}	{1,2,3,4,6,8,9,10,11}	{2,3,4,6,9,10,11}	
11	{2,3,4,5,6,7,9,10,11}	{1,3,6,8,9,10,11}	{3,6,9,10,11}	
12	{12}	{1,2,3,4,6,8,9,10,12}	{12}	1
Integration 2				
1	{1,2,3,4,5,6,8,9,10,11}	{1,8}	{1,8}	
2	{2,3,4,5,6,9,10}	{1,2,3,4,5,6,8,9,10,11}	{2,3,4,5,6,9,10}	2
3	{2,3,4,5,6,9,10,11}	{1,2,3,4,5,6,8,9,10,11}	{2,3,4,5,6,9,10,11}	2
4	{2,3,4,6,9,10}	{1,2,3,4,5,6,8,9,10,11}	{2,3,4,6,9,10}	2
5	{2,3,4,5,6}	{1,2,3,5,6,8,9,10,11}	{2,3,5,6}	
6	{2,3,4,5,6,9,10,11}	{1,2,3,4,5,6,8,9,10,11}	{2,3,4,5,6,9,10,11}	2
8	{1,2,3,4,5,6,8,9,10,11}	{1,8}	{1,8}	
9	{2,3,4,5,6,9,10,11}	{1,2,3,4,6,8,9,10,11}	{2,3,4,6,9,10,11}	
10	{2,3,4,5,6,9,10,11}	{1,2,3,4,6,8,9,10,11}	{2,3,4,6,9,10,11}	
11	{2,3,4,5,6,9,10,11}	{1,3,6,8,9,10,11}	{3,6,9,10,11}	
Integration 3				
1	{1,5,8,9,10,11}	{1,8}	{1,8}	
5	{5}	{1,5,8,9,10,11}	{5}	3
8	{1,5,8,9,10,11}	{1,8}	{1,8}	
9	{5,9,10,11}	{1,8,9,10,11}	{9,10,11}	
10	{5,9,10,11}	{1,8,9,10,11}	{9,10,11}	
11	{5,9,10,11}	{1,8,9,10,11}	{9,10,11}	
Integration 4				
1	{1,8,9,10,11}	{1,8}	{1,8}	
8	{1,8,9,10,11}	{1,8}	{1,8}	
9	{9,10,11}	{1,8,9,10,11}	{9,10,11}	4
10	{9,10,11}	{1,8,9,10,11}	{9,10,11}	4

(continued)

Table 4 (continued)

Obstacles	Reachability set	Antecedent set	Intersection set	Level
11	{9,10,11}	{1,8,9,10,11}	{9,10,11}	4
Integration 5				
1	{1,8}	{1,8}	{1,8}	5
8	{1,8}	{1,8}	{1,8}	5

Table 5 Final reachability matrix

Obstacles	1	2	3	4	5	6	7	8	9	10	11	12	Driver power
C1	1	1	1	1	1	1	1	1	1	1	1	1	12
C2	0	1	1	1	1	1	1	0	1	1	0	1	9
C3	0	1	1	1	1	1	1	0	1	1	1	1	10
C4	0	1	1	1	0	1	1	0	1	1	0	1	8
C5	0	1	1	1	1	1	1	0	0	0	0	0	6
C6	0	1	1	1	1	1	1	0	1	1	1	1	10
C7	0	0	0	0	0	0	1	0	0	0	0	0	1
C8	1	1	1	1	1	1	1	1	1	1	1	1	12
C9	0	1	1	1	1	1	1	0	1	1	1	1	10
C10	0	1	1	1	1	1	1	0	1	1	1	1	10
C11	0	1	1	1	1	1	1	0	1	1	1	0	9
C12	0	0	0	0	0	0	0	0	0	0	0	1	1
	2	10	10	10	9	10	11	2	9	9	7	9	

by the number of "1" entries in the columns. The dependency power of an obstacle is calculated by multiplying the number of "1" entries in the columns by the number of "1" entries in the columns.

The MICMAC analysis defines the device element's dependency and driving forces, and the analysis is based on the matrices' multiplication properties. If variable "a" influences variable "b", and variable "b" influences a third variable "c", then "a" and "c" have an indirect relationship. In the scheme, there are a variety of indirect relationships that are not represented in the direct relationship matrix. MICMAC research reveals a number of such indirect relationships that have an effect on the scheme. The second order matrix is obtained by squaring the matrix. The matrix is also multiplied n times to obtain the nth interconnecting variables.

When the direct matrix "A" (Table 5) is used as the input for MICMAC analysis, the multiplication of the matrix continues until the driving and dependency power ranks are saturated. The length of the circuit is represented by the power to which the matrix is multiplied.

Table 7 shows that the ranks of the driving and dependency powers are the same at A^4 and A^6, but the matrix becomes saturated at A^4 and repeats the same rank series
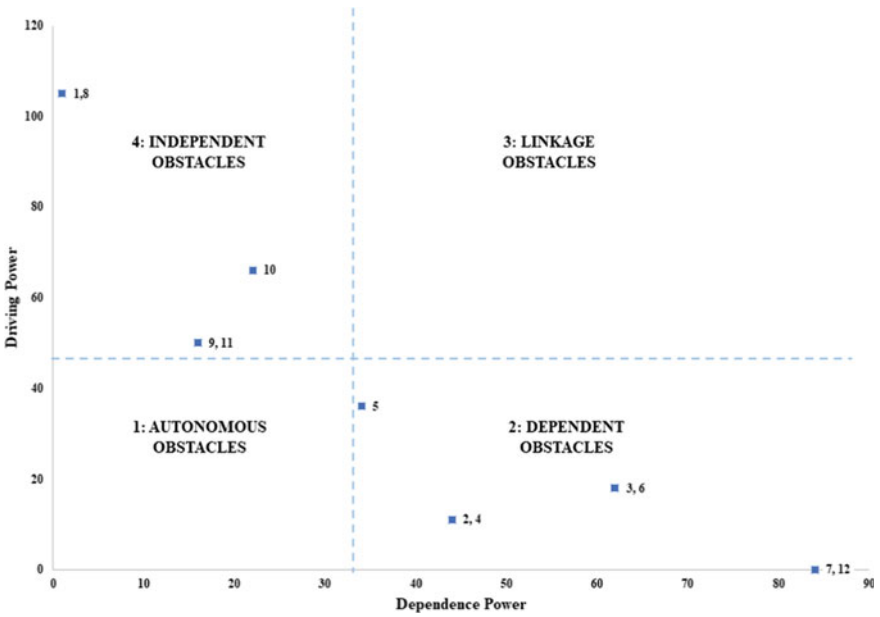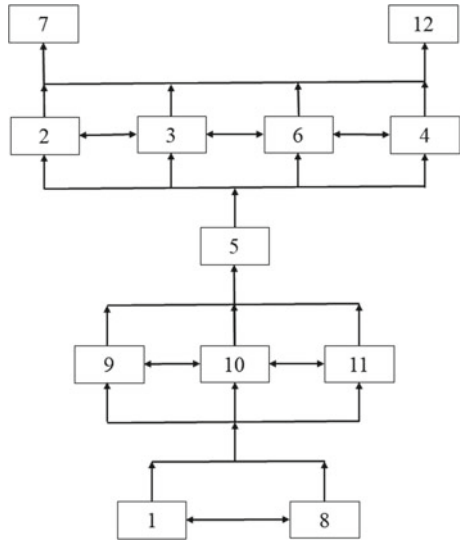
Fig. 5 MICMAC analysis of obstacles of DSC
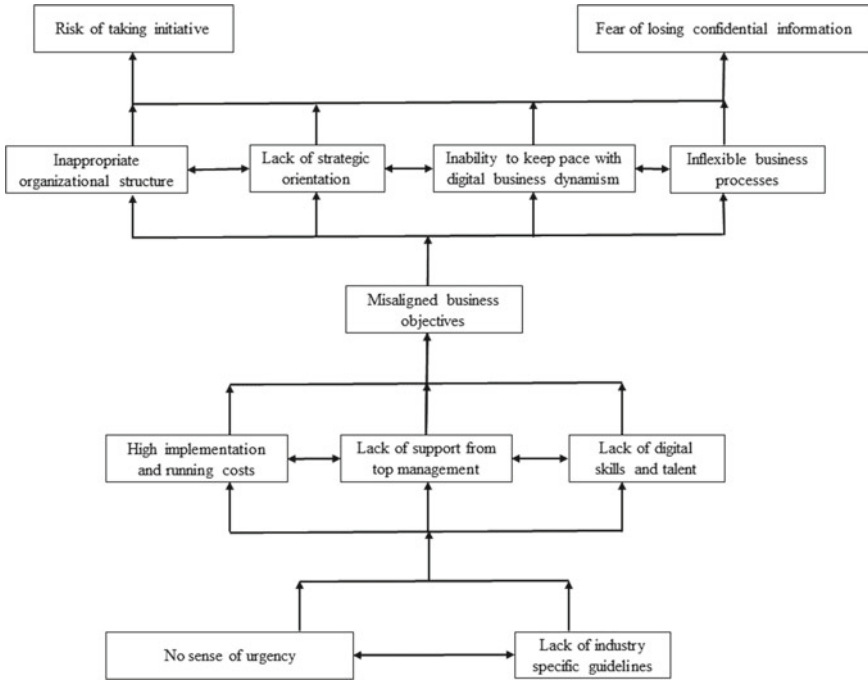
Fig. 6 Final digraph for barriers of DSC

Fig. 7 ISM-based model for the barriers of DSC

at A^6. As a result, Case 4 reflects the circuit's duration. Both the indirect relationship matrix's and direct relationship matrix's driving and dependency forces (Table 6) are determined in the same way (Table 8).

In MICMAC analysis, factors are divided into four clusters with respect to the driving power and dependence power. Therefore, the twelve obstacles are grouped into four clusters as Cluster 1: autonomous obstacles—this group includes obstacles with less driving and dependency control. These obstacles exist on the periphery of the system; Cluster 2: dependent obstacles—this group includes obstacles with little driving force but a lot of dependency. These obstacles can be removed by removing the obstacles that they depend on; Cluster 3: linkage obstacles—this category includes obstacles that have both powerful driving forces and dependencies. These are usually insecure and have bi-directional attraction to other obstacles; and Cluster 4: independent obstacles—this group includes obstacles with high driving power but low dependence. These obstacles have a high driving force and are known as independent obstacles. They are considered main device obstacles (Figs. 6 and 7).

Table 6 Direct relationship matrix (A)

Obstacles	1	2	3	4	5	6	7	8	9	10	11	12	Dr. P	Rank
1	0	0	0	0	0	0	0	1	1	1	1	0	4	1
2	0	0	1	0	0	0	1	0	0	0	0	1	3	2
3	0	1	0	0	0	1	1	0	0	0	0	1	4	1
4	0	0	0	0	0	1	1	0	0	0	0	1	3	2
5	0	1	1	1	0	1	0	0	0	0	0	0	4	1
6	0	0	0	0	0	0	1	0	0	0	0	1	4	1
7	0	0	0	0	0	0	0	0	0	0	0	0	0	4
8	1	0	0	0	0	0	0	0	1	1	1	0	4	1
9	0	0	0	0	1	0	0	0	0	1	0	0	2	3
10	0	0	0	0	1	0	0	0	1	0	1	0	3	2
11	0	0	0	0	1	0	0	0	0	1	0	0	2	3
12	0	0	0	0	0	0	0	0	0	0	0	0	0	4
DP	1	2	3	2	3	3	4	1	3	4	3	4		
Rank	4	3	2	3	2	2	1	4	2	1	2	1		

Note Dr. P = driving power, DP = dependence power

Table 7 Indirect relationship matrix (A4)

Obstacles	1	2	3	4	5	6	7	8	9	10	11	12	Dr. P	Rank
1	1	10	13	10	13	13	12	0	6	9	6	12	105	1
2	0	2	0	0	0	3	3	0	0	0	0	3	11	6
3	0	0	5	3	0	0	5	0	0	0	0	5	18	5
4	0	0	3	2	0	0	3	0	0	0	0	3	11	6
5	0	3	5	3	0	5	10	0	0	0	0	10	36	4
6	0	3	0	0	0	5	5	0	0	0	0	5	18	5
7	0	0	0	0	0	0	0	0	0	0	0	0	0	7
8	0	10	13	10	13	13	12	1	6	9	6	12	105	1
9	0	5	7	5	2	7	10	0	2	0	2	10	50	3
10	0	6	9	6	4	9	14	0	0	4	0	14	66	2
11	0	5	7	5	2	7	10	0	2	0	2	10	50	3
12	0	0	0	0	0	0	0	0	0	0	0	0	0	7
DP	1	44	62	44	34	62	84	1	16	22	16	84		
Rank	7	3	2	3	4	2	1	7	6	5	6	1		

Note Dr.P = driving power, DP = dependence power

Table 8 Matrix stabilization with MICMAC

Obstacles	A^2		A^4		A^6	
	Dr. Pr. R	DPr. R	Dr. Pr. R	DPr. R	Dr. Pr. R	DPr. R
1	2	4	1	7	1	7
2	5	3	6	3	6	3
3	4	2	5	2	5	2
4	5	3	6	3	6	3
5	1	1	4	4	4	4
6	4	2	5	2	5	2
7	6	1	7	1	7	1
8	2	4	1	7	1	7
9	4	3	3	6	3	6
10	3	2	2	5	2	5
11	4	3	3	6	3	6
12	6	1	7	1	7	1

Note Dr. Pr. R = driving power rank, DPr. R = dependence power rank

7 Results and Discussion

Transforming from traditional to DSC necessitates significant financial, time, and systemic adjustments. Different organizations would need to devise appropriate plans for a phased transition to DSC, taking into account their strengths and limitations. As a result, businesses must first determine "the competency needs to be transformed first; what are the major obstacles to DSC and relationships within them; and how these obstacles can be resolved" before embarking on such a transition initiative. This paper examines some of the main DSC roadblocks and organizes them into an ISM. The impediments to the supply chain's digital transition pose significant challenges for company executives and policy-makers. These roadblocks must be removed in order for a digital transition initiative to succeed. MICMAC research is used to classify DSC obstacles. As seen in Fig. 4, cluster 1 has no autonomous obstacles, implying that all of the obstacles considered are interconnected and have a major impact on DSC adoption. As a result, management must focus on all of the obstacles identified in this paper.

According to the ISM, the most important obstacles to DSC transition are "lack of urgency" and "lack of sector relevant guidance". These obstacles have a lot of pulling force and are the foundation of the ISM (Fig. 7). The next phase of the ISM is comprised of three major obstacles: a lack of digital expertise and talent, high deployment and operating costs, and top management support. There are self-contained inhibitors with a strong driving force. Similar findings can be seen in the MICMAC study, where these obstacles are listed as individual obstacles in the fourth cluster. These hurdles must be removed as soon as possible.

Obstacles such as misaligned market goals, inadequate operational structure, lack of strategic focus, failure to keep up with digital business dynamism, inflexible business processes, fear of losing sensitive knowledge, and the prospect of taking initiative make up the next cluster (Region 2 in Fig. 4). Such significant obstacles to digital technology adoption include the fear of destroying classified records, data protection, and the danger of taking action. This kind of obstacle is at the very top of the bureaucratic paradigm, and it is highly dependent on other types of obstacles. To limit, if not totally remove, security and other problems relevant to this hurdle, and to enable the implementation of DSC management (DSCM), the advances occurring in technology such as "Blockchain" must be recognized and applied.

The obstacle misaligned market priorities are found at the middle stage of the hierarchical paradigm. It is a contingent obstacle, but it often helps to push obstacles at the ISM's higher levels. Since the conventional supply chain's primary goal is to improve the quality of getting products and services from manufacturers to consumers through a sequence of intermediary measures, this obstacle requires focus.

DSC, on the other hand, is a customer-centric approach that collects and uses a wide range of real-time data from various sources to allow performance management by demand sensing and stimulation, as well as risk mitigation. As a result, rather than focusing solely on increasing performance, supply chain management must turn their emphasis to implementing the revolutionary innovations required by DSC in order to gain a potential competitive edge and delight their consumers.

The ISM's next step consists of four obstacles: an ineffective hierarchical structure, a lack of strategic focus, an inability to keep up with digital market dynamism, and rigid business processes. They are contingent obstacles with a strong reliance on lower-level obstacles and the potential to influence each other. This obstacle must be addressed once the lower-level obstacles have been addressed, so any action taken on the lower-level obstacles would have an impact on these obstacles. These impediments can be seen as strategic issues [92].

As a result, the following main conclusions can be drawn:

Since supply chains include a number of discrete and siloed phases ranging from manufacturers to ultimate consumers, such as product creation, manufacturing, promotion, and delivery, today's supply chains are struggling to meet a diverse variety of consumer demands. Organizations must break down these obstacles to create a more cohesive customer partnership by embracing horizontal integration in organizational structure, which facilitates agile business processes, lower risks and disruption visibility, stronger coordination among various supply chain partners, and more integrated and open supply chains.

To keep up with the dynamism of modern industry, new digital innovations are needed. In this unpredictable environment, digital technology such as "big data" and "edge" improve prediction quality and visibility throughout the supply chain. The exposure of the supply chain has real-time understanding of company processes. Big data analytics transforms raw data into actionable insights, while cloud eliminates different obstacles by allowing universal access to data.

Companies should form a team to regularly track selling trends and purchasing behaviour so demand sensing and up-to-date sales knowledge make for a greater

understanding of consumers' needs. It allows businesses to use modular products to meet a wide range of individual consumer needs. Companies can forecast consumers' shopping habits by viewing their browsing history across different mobile apps, and they can use predictive delivery to improve responsiveness through analysing real-time consumer demand data.

Since establishing the ideal organizational philosophy, process, and technology, attempts should be made to include consumers in the value chain in order to make the supply chain more customer-centric. For DSC transition programmes to thrive, good consumer relationships are needed. To do this, procedures and structures must be built to satisfy existing consumer needs while still being agile enough to respond as their desires and tastes evolve. Employees should be given the authority to modify procedures in accordance with consumer needs.

8   Conclusion

This paper focuses on supply chain digitization, which is a trending topic among both practitioners and academics. This framework assists in highlighting the key proposal, which is focused on a method for developing a DSC. The findings of this literature review are intended to address questions such as what the present state of digital transformation in the supply chain is in research and professional studies, as well as what the future progress of digital transformation would be like, and how the present value of digitalization can be incorporated into a supply chain or logistics, among other things.

Information gaps in the research sources are established, and the characteristics of previous research are combined to explain the state of the art inside the logistics sector. A DSC structure is built based on the benefits, disadvantages, and shortcomings of current literature, in addition to a detailed discussion on future developments in DSCs.

This paper finds a void in previous research regarding the creation of a comprehensive conceptual or theoretical structure. A proposed structure seeks to define the characteristics, materials, and technology enablers, as well as the obstacles and success factors involved in digitally transforming the supply chain. As a result, both academics and practitioners will gain from the current analysis and structure. More research is required to determine and evaluate the possible importance of the framework stages in a traditional supply chain, which can then be applied and validated.

The ISM and the driver dependency diagram discussed in this paper assist businesses in better understanding the barriers' significance and interrelationships. As this field develops, a few more roadblocks will arise. Nonetheless, it emphasizes the importance of taking a systematic approach to recognizing obstacles, judiciously allocating available resources, and creating the appropriate atmosphere for DSC adoption.

Customers and rivals put pressure on all businesses to accelerate digital transformation, which comes at a high cost and takes a lot of effort. However, since current resources must be reallocated to sustain this transition, the speed of transformation is sluggish. This paper lays out a step-by-step plan for overcoming the obstacles that stand in the way of implementing digital transformation of supply chain.

References

1. Sharma, S.K., Sharma, R.C., Choi, Y., Lee, J.: Experimental and mathematical study of flexible–rigid rail vehicle riding comfort and safety. Appl. Sci. **13**, 5252 (2023). https://doi.org/10.3390/app13095252
2. Qin, X., Huang, Y., Yang, Z., Li, X.: A Blockchain-based access control scheme with multiple attribute authorities for secure cloud data sharing. J. Syst. Archit. **112**, 101854 (2021). https://doi.org/10.1016/j.sysarc.2020.101854
3. Bosch, J., Olsson, H.H.: Digital for real: A multicase study on the digital transformation of companies in the embedded systems domain. J. Softw. Evol. Process, 1–25 (2021). https://doi.org/10.1002/smr.2333
4. Liu, M., Fang, S., Dong, H., Xu, C.: Review of digital twin about concepts, technologies, and industrial applications. J. Manuf. Syst. **58**, 346–361 (2021). https://doi.org/10.1016/j.jmsy.2020.06.017
5. Sharma, R.C., Palli, S., Sharma, S.K.: Ride analysis of railway vehicle considering rigidity and flexibility of the carbody. J. Chinese Inst. Eng. **46**, 355–366 (2023). https://doi.org/10.1080/02533839.2023.2194918
6. Ahmad, R., Alsmadi, I.: Machine learning approaches to IoT security: a systematic literature review. Internet Things **14**, 100365 (2021). https://doi.org/10.1016/j.iot.2021.100365
7. Sharma, S.K., Sharma, R.C., Lee, J.: In situ and experimental analysis of longitudinal load on carbody fatigue life using nonlinear damage accumulation. Int. J. Damage Mech. **31**, 605–622 (2022). https://doi.org/10.1177/10567895211046043
8. Sharma, R.C., Sharma, S.K.: Ride analysis of road surface-three-wheeled vehicle-human subject interactions subjected to random excitation. SAE Int. J. Commer. Veh. **15**, 02-15-03-0017 (2022). https://doi.org/10.4271/02-15-03-0017
9. Sharma, S.K., Lee, J., Jang, H.-L.: Mathematical modeling and simulation of suspended equipment impact on car body modes. Machines. **10**, 192 (2022). https://doi.org/10.3390/machines10030192
10. Sharma, S.K., Sharma, R.C., Lee, J., Jang, H.-L.: Numerical and experimental analysis of DVA on the flexible-rigid rail vehicle carbody resonant vibration. Sensors **22**, 1922 (2022). https://doi.org/10.3390/s22051922
11. Vishwakarma, P.N., Mishra, P., Sharma, S.K.: Characterization of a magnetorheological fluid damper a review. Mater. Today Proc. **56**, 2988–2994 (2022). https://doi.org/10.1016/j.matpr.2021.11.143
12. Sharma, S.K., Mohapatra, S., Sharma, R.C., Alturjman, S., Altrjman, C., Mostarda, L., Stephan, T.: Retrofitting existing buildings to improve energy performance. Sustainability **14**, 666 (2022). https://doi.org/10.3390/su14020666
13. Vishwakarma, P.N., Mishra, P., Sharma, S.K.: Formulation of semi-active suspension system and controls in rail vehicle. SSRN Electron. J. (2022). https://doi.org/10.2139/ssrn.4159616
14. Sharma, S.K., Lee, J.: Crashworthiness analysis for structural stability and dynamics. Int. J. Struct. Stab. Dyn. **21**, 2150039 (2021). https://doi.org/10.1142/S0219455421500395
15. Wu, Q., Cole, C., Spiryagin, M., Chang, C., Wei, W., Ursulyak, L., Shvets, A., Murtaza, M.A., Mirza, I.M., Zhelieznov, К., Mohammadi, S., Serajian, H., Schick, B., Berg, M., Sharma, R.C., Aboubakr, A., Sharma, S.K., Melzi, S., Di Gialleonardo, E., Bosso, N., Zampieri, N.,

Magelli, M., Ion, C.C., Routcliffe, I., Pudovikov, O., Menaker, G., Mo, J., Luo, S., Ghafourian, A., Serajian, R., Santos, A.A., Teodoro, Í.P., Eckert, J.J., Pugi, L., Shabana, A., Cantone, L.: Freight train air brake models. Int. J. Rail Transp. 1–49 (2021). https://doi.org/10.1080/232 48378.2021.2006808

16. Sharma, S.K., Sharma, R.C., Lee, J.: Effect of rail vehicle-track coupled dynamics on fatigue failure of coil spring in a suspension system. Appl. Sci. **11**, 2650 (2021). https://doi.org/10. 3390/app11062650

17. Mohapatra, S., Mohanty, D., Mohapatra, S., Sharma, S., Dikshit, S., Kohli, I., Samantaray, D.P., Kumar, R., Kathpalia, M.: Biomedical application of polymeric biomaterial: polyhydroxybutyrate. In: Bioresource Utilization and Management: Applications in Therapeutics, Biofuels, Agriculture, and Environmental Science, pp. 1–14. CRC Press (2021). https://doi. org/10.21203/rs.3.rs-1491519/v1

18. Bhardawaj, S., Sharma, R.C., Sharma, S.K., Sharma, N.: On the planning and construction of railway curved track. Int. J. Veh. Struct. Syst. **13**, 151–159 (2021). https://doi.org/10.4273/ ijvss.13.2.04

19. Sharma, R.C., Sharma, S., Sharma, N., Sharma, S.K.: Linear and nonlinear analysis of ride and stability of a three-wheeled vehicle subjected to random and bump inputs using bond graph and simulink methodology. SAE Int. J. Commer. Veh. **14**, 02-15-01-0001 (2021). https://doi. org/10.4271/02-15-01-0001

20. Sharma, R.C., Sharma, S., Sharma, S.K., Sharma, N., Singh, G.: Analysis of bio-dynamic model of seated human subject and optimization of the passenger ride comfort for three-wheel vehicle using random search technique. Proc. Inst. Mech. Eng. Part K J. Multi-body Dyn. **235**, 106–121 (2021). https://doi.org/10.1177/1464419320983711

21. Choi, S., Lee, J., Sharma, S.K.: A study on the performance evaluation of hydraulic tank injectors. In: Advances in Engineering Design: Select Proceedings of FLAME 2020, pp. 183– 190. Springer Singapore (2021). https://doi.org/10.1007/978-981-33-4684-0_19

22. Lee, J., Han, J., Sharma, S.K.: Structural analysis on the separated and integrated differential gear case for the weight reduction. In: Joshi, P., Gupta, S.S., Shukla, A.K., Gautam, S.S. (eds.) Advances in Engineering Design. Lecture Notes in Mechanical Engineering, pp. 175–181 (2021). https://doi.org/10.1007/978-981-33-4684-0_18

23. Sharma, S.K., Sharma, R.C.: Multi-objective design optimization of locomotive nose. In: SAE Technical Paper, pp. 1–10 (2021). https://doi.org/10.4271/2021-01-5053

24. Sharma, R.C., Palli, S., Sharma, N., Sharma, S.K.: Ride behaviour of a four-wheel vehicle using H infinity semi-active suspension control under deterministic and random inputs. Int. J. Veh. Struct. Syst. **13**, 234–237 (2021). https://doi.org/10.4273/ijvss.13.2.18

25. Sharma, S.K., Sharma, R.C., Sharma, N.: Combined multi-body-system and finite element analysis of a rail locomotive crashworthiness. Int. J. Veh. Struct. Syst. **12**, 428–435 (2020). https://doi.org/10.4273/ijvss.12.4.15

26. Sharma, R.C., Sharma, S.K., Palli, S.: Linear and non-linear stability analysis of a constrained railway wheelaxle. Int. J. Veh. Struct. Syst. **12**, 128–133 (2020). https://doi.org/10.4273/ijvss. 12.2.04

27. Palli, S., Sharma, R.C., Sharma, S.K., Chintada, V.B.: On methods used for setting the curve for railway tracks. J. Crit. Rev. **7**, 241–246 (2020)

28. Mohapatra, S., Pattnaik, S., Maity, S., Mohapatra, S., Sharma, S., Akhtar, J., Pati, S., Samantaray, D.P., Varma, A.: Comparative analysis of PHAs production by Bacillus megaterium OUAT 016 under submerged and solid-state fermentation. Saudi J. Biol. Sci. **27**, 1242–1250 (2020). https://doi.org/10.1016/j.sjbs.2020.02.001

29. Holmstrom, J.: From AI to digital transformation: the AI readiness framework. Bus. Horiz. (2021). https://doi.org/10.1016/j.bushor.2021.03.006

30. González Ramírez, P.L., Lloret, J., Tomás, J., Hurtado, M.: IoT-networks group-based model that uses AI for workgroup allocation. Comput. Netw. **186**, 107745 (2021). https://doi.org/10. 1016/j.comnet.2020.107745

31. He, Y., Zheng, Y., Jin, M., Yang, S., Zheng, X., Liu, Y.: RED: RFID-based eccentricity detection for high-speed rotating machinery. In: IEEE Transactions on Mobile Computing, pp. 1590– 1601 (2021). https://doi.org/10.1109/TMC.2019.2962770

32. Resources, D.T.: The Current State of Digital Supply Chain Transformation (2021). http://mkt forms.gtnexus.com/rs/979-MCL-531/images/GTNexus-Digital-Transformation-Report-US-FINAL.pdf
33. Tan, A., Shukkla, S.: Digital transformation of the supply chain. Digit. Transform. Supply Chain. (2021). https://doi.org/10.1142/12079
34. Sharma, R.C., Palli, S., Jha, A.K., Bhardawaj, S., Sharma, S.K.: Vibration and ride comfort analysis of railway vehicle system subjected to deterministic inputs. Resmilitaris **12**, 1345–1355 (2022).
35. Sharma, R.C., Sharma, S.K., Sharma, N., Sharma, S.: Analysis of ride and stability of an ICF railway coach. Int. J. Veh. Noise Vib. **16**, 127 (2020). https://doi.org/10.1504/IJVNV.2020.117820
36. Sharma, S.K., Phan, H., Lee, J.: An application study on road surface monitoring using DTW based image processing and ultrasonic sensors. Appl. Sci. **10**, 4490 (2020). https://doi.org/10.3390/app10134490
37. Sharma, R.C., Sharma, S., Sharma, S.K., Sharma, N.: Analysis of generalized force and its influence on ride and stability of railway vehicle. Noise Vib. Worldw. **51**, 95–109 (2020). https://doi.org/10.1177/0957456520923125
38. Lee, J., Sharma, S.K.: Numerical investigation of critical speed analysis of high-speed rail vehicle. 한국정밀공학회 학술발표대회 논문집 (Korean Soc. Precis. Eng. 696) (2020)
39. Sharma, S.K., Lee, J.: Finite element analysis of a fishplate rail joint in extreme environment condition. Int. J. Veh. Struct. Syst. **12**, 503–506 (2020). https://doi.org/10.4273/ijvss.12.5.03
40. Bhardawaj, S., Sharma, R.C., Sharma, S.K.: Ride analysis of track-vehicle-human body interaction subjected to random excitation. J. Chinese Soc. Mech. Eng. **41**, 237–236 (2020). https://doi.org/10.29979/JCSME
41. Bhardawaj, S., Sharma, R.C., Sharma, S.K.: Development in the modeling of rail vehicle system for the analysis of lateral stability. Mater. Today Proc. **25**, 610–619 (2020). https://doi.org/10.1016/j.matpr.2019.07.376
42. Bhardawaj, S., Sharma, R.C., Sharma, S.K.: Analysis of frontal car crash characteristics using ANSYS. Mater. Today Proc. **25**, 898–902 (2020). https://doi.org/10.1016/j.matpr.2019.12.358
43. Sharma, S., Sharma, R.C., Sharma, S.K., Sharma, N., Palli, S., Bhardawaj, S.: Vibration isolation of the quarter car model of road vehicle system using dynamic vibration absorber. Int. J. Veh. Struct. Syst. **12**, 513–516 (2020). https://doi.org/10.4273/ijvss.12.5.05
44. Acharya, A., Gahlaut, U., Sharma, K., Sharma, S.K., Vishwakarma, P.N., Phanden, R.K.: Crashworthiness analysis of a thin-walled structure in the frontal part of automotive chassis. Int. J. Veh. Struct. Syst. **12**, 517–520 (2020). https://doi.org/10.4273/ijvss.12.5.06
45. Bhardawaj, S., Sharma, R.C., Sharma, S.K.: Development of multibody dynamical using MR damper based semi-active bio-inspired chaotic fruit fly and fuzzy logic hybrid suspension control for rail vehicle system. Proc. Inst. Mech. Eng. Part K J. Multi-body Dyn. **234**, 723–744 (2020). https://doi.org/10.1177/1464419320953685
46. Sharma, S.K., Lee, J.: Design and development of smart semi active suspension for nonlinear rail vehicle vibration reduction. Int. J. Struct. Stab. Dyn. **20**, 2050120 (2020). https://doi.org/10.1142/S0219455420501205
47. Sharma, S.K.: Multibody analysis of longitudinal train dynamics on the passenger ride performance due to brake application. Proc. Inst. Mech. Eng. Part K J. Multi-body Dyn. **233**, 266–279 (2019). https://doi.org/10.1177/1464419318788775
48. Goyal, S., Anand, C.S., Sharma, S.K., Sharma, R.C.: Crashworthiness analysis of foam filled star shape polygon of thin-walled structure. Thin-Walled Struct. **144**, 106312 (2019). https://doi.org/10.1016/j.tws.2019.106312
49. Sharma, S.K., Sharma, R.C.: Pothole detection and warning system for indian roads. In: Advances in Interdisciplinary Engineering, pp. 511–519 (2019). https://doi.org/10.1007/978-981-13-6577-5_48
50. Goswami, B., Rathi, A., Sayeed, S., Das, P., Sharma, R.C., Sharma, S.K.: Optimization design for aerodynamic elements of indian locomotive of passenger train. In: Advances in Engineering Design, pp. 663–673. Lecture Notes in Mechanical Engineering. Springer, Singapore (2019). https://doi.org/10.1007/978-981-13-6469-3_61

51. Bhardawaj, S., Sharma, R.C., Sharma, S.K.: Development and advancement in the wheel-rail rolling contact mechanics. IOP Conf. Ser. Mater. Sci. Eng. **691**, 012034 (2019). https://doi.org/10.1088/1757-899X/691/1/012034

52. Choppara, R.K., Sharma, R.C., Sharma, S.K., Gupta, T.: Aero dynamic cross wind analysis of locomotive. In: IOP Conference Series: Materials Science and Engineering, p. 12035. IOP Publishing (2019)

53. Sinha, A.K., Sengupta, A., Gandhi, H., Bansal, P., Agarwal, K.M., Sharma, S.K., Sharma, R.C., Sharma, S.K.: Performance enhancement of an all-terrain vehicle by optimizing steering, powertrain and brakes. In: Advances in Engineering Design, pp. 207–215 (2019). https://doi.org/10.1007/978-981-13-6469-3_19

54. Sharma, S.K., Saini, U., Kumar, A.: Semi-active control to reduce lateral vibration of passenger rail vehicle using disturbance rejection and continuous state damper controllers. J. Vib. Eng. Technol. **7**, 117–129 (2019). https://doi.org/10.1007/s42417-019-00088-2

55. Bhardawaj, S., Chandmal Sharma, R., Kumar Sharma, S.: A survey of railway track modelling. Int. J. Veh. Struct. Syst. **11**, 508–518 (2019). https://doi.org/10.4273/ijvss.11.5.08

56. Sharma, R.C., Palli, S., Sharma, S.K., Roy, M.: Modernization of railway track with composite sleepers. Int. J. Veh. Struct. Syst. **9**, 321–329 (2018)

57. Sharma, R.C., Sharma, S.K., Palli, S.: Rail vehicle modelling and simulation using lagrangian method. Int. J. Veh. Struct. Syst. **10**, 188–194 (2018). https://doi.org/10.4273/ijvss.10.3.07

58. Palli, S., Koona, R., Sharma, S.K., Sharma, R.C.: A review on dynamic analysis of rail vehicle coach. Int. J. Veh. Struct. Syst. **10**, 204–211 (2018). https://doi.org/10.4273/ijvss.10.3.10

59. Fuller, A., Fan, Z., Day, C., Barlow, C.: Digital twin: enabling technologies, challenges and open research. In: IEEE Access, pp. 108952–108971, (2020). https://doi.org/10.1109/ACCESS.2020.2998358

60. Zheng, P., Xu, X., Chen, C.H.: A data-driven cyber-physical approach for personalised smart, connected product co-development in a cloud-based environment. J. Intell. Manuf. **31**, 3–18 (2020). https://doi.org/10.1007/s10845-018-1430-y

61. Jones, D., Snider, C., Nassehi, A., Yon, J., Hicks, B.: Characterising the digital twin: a systematic literature review. CIRP J. Manuf. Sci. Technol. **29**, 36–52 (2020). https://doi.org/10.1016/j.cirpj.2020.02.002

62. Hauge, J.B., Zafarzadeh, M., Jeong, Y., Li, Y., Khilji, W.A., Wiktorsson, M.: Employing digital twins within production logistics. Proc. 2020 IEEE Int. Conf. Eng. Technol. Innov. ICE/ITMC 2020. (2020). https://doi.org/10.1109/ICE/ITMC49519.2020.9198540

63. Cichosz, M., Wallenburg, C.M., Knemeyer, A.M.: Digital transformation at logistics service providers: barriers, success factors and leading practices. Int. J. Logist. Manag. **31**, 209–238 (2020). https://doi.org/10.1108/IJLM-08-2019-0229

64. Amanullah, M.A., Habeeb, R.A.A., Nasaruddin, F.H., Gani, A., Ahmed, E., Nainar, A.S.M., Akim, N.M., Imran, M.: Deep learning and big data technologies for IoT security (2020). https://doi.org/10.1016/j.comcom.2020.01.016

65. Sharma, R.C., Gopala Rao, L.V.V., Sharma, S.K., Palli, S., Satyanarayana, V.S.V.: Analysis of lateral stability and ride of an Indian railway constrained dual-axle bogie frame. SAE Int. J. Commer. Veh. **16**, 02-16-02–0014 (2022). https://doi.org/10.4271/02-16-02-0014

66. Sharma, S.K., Sharma, R.C.: An investigation of a locomotive structural crashworthiness using finite element simulation. SAE Int. J. Commer. Veh. **11**, 235–244 (2018). https://doi.org/10.4271/02-11-04-0019

67. Sharma, S.K., Sharma, R.C.: Simulation of quarter-car model with magnetorheological dampers for ride quality improvement. Int. J. Veh. Struct. Syst. **10**, 169–173 (2018). https://doi.org/10.4273/ijvss.10.3.03

68. Sharma, S.K., Kumar, A.: Impact of longitudinal train dynamics on train operations: a simulation-based study. J. Vib. Eng. Technol. **6**, 197–203 (2018). https://doi.org/10.1007/s42417-018-0033-4

69. Sharma, R.C., Sharma, S.K.: Sensitivity analysis of three-wheel vehicle's suspension parameters influencing ride behavior. Noise Vib. Worldw. **49**, 272–280 (2018). https://doi.org/10.1177/0957456518796846

70. Sharma, S.K., Kumar, A.: Ride comfort of a higher speed rail vehicle using a magnetorheological suspension system. Proc. Inst. Mech. Eng. Part K J. Multi-body Dyn. **232**, 32–48 (2018). https://doi.org/10.1177/1464419317706873

71. Sharma, S.K., Kumar, A.: Disturbance rejection and force-tracking controller of nonlinear lateral vibrations in passenger rail vehicle using magnetorheological fluid damper. J. Intell. Mater. Syst. Struct. **29**, 279–297 (2018). https://doi.org/10.1177/1045389X17721051

72. Sharma, S.K., Kumar, A.: Impact of electric locomotive traction of the passenger vehicle ride quality in longitudinal train dynamics in the context of Indian railways. Mech. Ind. **18**, 222 (2017). https://doi.org/10.1051/meca/2016047

73. Sharma, S.K., Kumar, A.: Ride performance of a high speed rail vehicle using controlled semi active suspension system. Smart Mater. Struct. **26**, 055026 (2017). https://doi.org/10.1088/1361-665X/aa68f7

74. Sharma, S.K., Kumar, A.: Dynamics analysis of wheel rail contact using FEA. Procedia Eng. **144**, 1119–1128 (2016). https://doi.org/10.1016/j.proeng.2016.05.076

75. Sharma, S.K., Kumar, A.: The impact of a rigid-flexible system on the ride quality of passenger bogies using a flexible carbody. In: Pombo, J. (ed.) Proceedings of the Third International Conference on Railway Technology: Research, Development and Maintenance, Stirlingshire, UK, p. 87. Civil-Comp Press, 2016, Stirlingshire, UK (2016). https://doi.org/10.4203/ccp.110.87

76. Sharma, S.K., Chaturvedi, S.: Jerk analysis in rail vehicle dynamics. Perspect. Sci. **8**, 648–650 (2016). https://doi.org/10.1016/j.pisc.2016.06.047

77. Kulkarni, D., Sharma, S.K., Kumar, A.: Finite element analysis of a fishplate rail joint due to wheel impact. In: International Conference on Advances in Dynamics, Vibration and Control (ICADVC-2016) NIT Durgapur, India February 25–27, 2016. National Institute of Technology Durgapur, Durgapur, India (2016)

78. Sharma, S.K., Sharma, R.C., Kumar, A., Palli, S.: Challenges in rail vehicle-track modeling and simulation. Int. J. Veh. Struct. Syst. **7**, 1–9 (2015). https://doi.org/10.4273/ijvss.7.1.01

79. Sharma, S.K., Kumar, A., Sharma, R.C.: Challenges in railway vehicle modeling and simulations. In: International Conference on Newest Drift in Mechanical Engineering (ICNDME-14), December 20–21, M. M. University, Mullana, INDIA. pp. 453–459. Maharishi Markandeshwar University, Mullana–Ambala (2014).

80. Sharma, S.K., Kumar, A.: A comparative study of Indian and Worldwide railways. Int. J. Mech. Eng. Robot. Res. **1**, 114–120 (2014)

81. Sharma, S.K.: Zero energy building envelope components: a review. Int. J. Eng. Res. Appl. **3**, 662–675 (2013)

82. Sharma, S.K., Lavania, S.: An autonomous metro: design and execution. In: Futuristic Trends in Mechanical and Industrial Engineering, pp. 1–8. JECRC UDML College of Engineering, Jaipur (2013)

83. Sharma, S.K., Lavania, S.: Green manufacturing and green supply chain management in India a review. In: Futuristic trends in Mechanical and Industrial Engineering, pp. 1–8. JECRC UDML College of Engineering (2013)

84. Sharma, S.K., Lavania, S.: Skin effect in high speed VLSI on-chip interconnects. In: International Conference on VLSI, Communication & Networks, V-CAN, pp. 1–8. Institute of Engineering & Technology, Alwar (2011)

85. Lavania, S., Sharma, S.K.: An explicit approach to compare crosstalk noise and delay in VLSI RLC interconnect modeled with skin effect with step and ramp input. J. VLSI Des. Tools Technol. **1**, 1–8 (2011)

86. Park, K.T., Im, S.J., Kang, Y.S., Noh, S. Do, Kang, Y.T., Yang, S.G.: Service-oriented platform for smart operation of dyeing and finishing industry. Int. J. Comput. Integr. Manuf. **32**, 307–326 (2019). https://doi.org/10.1080/0951192X.2019.1572225

87. Dupláková, D., Flimel, M., Duplák, J., Hatala, M., Radchenko, S., Botko, F.: Ergonomic rationalization of lighting in the working environment. Part I.: Proposal of rationalization algorithm for lighting redesign. Int. J. Ind. Ergon. **71**, 92–102 (2019). https://doi.org/10.1016/j.ergon.2019.02.012

88. Xie, J., Wang, X., Yang, Z., Hao, S.: Virtual monitoring method for hydraulic supports based on digital twin theory. Min. Technol. Trans. Inst. Min. Metall. **128**, 77–87 (2019). https://doi.org/10.1080/25726668.2019.1569367

89. Kumar, U., Kasvekar, R., Sharma, S.K., Upadhyay, R.K.: Wear of wheels and axle in locomotive and measures taken by Indian railway. In: Advances in Engine Tribology, pp. 77–96. Springer (2022). https://doi.org/10.1007/978-981-16-8337-4_5

90. Liu, L.L., Wan, X., Gao, Z., Li, X., Feng, B.: Research on modelling and optimization of hot rolling scheduling. J. Ambient Intell. Humaniz. Comput. **10**, 1201–1216 (2019). https://doi.org/10.1007/s12652-018-0944-7

91. Ivanov, D., Tsipoulanidis, A., Schönberger, J.: Supply chain risk management and resilience. In: Global Supply Chain and Operations Management: A Decision-Oriented Introduction to the Creation of Value. pp. 455–479. Springer International Publishing, Cham (2019). https://doi.org/10.1007/978-3-319-94313-8_15

92. Sharma, R.C., Palli, S., Gopala Rao, L.V. V., Duppala, A., Sharma, S.K.: Four-wheel vehicle response under bump, pothole, harmonic, and random excitations using bond graph/simulink technique. SAE Int. J. Commer. Veh. **16**, 02-16-02–0008 (2022). https://doi.org/10.4271/02-16-02-0008

Design and Modelling of Digital Twin Technology to Improve Freight Logistics

Hema Shreaya Sura, Mohd Avesh, and Swati Mohapatra

Abstract Logistics is all about making decisions based on the impact of real or potential risks and opportunities, faster than one's competitors. Logistics and supply chain networks are being modified to be agile, innovative, cheaper, and sustainable. Organizations must tackle volatile demand, uncertain supply, and constrained capacity to survive; hence, applying Industry 4.0 processes could improve production design and business models. The need for speed is the sole reason which has led to the digitization of freight logistics processes. The chapter elucidates the evolution of the concept, the characterization of the different components, and enabling technologies that are necessary to build a Digital Twin. Further, it discusses the role of this technology in making sustainable decisions in various sectors ranging from material to medical sciences. Based on the various aspects of Digital Twins covered, it examines if this technology is a viable opportunity to venture into freight logistics policy-making and infrastructure planning.

Keywords Digital Twin · Freight logistics · Physical-virtual systems

1 Introduction

The logistics industry has completely transformed over the last ten years as a direct result of the influence of technology, and adopting an agile approach has become extremely necessary to design and model complex and dynamic demand–supply networks. The availability of real-time data is a vital competitive advantage, and

H. S. Sura
Mahindra Logistics Limited, Mumbai 400060, India

M. Avesh
Star Saidham Services Solutions, Doiwala, Dehradun 248140, India

S. Mohapatra (✉)
School of Science, Gujarat State Fertilizers and Chemicals University, Vadodara, Gujarat 391750, India
e-mail: swatimohapatraiitr@gmail.com

with Industry 4.0 one can identify and analyse the events at a particular instant in time [1–4]. The industry's key competitive factors are digitization and automation of existing processes. Despite this, manual labour is often required in logistics operations, owing to the intricacy of human–computer/robot interaction, system interactions, and changes in operative processes. Companies will be able to begin their projects to build a Digital Twin with a lesser capital expenditure and a shorter period of time to value than before, thanks to advanced technologies, versatility, agility, and reduced costs [5–7]. A Digital Twin can be used through a product's life cycle and can answer questions in real time that couldn't be addressed previously, delivering value that was almost unthinkable just a few years ago. Since the technology is being developed and is in its initial phase, there is a lack of a universal definition, a framework for implementation, and protocol rules. The existing literature doesn't cover a deep-dive analysis from the point of view of concepts, current technologies, and applications in the industry [8–10].

The chapter describes how Digital Twin can help with the selection of the right components for freight logistics and provides a consolidated approach to what Digital Twin technology is. There is a lack of compatibility which has led to the identification of several characterizations for the Digital Twin and the twinning process. Therefore, through a deep-dive analysis, Sect. 2 in this review intends to provide an overview of the key concepts of the Digital Twin, its characteristics, and enabling technologies. Section 3 gives a detailed summary of the industrial applications. Section 4 shows the relationship of freight logistics with the Digital Twin, while Sect. 5 explains the implementation of this technology and provides further recommendations.

2 Digital Twin Technology

Digital technologies have accelerated the development of new supply chain management principles, paradigms, and models. Smart operations and digital supply chains are made easier by cyber-physical systems, the Internet of Things, smart, and connected products [11–14]. Recent surveys by proposed digital technology classifications and discussed their potential impacts on supply chain management. Advanced technologies in manufacturing with sensors, big data analytics, decentralised agent-driven control, augmented reality, robotics, tracing technologies, and advanced tracking are a few examples of digital technologies.

2.1 Origin of Digital Twin

The origin of the Digital Twin is attributed to Michael Grieves and his work along with John Vickers of NASA in 2003 [15]. They imagined a world in which a product's virtual model would serve as the basis for product life-cycle management. Grieves [15] elaborates on this by explaining that the Digital Twin is made up of three specific
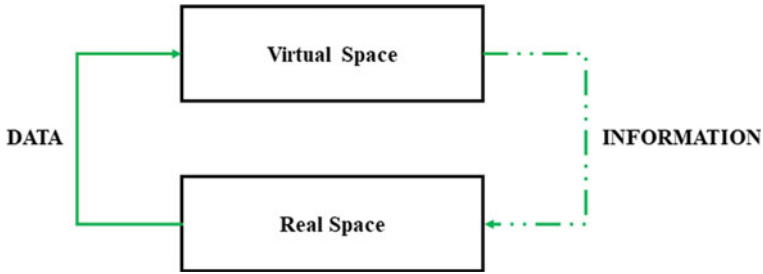
Fig. 1 Mirroring between the virtual and physical spaces [16]
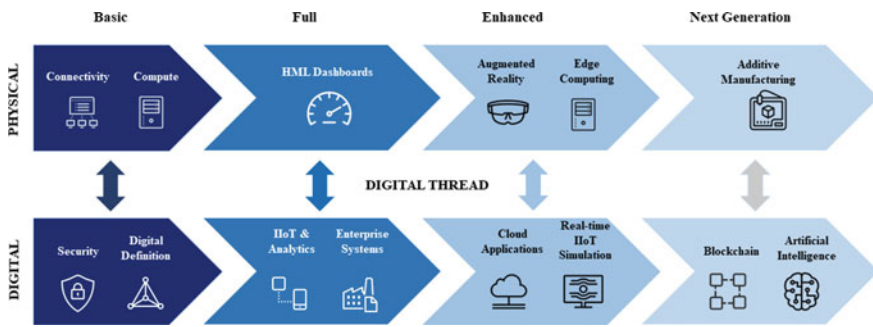

Fig. 2 Evolution of Digital Twin [17]

components: a digital representation of that product (virtual counterpart), a physical product, and a data channel that gets data from the sensors on the physical asset to the virtual counterpart, and information and actions from the virtual counterpart to the physical. Grieves shows this flow as cycles constantly between the virtual and physical entities of data from the physical to the virtual, and information and actions from the virtual to the physical (See Fig. 1). The virtual counterparts themselves consist of sub-spaces that enable specific virtual applications such as testing, modelling, and optimisation of operations. Figure 2 explains the evolution of multiple technologies that led to the creation of Digital Twin.

2.2 *Digital Twin Comes of Age*

Advancement in sensor and network technologies has allowed the interlinking of physical resources into a digital model. With time, mathematical models of real-world problems have successfully been replicated into a sophisticated digital reality world [18–21]. Technology is becoming popular and is being adopted across industries even though it has been available since the beginning of the twenty-first century. Data

storage resources at lower costs and higher computing power along with reliable high-speed wireless and wired networks have enabled Digital Twin to be implemented in organisations around the globe [22–25]. NASA, during its early years in space exploration, pioneered the use of a direct physical replica to support the maintenance and operation of an asset. During the Apollo 13 spacecraft crisis, the engineers at NASA tested and refined several plans and solutions with the replica module on Earth and communicated the best one to the panic-stricken crew aboard the spacecraft [26–29]. Since then, for all their missions, simulation has been an integral part of NASA's strategy for managing short- and long-term missions in space. Market analysis has shown that by 2025, the demand for Digital Twin would grow at an annual rate of 38%. Companies like SAP, Microsoft, and IBM are huge tech enterprises that see great potential as they have successfully established themselves in the artificial intelligence, cloud computing, and automation space which could boost the creation of Digital Twin solutions [30].

2.3 Constitutes of Digital Twin

The attributes which distinguish existing computer simulations from Digital Twin are: Digital Twin is the virtual model of a physical entity. Simulation of both the physical behaviour and state of the entity is done by Digital Twin. Digital Twin is specifically associated with only one entity at a particular instant of time; hence, they are unique [31–35]. It is then connected to a second entity that constantly tracks and adjusts the physical model's state, behaviour, condition, etc. With a Digital Twin, visualising, analysing, forecasting and optimising, becomes easy based on the requirements. Sometimes the digital model may be created even before the physical product has been produced, and it might exist longer than its physical counterpart. There could be several twins made depending on the various circumstances for only one asset, from planning to prediction for creating optimization models [36–39]. The United Kingdom is taking efforts to design a Digital Twin of the country to model all the input and output data concerning natural resources, infrastructure, and other utilities [40–44]. The smallest Digital Twin can represent the behaviour of specific materials, chemical reactions, or drug interactions and a larger Digital Twin can model entire metropolitan cities.

2.4 Underlying Technologies

In the development of the Digital Twin, the following technologies are essential to building a resilient virtual counterpart of the physical asset. Table 1 is about the underlying technologies and their features that support the Digital Twin in various industries [45–48].

Table 1 List of underlying technology and their descriptions

Technology	Description
Cloud computing	High data volumes, analytics capabilities [49], integration [50]
Internet of things	Connected assets, extended network [51], remote control
Artificial intelligence	Optimised design, predictive maintenance [52–57], adaptive behaviour
Block chain	Secure access, traceability [58], IP protection [59]
APIs & open standards	Data extraction [60], harmonise data [61], sharing data [62]
Augmented, mixed & virtual reality	Interaction, safety [63], training, field operations

2.5 Characterization Criteria

The subsequent sections provide a detailed summary of the characteristics of the physical and virtual entities of the technology along with their description and certain important use cases.

Environment

The physical environment points to the real-world conditions and space in which the physical asset exists. Attributes including temperature, humidity, pressure, etc., of the environment are measured and shared with the virtual twin environment to make sure that there is a correct virtual environment; therefore, when simulated, optimised, and decisions are made it achieves the purpose of simulating real-time physical conditions [64–67]. The physical environment might have to include all parameters that influence the physical asset, but they do not have to be limited to those captured concerning the Digital Twin, since measuring all parameters may not be feasible [68–71]. Many factors can influence the performance of a physical asset, and they should be included in the virtual environment. The virtual environment is in a digital domain and is the exact model of the physical environment, with twinning achieved using sensors sending information on critical measures from the physical asset to the virtual environment [72–75]. Terms such as virtual space, data model, virtual world, and multi-domain models are used to replace virtual environments. Most often, virtual environments are described using the underlying technologies used including API, cloud platform, and server, unlike the physical assets [76–79].

Connections

IoT, smart infrastructure, sensors, web services, availability of 5G, etc., are the factors that are restructured in the virtual model to mirror the physical environment. There are two phases: metrology, where the state of the physical object is captured while in the realization phase, the delta between the virtual and the physical objects is obtained to change the virtual parameters fittingly. As Grieves puts forth fact that

the movement of the material from the virtual model to the physical entity which is basically the Digital Twin technology allows the particular physical process to make modifications in its physical state [80–82]. Generally, the physical-to-virtual connection is more popular, but at the same time, it is to be realised that Digital Twin is a two-way/bidirectional connection which would be the fundamental paradigm of twinning. When both the connections are used together, it forms a closed loop and checks the hypothetical results which have been produced by the virtual environment in relation to the actual outcomes of the physical environment [83–86].

Parameters

Parameters describe the types of information, data, and processes that are fed between the physical and virtual twins [87–89]. Table 2 illustrates how parameters can be grouped into classes:

Process

Examples with respect to manufacturing have been stated in these papers which include automated factories, iron, and steel industries [90], 3D printing procedures [109], robot designing medical infrastructure [114], etc. Hence, physical processes are actions that are executed by that particular physical entity in its designated physical environment. While virtual processes are those which are executed by the virtual entity in its specific virtual environment. Activities like simulation, designing, modelling, analysing, and optimization are covered under the virtual processes. Examples include verifying the design [103], monitoring health, diagnostics and analysing and inferring from them, alternative management solutions [115], etc.

States

The term state refers to the present condition of the physical and virtual entities in the Digital Twin, or the values of the parameters that are measured right now. Examples of states are operational and health [116], disease within uman beings [96], process and behaviour [117], mechanical and thermodynamic [118], etc. Functionality such as real-time state estimation [119] and the prediction of past, present, and future states could be accomplished through understanding the state of the virtual representation which is the same as the physical twin. The state is therefore used for two parts in a Digital Twin: the physical and virtual entities.

Levels of Fidelity

Fidelity characterises the parameters, their accuracy, and pensiveness that are communicated and sent constantly between the virtual and physical representations. The fidelity of the virtual model is defined as a very accurate model of the physical asset. Grieves interprets the virtual representation as meticulous as a micro-atomic perspective. Fidelity is crucial in determining the activities that can be carried out in both virtual and physical ecosystems–the greater the fidelity, the more similar the virtual and physical environments are. Those cases found in the collection are usually located near the centre of a scale ranging from abstract (low) to specific (high), with medium fidelity in the middle. That is, the use cases only use a subset

Table 2 Parameter types, their descriptions and examples [16]

Parameter	Description	Examples
Form	Geometric structure of the entity	Geometry, dimensions, size [90], wear, tolerances [15, 91], work-piece parameters (strength, hardness) [92], coordinate system [91], space requirements [93]
Functionality	Movement and/or purpose of the entity	Functional capability [94], machine parameters (spindle speed, feed rate) [92], control [95], function model [93], general, biochemical [96]
Health	The actual state of the entity with respect to its ideal state	Analysis [97], management [97, 98]
Location	The geographic position of the entity	With respect to the entity [99], manufacturing [100], layouts [101], to the environment [97]
Process	Engagement of the entity within the activities	Scheduling parameters (sequence, idle time) [92], models [102], logistics [103], general [14, 104–106]
Time	Time is taken to complete an activity and the date/time that activity takes place	Timeliness [107], processing and production [108], idle and working time [92], exposure [109]
State	Current measured state of all environment parameters and entity	Entity, completeness [93], usage [110], processes [104], environment [94], general [109, 111], human stress [96]
Performance	Measured operation of the entity compared to its optimal operation	General, Part [112]
Environment	Existence of the entity in the Physical and virtual environment	General
Misc qualitative	Information that is qualitative and therefore not generally measurable by traditional Internet-of-Things type sensors	Product order [90, 100], requirements [93], employee qualifications [108], mission [113], diet [96]

of the parameters (medium fidelity), rather than the entire set (high fidelity) that the original Digital Twin definition required. There is yet to be a comprehensive high-fidelity application in the literature that captures parameters for every element of the physical twin. The truth of doing so may present challenges in device components such as network performance and computational processing capacity, implying that a true high-fidelity Digital Twin is not currently possible. The development of such abstract and early-stage Digital Twin has significant prospective advantages, with proposed benefits in the ability to model and to create information, and earlier process stages defined by a need for knowledge and up to 70% [120] of the budget dedicated to adolescent phases.

Twinning and Twinning Rate

Twinning is synchronising of the physical and virtual states, an illustration, the processes of aligning the physical entity's state and actualisation of that state in the virtual environment such that the states of both virtual and physical are the same or equal, where all the parameters have the same value for both the virtual representation and the physical asset. Figure 3 shows the twinning process. A change in either the virtual or physical entity is assessed before being released in its identical virtual/physical twin; the entities are said to be twinned. The bidirectional connections allow for continuous optimisation of the cycles, while physical states that could be feasible are predicted in the virtual counterpart and improved for a specific process. The virtual improvement process is carried out using the present states of the Physical asset/Virtual counterpart, and then this best set of virtual parameters is sent to the physical twin. The physical twin reacts to the transition, and the loop repeats itself to update the virtual twin with the new and measured state of the physical asset. The difference between the actual and predicted states can then be set side to side and the optimisation process is run again with the new information.

   Twinning rate is the frequency with which twinning happens. This rate is only described as real-time meaning that the changes in a physical state will almost immediately update the same change in the virtual state. The value of such an almost real-time state is that it allows the Digital Twin to act simultaneously, and results in an almost real-time reaction to change. Twinning rate and twinning are the real-time connections within the Physical Assets and the Virtual Representation/Environment. All the interactions between both the physical and virtual entities are stored in the virtual environment and are attainable to future virtual processes. This means that the Digital Twin can learn from its experience, in terms of past performance and virtual processes.
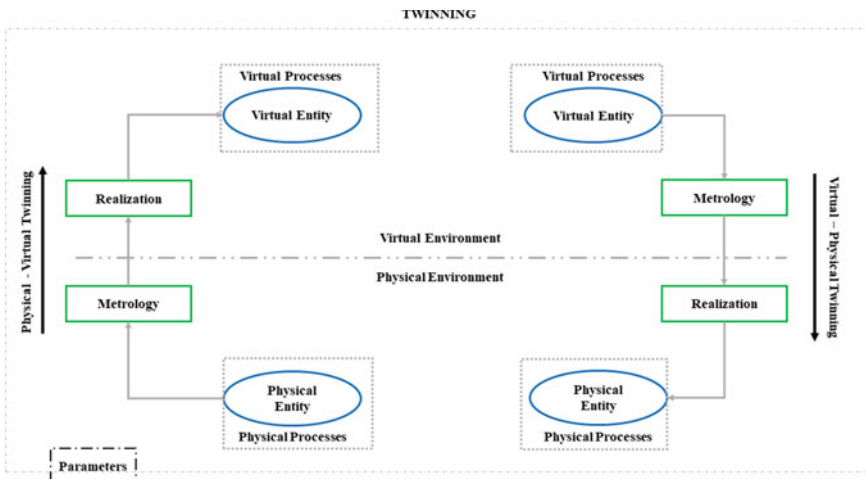

Fig. 3 Twinning process of physical to virtual and virtual to physical [16]

2.6 Key Technologies

In order to implement and develop Digital Twin, Table 3 lists several technologies that industries have used to build the digital model of the physical assets. The following table discusses the key technologies in the form of three different applications: Data related, high fidelity, and simulation models.

Table 3 List of key technologies to enable Digital Twin [121]

Applications	Functions	Technologies
Technologies related to data	Data collection	Industrial IoT, RFID, cameras, 3D scanning
	Data mapping	Automation, machine learning, XML
	Data transmission	5G, bluetooth, wireless sensor network
	Data processing	Signal processing, blockchain, edge computing
High-fidelity modelling	Semantic modelling	Machine learning, deep learning, data mining, expert system
	Model integration	Standard interface, flexible modelling, multiphysics modelling
	Physics modelling	Geometric modelling, material modelling, mechanical modelling, hydrodynamic modelling
Simulation-based on models	Multi-scale simulation	Analytical modelling, continuum modelling, network-based modelling
	Finite element analysis	Virtual element method, meshfree method, scaled boundary method
	Exchange interface	Network control technology, programmable control, embedded control
	Discrete event simulation	Dynamic stochastic systems, statistical analysis
	Bidirectional interaction	Follower modelling, despotic modelling, feedback-initiative modelling

2.7 Technical Implementation

Combining and integrating all these pre-existing technologies like 5G, wireless communication, ethernet, actuators, IoT, and RFID is how the Digital Twin technology can be placed at the centre of the process to collect data and give the appropriate results while connecting the virtual and physical environments. Sensors and RFID are used to acquire the required information, while the Internet of Things forms a network between all devices and actuators are used to identify the differences in the physical environment [1, 3–10, 18–25, 32, 33, 35]. Certain standards need to be maintained to implement the Digital Twin technology as it is being built from the present off-the-shelf technology.

Computer-Integrated Manufacturing

A reference manual for CIM was documented by the CIM Reference Model Committee International Purdue Manufacturing in the 1980s [122]. This way of manufacturing was considered to be a healthy and strong process to develop production lines, and it also could keep changing with the new modifications brought about by disorders or breakdowns and most importantly changes in customer preferences. Computers were enabled to both monitor and control a physical object by using closed information loops.

Virtual Manufacturing Systems

Onosato [114] introduced the concept of virtual manufacturing systems (VMS) which means manufacturing systems that pursue the informational equivalence with real manufacturing systems. Onosato, also designed a layout to set up a factory with the manufacturing and production processes and the main shop-floor organization using VMS to model, test and simulate the planning, forecasting, and timetabling. Building on this, Iwata et al. [11, 123] described the infrastructure needed for such systems. VMS is used to duplicate physical activities with high-fidelity digital representations.

Model-based Predictive Control

Digital Twin is similar to model-based predictive control in terms of analysing the present conditions and transposing them into the possible future states of the physical model. Initially, this type of predictive modelling was used to control the chemical reactions in the oil and gas industries [124]. Both the physical and virtual models and activities are analysed parallelly to balance them accordingly to get a better understanding of the behaviour of the system. Maynes review in 2014 [125] focused on the mathematical and theoretical features along with the challenges in ensuring the closed-loop control feature which was introduced by Grieves and Vickers, through sensor-to-controller and controller-to-actuator connections which is akin to the physical-to-virtual and virtual-to-physical characteristics of the Digital Twin technology.

Advanced Control System

The integration of artificial neural networks, fuzzy logic, and evolutionary algorithms has allowed various industries to adapt and apply them to the machinery. Dotoli et al. [126] explain how techniques involving computational thinking and intelligence, predictive systems have led to the development of adaptive control systems. These are advanced and measure the data from a physical environment and translate it into the virtual description of the same. Controlling the input parameters gives different outputs which in turn can be replicated in the physical environment to get optimal results.

Machine Health Monitoring

Heng et al. [127] state that it is necessary to keep track of the environmental changes where the physical entity is based in order to effectively connect the virtual twin and the physical model in real-world operations. The rotating machinery monitoring and prognostics are essentially forecasting the operational life and condition of the machine and the number of maintenance periods or repair works it might need. In order to protect the health and state of the machines, automated predictive systems are required which will collect data via the sensors, analyse, and report the findings. Any change in temperature, pressure, vibrations, acoustics, etc., will be instantly identified with the assistance of the mathematical models and the past and present states of the machine using the prognostic models.

Building Information Modelling

The objective is to create a single source of information to provide ease of access to the different stakeholders involved in the operations and to ensure the centralization of all the data. This is government legislation that absorbs the necessary information and then it is converted into a 3D representation of the building. Eastman et al. [128], in their handbook, describe the interoperability to standardise the formatting of the files, and lighter representations using CAD models [81] and with this, a virtual representation of any physical process can be built using this method which focuses on the users of the twin technology. The BIM Levels, which have been defined by the government of the UK, stress the likelihood of Digital Twin. Kritzinger et al. [129] talk about the BIM levels 1–3 which emphasise the Digital Shadow, Digital Model, and Digital Twin, respectively (See Fig. 4).

2.8   Challenges in DT

The widespread adoption of Digital Twin has considerable challenges. Trying to match sophisticated assets and their behaviour digitally will eventually overtake financial and computational capacity, data control abilities, and even corporate culture, with certainty and in real time [130].
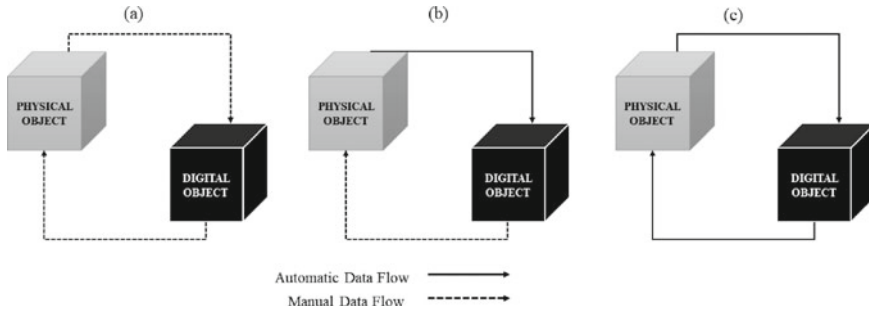
Fig. 4 Data flow in **a** Digital model **b** Digital shadow **c** Digital Twin [129]

Cost—Digital Twin requires substantial investment in new technologies, high maintenance cost, and system architecture while several of these expenses continue to decline, it is always essential to measure the decision to establish a Digital Twin to possible alternatives that could deliver similar benefits at a lower cost. If an organization is interested in a limited number of important factors, via an IoT environment with sensors and a regular database, these observations can be gathered in a more cost-friendly manner.

Precision—The Digital Twin can't be the same representation of their physical counterparts in the near future. It is both difficult and cost-intensive to match the chemical, electrical, physical, and thermal status of an intricately designed asset. Hence, engineers and programmers should make certain assumptions to enhance and sustain the desired features and simplify the Digital Twin models within the technical and financial limitations.

Quality—Good data will create good models, but it is difficult to get the same output from Digital Twin. Data is provided by around hundreds or even thousands of operations across various activities, information from sensors placed at various locations, and discussions over unstable networks. Organizations will have to build on techniques to identify and segregate bad data and improve the consistency of product data streams.

Interoperability—Economical and technical barriers continue to exist in spite of the transparency in procedures to transfer and exchange data. This technology is heavily dependent on simulation and AI software which might need to be provided by specific vendor companies. It could be hard to change or look for other providers as establishing and replicating the same features would be close to impossible. Hence, it is of utmost importance to ensure single-supplier relationships for longer durations.

Education—In order to effectively operate and use the system, organizations would need to train their employees and make sure ease of use for suppliers and customers. Changes for a smooth transition in the management to have a maximum capacity to build on skills and simulation tools for the staff to learn and interact with Digital Twin models. In order to fully understand the potential of new technology.

Cyber Security—A virtual model of the physical world would attract attention from cybercriminals. The data collected would be the link that connects every aspect

of the physical assets to their twin. This would create an opportunity for malware to hack the company's operations. Hence, cyber security becomes a critical part of a twin's efficient management to prevent any disruptive effects.

IP Protection—Digital Twin can be considered to be a reservoir of information. The features of the product or service need to be integrated into the models with a similar level of security due to data sensitivity issues. These present more challenges revolving around identity theft, data control and confidentiality, and authentication of information by a variety of participants.

2.9 Benefits

Many papers highlight the advantages of the Digital Twin technology implemented in various situations as depicted in Table 4.

3 Industrial Applications

Digital Twin is already being applied in multiple industries on a small scale. The following sections discuss the implementation of this technology in manufacturing, life sciences, infrastructure, etc.

Table 4 Benefits of implementing Digital Twin [16]

| Benefits	Citations
Reduction in costs	[15, 94, 109, 131]
Design and risk time	[131]
Reconfiguration and complexity time	[93]
Improvement in after-sales service	[112, 119]
Efficiency	[132]
Decision making maintenance	[133]
Security	[134]
Reliability and safety	[135]
Management in manufacturing	[110]
Tools and processes	[136]
Enhancing competitiveness and flexibility in manufacturing systems	[118]
Innovation incubators	[15]
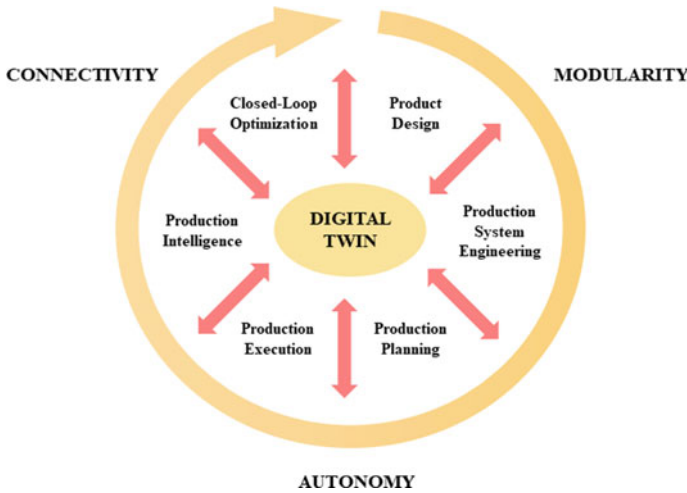
Fig. 5 Digital Twin during the product lifecycle [138]

3.1 Manufacturing

Manufacturing physical goods are the core operation of most major factories, and they are data rich (See Fig. 5). CNH Industrial, a company that manufactures vehicles for agricultural, commercial, and industrial purposes, partnered with a consultant called Fair Dynamics and a software provider called AnyLogic to use Digital Twin for optimising maintenance at its plant in Suzzara, Italy [137]. To find a more efficient method of maintaining CNH Industrials welding robots on the Iveco Van assembly line. A Digital Twin model of the assembly line was created by the company. Everything was included in the model, including different types of chassis and their welding requirements, automatic welding stations strategically placed along the assembly line, and individual robots in each welding station. They were able to forecast the maintenance and failure rate of the welding robot components using machine learning and simulations based on data obtained from the factory through its production planning and sensors added to each robot. This new learning enables the company to run multiple what-if scenarios comparing various decisions and maintenance routines in order to reduce downtime.

3.2 Materials Science

Materials science is an important aspect of production as product performance depends on the properties of materials used to make it. Math2Market, a German Software company, developed specialised software for the simulation of various materials and their properties. The company's GeoDict software models use AI-assisted

image processing and material Digital Twin for strength and stiffness analysis, fluid dynamics studies, and other variety of purposes [139]. The oil and gas industry is using this approach to model the flow through porous rocks in underground reservoirs. While the aviation industry is in search of a robust and lightweight material composition through extensive optimisation and digital simulation.

3.3 Healthcare

With accessible technology and innovation in the field of healthcare, even researchers, and doctors are exploring Digital Twin and its applications. Models of the human body and its parts can help doctors understand the human anatomy. Its behaviour and structure with greater detail while reducing the need for invasive tests. These models can also help in rehearsing complex operations safely. A Digital Twin model of the human heart was developed by Siemens Healthineers which simulates its electrical and mechanical behaviour [140]. Philips is exploring a range of additional Digital Twin applications other than human body models. The company is using AI to assist with remote support for complex medical machinery like CT scanners. Philips collects data from customers and analyses it to find early symptoms of diseases in its machines [141]. GE Healthcare's Hospital [142] of the Future Analytics Platform has the Digital Twin technology built into it and allows the modelling and simulation of complete hospital workflows for the first time. The inability to predict the effects and side effects of medicine on patients costs Europe's healthcare systems around 20% of its total budget. To counter this, the DigiTwins initiative [143], a far-reaching research consortium, wants to create a Digital Twin for every European Citizen [144].

3.4 Urban Planning

Some of the biggest Digital Twin that already exist are replicas of physical infrastructure including transportation networks, cities, and energy systems. In the UK, Alstom has a Digital Twin for its train maintenance operations, and it includes their operating timetables, details of every train in the fleet, and maintenance routines. To schedule maintenance, it uses a heuristic algorithm and allocates trains efficiently using an AnyLogic environment developed by the company. The system is connected and has a live location of every train and its planned movement. They also use What-if Analyses to see the effects of changes in the train operations and its schedule [145]. Fingrid collaborated with Siemens, IBM, [146] and other companies to create a Digital Twin of Finland's power network in energy transmission. The Electricity Verkko Information System integrates almost eight different systems into a single application that gives Fingrid a real-time model of its electric grid. In their day-to-day grid operations, the Digital Twin is used in assisting in the management of power flows and protection to meet deregulation targets. It also can handle designing and

planning activities, allowing the Fingrid to simulate the likely effect of investment in upgraded assets or changes to grid configuration.

3.5 Industrial Products

Companies with assets for industrial production often try to work on servitization strategies that help in mandating product uptime. After all, one can monitor assets when they are with the client. Sometimes, clients are willing to pay for the insights that could be gained from the analysis such as efficient maintenance strategies, remote repair, and diagnosis [147]. Major aero-engine manufacturers including GE, Pratt & Whitney, and Rolls-Royce use Digital Twin because it helps them to monitor and support the engines operating on customers' aircraft. On the ground, Kaeser Kompressoren, a compressed air systems manufacturer from the Netherlands developed a Digital Twin solution along with SAP covering its entire sales and product support lifecycle. The data collected and this system act as a repository for new installations and help in predictive maintenance capabilities [148].

3.6 Energy Sector

The energy sector has high operating costs and often involves complex and huge assets in remote locations. Digital Twin employed in this sector will help in improving safety and reliability while controlling operating costs. In the offshore oil and gas sector, Aker BP and Siemens worked on the BPs Ivar Aasen project which led to successful optimisation models for maintenance and reduced manpower requirement. They have an agreement where digital lifecycle automation and analytics solutions for performance which will be implemented in all future assets will be developed by Siemens [140]. While Royal Dutch Shell is developing a Digital Twin of an existing offshore production platform in the North Sea, the company has partnered with an R&D consultancy and a simulation company to find new methods of managing the structural integrity of the assets. They will use sensors to monitor and predict the health condition of the asset. DNV DL Group, a Norwegian engineering firm, has developed a WindGEMINI package for Digital Twin to monitor the structural integrity, fatigue, and life of turbines and their components [149]. While General Electric has developed a model where engineers can create virtual sensors using a thermal model of vital turbine components which are inaccessible otherwise.

4   Freight Logistics Digital Twin

The previous section covers the applications of Digital Twin technology in diverse industries and fields of applications such as Healthcare, Urban Planning, and Energy. There are multiple issues pertaining to logistics in every country developed or developing. It is also one of the major costs in the supply chain, costing at least 8% of a country's GDP per year. Efficiency and risk mitigation can be achieved by using technologies such as location tracking and automated vehicles to provide information and material at the required place, at the appropriate quality and quantity as well as at right time [134]. This is the future of manufacturing systems with seamless information systems, better handling of transport and cargo, visibility of material in the supply chain, and efficient use of energy and material [121]. It's important to have end-to-end visibility into the supply chain to detect disruptions and evaluate what's planned to what's happening [].

4.1   Implementation in Freight Logistics

This section will discuss how the implementation of technology like Digital Twin in logistics (See Fig. 6) will help optimise all the processes within this vertical and pass this cost-saving to critical stakeholders across the supply chain resulting in a more efficient value chain.
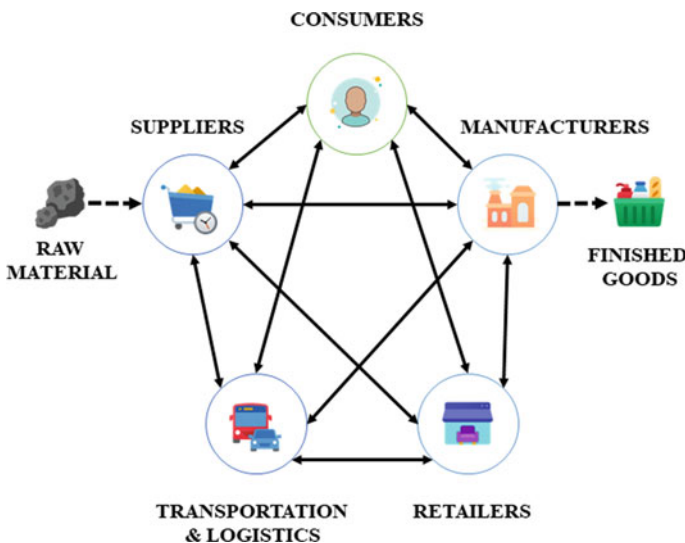

Fig. 6   Freight logistics Digital Twin network

4.2   Containers and Packaging

The logistics industry employs a large amount of single-use packaging as well as fleets of reusable containers that are either dedicated or general-purpose. The e-commerce boom has resulted in increased demand, seasonal volatility, and a variety of packaging options. As a result of the poor volume utilization, more waste is produced and operational efficiency is reduced. However, applying Digital Twin to materials science could aid in the development of more sustainable, light, and durable packaging. In order to reduce their carbon footprint, businesses are experimenting with different materials such as compostable plastics. IKEA, a Swedish furniture company, is replacing plastic foam with a mushroom-based alternative [150, 151]. Math2Markets Material Digital Twin could aid companies in studying and predicting the performance of the new material in packaging applications. Such twins can imitate how a material behaves under various physical conditions such as temperature, vibration, and shock loads when moving. Aircraft ULDs, standard ocean containers, reusable crates for transporting car parts between factories, and food and beverage containers are all examples of container fleets. In the case of container fleets, Digital Twin can assist logistics layers in more efficiently managing them. It can be difficult to keep track of them because companies must not only track their movement but also coordinate their next destination and inspect for damage and contamination that could affect future shipments or pose a threat to other assets. Metrilus, a German start-up, uses 3D photographic technologies to quickly create a model of a container, revealing potential issues like dents and cracks. These insights were combined with historical data on the movement of the containers to create a Digital Twin which can help determine when a container or asset should be repaired, used, or retired. Collecting this information across a fleet of containers could help owners make better data-driven decisions about the distribution and size of the fleet, as well as identify trends that can help predict or understand problems like container design flaws or rough handling at ports or other points along the supply chain.

4.3   Shipments

Adding models of the product in a package or a container is the next step. Combining the data of products and packaging will enable companies to improve efficiency and optimise utilisation through automated processes. High-value and sensitive products are already shipped with multiple sensors that monitor different parameters like temperature, package orientation, shock, and vibration. Roambee, Blulog, Kizy are a few companies that offer real-time data by incorporating different sensors during a shipment. This real-time data can act as a database and allow Digital Twin technologies to use it in new ways. Data could be extrapolated from external sensors about a package with thermal insulation and shock-absorbing packaging.

4.4 Warehouses and Distribution Centres

Once Digital Twin is implemented, it may have a noteworthy impact on the operation, design, and optimization of logistics infrastructures such as distribution centres, warehouses, and cross-dock facilities. These Digital Twins can combine a 3D model of the facility with inventory and operational data like size, location, and quantity and demand characteristics of everything along with data from connected warehouse platforms [152]. The Digital Twin could be updated continuously during warehousing with data collected from various automation technologies such as drone-based stock counting systems [153], automated guided vehicles, goods-to-person picking systems, and automated storage and retrieval equipment. Digital Twin will improve the performance of these automation systems even more by using sensor data, simulations, and monitoring. 3D facility data can help warehouse workers be more productive by allowing companies to use virtual-reality training tools like Google Glass Enterprise Edition or Microsoft HoloLens, which DHL Supply Chain already uses [154]. Facility managers can use simulations to evaluate and test the effect of changes in layout or operations due to the addition of innovative equipment or assets, before making changes on the ground. In a highly volatile and rapidly changing environment, Digital Twin can support the dynamic optimization of operations to accommodate current or forecasted demand.

4.5 Infrastructure for Logistics

Only 20% of logistics infrastructure and processes are made up of warehouses and distribution centres. The movement of goods from point of origin to point of destination is dependent on the coordination of various elements such as ships, trucks, and aeroplanes, as well as order and information systems and, most importantly, people. Singapore has been working on a project to address information exchange and offline processes using Digital Twin technologies. The Singapore Port Authority is developing a Digital Twin of Singapore's new mega-hub for container shipping in collaboration with many partners, including the National University of Singapore. In the design phase of the Singaporean project, the Digital Twin perspective is already yielding benefits. The Port Authority and project partners are using digital models to speed up the generation of potential layouts and simulation systems to assess various what-if scenarios. The Port Authority hopes that this technology will aid in the optimization of the new mega-management hubs. They can choose the best berthing location for any size vessel using simulation, taking into account the space, assets, and personnel needed for unloading and loading operations, as well as the requirements and constraints of sharing those resources among multiple vessels at the same time. Despite having a grand vision for using Digital Twin to improve logistics infrastructure, Singapore has yet to implement it.

4.6   Global Logistics Networks

In logistics, the ultimate Digital Twin will be a model of the entire network, including seas, railway lines, roads, streets, and consumer homes and workplaces, in addition to logistics properties. Geographic information system (GIS) technology is rapidly progressing due to developments in aerial and satellite photography, and digital mapping efforts from the ground. For several years, governments, utility companies, and navigation system providers have driven demand for geographic data, but with self-driving cars and trucks now being tested and examined on public roads, and a few automotive manufacturers announcing plans to introduce vehicles with autonomous capabilities within the next ten years, the demand for geographic data is growing. This has accelerated the need for extremely detailed geographic information [155].

Autonomous vehicles can alter geographic data in two ways: they will perform mapping functions themselves, and they will require extremely detailed maps to operate, gathering data from cameras that are on-board and radio or light-based detection and ranging (radar and lidar methods) systems and sharing it to constantly upgrade and enhance map databases. Traffic densities and speeds, delays on road, and restrictions in parking due to accidents or repair work are all included in modern GIS systems. Logistics companies now make substantial use of GIS data to schedule distribution routes based on weather forecast arrival times, delays, and congestion at airports, ports, and border crossings. The use of data on customer demand trends, locations, and travel times to plan inventory storage locations and delivery routes would aid providers in optimising their conventional logistics networks. The fragmented and heterogeneous structure of the logistics sector makes it even more challenging for Digital Twin to thrive.

5   Discussion and Recommendations

The purpose of this section is to support the usefulness of Digital Twin in Freight Logistics. Digital Twin is an amalgamation of simulation, optimization, and data: a data-driven approach for managing the risk of disruption in logistics. A digital freight logistics twin is a model that can represent the state of the transportation and process network at any time and enable transparency in logistics to develop better resilience and simulate what-if scenarios [156].

Tests and the data sets that were collected can be used for analytics and can predict and prevent failures from happening. The data snapshots including product logs drive the flow of tests based on use cases for application and test cases such as warehouse types, equipment layout, and stages of the workflow. Function libraries are the databases of scripts based on use cases in the application and interface layers (See Fig. 7). Logistics in an efficient production means handling and providing material at the right time, quantity, quality, and place. There is a lack of consideration for the human factor in the existing literature. The research effort is required about Digital
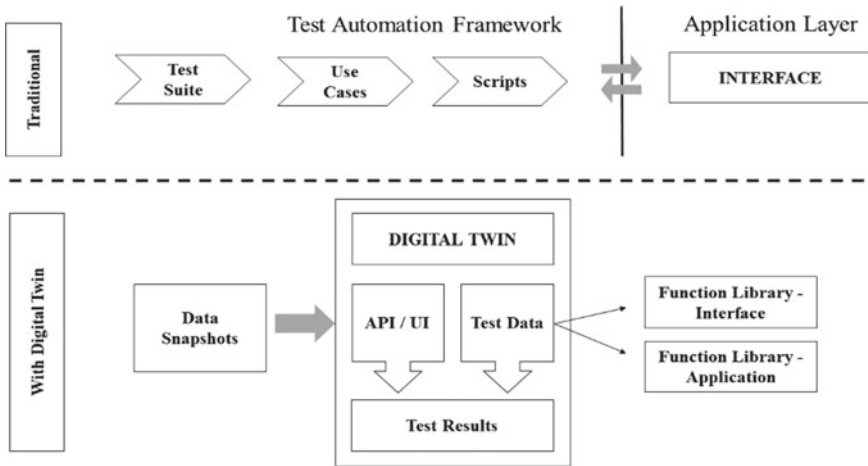
Fig. 7 Test Automation and application testing process using Digital Twin

Twin for people in logistics [121]. After a discussion about possible implementations in Freight Logistics, a few recommendations for improving this field further with this novel technology are mentioned in the subsequent sections.

5.1 Improving Freight Logistics

Figure 8 shows the interlinking between the virtual and the physical process involved when replicating a real product to make its Digital Twin counterpart.

5.2 Inbound to Manufacturing

Due to Digital Twin more customisable products twitch various configurations to match specific customer preferences will be available. There will be more flexible manufacturing operations due to new demands. Companies would have to create new processes to cope with the uncertainty without sacrificing lead times, logistics efficiencies, or inventory costs. All of this will necessitate a careful selection of supplier sites, as well as new shipping and freight management approaches. Manufacturers through exchanging demand forecasts which are derived from Digital Twin data and work along with suppliers to recognise their production processes' capability and limitations. At the same time, vendors may use vendor-managed inventory (VMI) to provide manufacturers and their customers with more flexibility and value.
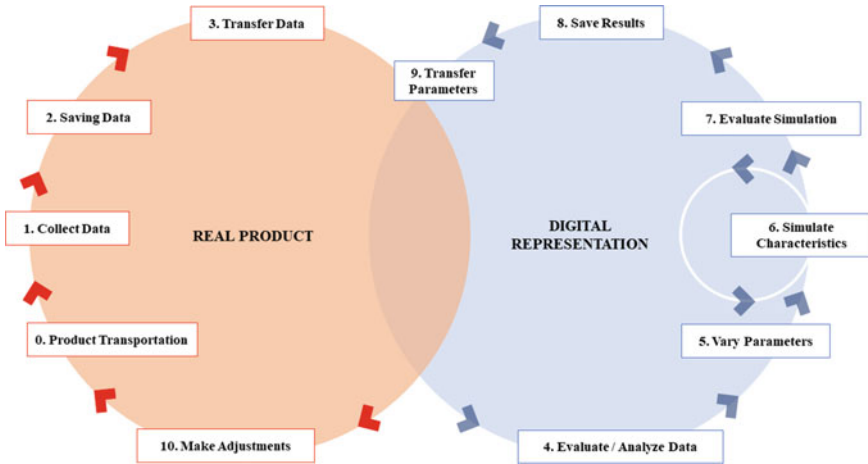
Fig. 8 Linking between the real product and digital representation

5.3   Logistics Within the Plant

The advent of Digital Twin-enabled manufacturing will change the requirement of in-plant material flows. To handle shorter lead times and higher product complexity, companies must adjust their Kanban replenishment strategies and their processes for just-in-time delivery. They must also maintain data related to materials and components to ensure that the Digital Twins of the products they create are connected to the correct components and materials. Depending on the specifications of Digital Twin-driven goods, the design of workstations and the layout of the plant need to be changed. Integrating with advanced storage and handling systems or using technology like augmented reality to help workers find and select parts quickly, Digital Twin technologies may help businesses handle the added complexity generated by new product workflows.

5.4   After-sales Logistics

Digital Twin can change the relationship between product manufacturers and their customers while adding tremendous value due to the new capabilities added by this technology. A third-party service partner or an OEM may track a product worldwide using a Digital Twin. This is why they are gaining popularity in the Industrial Products market. This capability can be used by companies to provide a variety of services to their customers, ranging from remote assistance to predictive maintenance. The success of these new offerings will be measured by the provider's aftermarket supply chain capabilities. An early warning system is only effective if a remedy is available

after the warning has been issued. Spare component procurement and distribution would be critical in the operating model for organizations that use a predictive maintenance system and constructive steps. Companies also need to consider their clients, the goods they purchase and use, and how they use those products in order to afford high-performing aftermarket logistics and service capabilities. To obtain lead times that suit their service level agreements, they would need to review the delivery and inventory of spare parts inventory regularly. The distribution must be linked to other aspects of a company's aftermarket and field service operations. They may need to coordinate the arrival of service technicians at customer locations with the distribution of appropriate parts and provide after-sales services through their dealer and distributor networks. Some pieces have reached the end of their useful life and are no longer in use by consumers. By recognising the exact type and content of equipment, Digital Twin will help businesses increase the future value of old equipment. However, capturing the value may necessitate complex reverse logistics systems that are combined with remanufacturing, recycling, and waste management systems.

5.5 Supply Chain Network Design

Through the complete view of the entire supply chain due to Digital Twin, companies can make holistic decisions that might impact the end-to-end journey of their products. Businesses need to find better ways to balance inventory costs, lead time, and supply across their networks. Doing this will maximise the value of products and associated services through the supply chain. The rise in the importance of the visibility of a product across the supply chain will push the customers to understand locations, availability of raw materials and goods in inventory, and procurement from suppliers, their sales channels, and distribution networks. For supply chains to be resilient, companies have to develop the ability to maintain service levels during disruptions in the supply chain like the bull-whip effect and recover quickly from black swan events, while maintaining responsiveness to demand.

5.6 Value Creation

Implementing this technology would ensure better intra- and inter-team synergy and collaboration between the various acting parties in the logistics industry (See Fig. 9). Centralised data sharing among the suppliers, retailers, manufacturers, producers, and distributors would ensure informed decision-making and better communication.

Descriptive Value—The digital reality world showcases a pictorial 3D model of the assets which could either be remote or treacherous, like huge gas turbines, factories, space centers, etc. Digital Twin creates information that is much more ubiquitous and understandable from afar.
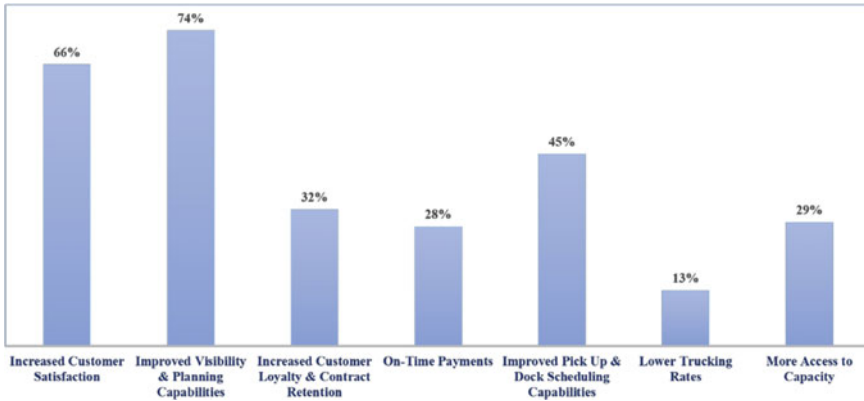
Fig. 9 Benefits of improved data sharing collaboration between shipper and 3PL counterparts

Analytical Value—Digital Twin is combining simulation technologies that can include evidence such as the output obtained within an entity that cannot be directly calculated on the physical body. This can be used with current products as a debugging technique and can help to enhance the efficiency of following generations of merchandise.

Diagnostic Value—Digital Twin could have diagnostic systems that indicate the most possible root triggers of specific states or behaviours using recorded or inferred evidence. These programmers can be applied in the form of specific guidelines based on business proficiency, or they can use analytics and approaches to machine learning to obtain existing evidence-based connections.

Predictive Value—Using a Digital Twin model, the potential future status of the physical system can be estimated. GE uses Digital Twin in wind farms to calculate power production is one examples. Rather than just forecasting the dilemma that will emerge, the most advanced Digital Twin does more; they also suggest the required solution. In order to optimise customer loyalty and profitability, Digital Twin can play a major role in the creation of potential smart factories which are capable of making autonomous decisions on when to make, what and how.

6 Conclusion and Future Scope

In the last few years, the growth of Digital Twin has seen a shift with several industry leaders heavily investing in the technology. The concept and the evolution of this technology have been made possible due to the tremendous advancements in IoT, AI, and cloud computing which are the key enablers. The review carried out is about the Digital Twin technology and the transformation it has brought about in industrial applications. Characterisation of this technology elaborates on the various features like the twinning rate, physical and virtual environment, virtual to physical

Connecting, etc. Further, it focuses on where it can be implemented with respect to the benefits one might receive, the technical implications it poses, and the gelling between the physical and virtual processes and also sheds light on the various underlying technologies which assist in the development of the Digital Twin. There are obstacles that remain in precise representation, computing resources, data quality, cost, organisational culture, and governance. Industries are restructuring and learning to conquer these challenges. The value added by Digital Twin will be better in scenarios where one would build powerful and resilient business models.

There is a wide range of applications for this technology from controlling a power grid, maintaining high-value assets, and running a metro service to monitoring the human heart and predicting operational discrepancies in a factory. This range showcases the scalability and flexibility which make it a perfect way to digitize a value chain and especially to cater freight logistics in a VUCA world while customer preferences keep changing regularly. Logistics is not only the flow of products but also the flow of information simultaneously. The basic parts of a Digital Twin: the physical asset caters to the product flow across the world, while the virtual counterpart deals with the flow of information and data. As the required technologies continue to become more attainable, the logistics industry is just starting its journey and examples of the first possible supply chain resources and development of logistics hubs are stated above. While the technology itself provides greater insights into and the prospect of the current and future state of an asset or operation, from a material used in the product to important infrastructure, more informed decisions can be taken about managing the operations during the actual field run. For Digital Twin and its physical counterparts to work together flawlessly, there is an increasing need for experts to improve the quality of service, responsiveness, availability, and accuracy in delivery to make sure that the physical counterpart performs harmoniously with its expected design and performance. A question that needs more attention for logistics experts to consider in the near future is how to take freight logistics to the next level and its evolution in an organisation when Digital Twin becomes an integral part of product, asset, and infrastructure operations. Several tech giants believe that Digital Twin in logistics is still in its inception phase, and it gives them the opportunity to explore and learn about the challenges and multiple opportunities that could be on the path of embracing this technology.

References

1. Sharma, S.K., Lee, J., Jang, H.-L.: Mathematical modeling and simulation of suspended equipment impact on car body modes. Machines **10**, 192 (2022). https://doi.org/10.3390/machines10030192
2. Vishwakarma, P.N., Mishra, P., Sharma, S.K.: Formulation of semi-active suspension system and controls in rail vehicle. SSRN Electron. J. (2022). https://doi.org/10.2139/ssrn.4159616
3. Vishwakarma, P.N., Mishra, P., Sharma, S.K.: Characterization of a magnetorheological fluid damper a review. Mater. Today Proc. **56**, 2988–2994 (2022). https://doi.org/10.1016/j.matpr.2021.11.143

4. Sharma, S.K., Sharma, R.C., Lee, J., Jang, H.-L.: Numerical and experimental analysis of DVA on the flexible-rigid rail vehicle carbody resonant vibration. Sensors **22**, 1922 (2022). https://doi.org/10.3390/s22051922

5. Sharma, S.K., Mohapatra, S., Sharma, R.C., Alturjman, S., Altrjman, C., Mostarda, L., Stephan, T.: Retrofitting existing buildings to improve energy performance. Sustainability **14**, 666 (2022). https://doi.org/10.3390/su14020666

6. Sharma, S.K., Sharma, R.C., Lee, J.: In situ and experimental analysis of longitudinal load on carbody fatigue life using nonlinear damage accumulation. Int. J. Damage Mech. **31**, 605–622 (2022). https://doi.org/10.1177/10567895211046043

7. Sharma, R.C., Sharma, S.K.: Ride analysis of road surface-three-wheeled vehicle-human subject interactions subjected to random excitation. SAE Int. J. Commer. Veh. **15**, 02-15-03-0017 (2022). https://doi.org/10.4271/02-15-03-0017

8. Sharma, S.K., Lee, J.: Crashworthiness analysis for structural stability and dynamics. Int. J. Struct. Stab. Dyn. **21**, 2150039 (2021). https://doi.org/10.1142/S0219455421500395

9. Wu, Q., Cole, C., Spiryagin, M., Chang, C., Wei, W., Ursulyak, L., Shvets, A., Murtaza, M.A., Mirza, I.M., Zhelieznov, К., Mohammadi, S., Serajian, H., Schick, B., Berg, M., Sharma, R.C., Aboubakr, A., Sharma, S.K., Melzi, S., Di Gialleonardo, E., Bosso, N., Zampieri, N., Magelli, M., Ion, C.C., Routcliffe, I., Pudovikov, O., Menaker, G., Mo, J., Luo, S., Ghafourian, A., Serajian, R., Santos, A.A., Teodoro, Í.P., Eckert, J.J., Pugi, L., Shabana, A., Cantone, L.: Freight train air brake models. Int. J. Rail Transp. 1–49 (2021). https://doi.org/10.1080/23248378.2021.2006808

10. Sharma, S.K., Sharma, R.C., Lee, J.: Effect of rail vehicle-track coupled dynamics on fatigue failure of coil spring in a suspension system. Appl. Sci. **11**, 2650 (2021). https://doi.org/10.3390/app11062650

11. Iwata, K., Onosato, M., Teramoto, K., Osaki, S.: Virtual manufacturing systems as advanced information infrastructure for integrating manufacturing resources and activities. CIRP Ann. Manuf. Technol. **46**, 335–338 (1997). https://doi.org/10.1016/s0007-8506(07)60837-3

12. Choi, S.S., Kim, B.H., Do Noh, S.: A diagnosis and evaluation method for strategic planning and systematic design of a virtual factory in smart manufacturing systems. Int. J. Precis. Eng. Manuf. **16**, 1107–1115 (2015). https://doi.org/10.1007/s12541-015-0143-9

13. Kuts, V., Modoni, G.E., Terkaj, W., Tähemaa, T., Sacco, M., Otto, T.: Exploiting factory telemetry to support virtual reality simulation in robotics cell. In: Lecture Notes in Computer Science (including subseries Lecture Notes in Artificial Intelligence and Lecture Notes in Bioinformatics), pp. 212–221 (2017). https://doi.org/10.1007/978-3-319-60922-5_16

14. Chhetri, S.R., Faezi, S., Al Faruque, M.A.: Digital Twin of Manufacturing Systems. Center for Embedded & Cyber-Physical Systems (2017)

15. Grieves, M.: Digital Twin : Manufacturing Excellence Through Virtual Factory Replication— A Whitepaper by Dr. Michael Grieves (2014)

16. Jones, D., Snider, C., Nassehi, A., Yon, J., Hicks, B.: Characterising the Digital Twin: a systematic literature review. CIRP J. Manuf. Sci. Technol. **29**, 36–52 (2020). https://doi.org/10.1016/j.cirpj.2020.02.002

17. David, I.: The Evolution of Difital Twin—and How Emerging Tech Is Driving Adoption

18. Mohapatra, S., Mohanty, D., Mohapatra, S., Sharma, S., Dikshit, S., Kohli, I., Samantaray, D.P., Kumar, R., Kathpalia, M.: Biomedical application of polymeric biomaterial: polyhydroxybutyrate. In: Bioresource Utilization and Management: Applications in Therapeutics, Biofuels, Agriculture, and Environmental Science, pp. 1–14. CRC Press (2021). https://doi.org/10.21203/rs.3.rs-1491519/v1

19. Bhardawaj, S., Sharma, R.C., Sharma, S.K., Sharma, N.: On the planning and construction of railway curved track. Int. J. Veh. Struct. Syst. **13**, 151–159 (2021). https://doi.org/10.4273/ijvss.13.2.04

20. Sharma, R.C., Sharma, S., Sharma, N., Sharma, S.K.: Linear and nonlinear analysis of ride and stability of a three-wheeled vehicle subjected to random and bump inputs using bond graph and simulink methodology. SAE Int. J. Commer. Veh. **14**, 02-15-01–0001 (2021). https://doi.org/10.4271/02-15-01-0001

21. Sharma, R.C., Sharma, S., Sharma, S.K., Sharma, N., Singh, G.: Analysis of bio-dynamic model of seated human subject and optimization of the passenger ride comfort for three-wheel vehicle using random search technique. Proc. Inst. Mech. Eng. Part K J. Multi-body Dyn. **235**, 106–121 (2021). https://doi.org/10.1177/1464419320983711

22. Choi, S., Lee, J., Sharma, S.K.: A study on the performance evaluation of hydraulic tank injectors. In: Advances in Engineering Design: Select Proceedings of FLAME 2020, pp. 183–190. Springer, Singapore (2021). https://doi.org/10.1007/978-981-33-4684-0_19

23. Lee, J., Han, J., Sharma, S.K.: Structural analysis on the separated and integrated differential gear case for the weight reduction. In: Joshi, P., Gupta, S.S., Shukla, A.K., and Gautam, S.S. (eds.) Advances in Engineering Design. Lecture Notes in Mechanical Engineering, pp. 175–181 (2021). https://doi.org/10.1007/978-981-33-4684-0_18

24. Sharma, S.K., Sharma, R.C.: Multi-objective Design Optimization of Locomotive Nose. In: SAE Technical Paper, pp. 1–10 (2021). https://doi.org/10.4271/2021-01-5053

25. Sharma, R.C., Palli, S., Sharma, N., Sharma, S.K.: Ride behaviour of a four-wheel vehicle using H infinity semi-active suspension control under deterministic and random inputs. Int. J. Veh. Struct. Syst. **13**, 234–237 (2021). https://doi.org/10.4273/ijvss.13.2.18

26. Sharma, S.K., Sharma, R.C., Sharma, N.: Combined multi-body-system and finite element analysis of a rail locomotive crashworthiness. Int. J. Veh. Struct. Syst. **12**, 428–435 (2020). https://doi.org/10.4273/ijvss.12.4.15

27. Sharma, R.C., Sharma, S.K., Palli, S.: Linear and non-linear stability analysis of a constrained railway wheelaxle. Int. J. Veh. Struct. Syst. **12**, 128–133 (2020). https://doi.org/10.4273/ijvss.12.2.04

28. Palli, S., Sharma, R.C., Sharma, S.K., Chintada, V.B.: On methods used for setting the curve for railway tracks. J. Crit. Rev. **7**, 241–246 (2020)

29. Mohapatra, S., Pattnaik, S., Maity, S., Mohapatra, S., Sharma, S., Akhtar, J., Pati, S., Samantaray, D.P., Varma, A.: Comparative analysis of PHAs production by Bacillus megaterium OUAT 016 under submerged and solid-state fermentation. Saudi J. Biol. Sci. **27**, 1242–1250 (2020). https://doi.org/10.1016/j.sjbs.2020.02.001

30. View, G.R.: Digital Twin Market Size Worth $26.07 Billion By 2025 | CAGR 38.2%, (2018)

31. Sharma, R.C., Sharma, S.K., Sharma, N., Sharma, S.: Analysis of ride and stability of an ICF railway coach. Int. J. Veh. Noise Vib. **16**, 127 (2020). https://doi.org/10.1504/IJVNV.2020.117820

32. Sharma, S.K., Phan, H., Lee, J.: An application study on road surface monitoring using DTW based image processing and ultrasonic sensors. Appl. Sci. **10**, 4490 (2020). https://doi.org/10.3390/app10134490

33. Sharma, R.C., Sharma, S., Sharma, S.K., Sharma, N.: Analysis of generalized force and its influence on ride and stability of railway vehicle. Noise Vib. Worldw. **51**, 95–109 (2020). https://doi.org/10.1177/0957456520923125

34. Lee, J., Sharma, S.K.: Numerical investigation of critical speed analysis of high-speed rail vehicle. 한국정밀공학회 학술발표대회 논문집 (Korean Soc. Precis. Eng. 696) (2020)

35. Sharma, S.K., Lee, J.: Finite element analysis of a fishplate rail joint in extreme environment condition. Int. J. Veh. Struct. Syst. **12**, 503–506 (2020). https://doi.org/10.4273/ijvss.12.5.03

36. Bhardawaj, S., Sharma, R.C., Sharma, S.K.: Ride analysis of track-vehicle-human body interaction subjected to random excitation. J. Chinese Soc. Mech. Eng. **41**, 237–236 (2020). https://doi.org/10.29979/JCSME

37. Bhardawaj, S., Sharma, R.C., Sharma, S.K.: Development in the modeling of rail vehicle system for the analysis of lateral stability. Mater. Today Proc. **25**, 610–619 (2020). https://doi.org/10.1016/j.matpr.2019.07.376

38. Bhardawaj, S., Sharma, R.C., Sharma, S.K.: Analysis of frontal car crash characteristics using ANSYS. Mater. Today Proc. **25**, 898–902 (2020). https://doi.org/10.1016/j.matpr.2019.12.358

39. Sharma, S., Sharma, R.C., Sharma, S.K., Sharma, N., Palli, S., Bhardawaj, S.: Vibration isolation of the quarter car model of road vehicle system using dynamic vibration absorber. Int. J. Veh. Struct. Syst. **12**, 513–516 (2020). https://doi.org/10.4273/ijvss.12.5.05

40. Acharya, A., Gahlaut, U., Sharma, K., Sharma, S.K., Vishwakarma, P.N., Phanden, R.K.: Crashworthiness analysis of a thin-walled structure in the frontal part of automotive chassis. Int. J. Veh. Struct. Syst. **12**, 517–520 (2020). https://doi.org/10.4273/ijvss.12.5.06

41. Bhardawaj, S., Sharma, R.C., Sharma, S.K.: Development of multibody dynamical using MR damper based semi-active bio-inspired chaotic fruit fly and fuzzy logic hybrid suspension control for rail vehicle system. Proc. Inst. Mech. Eng. Part K J. Multi-body Dyn. **234**, 723–744 (2020). https://doi.org/10.1177/1464419320953685

42. Sharma, S.K., Lee, J.: Design and development of smart semi active suspension for nonlinear rail vehicle vibration reduction. Int. J. Struct. Stab. Dyn. **20**, 2050120 (2020). https://doi.org/10.1142/S0219455420501205

43. Sharma, S.K.: Multibody analysis of longitudinal train dynamics on the passenger ride performance due to brake application. Proc. Inst. Mech. Eng. Part K J. Multi-body Dyn. **233**, 266–279 (2019). https://doi.org/10.1177/1464419318788775

44. Goyal, S., Anand, C.S., Sharma, S.K., Sharma, R.C.: Crashworthiness analysis of foam filled star shape polygon of thin-walled structure. Thin-Walled Struct. **144**, 106312 (2019). https://doi.org/10.1016/j.tws.2019.106312

45. Sharma, S.K., Sharma, R.C.: Pothole detection and warning system for Indian roads. In: Advances in Interdisciplinary Engineering, pp. 511–519 (2019). https://doi.org/10.1007/978-981-13-6577-5_48

46. Goswami, B., Rathi, A., Sayeed, S., Das, P., Sharma, R.C., Sharma, S.K.: Optimization design for aerodynamic elements of Indian locomotive of passenger train. In: Advances in Engineering Design, pp. 663–673. Lecture Notes in Mechanical Engineering. Springer, Singapore (2019). https://doi.org/10.1007/978-981-13-6469-3_61

47. Bhardawaj, S., Sharma, R.C, Sharma, S.K.: Development and advancement in the wheel-rail rolling contact mechanics. IOP Conf. Ser. Mater. Sci. Eng. **691**, 012034 (2019). https://doi.org/10.1088/1757-899X/691/1/012034

48. Choppara, R.K., Sharma, R.C., Sharma, S.K., Gupta, T.: Aero dynamic cross wind analysis of locomotive. In: IOP Conference Series: Materials Science and Engineering, p. 12035. IOP Publishing (2019)

49. Kalra, M., Singh, S.: A review of metaheuristic scheduling techniques in cloud computing. Egypt Inform. J. **16**, 275–295 (2015). https://doi.org/10.1016/j.eij.2015.07.001

50. Novais, L., Maqueira, J.M., Ortiz-Bas, Á.: A systematic literature review of cloud computing use in supply chain integration. Comput. Ind. Eng. **129**, 296–314 (2019). https://doi.org/10.1016/j.cie.2019.01.056

51. González Ramírez, P.L., Lloret, J., Tomás, J., Hurtado, M.: IoT-networks group-based model that uses AI for workgroup allocation. Comput. Netw. **186**, 107745 (2021). https://doi.org/10.1016/j.comnet.2020.107745

52. Lee, W.J., Wu, H., Yun, H., Kim, H., Jun, M.B.G., Sutherland, J.W.: Predictive maintenance of machine tool systems using artificial intelligence techniques applied to machine condition data. In: Procedia CIRP, pp. 506–511. Elsevier B.V. (2019). https://doi.org/10.1016/j.procir.2018.12.019

53. Thoben, K.D., Wiesner, S.A., Wuest, T.: "Industrie 4.0" and smart manufacturing-a review of research issues and application examples. Int. J. Autom. Technol. **11**, 4–16 (2017). https://doi.org/10.20965/ijat.2017.p0004

54. Lu, S.C.Y.: Machine learning approaches to knowledge synthesis and integration tasks for advanced engineering automation (1990). https://doi.org/10.1016/0166-3615(90)90088-7

55. Wuest, T., Weimer, D., Irgens, C., Thoben, K.D.: Machine Learning in Manufacturing: Advantages, Challenges, and Applications (2016). https://doi.org/10.1080/21693277.2016.1192517

56. Moyne, J., Iskandar, J.: Big Data Analytics for Smart Manufacturing: Case Studies in Semiconductor Manufacturing (2017). https://doi.org/10.3390/pr5030039

57. Lee, J., Bagheri, B., Kao, H.A.: A Cyber-Physical Systems architecture for Industry 4.0-based manufacturing systems (2015). https://doi.org/10.1016/j.mfglet.2014.12.001

58. Sunny, J., Undralla, N., Madhusudanan Pillai, V.: Supply chain transparency through blockchain-based traceability: an overview with demonstration. Comput. Ind. Eng. **150**, 106895 (2020). https://doi.org/10.1016/j.cie.2020.106895

59. Ragot, S., Rey, A., Shafai, R.: IP lifecycle management using blockchain and machine learning: application to 3D printing datafiles. World Pat. Inf. **62**, 101966 (2020). https://doi.org/10.1016/j.wpi.2020.101966

60. Gao, S., Liu, L., Liu, Y., Liu, H., Wang, Y.: API recommendation for the development of Android App features based on the knowledge mined from App stores. Sci. Comput. Program. **202**, 102556 (2021). https://doi.org/10.1016/j.scico.2020.102556

61. Avazpour, I., Grundy, J., Zhu, L.: Engineering complex data integration, harmonization and visualization systems. J. Ind. Inf. Integr. **16**, 100103 (2019). https://doi.org/10.1016/j.jii.2019.08.001

62. Borgogno, O., Colangelo, G.: Data sharing and interoperability: fostering innovation and competition through APIs. Comput. Law Secur. Rev. **35**, 105314 (2019). https://doi.org/10.1016/j.clsr.2019.03.008

63. Chen, H., Hou, L., Zhang, G. (Kevin), Moon, S.: Development of BIM, IoT and AR/VR technologies for fire safety and upskilling. Autom. Constr. **125**, 103631 (2021). https://doi.org/10.1016/j.autcon.2021.103631

64. Sinha, A.K., Sengupta, A., Gandhi, H., Bansal, P., Agarwal, K.M., Sharma, S.K., Sharma, R.C., Sharma, S.K.: Performance enhancement of an all-terrain vehicle by optimizing steering, powertrain and brakes. In: Advances in Engineering Design, pp. 207–215 (2019). https://doi.org/10.1007/978-981-13-6469-3_19

65. Sharma, S.K., Saini, U., Kumar, A.: Semi-active control to reduce lateral vibration of passenger rail vehicle using disturbance rejection and continuous state damper controllers. J. Vib. Eng. Technol. **7**, 117–129 (2019). https://doi.org/10.1007/s42417-019-00088-2

66. Bhardawaj, S., Chandmal Sharma, R., Kumar Sharma, S.: A survey of railway track modelling. Int. J. Veh. Struct. Syst. **11**, 508–518 (2019). https://doi.org/10.4273/ijvss.11.5.08

67. Sharma, R.C., Palli, S., Sharma, S.K., Roy, M.: Modernization of railway track with composite sleepers. Int. J. Veh. Struct. Syst. **9**, 321–329 (2018)

68. Sharma, R.C., Sharma, S.K., Palli, S.: Rail vehicle modelling and simulation using Lagrangian method. Int. J. Veh. Struct. Syst. **10**, 188–194 (2018). https://doi.org/10.4273/ijvss.10.3.07

69. Palli, S., Koona, R., Sharma, S.K., Sharma, R.C.: A review on dynamic analysis of rail vehicle coach. Int. J. Veh. Struct. Syst. **10**, 204–211 (2018). https://doi.org/10.4273/ijvss.10.3.10

70. Sharma, S.K., Sharma, R.C.: An investigation of a locomotive structural crashworthiness using finite element simulation. SAE Int. J. Commer. Veh. **11**, 235–244 (2018). https://doi.org/10.4271/02-11-04-0019

71. Sharma, S.K., Sharma, R.C.: Simulation of quarter-car model with magnetorheological dampers for ride quality improvement. Int. J. Veh. Struct. Syst. **10**, 169–173 (2018). https://doi.org/10.4273/ijvss.10.3.03

72. Sharma, S.K., Kumar, A.: Impact of longitudinal train dynamics on train operations: a simulation-based study. J. Vib. Eng. Technol. **6**, 197–203 (2018). https://doi.org/10.1007/s42417-018-0033-4

73. Sharma, R.C., Sharma, S.K.: Sensitivity analysis of three-wheel vehicle's suspension parameters influencing ride behavior. Noise Vib. Worldw. **49**, 272–280 (2018). https://doi.org/10.1177/0957456518796846

74. Sharma, S.K., Kumar, A.: Ride comfort of a higher speed rail vehicle using a magnetorheological suspension system. Proc. Inst. Mech. Eng. Part K J. Multi-body Dyn. **232**, 32–48 (2018). https://doi.org/10.1177/1464419317706873

75. Sharma, S.K., Kumar, A.: Disturbance rejection and force-tracking controller of nonlinear lateral vibrations in passenger rail vehicle using magnetorheological fluid damper. J. Intell. Mater. Syst. Struct. **29**, 279–297 (2018). https://doi.org/10.1177/1045389X17721051

76. Sharma, S.K., Kumar, A.: Impact of electric locomotive traction of the passenger vehicle Ride quality in longitudinal train dynamics in the context of Indian railways. Mech. Ind. **18**, 222 (2017). https://doi.org/10.1051/meca/2016047

77. Sharma, S.K., Kumar, A.: Ride performance of a high speed rail vehicle using controlled semi active suspension system. Smart Mater. Struct. **26**, 055026 (2017). https://doi.org/10.1088/1361-665X/aa68f7

78. Sharma, S.K., Kumar, A.: Dynamics analysis of wheel rail contact using FEA. Procedia Eng. **144**, 1119–1128 (2016). https://doi.org/10.1016/j.proeng.2016.05.076

79. Sharma, S.K., Kumar, A.: The impact of a rigid-flexible system on the ride quality of passenger bogies using a flexible carbody. In: Pombo, J. (ed.) Proceedings of the Third International Conference on Railway Technology: Research, Development and Maintenance, Stirlingshire, UK, p. 87. Civil-Comp Press, 2016, Stirlingshire, UK (2016). https://doi.org/10.4203/ccp.110.87

80. Sharma, S.K., Chaturvedi, S.: Jerk analysis in rail vehicle dynamics. Perspect. Sci. **8**, 648–650 (2016). https://doi.org/10.1016/j.pisc.2016.06.047

81. Kulkarni, D., Sharma, S.K., Kumar, A.: Finite element analysis of a fishplate rail joint due to wheel impact. In: International Conference on Advances in Dynamics, Vibration and Control (ICADVC-2016) NIT Durgapur, India February 25–27, 2016. National Institute of Technology Durgapur, Durgapur, India (2016)

82. Sharma, S.K., Sharma, R.C., Kumar, A., Palli, S.: Challenges in rail vehicle-track modeling and simulation. Int. J. Veh. Struct. Syst. **7**, 1–9 (2015). https://doi.org/10.4273/ijvss.7.1.01

83. Sharma, S.K., Kumar, A., Sharma, R.C.: Challenges in railway vehicle modeling and simulations. In: International Conference on Newest Drift in Mechanical Engineering (ICNDME-14), December 20–21, M. M. University, Mullana, INDIA, pp. 453–459. Maharishi Markandeshwar University, Mullana–Ambala (2014)

84. Sharma, S.K., Kumar, A.: A comparative study of Indian and Worldwide railways. Int. J. Mech. Eng. Robot. Res. **1**, 114–120 (2014)

85. Sharma, S.K.: Zero energy building envelope components: a review. Int. J. Eng. Res. Appl. **3**, 662–675 (2013)

86. Sharma, S.K., Lavania, S.: An autonomous metro: design and execution. In: Futuristic trends in Mechanical and Industrial Engineering, pp. 1–8. JECRC UDML College of Engineering, Jaipur (2013)

87. Sharma, S.K., Lavania, S.: Green manufacturing and green supply chain management in India a review. In: Futuristic trends in Mechanical and Industrial Engineering, pp. 1–8. JECRC UDML College of Engineering (2013)

88. Sharma, S.K., Lavania, S.: Skin effect in high speed VLSI on-chip interconnects. In: International Conference on VLSI, Communication & Networks, V-CAN, pp. 1–8. Institute of Engineering & Technology, Alwar (2011)

89. Lavania, S., Sharma, S.K.: An explicit approach to compare crosstalk noise and delay in VLSI RLC interconnect modeled with skin effect with step and ramp input. J. VLSI Des. Tools Technol. **1**, 1–8 (2011)

90. Xiang, F., Zhi, Z., Jiang, G.: Digital twins technolgy and its data fusion in iron and steel product life cycle. In: ICNSC 2018—15th IEEE International Conference on Networking, Sensing and Control, pp. 1–5 (2018). https://doi.org/10.1109/ICNSC.2018.8361293

91. Guo, F., Zou, F., Liu, J., Wang, Z.: Working mode in aircraft manufacturing based on digital coordination model. Int. J. Adv. Manuf. Technol. **98**, 1547–1571 (2018). https://doi.org/10.1007/s00170-018-2048-0

92. Zhang, M., Zuo, Y., Tao, F.: Equipment energy consumption management in digital twin shop-floor: a framework and potential applications. In: ICNSC 2018—15th IEEE International Conference on Networking, Sensing and Control, pp. 1–5 (2018). https://doi.org/10.1109/ICNSC.2018.8361272

93. Talkhestani, B.A., Jazdi, N., Schloegl, W., Weyrich, M.: Consistency check to synchronize the Digital Twin of manufacturing automation based on anchor points. Procedia CIRP. **72**, 159–164 (2018). https://doi.org/10.1016/j.procir.2018.03.166

94. Ben Miled, Z., French, M.O., Miled, Z. Ben: Towards a reasoning framework for digital clones using the digital thread. 55th AIAA Aerosp. Sci. Meet. 0873 (2017). https://doi.org/10.2514/6.2017-0873

95. Lohtander, M., Ahonen, N., Lanz, M., Ratava, J., Kaakkunen, J.: Micro manufacturing unit and the corresponding 3D-model for the Digital Twin. Procedia Manuf. **25**, 55–61 (2018). https://doi.org/10.1016/j.promfg.2018.06.057

96. Torkamani, A., Andersen, K.G., Steinhubl, S.R., Topol, E.J.: High-definition medicine. Cell **170**, 828–843

97. Verdouw, C., Kruize, J.W., Wolfert, S., Chatzikostas, G.: Digital Twins in farm management. In: PA17–The International Tri-Conference for Precision Agriculture in 2017, Hamilton (2017)

98. Glaessgen, E.H., Stargel, D.S.: The digital twin paradigm for future NASA and U.S. Air force vehicles. In: Collection of Technical Papers—AIAA/ASME/ASCE/AHS/ASC Structures, Structural Dynamics and Materials Conference (2012). https://doi.org/10.2514/6.2012-1818

99. Cai, Y., Starly, B., Cohen, P., Lee, Y.S.: Sensor data and information fusion to construct digital-twins virtual machine tools for cyber-physical manufacturing. Procedia Manuf. **10**, 1031–1042 (2017). https://doi.org/10.1016/j.promfg.2017.07.094

100. Cheng, J., Chen, W., Tao, F., Lin, C.L.: Industrial IoT in 5G environment towards smart manufacturing. J. Ind. Inf. Integr. **10**, 10–19 (2018). https://doi.org/10.1016/j.jii.2018.04.001

101. Zhang, H., Liu, Q., Chen, X., Zhang, D., Leng, J.: A Digital Twin-based approach for designing and multi-objective optimization of hollow glass production line. IEEE Access. **5**, 26901–26911 (2017). https://doi.org/10.1109/ACCESS.2017.2766453

102. Damiani, L., Demartini, M., Giribone, P., Maggiani, M., Revetria, R., Tonelli, F.: Simulation and digital twin based design of a production line: a case study. In: Lecture Notes in Engineering and Computer Science (2018)

103. Guo, J., Zhao, N., Sun, L., Zhang, S.: Modular based flexible digital twin for factory design. J. Ambient Intell. Humaniz. Comput. **10**, 1189–1200 (2019). https://doi.org/10.1007/s12652-018-0953-6

104. Stojanovic, V., Trapp, M., Richter, R., Hagedorn, B., Döllner, J.: Towards the Generation of Digital Twins for Facility Management Based on 3D Point Clouds (2018)

105. Uhlemann, T.H.J., Schock, C., Lehmann, C., Freiberger, S., Steinhilper, R.: The Digital Twin: demonstrating the potential of real time data acquisition in production systems. Procedia Manuf. **9**, 113–120 (2017). https://doi.org/10.1016/j.promfg.2017.04.043

106. Schroeder, G.N., Steinmetz, C., Pereira, C.E., Espindola, D.B.: Digital Twin data modeling with AutomationML and a communication methodology for data exchange. IFAC-PapersOnLine **49**, 12–17 (2016). https://doi.org/10.1016/j.ifacol.2016.11.115

107. Kraft, E.M.: Approach to the development and application of a digital thread/digital twin authoritative truth source (2018). https://doi.org/10.2514/6.2018-4003

108. Uhlemann, E., Hohwieler, E., Geisert, C.: Intelligent production systems in the era of industrie 4.0-Changing mindsets and business models. J. Mach. Eng. **17**, 5–24 (2017)

109. Hu, L., Nguyen, N.T., Tao, W., Leu, M.C., Liu, X.F., Shahriar, M.R., Al Sunny, S.M.N.: Modeling of cloud-based digital twins for smart manufacturing with MT connect. Procedia Manuf. **26**, 1193–1203.

110. Qi, Q., Tao, F.: Digital Twin and big data towards smart manufacturing and industry 4.0: 360 degree comparison. IEEE Access. **6**, 3585–3593 (2018). https://doi.org/10.1109/ACCESS.2018.2793265

111. Schleich, B., Anwer, N., Mathieu, L., Wartzack, S.: Shaping the digital twin for design and production engineering. CIRP Ann. Manuf. Technol. **66**, 141–144 (2017). https://doi.org/10.1016/j.cirp.2017.04.040

112. Rubmann, M., Lorenz, M., Gerbert, P., Waldner, M., Justus, J., Engel, P., Harnisch, M.: Industry 4.0: the future of productivity and growth in manufacturing industries. Bost. Consult. Gr. **9**, 1–14 (2015)

113. Shafto, M., Conroy, M., Doyle, R., Glaessgen, E., Kemp, C., LeMoigne, J., Wang, L.: Modeling, simulation, information technology & processing road- map. National Aeronautics and Space Administration

114. Onosato, M., Iwata, K.: Development of a virtual manufacturing system by integrating product models and factory models. CIRP Ann. Manuf. Technol. **42**, 475–478 (1993). https://doi.org/10.1016/S0007-8506(07)62489-5

115. Baruffaldi, G., Accorsi, R., Manzini, R.: Warehouse management system customization and information availability in 3pl companies: a decision-support tool. Ind. Manag. Data Syst. **119**, 251–273 (2019). https://doi.org/10.1108/IMDS-01-2018-0033

116. Qi, Q., Tao, F., Zuo, Y., Zhao, D.: Digital Twin service towards smart manufacturing. Procedia CIRP. **72**, 237–242 (2018). https://doi.org/10.1016/j.procir.2018.03.103

117. Yang, W., Yoshida, K., Takakuwa, S.: Digital twin-driven simulation for a cyber-physical system in Industry 4. 0. DAAAM International Scientific Book

118. Zheng, Y., Yang, S., Cheng, H.: An application framework of digital twin and its case study. J. Ambient Intell. Humaniz. Comput. **10**, 1141–1153 (2019). https://doi.org/10.1007/s12652-018-0911-3

119. Cheng, Y., Zhang, Y., Ji, P., Xu, W., Zhou, Z., Tao, F.: Cyber-physical integration for moving digital factories forward towards smart manufacturing: a survey. Int J Adv Manuf Technol (2018). https://doi.org/10.1007/s00170-018-2001-2

120. Culley, S.J.: The mechanical design process. McGraw-Hill (1994). https://doi.org/10.1016/0142-694x(94)90041-8

121. Liu, M., Fang, S., Dong, H., Xu, C.: Review of digital twin about concepts, technologies, and industrial applications. J. Manuf. Syst. **58**, 346–361 (2021). https://doi.org/10.1016/j.jmsy.2020.06.017

122. Automation, I.: A Reference Model For Computer Integrated Manufacturing (CIM). International Purdue Works

123. Iwata, K., Onosato, M., Teramoto, K., Osaki, S.: A modelling and simulation architecture for virtual manufacturing systems. CIRP Ann. Manuf. Technol. **44**, 399–402 (1995). https://doi.org/10.1016/S0007-8506(07)62350-6

124. Morari, M., Garcia, C.E., Prett, D.M.: Model predictive control: theory and practice. IFAC Proc. **21**, 1–12 (1988). https://doi.org/10.1016/b978-0-08-035735-5.50006-1

125. Mayne, D.Q.: Model predictive control: recent developments and future promise. Automatica **50**, 2967–2986 (2014). https://doi.org/10.1016/j.automatica.2014.10.128

126. Dotoli, M., Fay, A., Miśkowicz, M., Seatzu, C.: Advanced control in factory automation: a survey. Int. J. Prod. Res. **55**, 1243–1259 (2017). https://doi.org/10.1080/00207543.2016.1173259

127. Heng, A., Zhang, S., Tan, A.C.C., Mathew, J.: Rotating machinery prognostics: State of the art, challenges and opportunities. Mech. Syst. Signal Process. **23**, 724–739 (2009). https://doi.org/10.1016/j.ymssp.2008.06.009

128. Wang, X.: BIM handbook: a guide to building information modeling for owners, managers, designers, engineers and contractors. John Wiley & Sons (2012). https://doi.org/10.5130/ajceb.v12i3.2749

129. Kritzinger, W., Karner, M., Traar, G., Henjes, J., Sihn, W.: Digital Twin in manufacturing: a categorical literature review and classification. IFAC-PapersOnLine **51**, 1016–1022 (2018). https://doi.org/10.1016/j.ifacol.2018.08.474

130. Wagner, R., Schleich, B., Haefner, B., Kuhnle, A., Wartzack, S., Lanza, G.: Challenges and potentials of digital twins and industry 4.0 in product design and production for high performance products. In: Procedia CIRP, pp. 88–93. Elsevier B.V. (2019). https://doi.org/10.1016/j.procir.2019.04.219

131. Damjanovic-Behrendt, V.: A Digital Twin-based privacy enhancement mechanism for the automotive industry. In: 9th International Conference on Intelligent Systems 2018: Theory, Research and Innovation in Applications, IS 2018—Proceedings, pp. 272–279 (2018). https://doi.org/10.1109/IS.2018.8710526

132. Ayani, M., Ganebäck, M., Ng, A.H.C.: Digital Twin: applying emulation for machine reconditioning. In: Procedia CIRP, pp. 243–248 (2018). https://doi.org/10.1016/j.procir.2018.03.139

133. Macchi, M., Roda, I., Negri, E., Fumagalli, L.: Exploring the role of digital twin for asset lifecycle management. IFAC-PapersOnLine **51**, 790–795

134. Bitton, R., Gluck, T., Stan, O., Inokuchi, M., Ohta, Y., Yamada, Y., Yagyu, T., Elovici, Y., Shabtai, A.: Deriving a cost-effective digital twin of an ICS to facilitate security evaluation. In: Lecture Notes in Computer Science (including subseries Lecture Notes in Artificial Intelligence and Lecture Notes in Bioinformatics), pp. 533–554 (2018). https://doi.org/10.1007/978-3-319-99073-6_26

135. Söderberg, R., Wärmefjord, K., Carlson, J.S., Lindkvist, L.: Toward a Digital Twin for real-time geometry assurance in individualized production. CIRP Ann. Manuf. Technol. **66**, 137–140 (2017). https://doi.org/10.1016/j.cirp.2017.04.038

136. Botkina, D., Hedlind, M., Olsson, B., Henser, J., Lundholm, T.: Digital Twin of a cutting tool. Procedia CIRP. **72**, 215–218 (2018). https://doi.org/10.1016/j.procir.2018.03.178

137. AnyLogic: Digital Twin of a Manufacturing Line: Helping Maintenance Decision-making

138. Rosen, R., von Wichert, G., Lo, G., Bettenhausen, K.D.: About the importance of autonomy and digital twins for the future of manufacturing. IFAC-PapersOnLine **48**, 567–572 (2015). https://doi.org/10.1016/j.ifacol.2015.06.141

139. GeoDict (landing page). https://www.geodict.com Metrilus (2019) MetriXFreight Smart Dimensioning

140. Siemens: Optimizing offshore production with Siemens Topsides 4.0 digital lifecycle solutions

141. Sharma, R.C., Palli, S., Sharma, S.K.: Ride analysis of railway vehicle considering rigidity and flexibility of the carbody. J. Chinese Inst. Eng. **46**, 355–366 (2023). https://doi.org/10.1080/02533839.2023.2194918

142. Partners, G.E.H.: What's a Digital Twin? https://uscan.gehealthcarepartners.com/service-about/digital-twin

143. Sharma, R.C., Palli, S., Jha, A.K., Bhardawaj, S., Sharma, S.K.: Vibration And Ride Comfort Analysis of Railway Vehicle System Subjected to Deterministic Inputs. resmilitaris. **12**, 1345–1355 (2022)

144. Copley, C.: Medtech Firms get Personal with Digital Twins (2019)

145. Sharma, R.C., Rao, L.V.V.G., Sharma, S.K., Palli, S., Satyanarayana, V.S. V: Analysis of Lateral Stability and Ride of an Indian Railway Constrained Dual-Axle Bogie Frame. SAE Int. J. Commer. Veh. **16**, (2022)

146. AG, S.: For a digital twin of the grid (2017) https://www.siemens.com/press/pool/de/events/2017/corporate/2017-12-innovation/inno2017-digitaltwin-e.pdf (2017)

147. Sharma, R.C., Palli, S., Rao, L.V.V.G., Duppala, A., Sharma, S.K.: Four-Wheel Vehicle Response under Bump, Pothole, Harmonic, and Random Excitations Using Bond Graph/Simulink Technique. SAE Int. J. Commer. Veh. **16**, (2022)

148. Kumar, U., Kasvekar, R., Sharma, S.K., Upadhyay, R.K.: Wear of Wheels and Axle in Locomotive and Measures Taken by Indian Railway. Adv. Engine Tribol. 77–96 (2022)

149. DNV GL: WindGEMINI digital twin for wind turbine operations (2018)

150. Steffen, A.D.: IKEA Starts Using Compostable Mushroom-Based Packaging For Its Products (2019)

151. Lempert, P.: Ikea Switches to Packaging Made From Mushrooms (2018)

152. Hippold, S.: How Digital Twins Simplify the IoT (2019)

153. DroneScan: Homepage. http://www.dronescan.co

154. Sharma, S.K., Sharma, R.C., Choi, Y., Lee, J.: Experimental and Mathematical Study of Flexible–Rigid Rail Vehicle Riding Comfort and Safety. Appl. Sci. **13**, 5252 (2023). https://doi.org/10.3390/app13095252

155. Daniel, F.: The Self-Driving Car Timeline—Predictions from the Top 11 Global Automakers | Emerj (2014). https://emerj.com/ai-adoption-timelines/self-driving-car-timeline-themselves-top-11-automakers/

156. Ivanov, D., Dolgui, A., Das, A., Sokolov, B.: Digital Supply Chain Twins: Managing the Ripple Effect, Resilience, and Disruption Risks by Data-Driven Optimization, Simulation, and Visibility. Springer International Publishing (2019). https://doi.org/10.1007/978-3-030-14302-2_15